THE ROLE OF NEUROVASCULAR UNIT IN NEURODEGENERATION

EDITED BY: Dennis Qing Wang and Eng-King Tan
PUBLISHED IN: Frontiers in Cellular Neuroscience, Frontiers in Aging Neuroscience and Frontiers in Neuroscience

frontiers Research Topics

frontiers

ISSN 1664-8714
ISBN 978-2-88976-126-5
DOI 10.3389/978-2-88976-126-5

About Frontiers

Frontiers is more than just an open-access publisher of scholarly articles: it is a pioneering approach to the world of academia, radically improving the way scholarly research is managed. The grand vision of Frontiers is a world where all people have an equal opportunity to seek, share and generate knowledge. Frontiers provides immediate and permanent online open access to all its publications, but this alone is not enough to realize our grand goals.

Frontiers Journal Series

The Frontiers Journal Series is a multi-tier and interdisciplinary set of open-access, online journals, promising a paradigm shift from the current review, selection and dissemination processes in academic publishing. All Frontiers journals are driven by researchers for researchers; therefore, they constitute a service to the scholarly community. At the same time, the Frontiers Journal Series operates on a revolutionary invention, the tiered publishing system, initially addressing specific communities of scholars, and gradually climbing up to broader public understanding, thus serving the interests of the lay society, too.

Dedication to Quality

Each Frontiers article is a landmark of the highest quality, thanks to genuinely collaborative interactions between authors and review editors, who include some of the world's best academicians. Research must be certified by peers before entering a stream of knowledge that may eventually reach the public - and shape society; therefore, Frontiers only applies the most rigorous and unbiased reviews.
Frontiers revolutionizes research publishing by freely delivering the most outstanding research, evaluated with no bias from both the academic and social point of view. By applying the most advanced information technologies, Frontiers is catapulting scholarly publishing into a new generation.

What are Frontiers Research Topics?

Frontiers Research Topics are very popular trademarks of the Frontiers Journals Series: they are collections of at least ten articles, all centered on a particular subject. With their unique mix of varied contributions from Original Research to Review Articles, Frontiers Research Topics unify the most influential researchers, the latest key findings and historical advances in a hot research area! Find out more on how to host your own Frontiers Research Topic or contribute to one as an author by contacting the Frontiers Editorial Office: frontiersin.org/about/contact

THE ROLE OF NEUROVASCULAR UNIT IN NEURODEGENERATION

Topic Editors:
Dennis Qing Wang, Southern Medical University, China
Eng-King Tan, National Neuroscience Institute (NNI), Singapore

Citation: Wang, D. Q., Tan, E.-K., eds. (2022). The Role of Neurovascular Unit in Neurodegeneration. Lausanne: Frontiers Media SA.
doi: 10.3389/978-2-88976-126-5

Table of Contents

frontiers | Frontiers in Cellular Neuroscience

EDITORIAL
published: 19 April 2022
doi: 10.3389/fncel.2022.870631

Editorial: The Role of Neurovascular Unit in Neurodegeneration

Zhi Dong Zhou[1,2]*, *Dennis Qing Wang*[3] and *Eng-King Tan*[1,2,4]*

[1] Department of Research, National Neuroscience Institute, Singapore, Singapore, [2] Neuroscience and Behavioural Disorders Programme (NBD), Duke-National University of Singapore Medical School, Singapore, Singapore, [3] Zhujiang Hospital of Southern Medical University, Guangzhou, China, [4] Department of Neurology, Singapore General Hospital, Singapore, Singapore

Keywords: blood-brain barrier, cerebral blood flow, cerebral vasculature system, neurovascular unit (NVU), neurovascular coupling (NC), pathogenesis and therapy

Editorial on the Research Topic

The Role of Neurovascular Unit in Neurodegeneration

The neurovascular unit (NVU) is a novel concept which refers to the dynamic multicellular complex and functional interactions between brain tissues and blood vessels (Schaeffer and Iadecola, 2021). Neurons, perivascular astrocytes, microglia, pericytes, and endothelial cells (ECs), as well as the basement membrane (BM) form a functional NVU complex (Bell et al., 2020). These components interact with each other in order to maintain the physiological integrity of the NVU. It is suggested that the NVU modulates neurovascular coupling (NVC) and maintains blood–brain barrier (BBB) functions, which are vital to brain homeostasis and functions (Bell et al., 2020). In NVC, the cerebral blood flow (CBF) and cerebral nutrition supplement demand are closely linked *via* molecular events to regulate the intraluminal diameter of cerebral blood vessels (Bell et al., 2020). The other major function of the NVU is to maintain BBB barrier functions, leading to formation of a specific circumstance for cerebral function and development (Bell et al., 2020). Under physiological conditions, NVU component cells and the BM cooperate in multicellular complex for BBB development and maintenance (Xu et al., 2019; Bell et al., 2020).

Increasing evidence suggests that dysfunction of the NVU can be associated with Alzheimer's disease (AD), Parkinson's disease (PD), sleep disorders, neurovascular diseases, and traumatic brain injury (Schaeffer and Iadecola, 2021). Recent studies demonstrate that amyloid β (Aβ) disrupts cerebral circulation and disturbs capillary blood flow distribution through targeting pericytes (Schaeffer and Iadecola, 2021). The hyperphosphorylated tau, the other main pathogenic factor of AD, selectively inhibits artery dilatation in the process of NVC, contributing to neurodegeneration in AD (Schaeffer and Iadecola, 2021). Studies suggest that dysfunction of NVC and disturbance of cerebral blood flow are also implicated in the pathogenesis of PD, sleep disorders, traumatic brain injury, and other cerebral disorders (Schaeffer and Iadecola, 2021). We still know little about the pathophysiological roles of the NVU in human neurological diseases. In this issue, three articles provide new insights which advance our understanding of the pathophysiological role of the NVU in neurological disorders (Kisler et al.; Rust et al.; Schaeffer and Iadecola, 2021).

The first study by Kisler et al. highlighted that ablation of pericytes can disturb the NVC process in transgenic mice models. Drug-induced loss of pericyte coverage of cortical capillaries was associated with a significant decrease of stimulus-induced CBF responses. Their findings confirm the vital role of pericytes in modulating the NVC process, which suggests that they may play a part in neurological conditions associated with acute or chronic pericyte depletion (such as hypoperfusion and stroke, as well as human neurodegenerative conditions such as AD).

OPEN ACCESS

Edited and reviewed by:
Marie-Ève Tremblay,
University of Victoria, Canada

***Correspondence:**
Eng-King Tan
gnrtek@sgh.com.sg
Zhi Dong Zhou
zhidong_zhou@nni.com.sg

Specialty section:
This article was submitted to Non-Neuronal Cells, a section of the journal Frontiers in Cellular Neuroscience

Received: *07 February 2022*
Accepted: *02 March 2022*
Published: *19 April 2022*

Citation:
Zhou ZD, Wang DQ and Tan E-K (2022) Editorial: The Role of Neurovascular Unit in Neurodegeneration. Front. Cell. Neurosci. 16:870631. doi: 10.3389/fncel.2022.870631

In the second study by Rust et al., the authors developed a fast, automated, and highly reproducible protocol [utilizing the open source software Fiji (ImageJ)] for quantitative analysis and monitoring of various vascular parameters and their alterations. Their novel method provides a practical and reliable guide to monitor dynamic changes in cerebral NVC and the vasculature system under various pathological and physiological conditions in mice and humans, including pharmacological drug-induced alteration of NVC or the cerebral vasculature system.

In the third study, Schaeffer and Iadecola highlighted that dysfunction of the BBB can be associated with neurodegeneration in PD. The increased permeability of the BBB was identified in advanced PD, which was associated with leakage of red blood cells (RBCs) and neurotoxic factors from circulation into parenchymal brain tissue (Schaeffer and Iadecola, 2021). The penetration of RBCs into the brain can cause accumulation of iron species and generation of neurotoxic reactive oxygen species (ROS) (Schaeffer and Iadecola, 2021). In a recent study, Yang et al. studied 204 PD patients and 204 aging healthy controls (HCs), and found that serum SOD level was decreased, while serum hsCRP, an inflammation marker, increased in PD patients. Furthermore, abnormalities in lipid metabolism with decreased cholesterol, HDL-C, and LDL-C were identified in PD, compared with HCs. Plasma HDL and cholesterol were closely related to the integrity of the BBB, and dyslipidemia can cause BBB impairment (Bowman et al., 2012). These findings suggest a link between BBB impairment and PD pathogenesis.

While the findings of the three studies have provided additional pathophysiologic insights, the exact role of the NVU in neurodegenerative diseases still remains to be elucidated. Recent findings demonstrate the molecular heterogeneity of brain NVU cells, suggesting no prototypical neurovascular unit may exist at distinct levels of cerebral NVU networks (Schaeffer and Iadecola, 2021). The cerebral NVU network seems to be more complicated than we expected. Further studies from *in vitro* to *in vivo* models are needed to investigate the role of the NVU in the pathogenesis of various neurological diseases with the hope of identifying potential therapeutic targets.

AUTHOR CONTRIBUTIONS

All authors contributed to conceptual design, writing, and approval of the manuscript.

FUNDING

This study was supported by the Singapore National Medical Research Council (NMRC; STaR and SPARK II Programe, OF PD LCG 0002).

REFERENCES

Bell, A. H., Miller, S. L., Castillo-Melendez, M., and Malhotra, A. (2020). The neurovascular unit: effects of brain insults during the perinatal period. *Front Neurosci.* 13:1452. doi: 10.3389/fnins.2019.01452

Bowman, G. L., Kaye, J. A., and Quinn, J. F. (2012). Dyslipidemia and blood-brain barrier integrity in Alzheimer's disease. *Curr Gerontol Geriatr Res.* 2012:184042. doi: 10.1155/2012/184042

Schaeffer, S., and Iadecola, C. (2021). Revisiting the neurovascular unit. *Nat Neurosci.* 24, 1198–1209. doi: 10.1038/s41593-021-00904-7

Xu, L., Nirwane, A., and Yao, Y. (2019). Basement membrane and blood-brain barrier. *Stroke Vasc. Neurol.* 4, 78–82. doi: 10.1136/svn-2018-000198

Conflict of Interest: The authors declare that the research was conducted in the absence of any commercial or financial relationships that could be construed as a potential conflict of interest.

frontiers in Cellular Neuroscience

BRIEF RESEARCH REPORT
published: 14 February 2020
doi: 10.3389/fncel.2020.00027

Acute Ablation of Cortical Pericytes Leads to Rapid Neurovascular Uncoupling

*Kassandra Kisler[1†], Angeliki M. Nikolakopoulou[1†], Melanie D. Sweeney[1], Divna Lazic[1,2], Zhen Zhao[1] and Berislav V. Zlokovic[1]**

[1]*Department of Physiology and Neuroscience, The Zilkha Neurogenetic Institute, Keck School of Medicine of the University of Southern California, Los Angeles, CA, United States,* [2]*Department of Neurobiology, Institute for Biological Research, University of Belgrade, Belgrade, Serbia*

Pericytes are perivascular mural cells that enwrap brain capillaries and maintain blood-brain barrier (BBB) integrity. Most studies suggest that pericytes regulate cerebral blood flow (CBF) and oxygen delivery to activated brain structures, known as neurovascular coupling. While we have previously shown that congenital loss of pericytes leads over time to aberrant hemodynamic responses, the effects of acute global pericyte loss on neurovascular coupling have not been studied. To address this, we used our recently reported inducible pericyte-specific Cre mouse line crossed to iDTR mice carrying Cre-dependent human diphtheria toxin (DT) receptor, which upon DT treatment leads to acute pericyte ablation. As expected, DT led to rapid progressive loss of pericyte coverage of cortical capillaries up to 50% at 3 days post-DT, which correlated with approximately 50% reductions in stimulus-induced CBF responses measured with laser doppler flowmetry (LDF) and/or intrinsic optical signal (IOS) imaging. Endothelial response to acetylcholine, microvascular density, and neuronal evoked membrane potential responses remained, however, unchanged, as well as arteriolar smooth muscle cell (SMC) coverage and functional responses to adenosine, as we previously reported. Together, these data suggest that neurovascular uncoupling in this model is driven by pericyte loss, but not other vascular deficits or neuronal dysfunction. These results further support the role of pericytes in CBF regulation and may have implications for neurological conditions associated with rapid pericyte loss such as hypoperfusion and stroke, as well as conditions where the exact time course of global regional pericyte loss is less clear, such as Alzheimer's disease (AD) and other neurogenerative disorders.

Keywords: neurovascular coupling, acute pericyte ablation, cerebral blood flow, capillary, laser doppler flowmetry, intrinsic optical signal imaging, voltage-sensitive dye imaging

OPEN ACCESS

Edited by:
Eng-King Tan, National Neuroscience Institute (NNI), Singapore

Reviewed by:
Hajime Hirase, University of Copenhagen, Denmark
Farida Hellal, Institute for Stroke and Dementia Research (ISD), Germany

****Correspondence:***
Berislav V. Zlokovic
zlokovic@usc.edu

†These authors have contributed equally to this work and share first authorship

Received: *26 October 2019*
Accepted: *29 January 2020*
Published: *14 February 2020*

Citation:
Kisler K, Nikolakopoulou AM, Sweeney MD, Lazic D, Zhao Z and Zlokovic BV (2020) Acute Ablation of Cortical Pericytes Leads to Rapid Neurovascular Uncoupling. Front. Cell. Neurosci. 14:27. doi: 10.3389/fncel.2020.00027

INTRODUCTION

Proper brain functioning depends on delivery of oxygen and nutrients *via* cerebral blood flow (CBF). Neurovascular coupling, the unique mechanism of CBF control in the mammalian brain, ensures a rapid increase in the rate of CBF and oxygen delivery to activated brain structures (Kisler et al., 2017a). Pericytes are perivascular mural

cells that enwrap brain capillaries. They are centrally positioned within the neurovascular unit, a collection of different cell types that at the level of brain capillaries includes pericytes, endothelial cells, astrocytes and neurons (Kisler et al., 2017a). Our group and others have shown that pericytes play vital roles in regulation of CBF (Bell et al., 2010; Tachibana et al., 2018; Nikolakopoulou et al., 2019; Nortley et al., 2019), neurovascular coupling (Peppiatt et al., 2006; Hall et al., 2014; Biesecker et al., 2016; Mishra et al., 2016; Kisler et al., 2017b; Cai et al., 2018; Rungta et al., 2018; Nortley et al., 2019), and blood-brain barrier (BBB) integrity (Armulik et al., 2010; Bell et al., 2010; Daneman et al., 2010).

Previously studied models of congenital pericyte deficiency rely on either reduced bioavailability of endothelial platelet-derived growth factor-B (PDGF-BB; Armulik et al., 2010; Keller et al., 2013) or globally inherited platelet-derived growth factor receptor-β (PDGFRβ) deficiency in pericytes (Bell et al., 2010; Daneman et al., 2010; Nikolakopoulou et al., 2017). *Pdgfrb*-deficient mice develop progressive but slow pericyte loss over time associated with CBF reductions and dysregulation, eventually leading to neuronal dysfunction as they age that may take months to develop (Bell et al., 2010; Kisler et al., 2017b; Montagne et al., 2018). While we have previously shown that moderate loss of pericytes in *Pdgfrb* pericyte-deficient mice leads to neurovascular uncoupling and diminished oxygen delivery preceding late-appearing neuronal changes (Kisler et al., 2017b), it is not clear if any developmental compensation occurred in this model that might contribute to aberrant neurovascular coupling. Using an *in vivo* laser ablation technique, another study has shown that acute single pericyte ablation leads to localized temporary loss of vascular tone and capillary dilation (Berthiaume et al., 2018). However, neither of these studies examined the effect of the rapid and global loss of brain pericytes on hemodynamic responses, as it may occur in some acute and chronic neurological disorders (Sweeney et al., 2018a,b, 2019).

To disentangle alterations in neurovascular coupling from developmental aspects of pericyte loss, and determine the effect of global acute pericyte loss on neurovascular coupling, we used a recently developed mouse model of pericyte-specific ablation to rapidly deplete pericytes from the brains of living mice (Nikolakopoulou et al., 2019). We hypothesized that rapid loss of capillary pericyte coverage would lead to rapid aberrant hemodynamic responses to neuronal stimulus.

MATERIALS AND METHODS

Animals

Mice were housed in plastic cages on a 12 h light cycle with *ad libitum* access to water and a standard laboratory diet. All procedures were approved by the Institutional Animal Care and Use Committee at the University of Southern California with the National Institutes of Health guidelines. Animals of both sexes 2–3 months old were used in the experiments. All animals were randomized for their genotype information. All experiments were blinded: the operators responsible for the experimental procedures and data analysis were blinded and unaware of group allocation throughout the experiments.

Pericyte-CreER mice, which express Cre recombinase specifically in pericytes after induction with tamoxifen (TAM) treatment, were generated using a double-promoter approach combining a Pdgfrb-Flp construct that expresses Flp recombinase under the control of the Pdgfrb promoter (Foo et al., 2006; Cuttler et al., 2011) and a Cspg4-FSF-CreER construct carrying a Frt-Stop-Frt-CreER cassette under the control of Cspg4 promoter (Zhu et al., 2008, 2011), as we described previously (Nikolakopoulou et al., 2019). These mice were crossed with iDTR mice (Jackson Laboratory, Bar Harbor, ME, USA #: 007900) for Cre-dependent expression of diphtheria toxin (DT) receptor (DTR; from simian Hbegf; Buch et al., 2005) in pericytes. Tamoxifen (TAM) was administered intraperitoneally (i.p) to mice (40 mg/kg daily) for 7 days to induce DTR expression. Two weeks after the end of TAM treatment, 2–3 months old Pericyte-CreER; iDTR mice were administered i.p. 0.1 μg DT (Sigma–Aldrich, St. Louis, MO, USA #D0564) or vehicle per day for 10 consecutive days, as we reported previously (Nikolakopoulou et al., 2019). Animals were studied at day 0, 3, 6, and 9 of DT or vehicle treatment including laser doppler flowmetry (LDF), intrinsic optical signal (IOS) imaging, and pericyte coverage) and 3 days post-DT or vehicle (LDF, IOS imaging, pericyte coverage, neuronal response by voltage-sensitive dye (VSD) imaging, vascular density).

Immunohistochemistry

Immunostaining was performed as described previously (Bell et al., 2010; Nikolakopoulou et al., 2017, 2019). Briefly, animals were anesthetized with an i.p. injection of 100 mg/kg of ketamine and 10 mg/kg of xylazine, and transcardially perfused first with 15 ml saline, followed by 20 ml of 4% paraformaldehyde (PFA) in PBS. Brains were removed and postfixed overnight with 4% PFA at 4°C before brain sections were cut at 30 μm thickness. The sections were blocked with 5% normal donkey serum (Vector Laboratories, Burlingame, CA, USA)/0.1%Triton-X/0.01M PBS and incubated with primary antibody for pericytes, polyclonal goat anti-mouse aminopeptidase N/ANPEP (CD13; R&D Systems, AF2335; 1:250), diluted in blocking solution overnight at 4°C. The sections were then washed in PBS and incubated with fluorophore-conjugated secondary antibody Alexa fluor 647-conjugated donkey anti-goat (Invitrogen, Waltham, MA, USA, A-21447, 1:500) for 1 h. To visualize brain microvessels, sections were incubated with Dylight 488-conjugated L. esculentum Lectin as we have previously reported (Bell et al., 2010; Nikolakopoulou et al., 2017) with the secondary antibodies. The sections were then washed in PBS and mounted onto slides with 4′,6-diamidino-2-phenylindole (DAPI) fluorescence mounting medium (Dako). The sections were imaged with a Zeiss LSM 510 confocal laser-scanning microscope, as we described previously (Montagne et al., 2018). Z-stack projections and pseudo-coloring were performed using ZEN software (Carl Zeiss Microimaging, Jena, Germany), and image post-analysis was performed using ImageJ software.

To determine pericyte coverage, 10 μm maximum projection z-stacks (area 640 × 480 μm) were reconstructed, and

the areas occupied by CD13-positive (pericyte) and lectin-positive (endothelium) fluorescent signals on vessels <6 μm in diameter were analyzed using ImageJ as we described previously (Nikolakopoulou et al., 2017). For each animal, four to six randomly selected fields in the S1 somatosensory cortex region were analyzed in three to four non-adjacent sections (∼100 μm apart) and averaged per mouse. Pericyte coverage of control mice that were not treated with DT was taken arbitrarily as zero loss of pericyte coverage (day 0).

To determine microvascular density, 10-micron maximum projection Z-stacks were reconstructed, and the length of lectin-positive capillary profiles (≤6 μm in diameter) were measured using the ImageJ plugin "Neuro J" length analysis tool. In each animal, 4–6 randomly selected fields (640 × 480 μm) in the somatosensory cortex were analyzed from four non-adjacent sections (∼100 μm apart), and averaged per mouse, as we have previously described (Bell et al., 2010; Nikolakopoulou et al., 2017). The length was expressed in mm of lectin-positive vascular profiles per mm^3 of brain tissue.

Cranial Window

Cranial windows were implanted as previously described (Kisler et al., 2017b, 2018). Briefly, animals were initially anesthetized with 100 mg/kg of ketamine and 10 mg/kg of xylazine and were placed on a heating pad (37°C). The cranium of the mouse was firmly secured in a stereotaxic frame (Kopf Instruments, Tujunga, CA, USA). A high-speed dental drill (tip FST 19007-05, Fine Science Tools Inc., Foster City, CA, USA) was used to delineate a cranial window about 5 mm in diameter over the somatosensory cortex, and 45° forceps were used to remove the piece of skull. Gelfoam (Pharmacia and Upjohn Company, Kalamazoo, MA, USA) was applied immediately to control any cranial or dural bleeding. A sterile 5 mm glass coverslip was then placed on the dura mater and sealed with cyanoacrylate based glue.

Laser-Doppler Flowmetry (LDF)

CBF responses to hind-limb stimulation in anesthetized mice (1% isoflurane) were determined using laser-Doppler flowmetry measured through a cranial window. The tip of the laser-Doppler probe (Transonic Systems Inc., Ithaca, NY, USA) was stereotaxically placed 0.5 mm above the cranial window. CBF was recorded from the somatosensory cortex hind-limb region following electrical stimulation of the hind-limb using a 60 s long stimulus (7 Hz, 2 ms pulse duration). The percent increase in CBF due to stimulation was obtained by subtracting the baseline CBF from the maximum value reached during stimulus, and averaged over three trials per mouse. For CBF response to acetylcholine application, the LDF probe was stereotaxically placed over the center of an open cranial window (center at AP = −1.5 mm, L = 2 mm). Acetylcholine (10 μM, Sigma–Aldrich, St. Louis, MO, USA) was superfused over the open window, and responses recorded, as we reported previously (Kisler et al., 2017b; Nikolakopoulou et al., 2019).

Intrinsic Optical Signal Imaging (IOS)

IOSs were imaged through a cranial window over the hind-limb region in the somatosensory cortex, as we previously described (Kisler et al., 2017b, 2018). Under isoflurane anesthesia set at 1%, images were captured at 30 ms/frame using a 1/2 inch CCD MiCAM02-HR camera (SciMedia; 2× binned to 184 × 124-pixel resolution; 1 pixel = 16.5 μm) with accompanying BV_ANA acquisition software. Images were captured under a 530 nm green LED light source and collected through a 522/36 nm bandpass filter (Chroma). The contralateral hind-limb was stimulated by a brief mechanical vibration lasting 300 ms. The resulting image sets were low pass filtered at 2 Hz, and the baselines corrected for any drift using the BV_ANA software. Signal time courses were evaluated using 10-pixel radius ROIs chosen in the region of peak signal change such that the regions did not include any large visible vessels, and were at least 30 μm away from any large vessels. Time courses were plotted using Igor Pro 6 and analyzed with Igor Pro 6 and GraphPad Prism 8. Pseudocolor images for presentation were generated in ImageJ.

Voltage-Sensitive Dye (VSD) Imaging

VSD imaging was performed as described previously (Kisler et al., 2017b). Briefly, a cranial window was created over the hind-limb region in the somatosensory cortex, as described above. RH-1692 VSD (1 mg/ml; Optical Imaging) dissolved in aCSF was applied to the exposed cortex for 90 min. The brain was then washed with aCSF and sealed with a coverslip as above. Under isoflurane anesthesia (1%), images were captured at 5 ms/frame (184 × 124 resolution) using a 1/2 inch CCD MiCAM02-HR camera (SciMedia, Costa Mesa, CA, USA) coupled with MiCAM BV_ANA acquisition software. RH-1692 was excited using an MHAB-150W (Moritex Corp.) light source with a 632/22 filter, and fluorescence collected with a 665 nm long-pass filter. The contralateral hind-limb was stimulated by a brief mechanical vibration lasting 300 ms. Alternating image sets were taken with and without stimulus to generate "stimulus trial" and "baseline" responses. Next, the baseline image set was subtracted from the stimulus trials to eliminate any background signal. Ten baseline subtracted trials were averaged to make up the final profile for each mouse. Time courses were evaluated using a circular ROI centered over the hind-limb region as described previously (Bell et al., 2012; Kisler et al., 2017b). Time courses were plotted using Igor Pro 6 and analyzed with Igor Pro 6 and GraphPad Prism 8. Pseudocolor images for presentation were generated in ImageJ.

Statistical Analysis

Sample sizes were calculated using nQUERY assuming a two-sided alpha-level of 0.05, 80% power, and homogeneous variances for the samples to be compared, with the means and common standard deviation for different parameters estimated based on our previous studies (Kisler et al., 2017b; Nikolakopoulou et al., 2017, 2019; Montagne et al., 2018). Data are presented as mean ± SEM. For comparison between two groups, an F-test was conducted to determine the similarity in variances between the groups that are statistically compared, and statistical significance was analyzed by two-tailed Student's t-test. For multiple comparisons, Brown–Forsythe test was used to determine the similarity in variances between the groups, and one-way analysis of variance (ANOVA) followed by Bonferroni

or Tukey's *post hoc* test was used as indicated in figure legends to test statistical significance, using GraphPad Prism 8 software. A *P*-value of less than 0.05 was considered statistically significant. Pearson correlation coefficient and significance were calculated using a two-tailed test in GraphPad Prism 8 software.

RESULTS

To study the effect of acute and global pericyte loss on neurovascular coupling, we used our recently developed inducible pericyte-specific Cre mouse line (pericyte-CreER; Nikolakopoulou et al., 2019) crossed to iDTR mice carrying Cre-dependent human diphtheria toxin receptor (DTR; Buch et al., 2005; pericyte-CreER; iDTR), as we previously reported (Nikolakopoulou et al., 2019). Treatment of pericyte-CreER; iDTR mice with tamoxifen (TAM) induces DTR expression specifically in pericytes (and not in any other cell types), and subsequent treatment with DT leads exclusively to pericyte cell death, as previously reported (Nikolakopoulou et al., 2019). Deficits in neurovascular coupling were evaluated by LDF and IOS imaging of CBF responses to hindlimb stimulus at 0, 3, 6 and 9 days of DT or vehicle treatment, and 3 days post-DT or vehicle (**Figure 1A**). Pericyte coverage was determined at 0, 3, 6 and 9 days of DT treatment, and 3 days post-DT or vehicle, while VSD measurements of neuronal evoked membrane potential responses and cortical capillary density were evaluated at 3 days post-DT or vehicle treatment (**Figure 1A**).

As we reported (Nikolakopoulou et al., 2019), DT treatment of TAM-treated pericyte-CreER; iDTR mice compared to vehicle led to progressive loss of CD13-positive pericyte coverage (**Figure 1B**) as shown in the S1 somatosensory cortex by ∼37% loss after 6 days of DT treatment, and by approximately 50% loss at 3 days post-DT treatment (**Figure 1C**) consistent with our previous report (Nikolakopoulou et al., 2019). Analysis of CBF responses to hind-limb stimulation as measured by LDF in the S1 cortex hind-limb region in TAM-treated pericyte-CreER; iDTR mice revealed progressive neurovascular dysregulation beginning with a 36% reduction in CBF response at day 6 of DT treatment compared to vehicle, and reaching 57% reduction in CBF response at 3 days post-DT compared to vehicle (**Figure 1D**). Diminished CBF responses in pericyte-CreER; iDTR mice treated with TAM and vehicle, or TAM and DT, correlated positively with the loss in pericyte coverage as shown at 3 days post-DT or vehicle treatment (**Figure 1E**).

The length of lectin-positive capillary (diameter <6 μm) profiles in the S1 cortex (**Figures 1B,F**) was unchanged in pericyte-CreER; iDTR mice at 3 days post-DT or vehicle treatment, indicating that the observed differences in CBF responses could not be attributed to differences in brain capillary density. To determine whether endothelial dysfunction can contribute to CBF dysregulation as seen in TAM-treated pericyte-CreER; iDTR mice after DT treatment, we tested CBF response to acetylcholine, an endothelium-dependent receptor-mediated vasodilator (**Figure 1G**; Kisler et al., 2017b). These experiments showed no difference in CBF response in the presence of acetylcholine at 3 days post-DT or vehicle treatment, thus ruling out endothelial dysfunction as a contributor to the observed changes in neurovascular coupling.

To independently test whether DT-induced pericyte-deficiency can lead to a global deficit in neurovascular coupling in the parenchyma over the course of DT treatment, we studied hemodynamic responses to a mechanical hind-limb stimulus at key time points by IOS imaging acquired under 530 nm illumination (**Figures 2A–C**). IOS changes at this wavelength reflect changes in the total hemoglobin content in the brain tissue due to changes in blood flow and blood volume in response to stimulus (Hillman, 2007; Kisler et al., 2017b, 2018). At days 6 and 9 of DT treatment and 3 days post-DT treatment compared to vehicle, TAM-treated pericyte-CreER; iDTR mice showed a decrease in the peak signal IOS amplitude by approximately 50% starting at day 6 of DT treatment (**Figure 2C**), corroborating our LDF data by suggesting impaired neurovascular coupling immediately after pericyte loss.

Next, we investigated whether neurovascular coupling deficits could be due to changes in neuronal activation as evaluated by VSD imaging of neuronal evoked membrane potential responses to hind limb stimulus at 3 days post-DT or vehicle treatment. VSD imaging in the hind-limb S1 cortical area of TAM-treated pericyte-CreER; iDTR mice revealed no differences in depolarization pattern (**Figures 3A–D**), with similar signal amplitude (**Figure 3C**) and response latency (**Figure 3D**) at 3 days post-DT treatment compared to vehicle, consistent no changes in neuronal counts, neuritic density or behavior as previously reported in TAM-treated pericyte-CreER; iDTR mice at 3 days post-DT (Nikolakopoulou et al., 2019).

DISCUSSION

Using our recently developed pericyte-specific Cre line crossed to iDTR mice (Nikolakopoulou et al., 2019), we found that deficits in neurovascular coupling develop rapidly after global pericyte ablation from the cortex of adult mice. Furthermore, we also found that endothelial function and capillary density remain normal over the course of DT-induced pericyte loss, and that neuronal function evaluated by neuronal evoked membrane potential responses to hind limb stimulus was also unchanged 3 days after DT treatment in pericyte-CreER; iDTR mice. This data, together with our previous findings demonstrating unchanged arteriole smooth muscle cell (SMC) coverage and SMC functional response to adenosine after pericyte ablation with DT in TAM-treated pericyte-CreER; iDTR mice (Nikolakopoulou et al., 2019), suggests that acute loss of pericyte coverage, but not other vascular deficits or neuronal dysfunction, drives the observed deficits in neurovascular coupling.

We observe aberrant hemodynamic responses in TAM-treated pericyte-CreER; iDTR mice very early after an initial 37% loss of pericyte coverage occurring at 6 days of DT treatment. Multiple *in vivo* studies have indicated that pericytes regulate neurovascular coupling, playing an active role in capillary dilation (Hall et al., 2014; Biesecker et al., 2016; Mishra et al., 2016; Kisler et al., 2017b; Cai et al., 2018; Rungta et al., 2018; Nortley et al., 2019) that according

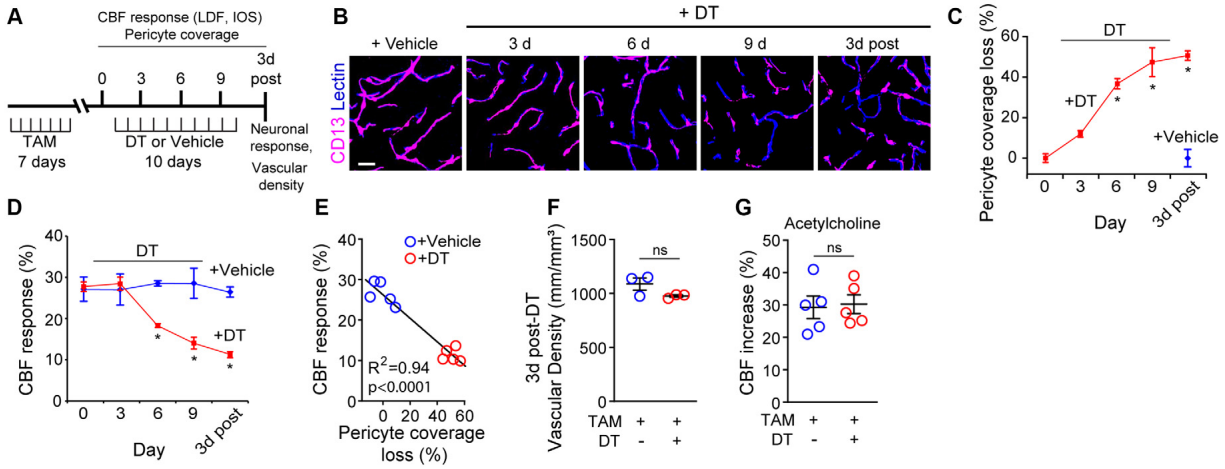

FIGURE 1 | Ablation of cortical pericytes from the adult mouse brain leads to acute dysregulation of neurovascular coupling. **(A)** A diagram of the injection protocol of pericyte-CreER; iDTR mice with tamoxifen (TAM; 40 mg/kg daily for seven consecutive days), diphtheria toxin (DT; 0.1 μg per day for 10 consecutive days) or vehicle, and the time points when cerebral blood flow (CBF) responses to stimulus measured by laser Doppler flowmetry (LDF) and intrinsic optical signal (IOS) imaging, neuronal response to stimulus, and capillary density measurements were performed. **(B)** Representative confocal microscopy images of CD13-positive pericyte coverage of lectin-positive endothelial profiles in the S1 cortex hind-limb region at 3, 6, and 9 days of DT or vehicle administration, and 3 days post-DT or vehicle. Bar = 20 μm. **(C)** Quantification of pericyte coverage loss on capillaries (<6 μm in diameter) in the S1 cortex in TAM-treated pericyte-CreER; iDTR mice at 0, 3, 6 and 9 days of DT administration, and 3 days post-DT or vehicle treatment; $n = 5$ mice per group. $^*P < 0.05$ vs. day 0 of DT treatment by analysis of variance (ANOVA) followed by Tukey's *post hoc* test. **(D)** CBF response to an electrical hind limb stimulus (60 s duration, 7 Hz, 2 ms pulse duration) in 3-month-old TAM-treated pericyte-CreER; iDTR mice determined by LDF in the S1 cortex hind-limb region at 0, 3, 6, and 9 days of DT or vehicle administration, and 3 days post-DT or vehicle treatment. CBF response is expressed as the percentage increase relative to baseline; $n = 5$ mice per group; $^*P < 0.05$, by ANOVA followed by Tukey's *post hoc* test. **(E)** Pearson's correlation between CBF response to a stimulus as in **(D)** and loss of pericyte coverage determined at 3 days post-DT or vehicle treatment of TAM-treated pericyte-CreER; iDTR mice. Each point represents an individual response per mouse of 10 studied mice; $P < 0.0001$. Significance by two-tailed Pearson correlation; R, Pearson correlation coefficient. **(F)** Capillary (diameter <6 μm) density in the S1 cortex hind-limb region in TAM-treated pericyte-CreER; iDTR mice at 3 days post-DT or vehicle treatment; $n = 3$ mice per group. **(G)** LDF measurements of CBF response to endothelium-dependent vasodilator acetylcholine (10 μM) in TAM-treated pericyte-CreER; iDTR mice determined 3 days post-DT or vehicle treatment; $n = 5$ mice per group. Data in **(C,D,F,G)** represented as Mean ± SEM; in **(F,G)** ns, non-significant by Student's *t*-test. Circles denote individual values per mouse in **(E–G)**.

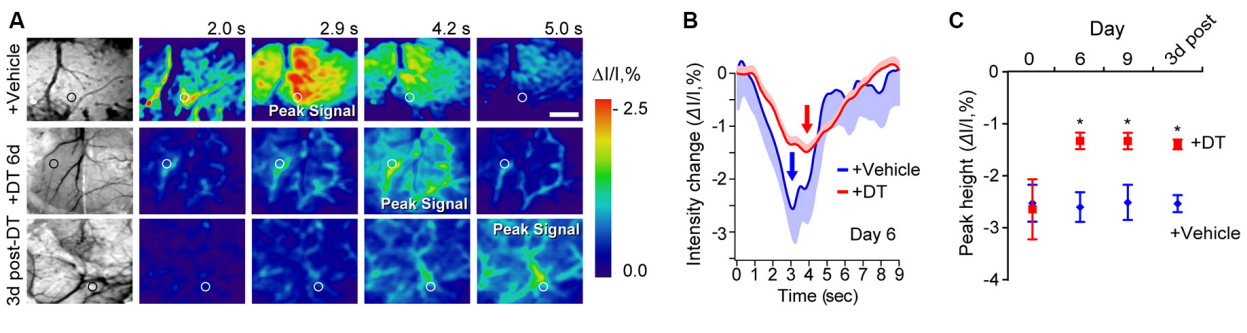

FIGURE 2 | Neurovascular coupling deficits in pericyte-CreER; iDTR mice at key time points during pericyte ablation with DT and 3 days post-DT determined by IOS imaging. **(A)** Example of grayscale images of the visualized somatosensory cortex of TAM-treated pericyte-CreER; iDTR mice showing vasculature (far left), and pseudocolored images of the somatosensory cortex showing IOS imaging under 530 nm illumination in response to a 300 ms mechanical hind limb stimulus beginning at 0 s at key time points during DT (+DT) or vehicle administration. Peak signals and peak signal times are indicated. Circles indicate regions of interest (ROIs) for curves shown in panel **(B)** for day 6 of DT treatment. Scale bar = 0.5 mm. **(B)** IOS time courses for vehicle and 6 days DT-treated mice in parenchymal ROIs shown in **(A)**. Mean ± SEM from 10 trials in each representative mouse is shown. Arrows indicate peak signal intensity. **(C)** IOS peak intensity quantification at 0, 6, and 9 days of DT or vehicle administration, and 3 days post-DT or vehicle treatment in response to stimulus in ROIs away from large surface vessels in mice as in **(A)**. Mean ± SEM, $n = 4$–6 mice per group. $^*P < 0.05$, one-way ANOVA followed by Bonferroni *post hoc* test.

to some studies precedes arteriolar dilation after neuronal stimulus (Hall et al., 2014; Mishra et al., 2016; Kisler et al., 2017b). Consistent with the present findings, recent work from our lab using a model of congenital pericyte deficiency due to globally inherited PDGFRβ deficiency in pericytes also revealed that loss of pericyte coverage delayed capillary vessel dilation upon neuronal stimulus (Kisler et al., 2017b). These studies suggest that acute pericyte loss may lead to aberrant

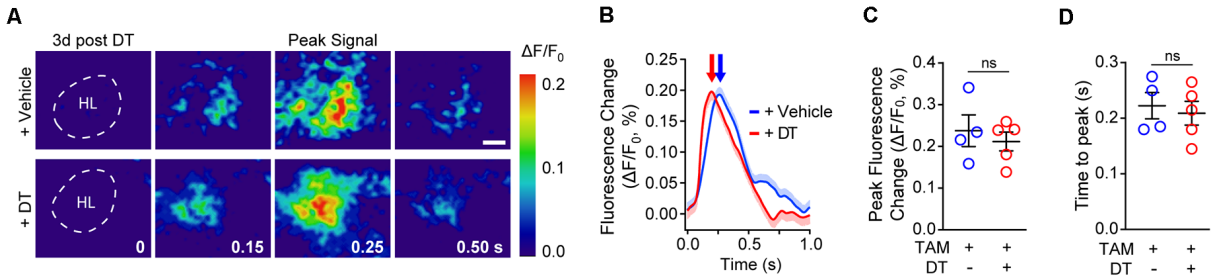

FIGURE 3 | Cortical neuronal activity determined by voltage-sensitive dye (VSD) imaging in response to sensory stimulation in pericyte-CreER; iDTR mice 3 days post-DT treatment. **(A)** Representative pseudocolored image sequences of cortical depolarization pattern in the hind limb S1 cortical region obtained by VSD imaging in response to a 300 ms hind limb mechanical stimulus in TAM-treated pericyte-CreER; iDTR mice treated with DT or vehicle determined 3 days post-DT or vehicle treatment. The dashed line indicates hind limb (HL) region. Peak signals and peak signal times are indicated. Scale bar = 0.25 mm. **(B–D)** Representative VSD intensity traces from individual mice (average ± SEM for 10 trials per mouse; **B**), average peak fluorescence change **(C)**, and average time to peak **(D)** in pericyte-CreER; iDTR mice 3 days post-DT or vehicle treatment. In **(C**,**D)**, mean ± SEM, from n = 4–5 mice per group; circles denote individual values per mouse. ns, non-significant by Student's t-test.

hemodynamic responses due to a loss of active capillary dilation in response to neuronal stimulus. However, present literature also does not rule out a role for capillaries in the retrograde propagation of intramural vascular signals from the capillary level upstream influencing neurovascular coupling (Hillman, 2014; Longden et al., 2017), which would likely be compromised by the loss of pericytes and subsequent BBB breakdown, as discussed below.

A previous study found that significant resting-state CBF reductions and low but detectable BBB breakdown also develop after 6 days of DT treatment of TAM-treated pericyte-CreER; iDTR mice (Nikolakopoulou et al., 2019). Vasogenic edema, likely caused by a substantial BBB breakdown after 9 days of DT treatment (Nikolakopoulou et al., 2019), cannot be ruled out as a contributor to aberrant neurovascular coupling observed at later time points during and after the DT treatment regimen. Nonetheless, that we observe a neurovascular coupling deficit at a time point prior to edema development implies also that loss of pericyte coverage may be sufficient to initially drive changes in neurovascular coupling. Since our previous report found no changes in the number of Iba1-positive microglia and GFAP-positive astrocytes after pericyte ablation in the presently crossed pericyte-CreER; iDTR line (Nikolakopoulou et al., 2019), it is unlikely that the changes we observe in neurovascular coupling after pericyte loss are influenced by an inflammatory response. Given the apparent role that pericytes play in regulating the dynamic changes in hemodynamic responses (Hall et al., 2014; Biesecker et al., 2016; Mishra et al., 2016; Kisler et al., 2017b; Cai et al., 2018; Rungta et al., 2018; Nortley et al., 2019), it is possible that deficits in neurovascular coupling observed in the present study might also contribute to CBF reductions reported previously in this model (Nikolakopoulou et al., 2019).

A previous study investigating acute ablation of individual pericytes from the adult mouse brain found temporary loss of vascular tone and capillary dilation, but also revealed that neighboring pericytes possess the plasticity to extend processes into the region vacated by the ablated cell to restore pericyte coverage and tone of the affected capillary (Berthiaume et al., 2018). The effect of blood flow after single pericyte ablation in this model was not evaluated, but it is reasonable to assume that single pericyte loss likely would not cause large alterations to CBF. While single pericyte ablation technique yields important insights into the plasticity of pericytes and their regulation of resting vascular tone, it is difficult to directly compare these previous findings to the conditions presented here where brain-wide pericyte loss is rapidly induced. Such rapid, large scale pericyte loss as we observe in the present pericyte-CreER; iDTR model likely does not allow for sufficient numbers of pericytes to effectively compensate for lost pericyte coverage.

Rapid global pericyte loss from central nervous system occurs after cerebral hypoperfusion, stroke, and spinal cord injury (Melgar et al., 2005; Göritz et al., 2011; Fernández-Klett et al., 2013; Dias et al., 2018; Liu et al., 2019). While it is thought that some of these pericytes can detach from capillaries to allow neovascularization (Shimauchi-Ohtaki et al., 2019), contribute to scar formation (Göritz et al., 2011; Dias et al., 2018), or transform cell phenotype through their multipotent properties (Dore-Duffy, 2008; Nakagomi et al., 2015), the effects of rapid global pericyte loss on neurovascular coupling has still not been examined prior to the present study. Substantial regional pericyte loss (≥50%) in cortex and hippocampus is also observed in neurodegenerative diseases such as Alzheimer's disease (AD; Sengillo et al., 2013; Halliday et al., 2016), but whether it occurs rapidly or more slowly over time is less clear. Aberrant neurovascular coupling and CBF reductions have been reported in humans with dementia, AD and other neurodegenerative diseases (reviewed in Iadecola, 2017; Sweeney et al., 2018a,b), and more recent studies suggest that pericyte injury is an early independent biomarker of human cognitive dysfunction (Montagne et al., 2015; Nation et al., 2019). Thus, the present findings, in addition to further supporting the role of pericytes in CBF regulation, may also have implications for understanding neurovascular dysfunction in disorders associated with global and rapid pericyte loss such as stroke, as well as conditions where the exact time course of

global regional pericyte loss is less clear, such as AD and other neurogenerative disorders.

DATA AVAILABILITY STATEMENT

The data that support the findings of this study are available from the corresponding author upon reasonable request.

ETHICS STATEMENT

All procedures performed on animals were reviewed and approved by the Institutional Animal Care and Use Committee at the University of Southern California.

AUTHOR CONTRIBUTIONS

KK, AN, ZZ, and BZ contributed to the project and experimental design. KK, AN, and MS conducted experiments and analyzed data. DL performed experiments. BZ supervised experiments. KK and BZ wrote the manuscript.

FUNDING

This work is supported by National Institutes of Health (NIH) grants R01AG039452, R01NS100459, R01AG023084, R01NS090904, R01NS034467 to BZ and the Foundation Leducq Transatlantic Network of Excellence for the Study of Perivascular Spaces in Small Vessel Disease reference No. 16 CVD 05.

REFERENCES

Armulik, A., Genové, G., Mäe, M., Nisancioglu, M. H., Wallgard, E., Niaudet, C., et al. (2010). Pericytes regulate the blood-brain barrier. *Nature* 468, 557–561. doi: 10.1038/nature09522

Bell, R. D., Winkler, E. A., Sagare, A. P., Singh, I., LaRue, B., Deane, R., et al. (2010). Pericytes control key neurovascular functions and neuronal phenotype in the adult brain and during brain aging. *Neuron* 68, 409–427. doi: 10.1016/j.neuron.2010.09.043

Bell, R. D., Winkler, E. A., Singh, I., Sagare, A. P., Deane, R., Wu, Z., et al. (2012). Apolipoprotein E controls cerebrovascular integrity *via* cyclophilin A. *Nature* 485, 512–516. doi: 10.1038/nature11087

Berthiaume, A.-A., Grant, R. I., McDowell, K. P., Underly, R. G., Hartmann, D. A., Levy, M., et al. (2018). Dynamic remodeling of pericytes *in vivo* maintains capillary coverage in the adult mouse brain. *Cell Rep.* 22, 8–16. doi: 10.1016/j.celrep.2017.12.016

Biesecker, K. R., Srienc, A. I., Shimoda, A. M., Agarwal, A., Bergles, D. E., Kofuji, P., et al. (2016). Glial cell calcium signaling mediates capillary regulation of blood flow in the retina. *J. Neurosci.* 36, 9435–9445. doi: 10.1523/JNEUROSCI.1782-16.2016

Buch, T., Heppner, F. L., Tertilt, C., Heinen, T. J. A. J., Kremer, M., Wunderlich, F. T., et al. (2005). A Cre-inducible diphtheria toxin receptor mediates cell lineage ablation after toxin administration. *Nat. Methods* 2, 419–426. doi: 10.1038/nmeth762

Cai, C., Fordsmann, J. C., Jensen, S. H., Gesslein, B., Lønstrup, M., Hald, B. O., et al. (2018). Stimulation-induced increases in cerebral blood flow and local capillary vasoconstriction depend on conducted vascular responses. *Proc. Natl. Acad. Sci. U S A* 115, E5796–E5804. doi: 10.1073/pnas.1707702115

Cuttler, A. S., LeClair, R. J., Stohn, J. P., Wang, Q., Sorenson, C. M., Liaw, L., et al. (2011). Characterization of Pdgfrb-Cre transgenic mice reveals reduction of ROSA26 reporter activity in remodeling arteries. *Genesis* 49, 673–680. doi: 10.1002/dvg.20769

Daneman, R., Zhou, L., Kebede, A. A., and Barres, B. A. (2010). Pericytes are required for blood-brain barrier integrity during embryogenesis. *Nature* 468, 562–566. doi: 10.1038/nature09513

Dias, D. O., Kim, H., Holl, D., Werne Solnestam, B., Lundeberg, J., Carlén, M., et al. (2018). Reducing pericyte-derived scarring promotes recovery after spinal cord injury. *Cell* 173, 153.e22–165.e22. doi: 10.1016/j.cell.2018.02.004

Dore-Duffy, P. (2008). Pericytes: pluripotent cells of the blood brain barrier. *Curr. Pharm. Des.* 14, 1581–1593. doi: 10.2174/138161208784705469

Fernández-Klett, F., Potas, J. R., Hilpert, D., Blazej, K., Radke, J., Huck, J., et al. (2013). Early loss of pericytes and perivascular stromal cell-induced scar formation after stroke. *J. Cereb. Blood Flow Metab.* 33, 428–439. doi: 10.1038/jcbfm.2012.187

Foo, S. S., Turner, C. J., Adams, S., Compagni, A., Aubyn, D., Kogata, N., et al. (2006). Ephrin-B2 controls cell motility and adhesion during blood-vessel-wall assembly. *Cell* 124, 161–173. doi: 10.1016/j.cell.2005.10.034

Göritz, C., Dias, D. O., Tomilin, N., Barbacid, M., Shupliakov, O., and Frisén, J. (2011). A pericyte origin of spinal cord scar tissue. *Science* 333, 238–242. doi: 10.1126/science.1203165

Hall, C. N., Reynell, C., Gesslein, B., Hamilton, N. B., Mishra, A., Sutherland, B. A., et al. (2014). Capillary pericytes regulate cerebral blood flow in health and disease. *Nature* 508, 55–60. doi: 10.1038/nature13165

Halliday, M. R., Rege, S. V., Ma, Q., Zhao, Z., Miller, C. A., Winkler, E. A., et al. (2016). Accelerated pericyte degeneration and blood-brain barrier breakdown in Apolipoprotein E4 carriers with Alzheimer's disease. *J. Cereb. Blood Flow Metab.* 36, 216–227. doi: 10.1038/jcbfm.2015.44

Hillman, E. M. C. (2007). Optical brain imaging *in vivo*: techniques and applications from animal to man. *J. Biomed. Opt.* 12:051402. doi: 10.1117/1.2789693

Hillman, E. M. C. (2014). Coupling mechanism and significance of the BOLD signal: a status report. *Annu. Rev. Neurosci.* 37, 161–181. doi: 10.1146/annurev-neuro-071013-014111

Iadecola, C. (2017). The neurovascular unit coming of age: a journey through neurovascular coupling in health and disease. *Neuron* 96, 17–42. doi: 10.1016/j.neuron.2017.07.030

Keller, A., Westenberger, A., Sobrido, M. J., García-Murias, M., Domingo, A., Sears, R. L., et al. (2013). Mutations in the gene encoding PDGF-B cause brain calcifications in humans and mice. *Nat. Genet.* 45, 1077–1082. doi: 10.1038/ng.2723

Kisler, K., Lazic, D., Sweeney, M. D., Plunkett, S., El Khatib, M., Vinogradov, S. A., et al. (2018). *In vivo* imaging and analysis of cerebrovascular hemodynamic responses and tissue oxygenation in the mouse brain. *Nat. Protoc.* 13, 1377–1402. doi: 10.1038/nprot.2018.034

Kisler, K., Nelson, A. R., Montagne, A., and Zlokovic, B. V. (2017a). Cerebral blood flow regulation and neurovascular dysfunction in Alzheimer disease. *Nat. Rev. Neurosci.* 18, 419–434. doi: 10.1038/nrn.2017.48

Kisler, K., Nelson, A. R., Rege, S. V., Ramanathan, A., Wang, Y., Ahuja, A., et al. (2017b). Pericyte degeneration leads to neurovascular uncoupling and limits oxygen supply to brain. *Nat. Neurosci.* 20, 406–416. doi: 10.1038/nn.4489

Liu, Q., Radwanski, R., Babadjouni, R., Patel, A., Hodis, D. M., Baumbacher, P., et al. (2019). Experimental chronic cerebral hypoperfusion results in decreased pericyte coverage and increased blood-brain barrier permeability in the corpus callosum. *J. Cereb. Blood Flow Metab.* 39, 240–250. doi: 10.1177/0271678x17743670

Longden, T. A., Dabertrand, F., Koide, M., Gonzales, A. L., Tykocki, N. R., Brayden, J. E., et al. (2017). Capillary K^+-sensing initiates retrograde hyperpolarization to increase local cerebral blood flow. *Nat. Neurosci.* 20, 717–726. doi: 10.1038/nn.4533

Melgar, M. A., Rafols, J., Gloss, D., and Diaz, F. G. (2005). Postischemic reperfusion: ultrastructural blood-brain barrier and hemodynamic correlative changes in an awake model of transient forebrain ischemia. *Neurosurgery* 56, 571–581. doi: 10.1227/01.neu.0000154702.23664.3d

Mishra, A., Reynolds, J. P., Chen, Y., Gourine, A. V., Rusakov, D. A., and Attwell, D. (2016). Astrocytes mediate neurovascular signaling to capillary

pericytes but not to arterioles. *Nat. Neurosci.* 19, 1619–1627. doi: 10.1038/nn.4428

Montagne, A., Barnes, S. R., Sweeney, M. D., Halliday, M. R., Sagare, A. P., Zhao, Z., et al. (2015). Blood-brain barrier breakdown in the aging human hippocampus. *Neuron* 85, 296–302. doi: 10.1016/j.neuron.2014.12.032

Montagne, A., Nikolakopoulou, A. M., Zhao, Z., Sagare, A. P., Si, G., Lazic, D., et al. (2018). Pericyte degeneration causes white matter dysfunction in the mouse central nervous system. *Nat. Med.* 24, 326–337. doi: 10.1038/nm.4482

Nakagomi, T., Kubo, S., Nakano-Doi, A., Sakuma, R., Lu, S., Narita, A., et al. (2015). Brain vascular pericytes following ischemia have multipotential stem cell activity to differentiate into neural and vascular lineage cells: brain vascular pericytes and neurovasculogenesis. *Stem Cells* 33, 1962–1974. doi: 10.1002/stem.1977

Nation, D. A., Sweeney, M. D., Montagne, A., Sagare, A. P., D'Orazio, L. M., Pachicano, M., et al. (2019). Blood-brain barrier breakdown is an early biomarker of human cognitive dysfunction. *Nat. Med.* 25, 270–276. doi: 10.1038/s41591-018-0297-y

Nikolakopoulou, A. M., Montagne, A., Kisler, K., Dai, Z., Wang, Y., Huuskonen, M. T., et al. (2019). Pericyte loss leads to circulatory failure and pleiotrophin depletion causing neuron loss. *Nat. Neurosci.* 22, 1089–1098. doi: 10.1038/s41593-019-0434-z

Nikolakopoulou, A. M., Zhao, Z., Montagne, A., and Zlokovic, B. V. (2017). Regional early and progressive loss of brain pericytes but not vascular smooth muscle cells in adult mice with disrupted platelet-derived growth factor receptor-β signaling. *PLoS One* 12:e0176225. doi: 10.1371/journal.pone.0176225

Nortley, R., Korte, N., Izquierdo, P., Hirunpattarasilp, C., Mishra, A., Jaunmuktane, Z., et al. (2019). Amyloid β oligomers constrict human capillaries in Alzheimer's disease *via* signaling to pericytes. *Science* 365:eaav9518. doi: 10.1126/science.aav9518

Peppiatt, C. M., Howarth, C., Mobbs, P., and Attwell, D. (2006). Bidirectional control of CNS capillary diameter by pericytes. *Nature* 443, 700–704. doi: 10.1038/nature05193

Rungta, R. L., Chaigneau, E., Osmanski, B.-F., and Charpak, S. (2018). Vascular compartmentalization of functional hyperemia from the synapse to the pia. *Neuron* 99, 362.e4–375.e4. doi: 10.1016/j.neuron.2018.06.012

Sengillo, J. D., Winkler, E. A., Walker, C. T., Sullivan, J. S., Johnson, M., and Zlokovic, B. V. (2013). Deficiency in mural vascular cells coincides with blood-brain barrier disruption in Alzheimer's disease. *Brain Pathol.* 23, 303–310. doi: 10.1111/bpa.12004

Shimauchi-Ohtaki, H., Kurachi, M., Naruse, M., Shibasaki, K., Sugio, S., Matsumoto, K., et al. (2019). The dynamics of revascularization after white matter infarction monitored in Flt1-tdsRed and Flk1-GFP mice. *Neurosci. Lett.* 692, 70–76. doi: 10.1016/j.neulet.2018.10.057

Sweeney, M. D., Kisler, K., Montagne, A., Toga, A. W., and Zlokovic, B. V. (2018a). The role of brain vasculature in neurodegenerative disorders. *Nat. Neurosci.* 21, 1318–1331. doi: 10.1038/s41593-018-0234-x

Sweeney, M. D., Sagare, A. P., and Zlokovic, B. V. (2018b). Blood-brain barrier breakdown in Alzheimer disease and other neurodegenerative disorders. *Nat. Rev. Neurol.* 14, 133–150. doi: 10.1038/nrneurol.2017.188

Sweeney, M. D., Zhao, Z., Montagne, A., Nelson, A. R., and Zlokovic, B. V. (2019). Blood-brain barrier: from physiology to disease and back. *Physiol. Rev.* 99, 21–78. doi: 10.1152/physrev.00050.2017

Tachibana, M., Yamazaki, Y., Liu, C.-C., Bu, G., and Kanekiyo, T. (2018). Pericyte implantation in the brain enhances cerebral blood flow and reduces amyloid-β pathology in amyloid model mice. *Exp. Neurol.* 300, 13–21. doi: 10.1016/j.expneurol.2017.10.023

Zhu, X., Bergles, D. E., and Nishiyama, A. (2008). NG2 cells generate both oligodendrocytes and gray matter astrocytes. *Development* 135, 145–157. doi: 10.1242/dev.004895

Zhu, X., Hill, R. A., Dietrich, D., Komitova, M., Suzuki, R., and Nishiyama, A. (2011). Age-dependent fate and lineage restriction of single NG2 cells. *Development* 138, 745–753. doi: 10.1242/dev.047951

Conflict of Interest: The authors declare that the research was conducted in the absence of any commercial or financial relationships that could be construed as a potential conflict of interest.

frontiers in Aging Neuroscience

ORIGINAL RESEARCH
published: 06 March 2020
doi: 10.3389/fnagi.2020.00053

Contra-Directional Expression of Plasma Superoxide Dismutase with Lipoprotein Cholesterol and High-Sensitivity C-reactive Protein as Important Markers of Parkinson's Disease Severity

Wanlin Yang[1†], Zihan Chang[1†], Rongfang Que[1†], Guomei Weng[2], Bin Deng[1], Ting Wang[1], Zifeng Huang[1], Fen Xie[1], Xiaobo Wei[1], Qin Yang[1], Mengyan Li[3], Kefu Ma[4], Fengli Zhou[5], Beisha Tang[6], Vincent C. T. Mok[7], Shuzhen Zhu[1] and Qing Wang[1]**

[1]Department of Neurology, Zhujiang Hospital of Southern Medical University, Guangzhou, China, [2]Department of Neurology, The First People Hospital of Zhaoqing, Zhaoqing, China, [3]Department of Neurology, Guangzhou First People's Hospital, Guangzhou, China, [4]Department of Neurology, Shenzhen People Hospital, Shenzhen, China, [5]Department of Respiratory Medicine, The Third Affiliated Hospital of Sun Yat-Sen University, Guangzhou, China, [6]Department of Neurology, Xiangya Hospital of Central South University, Changsha, China, [7]Gerald Choa Neuroscience Centre, Department of Medicine and Therapeutics, Faculty of Medicine, Prince of Wales Hospital, The Chinese University of Hong Kong, Shatin, China

OPEN ACCESS

Edited by:
Rubem C. A. Guedes, Federal University of Pernambuco, Brazil

Reviewed by:
Huifang Shang, Sichuan University, China
Boon-Seng Wong, Singapore Institute of Technology, Singapore

***Correspondence:**
Shuzhen Zhu
453951712@qq.com
Qing Wang
denniswq@yahoo.com

[†]These authors have contributed equally to this work

Received: 28 November 2019
Accepted: 18 February 2020
Published: 06 March 2020

Citation:
Yang W, Chang Z, Que R, Weng G, Deng B, Wang T, Huang Z, Xie F, Wei X, Yang Q, Li M, Ma K, Zhou F, Tang B, Mok VCT, Zhu S and Wang Q (2020) Contra-Directional Expression of Plasma Superoxide Dismutase With Lipoprotein Cholesterol and High-Sensitivity C-reactive Protein as Important Markers of Parkinson's Disease Severity. Front. Aging Neurosci. 12:53. doi: 10.3389/fnagi.2020.00053

Aim: Oxidative stress and inflammation play critical roles in the neuropathogenesis of PD. We aimed to evaluate oxidative stress and inflammation status by measuring serum superoxide dismutase (SOD) with lipoprotein cholesterol and high-sensitivity C-reactive protein (hsCRP) respectively in PD patients, and explore their correlation with the disease severity.

Methods: We performed a cross-sectional study that included 204 PD patients and 204 age-matched healthy controls (HCs). Plasma levels of SOD, hsCRP, total cholesterol, high-density lipoprotein cholesterol (HDL-C) and low-density lipoprotein cholesterol (LDL-C) were measured. A series of neuropsychological assessments were performed to rate the severity of PD.

Results: The plasma levels of SOD (135.7 ± 20.14 vs. 147.2 ± 24.34, $P < 0.0001$), total cholesterol, HDL-C and LDL-C in PD were significantly lower than those in HCs; the hsCRP level was remarkably increased in PD compared to HC (2.766 ± 3.242 vs. 1.637 ± 1.597, $P < 0.0001$). The plasma SOD was negatively correlated with the hsCRP, while positively correlated with total cholesterol, HDL-C, and LDL-C in PD patients. The plasma SOD were negatively correlated with H&Y, total UPDRS, UPDRS (I), UPDRS (II), and UPDRS (III) scores, but positively correlated with MoCA and MMSE scores. Besides,

Abbreviations: AD, Alzheimer's disease; BMI, body mass index; Chol, cholesterol; HDL-C, high-density lipoprotein cholesterol; H&Y, Hoehn and Yahr scale; H_2O_2, hydrogen peroxide; hsCRP, high-sensitivity C-reactive protein; LDL-C, low-density lipoprotein cholesterol; MMSE, Mini-Mental State Examination; MoCA, Montreal Cognitive Assessment; O_{2-}, superoxide radicals; PD, Parkinson's disease; ROC, receiver operating characteristic; ROS, reactive oxygen species; SNpc, substantia nigra pars compacta; SOD, superoxide dismutase; UPDRS, Unified PD rating scale.

hsCRP was negatively correlated with MoCA; while total cholesterol, HDL-C and LDL-C were positively correlated with the MoCA, respectively.

Conclusion: Our findings suggest that lower SOD along with cholesterol, HDL-C and LDL-C, and higher hsCRP levels might be important markers to assess the PD severity. A better understanding of SOD and hsCRP may yield insights into the pathogenesis of PD.

Keywords: superoxide dismutase, high-sensitivity C-reactive protein, lipoprotein cholesterol, Parkinson's disease, inflammation, oxidative stress

INTRODUCTION

Parkinson's disease (PD) is the second common age-related neurodegenerative disease following Alzheimer's disease (AD) due to the progressive loss of dopaminergic neurons in the substantia nigra pars compacta (SNpc) and striatum (Zhao et al., 2018; Li et al., 2019; Qian and Huang, 2019). It is clinically characterized by resting tremor, rigidity, bradykinesia, and postural instability (Chomiak et al., 2018; Gao et al., 2018; Ray Chaudhuri et al., 2018; Sun et al., 2018). Increasing evidence points to the importance of neuroinflammation and oxidative stress in the pathophysiology of PD (Adams et al., 2019), but the underlying exact mechanisms remain unclear and need to be elucidated.

Superoxide dismutase (SOD) is one of the most important antioxidant enzymes both inside and outside cell membranes, and it catalyzes the dismutation of superoxide radicals (O_2–) to hydrogen peroxide (H_2O_2), which is converted to water and oxygen by catalase and glutathione peroxidase (Zhu et al., 2019). Some Neurologists have even suggested that SOD is the first-line defense against increased reactive oxygen species (ROS) production in PD patients (de Farias et al., 2016). The onsets of cerebrovascular inflammation are considered as stimuli that trigger or facilitate the development of all kinds of neurological disorders. The excessive inflammatory response can influence blood brain barrier (BBB) integrity, and various inflammation markers have been investigated as potential predictors of PD (Mosley et al., 2006). Among those markers, high-sensitivity C-reactive protein (hsCRP) is one of the most frequently investigated potential biomarkers during the screening and monitoring of inflammatory activity in all kinds of system diseases (Kuo et al., 2005). Previous studies have indicated that high concentrations of hsCRP could increase the paracellular permeability of the BBB, which is associated with increased risk, severity and progression of PD (Nawaz and Mohammad, 2015).

Lipids are molecules that contain fatty acids or a steroid nucleus (e.g., cholesterol) and are the main compositions that constitute cellular membranes, part of membrane rafts and protein anchors, and signaling and transport molecules across BBB (Chen et al., 2018; Shi et al., 2019; Xicoy et al., 2019). A previous study found that dyslipidemia is causally related to BBB impairment and plasma high-density lipoprotein cholesterol (HDL-C) were the lipids most associated with BBB integrity (Bowman et al., 2012; Chen et al., 2018). The association of PD with peripheral blood lipids has been investigated in many studies, but the results are inconsistent. For example, some previous studies found that plasma level of cholesterol was inversely associated with the risk of PD, while others showed opposite tendencies or no significant association (Hu, 2010; Guo et al., 2015; Zhang et al., 2017). Lower plasma levels of HDL-C or no difference in PD patients compared to HCs were also reported. The efficacy of lipid-lowering therapies against neurodegenerative diseases is also controversial (Wei et al., 2013; Xicoy et al., 2019). A previous study has shown that statins, a lipid-lowering drug, may interfere with Aβ metabolism and reduce Aβ-mediated neurodegeneration (Ng and Tan, 2017; Shakour et al., 2019). Whereas, possible adverse effects of intensive lipid-lowering treatment in neurocognitive disorders have been indicated, as cholesterol is a component of the CNS (Mannarino et al., 2018).

Identification of markers in the circulation of PD patients may help us to assess and monitor the disease severity and progression of PD (He et al., 2018). There are evidences suggesting that oxidative stress, lipid metabolism, and inflammatory responses play critical roles in the pathogenesis of PD. Whether oxidative, lipid metabolism and inflammatory mediators could be used as potential biomarkers to detect the severity of PD remains largely unknown. Therefore, we aimed to investigate the value of combined SOD, cholesterol, HDL-C, LDL-C and hsCRP in evaluating and monitoring the severity of PD.

MATERIALS AND METHODS

Subjects and Ethics Statement

This study was approved by the ethics committee of the Zhujiang Hospital of Southern Medical University (2019-KY-071-02) and was conducted according to the principles outlined in the revised Declaration of Helsinki of 1975 and the National Institutes of Health Human Subjects Policies and Guidelines released in 1999. All participants provided written consent to participate in the investigation and allowed investigators to measure their blood sample levels. The PD patients recruited in this present study met the 2015 Movement Disorder Society criteria for the diagnosis of idiopathic PD (Postuma et al., 2015). The exclusion criteria for patients were: The exclusion criteria for patients were: (1) PD patients with other neurological conditions or neuropsychiatric comorbidities, such as cerebrovascular disease or psychiatric disorders (psychosis

and severe depression); (2) PD patients with somatic diseases, such as endocrine and malignant diseases, cardiac, hepatic or renal failure, or other life-threatening diseases; (3) PD patients who are taking antilipemic agent, such as statins, fibrates and nicotinic acid; and (4) PD patients who refused to participate in the study. The healthy controls (HCs) subjects were recruited from the Medical Examination Centre of Zhujiang Hospital of Southern Medical University, and those with hypertension, cerebral ischemia, cardiovascular disease, diabetes, psychiatric disorders, hepatic or renal dysfunction were excluded from this study. A total of 204 PD patients (92 males and 112 females) and 204 healthy age- and gender-matched subjects (92 males and 112 females) were recruited in this present study. The control group was created by randomly selecting 1:1 age- and gender-matched subjects.

Clinical Evaluation and Blood Collection and Measurement

Experienced neurologists performed clinical evaluations, which were conducted in a blinded manner. All PD participants underwent a series of neuropsychological assessments including the unified Parkinson's disease rating scale (UPDRS; Movement Disorder Society Task Force on Rating Scales for Parkinson's, 2003) and modified Hoehn and Yahr staging scale (H&Y; Hoehn and Yahr, 1967). UPDRS (I) subscale was applied to measure the mentation, behavior, and mood of PD patients including intellectual impairment, thought disorder, depression and motivation/initiative. UPDRS (II) subscale was applied to measure the daily life functionality of PD patients such as speech, swallowing, handwriting, turning in bed etc. UPDRS (III) subscale was applied to measure the motor dysfunction of PD patients such as hand movements, tremors, rigidity, arising from chair and gait etc. H&Y was used to measure clinical stages and disease progression of PD patients. Mini-Mental State Examination (MMSE; Folstein et al., 1975) and Montreal Cognitive Assessment (MoCA; Smith et al., 2007) were used to measure the cognitive function of PD patients. Venous blood samples from all participants were collected into EDTA tubes by trained nurses in the morning. Blood samples were sent to the clinical pathology department and analyzed immediately, and triple replicates have been performed to assess protein and cholesterol levels. The plasma SOD level was measured with a Cu/Zn SOD ELISA kit (Bio-Techne Corporation, R&D system, Minnesota, MN, USA) according to the manufacturer's instructions. The hsCRP and lipids levels were measured by latex immunoturbidimetric assay and direct enzymatic methods, respectively.

Statistical Analysis

All data were analyzed using SPSS 25.0 (IBM Corporation, Armonk, NY, USA). For continuous variables, the results were presented as mean values ± SD. For categorical variables, the results are presented as percentages. When the data were normally distributed, the Student's *t*-test was performed for two-group comparisons. Correlation coefficients were performed with Spearman's rank correlation or Pearson correlation analysis to determine the correlation between different clinical parameters. A receiver operating characteristic (ROC) analysis was conducted to assess the performance of clinical markers as discriminative criteria for PD. A value of $P < 0.05$ was considered statistically significant.

RESULTS

Demographic and Clinical Characteristics of PD Patients and Healthy Controls

Detailed demographic and clinical characteristics are described in **Table 1**. A total of 204 PD patients [92 (45.1%) males and 112 (54.9%) females], and 204 healthy control (HC) subjects [92 (45.1%) males and 112 (54.9%) females] were enrolled in this study. The mean ages of the PD patients and HC subjects were 63.94 ± 11.15 and 63.78 ± 11.42 years, respectively. The mean BMI of PD patients and HC subjects were 23.68 ± 3.807 and 24.32 ± 3.290 kg/m^2, respectively. There were no significant differences in age (P = 0.9112) and BMI (P = 0.2353) between PD patients and HC subjects. The mean H&Y stage PD patient was 2.385 ± 0.9547. The mean of MoCA and MMSE score for PD patients was 18.40 ± 5.671 and 22.80 ± 4.691, respectively. The mean total UPDRS score was 39.31 ± 18.61, mean UPDRS (I) was 4.348 ± 3.309, mean UPDRS (II) was 14.50 ± 7.180 and mean UPDRS (III) was 21.33 ± 11.05.

Comparisons of Plasma Markers Between PD Patients and Healthy Controls

As shown in **Table 1** and **Figure 1**, significant differences in plasma SOD, hsCRP, cholesterol, HDL-C, and LDL-C levels were observed between PD and HC. Plasma SOD levels of PD patients were remarkably lower than those of HC (135.7 ± 20.14 vs. 147.2 ± 24.34, $P < 0.0001$). PD patients exhibited significantly decreased levels of plasma cholesterol, HDL-C and LDL-C relative to HC (4.665 ± 1.024 vs. 5.025 ± 0.893 for cholesterol, P = 0.0002, 1.320 ± 0.3494 vs. 1.435 ± 0.365 for HDL-C, P = 0.0013, 2.744 ± 0.8474 vs. 3.051 ± 0.754 for LDL-C, P = 0.0001). In addition, plasma hsCRP levels were significantly higher in PD patients than in HC (2.766 ± 3.242 vs. 1.637 ± 1.597, $P < 0.0001$).

When PD patients and HC were divided into specific gender groups, the plasma levels of SOD, cholesterol, and LDL-C in the male and female PD patients were significantly lower than those of HC (**Table 2**, **Figure 1**). Plasma HDL-C level in male patients was lower than in female patients (**Table 2**, **Figure 1**), while there was no significant difference between female PD patients and female HC. Besides, we found that plasma hsCRP levels in both male and female PD patients were remarkably higher than male and female PD patients (**Table 2**, **Figure 1**). Additionally, in PD patients, levels of HDL-C in male patients were lower than in female patients (**Table 2**), while there were no significant differences in plasma levels of SOD, hsCRP, cholesterol and LDL-C between male and female PD patients. The above results indicated that plasma antioxidant status such as the decreased SOD levels is obviously impaired in PD patients,

TABLE 1 | Demographic profiles and clinical characteristics of PD patients and healthy controls.

Clinical parameters		Healthy controls			Patients with PD			PD vs. Control
		mean ± SD	Min	Max	mean ± SD	Min	Max	*P*-value
Gender	Male n (%)	92 (45.10%)	/	/	92 (45.10%)	/	/	/
	Female n (%)	112 (54.90%)	/	/	112 (54.90%)	/	/	/
Age (years)		63.78 ± 11.42	33	91	63.94 ± 11.15	33	91	0.9112
BMI (kg/m^2)		24.32 ± 3.290	18.36	32.39	23.68 ± 3.807	16.71	32.87	0.2353
Duration (years)		/	/	/	4.780 ± 3.653	0.1	20	/
UPDRS		/	/	/	39.31 ± 18.61	6	108	/
	UPDRS(I)	/	/	/	4.348 ± 3.309	1	21	/
	UPDRS(II)	/	/	/	14.50 ± 7.180	2	48	/
	UPDRS(III)	/	/	/	21.33 ± 11.05	2	54	/
H&Y		/	/	/	2.385 ± 0.9547	1	5	/
MoCA		/	/	/	18.40 ± 5.671	4	28	/
MMSE		/	/	/	22.80 ± 4.691	9	30	/
SOD		147.2 ± 24.34	101.0	208.0	135.7 ± 20.14	68.00	184.0	<0.0001****
hsCRP		1.637 ± 1.597	0.500	11.70	2.766 ± 3.242	0.500	18.00	<0.0001****
UA		352.7 ± 97.55	107.0	660.0	326.9 ± 91.84	139.0	634.0	0.0069**
FN		215.4 ± 36.46	124.7	399.0	211.9 ± 32.32	136.0	327.0	0.3211
RBP		42.25 ± 12.45	13.10	90.00	41.41 ± 11.76	17.00	83.01	0.4942
CysC		0.927 ± 0.207	0.030	1.820	1.036 ± 0.3206	0.630	3.650	<0.0001****
Cr		71.01 ± 17.17	37.60	120.0	74.80 ± 30.85	35.90	312.0	0.1278
Urea		5.325 ± 1.486	2.500	9.500	5.377 ± 1.966	2.140	18.640	0.7634
TG		1.498 ± 1.063	0.290	9.540	1.423 ± 0.8207	0.370	6.460	0.4348
Chol		5.025 ± 0.893	2.490	9.220	4.665 ± 1.024	2.460	8.550	0.0002***
HDL-C		1.435 ± 0.365	0.830	2.550	1.320 ± 0.3494	0.660	2.440	0.0013**
LDL-C		3.051 ± 0.754	1.110	5.160	2.744 ± 0.8474	0.990	5.810	0.0001***

*Abbreviations: PD, Parkinson's disease; BMI, body mass index; UPDRS, Unified Parkinson's Disease Rating Scale; H&Y, Hoehn, and Yahr staging scale; MoCA, Montreal Cognitive Assessment; MMSE, Mini-Mental State Examination; SOD, superoxide dismutase; hsCRP, high-sensitivity C-reactive protein; UA, urine acid; FN, fibronectin; RBP, retinol-binding protein; CysC, cystatin C; Cr, creatinine; TG, triglyceride; Chol, cholesterol; HDL-C, high-density lipoprotein cholesterol; LDL-C, low-density lipoprotein cholesterol. Data shown are mean ± SD. A comparison of variables between PD and healthy subjects was performed by Student's t-test. A value of P < 0.05 was considered statistically significant. **P < 0.01, ***P < 0.001, ****P < 0.0001.*

TABLE 2 | Comparisons of SOD, hsCRP, cholesterol, HDL-C, and LDL-C between PD patients and healthy controls according to genders.

Clinical parameters	Gender	Control mean ± SD	PD mean ± SD	PD vs. Control *P*-value	PD (male vs. female) *P*-value
SOD	Male	147.9 ± 23.89	137.2 ± 20.80	0.0014**	0.3230
	Female	146.6 ± 24.80	134.4 ± 19.58	<0.0001****	
hsCRP	Male	1.402 ± 0.9463	2.963 ± 3.471	<0.0001****	0.4318
	Female	1.831 ± 1.962	2.604 ± 3.047	0.0250*	
Chol	Male	4.914 ± 0.9586	4.557 ± 0.9071	0.0104*	0.1729
	Female	5.117 ± 0.8287	4.754 ± 1.107	0.0060**	
HDL-C	Male	1.373 ± 0.3308	1.237 ± 0.3171	0.0047**	0.0018**
	Female	1.486 ± 0.3850	1.389 ± 0.3609	0.0529	
LDL-C	Male	3.000 ± 0.8401	2.666 ± 0.7620	0.0054**	0.2353
	Female	3.093 ± 0.6754	2.808 ± 0.9101	0.0083**	

*Data shown are mean ± SD. A comparison of variables between PD and healthy subjects according to gender was performed by Student's t-test. A comparison of variables between male and female PD patients was performed by Student's t-test. A value of P < 0.05 was considered statistically significant. *P < 0.05, **P < 0.01, ****P < 0.0001.*

while plasma levels of inflammatory mediators such as hsCRP are increased.

Correlation Analysis Among UPDRS, H&Y, MoCA, MMSE, SOD, hsCRP, Cholesterol, HDL-C and LDL-C Levels in PD Patients

To evaluate correlations between the disease severity and clinical variables in PD patients, we conducted Pearman's correlation or Spearman's rank correlation analysis among mediator variables and various assessments. We found that plasma SOD level was negatively correlated with hsCRP ($\gamma = -0.3513$, $P < 0.0001$) and positively correlated with cholesterol, HDL-C and LDL-C ($\gamma = 0.\ 0.3553$, $P < 0.0001$ for cholesterol, $\gamma = 0.3121$, $P < 0.0001$ for HDL-C, $\gamma = 0.3678$, $P < 0.0001$ for LDL-C, **Table 3**, **Figure 2**). The plasma SOD level was negatively correlated with UPDRS, UPDRS (I), UPDRS (II), UPDRS (III) and H&Y scores ($\gamma = -0.4856$, $P < 0.0001$ for total UPDRS; $\gamma = -0.3246$, $P < 0.0001$ for UPDRS (I); $\gamma = -0.4422$, $P < 0.0001$ for UPDRS (II); $\gamma = -0.4204$, $P < 0.0001$ for UPDRS (III); $\gamma = -0.4903$, $P < 0.0001$ for H&Y; **Table 3**, **Figure 3**). While, the plasma SOD level was positively correlated with MoCA ($\gamma = 0.4271$, $P < 0.0001$) and MMSE ($\gamma = 0.3443$, $P < 0.0001$). Besides, plasma hsCRP ($\gamma = -0.2640$, $P = 0.0001$) was negatively

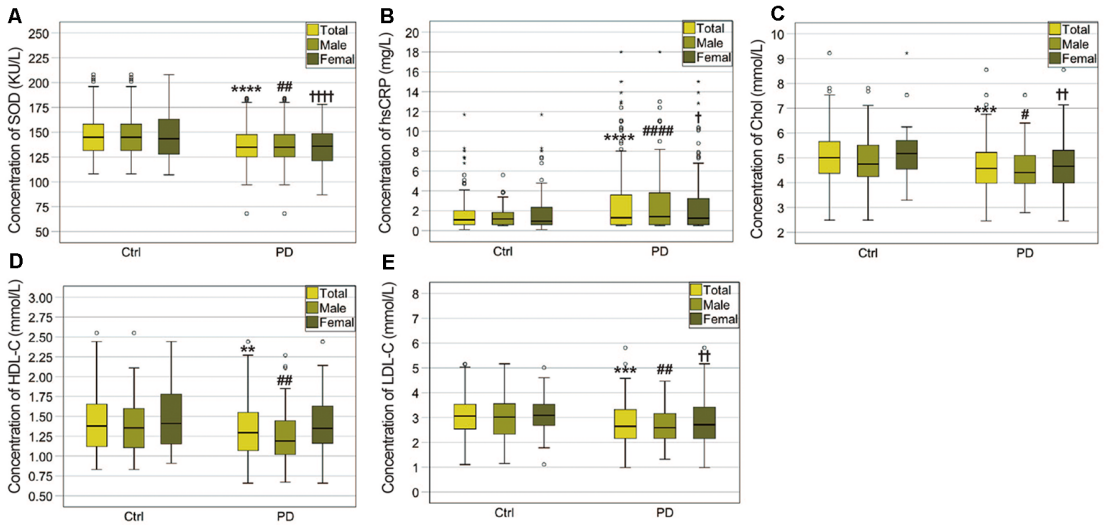

FIGURE 1 | Comparisons of plasma biomarker levels between PD patients and healthy controls (HCs). **(A)** Comparison of superoxide dismutase (SOD) levels between the PD patients and HCs. ****PD (total) vs. Ctrl (total), $P < 0.0001$; $^{\#\#}$PD (male) vs. Ctrl (male), $P < 0.01$; ††††PD (female) vs. Ctrl (female), $P < 0.0001$. **(B)** Comparison of high-sensitivity C-reactive protein (hsCRP) levels between the PD patients and HCs. ****PD (total) vs. Ctrl (total), $P < 0.0001$; $^{\#\#\#\#}$PD (male) vs. Ctrl (male), $P < 0.0001$; †PD (female) vs. Ctrl (female), $P < 0.05$. **(C)** Comparison of cholesterol levels between the PD patients and HCs. ***PD (total) vs. Ctrl (total), $P < 0.001$; $^{\#}$PD (male) vs. Ctrl (male), $P < 0.05$; ††PD (female) vs. Ctrl (female), $P < 0.01$. **(D)** Comparison of high-density lipoprotein cholesterol (HDL-C) levels between the PD patients and HCs. **PD (total) vs. Ctrl (total), $P < 0.01$; $^{\#\#}$PD (male) vs. Ctrl (male), $P < 0.01$. **(E)** Comparison of low-density lipoprotein cholesterol (LDL-C) levels between the PD patients and HCs. ***PD (total) vs. Ctrl (total), $P < 0.001$; $^{\#\#}$PD (male) vs. Ctrl (male), $P < 0.01$. ††PD (female) vs. Ctrl (female), $P < 0.01$.

TABLE 3 | Correlation analysis of all variables in PD patients.

Variable	SOD		hsCR*P*		Chol		HDL-C		LDL-C	
	γ	*P*	Γ	*P*	γ	*P*	γ	*P*	γ	*P*
UPDRS	−0.4856	<0.0001****	0.0975	0.1656	−0.1634	0.0195*	−0.1091	0.1204	−0.1300	0.0638
UPDRS(I)	−0.3246	<0.0001****	0.1445	0.0392*	−0.1026	0.1441	−0.0292	0.6787	−0.1057	0.1324
UPDRS(II)	−0.4422	<0.0001****	0.1491	0.0333*	−0.1356	0.0532	−0.1023	0.1452	−0.1380	0.0490*
UPDRS(III)	−0.4204	<0.0001****	−0.0011	0.9870	−0.1318	0.0602	−0.0736	0.2954	−0.1030	0.1427
H&Y	−0.4903	<0.0001****	0.2264	0.0011**	−0.1626	0.0202*	−0.1156	0.0996	−0.1662	0.0175*
MoCA	0.4271	<0.0001****	−0.2640	0.0001***	0.2008	0.0040**	0.2539	0.0002***	0.1665	0.0173*
MMSE	0.3443	<0.0001****	−0.2150	0.0020**	0.1550	0.0268*	0.1217	0.0830	0.1241	0.0769
SOD	/	/	−0.3513	<0.0001****	0.3553	<0.0001****	0.3121	<0.0001****	0.3678	<0.0001****
hsCRP	−0.3513	<0.0001****	/	/	−0.0956	0.1737	−0.1657	0.0179*	−0.0139	0.8435
Chol	0.3553	<0.0001****	−0.0956	0.1737	/	/	0.3771	<0.0001****	0.8761	<0.0001****
HDL-C	0.3121	<0.0001****	−0.1657	0.0179*	0.3771	<0.0001****	/	/	0.2607	0.0002***
LDL-C	0.3678	<0.0001****	−0.0139	0.8435	0.8761	<0.0001****	0.2607	0.0002***	/	/

*The Pearson correlation was performed to evaluate the relationship between two continuous variables. The Spearman's rank correlation was performed to evaluate the relationship between two continuous or ordinal variables. A value of P < 0.05 was considered statistically significant. *P < 0.05, **P < 0.01, ***P < 0.001, ****P < 0.0001.*

correlated with MoCA, while total cholesterol ($\gamma = 0.2008$, $P = 0.0040$), HDL-C ($\gamma = 0.2539$, $P = 0.0002$) and LDL-C ($\gamma = 0.1665$, $P = 0.0173$) were positively correlated with the MoCA, respectively (**Table 3**). This finding strongly suggests that decreased plasma SOD level is associated with the disease severity in PD patients.

ROC Curves for SOD, hsCRP, Cholesterol, HDL-C, and LDL-C in the Diagnosis of PD

ROC curves were performed to investigate whether plasma SOD, hsCRP, cholesterol, HDL-C, and LDL-C levels could provide potential discrimination between PD patients and HCs. The area under the curve (AUC) value for SOD was 0.6252 (95% CI: 0.5715–0.6790, $P < 0.0001$), the cut-off was 145.7, with a sensitivity of 47.1% and a specificity of 74% (**Figure 4**). AUC for hsCRP was 0.5641 (95% CI: 0.5081–0.6202, $P = 0.0251$), and cut-off was 3.05, with a sensitivity of 29.9% and a specificity of 88.2% (**Figure 4A**). The AUC for cholesterol was 0.6161 (95% CI: 0.5613–0.6708, $P < 0.0001$), the cut-off was 4.21, with a sensitivity of 84.8% and a specificity of 36.8% (**Figure 4B**). The AUC for HDL-C was 0.5810 (95% CI: 0.5258–0.6362, $P = 0.0047$), and the cut-off was 1.05, with a sensitivity of 90.2% and a specificity of 24% (**Figure 4C**). The AUC for LDL-C was 0.6182 (95% CI: 0.5635–0.6729, $P < 0.0001$), and the cut-off was 2.86,

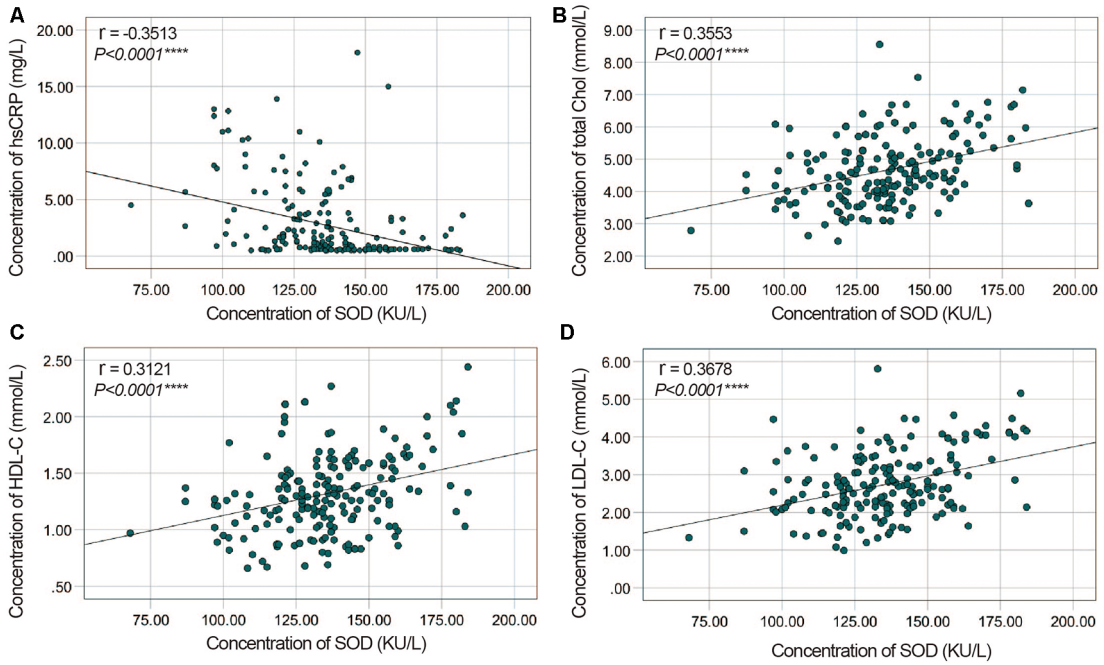

FIGURE 2 | Correlation analysis between plasma SOD and hsCRP/cholesterol/HDL-C/LDL-C in PD Patients. **(A)** A significant negative correlation between SOD and hsCRP in PD Patients. **(B)** A significant positive correlation between SOD and cholesterol in PD Patients. **(C)** A significant positive correlation between SOD and HDL-C in PD Patients. **(D)** A significant positive correlation between SOD and LDL-C in PD Patients. ****$P < 0.0001$.

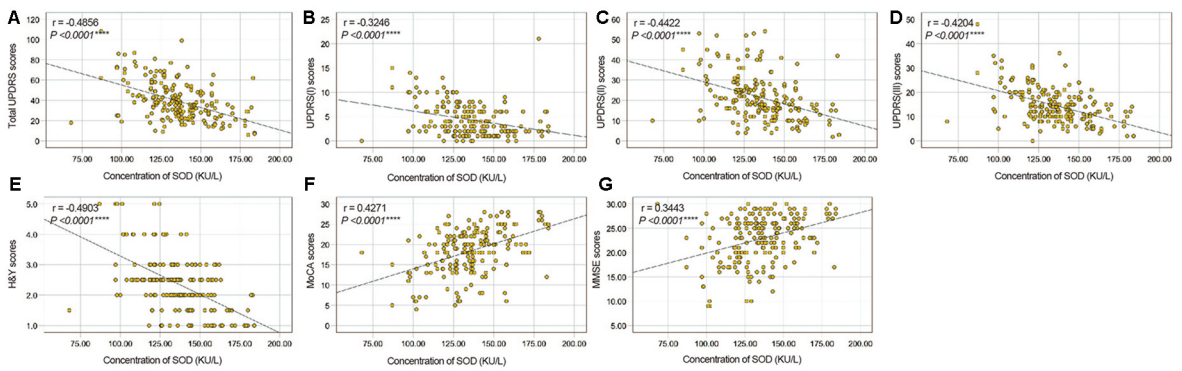

FIGURE 3 | Correlation analysis between plasma SOD and UPDRS/H&Y/MoCA/MMSE scores in PD Patients. **(A)** A significant negative correlation between SOD and total UPDRS scores in PD Patients. **(B)** A significant negative correlation between SOD and UPDRS (I) scores in PD Patients. **(C)** A significant negative correlation between SOD and UPDRS (II) scores in PD Patients. **(D)** A significant negative correlation between SOD and UPDRS (III) scores in PD Patients. **(E)** A significant negative correlation between SOD and H&Y scores in PD Patients. **(F)** A significant positive correlation between SOD and MoCA scores in PD Patients. **(G)** A significant positive correlation between SOD and MMSE scores in PD Patients. ****$P < 0.0001$.

with a sensitivity of 62.7% and a specificity of 62.3% (**Figure 4D**). These data indicate that hsCRP, SOD, cholesterol, HDL-C and LDL-C alone have a diagnostic value in distinguishing PD patients from HC.

In addition, we also conducted a ROC analysis for the combination of SOD and hsCRP/cholesterol/HDL-C/LDL-C levels in the discrimination between PD patients and HCs. The AUC for SOD and hsCRP was 0.6473 (95% CI: 0.5945–0.7000, $P < 0.0001$ 0.06107), with a sensitivity of 41.2% and a specificity of 82.8%, and the cut-off was 0.57, depending on the predicted risk algorithm (**Figure 4A**). The AUC for SOD and cholesterol was 0.6607 (95% CI: 0.6084–0.7130, $P < 0.0001$), with a sensitivity of 52% and a specificity of 72.5%, and cut-off was 0.54 (**Figure 4B**). The AUC for SOD and HDL-C was 0.6472 (95% CI: 0.5944–0.7000, $P < 0.0001$), with a sensitivity of 47.5% and a specificity of 75%, and the cut-off was 0.57 (**Figure 4C**). The AUC for SOD and LDL-C was 0.6712 (95% CI: 0.6191–0.7233, $P < 0.0001$), with a sensitivity of 69.1% and a specificity of

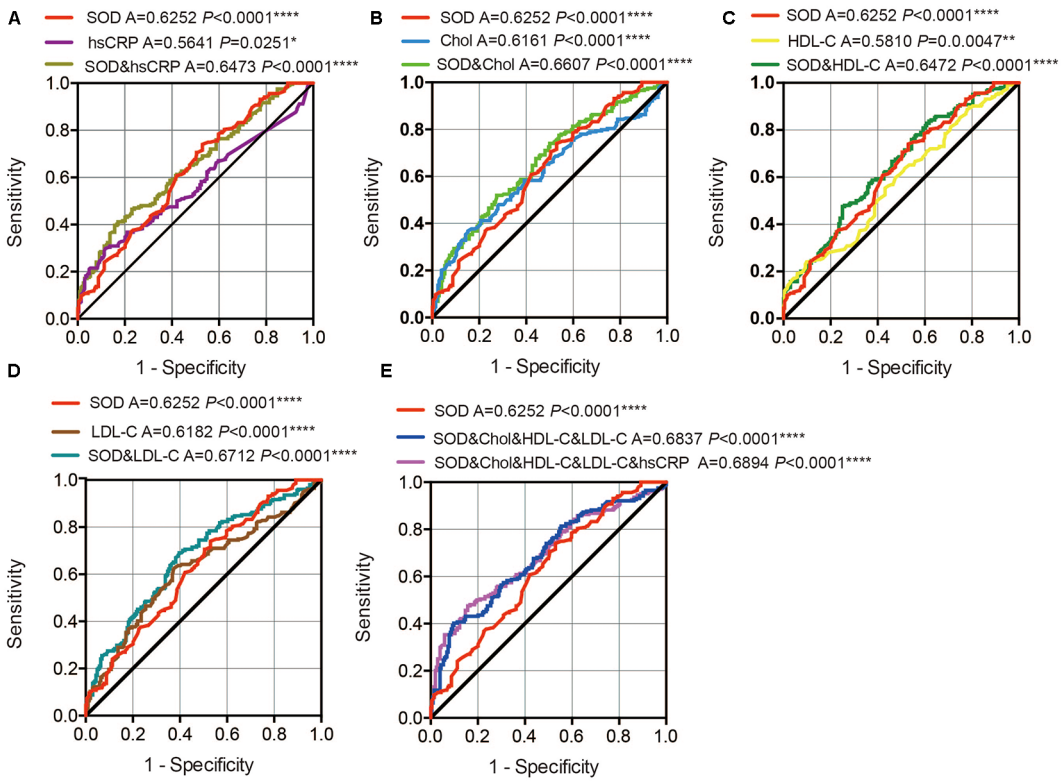

FIGURE 4 | ROC curves to evaluate the utility of plasma levels of SOD, hsCRP, cholesterol, HDL-C and LDL-C for the discrimination of PD patients from healthy controls. **(A)** The area under the curves (AUCs) of the ROC curves for SOD, hsCRP and SOD+hsCRP. **(B)** The AUCs of the ROC curves for SOD, Chol, and SOD+Chol. **(C)** The AUCs of the ROC curves for SOD, HDL-C and SOD+HDL-C. **(D)** The AUCs of the ROC curves for SOD, LDL-C and SOD+LDL-C. **(E)** The AUCs of the ROC curves for SOD, SOD+Chol+HDL-C+LDL-C and SOD+Chol+HDL-C+LDL-C+hsCRP. A, area under the curves. $^{*}P < 0.05$, $^{**}P < 0.01$, $^{****}P < 0.0001$.

60.3%, and the cut-off was 0.49 (**Figure 4D**). When we combined the SOD, cholesterol, HDL-C and LDL-C values, the AUC was 0.6837 (95% CI:0.6323–0.7351, $P < 0.0001$), with a sensitivity of 40.2% and a specificity of 90.2% at the cut-off of 0.60 (**Figure 4E**). When we combined the SOD, cholesterol, HDL-C, LDL-C and hsCRP values, the AUC was 0.6894 (95% CI: 0.6382–0.7405, $P < 0.0001$), with a sensitivity of 47.5% and a specificity of 84.3% at the cut-off of 0.58 (**Figure 4E**). These data indicate that the combination SOD with cholesterol, HDL-C, LDL-C and hsCRP levels was more robust than SOD, cholesterol, HDL-C and LDL-C alone in distinguishing PD patients from HC.

DISCUSSION

In this present study, we explored the variations of plasma levels of SOD, hsCRP, cholesterol, HDL-C and LDL-C in PD patients and noted several interesting results. First, we found a pronounced decrease in the plasma levels of SOD, cholesterol, HDL-C, and LDL-C and an increase in the plasma level of hsCRP in PD patients when compared to HC. Second, the plasma level of SOD was negatively correlated with the plasma level of hsCRP but positively correlated with the plasma levels of cholesterol, HDL-C and LDL-C in PD patients. Third, there were significant correlations between the decreased plasma SOD level and the disease severity of PD. The interesting finding of an inversed correlation between plasma levels of SOD and hsCRP may shed light on the underlying neuro-pathogenesis of PD.

More and more evidence indicates that BBB dysfunction contributes to the pathophysiological process of PD (Iadecola, 2017). A post-mortem study of advanced PD cases showed vessel degeneration in multiple brain regions, especially in the substantia nigra, middle frontal cortex and brain stem nuclei (Guan et al., 2013; Zheng et al., 2018; Calvo-Rodriguez et al., 2019; Wei et al., 2019). Other studies also demonstrated that BBB permeability was increased in the late stages of PD (Kortekaas et al., 2005; Pisani et al., 2012). Since the BBB was impaired, various neurotoxic molecules and red blood cells (RBCs) can leak from peripheral circulation into brain parenchyma. RBCs invasion causes accumulation of hemoglobin-derived neurotoxic products including iron, which generates neurotoxic ROS (Zlokovic, 2011; Cai et al., 2017). Dopaminergic cells are equipped with abundant amounts of mitochondria, and therefore more vulnerable to ROS attacks (Calvo-Rodriguez et al., 2019). SOD, as one of the most important antioxidant enzymes, is supposed to be the first-line defense against increased ROS production in PD (Peng et al., 2005; Botella et al., 2008; de Farias et al., 2016). The decrease in SOD reduces the scavenging of O_2– and the balance was shifted towards oxidative stress in

PD patients, which eventually lead to the development of PD. In this study, we found that the plasma level of SOD in PD patients was remarkably lower than HC, indicating that lower plasma levels of SOD may contribute to the neuro-pathogenesis of PD, and may be correlated to the disease severity. Our finding is in agreement with the results of previous studies. Gruden et al. (2012) demonstrated that the plasma activity of SOD in PD patients was diminished. Yuan et al. (2016) found that plasma activity of SOD in *de novo* Chinese PD patients were lower than in HCs. Furthermore, Li et al., 2017 generated MPTP-treated PD monkey model and found that serum SOD showed continuously decrease. However, there are also some contradictory results in PD patients showing increased SOD in the peripheral blood when compared with HC (Serra et al., 2001; Sharma et al., 2008; de Farias et al., 2016). Whereas in some other studies, although a slight decrease in PD was indicated, they did not find a statistical difference in plasma SOD between PD patients and HC (Watfa et al., 2011). The significant heterogeneity among those studies might be due to the different ethnic groups, disease severity, disease duration, medication status, limited number of subjects. Therefore, we specifically examined the relationship between plasma SOD level and PD severity. In this study, we found that the plasma SOD concentration was significantly negatively correlated with the scores of UPDRS, UPDRS (I), UPDRS (II), UPDRS (III), and H&Y. UPDRS (I) subscale was applied to measure the mentation, behavior and mood including intellectual impairment, thought disorder, depression and motivation/initiative. UPDRS (II) subscale was applied to measure the daily life functions such as speech, swallowing, handwriting, turning in bed etc. UPDRS (III) subscale was applied to measure the motor dysfunction such as hand movements, tremors, rigidity, arising from chair and gait. Previous study has also demonstrated that SOD change was closely related to the appearance of clinical symptoms in MPTP-treated monkeys such as akinesia, rigidity and tremor (Li et al., 2017). Furthermore, we noted the significantly positive correlation between plasma SOD level and MoCA/MMSE scores in PD patients, indicating that decreased plasma SOD level in PD might, at least partially, correlate to the cognitive impairment of PD patients. Previous studies have also demonstrated that higher SOD level is associated with a decreased risk of dementia (Casado et al., 2008). Based on our findings, the decreased SOD might be an important marker to assess the disease severity of PD patients.

Lipids are molecules that contain fatty acids or a steroid nucleus (e.g., cholesterol). They are the main compositions that constitute cellular membranes, part of membrane rafts and protein anchors, and signaling and transport molecules across BBB (Shi et al., 2019). Several lines of evidence already indicated that abnormalities in lipid metabolism are involved in the pathophysiological process of PD (Chung et al., 2019; Xicoy et al., 2019). A previous study demonstrated that dyslipidemia is causally related to BBB impairment and plasma HDL cholesterol were the lipids most associated with BBB integrity (Bowman et al., 2012; Deng et al., 2018; Eiden et al., 2019; Miao et al., 2019). α-synuclein is a small protein abundantly expressed in the brain. It is well-established that the folding and aggregation of α-synuclein is a pathological hallmark of Parkinson's disease. Previous study indicated that the disruption of lipids homeostasis may lead to the accumulation of α-synuclein *via* a direct lipid-protein interaction (Galvagnion, 2017). In this present study, we found that plasma levels of cholesterol, HDL-C and LDL-C were significantly decreased in PD patients compared to HC. Our findings are in agreement with previous studies, showing lower levels of plasma total cholesterol, LDL-C, HDL-C in PD patients compared with HCs (Guo et al., 2015; Zhang et al., 2017). Fang et al. (2019) found that higher levels of total cholesterol, LDL-C, and triglycerides were associated with a lower future risk of PD. Furthermore, previous studies indicated that a higher plasma level of cholesterol has been associated with reduced PD risk and slower clinical progression of PD (Huang et al., 2011, 2015; Rozani et al., 2018). cholesterol intake has been suggested to be negatively correlated with PD risk (Powers et al., 2009). Lower plasma level of HDL has also been found to be associated with earlier PD onset and higher PD risk (Qiang et al., 2013; Lu et al., 2014; Swanson et al., 2015a,b). Lower level of LDL-C was reportedly associated with higher PD risk, while higher level of LDL-C might be protective for PD and associated with preserved executive and fine motor functions in PD (Huang et al., 2008; Du et al., 2012; Rozani et al., 2018). These results suggested that the disruption of lipids homeostasis may be involved in the pathogenesis of PD.

Interestingly, we noticed a significant and positive correlation between SOD and cholesterol, HDL-C and LDL-C in PD patients. It has been shown that increased cholesterol, either *in vivo* in cholesterol-fed wt mice or *in vitro* in genetically induced cholesterol accumulation due to NPC1 loss-of-function, could potentiate SOD activity, suggesting that SOD might be a prime target and the first defense mechanism of oxidative stress response upon increased cholesterol (Dominko et al., 2018). Multiple lines of evidence already indicate that a high level of LDL-C could cause the free radical formation and excessive oxidative stress, which initially leads to a progressive increase in endogenous enzymatic scavengers like SOD (Gupta et al., 2009). Therefore, we propose that both SOD, cholesterol, HDL-C and LDL-C would directly participate in the pathophysiological mechanism of PD.

Evidence is now overwhelming that inflammatory responses manifested by glial reactions, increased expression of inflammatory cytokines, and other toxic mediators are important contributors to the progressive loss of nigral dopaminergic (DA) neurons in PD patients. Previous studies found that the aging process can exaggerate the inflammatory responses and aggravate the DA neurons loss in the brain (Zhao et al., 2018). Additionally, the existence of ongoing inflammatory processes affects the modulation of neurogenesis, for example, TNFα affects the differentiation and proliferation of neural stem cells by up-regulation of Ascl2 (Liu et al., 2019). Previous studies demonstrated that systemic inflammation may exacerbate the symptoms of chronic neurodegenerative diseases, indicating that systemic inflammation may promote neurodegeneration (Cunningham et al., 2009; Perry, 2010). The level of hsCRP in the peripheral blood is a well-studied non-specific marker

of low-grade systemic inflammation. Previous studies have indicated that high concentration of hsCRP may disrupt BBB (Schmidt et al., 2002) and increase the paracellular permeability by binding to the Fcγ receptor, which results in the entrance of hsCRP and other peripheral inflammatory proteins into the central nervous system and eventually leads to reactive gliosis and development of PD (Wilms et al., 2007; Chen et al., 2008). In this case, the level of hsCRP in the peripheral blood may reflect the neuro-inflammatory status in the central nervous system. In the present study, we found a pronounced increase in the plasma level of hsCRP in PD patients compared to HC, which is in line with previous reports (Baran et al., 2019). Besides, in this present study, we found that plasma hsCRP level was negatively correlated with MoCA in PD, suggesting that elevated hsCRP level was associated with poor cognitive performance. Our finding is in accord with previous studies that higher level of hsCRP was associated with cognitive decline in the general population and AD (Kuo et al., 2005; Komulainen et al., 2007; Marioni et al., 2009; Xu et al., 2009). Several underlying mechanisms might explain the involvement of hsCRP in the process that contributes to cognitive impairment in PD patients. Accumulating evidence suggests that inflammation is associated with cardio-cerebrovascular diseases (Kuo et al., 2005; Wichmann et al., 2014). The hsCRP, rather than just simply acting as a systemic inflammatory marker, is also a proatherogenic role and involved in atherogenesis through the mediation of LDL uptake by macrophages, facilitation of foam-cell formation and low nitric-oxide production, stimulation of monotype recruitment and vascular smooth muscle proliferation, thus leading to cerebral microangiopathy and macroangiopathy. All of these finally would result in the disruption of the frontal-subcortical circuit and cognitive impairment (Kuo et al., 2005). These results strongly imply that the plasma hsCRP level could be used to assess cognitive impairment in PD patients.

Interestingly, in this present study, our findings indicated the decreased SOD in PD, and we proposed that this decrease might contribute to the cognitive impairment in PD patients; while the increased hsCRP might aggravate cognitive impairment in PD patients. This contra-directional effect of SOD and hsCRP in cognitive function indicating they might perform the opposite function in PD patients. The hsCRP not only performs an important role in the inflammatory mechanisms but also induces oxidative stress. Kobayashi et al., 2003 found that hsCRP could induce the generation of ROS in cultured coronary artery smooth muscle cells by enhancing p22phox protein expression. Venugopal et al. (2003) showed that hsCRP could stimulate O_2– release and resulted in decreased prostacyclin release in human aortic endothelial cells. On the other hand, O_2– has involved not just oxidative stress but also pro-inflammatory roles, which may contribute to the recruitment of neutrophils to sites of inflammation, the formation of chemotactic factors, cytokine release, neurotransmitter and hormone inactivation, adhesion molecules expression, lipid peroxidation and oxidation and DNA damage. Previous studies also indicated that O_2– could activate nuclear factor-κB, which finally induced hsCRP expression (Zhao et al., 2019). SOD is the major antioxidant enzyme in the human antioxidant system to protect against oxidative stress, which catalyzes the dismutation of highly reactive O_2– to less reactive H_2O_2 and oxygen. Therefore, SOD can be considered to be anti-inflammatory and anti-oxidative stress. Indeed, SOD mimetic has been successfully used to prevent the extent of inflammation (De Lazzari et al., 2018; Ren et al., 2018). As mentioned above, SOD is the prime target and the first defense mechanism of oxidative stress response upon increased cholesterol /LDL-C (Gupta et al., 2009; Dominko et al., 2018), which may prevent the inflammatory response caused by cholesterol /LDL-C to some extent. Therefore, there seems to be a strong and complicated interaction between hsCRP/cholesterol/LDL-C pro-inflammatory function and SOD anti-inflammatory function, which may influence the cognitive dysfunctions in PD patients.

There are several limitations to this study: (1) a relatively small number of participants (204 PD patients and 204 healthy subjects) were recruited. In the future, a large number of participants would be recruited; (2) this study is a cross-sectional study. Therefore, longitudinal cohort studies with a larger population need to be performed in the future; and (3) absence of the assessment of other inflammatory markers like cytokines. Furthermore, the indexes of oxidative stress and inflammation status should be further investigated to comprehensively understand the roles of oxidative stress and inflammation in PD.

In summary, plasma antioxidant status such as the SOD is obviously impaired in PD patients, while plasma inflammation such as hsCRP is increased. This finding supports the idea that oxidative stress and inflammation in the peripheral blood may contribute to the pathogenesis of PD. Decreased SOD along with cholesterol, HDL-C and LDL-C and increased hsCRP might be important markers to assess the disease severity of PD patients. Further prospective studies are needed to validate these findings that will help us better understand PD pathogenesis and potential neuroprotection effects of SOD.

DATA AVAILABILITY STATEMENT

All datasets generated for this study are included in the article.

ETHICS STATEMENT

The studies involving human participants were reviewed and approved by the ethics committee of the Zhujiang Hospital of Southern Medical University. The patients/participants provided their written informed consent to participate in this study.

AUTHOR CONTRIBUTIONS

WY, SZ, and QW conceived and designed the study. WY, ZC, RQ, GW, BD, ZH, FX, XW, QY, and TW performed the study. ML, KM, BT, VM, and FZ revised the article for intellectual content. WY and ZC performed data statistics and analysis. WY and QW wrote the article. All authors read and approved the final manuscript.

FUNDING

This work was supported by the National Key R&D Program of China (No. 2017YFC1310200), National Natural Science Foundation of China (No. 81873777), Natural Science Foundations of Guangdong of China (Grant No. 2017A030311010), Leading Talent in Talents Project Guangdong High-level Personnel of Special Support Program, and Scientific Research Foundation of Guangzhou (Grant No. 201704030080) to QW, China Postdoctoral Science Foundation funded project (Grant No. 2019M652971) and Natural Science Foundations of Guangdong of China (Grant No. 2017A030313672 and Grant No. 2019A1515010281) to SZ, China Postdoctoral Science Foundation funded project (Grant No. 2019M662987) to WY.

REFERENCES

Adams, B., Nunes, J. M., Page, M. J., Roberts, T., Carr, J., Nell, T. A., et al. (2019). Parkinson's disease: a systemic inflammatory disease accompanied by bacterial inflammagens. *Front. Aging Neurosci.* 11:210. doi: 10.3389/fnagi.2019.00210

Baran, A., Bulut, M., Kaya, M. C., Demirpence, Ö., Sevim, B., Akil, E., et al. (2019). High-sensitivity C-reactive protein and high mobility group box-1 levels in Parkinson's disease. *Neurol. Sci.* 40, 167–173. doi: 10.1007/s10072-018-3611-z

Botella, J. A., Bayersdorfer, F., and Schneuwly, S. (2008). Superoxide dismutase overexpression protects dopaminergic neurons in a *Drosophila* model of Parkinson's disease. *Neurobiol. Dis.* 30, 65–73. doi: 10.1016/j.nbd.2007.11.013

Bowman, G. L., Kaye, J. A., and Quinn, J. F. (2012). Dyslipidemia and blood-brain barrier integrity in Alzheimer's disease. *Curr. Gerontol. Geriatr. Res.* 2012:184042. doi: 10.1155/2012/184042

Cai, W., Zhang, K., Li, P., Zhu, L., Xu, J., Yang, B., et al. (2017). Dysfunction of the neurovascular unit in ischemic stroke and neurodegenerative diseases: an aging effect. *Ageing Res. Rev.* 34, 77–87. doi: 10.1016/j.arr.2016.09.006

Calvo-Rodriguez, M., Hernando-Perez, E., Nuñez, L., and Villalobos, C. (2019). Amyloid β oligomers increase ER-Mitochondria Ca^{2+} Cross talk in young hippocampal neurons and exacerbate aging-induced intracellular Ca^{2+} remodeling. *Front. Cell. Neurosci.* 13:22. doi: 10.3389/fncel.2019.00022

Casado, A., Encarnación López-Fernańdez, M., Concepcion Casado, M., and de La Torre, R. (2008). Lipid peroxidation and antioxidant enzyme activities in vascular and Alzheimer dementias. *Neurochem. Res.* 33, 450–458. doi: 10.1007/s11064-007-9453-3

Chen, H., O'Reilly, E. J., Schwarzschild, M. A., and Ascherio, A. (2008). Peripheral inflammatory biomarkers and risk of Parkinson's disease. *Am. J. Epidemiol.* 167, 90–95. doi: 10.1093/aje/kwm260

Chen, Y., Yin, M., Cao, X., Hu, G., and Xiao, M. (2018). Pro- and anti-inflammatory effects of high cholesterol diet on aged brain. *Aging Dis.* 9, 374–390. doi: 10.14336/ad.2017.0706

Chomiak, T., Watts, A., Burt, J., Camicioli, R., Tan, S. N., McKeown, M. J., et al. (2018). Differentiating cognitive or motor dimensions associated with the perception of fall-related self-efficacy in Parkinson's disease. *NPJ Parkinsons. Dis.* 4:26. doi: 10.1038/s41531-018-0059-z

Chung, H. Y., Kim, D. H., Lee, E. K., Chung, K. W., Chung, S., Lee, B., et al. (2019). Redefining chronic inflammation in aging and age-related diseases: proposal of the senoinflammation concept. *Aging Dis.* 10, 367–382. doi: 10.14336/ad.2018.0324

Cunningham, C., Campion, S., Lunnon, K., Murray, C. L., Woods, J. F., Deacon, R. M., et al. (2009). Systemic inflammation induces acute behavioral and cognitive changes and accelerates neurodegenerative disease. *Biol. Psychiatry* 65, 304–312. doi: 10.1016/j.biopsych.2008.07.024

de Farias, C. C., Maes, M., Bonifacio, K. L., Bortolásci, C. C., de Souza Nogueira, A., Brinholi, F. F., et al. (2016). Highly specific changes in antioxidant levels and lipid peroxidation in Parkinson's disease and its progression: disease and staging biomarkers and new drug targets. *Neurosci Lett.* 617, 66–71. doi: 10.1016/j.neulet.2016.02.011

De Lazzari, F., Bubacco, L., Whitworth, A. J., and Bisaglia, M. (2018). Superoxide radical dismutation as new therapeutic strategy in Parkinson's disease. *Aging Dis.* 9, 716–728. doi: 10.14336/ad.2017.1018

Deng, Q. W., Li, S., Wang, H., Lei, L., Zhang, H. Q., Gu, Z. T., et al. (2018). The short-term prognostic value of the triglyceride-to-high-density lipoprotein cholesterol ratio in acute ischemic stroke. *Aging Dis.* 9, 498–506. doi: 10.14336/ad.2017.0629

Dominko, K., Dikic, D., and Hecimovic, S. (2018). Enhanced activity of superoxide dismutase is a common response to dietary and genetically induced increased cholesterol levels. *Nutr. Neurosci.* 17, 1–13. doi: 10.1080/1028415x.2018.1511027

Du, G., Lewis, M. M., Shaffer, M. L., Chen, H., Yang, Q. X., Mailman, R. B., et al. (2012). Serum cholesterol and nigrostriatal R2* values in Parkinson's disease. *PLoS One* 7:e35397. doi: 10.1371/journal.pone.0035397

Eiden, M., Christinat, N., Chakrabarti, A., Sonnay, S., Miroz, J. P., Cuenoud, B., et al. (2019). Discovery and validation of temporal patterns involved in human brain ketometabolism in cerebral microdialysis fluids of traumatic brain injury patients. *EBioMedicine* 44, 607–617. doi: 10.1016/j.ebiom.2019.05.054

Fang, F., Zhan, Y., Hammar, N., Shen, X., Wirdefeldt, K., Walldius, G., et al. (2019). Lipids, apolipoproteins and the risk of parkinson disease. *Circ. Res.* 125, 643–652. doi: 10.1161/CIRCRESAHA.119.314929

Folstein, M. F., Folstein, S. E., and McHugh, P. R. (1975). "Mini-mental state". A practical method for grading the cognitive state of patients for the clinician. *J. Psychiatr. Res.* 12, 189–198. doi: 10.1016/0022-3956(75)90026-6

Galvagnion, C. (2017). The role of lipids interacting with α-synuclein in the pathogenesis of Parkinson's disease. *J. Parkinsons Dis.* 7, 433–450. doi: 10.3233/JPD-171103

Gao, C., Smith, S., Lones, M., Jamieson, S., Alty, J., Cosgrove, J., et al. (2018). Objective assessment of bradykinesia in Parkinson's disease using evolutionary algorithms: clinical validation. *Transl. Neurodegener.* 7:18. doi: 10.5220/0006601700630069

Gruden, M. A., Yanamandra, K., Kucheryanu, V. G., Bocharova, O. R., Sherstnev, V. V., Morozova-Roche, L. A., et al. (2012). Correlation between protective immunity to α-synuclein aggregates, oxidative stress and inflammation. *Neuroimmunomodulation* 19, 334–342. doi: 10.1159/000341400

Guan, J., Pavlovic, D., Dalkie, N., Waldvogel, H. J., O'Carroll, S. J., Green, C. R., et al. (2013). Vascular degeneration in Parkinson's disease. *Brain Pathol.* 23, 154–164. doi: 10.1111/j.1750-3639.2012.00628.x

Guo, X., Song, W., Chen, K., Chen, X., Zheng, Z., Cao, B., et al. (2015). The serum lipid profile of Parkinson's disease patients: a study from China. *Int. J. Neurosci.* 125, 838–844. doi: 10.3109/00207454.2014.979288

Gupta, S., Sodhi, S., and Mahajan, V. (2009). Correlation of antioxidants with lipid peroxidation and lipid profile in patients suffering from coronary artery disease. *Expert Opin. Ther. Targets* 13, 889–894. doi: 10.1517/14728220903099668

He, R., Yan, X., Guo, J., Xu, Q., Tang, B., and Sun, Q. (2018). Recent advances in biomarkers for Parkinson's disease. *Front. Aging Neurosci.* 10:305. doi: 10.3389/fnagi.2018.00305

Hoehn, M. M., and Yahr, M. D. (1967). Parkinsonism: onset, progression and mortality. *Neurology* 17, 427–442. doi: 10.1212/wnl.17.5.427

Hu, G. (2010). Total cholesterol and the risk of Parkinson's disease: a review for some new findings. *Parkinsons Dis.* 2010:836962. doi: 10.4061/2010/836962

Huang, X., Abbott, R. D., Petrovitch, H., Mailman, R. B., and Ross, G. W. (2008). Low LDL cholesterol and increased risk of Parkinson's disease: prospective results from Honolulu-Asia Aging Study. *Mov. Disord.* 23, 1013–1018. doi: 10.1002/mds.22013

Huang, X., Alonso, A., Guo, X., Umbach, D. M., Lichtenstein, M. L., Ballantyne, C. M., et al. (2015). Statins, plasma cholesterol and risk of Parkinson's disease: a prospective study. *Mov. Disord.* 30, 552–559. doi: 10.1002/mds.26152

Huang, X., Auinger, P., Eberly, S., Oakes, D., Schwarzschild, M., Ascherio, A., et al. (2011). Serum cholesterol and the progression of Parkinson's disease: results from DATATOP. *PLoS One* 6:e22854. doi: 10.1371/journal.pone.0022854

Iadecola, C. (2017). The neurovascular unit coming of age: a journey through neurovascular coupling in health and disease. *Neuron* 96, 17–42. doi: 10.1016/j.neuron.2017.07.030

Kobayashi, S., Inoue, N., Ohashi, Y., Terashima, M., Matsui, K., Mori, T., et al. (2003). Interaction of oxidative stress and inflammatory response in coronary plaque instability: important role of C-reactive protein. *Arterioscler. Thromb. Vasc. Biol.* 23, 1398–1404. doi: 10.1161/01.atv.0000081637.36475.bc

Komulainen, P., Lakka, T. A., Kivipelto, M., Hassinen, M., Penttila, I. M., Helkala, E. L., et al. (2007). Serum high sensitivity C-reactive protein and cognitive function in elderly women. *Age Ageing* 36, 443–448. doi: 10.1093/ageing/afm051

Kortekaas, R., Leenders, K. L., van Oostrom, J. C., Vaalburg, W., Bart, J., Willemsen, A. T., et al. (2005). Blood-brain barrier dysfunction in parkinsonian midbrain *in vivo*. *Ann. Neurol.* 57, 176–179. doi: 10.1002/ana.20369

Kuo, H. K., Yen, C. J., Chang, C. H., Kuo, C. K., Chen, J. H., and Sorond, F. (2005). Relation of C-reactive protein to stroke, cognitive disorders, and depression in the general population: systematic review and meta-analysis. *Lancet. Neurol.* 4, 371–380. doi: 10.1016/s1474-4422(05)70099-5

Li, G., Ma, J., Cui, S., He, Y., Xiao, Q., Liu, J., et al. (2019). Parkinson's disease in China: a forty-year growing track of bedside work. *Transl. Neurodegener.* 8:22. doi: 10.1186/s40035-019-0162-z

Li, L., Shi, L., Liu, H., Luo, Q., Huang, C., Liu, W., et al. (2017). Changes in blood anti-oxidation enzyme levels in MPTP-treated monkeys. *Neurosci. Lett.* 649, 93–99. doi: 10.1016/j.neulet.2017.04.004

Liu, Z., Wang, X., Jiang, K., Ji, X., Zhang, Y. A., and Chen, Z. (2019). TNFα-induced Up-regulation of Ascl2 affects the differentiation and proliferation of neural stem cells. *Aging Dis.* 10, 1207–1220. doi: 10.14336/ad.2018.1028

Lu, W., Wan, X., Liu, B., Rong, X., Zhu, L., Li, P., et al. (2014). Specific changes of serum proteins in Parkinson's disease patients. *PLoS One* 9:e95684. doi: 10.1371/journal.pone.0095684

Mannarino, M. R., Sahebkar, A., Bianconi, V., Serban, M. C., Banach, M., and Pirro, M. (2018). PCSK9 and neurocognitive function: Should it be still an issue after FOURIER and EBBINGHAUS results?. *J. Clin. Lipidol.* 12, 1123–1132. doi: 10.1016/j.jacl.2018.05.012

Marioni, R. E., Stewart, M. C., Murray, G. D., Deary, I. J., Fowkes, F. G., Lowe, G. D., et al. (2009). Peripheral levels of fibrinogen, C-reactive protein, and plasma viscosity predict future cognitive decline in individuals without dementia. *Psychosom. Med.* 71, 901–906. doi: 10.1097/psy.0b013e3181b1e538

Miao, H., Yang, Y., Wang, H., Huo, L., Wang, M., Zhou, Y., et al. (2019). Intensive lipid-lowering therapy ameliorates asymptomatic intracranial atherosclerosis. *Aging Dis.* 10, 258–266. doi: 10.14336/ad.2018.0526

Mosley, R. L., Benner, E. J., Kadiu, I., Thomas, M., Boska, M. D., Hasan, K., et al. (2006). Neuroinflammation, oxidative stress and the pathogenesis of Parkinson's disease. *Clin. Neurosci. Res.* 6, 261–281. doi: 10.1016/j.cnr.2006.09.006

Movement Disorder Society Task Force on Rating Scales for Parkinson's, D. (2003). The Unified Parkinson's Disease Rating Scale (UPDRS): status and recommendations. *Mov. Disord.* 18, 738–750. doi: 10.1002/mds.10473

Nawaz, M. I., and Mohammad, G. (2015). Role of high-mobility group box-1 protein in disruption of vascular barriers and regulation of leukocyte-endothelial interactions. *J. Recept. Signal Transduct. Res.* 35, 340–345. doi: 10.3109/10799893.2014.984309

Ng, A. S. L., and Tan, E. K. (2017). Linking statins and lipids in Parkinson's disease. *Mov. Disord.* 32, 807–809. doi: 10.1002/mds.27053

Peng, J., Stevenson, F. F., Doctrow, S. R., and Andersen, J. K. (2005). Superoxide dismutase/catalase mimetics are neuroprotective against selective paraquat-mediated dopaminergic neuron death in the substantial nigra: implications for Parkinson disease. *J. Biol. Chem.* 280, 29194–29198. doi: 10.1074/jbc.m500984200

Perry, V. H. (2010). Contribution of systemic inflammation to chronic neurodegeneration. *Acta Neuropathol.* 120, 277–286. doi: 10.1007/s00401-010-0722-x

Pisani, V., Stefani, A., Pierantozzi, M., Natoli, S., Stanzione, P., Franciotta, D., et al. (2012). Increased blood-cerebrospinal fluid transfer of albumin in advanced Parkinson's disease. *J. Neuroinflammation* 9:188. doi: 10.1186/1742-2094-9-188

Postuma, R. B., Berg, D., Stern, M., Poewe, W., Olanow, C. W., Oertel, W., et al. (2015). MDS clinical diagnostic criteria for Parkinson's disease. *Mov. Disord.* 30, 1591–1601. doi: 10.1002/mds.26424

Powers, K. M., Smith-Weller, T., Franklin, G. M., Longstreth, W. T. Jr., Swanson, P. D., and Checkoway, H. (2009). Dietary fats, cholesterol and iron as risk factors for Parkinson's disease. *Parkinsonism Relat. Disord.* 15, 47–52. doi: 10.1016/j.parkreldis.2008.03.002

Qian, E., and Huang, Y. (2019). Subtyping of Parkinson's disease—where are we up to?. *Aging Dis.* 10, 1130–1139. doi: 10.14336/ad.2019.0112

Qiang, J. K., Wong, Y. C., Siderowf, A., Hurtig, H. I., Xie, S. X., Lee, V. M., et al. (2013). Plasma apolipoprotein A1 as a biomarker for Parkinson disease. *Ann. Neurol.* 74, 119–127. doi: 10.1002/ana.23872

Ray Chaudhuri, K., Poewe, W., and Brooks, D. (2018). Motor and nonmotor complications of levodopa: phenomenology, risk factors, and imaging features. *Mov Disord* 33, 909–919. doi: 10.1002/mds.27386

Ren, C., Wu, H., Li, D., Yang, Y., Gao, Y., Jizhang, Y., et al. (2018). Remote ischemic conditioning protects diabetic retinopathy in streptozotocin-induced diabetic rats *via* anti-inflammation and antioxidation. *Aging Dis.* 9, 1122–1133. doi: 10.14336/ad.2018.0711

Rozani, V., Gurevich, T., Giladi, N., El-Ad, B., Tsamir, J., Hemo, B., et al. (2018). Higher serum cholesterol and decreased Parkinson's disease risk: a statin-free cohort study. *Mov. Disord.* 33, 1298–1305. doi: 10.1002/mds.27413

Schmidt, R., Schmidt, H., Curb, J. D., Masaki, K., White, L. R., and Launer, L. J. (2002). Early inflammation and dementia: a 25-year follow-up of the Honolulu-Asia Aging Study. *Ann. Neurol.* 52, 168–174. doi: 10.1002/ana.10265

Serra, J. A., Dominguez, R. O., de Lustig, E. S., Guareschi, E. M., Famulari, A. L., Bartolome, E. L., et al. (2001). Parkinson's disease is associated with oxidative stress: comparison of peripheral antioxidant profiles in living Parkinson's, Alzheimer's and vascular dementia patients. *J. Neural. Transm.* 108, 1135–1148. doi: 10.1007/s007020170003

Shakour, N., Bianconi, V., Pirro, M., Barreto, G. E., Hadizadeh, F., and Sahebkar, A. (2019). *In silico* evidence of direct interaction between statins and β-amyloid. *J. Cell. Biochem.* 120, 4710–4715. doi: 10.1002/jcb.27761

Sharma, A., Kaur, P., Kumar, B., Prabhakar, S., and Gill, K. D. (2008). Plasma lipid peroxidation and antioxidant status of Parkinson's disease patients in the Indian population. *Parkinsonism Relat. Disord.* 14, 52–57. doi: 10.1016/j.parkreldis.2007.06.009

Shi, M., Sheng, L., Stewart, T., Zabetian, C. P., and Zhang, J. (2019). New windows into the brain: central nervous system-derived extracellular vesicles in blood. *Prog. Neurobiol.* 175, 96–106. doi: 10.1016/j.pneurobio.2019.01.005

Smith, T., Gildeh, N., and Holmes, C. (2007). The montreal cognitive assessment: validity and utility in a memory clinic setting. *Can. J. Psychiatry* 52, 329–332. doi: 10.1177/070674370705200508

Sun, Q., Wang, T., Jiang, T. F., Huang, P., Wang, Y., Xiao, Q., et al. (2018). Clinical profile of chinese long-term Parkinson's disease survivors with 10 years of disease duration and beyond. *Aging Dis.* 9, 8–16. doi: 10.14336/ad.2017.0204

Swanson, C. R., Berlyand, Y., Xie, S. X., Alcalay, R. N., Chahine, L. M., and Chen-Plotkin, A. S. (2015a). Plasma apolipoprotein A1 associates with age at onset and motor severity in early Parkinson's disease patients. *Mov. Disord.* 30, 1648–1656. doi: 10.1002/mds.26290

Swanson, C. R., Li, K., Unger, T. L., Gallagher, M. D., Van Deerlin, V. M., Agarwal, P., et al. (2015b). Lower plasma apolipoprotein A1 levels are found in Parkinson's disease and associate with apolipoprotein A1 genotype. *Mov. Disord.* 30, 805–812. doi: 10.1002/mds.26022

Venugopal, S. K., Devaraj, S., and Jialal, I. (2003). C-reactive protein decreases prostacyclin release from human aortic endothelial cells. *Circulation* 108, 1676–1678. doi: 10.1161/01.cir.0000094736.10595.a1

Watfa, G., Dragonas, C., Brosche, T., Dittrich, R., Sieber, C. C., Alecu, C., et al. (2011). Study of telomere length and different markers of oxidative stress in patients with Parkinson's disease. *J. Nutr. Health Aging* 15, 277–281. doi: 10.1007/s12603-010-0275-7

Wei, Q., Wang, H., Tian, Y., Xu, F., Chen, X., and Wang, K. (2013). Reduced serum levels of triglyceride, very low density lipoprotein cholesterol and apolipoprotein B in Parkinson's disease patients. *PLoS One* 8:e75743. doi: 10.1371/journal.pone.0075743

Wei, P., Yang, F., Zheng, Q., Tang, W., and Li, J. (2019). The Potential Role of the NLRP3 Inflammasome Activation as a Link Between Mitochondria ROS

Generation and Neuroinflammation in Postoperative Cognitive Dysfunction. *Front. Cell. Neurosci.* 13:73. doi: 10.3389/fncel.2019.00073

Wichmann, M. A., Cruickshanks, K. J., Carlsson, C. M., Chappell, R., Fischer, M. E., Klein, B. E., et al. (2014). Long-term systemic inflammation and cognitive impairment in a population-based cohort. *J. Am. Geriatr. Soc.* 62, 1683–1691. doi: 10.1111/jgs.12994

Wilms, H., Zecca, L., Rosenstiel, P., Sievers, J., Deuschl, G., and Lucius, R. (2007). Inflammation in Parkinson's diseases and other neurodegenerative diseases: cause and therapeutic implications. *Curr. Pharm. Des.* 13, 1925–1928. doi: 10.2174/138161207780858429

Xicoy, H., Wieringa, B., and Martens, G. J. M. (2019). The role of lipids in Parkinson's disease. *Cells* 8:E27. doi: 10.3390/cells8010027

Xu, G., Zhou, Z., Zhu, W., Fan, X., and Liu, X. (2009). Plasma C-reactive protein is related to cognitive deterioration and dementia in patients with mild cognitive impairment. *J. Neurol. Sci.* 284, 77–80. doi: 10.1016/j.jns.2009.04.018

Yuan, Y., Tong, Q., Zhang, L., Jiang, S., Zhou, H., Zhang, R., et al. (2016). Plasma antioxidant status and motor features in *de novo* Chinese Parkinson's disease patients. *Int. J. Neurosci.* 126, 641–646. doi: 10.3109/00207454.2015.1054031

Zhang, L., Wang, X., Wang, M., Sterling, N. W., Du, G., Lewis, M. M., et al. (2017). Circulating cholesterol levels may link to the factors influencing Parkinson's risk. *Front. Neurol.* 8:501. doi: 10.3389/fneur.2017.00501

Zhao, Y. F., Qiong, Z., Zhang, J. F., Lou, Z. Y., Zu, H. B., Wang, Z. G., et al. (2018). The synergy of aging and LPS exposure in a mouse model of Parkinson's disease. *Aging Dis.* 9, 785–797. doi: 10.14336/ad.2017.1028

Zhao, J., Xu, S. Z., and Liu, J. (2019). Fibrinopeptide A induces C-reactive protein expression through the ROS-ERK1/2/p38-NF-kB signal pathway in the human umbilical vascular endothelial cells. *J. Cell. Physiol.* 234, 13481–13492. doi: 10.1002/jcp.28027

Zheng, C., Chen, G., Tan, Y., Zeng, W., Peng, Q., Wang, J., et al. (2018). TRH analog, taltirelin protects dopaminergic neurons from neurotoxicity of MPTP and rotenone. *Front. Cell. Neurosci.* 12:485. doi: 10.3389/fncel.2018.00485

Zhu, S., Wei, X., Yang, X., Huang, Z., Chang, Z., Xie, F., et al. (2019). Plasma lipoprotein-associated Phospholipase A2 and superoxide dismutase are independent predicators of cognitive impairment in cerebral small vessel disease patients: diagnosis and assessment. *Aging Dis.* 10, 834–846. doi: 10.14336/ad.2019.0304

Zlokovic, B. V. (2011). Neurovascular pathways to neurodegeneration in Alzheimer's disease and other disorders. *Nat. Rev. Neurosci.* 12, 723–738. doi: 10.1038/nrn3114

Conflict of Interest: The authors declare that the research was conducted in the absence of any commercial or financial relationships that could be construed as a potential conflict of interest.

frontiers in Cellular Neuroscience

ORIGINAL RESEARCH
published: 10 March 2020
doi: 10.3389/fncel.2020.00047

Hepcidin-to-Ferritin Ratio Is Decreased in Astrocytes With Extracellular Alpha-Synuclein and Iron Exposure

Juntao Cui, Xinli Guo, Qijun Li, Ning Song and Junxia Xie**

Institute of Brain Science and Disease, Shandong Provincial Key Laboratory of Pathogenesis and Prevention of Neurological Disorders, Shandong Provincial Collaborative Innovation Center for Neurodegenerative Disorders, Qingdao University, Qingdao, China

Astrocytes are the most abundant glial cells in the central nervous system (CNS). As indispensable elements of the neurovascular unit, they are involved in the inflammatory response and disease-associated processes. Alpha-synuclein (α-syn) is released into the extracellular space by neurons and can be internalized by adjacent astrocytes, which activates glial cells to induce neuroinflammation. We were interested in whether astrocyte-mediated neuroinflammation is modulated by intracellular iron status and extracellular α-syn. Our results showed that recombinant α-syn (1 μg/ml and 5 μg/ml) treatment for 24 h did not affect the expression of the iron transporters divalent metal transporter 1 (DMT1) and ferroportin 1 (FPN1), nor those of iron regulatory protein (IRP) 1 or IRP2. Several proinflammatory cytokines, including tumor necrosis factor-α (TNF-α), interleukin (IL)-1β, and IL-6 exhibited up-regulated mRNA levels in 5 μg/ml α-syn-treated astrocytes. TNF-α release was increased, indicating that inflammatory responses were triggered in these cells. Pretreatment with the iron-overload reagent ferric ammonium citrate (FAC, 100 μmol/L) for 24 h had no effects on mRNA levels and release of proinflammatory cytokines. Inflammatory responses triggered by α-syn were not affected by iron overload. The iron chelator desferrioxamine (DFO, 100 μmol/L) exerted suppressive effects on TNF-α mRNA levels, although no change was observed for TNF-α release. Hepcidin mRNA levels were down-regulated significantly in astrocytes co-treated with FAC and α-syn, although independent treatment with either FAC or α-syn did not alter hepcidin levels. In contrast, hepcidin mRNA levels were up-regulated in DFO and α-syn co-treated cells. As expected, ferritin protein levels were up-regulated or down-regulated with FAC or DFO treatment, respectively. Following the up-regulation of ferritin mediated by α-syn, hepcidin-to-ferritin levels were indicative of modulatory effects in α-syn-treated astrocytes with altered iron status. Therefore, we propose that the hepcidin-to-ferritin ratio is indicative of a detrimental response in primary cultured astrocytes experiencing iron and extracellular α-syn.

Keywords: neuroinflammation, ferritin, hepcidin, alpha-synuclein, primary astrocytes

OPEN ACCESS

Edited by:
Dennis Qing Wang,
Southern Medical University, China

Reviewed by:
Xuping Li,
Houston Methodist Research Institute, United States
Shuzhen Zhu,
Southern Medical University, China
Mingtao Li,
Sun Yat-sen University, China

****Correspondence:***
Ning Song
ningsong@qdu.edu.cn
Junxia Xie
jxiaxie@163.com;
jxiaxie@public.qd.sd.cn

Received: *29 December 2019*
Accepted: *20 February 2020*
Published: *10 March 2020*

Citation:
Cui J, Guo X, Li Q, Song N and Xie J (2020) Hepcidin-to-Ferritin Ratio Is Decreased in Astrocytes With Extracellular Alpha-Synuclein and Iron Exposure. Front. Cell. Neurosci. 14:47. doi: 10.3389/fncel.2020.00047

INTRODUCTION

Parkinson's disease (PD) is characterized by a progressive loss of midbrain dopaminergic neurons in the substantia nigra (SN), resulting in motor symptoms including rigidity, postural instability, tremor at rest, and bradykinesia. A defining pathological feature of PD is the presence of intracellular protein aggregates termed Lewy bodies (LBs) in degenerated dopaminergic neurons, whose major components are aggregated alpha-synuclein (α-syn; Goedert, 2001; Dickson, 2012; Kalia and Lang, 2015; Przedborski, 2017). In addition to the presence of LBs in the most affected SN, α-syn aggregates have also been found in other brain regions, including the locus coeruleus, nucleus basalis of Meynert, hypothalamus, cerebral cortex, and cranial nerve motor nuclei, as well as in the central and peripheral divisions of the autonomic nervous system (Spillantini et al., 1997; Braak et al., 2010). Based on these findings, the prion hypothesis suggests that in the brain, α-syn released from degenerating neurons into extracellular spaces is taken up by neighboring neurons and non-neuronal cells (Volpicelli-Daley et al., 2011; Luk et al., 2012; Paumier et al., 2015; Brundin and Melki, 2017).

Astrocytes are the most abundant glial cells in the central nervous system (CNS). With widespread distribution throughout the whole CNS, astrocytes are responsible for extracellular homeostasis of water, ions, and neurotransmitters. Astrocytes act as indispensable elements of the neurovascular unit, which was an important participant in PD pathogenesis and treatment (Zou et al., 2017; Zhu et al., 2019). In a healthy brain as well as disease-associated processes, astrocytes were closely involved in inflammatory responses (Banks et al., 2015; Wang et al., 2018; Li et al., 2019). Neuroinflammation mediated by activated astrocytes/microglia were believed to be targeted to curb pathogenesis of neurodegeneration, or even promote the differentiation and proliferation of neural stem cells (Cho, 2019; Eremenko et al., 2019; Liu et al., 2019; Sn et al., 2019; Tu et al., 2019). Hepcidin, an antimicrobial peptide primarily secreted by the liver, is induced by inflammatory stimuli (Nicolas et al., 2002; Schmidt, 2015). In the brain, hepcidin is widely distributed in different brain areas and can be primarily induced in astrocytes by lipopolysaccharide (LPS) administration or by intracerebral hemorrhage (Xiong et al., 2016; You et al., 2017). Astrocytes have been reported to be able to internalize extracellular α-syn and activated to induce neuroinflammation (Lee et al., 2010, 2014). *In vitro* evidence showed that the co-culture of primary astrocytes with SH-SY5Y human neuroblastoma cells secreting α-syn resulted in the formation of astrocytic inclusion bodies. The induction of proinflammatory cytokines was correlated with the extent of intracellular accumulation of α-syn (Lee et al., 2010). More recently, amyloid-β (Aβ), another disease-associated misfolded protein was shown to induce inflammatory responses in astrocytes both *in vivo* and *in vitro* (Urrutia et al., 2013).

Iron is an essential trace element involved in various physiological processes, including oxygen transport (*via* hemoglobin), redox reactions, neurotransmitter synthesis, myelin production, and a number of mitochondrial functions. However, due to its propensity to release electrons and produce reactive oxygen species (ROS), excessive iron accumulation enables the occurrence of oxidative stress and ferroptosis, therefore contributing to the vulnerability of dopaminergic neurons in PD (Moreau et al., 2018; Trist et al., 2019). Astrocytes show robust expression of iron metabolism-related proteins. They set up the relative independence of iron balance in the brain by constituting the blood-brain barrier (BBB), and in addition, modulate synaptic activities by buffering iron concentration in the synaptic environment (Codazzi et al., 2015; Song et al., 2018). Under pathological conditions, astrocytes have the capacity to efficiently transport/recycle iron, thus potentially buffering excess iron and playing a crucial role in proper iron handling within the CNS (Pelizzoni et al., 2013; Zhang et al., 2013; Zarruk et al., 2015). As a regulator of brain iron homeostasis, hepcidin plays a key role in controlling the transport of iron across the BBB (Du et al., 2011; Urrutia et al., 2013). When treated with hepcidin peptide or infected with hepcidin expression adenovirus, astrocytes showed a significant capacity to reduce iron uptake and release (Du et al., 2011). There were controversial data that astrocytic hepcidin participated in LPS-induced neuronal apoptosis (You et al., 2017), or attenuate Aβ-induced inflammatory and pro-oxidant responses (Urrutia et al., 2017). However, the mechanisms by which astrocytic hepcidin responds to both altered iron metabolism and neuroinflammation has not been elucidated.

In the present study, we were interested in whether astrocyte-mediated neuroinflammation is modulated by intracellular iron status and extracellular α-syn. We demonstrated that extracellular α-syn did not affect iron metabolism-related proteins. Iron manipulations have limited effects on inflammatory response in primary cultured astrocytes triggered by α-syn. However, decreased hepcidin levels and a decreased ratio of hepcidin-to-ferritin were noted in astrocytes with co-administration of α-syn and iron. We further propose that the hepcidin-to-ferritin ratio could be indicative of detrimental interaction between iron and α-syn in primary cultured astrocytes.

MATERIALS AND METHODS

Pharmacological Agents and Antibodies

α-syn was purchased from rPeptide (Bogart, GA, USA). The antibodies for ferric ammonium citrate (FAC), deferoxamine mesylate salt (DFO), and ferroportin1 (FPN1) were from Sigma–Aldrich (St. Louis, MO, USA). Fetal bovine serum (FBS) was from Gibco (Grand Island, NY, USA), and DMEM/F12 was from Hyclone (Logan, Utah, USA). Divalent metal transporter 1 (DMT1) antibody was from OriGene (Rockville, MD, USA), antibodies against ferritin, iron regulatory protein (IRP) 1 and IRP2 antibody were from Abcam (Cambridge, UK). The beta-actin antibody was from Bioss (Beijing, China). The Rat tumor necrosis factor-α (TNF-α), interleukin (IL)-1β, IL-6 Duoset ELISA Kit was from R&D Systems (Minnesota, MN, USA). All other chemicals and reagents were of the highest grade available from local commercial sources.

Cell Culture and Treatment

Animals were handled in accordance with the National Institutes of Health Guide for the Care and Use of Laboratory Animals and were approved by the Ethical Committee of the Medical College of Qingdao University. Neonatal Wistar rats were sacrificed by cervical dislocation within postnatal days 1–2, and their mesencephalons were harvested. Several superficial washings were performed with phosphate-buffered saline (PBS) containing 100 U/ml penicillin and 100 μg/ml streptomycin, in order to limit contamination. Superficial blood vessels were carefully extracted using dissection pliers, and the tissues were mechanically dissociated to yield single cells. After filtration through a 100 μm pore mesh, the cell suspension was centrifuged at 1,000 *g* for 5 min and resuspended in DMEM/F12 cell culture medium containing 10% FBS, 100 U/ml penicillin, and 100 μg/ml streptomycin. The cells were plated in tissue culturing flasks pre-coated with poly-D-lysine at a density of five mouse brains per 75 cm^2, then cultured at 37°C in a 5% CO_2 incubator. After incubation for 24 h, the medium was changed and non-adherent cells were removed. Next, the adherent cells were incubated in culture medium for 10 d, with a medium change every 3–4 days. When cells had grown to confluence (after 10–14 days), the culture flasks were shaken on a rotary shaker at 200 rpm for 18–20 h at 37°C to remove any loosely attached microglia and oligodendrocyte precursor cells. The attached, enriched astrocytes were subsequently detached using trypsin-EDTA and then subjected to the different treatments. Recombinant α-syn was dissolved in sterile deionized water as a storage solution (1 mg/ml) and diluted to the appropriate concentration. FAC or DFO was dissolved in cell culture medium and diluted to 100 μmol/L. Astrocytes were treated by incubation with either α-syn (1 μg/ml or 5 μg/ml; Lee et al., 2010; Yu et al., 2016), FAC or DFO for 24 h. Alternatively, FAC or DFO pretreatment was applied for 24 h, followed by treatment with culture medium or α-syn (5 μg/ml) for a further 24 h. Astrocytes as control were treated with culture medium.

Western Blotting

The cell lysate was prepared in ice-cold radio immunoprecipitation assay (RIPA) lysis buffer with a protease inhibitor (CWBIO, Beijing, China). Protein samples (20 μg) were loaded and separated by 8% or 10% sodium dodecyl sulfate-polyacrylamide gel electrophoresis (SDS-PAGE) at 80 V for 30 min, followed by 120 V for 90 min. The proteins were subsequently transferred onto a polyvinylidene fluoride (PVDF) membrane and the transfer was performed at 300 mA for 120 min on cold ice. Membranes were blocked for 1 h with 5% skimmed milk in Tris-buffered saline-tween-20 (TBST), and incubated overnight with the following primary antibodies at 4°C: DMT1 (1:800); FPN1 (1:800); IRP1 (1:2,000); IRP2 (1:1,000); ferritin (1:1,000); and Beta-Actin (1:5,000). Membranes were washed with TBST and incubated with goat anti-rabbit IgG-horseradish peroxidase secondary antibodies (1:5,000; Absin, Shanghai, China) for 1 h at room temperature. The blots were stained with the Clarity Western enhanced chemiluminescence (ECL) substrate (Millipore Corp, Billerica, MA, USA), and target bands were visualized using a UVP BioDoc-It Imaging System (Upland CA, USA). The target bands were quantified using the ImageJ software (NIH Image, Bethesda, MD, USA), and the density of each band was normalized against Beta-Actin.

Real-Time Quantitative PCR

Total RNA was extracted from primary astrocytes with Trizol reagent (Invitrogen, Pittsburgh, PA, USA). According to the manufacturer's instructions, the first-strand cDNA was synthesized using a RevertAid First Strand cDNA Synthesis Kit (Thermo Scientific Fermentas, Pittsburgh, PA, USA). Quantitative PCR was performed using specific primers for TNF-α (F5′-TCAGTTCCATGGCCCAGAC-3′, R5′-GTTGTC TTTGAGATCCATGCCATT-3′), IL-1β (F5′-CCCTGAACTCA ACTGTGAAATAGCA-3′, R5′-CCCAAGTCAAGGGCTTGGA A-3′), hepcidin (F5′-GCCTGAGCAGCACCACCTAT-3′, R5′-AGCATTTACAGCAGAAGATGCAGA-3′), and GAPDH (F5′-AAATGGTGAAGGTCGGTGTGAAC-3′, R5′-CAACAATCTC CACTTTGCCACTG-3′). Gene expression was expressed as the mRNA level, normalized to that of the standard housekeeping gene GAPDH. Relative levels of target mRNA expression were calculated using the $2^{-\Delta\Delta ct}$ method. At least three independent experiments were performed for each measurement.

Enzyme-Linked Immunosorbent Assay (ELISA)

The medium was collected and centrifuged for 20 min at 1,000 *g* to remove the pellet. The levels of TNF-α, IL-1β, IL-6 protein in culture medium were determined using the Rat TNF-α, IL-1β, IL-6 Duoset ELISA Kit, according to the manufacturer's instructions. The optical densities of the standards and samples were measured by subtracting the readings at 540 nm from the readings at 450 nm using a multifunctional microplate reader (SpectraMax M5, Molecular Devices, San Jose, CA, USA).

Statistical Analysis

All data were analyzed using GraphPad Prism version 6.0 software (GraphPad Software Inc., San Diego, CA, USA) All data were expressed as the mean ± SEM. Statistical analyses were performed by comparing the means of different groups using one-way ANOVAs with Tukey's multiple comparisons test, with $P < 0.05$ considered significant.

RESULTS

Extracellular α-Syn Did Not Affect the Expression Levels of Iron Metabolism-Related Proteins in Primary Cultured Astrocytes

We first investigated whether the expression levels of iron metabolism-related proteins in primary cultured astrocytes were affected by 1 μg/ml or 5 μg/ml α-syn treatment for 24 h. The protein levels of the iron importer DMT1, the iron exporter FPN1, and IRP1 and IRP2 were evaluated, as well as the mRNA levels of hepcidin. The results showed that there were no changes in any of these protein or hepcidin mRNA levels (**Figures 1**, **4**), suggesting that neither 1 μg/ml nor 5 μg/ml α-syn had any

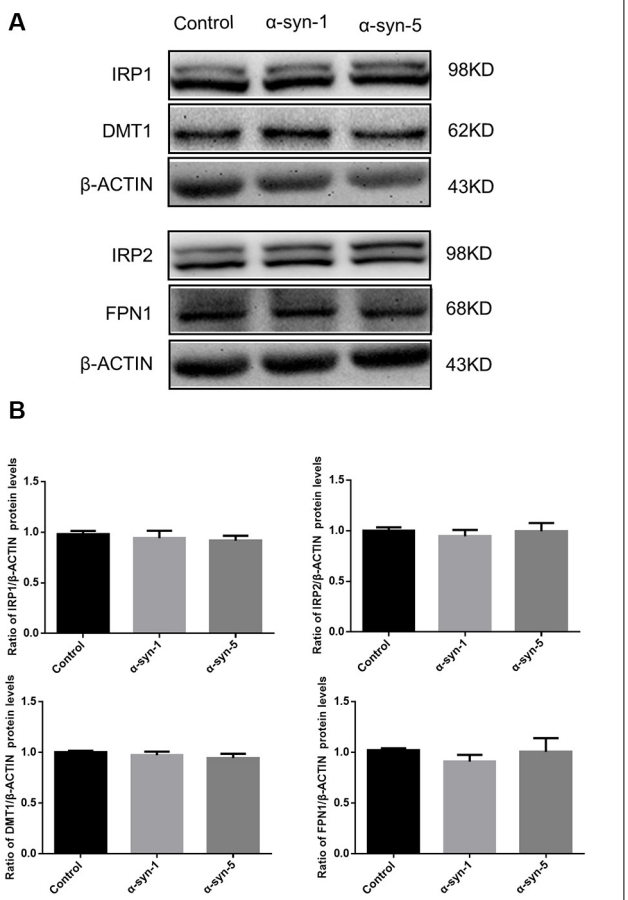

FIGURE 1 | Changes in iron metabolism-related proteins in α-syn-treated primary cultured astrocytes. Proteins levels of DMT1, FPN1, IRP1 and IRP2 were unchanged **(A)**. Quantitative analysis of the proteins was shown in **(B)**. Data are presented as the ratio of DMT1, FPN1, IRP1 and IRP2 protein levels to β-actin. Each bar represents the mean ± SEM of three independent experiments.

effects on the iron transporting or iron regulatory components of astrocytes.

The Extracellular α-Syn Induced Inflammatory Response Was Largely Unaffected by Iron Status in Primary Cultured Astrocytes

Extracellular α-syn can be taken up by primary cultured astrocytes to trigger an inflammatory response (Lee et al., 2010). Therefore, we next investigated the effects of extracellular α-syn on TNF-α and IL-1β mRNA levels and on the release of the corresponding proteins by astrocytes. The results showed that treatment with 5 μg/ml, but not 1 μg/ml α-syn, induced a significant increase in TNF-α mRNA and IL-1β mRNA expression, indicating that inflammatory responses were triggered in these cells. Pretreatment with the iron-overload reagent FAC for 24 h had no effects on the mRNA levels of these proinflammatory cytokines, and also no effects on α-syn-triggered responses (**Figures 2A,B**). Release of TNF-α changed in parallel with the change in its mRNA expression; that is, TNF-α release was up-regulated in 5 μg/ml α-syn-treated astrocytes, with or without FAC pretreatment (**Figure 2E**).

Similar to FAC, the iron chelator DFO itself had no effects on the mRNA levels of these proinflammatory cytokines. DFO pretreatment exerted a suppressive effect on TNF-α mRNA levels, but not on IL-1β mRNA levels, induced by 5 μg/ml α-syn treatment (**Figures 2C,D**). However, no effects were observed on α-syn-induced TNF-α release (**Figure 2G**). Unfortunately, the release of IL-1β showed no change under any of these experimental manipulations (**Figures 2F,H**). More strikingly, we observed a stimulative effect of DFO on α-syn-induced IL-6 release, which was not observed in FAC-pretreated cells (**Figures 2I,J**). Overall, these results demonstrate that the extracellular α-syn-induced inflammatory response was not affected much by iron status in primary cultured astrocytes.

Ferritin Protein Levels Were Tightly Regulated by Both Iron Status and by Extracellular α-Syn in Primary Cultured Astrocytes

We detected the expression of ferritin protein levels in astrocytes during extracellular α-syn treatment. We observed higher ferritin protein levels in α-syn-treated cells (1 μg/ml or 5 μg/ml; **Figures 3A,B**). As expected, robust regulation of ferritin expression was observed in FAC or DFO-treated cells; that is, ferritin protein levels were up-regulated or down-regulated by FAC or DFO treatment, respectively. Ferritin up-regulation induced by 5 μg/ml α-syn was enhanced by FAC pretreatment, whereas it was suppressed by DFO pretreatment.

Hepcidin mRNA and Hepcidin-to-Ferritin Ratio Were Modulated by Iron Status in Primary Cultured Astrocytes Under Treatment of Extracellular α-Syn

Hepcidin is the key link between iron homeostasis and the regulation of acute inflammatory responses in the CNS (Raha et al., 2013; Vela, 2018). To explore the possible mechanisms involved in the modulatory effects of intracellular iron status and extracellular α-syn, we investigated the mRNA levels of hepcidin in primary astrocytes. As mentioned above, hepcidin mRNA levels were unchanged by either FAC or DFO treatment. Neither the 1 μg/ml nor the 5 μg/ml α-syn treatment had any effect on hepcidin, although there were increased mRNA or protein levels of proinflammatory cytokines, such as TNF-α, IL-1β, and IL-6. Unexpectedly, hepcidin mRNA levels were down-regulated significantly in astrocytes co-treated with FAC and α-syn (**Figure 4A**). In contrast, hepcidin mRNA levels were up-regulated in DFO and α-syn co-treated cells (**Figure 4B**), in parallel with an increase of IL-6 release in these cells (**Figure 2J**).

We then calculated the ratio of hepcidin mRNA levels to ferritin protein levels in astrocytes with altered iron status treated with extracellular α-syn. As shown in **Figure 5A**, the ratio of these two molecules in astrocytes with FAC and α-syn

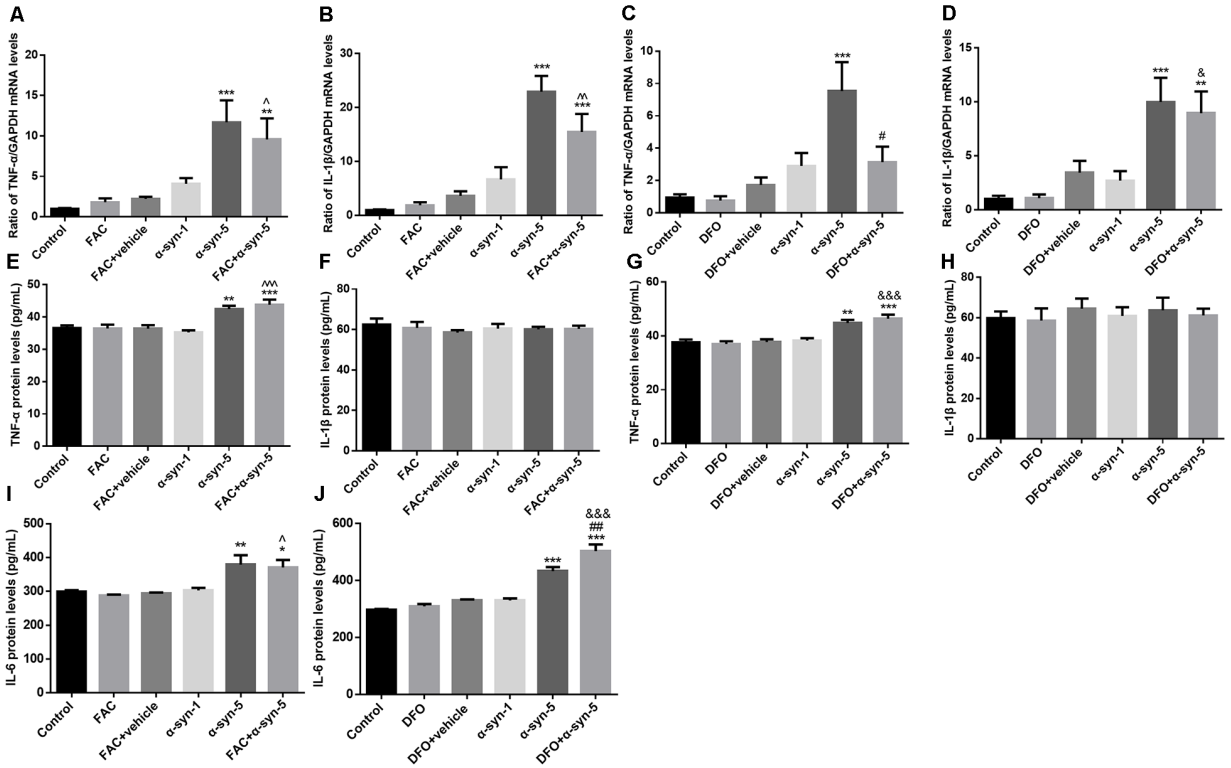

FIGURE 2 | Effects of intracellular iron status and extracellularly administered α-syn on the mRNA levels of tumor necrosis factor-α (TNF-α) and IL1β and the release of TNF-α, IL1β, and IL-6 in primary cultured astrocytes. Treatment with 5 μg/ml α-syn induced a significant increase in TNF-α **(A,C)** and IL-1β **(B,D)** mRNA expression, as well as TNF-α **(E,G)** and IL-6 **(I,J)** release. DFO pretreatment suppressed the increase in TNF-α mRNA levels induced by 5 μg/ml α-syn **(C)** but enhanced IL-6 release **(J)**. IL-1β release is not affected by ferric ammonium citrate (FAC), DFO or α-syn **(F,H)**. Data are presented as the TNF-α and IL-1β mRNA levels relative to the level of GAPDH mRNA. Each bar represents the mean ± SEM of three independent experiments (*$P < 0.05$, **$P < 0.01$, and ***$P < 0.001$ compared with the control group; $^{\#}P < 0.05$ and $^{\#\#}P < 0.01$ compared with the α-syn-5 group; ^$P < 0.05$, ^^$P < 0.01$, and ^^^$P < 0.001$ compared with the FAC + vehicle group; $^{\&}P < 0.05$ and $^{\&\&\&}P < 0.001$ compared with the DFO+vehicle group).

co-treatments differed from those with α-syn treatment alone, although there was no difference in the levels of proinflammatory cytokines (**Figure 2**). Similarly, this ratio was significantly higher in astrocytes during DFO and α-syn co-treatment (**Figure 5B**) and was therefore much more sensitive than the undetectable changes in proinflammatory cytokine levels.

DISCUSSION

Aggregation of α-syn is a central hallmark of neurodegeneration in PD and occurs extensively in the central and peripheral nervous systems (Cooper et al., 2018; Manfredsson et al., 2018). In recent years, cell-to-cell transfer of α-syn was believed to contribute to the progression of PD; that is, that α-syn may be released from neurons and then act on neighboring cells. Despite the fact that glial cells express low levels of α-syn, they are able to take up α-syn and thus contribute to the spread of α-syn pathology (Lee et al., 2010; Rey et al., 2016; Xia et al., 2019). As one of the functions of glial cells, neuroinflammation is a typical pathological trait characterizing various neurodegenerative diseases, including PD. Primary cultured astrocytes have higher uptake rate constants of extracellular α-syn compared to primary cultured neurons and microglia (Lee et al., 2008). Upon neuron-to-astrocyte transfer of α-syn, astrocytes display proinflammatory responses, producing multiple proinflammatory cytokines and chemokines (Fellner et al., 2013). *In vivo*, accumulation of α-syn in astrocytes, therefore an increased number of α-syn-positive astrocytes, is accompanied by an increase in proinflammatory cytokine levels in the Major Basic Protein (MBP)1-hα-syn transgenic mouse model of multiple system atrophy; these effects were reduced by antidepressant treatment (Valera et al., 2014). In the present study, we observed that 5 μg/ml α-syn induced a significant increase in TNF-α and IL-1β mRNA expression, as well as an increase of TNF-α and IL-6 release in primary astrocytes. Therefore, our results confirm that extracellular α-syn can cause an inflammatory response in primary cultured astrocytes.

Astrocytes are considered to be key regulators of the iron metabolism of the brain. The neurotoxin 6-hydroxydopamine (6-OHDA) induces iron deposits in primary cultured neurons but promotes iron transport rate in primary cultured astrocytes, suggesting distinct regulation of iron metabolism in neurons vs. astrocytes (Song et al., 2010; Zhang et al., 2013). Astrocytes have a high capacity for rapidly accumulating iron ions and

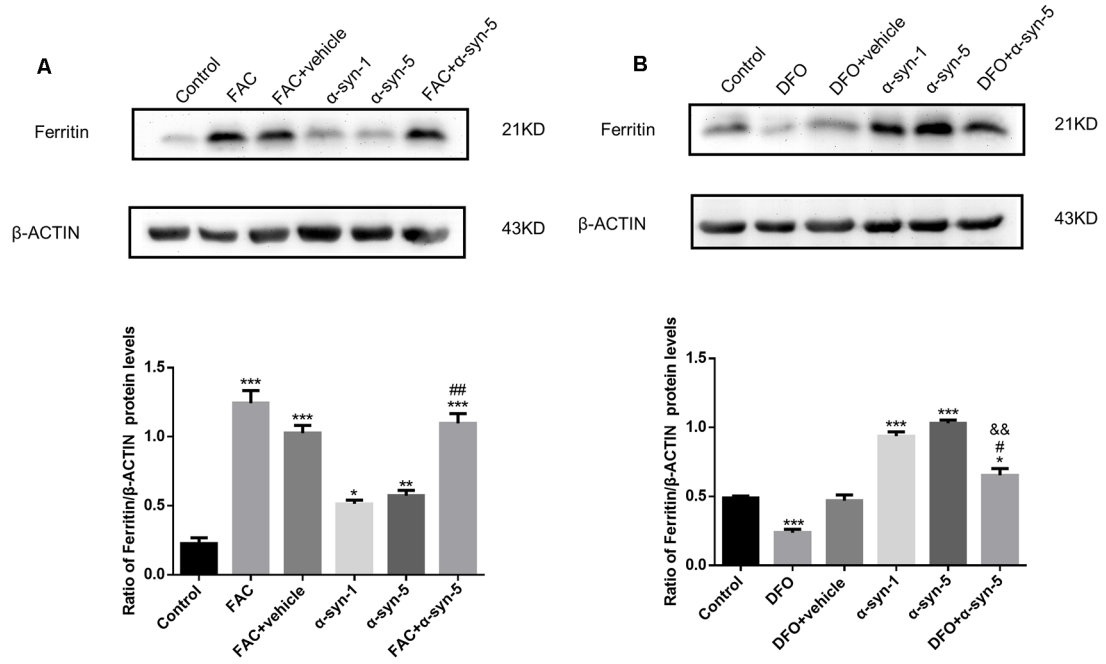

FIGURE 3 | Effects of intracellular iron status and extracellularly administered α-syn on the protein levels of ferritin in primary cultured astrocytes. Both FAC and α-syn (1 μg/ml and 5 μg/ml) induced an up-regulation of ferritin protein levels. Ferritin protein levels were further increased in astrocytes co-treated with FAC and α-syn **(A)** and decreased in DFO/α-syn treated cells **(B)**, as compared to those in cells treated with α-syn treatment alone. Data are presented as the ratio of ferritin levels to β-actin. Each bar represents the mean ± SEM of three independent experiments (*$P < 0.05$, **$P < 0.01$ and ***$P < 0.001$ compared with the control group; $^{\#}P < 0.05$ and $^{\#\#}P < 0.01$ compared with the α-syn-5 group; $^{\&\&}P < 0.01$ compared with the DFO + vehicle group).

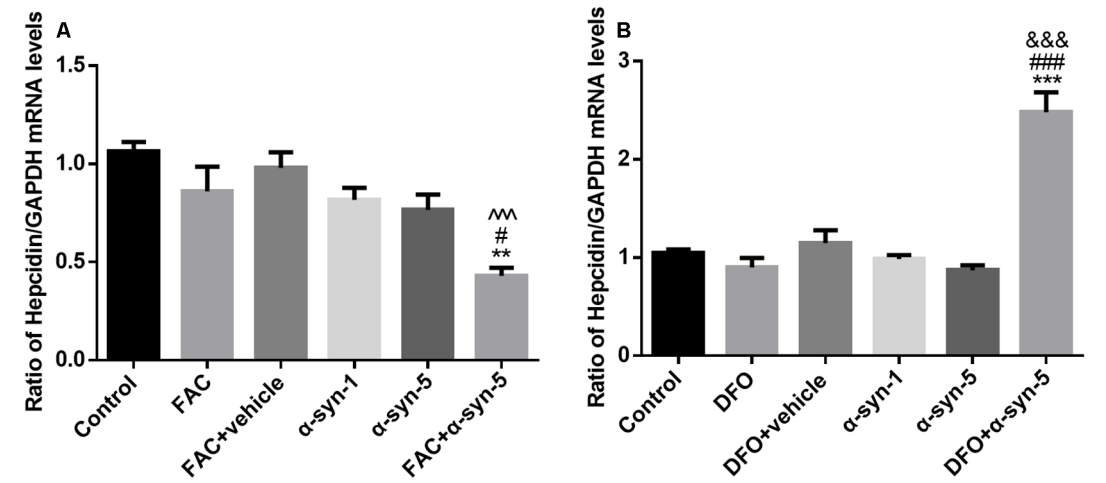

FIGURE 4 | Effects of intracellular iron status and extracellularly administered α-syn on the mRNA levels of hepcidin in primary cultured astrocytes. Hepcidin mRNA levels were down-regulated significantly in astrocytes co-treated with FAC and α-syn **(A)** and up-regulated in DFO/α-syn treated cells **(B)**. Data are presented as the relative level of hepcidin mRNA to GAPDH mRNA. Each bar represents the mean ± SEM of three independent experiments (**$P < 0.01$ and ***$P < 0.001$ compared with the control group; $^{\#}P < 0.05$ and $^{\#\#\#}P < 0.001$ compared with the α-syn-5 group; $^{\wedge\wedge\wedge}P < 0.001$ compared with the FAC + vehicle group; $^{\&\&\&}P < 0.001$ compared with the DFO + vehicle group).

various iron-containing compounds; they are able to store the iron in ferritin, although they do not normally contain large amounts of iron or ferritin (Bartzokis et al., 2007; Dringen et al., 2007). Ferritin sequesters iron in a non-toxic form, while the levels of free iron regulate cellular ferritin levels. Therefore, cytoplasmic ferritin synthesis is stimulated by an increase of

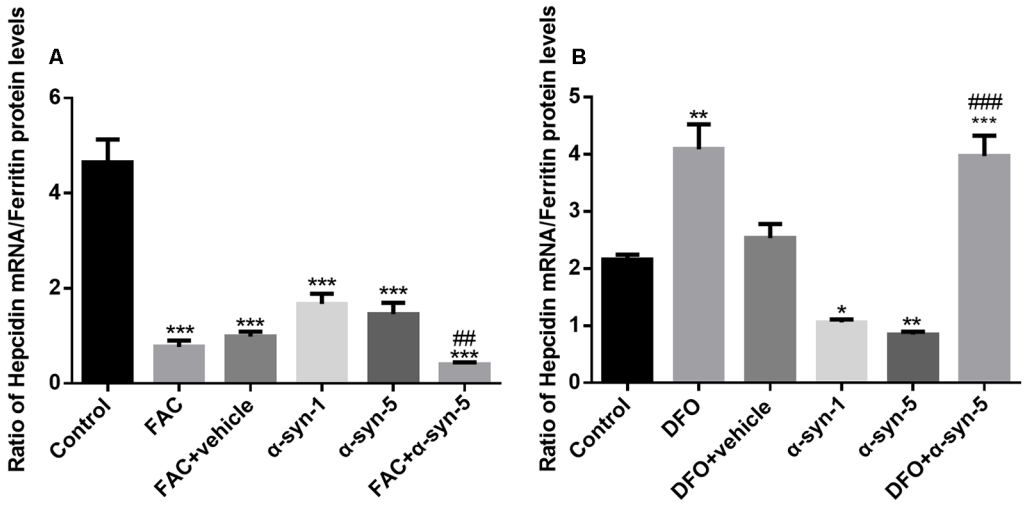

FIGURE 5 | Effects of intracellular iron status and extracellularly administered α-syn on the ratio of hepcidin mRNA to ferritin protein levels in primary cultured astrocytes. The ratio of hepcidin mRNA to ferritin protein levels in astrocytes co-treated with FAC and α-syn was much lower than that in cells treated with α-syn alone **(A)**. However, the ratio was significantly higher in astrocytes co-treated with DFO and α-syn (**B**; $^{*}P < 0.05$, $^{**}P < 0.01$ and $^{***}P < 0.001$ compared with the control group; $^{\#\#}P < 0.01$, $^{\#\#\#}P < 0.001$ compared with the α-syn-5 group).

iron, whereas it is decreased by iron depletion (Torti and Torti, 2002). When astrocytes are exposed to large concentrations of iron *in vitro*, their iron uptake rate temporarily exceeds the storage capacity of their ferritin and the cells experience transient oxidative stress (Hoepken et al., 2004). In the present study, cell iron status almost had no effect on the mRNA levels and release of pro-inflammatory factors in α-syn-treated primary astrocytes, although there seemed to be a suppression of TNF-α mRNA expression by DFO. We observed that the protein levels of the iron importer DMT1 and the iron exporter FPN1 were unchanged, indicating that extracellular α-syn does not affect iron transport in astrocytes. Ferritin protein levels were up-regulated or down-regulated with FAC or DFO treatment, respectively. We suppose that ferritin might efficiently buffer the intracellular free iron in astrocytes; thus, a negligible modulation of the α-syn-induced pro-inflammatory response was observed when iron levels were altered. Notably, ferritin levels were up-regulated in both the 1 μg/ml and 5 μg/ml in α-syn treated astrocytes, although IRP1 and IRP2 protein levels were unchanged. Ferritin responds to both inflammation and iron metabolism. Elevated ferritin in α-syn treated astrocytes may be due to the enhanced cytokine levels accompanying inflammation, considering that marked ferritin synthesis occurs at the post-transcriptional level during inflammation (Rogers et al., 1994; Thomsen et al., 2015).

Hepcidin is a key regulator of systemic iron homeostasis and modulates immune function in part by its ability to decrease iron absorption and serum iron content in response to infection and inflammation (Urrutia et al., 2017). Hepcidin acts on FPN1, the only iron efflux channel, inducing its internalization and degradation, eventually leading to iron retention in cells (Nemeth et al., 2004b). In macrophages, elevated hepcidin levels favor iron retention in these cells to encounter increased iron intake, infection, and inflammation. Whereas reduced hepcidin levels are associated with iron deficiency, hypoxia, anemia and homozygous hemochromatosis (Nemeth et al., 2004a; Sullivan, 2007). In the brain, hepcidin is produced in response to inflammatory stimuli in astrocytes. By modulating the levels of iron transporters, such as FPN1 and transferrin receptor 1, hepcidin is believed to contribute to brain iron homeostasis (Du et al., 2011; Urrutia et al., 2013). Both hepcidin and FPN1 are significantly reduced in hippocampal lysates from Alzheimer's disease brains, although the reasons are unclear, this probably results from an imbalance in iron metabolism (Raha et al., 2013; Urrutia et al., 2013). At the cellular level, hepcidin promoter activity is significantly increased by the occupancy of c-Jun N-terminal kinase (JNK) or activator protein-1 (AP-1), which are enhanced through the direct activation of toll-like receptors (TLRs) induced by LPS (Lee et al., 2017). During infection, proinflammatory cytokines such as IL-6 promote transcriptional induction of hepcidin *via* signal transducer and activator of transcription (STAT) signaling (Hood and Skaar, 2012; Fillebeen et al., 2018). In the present study, hepcidin mRNA levels were unchanged under conditions of either altered iron levels (FAC/DFO treatment) or α-syn treatment. However, hepcidin mRNA levels were down-regulated significantly in astrocytes co-treated with FAC and α-syn; while they were up-regulated in DFO and α-syn co-treated cells, in parallel with an increase of IL-6 release in these cells. As ferritin is up-regulated dramatically and consistently in FAC treated astrocytes with/without α-syn, that means ferritin is not such a good indicator of α-syn exposure in iron-overloaded astrocytes, although ferritin could be moderately up-regulated by α-syn itself. More strikingly, we observed the calculated hepcidin-to-ferritin ratio was decreased in astrocytes with co-administration of α-syn and iron. The co-existence of iron

and α-syn shifts the high/normal-hepcidin to low-hepcidin levels; the low hepcidin-to-ferritin ratio is efficient to reflect the situation in overloaded astrocytes experiencing extracellular α-syn, facilitating the iron-releasing phenotype in these cells. This might be detrimental for neighboring neurons who were vulnerable to both elevated iron and spreading α-syn. In contrast, in astrocytes with low iron levels and extracellular α-syn exposure, increased hepcidin levels and high hepcidin-to-ferritin ratio might be beneficial because of the possible iron retention in astrocytes and actually prevent iron elevation in the local environment *via* the large buffering capacity of the astrocytes. Given the importance of hepcidin and ferritin on iron homeostasis, the hepcidin-to-ferritin ratio, reflecting the amount of hepcidin relative to ferritin, underscores their roles in determining transcellular iron distribution. The relationship between this ratio and iron-inflammation interactions has not been reported previously, our study suggested a low hepcidin-to-ferritin ratio indicates a more unbeneficial situation occurring under conditions of both iron overload and proinflammatory insult.

In summary, in this study, we showed that the extracellular α-syn-induced inflammatory response was largely unaffected by iron status. Ferritin protein levels were tightly regulated by both iron status and inflammation. We observed decreased hepcidin and hepcidin-to-ferritin ratio in astrocytes with co-administration of iron and α-syn, and we propose the hepcidin-to-ferritin ratio is indicative of a detrimental response in primary cultured astrocytes experiencing extracellular α-syn and iron overload.

DATA AVAILABILITY STATEMENT

The datasets generated for this study are available on request to the corresponding author.

ETHICS STATEMENT

The animal study was reviewed and approved by Ethical Committee of the Medical College of Qingdao University.

AUTHOR CONTRIBUTIONS

JX and NS designed the research. JC, XG and QL performed the research. JC and QL analyzed the data. NS and JC wrote the article, and all authors had access to the study data, and have reviewed and approved the final manuscript.

FUNDING

This work was supported by grants from the National Foundation of Natural Science of China (31771124 and 31871049), the Excellent Innovative Team of Shandong Province, and the Taishan Scholars Construction Project.

REFERENCES

Banks, W. A., Gray, A. M., Erickson, M. A., Salameh, T. S., Damodarasamy, M., Sheibani, N., et al. (2015). Lipopolysaccharide-induced blood-brain barrier disruption: roles of cyclooxygenase, oxidative stress, neuroinflammation, and elements of the neurovascular unit. *J. Neuroinflammation* 12:223. doi: 10.1186/s12974-015-0434-1

Bartzokis, G., Tishler, T. A., Lu, P. H., Villablanca, P., Altshuler, L. L., Carter, M., et al. (2007). Brain ferritin iron may influence age- and gender-related risks of neurodegeneration. *Neurobiol. Aging* 28, 414–423. doi: 10.1016/j.neurobiolaging.2006.02.005

Braak, H., Bohl, J. R., Müller, C. M., Rüb, U., de Vos, R. A., and Kelly, D. T. (2010). Stanley Fahn Lecture 2005: the staging procedure for the inclusion body pathology associated with sporadic Parkinson's disease reconsidered. *Mov. Disord.* 21, 2042–2051. doi: 10.1002/mds.21065

Brundin, P., and Melki, R. (2017). Prying into the prion hypothesis for Parkinson's disease. *J. Neurosci.* 37, 9808–9818. doi: 10.1523/JNEUROSCI.1788-16.2017

Cho, K. (2019). Emerging roles of complement protein C1q in neurodegeneration. *Aging Dis.* 10, 652–663. doi: 10.14336/AD.2019.0118

Codazzi, F., Pelizzoni, I., Zacchetti, D., and Grohovaz, F. (2015). Iron entry in neurons and astrocytes: a link with synaptic activity. *Front. Mol. Neurosci.* 8:18. doi: 10.3389/fnmol.2015.00018

Cooper, J. F., Spielbauer, K. K., Senchuk, M. M., Nadarajan, S., Colaiácovo, M. P., and Van Raamsdonk, J. M. (2018). α-synuclein expression from a single copy transgene increases sensitivity to stress and accelerates neuronal loss in genetic models of Parkinson's disease. *Exp. Neurol.* 310, 58–69. doi: 10.1016/j.expneurol.2018.09.001

Dickson, D. W. (2012). Parkinson's disease and parkinsonism: neuropathology. *Cold Spring Harb. Perspect. Med.* 2:a009258. doi: 10.1101/cshperspect.a009258

Dringen, R., Bishop, G. M., Koeppe, M., Dang, T. N., and Robinson, S. R. (2007). The pivotal role of astrocytes in the metabolism of iron in the brain. *Neurochem. Res.* 32, 1884–1890. doi: 10.1007/s11064-007-9375-0

Du, F., Qian, C., Qian, Z. M., Wu, X.-M., Xie, H., Yung, W.-H., et al. (2011). Hepcidin directly inhibits transferrin receptor 1 expression in astrocytes *via* a cyclic AMP-protein kinase A pathway. *Glia* 59, 936–945. doi: 10.1002/glia.21166

Eremenko, E., Mittal, K., Berner, O., Kamenetsky, N., Nemirovsky, A., Elyahu, Y., et al. (2019). BDNF-producing, amyloid β-specific CD4 T cells as targeted drug-delivery vehicles in Alzheimer's disease. *EBioMedicine* 43, 424–434. doi: 10.1016/j.ebiom.2019.04.019

Fellner, L., Irschick, R., Schanda, K., Reindl, M., Klimaschewski, L., Poewe, W., et al. (2013). Toll-like receptor 4 is required for α-synuclein dependent activation of microglia and astroglia. *Glia* 61, 349–360. doi: 10.1002/glia.22437

Fillebeen, C., Wilkinson, N., Charlebois, E., Katsarou, A., Wagner, J., and Pantopoulos, K. (2018). Hepcidin-mediated hypoferremic response to acute inflammation requires a threshold of Bmp6/Hjv/Smad signaling. *Blood* 132, 1829–1841. doi: 10.1182/blood-2018-03-841197

Goedert, M. (2001). α-synuclein and neurodegenerative diseases. *Nat. Rev. Neurosci.* 2, 492–501. doi: 10.1038/35081564

Hoepken, H. H., Korten, T., Robinson, S. R., and Dringen, R. (2004). Iron accumulation, iron-mediated toxicity and altered levels of ferritin and transferrin receptor in cultured astrocytes during incubation with ferric ammonium citrate. *J. Neurochem.* 88, 1194–1202. doi: 10.1046/j.1471-4159.2003.02236.x

Hood, M. I., and Skaar, E. P. (2012). Nutritional immunity: transition metals at the pathogen-host interface. *Nat. Rev. Microbiol.* 10, 525–537. doi: 10.1038/nrmicro2836

Kalia, L. V., and Lang, A. E. (2015). Parkinson's disease. *Lancet* 386, 896–912. doi: 10.1016/S0140-6736(14)61393-3

Lee, H. J., Bae, E. J., and Lee, S. J. (2014). Extracellular α—synuclein-a novel and crucial factor in Lewy body diseases. *Nat. Rev. Neurol.* 10, 92–98. doi: 10.1038/nrneurol.2013.275

Lee, Y.-S., Kim, Y.-H., Jung, Y. S., Kim, K.-S., Kim, D.-K., Na, S.-Y., et al. (2017). Hepatocyte toll-like receptor 4 mediates lipopolysaccharide-induced hepcidin expression. *Exp. Mol. Med.* 49:e408. doi: 10.1038/emm.2017.207

Lee, H.-J., Suk, J.-E., Bae, E.-J., and Lee, S.-J. (2008). Clearance and deposition of extracellular α-synuclein aggregates in microglia. *Biochem. Biophys. Res. Commun.* 372, 423–428. doi: 10.1016/j.bbrc.2008.05.045

Lee, H.-J., Suk, J.-E., Patrick, C., Bae, E.-J., Cho, J.-H., Rho, S., et al. (2010). Direct transfer of α-synuclein from neuron to astroglia causes inflammatory responses in synucleinopathies. *J. Biol. Chem.* 285, 9262–9272. doi: 10.1074/jbc.M109.081125

Li, K., Li, J., Zheng, J., and Qin, S. (2019). Reactive astrocytes in neurodegenerative diseases. *Aging Dis.* 10, 664–675. doi: 10.14336/ad.2018.0720

Liu, Z., Wang, X., Jiang, K., Ji, X., Zhang, Y. A., and Chen, Z. (2019). TNFα-induced up-regulation of *Ascl2* affects the differentiation and proliferation of neural stem cells. *Aging Dis.* 10, 1207–1220. doi: 10.14336/AD.2018.1028

Luk, K. C., Victoria, K., Jenna, C., Bin, Z., Patrick, O. B., Trojanowski, J. Q., et al. (2012). Pathological α-synuclein transmission initiates Parkinson-like neurodegeneration in nontransgenic mice. *Science* 338, 949–953. doi: 10.1126/science.1227157

Manfredsson, F. P., Luk, K. C., Benskey, M. J., Gezer, A., Garcia, J., Kuhn, N. C., et al. (2018). Induction of α-synuclein pathology in the enteric nervous system of the rat and non-human primate results in gastrointestinal dysmotility and transient CNS pathology. *Neurobiol. Dis.* 112, 106–118. doi: 10.1016/j.nbd.2018.01.008

Moreau, C., Duce, J. A., Rascol, O., Devedjian, J. C., Berg, D., Dexter, D., et al. (2018). Iron as a therapeutic target for Parkinson's disease. *Mov. Disord.* 33, 568–574. doi: 10.1002/mds.27275

Nemeth, E., Rivera, S., Gabayan, V., Keller, C., Taudorf, S., Pedersen, B. K., et al. (2004a). IL-6 mediates hypoferremia of inflammation by inducing the synthesis of the iron regulatory hormone hepcidin. *J. Clin. Invest.* 113, 1271–1276. doi: 10.1172/JCI20945

Nemeth, E., Tuttle, M. S., Powelson, J., Vaughn, M. B., Donovan, A., Ward, D. M., et al. (2004b). Hepcidin regulates cellular iron efflux by binding to ferroportin and inducing its internalization. *Science* 306, 2090–2093. doi: 10.1126/science.1104742

Nicolas, G., Chauvet, C., Viatte, L., Danan, J. L., Bigard, X., Devaux, I., et al. (2002). The gene encoding the iron regulatory peptide hepcidin is regulated by anemia, hypoxia and inflammation. *J. Clin. Invest.* 110, 1037–1044. doi: 10.1172/jci0215686

Paumier, K. L., Luk, K. C., Manfredsson, F. P., Kanaan, N. M., Lipton, J. W., Collier, T. J., et al. (2015). Intrastriatal injection of pre-formed mouse α-synuclein fibrils into rats triggers α-synuclein pathology and bilateral nigrostriatal degeneration. *Neurobiol. Dis.* 82, 185–199. doi: 10.1016/j.nbd.2015.06.003

Pelizzoni, I., Zacchetti, D., Campanella, A., Grohovaz, F., and Codazzi, F. (2013). Iron uptake in quiescent and inflammation-activated astrocytes: a potentially neuroprotective control of iron burden. *Biochim. Biophys. Acta* 1832, 1326–1333. doi: 10.1016/j.bbadis.2013.04.007

Przedborski, S. (2017). The two-century journey of Parkinson disease research. *Nat. Rev. Neurosci.* 18, 251–259. doi: 10.1038/nrn.2017.25

Raha, A. A., Vaishnav, R. A., Friedland, R. P., Bomford, A., and Raha-Chowdhury, R. (2013). The systemic iron-regulatory proteins hepcidin and ferroportin are reduced in the brain in Alzheimer's disease. *Acta Neuropathol. Commun.* 1:55. doi: 10.1186/2051-5960-1-55

Rey, N. L., George, S., and Brundin, P. (2016). Review: spreading the word: precise animal models and validated methods are vital when evaluating prion-like behaviour of α-synuclein. *Neuropathol. Appl. Neurobiol.* 42, 51–76. doi: 10.1111/nan.12299

Rogers, J. T., Andriotakis, J. L., Lacroix, L., Durmowicz, G. P., Kasschau, K. D., and Bridges, K. R. (1994). Translational enhancement of H-ferritin mRNA by interleukin-1 β acts through 5' leader sequences distinct from the iron responsive element. *Nucleic Acids Res.* 22, 2678–2686. doi: 10.1093/nar/22.13.2678

Schmidt, P. J. (2015). Regulation of iron metabolism by hepcidin under conditions of inflammation. *J. Biol. Chem.* 290, 18975–18983. doi: 10.1074/jbc.r115.650150

Sn, S., Pandurangi, J., Murumalla, R., Dj, V., Garimella, L., Acharya, A., et al. (2019). Small molecule modulator of aggrephagy regulates neuroinflammation to curb pathogenesis of neurodegeneration. *EBioMedicine* 50, 260–273. doi: 10.1016/j.ebiom.2019.10.036

Song, N., Wang, J., Jiang, H., and Xie, J. (2018). Astroglial and microglial contributions to iron metabolism disturbance in Parkinson's disease. *Biochim. Biophys. Acta Mol. Basis Dis.* 1864, 967–973. doi: 10.1016/j.bbadis.2018.01.008

Song, N., Wang, J., Jiang, H., and Xie, J. (2010). Ferroportin 1 but not hephaestin contributes to iron accumulation in a cell model of Parkinson's disease. *Free Radic. Biol. Med.* 48, 332–341. doi: 10.1016/j.freeradbiomed.2009.11.004

Spillantini, M. G., Schmidt, M. L., Lee, V. M., Trojanowski, J. Q., Jakes, R., and Goedert, M. (1997). α-synuclein in Lewy bodies. *Nature* 388, 839–840. doi: 10.1038/42166

Sullivan, J. L. (2007). Macrophage iron, hepcidin, and atherosclerotic plaque stability. *Exp. Biol. Med.* 232, 1014–1020. doi: 10.3181/0703-mr-54

Thomsen, M. S., Andersen, M. V., Christoffersen, P. R., Jensen, M. D., Lichota, J., and Moos, T. (2015). Neurodegeneration with inflammation is accompanied by accumulation of iron and ferritin in microglia and neurons. *Neurobiol. Dis.* 81, 108–118. doi: 10.1016/j.nbd.2015.03.013

Torti, F. M., and Torti, S. V. (2002). Regulation of ferritin genes and protein. *Blood* 99, 3505–3516. doi: 10.1182/blood.v99.10.3505

Trist, B. G., Hare, D. J., and Double, K. L. (2019). Oxidative stress in the aging substantia nigra and the etiology of Parkinson's disease. *Aging Cell* 16:e13031. doi: 10.1111/acel.13031

Tu, W., Wang, H., Li, S., Liu, Q., and Sha, H. (2019). The anti-inflammatory and anti-oxidant mechanisms of the Keap1/Nrf2/ARE signaling pathway in chronic diseases. *Aging Dis.* 10, 637–651. doi: 10.14336/ad.2018.0513

Urrutia, P., Aguirre, P., Esparza, A., Tapia, V., Mena, N. P., Arredondo, M., et al. (2013). Inflammation alters the expression of DMT1, FPN1 and hepcidin, and it causes iron accumulation in central nervous system cells. *J. Neurochem.* 126, 541–549. doi: 10.1111/jnc.12244

Urrutia, P. J., Hirsch, E. C., González-Billault, C., and Núñez, M. T. (2017). Hepcidin attenuates amyloid β-induced inflammatory and pro-oxidant responses in astrocytes and microglia. *J. Neurochem.* 142, 140–152. doi: 10.1111/jnc.14005

Valera, E., Ubhi, K., Mante, M., Rockenstein, E., and Masliah, E. (2014). Antidepressants reduce neuroinflammatory responses and astroglial α-synuclein accumulation in a transgenic mouse model of multiple system atrophy. *Glia* 62, 317–337. doi: 10.1002/glia.22610

Vela, D. (2018). Hepcidin, an emerging and important player in brain iron homeostasis. *J. Transl. Med.* 16:25. doi: 10.1186/s12967-018-1399-5

Volpicelli-Daley, L. A., Luk, K. C., Patel, T. P., Tanik, S. A., Riddle, D. M., Stieber, A., et al. (2011). Exogenous α-synuclein fibrils induce lewy body pathology leading to synaptic dysfunction and neuron death. *Neuron* 72, 57–71. doi: 10.1016/j.neuron.2011.08.033

Wang, Y., Chen, Y., Zhou, Q., Xu, J., Qian, Q., Ni, P., et al. (2018). Mild endoplasmic reticulum stress protects against lipopolysaccharide-induced astrocytic activation and blood-brain barrier hyperpermeability. *Front. Cell. Neurosci.* 12:222. doi: 10.3389/fncel.2018.00222

Xia, Y., Zhang, G., Han, C., Ma, K., Guo, X., Wan, F., et al. (2019). Microglia as modulators of exosomal α-synuclein transmission. *Cell Death Dis.* 10:174. doi: 10.1038/s41419-019-1404-9

Xiong, X. Y., Liu, L., Wang, F. X., Yang, Y. R., Hao, J. W., Wang, P. F., et al. (2016). Toll-like receptor 4/MyD88-mediated signaling of hepcidin expression causing brain iron accumulation, oxidative injury, and cognitive impairment after intracerebral hemorrhage. *Circulation* 134, 1025–1038. doi: 10.1161/circulationaha.116.021881

You, L. H., Yan, C. Z., Zheng, B. J., Ci, Y. Z., Chang, S. Y., Yu, P., et al. (2017). Astrocyte hepcidin is a key factor in LPS-induced neuronal apoptosis. *Cell Death Dis.* 8:e2676. doi: 10.1038/cddis.2017.93

Yu, X., Song, N., Guo, X., Jiang, H., Zhang, H., and Xie, J. (2016). Differences in vulnerability of neurons and astrocytes to heme oxygenase-1 modulation: implications for mitochondrial ferritin. *Sci. Rep.* 6:24200. doi: 10.1038/srep24200

Zarruk, J. G., Berard, J. L., Passos dos Santos, R., Kroner, A., Lee, J., Arosio, P., et al. (2015). Expression of iron homeostasis proteins in the spinal cord in experimental autoimmune encephalomyelitis and their implications for iron accumulation. *Neurobiol. Dis.* 81, 93–107. doi: 10.1016/j.nbd.2015.02.001

Zhang, H.-Y., Wang, N.-D., Song, N., Xu, H.-M., Shi, L.-M., Jiang, H., et al. (2013). 6-Hydroxydopamine promotes iron traffic in primary

cultured astrocytes. *Biometals* 26, 705–714. doi: 10.1007/s10534-013-9647-x

Zhu, S., Wei, X., Yang, X., Huang, Z., Chang, Z., Xie, F., et al. (2019). Plasma lipoprotein-associated phospholipase A2 and superoxide dismutase are independent predicators of cognitive impairment in cerebral small vessel disease patients: diagnosis and assessment. *Aging Dis.* 10, 834–846. doi: 10.14336/ad.2019.0304

Zou, J., Chen, Z., Wei, X., Chen, Z., Fu, Y., Yang, X., et al. (2017). Cystatin C as a potential therapeutic mediator against Parkinson's disease *via* VEGF-induced angiogenesis and enhanced neuronal autophagy in neurovascular units. *Cell Death Dis.* 8:e2854. doi: 10.1038/cddis.2017.240

Conflict of Interest: The authors declare that the research was conducted in the absence of any commercial or financial relationships that could be construed as a potential conflict of interest.

frontiers in Neuroscience

METHODS
published: 20 March 2020
doi: 10.3389/fnins.2020.00244

A Practical Guide to the Automated Analysis of Vascular Growth, Maturation and Injury in the Brain

Ruslan Rust[1,2,3], Tunahan Kirabali[1,3], Lisa Grönnert[1], Berre Dogancay[3], Yanuar D. P. Limasale[4], Andrea Meinhardt[4], Carsten Werner[4], Bàrbara Laviña[5], Luka Kulic[1,3], Roger M. Nitsch[1,3], Christian Tackenberg[1,3] and Martin E. Schwab[1,2,3]*

[1] Institute for Regenerative Medicine, University of Zurich, Zurich, Switzerland, [2] Department of Health Sciences and Technology, ETH Zürich, Zurich, Switzerland, [3] Neuroscience Center Zurich, University of Zurich and ETH Zürich, Zurich, Switzerland, [4] Leibniz Institute for Polymer Research, Dresden, Germany, [5] Department of Immunology, Genetics and Pathology, Uppsala University, Uppsala, Sweden

The distinct organization of the brain's vasculature ensures the adequate delivery of oxygen and nutrients during development and adulthood. Acute and chronic pathological changes of the vascular system have been implicated in many neurological disorders including stroke and dementia. Here, we describe a fast, automated method that allows the highly reproducible, quantitative assessment of distinct vascular parameters and their changes based on the open source software Fiji (ImageJ). In particular, we developed a practical guide to reliably measure aspects of growth, repair and maturation of the brain's vasculature during development and neurovascular disease in mice and humans. The script can be used to assess the effects of different external factors including pharmacological treatments or disease states. Moreover, the procedure is expandable to blood vessels of other organs and vascular *in vitro* models.

Keywords: quantification, image processing, angiogenesis, blood vessels, stroke, development, central nervous system (CNS)

OPEN ACCESS

Edited by:
Dennis Qing Wang, Southern Medical University, China

Reviewed by:
Shuzhen Zhu, Southern Medical University, China
Axel Montagne, University of Southern California, United States
Marco Bacigaluppi, San Raffaele Scientific Institute (IRCCS), Italy

****Correspondence:***
Ruslan Rust
ruslan.rust@irem.uzh.ch

Specialty section:
This article was submitted to Neurodegeneration, a section of the journal Frontiers in Neuroscience

Received: *13 November 2019*
Accepted: *04 March 2020*
Published: *20 March 2020*

Citation:
Rust R, Kirabali T, Grönnert L, Dogancay B, Limasale YDP, Meinhardt A, Werner C, Laviña B, Kulic L, Nitsch RM, Tackenberg C and Schwab ME (2020) A Practical Guide to the Automated Analysis of Vascular Growth, Maturation and Injury in the Brain. Front. Neurosci. 14:244. doi: 10.3389/fnins.2020.00244

INTRODUCTION

Structural and functional integrity of blood vessels are essential for normal brain function. A complex vascular network supplies the brain with oxygen and nutrients, removes metabolic waste products, conveys hormonal signaling and allows rapid distribution of immune cells (Rust et al., 2018, 2019c; Sweeney et al., 2018). As opposed to the periphery, brain vasculature also forms a highly selective border, the BBB (Zhao et al., 2015; Sweeney et al., 2019b). The BBB consists of a continuous brain microvascular endothelium, its underlying basement membrane, pericytes, astrocytes and microglia. It maintains the homeostatic environment within the brain, which is required for proper functioning of neuronal circuits (Sweeney et al., 2016; Iadecola, 2017; Brown et al., 2019).

Since the brain is highly vulnerable to compromises of blood supply, brain vasculature has long been an object of scientific interest due to its central role in major neurovascular diseases including strokes and dementia. Correct interpretation of structural changes in the vasculature is therefore

Abbreviations: BBB, blood brain barrier; Cldn5, claudin-5; CNS, central nervous system; fMRI, functional magnetic resonance imaging; GFP, green fluorescent protein; GM, gray matter; NIRS, near-infrared spectroscopy; PET, positron emission tomography; ROI, region of interest; WM, white matter.

fundamental to understand its underlying (patho-)physiologies (Potente and Carmeliet, 2017; Sweeney et al., 2018). Advances in high resolution laser microscopy and *in vivo* imaging techniques reinforced the use of image-based analysis in vascular research for both animal experiments and human pathologies (Ertürk et al., 2014; Zhang et al., 2018). Despite improvements in imaging techniques, interpretation of these data can be challenging, time-consuming and laborious due to the 3D nature and high complexity of the brain vasculature. A consequence are poor levels of quantification and high variation between analysis methods and investigators.

Computational methods have facilitated the quantification of vascular networks. However, most of them currently rely on commercial software (e.g., Matlab, Imaris, Vesselucida) that can be expensive and require considerable expertise (Walter et al., 2010; Reyes-Aldasoro et al., 2011; Craver et al., 2016; Montoya-Zegarra et al., 2019). Alternatives are open-source packages that also provide excellent extensions tailored for specific applications to trace and analyze the features of the vasculature. Nonetheless, many extensions are not well maintained and might not be compatible with one another.

Here, we provide a straightforward practical guideline how to process vascular images, identify biologically relevant vascular parameters and automatize these processes with a script based on the open source Fiji (ImageJ) software. The script implements pre-processing steps to binarize the raw image and visualize it with a heatmap. Quantitative assessment provides information about the vascular area fraction, vascular segment length, number of branch points and the distance and distribution between single vessels. Moreover, we have developed a pipeline how to measure pericyte coverage of the vasculature that has been shown to be a critical factor for vascular integrity and physiological function. All features have been tested for compatibility across different ImageJ versions. The script is applicable to vascular development and vascular pathologies in mice and humans but has also been validated on retinal vascular development *in vitro* models.

RESULTS

Quantification of Key Anatomical Features of the Developing Brain Vasculature

Mouse brain vasculature can be visualized by different procedures such as the use of specific ligands or immunohistological markers (e.g., lectins or antibodies against CD31), intravascular perfusion with fluorophore-coupled substances (e.g., Lectin Dylight594) or the use of genetic mouse models that express a reporter under the control of a vascular-specific gene (e.g., Cldn5-GFP). Here, we show that these methods result in the specific visualization of the brain vasculature, and therefore are suitable to perform quantitative analyses with our automated image processing and data analysis pipeline (**Figures 1A,B**). All methods led to visualization of the entire vascular system including the smallest vessels and newly formed capillaries, including endothelial tip cells (**Supplementary Figure S1**).

As an example, images of cortical regions from Cldn5-GFP mice at the age of postnatal day p3, p7, p30, p60, and p120 were processed and automatically analyzed for the vascular area fraction, vessel segment length, vascular branching and the distance between single vessels (according to Script in **Supplementary Figure S2**) with the developed Fiji (ImageJ) protocol (**Figures 1C,D**). The analysis revealed a steady increase of vascular area fraction (p3: 0.027 ± 0.003; p120: 0.106 ± 0.004, $p < 0.001$), vascular length in mm per mm2 (p3: 17.12 ± 6.45; p120: 25.47 ± 0.95, $p = 0.028$), number of vascular branches per mm2 (p3: 232.09 ± 92.16; p120: 310.74 ± 16.29, $p = 0.449$); and a decrease in distance between the vessels in μm (p3: 50.49 ± 9.50; p120: 23.72 ± 0.23, $p < 0.001$). Interestingly, we also observed a continuous reduction in the number of branch points per mm^2 starting from p10, indicating the decrease in anastomoses that is known to occur during normal development and maturation of the vasculature (Wang et al., 1992) (p10: 423.43 ± 62.37; p120: 310.74 ± 16.29, $p = 0.137$) (**Figure 1D**).

In addition to cerebrovascular development, we confirmed the applicability of our automated analysis pipeline for blood vessel development in the retina from postnatal day 3 to 120 (**Supplementary Figure S3**). Moreover, we also validated its application for *in vitro* systems of 3D vascular networks derived from human umbilical vein endothelial cells (HUVECs) grown in a matrix with and without inhibitory factors for vascular growth (**Supplementary Figure S4**).

Disruption of Cerebral Vascular Network and Pericyte Coverage Following Ischemic Stroke

Ischemic strokes (the most frequent kind of vascular failure in the brain) lead to a partially blocked and disrupted vascular network. Often, a central stroke core with severely compromised blood flow develops, surrounded by a rim of partially ischemic tissue (ischemic border zone) with impaired function but in part preserved cellular viability (Sweeney et al., 2018).

Here, we use the photothrombotic stroke model in the sensorimotor cortex of mice to analyze the vasculature in the ischemic border zone 3 weeks following stroke (**Figures 2A,B**). We detected changes in all vascular parameters between the intact and the peri-infarct cortex (**Figure 2C**). There was a decrease in vascular area fraction (−39%; intact: 0.100 ± 0.017; injury: 0.060 ± 0.014, $p < 0.001$), vessel segment length in mm/mm2 (−44%; intact: 57.74 ± 4.83, injury: 31.89 ± 5.83, $p < 0.001$), number of branches per mm2 (−68%; intact: 396.31 ± 18.81, injury: 126.57 ± 58.30, $p < 0.001$). Moreover, the distance between the vessels in μm increased in the peri-infarct region (+21.4%; intact: 30.34 ± 1.76, injury: 36.85 ± 3.96, $p < 0.001$).

Pericyte coverage is an important parameter for physiological function and maturity of cerebral blood vessels. As perivascular multi-potent cells and an important component of the BBB (Sweeney et al., 2018, 2019b), pericytes have been shown to play important roles during vascular growth and maturation, immune functions and BBB maintenance (Zlokovic, 2010; Gautam and Yao, 2018). Therefore, we included the analysis of the vascular pericyte coverage in our script. At 3 weeks after the stroke, the

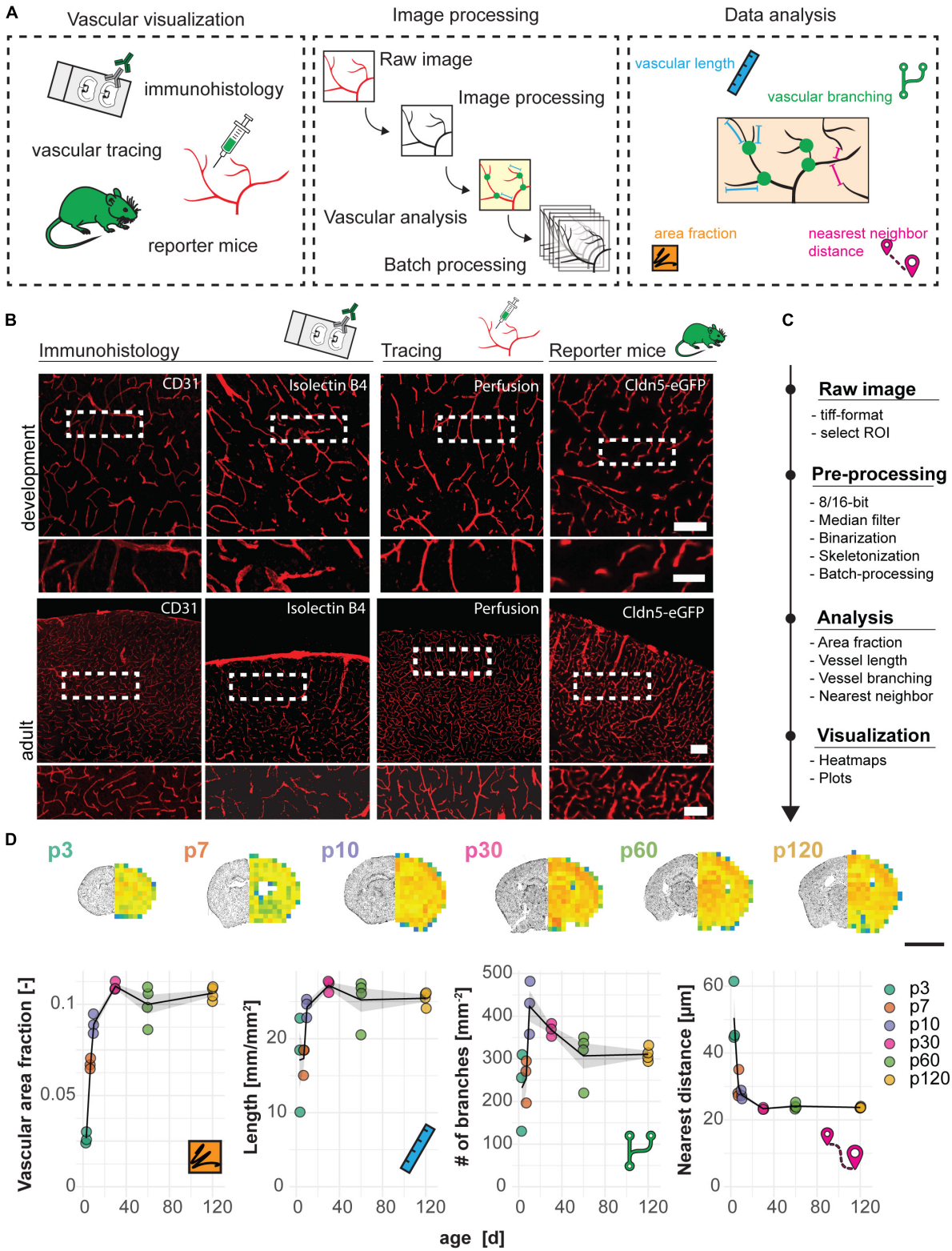

FIGURE 1 | Visualization and quantification of cortical vasculature in the developing mouse brain. **(A)** Experimental design. **(B)** Visualization of the vasculature with immune- or lectin-histofluorescence, transcardial perfusion with Lectin-Dylight594 or the use of Cldn5-GFP reporter mice at the age of p10 (development) and 3 months (adult). Scale bar 50 µm. **(C)** Step-by-step analysis pipeline for vascular quantification. **(D)** Heatmap and quantification of vascular area fraction, length, branching and nearest distance between blood vessels in cortical brain sections. Scale bar: 2 mm. Data are represented as means ± SD. Each dot represents one animal.

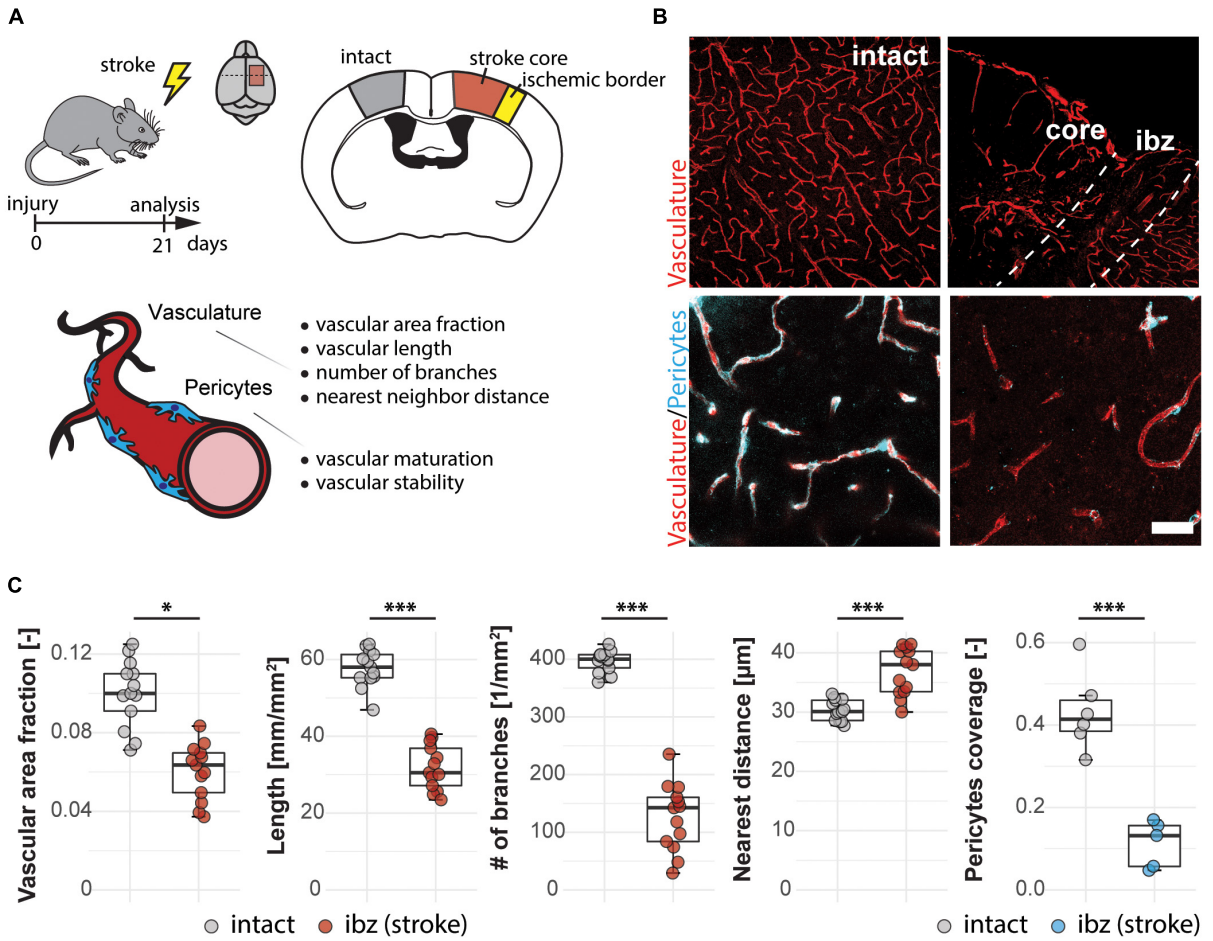

FIGURE 2 | Vascular changes in the peri-infarct ischemic border zone around the stroke core in the mouse cortex. **(A)** Experimental design. **(B)** Representative images of intact cortex vasculature (left panels) and endothelial network (CD31+; red) and pericytes (CD13+; blue) in the ischemic border zone. Scale bar: 100 μm (overview), 20 μm (close-up). **(C)** Quantitative assessment of vascular parameters (area fraction, length, branching, distance) and pericyte coverage of the vasculature. Data are represented as boxplots (median, two hinges and two whiskers); the upper and lower hinges correspond to the first and third quantiles. The whiskers extend until 1.5 × IQR from the hinges; data beyond the end of the whiskers are defined as outlying points. Each dot represents one animal, and significance of mean differences between the groups was assessed using two-tailed unpaired one-sample *t*-test. Asterisks indicate significance: $^{*}P < 0.05$, $^{***}P < 0.001$. IQR, interquartile range.

peri-infarct regions around the stroke core still showed a 74% lower pericyte coverage (0.112 ± 0.056) compared to the intact hemisphere (0.432 ± 0.096, $p < 0.001$).

Vascular Pericyte Coverage Is Reduced in Alzheimer's Patients in the Medial Frontal Cortex

Vascular changes and BBB disruption are also major contributors of Alzheimer's disease pathophysiology and therefore widely investigated with post-mortem studies (Nelson et al., 2016). Within these changes, decreased pericyte coverage of vessels was reported by various groups both in transgenic animal models and in human brain samples (Visser et al., 1990; Halliday et al., 2016; Ma et al., 2018; Miners et al., 2018).

To test our automated image processing pipeline in a human post-mortem vascular analysis, we applied the script for quantification of the vascular area fraction and pericyte coverage in gray and white matter tissue samples of the medial frontal cortex (**Figures 3A,B**) from five Alzheimer patients and five age-matched controls (**Supplementary Table S1**). In line with the earlier reports (Nyúl-Tóth et al., 2016; Kubíková et al., 2018; Hase et al., 2019), our analysis showed a higher vascular area fraction in GM compared to white matter (GM: 0.028 ± 0.003; WM: 0.015 ± 0.003, $p < 0.001$) (**Figure 3C**) whereas pericyte coverage was not significantly different between gray and white matter (GM: 0.279 ± 0.168, WM: 0.489 ± 0.304, $p = 0.078$) (**Figure 3C**). Quantification of vascular area fraction didn't reveal any significant changes between non-demented controls and AD patients in neither cortical GM (Ctrl 0.029 ± 0.001, AD: 0.026 ± 0.003, $p = 0.130$), nor white matter regions (Ctrl: 0.016 ± 0.004, AD: 0.015 ± 0.003, $p = 0.554$) (**Figure 3C**). On the other hand, pericyte coverage showed a significant reduction of PDGFR-β immunoreactivity in AD patients compared to

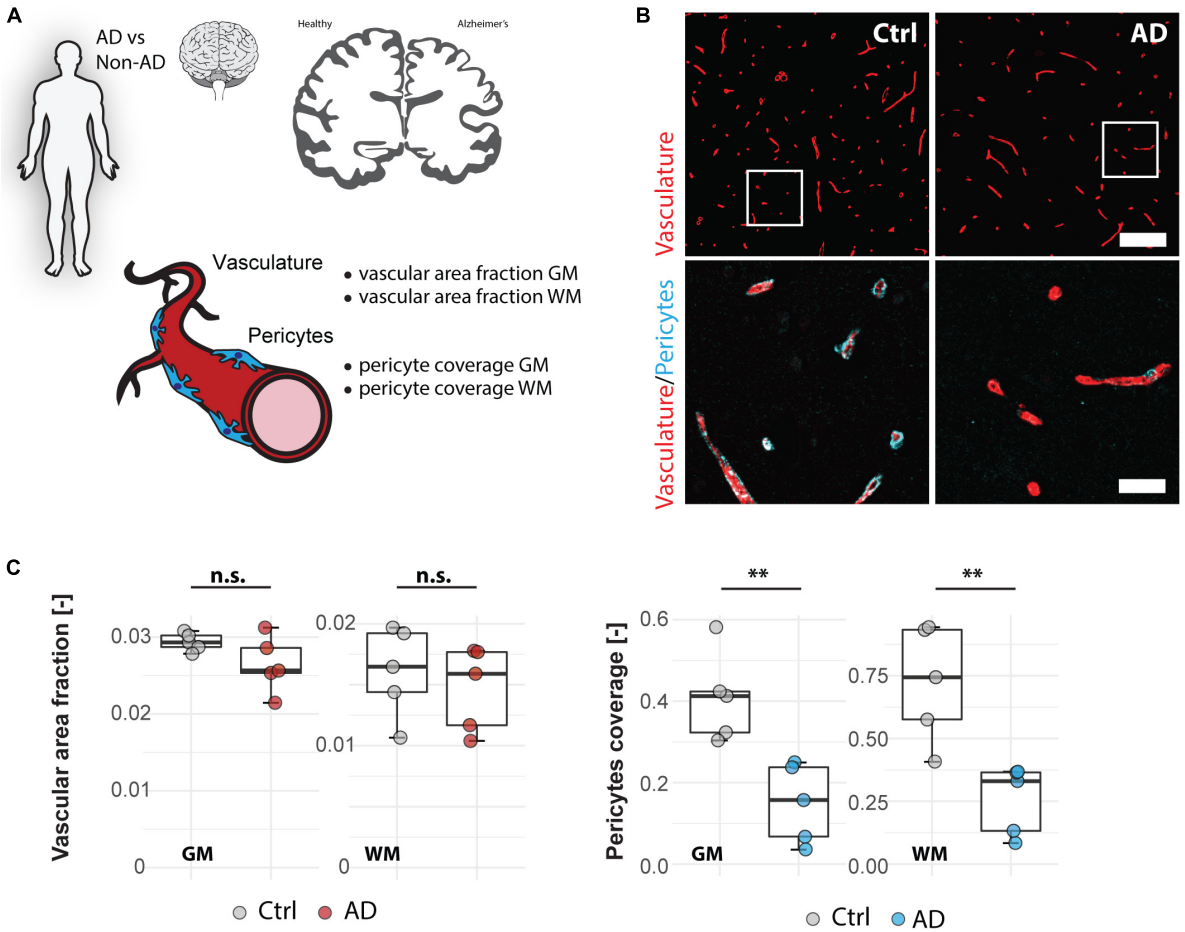

FIGURE 3 | Vascular changes in human Alzheimer's disease brains. **(A)** Experimental design. **(B)** Representative images of Alzheimer's brain sections. Scale bar 100 μm (overview), 20 μm (close-up). **(C)** Quantitative assessment of brain vasculature and pericyte coverage in cortical gray and white matter sections of AD patients and healthy controls. Data are represented as boxplots (median, two hinges and two whiskers); the upper and lower hinges correspond to the first and third quantiles. The whiskers extend until 1.5 × IQR from the hinges; data beyond the end of the whiskers are defined as outlying points. Each dot represents one subject and significance of mean differences between the groups was assessed using a two two-tailed unpaired one-sample *t*-test. Asterisks indicate significance: $^{**}P < 0.01$. GM, gray matter; WM, white matter; AD, Alzheimer's disease; Ctrl, control; n.s., not significant; IQR: interquartile range.

controls both in the GM: −63% (Ctrl: 0.408 ± 0.110, AD: 0.149 ± 0.097, $p = 0.004$) and in the white matter −64% (Ctrl: 0.721 ± 0.231, AD: 0.256 ± 0.137, $p = 0.004$). Thus, our automated analysis pipeline confirmed the reduction in pericyte coverage in AD patients both in white and GM of the medial frontal cortex, but the overall vascular density seemed not be affected in our patient sample.

DISCUSSION

We describe a practical toolbox based on open-source software for the analysis of complex blood vessel networks during development and following cerebrovascular diseases. The pipeline allows to quantitatively assess the important parameters vascular area fraction, vessel segment length, vascular branching, nearest distance between single vessels and pericyte coverage in a fast and reliable way in developing, adult and diseased brains of mice and humans. Moreover, we validated the versatile applicability of the toolbox for mouse retinal tissue and vascular *in vitro* models.

Reliable quantification of the vasculature and its supporting cells is fundamental to detect pathological changes in several major diseases. Consequently, many research institutes and pharmaceutical companies are assessing drugs and treatments to either predict early changes in the vasculature or to find an effective treatment. In the field of cancer, tumor growth is strongly promoted by the formation of new vessels – and treatment strategies are developed to inhibit vascular growth (Rust et al., 2018; Alcala et al., 2019; Jiang et al., 2019). In diabetic retinopathy (DR), a major vascular complication of diabetes mellitus, the dysfunction is characterized by the formation of new vessels inside the retina. New mechanisms and targets are currently discovered to alleviate the vascular pathology in DR (Zhu et al., 2019a). Moreover, alterations in the vasculature and vascular supporting cells have been proven to be a hallmark of

hypertension, atherosclerosis and advanced chronic liver disease (Li et al., 2019; Maeso-Díaz et al., 2019; Miao et al., 2019). In the CNS, regulation of vascular remodeling and repair has been shown influence pathological progression of e.g., stroke, cerebral small vessel disease, Parkinson's, and Alzheimer's (Wei et al., 2016; Zou et al., 2017; Shen et al., 2019; Sweeney et al., 2019a; Zhu et al., 2019b). Consequently, the development of tools to reliably describe early changes in the vascular anatomy are relevant for a large variety of research.

Comparison of different visualization methods for brain blood vessels including immune- and lectin-histochemistry, vascular tracer perfusion and genetic reporter mice revealed similar patterns of the brain blood vessels. Nonetheless, since perfusion methods only label vasculature that is supplied with blood, newly formed blood vessels with their tip cells and filopodia remain undetected. by intravascular tracer perfusion. Methods may be chosen dependent on the experimental questions and set up.

Several methods were proposed for the quantitative assessment of vascular networks (Seaman et al., 2011; Zudaire et al., 2011; Zhang et al., 2018; Montoya-Zegarra et al., 2019). However, most rely on commercial, often expensive software, may require considerable expertise or are specialized for specific vascular networks, e.g., the retina (Walter et al., 2010; Reyes-Aldasoro et al., 2011; Craver et al., 2016; Montoya-Zegarra et al., 2019).

A main advantage of the present toolbox is that it is free of charge, easy and straightforward in practice and has a broad application. It does not require any technical knowledge in coding to adapt the script. Moreover, it has been tested and validated across different operating systems and ImageJ versions. It only requires the initial installation of two plugins for the measurement of vessel segment length (Measure Skeleton Length) and distance calculations (Nearest Neighbor Distances Calculation with ImageJ) before starting. The toolbox covers the entire process of image processing, visualization and analysis of relevant biological parameters. We decided to include a quantitative assessment of vascular area fraction for a general overview of vascular density. In addition to vessel density, length and branching are relevant for an understanding of exchange of oxygen and nutrients between the capillary network and the brain tissue (Kopylova et al., 2017). The distance and its variability between blood vessels additionally allows the detection of local hypoxic regions that may not entirely be represented by the overall mean vascular density. Previous versions of the script have been used to assess post-stroke angiogenesis and retinal vascular growth (Rust et al., 2019a,b,d). Interestingly, we observe very high levels of vascular density in the adult mouse retina (higher than in the mouse brain), which has been previously observed (Chintala et al., 2015; Zhang et al., 2018; Rust et al., 2019a,d).

The measured pericyte coverage of blood vessels in our samples (both human and mice) ranged between 40–60% and has been previously reported to be around 80% (Nikolakopoulou et al., 2017; Montagne et al., 2018). These discrepancies are likely to occur due to the use of different antibodies and/or different epitopes (CD13, PDGFRβ for pericytes or CD31, lectin, Laminin, Collagen IV for vasculature). Moreover, further studies are needed to evaluate differences between animal Alzheimer's disease (AD) models and a large cohort of human AD samples. The presented study was designed to evaluate and validate the automated script for vascular analysis. Accordingly, we had only 5 human AD subjects and 5 non-demented controls. All AD subjects were female, APOE E4 carriers and had a Braak Score of 5–6. Larger cohorts are required to reliably interpret the observed vascular and pericyte phenotypes between AD and control cohorts.

The performed immunostainings resulted in a uniform visualization of all blood vessels; however, we did not intent to distinguish between different types of blood vessels (such as arteries, arterioles, capillaries, venules, and veins). Several antigens were previously reported to be expressed specifically in either veins or arteries (Kretschmer et al., 2013) and might be also used for analysis. The sensitivity and reliability of the script strongly depends on the quality of vascular visualization and imaging. To our experiences we observe the best signal to noise ratio by using transgenic models or performing transcranial perfusion with fluorescent dyes. We have observed that especially old human tissue might show heterogeneity between brains and therefore all automated steps should be manually controlled.

A limitation of the script is that it does not provide information about the vascular integrity. Many neurological diseases including stroke and Alzheimer's disease have damage of the BBB and extravasation of blood-derived neurotoxic molecules as a hallmark. There are many approaches to study BBB integrity in mice and human including the use of vascular fluorescent tracers or immunostaining of extravasated endogenous molecules e.g., fibrinogen. Especially in human, BBB integrity can also be assessed using magnetic resonance imaging (MRI) and NIRS. Automated quantification of BBB integrity has been previously described (Michalski et al., 2010; Tang et al., 2010; Saunders et al., 2015).

Vascular damage is an important hallmark of many neurological diseases, but, the underlying changes in vascular anatomy and physiology may differ. Studies should ideally combine structural end-point measures with physiological data from the different brain imaging techniques including functional MRI (fMRI) and PET (Mier and Mier, 2015).

CONCLUSION

We established and validated a straightforward and versatile toolbox based on the open-source software ImageJ to reliably describe brain vasculature in tissue sections. It is applicable to the developmental, adult and diseases vasculature and has been also tested outside the CNS. The protocol will facilitate the detection of pathological changes or results of genetic or pharmacological manipulations of the vascular anatomy.

MATERIALS AND METHODS

Animals

We used wildtype and Claudin-eGFP (Cldn5-GFP) C57BL/6[13] mice. Cldn5-GFP were generated using bacterial artificial

chromosome (BAC) technology. Animals were maintained at the Brain Research Institute and at the Laboratory Animal Services Center in Zürich on a 12 h light/dark cycle with food and water provided *ad libitum*. Mice were housed in standard Type II/III cages at least in pairs. Animals used were 7 days to 3-month-old males and females. All experiments were conducted in accordance with the applicable national regulations and approved by the Cantonal Veterinary Department of Zürich.

Human Brain Tissue

Paraffin-embedded middle-frontal cortex tissue blocks were provided by the Netherlands Brain Bank (NBB), the Netherlands Institute for Neuroscience, Amsterdam, Netherlands. Post-mortem samples were collected from donors with a written informed consent for brain autopsy and the use of the material for research purposes was obtained by the NBB. Braak stage (Braak and Braak, 1995), CERAD (Consortium to Establish a Registry for Alzheimer's Disease) score for amyloid load (Hyman et al., 2012), APOE genotype and clinical diagnosis for each subject were determined and provided by NBB. Demographics of all subjects were listed in **Supplementary Table S1**.

Tissue Processing for Mouse Brain Sections

Animals were deeply anesthetized by intraperitoneal injection of pentobarbital (150 mg/kg bodyweight) and subsequently transcardially perfused with isotonic Ringer solution (5 ml/l Heparin, B. Braun) and 4% Paraformaldehyde (PFA, in 0.2 M phosphate buffer, pH 7.4). Brains were removed from the skulls and post-fixed for 4 h at 4°C. For cryoprotection, brains were transferred to 30% sucrose and kept overnight at 4°C. Coronal sections with a thickness of 40 μm were cut using a sliding microtome (Microm HM430, Leica). Sections were collected and stored as free-floating sections in cryoprotectant solution at −20°C until further processing. For immunohistochemical staining brain sections were washed with 0.1 M phosphate buffer (PB) and then incubated with a blocking and permeabilization solution (TNB, 0.1% TBST, 3% normal goat serum) for 30 min at RT shaking. Sections were incubated with primary antibody (rat-CD31, BD Biosciences, 1:100) overnight at 4°C. The next day sections were washed and incubated with corresponding secondary antibodies for 2 h at RT. All antibodies were diluted in blocking and permeabilization solution (TNB, 0.1% TBST, 3% normal goat serum). Nuclei were counterstained with DAPI (1:2000 in 0.1 M PB). Sections were mounted in 0.1 M PB on Superfrost PlusTM microscope slides (Thermo Fisher) and coverslipped using Mowiol.

Tissue Processing for Human Brain Sections

Five μm thick sections of paraffin-embedded human middle frontal cortex blocks were prepared with Leica RM2135 rotary microtome and mounted on slides. Sections were placed in xylol, 100% ethanol, 95% ethanol, 70% ethanol and water in respective order and kept in each solvent for 3 min. For antigen retrieval, sections were boiled in 0.1M citrate buffer. After washing with phosphate-buffered saline (PBS), sections were blocked with 10% horse serum in PBS with 0.2% Triton X-100 (PBS-T) for 2 h at room temperature. After blocking, primary antibody cocktail (1:500 dilution of biotinylated-lectin (B-1065, Vector Laboratories) and 1:50 dilution of goat anti-PDGFR-β antibody (AF385, R&D systems) in 5% horse serum in PBS-T) was applied and incubated overnight at 4°C. Next day, sections were incubated for 2 h at room temperature with secondary antibodies [1:200 dilution in 5% horse serum in PBS-T, streptavidin conjugated to Alexa488 and donkey anti-goat conjugated to Cy3 (Jackson Immunoresearch)] and for 5 min with 0.2% Sudan Black (Sigma Aldrich) in 70% ethanol. Coverslips were mounted with Histomount (National Diagnostics) mounting medium. No white matter lesions were observed in AD samples.

Transcardial Perfusion With Vascular Tracers

After deep anesthesia and shortly before perfusion, 50 μl of 1 mg/ml Lycopersicon Esculentum lectin conjugated to DyLight594 (DL-1177, VactorLabs) were transcardially injected. After 1 min animals were transcardially perfused with isotonic Ringer solution (5 ml/l Heparin, B. Braun) and 4% Paraformaldehyde (PFA, in 0.2 M phosphate buffer, pH 7.4.

Photothrombotic Stroke

Animals were anesthetized with 2% isoflurane followed by an intraperitoneal injection of fentanyl (20 ug/kg), midazolam (1 mg/kg), medetomidine (200 ug/kg). A photo-thrombotic stroke to unilaterally lesion the sensorimotor cortex was introduced on the right hemisphere. Animal was fixed in a stereotactic frame, the skull exposed through a midline incision, cleared of connective tissue and dried. A cold light source (Olympus KL 1500LCS, 150W, 3000 K) was positioned over an opaque template with an opening for the light source (5 × 3 mm) 2.5 mm to −2.5 mm anterior and 0 mm to 3 mm lateral to Bregma. Rose Bengal (13 mg/kg body weight, 10 mg/ml Rose Bengal in 0.9% NaCl solution) was intraperitoneally injected and after 5 min, the brain was illuminated through the intact skull for 8 min. For postoperative care, all animals received analgesics (Dafalgan Sirup, Braun, *per os* in the drinking water) and antibiotics (Baytril, 5 mg/kg body weight, Bayer, s.c.) once a day for at least 3 days after surgery. Sham operated animals underwent the entire surgical process but did not received Rose Bengal. Vascular analysis was performed 3 weeks following stroke injury; however, it has also been validated to other time points (day 1, 3, 7, 28, data not shown).

Microscopy and Vascular and Pericyte Quantification

Imaging of brain sections was performed with Leica SP8 laser scanning confocal microscope equipped with 10x, 20x, 40x objectives. Images were processed using Fiji (ImageJ) and Adobe Illustrator CC. First, regions of interest were chosen for the respective experiments. The regions were defined as stroke core (no surviving neurons), ischemic border zone (ibz; a region of 300 um distal to the stroke core with hypovascularization) and intact (cortical contralesional site) as previously described (Rust et al.,

2019b,d). Images were pre-processed and binarized according to **Figure 1**. To assess vascular growth and repair an ImageJ (Fiji) script was established to automatically calculate (1) area fraction of blood vessels, (2) vessel segment length (3) vascular branching (4) distance between blood vessels. Maturation of blood vessels was assessed by the ratio of pericyte coverage to total vascular area fraction. To assess the information images are duplicated, processed (to remove noise) and binarized. Area fraction calculation measures the percentage of pixels with non-zero pixels. Vessel segment length and vascular branching is assessed by skeletonizing the binary image. This allows to tag all pixels in a skeleton image and then count all its branches and measures their average and maximum length. The distance between single vessels is calculated by the nearest neighbor distance that displays the distance between closest individual single non-zero pixels. Quantification of the pericyte coverage is measured by dividing the pericyte area fraction signal from the previously acquired vascular area fraction signal. The relative ratio provides the pericyte coverage of the blood vessels. Heatmap analysis is performed by selecting the number of squared per row/column. For each square the area fraction is calculated (as described above) and the values are visualized with a heatmap. The size of squared is adjustable and should be adapted to the used magnification and sample. The corresponding script can be found in **Supplementary Data Sheet S1**.

Hydrogel Formation

Biohybrid GAG-PEG hydrogels for *in vitro* HUVEC morphogenesis studies were prepared as described previously with slight modifications. In brief, a degradable starPEG-MMP conjugate (MW 16,489) was dissolved in HUVEC culture medium at a final concentration of 0.75 mM and a heparin-maleimide conjugate (MW 15,000) was dissolved in the medium and supplemented with the adhesive peptide CWGGRGDSP (cRGD, MW 990) to reach a final concentration of 1 mM and 2 mM, respectively. Thereafter, the heparin-RGD mixture was (non-reactively) functionalized with VEGF165 (PeproTech, United States), SDF1 (Miltenyi Biotec, Germany) and FGF2 (Miltenyi Biotec, Germany) each at a final concentration of 5 μg/ml. The myelin was added in concentrations of rat Myelin at 10 μg/ml) before adding a HUVEC suspension to generate a cell-heparin conjugate mixture. For the formation of hydrogels, the cell-heparin conjugate mixture was mixed with the starPEG conjugate solution in a 1:1 volume ratio to form 15 μl hydrogel droplets which were casted onto hydrophobic 12 well chamber slides (Ibidi, Germany). Following the *in situ* crosslinking, the gels were immediately immersed in cell culture medium and 70% of the medium was exchanged with fresh medium every other day. Three to five replicates per condition were produced for all seven conditions investigated. On day 3 the samples were fixed with 4% paraformaldehyde for 15 min at RT and immunostained thereafter.

Immunocytochemistry for *in vitro* Experiments

After fixation and washing with PBS the samples were permeabilized using 0.1% Triton X-100 for 10 min. The samples were blocked with 2% BSA and 2% goat serum in PBS for 3 h and incubated over night with the primary antibodies mouse anti-CD31 (BD 555444; 1:100) at 4°C. After 3 washes with PBS/0.1% BSA, the secondary antibody Alexa Flour 488 goat anti-mouse (Life Technologies 1:200) was added and incubated over night at 4°C. Samples were washed and incubated with Hoechst 33342 (Life Technologies; 1:200) over night at 4°C. Fluorescent images were captured using a Dragonfly Spinning Disk confocal microscope (Andor). At least three images were taken at different positions within each hydrogel. Fields and samples for imaging and quantification were chosen randomly for all experiments.

Statistical Analysis

Statistical analysis was performed using RStudio. Sample sizes were designed with adequate power according to our previous studies and to the literature. All data were tested for normal distribution by using the Shapiro–Wilk test. Normally distributed data was tested for differences with a two-tailed unpaired one-sample *t*-test to compare differences between two groups (vascular repair in stroke mice, retinal development, *in vitro* model, Alzheimer's patients). Multiple comparisons were assessed using ANOVA followed by Tukey's HSD *post hoc* test (time course of developmental brain vasculature). Data are expressed as mean ± SD and statistical significance was defined as $^{*}p < 0.05$, $^{**}p < 0.01$, and $^{***}p < 0.001$.

DATA AVAILABILITY STATEMENT

The datasets generated for this study are available on request to the corresponding author.

ETHICS STATEMENT

The animal study was reviewed and approved by the Cantonal Veterinary Department of Zurich. The studies involving human participants were reviewed and approved by the Netherlands Brain Bank. The patients/participants provided their written informed consent to participate in this study.

AUTHOR CONTRIBUTIONS

RR, TK, and MS designed the study, prepared the figures, and wrote the manuscript. RR, TK, LG, BD, YL, and AM carried out the experiments. TK, BL, LK, RN, CW, and CT provided tissue and/or the Cldn5-eGFP mouse model. TK, LG, MS, and CT proof-read and revised the manuscript. All authors read and approved the final manuscript.

SUPPLEMENTARY MATERIAL

The Supplementary Material for this article can be found online at: https://www.frontiersin.org/articles/10.3389/fnins.2020.00244/full#supplementary-material

REFERENCES

Alcala, N., Mangiante, L., Le-Stang, N., Gustafson, C. E., Boyault, S., Damiola, F., et al. (2019). Redefining malignant pleural mesothelioma types as a continuum uncovers immune-vascular interactions. *Ebiomedicine* 48, 191–202. doi: 10.1016/j.ebiom.2019.09.003

Braak, H., and Braak, E. (1995). Staging of Alzheimer's disease-related neurofibrillary changes. *Neurobiol. Aging* 16, 271–278. doi: 10.1016/0197-4580(95)00021-6

Brown, L. S., Foster, C. G., Courtney, J.-M., King, N. E., Howells, D. W., and Sutherland, B. A. (2019). Pericytes and neurovascular function in the healthy and diseased brain. *Front. Cell. Neurosci.* 13:282. doi: 10.3389/fncel.2019.00282

Chintala, H., Krupska, I., Yan, L., Lau, L., Grant, M., and Chaqour, B. (2015). The matricellular protein CCN1 controls retinal angiogenesis by targeting VEGF, Src homology 2 domain phosphatase-1 and Notch signaling. *Dev. Camb. Engl.* 142, 2364–2374. doi: 10.1242/dev.121913

Craver, B. M., Acharya, M. M., Allen, B. D., Benke, S. N., Hultgren, N. W., Baulch, J. E., et al. (2016). 3D surface analysis of hippocampal microvasculature in the irradiated brain. *Environ. Mol. Mutagen.* 57, 341–349. doi: 10.1002/em.22015

Ertürk, A., Lafkas, D., and Chalouni, C. (2014). Imaging cleared intact biological systems at a cellular level by 3DISCO. *J. Vis. Exp.* 89:e51382. doi: 10.3791/51382

Gautam, J., and Yao, Y. (2018). Roles of pericytes in stroke pathogenesis. *Cell Transplant.* 27, 1798–1808. doi: 10.1177/0963689718768455

Halliday, M. R., Rege, S. V., Ma, Q., Zhao, Z., Miller, C. A., Winkler, E. A., et al. (2016). Accelerated pericyte degeneration and blood-brain barrier breakdown in apolipoprotein E4 carriers with Alzheimer's disease. *J. Cereb. Blood Flow Metab.* 36, 216–227. doi: 10.1038/jcbfm.2015.44

Hase, Y., Ding, R., Harrison, G., Hawthorne, E., King, A., Gettings, S., et al. (2019). White matter capillaries in vascular and neurodegenerative dementias. *Acta Neuropathol. Commun.* 7:16. doi: 10.1186/s40478-019-0666-x

Hyman, B. T., Phelps, C. H., Beach, T. G., Bigio, E. H., Cairns, N. J., Carrillo, M. C., et al. (2012). National institute on Aging-Alzheimer's association guidelines for the neuropathologic assessment of Alzheimer's disease. *J. Alzheimers Assoc.* 8, 1–13. doi: 10.1016/j.jalz.2011.10.007

Iadecola, C. (2017). The neurovascular unit coming of age: a journey through neurovascular coupling in health and disease. *Neuron* 96, 17–42. doi: 10.1016/j.neuron.2017.07.030

Jiang, Y., Zhou, J., Zou, D., Hou, D., Zhang, H., Zhao, J., et al. (2019). Overexpression of Limb-Bud and Heart (LBH) promotes angiogenesis in human glioma via VEGFA-mediated ERK signalling under hypoxia. *Ebiomedicine* 48, 36–48. doi: 10.1016/j.ebiom.2019.09.037

Kopylova, V. S., Boronovskiy, S. E., and Nartsissov, Y. R. (2017). Fundamental principles of vascular network topology. *Biochem. Soc. Trans.* 45, 839–844. doi: 10.1042/BST20160409

Kretschmer, S., Dethlefsen, I., Hagner-Benes, S., Marsh, L. M., Garn, H., and König, P. (2013). Visualization of intrapulmonary lymph vessels in healthy and inflamed murine lung using CD90/Thy-1 as a marker. *PLoS One* 8:e55201. doi: 10.1371/journal.pone.0055201

Kubíková, T., Kochová, P., Tomášek, P., Witter, K., and Tonar, Z. (2018). Numerical and length densities of microvessels in the human brain: correlation with preferential orientation of microvessels in the cerebral cortex, subcortical grey matter and white matter, pons and cerebellum. *J. Chem. Neuroanat.* 88, 22–32. doi: 10.1016/j.jchemneu.2017.11.005

Li, F.-J., Zhang, C.-L., Luo, X.-J., Peng, J., and Yang, T.-L. (2019). Involvement of the MiR-181b-5p/HMGB1 pathway in ang II-induced phenotypic transformation of smooth muscle cells in hypertension. *Aging Dis.* 10, 231–248. doi: 10.14336/AD.2018.0510

Ma, Q., Zhao, Z., Sagare, A. P., Wu, Y., Wang, M., Owens, N. C., et al. (2018). Blood-brain barrier-associated pericytes internalize and clear aggregated amyloid-β42 by LRP1-dependent apolipoprotein E isoform-specific mechanism. *Mol. Neurodegener.* 13:57. doi: 10.1186/s13024-018-0286-0

Maeso-Díaz, R., Ortega-Ribera, M., Lafoz, E., Lozano, J. J., Baiges, A., Francés, R., et al. (2019). Aging influences hepatic microvascular biology and liver fibrosis in advanced chronic liver disease. *Aging Dis.* 10, 684–698. doi: 10.14336/AD.2019.0127

Miao, H., Yang, Y., Wang, H., Huo, L., Wang, M., Zhou, Y., et al. (2019). Intensive lipid-lowering therapy ameliorates asymptomatic intracranial atherosclerosis. *Aging Dis.* 10, 258–266. doi: 10.14336/AD.2018.0526

Michalski, D., Grosche, J., Pelz, J., Schneider, D., Weise, C., Bauer, U., et al. (2010). A novel quantification of blood-brain barrier damage and histochemical typing after embolic stroke in rats. *Brain Res.* 1359, 186–200. doi: 10.1016/j.brainres.2010.08.045

Mier, W., and Mier, D. (2015). Advantages in functional imaging of the brain. *Front. Hum. Neurosci.* 9:249. doi: 10.3389/fnhum.2015.00249

Miners, J. S., Schulz, I., and Love, S. (2018). Differing associations between Aβ accumulation, hypoperfusion, blood-brain barrier dysfunction and loss of PDGFRB pericyte marker in the precuneus and parietal white matter in Alzheimer's disease. *J. Cereb. Blood Flow Metab.* 38, 103–115. doi: 10.1177/0271678X17690761

Montagne, A., Nikolakopoulou, A. M., Zhao, Z., Sagare, A. P., Si, G., Lazic, D., et al. (2018). Pericyte degeneration causes white matter dysfunction in the mouse central nervous system. *Nat. Med.* 24, 326–337. doi: 10.1038/nm.4482

Montoya-Zegarra, J. A., Russo, E., Runge, P., Jadhav, M., Willrodt, A.-H., Stoma, S., et al. (2019). AutoTube: a novel software for the automated morphometric analysis of vascular networks in tissues. *Angiogenesis* 22, 223–236. doi: 10.1007/s10456-018-9652-3

Nelson, A. R., Sweeney, M. D., Sagare, A. P., and Zlokovic, B. V. (2016). Neurovascular dysfunction and neurodegeneration in dementia and Alzheimer's disease. *Biochim. Biophys. Acta* 1862, 887–900. doi: 10.1016/j.bbadis.2015.12.016

Nikolakopoulou, A. M., Zhao, Z., Montagne, A., and Zlokovic, B. V. (2017). Regional early and progressive loss of brain pericytes but not vascular smooth muscle cells in adult mice with disrupted platelet-derived growth factor receptor-β signaling. *PLoS One* 12:e0176225. doi: 10.1371/journal.pone.0176225

Nyúl-Tóth, Á, Suciu, M., Molnár, J., Fazakas, C., Haskó, J., Herman, H., et al. (2016). Differences in the molecular structure of the blood-brain barrier in the cerebral cortex and white matter: an in silico, in vitro, and ex vivo study. *Am. J. Physiol. Heart Circ. Physiol.* 310, H1702–H1714. doi: 10.1152/ajpheart.00774.2015

Potente, M., and Carmeliet, P. (2017). The link between angiogenesis and endothelial metabolism. *Annu. Rev. Physiol.* 79, 43–66. doi: 10.1146/annurev-physiol-021115-105134

Reyes-Aldasoro, C. C., Williams, L. J., Akerman, S., Kanthou, C., and Tozer, G. M. (2011). An automatic algorithm for the segmentation and morphological analysis of microvessels in immunostained histological tumour sections. *J. Microsc.* 242, 262–278. doi: 10.1111/j.1365-2818.2010.03464.x

Rust, R., Gantner, C., and Schwab, M. E. (2018). Pro- and antiangiogenic therapies: current status and clinical implications. *FASEB J.* 33, 34–48. doi: 10.1096/fj.201800640RR

Rust, R., Grönnert, L., Dogançay, B., and Schwab, M. E. (2019a). A revised view on growth and remodeling in the retinal vasculature. *Sci. Rep.* 9:3263. doi: 10.1038/s41598-019-40135-2

Rust, R., Grönnert, L., Gantner, C., Enzler, A., Mulders, G., Weber, R. Z., et al. (2019b). Nogo-A targeted therapy promotes vascular repair and functional recovery following stroke. *Proc. Natl. Acad. Sci. U.S.A.* 116, 14270–14279. doi: 10.1073/pnas.1905309116

Rust, R., Grönnert, L., Weber, R. Z., Mulders, G., and Schwab, M. E. (2019c). Refueling the ischemic CNS: guidance molecules for vascular repair. *Trends Neurosci.* 42, 644–656. doi: 10.1016/j.tins.2019.05.006

Rust, R., Weber, R. Z., Grönnert, L., Mulders, G., Maurer, M. A., Hofer, A.-S., et al. (2019d). Anti-Nogo-A antibodies prevent vascular leakage and act as pro-angiogenic factors following stroke. *Sci. Rep.* 9, 1–10. doi: 10.1038/s41598-019-56634-1

Saunders, N. R., Dziegielewska, K. M., Møllgård, K., and Habgood, M. D. (2015). Markers for blood-brain barrier integrity: how appropriate is Evans blue in the twenty-first century and what are the alternatives? *Front. Neurosci.* 9:385. doi: 10.3389/fnins.2015.00385

Seaman, M. E., Peirce, S. M., and Kelly, K. (2011). Rapid analysis of vessel elements (RAVE): a tool for studying physiologic, pathologic and tumor angiogenesis. *PLoS One* 6:e20807. doi: 10.1371/journal.pone.0020807

Shen, F., Jiang, L., Han, F., Degos, V., Chen, S., and Su, H. (2019). Increased inflammatory response in old mice is associated with more severe neuronal injury at the acute stage of ischemic stroke. *Aging Dis.* 10, 12–22. doi: 10.14336/AD.2018.0205

Sweeney, M. D., Ayyadurai, S., and Zlokovic, B. V. (2016). Pericytes of the neurovascular unit: key functions and signaling pathways. *Nat. Neurosci.* 19, 771–783. doi: 10.1038/nn.4288

Sweeney, M. D., Kisler, K., Montagne, A., Toga, A. W., and Zlokovic, B. V. (2018). The role of brain vasculature in neurodegenerative disorders. *Nat. Neurosci.* 21, 1318–1331. doi: 10.1038/s41593-018-0234-x

Sweeney, M. D., Montagne, A., Sagare, A. P., Nation, D. A., Schneider, L. S., Chui, H. C., et al. (2019a). Vascular dysfunction–The disregarded partner of Alzheimer's disease. *Alzheimers Dement.* 15, 158–167. doi: 10.1016/j.jalz.2018.07.222

Sweeney, M. D., Zhao, Z., Montagne, A., Nelson, A. R., and Zlokovic, B. V. (2019b). Blood-brain barrier: from physiology to disease and back. *Physiol. Rev.* 99, 21–78. doi: 10.1152/physrev.00050.2017

Tang, X. N., Berman, A. E., Swanson, R. A., and Yenari, M. A. (2010). Digitally quantifying cerebral hemorrhage using photoshop and image J. *J. Neurosci. Methods* 190, 240–243. doi: 10.1016/j.jneumeth.2010.05.004

Visser, G., Reinten, C., Coplan, P., Gilbert, D. A., and Hammond, K. (1990). Oscillations in cell morphology and redox state. *Biophys. Chem.* 37, 383–394. doi: 10.1016/0301-4622(90)88037-s

Walter, T., Shattuck, D. W., Baldock, R., Bastin, M. E., Carpenter, A. E., Duce, S., et al. (2010). Visualization of image data from cells to organisms. *Nat. Methods* 7, S26–S41. doi: 10.1038/nmeth.1431

Wang, D. B., Blocher, N. C., Spence, M. E., Rovainen, C. M., and Woolsey, T. A. (1992). Development and remodeling of cerebral blood vessels and their flow in postnatal mice observed with in vivo videomicroscopy. *J. Cereb. Blood Flow Metab.* 12, 935–946. doi: 10.1038/jcbfm.1992.130

Wei, X., Gao, H., Zou, J., Liu, X., Chen, D., Liao, J., et al. (2016). Contra-directional Coupling of Nur77 and Nurr1 in Neurodegeneration: a novel mechanism for memantine-induced anti-inflammation and anti-mitochondrial impairment. *Mol. Neurobiol.* 53, 5876–5892. doi: 10.1007/s12035-015-9477-7

Zhang, L.-Y., Lin, P., Pan, J., Ma, Y., Wei, Z., Jiang, L., et al. (2018). CLARITY for high-resolution imaging and quantification of vasculature in the whole mouse brain. *Aging Dis.* 9, 262–272. doi: 10.14336/AD.2017.0613

Zhao, Z., Nelson, A. R., Betsholtz, C., and Zlokovic, B. V. (2015). Establishment and dysfunction of the blood-brain barrier. *Cell* 163, 1064–1078. doi: 10.1016/j.cell.2015.10.067

Zhu, K., Hu, X., Chen, H., Li, F., Yin, N., Liu, A.-L., et al. (2019a). Downregulation of circRNA DMNT3B contributes to diabetic retinal vascular dysfunction through targeting miR-20b-5p and BAMBI. *Ebiomedicine* 49, 341–353. doi: 10.1016/j.ebiom.2019.10.004

Zhu, S., Wei, X., Yang, X., Huang, Z., Chang, Z., Xie, F., et al. (2019b). Plasma lipoprotein-associated Phospholipase A2 and superoxide dismutase are independent predicators of cognitive impairment in cerebral small vessel disease patients: diagnosis and assessment. *Aging Dis.* 10, 834–846. doi: 10.14336/AD.2019.0304

Zlokovic, B. V. (2010). Neurodegeneration and the neurovascular unit. *Nat. Med.* 16, 1370–1371. doi: 10.1038/nm1210-1370

Zou, J., Chen, Z., Wei, X., Chen, Z., Fu, Y., Yang, X., et al. (2017). Cystatin C as a potential therapeutic mediator against Parkinson's disease via VEGF-induced angiogenesis and enhanced neuronal autophagy in neurovascular units. *Cell Death Dis.* 8:e2854. doi: 10.1038/cddis.2017.240

Zudaire, E., Gambardella, L., Kurcz, C., and Vermeren, S. (2011). A computational tool for quantitative analysis of vascular networks. *PLoS One* 6:e0027385. doi: 10.1371/journal.pone.0027385

Conflict of Interest: The authors declare that the research was conducted in the absence of any commercial or financial relationships that could be construed as a potential conflict of interest.

frontiers in Cellular Neuroscience

ORIGINAL RESEARCH
published: 03 April 2020
doi: 10.3389/fncel.2020.00077

Delayed PARP-1 Inhibition Alleviates Post-stroke Inflammation in Male Versus Female Mice: Differences and Similarities

Jian Chen[1,2,3†], Xiaoxi Li[1,2,3†], Siyi Xu[1,2,3], Meijuan Zhang[1,2,3], Zhengzheng Wu[1], Xi Zhang[1], Yun Xu[1,2,3] and Yanting Chen[1,2,3*]*

[1] The State Key Laboratory of Pharmaceutical Biotechnology, Department of Neurology, Drum Tower Hospital, Medical School of Nanjing University, Nanjing, China, [2] Jiangsu Key Laboratory for Molecular Medicine, Medical School of Nanjing University, Nanjing, China, [3] Jiangsu Province Stroke Center for Diagnosis and Therapy, Nanjing, China

Post-stroke inflammation is almost involved in the whole process of stroke pathogenesis, which serves as a prime target for developing new stroke therapies. Despite known sex differences in the incidence and outcome of stroke, few preclinical or clinical studies take into account sex bias in treatment. Recent evidence suggests that poly (ADP-ribose) polymerase (PARP)-1 inhibitor exerts sex-specific neuroprotection in the ischemic stroke. This study was aimed to investigate the effects of delayed PARP-1 inhibition on post-stroke inflammation and possible sexual dimorphism, and explore the possible relevant mediators. In male and female C57BL/6 mice subjected to transit middle cerebral artery occlusion (MCAO), we found that delayed treatment of PARP-1 inhibitor at 48 h following reperfusion could comparably alleviate neuro-inflammation at 72 h after stroke. Whereas, more remarkable reduction of iNOS and MMP9 induced by PARP-1 inhibition were found in male MCAO mice, and the improvement of behavioral outcomes was more prominent in male MCAO mice. In addition, we further identified that PARP-1 inhibitor might equivalently suppress microglial activation in males and females *in vivo* and *in vitro.* With proteomic analysis and western blotting assay, it was found that stroke-induced peroxiredoxin-1 (Prx1) expression was significantly affected by PARP-1 inhibition. Interestingly, injection of recombinant Prx1 into the ischemic core could block the anti-inflammatory effects of PARP-1 inhibitor in the experimental stroke. These findings suggest that PARP-1 inhibitor has effects on regulating microglial activation and post-stroke inflammation in males and females, and holds promise as a novel therapeutic agent for stroke with extended therapeutic time window. Efforts need to be made to delineate the actions of PARP-1 inhibition in stroke, and here we propose that Prx1 might be a critical mediator.

Keywords: gender, inflammation, ischemic stroke, PARP-1, microglia

OPEN ACCESS

Edited by:
Dennis Qing Wang,
Southern Medical University, China

Reviewed by:
Heng Zhao,
Stanford University, United States
Wanlin Yang,
Southern Medical University, China

****Correspondence:***
Yun Xu
xuyun20042001@aliyun.com
Yanting Chen
y.chen860606@gmail.com

† These authors have contributed equally to this work and share first authorship

Specialty section:
This article was submitted to Non-Neuronal Cells, a section of the journal Frontiers in Cellular Neuroscience

Received: *12 January 2020*
Accepted: *17 March 2020*
Published: *03 April 2020*

Citation:
Chen J, Li X, Xu S, Zhang M, Wu Z, Zhang X, Xu Y and Chen Y (2020) Delayed PARP-1 Inhibition Alleviates Post-stroke Inflammation in Male Versus Female Mice: Differences and Similarities. Front. Cell. Neurosci. 14:77. doi: 10.3389/fncel.2020.00077

INTRODUCTION

Ischemic stroke is one of the major causes of morbidity and mortality worldwide. To date, intravenous thrombolysis, and thrombectomy are approved efficient therapies for ischemic stroke patients (Lambertsen et al., 2019; Tao et al., 2019; Yang et al., 2019). However, due to the narrow therapeutic time window and a cascade of pathophysiological events induced by reperfusion, the

recanalization therapies are only available for a small fraction of stroke patients (Bosetti et al., 2017; Ma et al., 2019). Therefore, novel therapeutic options for cerebral ischemia are urgently needed. New treatments targeting key pathogenic mechanisms are currently being explored in the preclinical and clinical stroke research, either alone or in combination with reperfusion therapies (George and Steinberg, 2015; Bosetti et al., 2017). Inflammation is integral to the whole process of stroke pathogenesis, thus serving as a prime target for the development of new stroke therapies (Shao et al., 2019; Zhu et al., 2019), and potentially providing a clinically accessible time window for initiating therapy (Chen et al., 2014).

Poly (ADP-ribose) polymerase (PARP)-1 is an abundant nuclear protein, which plays a critical role in various DNA repair pathways and in the maintenance of genomic stability (Wang et al., 2016; Ray Chaudhuri and Nussenzweig, 2017). Accumulating evidence reveals that excessive activation of PARP-1 contribute to pathogenesis of many diseases including ischemic stroke (Bai and Canto, 2012; Charriaut-Marlangue et al., 2018). Several PARP inhibitors have entered clinical trials for cancer and other diseases (Curtin and Szabo, 2013; Wang et al., 2016). PARP-1 inhibitor also displays exciting therapeutic potential in experimental and clinical stroke studies. PJ34, a PARP inhibitor, can inhibit the activation from PARP to PAR and preserve intracellular NAD + levels, thus improves mitochondrial function (Zha et al., 2018). Xu et al. (2016) suggested that PJ34 (given immediately after ischemia followed by one injection per day until the third day) along could block microglial activation and alleviate post-stroke neuro-inflammation. Besides, PJ34 (given combined with rt-PA at 6 h after ischemia) was also proven to reduce rt-PA-induced BBB breakage and hemorrhagic transformations (Haddad et al., 2013; Teng et al., 2013). Moreover, the recent clinical availability of the PARP inhibitor Lynparza (olaparib) has been proposed for potential therapeutic repurposing for non-oncological indications including stroke (Berger et al., 2018).

Sexual dimorphism was well-documented in the pathophysiology, incidence and severity of stroke. Importantly, post-stroke inflammation was sex-specific, for instance, inflammatory cells like resident microglia and peripheral T cells, and response to CNS injury with sextual difference (Ahnstedt and McCullough, 2019; Kerr et al., 2019). However, few investigations take into account possible gender bias of stroke patients in the response to treatments in the preclinical research (Sohrabji et al., 2017), thereby potential gender associated pathogenesis could be neglected. Recent evidence indicates that PARP activation plays a key role in the ischemic sexual dimorphism (Yuan et al., 2009). PARP-1 stimulates the production of poly (ADP-ribose) polymerase (PAR) and release of apoptosis inducing factor (AIF) from the mitochondria in males, leading to cell death, whereas the PARP-1/AIF pathway does not play a causal role in stroke-induced cell death in females, which might be associated the finding that immediately PARP-1 inhibition after ischemia alleviate ischemic brain injury only in males (Lang and McCullough, 2008; Yuan et al., 2009). Interestingly, several previous studies have shown that PARP inhibition preferentially protects males in the experimental stroke (Hagberg et al., 2004; Waye, 2009; Yuan et al., 2009). Moreover, in an open-label evaluator-blinded clinical study, gender-dependent effects were observed in the neuroprotection of oral minocycline (a putative PARP inhibitor) treatment in the ischemic stroke (Amiri-Nikpour et al., 2015). Recognition of the possible sex differences in the stroke research will play an critical role in the translational success of novel therapeutic agents.

In this study, we attempted to investigate the effects of delayed PARP-1 inhibition on post-stroke neuro-inflammation and behavioral performance in male and female mice. We further aimed to identify key mediators underlying the actions of PARP-1 inhibitor in the ischemic stroke. Moreover, PARP-1 inhibitor was administrated at 48 h following ischemia/referfusion, in order to comfirm that whether PARP-1 inhibitor could potentially provide an extended time window for stroke treatment.

MATERIALS AND METHODS

Animals

Adult male and female C57BL/6 mice (22–26 g, 8 to 10 weeks old) were purchased from the Model Animal Research Center of Nanjing University (Nanjing, China). All animals were housed in a specific pathogen-free facility with a 12 h light/dark cycle. Food and water were available *ad libitum*. All efforts were made to minimize animal suffering and the number of animals used. All animal experiments were approved by the Institutional Animal Care and Use Committee of Nanjing University.

Middle Cerebral Artery Occlusion

The transient middle cerebral artery occlusion (MCAO) was conducted to induce focal ischemia as previously described (Chen et al., 2019). Briefly, mice were anesthetized with 1.5% isoflurane in a 68.5% N_2O/30% O_2 mixture. Transient focal ischemia was induced by intraluminal occlusion of the right middle cerebral artery (MCA) for 50 min. At first, a 1-cm long midline neck incision was made and the right external carotid artery (ECA) was exposed and isolated from the adjacent tissue. Then, a silicone-rubber-coated 6-0 nylon filament (Doccol, United States) was inserted into the internal carotid artery via the proximal ECA and further inserted to the circle of Willis to achieve the MCAO. After 50 min of occlusion, the monofilament was withdrawn to allow reperfusion. Sham-operated mice were subjected to the same procedure without occlusion of MCA. Mice exposed to MCAO were placed in a 35°C nursing box for anesthesia recovery.

PARP-1 Inhibitor PJ34 and Recombinant Mouse Peroxiredoxin 1 (Prx1) Injection

The MCAO mice were intraperitoneally (i.p.) administrated with either vehicle or N-(6-Oxo-5.6-dihydrophenanthridin-2-yl)- (N, N-dimethylamino) acetamide hydrochloride (PJ34, 30 mg/kg, Tocris Bioscience, United States) 48 h after MCAO. For Prx1 injection, 48 h after MCAO, mice were fixed in a stereotactic frame, and Prx1 (Sigma, United States, 2 μl/mouse) was injected

to the right ischemic striatum using the following microinjection coordinates: anteroposterior, −0.5 mm; lateral, 2.0 mm; and ventral, 3.5 mm.

Quantitative Real-Time Polymerase Chain Reaction

Total RNA was extracted from mouse brain tissue (mainly include cortex and striatum) and cultures using Trizol reagent (Invitrogen, United States). The cDNA was synthesized using a Prime Script RT reagent kit (Takara, United States) according to the protocol of the manufacturer. Real-time PCR was performed using SYBR Green (Takara, United States) with the ABI 7500 PCR instrument (Applied Biosystems, United States) as previously described (Liu et al., 2019). The primer sequences used in this study were listed as follows:

GAPDH forward primer, 5′-GCCAAGGCTGTGGGCAAGGT-3′';
GAPDH reverse primer, 5′'-TCTCCAGGCGGCACGTCAGA-3′';
INOS forward primer, 5′'-CAAGCACCTTGGAAGAGGAG-3′';
INOS reverse primer, 5′'-AAGGCCAAACACAGCATACC-3′';
IL-1β forward primer, 5′'-GCAACTGTTCCTGAACTCAACT-3′';
IL-1β reverse primer, 5′'-ATCTTTTGGGGTCCGTCAACT-3′';
TNFα forward primer, 5′'-CCCTCACACTCAGATCATCTTCT-3′';
TNFα reverse primer, 5′'-GCTACGACGTGGGCTACAG -3′';
MMP9 forward primer, 5′'-CTGGACAGCCAGACACTAAAG-3′';
MMP9 reverse primer, 5′'-CTCGCGGCAAGTCTTCAGAG-3′';
CD11b forward primer, 5′'-CCAAGACGATCTCAGCATCA-3′';
CD11b reverse primer, 5′'-TTCTGGCTTGCTGAATCCTT-3′';
Iba-1 forward primer, 5′'-TCCTCCGGCCCATGATTAAAG-3′';
Iba-1 reverse primer, 5′'-CTGTCTGGCTGCCCATTCT-3′';
GFAP forward primer, 5′'-CGGAGACGCATCACCTCTG-3′';
GFAP reverse primer, 5′'-AGGGAGTGGAGGAGTCATTCG-3′';
CD16 forward primer, 5′'-TTTGGACACCCAGATGTTTCAG-3′';
CD16 reverse primer, 5′'-GTCTTCCTTGAGCACCTGGATC-3′';
CD206 forward primer, 5′'-CAAGGAAGGTTGGCATTTGT-3′';
CD206 reverse primer, 5′'-CCTTTCAGTCCTTTGCAAGC-3′';
TGF-β forward primer, 5′'-AACTATTGCTTCAGCTCCACAGAG-3′';
TGF-β reverse primer, 5′'-AGTTGGATGGTAGCCCTTG-3′';
Prx1 forward primer, 5′'- CAA GTG ATT GGC GCT-3′';
Prx1 reverse primer, 5′'-GGT CCC AAT CCT CCT TG-3′';
Prx6 forward primer, 5′'-CCAGCACTGATCTAGGTCTCC-3′';
Prx6 reverse primer, 5′'-ATGCCCCATGAATCTCCCAG-3′'.

Western Blotting

Tissues were resected from the brain of MCAO mice and further homogenized and lysed using the lysis buffer (Thermo Fisher Scientific, United States) containing 1% protease inhibitor cocktail (Sigma-Aldrich, United States) as described previously (Deng et al., 2019). Protein concentration was determined using Bicinchoninic Acid assay (Beyotime Biotechnology, China). Equal amounts of total protein from each sample were separated by SDS-PAGE and blotted onto PVDF membranes. Then, the membranes were incubated with primary antibodies, including CD11b (1:1000; Abcam, United States), GFAP (1:1000; Abcam, United States), Prx1 (1:1000; Abcam, United States), Prx6 (1:1000; Abcam, United States), and β-Actin (1:5000; Bio-Rad, United States). Secondary antibodies were horseradish peroxidase (HRP)–conjugated antibodies (Bio-Rad, United States). Protein bands were detected using a chemiluminescent substrate kit (Millipore, United States). Image-Pro Plus (National Institutes of Health, United States) was used to analyze the intensities of the bands.

Behavior Test

The modified neurological severity score (mNSS) and grip strength were employed to assess the neurological performance of the MCAO mice 24 h after PJ34 administration as described previously (Meng et al., 2019). mNSS score: the test was performed mainly to assess the motor, reflex, sensory, and balance deficits with a score range from 0 to 18 (0: normal; 18: maximal deficit score). Grip strength: Grip strength was measured using a Panlab machine (LE902, United States). Briefly, the mouse was allowed to hold the platform of the grip-strength machine using the front paws and then the mouse was pulled in a straight line away from the platform, each mouse was tested for three times and maximum grip strength was recorded. Neurobehavioral performance was evaluated by an observer blinded to the experiments.

Primary Microglial Culture and Drug Treatment

Primary microglia were isolated and purified from brains from postnatal 1–2 days C57BL/6 mice, with sex determined via identifying sex chromosomes as described previously (Posynick and Brown, 2019). The cerebral cortex tissues of mice were dissected and digested in Tryple (Thermo Fisher Scientific, United States) for 5 min at 37°C. After centrifugation, the cell mixture was suspended and passed through a 70 μM pore filter. Finally, cells were planted in 75 cm^2 flasks in 5% CO2 at 37°C, and the medium was half-changed at day 5. After culturing for 2 weeks, microglial cells were obtained by gently shaking the flasks. The microglia were collected, centrifuged, and then replated onto 12-well plates at a density of 2×10^5/well.

For drug administration, PARP-1 inhibitor DPQ (25 μM) was applied to the microglial culture medium combined with 500 ng/μl lipopolysaccharide (LPS) (Sigma-Aldrich, United States). After 24 h, cells were harvested for the following experiments.

Proteomic and Microarray Processing Analysis

Proteomics analysis was performed by AB SCIEX TripleTOF 5600 mass spectrometer (AB SCIEX, United States) equipped with a liquid chromatography-tandem mass spectrometry (LC-MS/MS) system. Proteins (100 μg) of each sample were resolved on SDS polyacry-lamide gels and then stained with Coomassie Blue G-250 for 4 h. After distaining in ultrapure H_2O, the gel was cut into blocks, and digested using trypsin. After being cleaned, desalted, and vacuum-dried, the peptides were analyzed. The Agilent Sure Print G3 Mouse GE V2.0 Microarray plates were conducted by Shanghai oebiotech Company of China.

Briefly, total RNA was acquired from mouse brain tissue and quantified by the NanoDrop ND-2000 (Thermo Fisher Scientific, United States). Then, RNA was purified and transcribed to double strand cDNA. Then, the cDNA was synthesized into cRNA to be hybridized onto the microarray and scanned by Agilent Scanner G2505C (Agilent Technologies, China) to acquire images and analyzed using Feature Extraction software (version10.7.1.1, Agilent Technologies, China). The bioinformatics analysis of differentially expression proteins and genes were conducted by GO (Gene Ontology) and KEGG (Kyoto Encyclopedia of Genes and Genomes) analysis.

Nitric Oxide Measurements

Production of nitric oxide (NO) *in vitro* was determined as described previously (Zhang et al., 2018). Briefly, after co-treatment of DPQ (25 μM) and LPS (500 ng/μl) for 24 h, the supernatant was mixed with an equal volume of Griess reagent and then incubated at room temperature for 15 min. Absorbance at 540 nm was measured to determine NO production. Four replicate wells were used in this experiment.

Statistical Analysis

Comparisons between groups were carried out by one-way analysis of variance (ANOVA) followed by Bonferroni-corrected *post hoc* tests. Comparative differences were considered significant at $P < 0.05$. The statistical software package Sigma Stat 11.5 (SPSS) was used to perform all analysis. Data are presented as means ± SEM.

RESULTS

PARP-1 Inhibitor PJ34 Alleviated Post-stroke Neuro-Inflammation and Neurological Deficits in Males Versus Females

This study was commenced by investigating whether delayed PARP-1 inhibition could mitigate post-stroke inflammation and neurological deficits, and whether there was a sex bias in the effects of PARP-1 inhibition. PARP-1 inhibitor PJ34 was given to both male and female MCAO mice after 48 h of reperfusion, 24 h following PJ34 administration, inflammatory profiles in all groups of mice were assessed. Quantitative real-time PCR was employed to detect inflammatory cytokines in the ipsilateral cortex of the MCAO mice. As shown in **Figure 1A**, cerebral ischemia induced substantial inducible nitric oxide synthase (iNOS) expression in males, which was significantly attenuated by PJ34 treatment. Whereas, no evident induction of iNOS was observed in female MCAO mice. In addition, we found that cerebral ischemia resulted in remarkably increased mRNA expression of interleukin (IL)-1β in both male and female mice, which were consistently reversed by PRAP-1 inhibition (**Figure 1B**). Alteration of matrix metallopeptidase 9 (MMP9) displayed a similar pattern as iNOS (**Figure 1C**). Tumor necrosis factor (TNF) -α was significantly increased in males and females after ischemia. A downward trend of TNF -α by PARP-1 inhibition was observed in both genders (**Figure 1D**). Behavioral

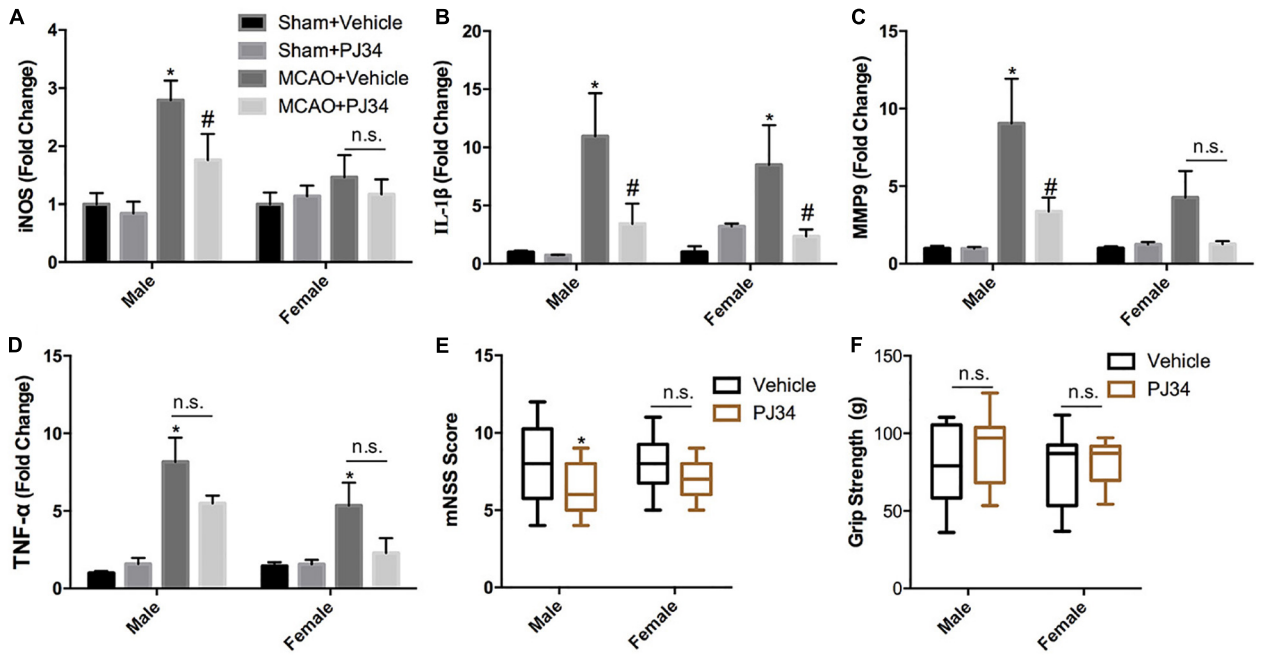

FIGURE 1 | PARP-1 inhibitor PJ34 alleviated post-stroke neuro-inflammation and neurological deficits in males versus females. PARP-1 inhibitor PJ34 was administrated to both males and females at 48 h after MCAO, 24 h later, ipsilateral cortexes were isolated and real-time PCR was performed to detect the mRNA level of pro-inflammatory cytokines, including **(A)** iNOS, **(B)** IL-1β, **(C)** MMP9, and **(D)** TNF-α. Values are presented as mean ± SEM for three mice in each group. $^*P < 0.05$ versus sham + Vehicle groups, $\#P < 0.05$ versus MCAO + Vehicle groups. The behavioral performance of male and female MCAO mice was evaluated by **(E)** mNSS and **(F)** Grip strength. Values are the median (25th and 75th percentiles), $n = 14–16$. $^*P < 0.05$ versus Vehicle groups. n.s., no significance.

tests were further performed to evaluate the therapeutic effects of delayed PARP-1 inhibition on neurological deficit of MCAO mice. As shown in **Figure 1E**, delayed administration of PJ34 improved neurological functions in the male group with a lower mNSS, whereas a minor improvement of the neurological deficits was found in the female group (**Figure 1E**). No significant improvement of grip strength was observed in both male and female MCAO mice (**Figure 1F**). These data demonstrated that delayed PARP-1 inhibitor PJ34 administration could mitigate post-stroke neuro-inflammation in both males and females. This regulatory effects of delayed PARP-1 inhibition, however, were not completely consistent in both genders, and the improvement of neurological deficits was more pronounced in male MCAO mice.

PARP-1 Regulates Inflammatory Response After Stroke in Males Versus Females

In addition, mRNA microarray was further performed to explore the influence of delayed administration of PJ34 on the molecular profile in the ischemic cortex in both males and females ($n = 3$ mice per group). GO analysis was employed to evaluate the biological characteristics of the differentially expressed genes (fold change ≥ 2.0 and $p < 0.05$) in three aspects: biological process, molecular function and cellular component. As shown in **Figures 2A,B**, GO analysis indicated that differentially expressed genes affected by delayed PJ34 treatment after MCAO were mainly associated with inflammatory response regulation in both males and females. Briefly, in the male group, differentially expressed genes were mainly enriched in inflammatory response, cellular response to IL-1 and leukocyte migration involved in inflammatory response, et cetera. Whereas, in the female group, differentially expressed genes were mostly related to immune system process, positive regulation of blood coagulation and peptidyl- cysteine S- nitrosylation. Moreover, KEGG pathway analysis was performed to analyze the potential pathways altered by PJ34 in males and females in stroke. Consistent with the results of GO analysis, the differentially expressed genes affected by PJ34 were abundantly enriched in pathways that are implicated in modulating inflammation. In the male MCAO mice, the differentially expressed genes were mainly located in IL-17 signaling pathway, cytokine-cytokine receptor interaction and Natural killer cell mediated cytotoxicity, et cetera (**Figure 2C**). In the female group, complement and coagulation cascades, ECM-receptor interaction, and IL-17 signaling pathways were significantly influenced by delayed treatment of PARP-1 inhibitor in the ischemic stroke (**Figure 2D**). These markedly affected biological processes and pathways might account for the similarities and differences underlying the effects of PARP-1 inhibition in post-stroke inflammation.

PARP-1 Inhibition Modulates Microglial Activation After Cerebral Ischemia

Microglia and astrocytes are the two main resident components of resident immune cells in the ischemic brain (Cserep et al., 2019). Since delayed treatment of PJ34 was found to suppress neuro-inflammation in the ischemic brain, we further explored whether delayed PARP-1 inhibition could block the activation of microglia or astrocytes. Microglial and astrocytic activation were evaluated as described previously (Cheon et al., 2017; Jiang et al., 2017). CD11b and Iba-1 were used as microglial activation markers, and GFAP was used to assess the activation level of astrocytes. At first, we evaluated the mRNA expression of CD11b, Iba-1, and GFAP via quantitative real-time PCR. It was demonstrated that delayed PJ34 administration significantly reduced the mRNA level of CD11b in the ischemic brain in both of the male and female groups (**Figure 3A**). In addition, Iba-1 expression was also down-regulated by PARP-1 inhibition in both males and females (**Figure 3B**). On the contrary, delayed PARP-1 suppression did not affect GFAP mRNA level (**Figure 3C**). To further examine whether PJ34 affected the polarization of microglia in the ischemic brain, pro-inflammatory microglial marker (CD16) and anti-inflammatory microglial markers (CD206 and TGF-β) were detected using real-time PCR, our findings indicated that PJ34 reduced expression of both CD16, CD206, and TGF-β in the MCAO mice of both genders (**Figures 3D–F**), which suggested that PARP-1 inhibitor simultaneously affected the pro-inflammatory and anti-inflammatory microglial activation induced by cerebral ischemia. Furthermore, western blotting assay was further performed to validate the protein levels of inflammatory markers. In consistent with the alteration of mRNA expression, PJ34 down-regulated the protein level of CD11b in both of the male and female MCAO mice, while GFAP protein level was not affected (**Figure 3G** and **Supplementary Figure S1**). Thus, our results indicated that PARP-1 inhibitor might attenuate neuro-inflammation by targeting the microglial activation after stroke.

PARP-1 Inhibition Alleviates Microglial Activation *in vitro*

To further validate that PARP-1 inhibition block microglial activation *in vitro*, primary microglia with sex identified were cultured and subjected to co-treatment of LPS and PARP-1 inhibitor DPQ. Real-time PCR results demonstrated that PARP-1 inhibitor DPQ blocked microglial activation induced by LPS, with decreased mRNA levels of CD11b and CD32 in both of the male and female groups (**Figures 4A,B**). In addition, PARP-1 inhibitor could also mitigate the LPS- induced elevation of iNOS mRNA levels and NO release (**Figures 4C,D**).

PARP-1 Suppression Affects Peroxiredoxins in MCAO Mice

To elucidate the molecular mechanisms underlying the effects of PARP-1 inhibition in stroke, protein mass spectrometry was conducted to screen key mediators. Peroxiredoxins (Prxs) are a family of thioredoxin peroxidases that activate the Toll-like receptor 4 in immune cells and initiate neuro-inflammation after ischemic stroke (Garcia-Bonilla and Iadecola, 2012; Liu et al., 2018). As shown in **Figures 5A,B**, Prxs were significantly altered by PJ34 both in male and female MCAO mice. Real-time PCR was used to detect the mRNA levels of peroxiredoxin 1 (Prx1) and peroxiredoxin 6 (Prx6),which are abundant in microglia.

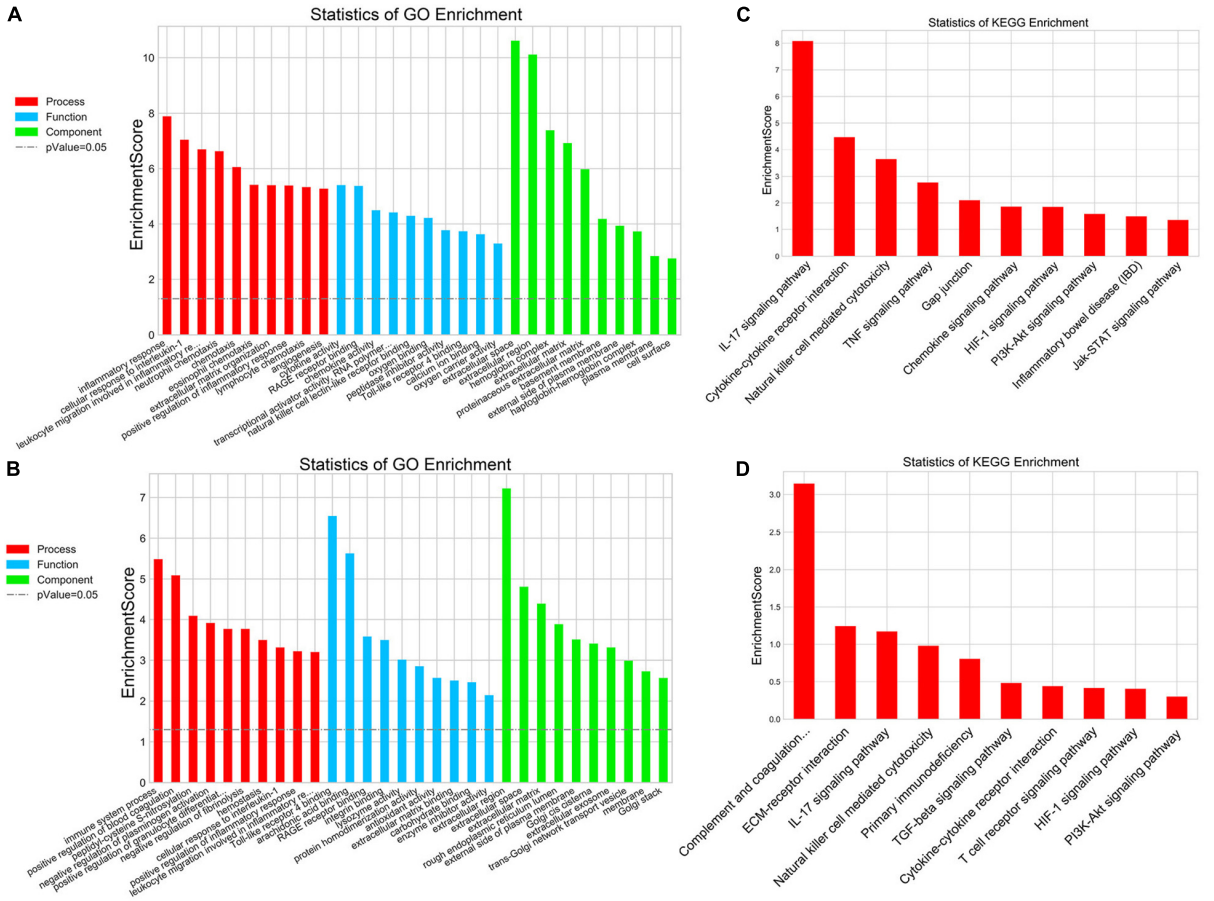

FIGURE 2 | PARP-1 regulated inflammatory response after stroke in males and females. GO analysis of the differentially expressed genes (MCAO + Vehicle versus MCAO + PJ34, fold change ≥ 2, $p < 0.05$) in **(A)** the male group and **(B)** the female group, including three aspects: biological process, cellular component, and molecular function. KEGG pathway analysis of the differentially expressed genes (MCAO + Vehicle versus MCAO + PJ34, fold change ≥ 2, $p < 0.05$) in **(C)** the male group and **(D)** the female group, $n = 3$ mice per group.

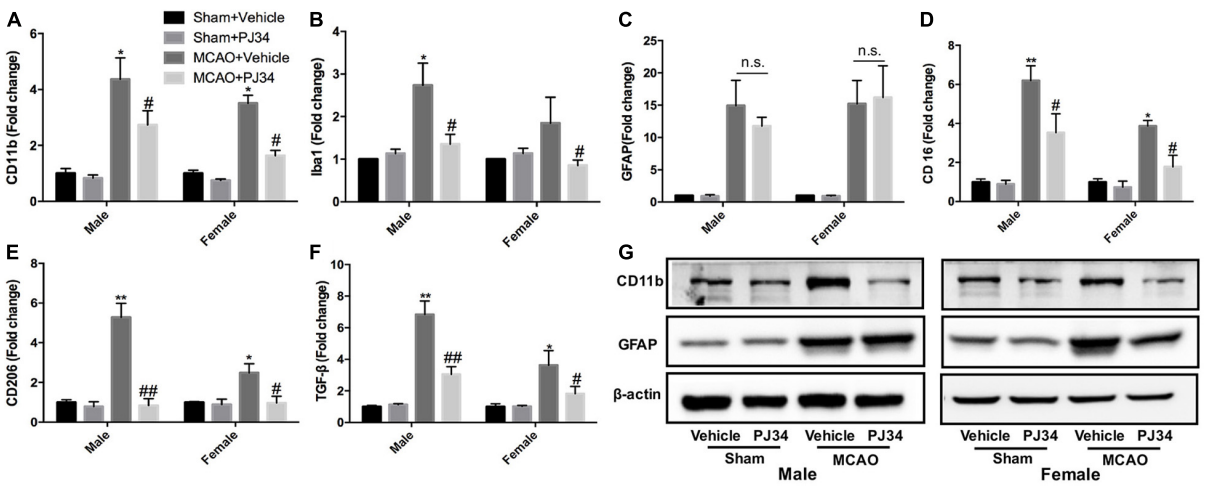

FIGURE 3 | PARP-1 inhibition modulated microglial activation after cerebral ischemia. Relative mRNA level of inflammatory mediators in cortexes from male and female groups were detected via real-time PCR, including **(A)** CD11b, **(B)** Iba-1, **(C)** GFAP, **(D)** CD16, **(E)** CD206, and **(F)** TGF-β. Values are presented as mean ± SEM for three mice in each group. $^*P < 0.05$ and $^{**}P < 0.01$ versus sham + Vehicle groups, $\#P < 0.05$ and $\#\#P < 0.01$ versus MCAO + Vehicle groups. **(G)** CD11b and GFAP protein level were detected via western blotting. n.s., no significance.

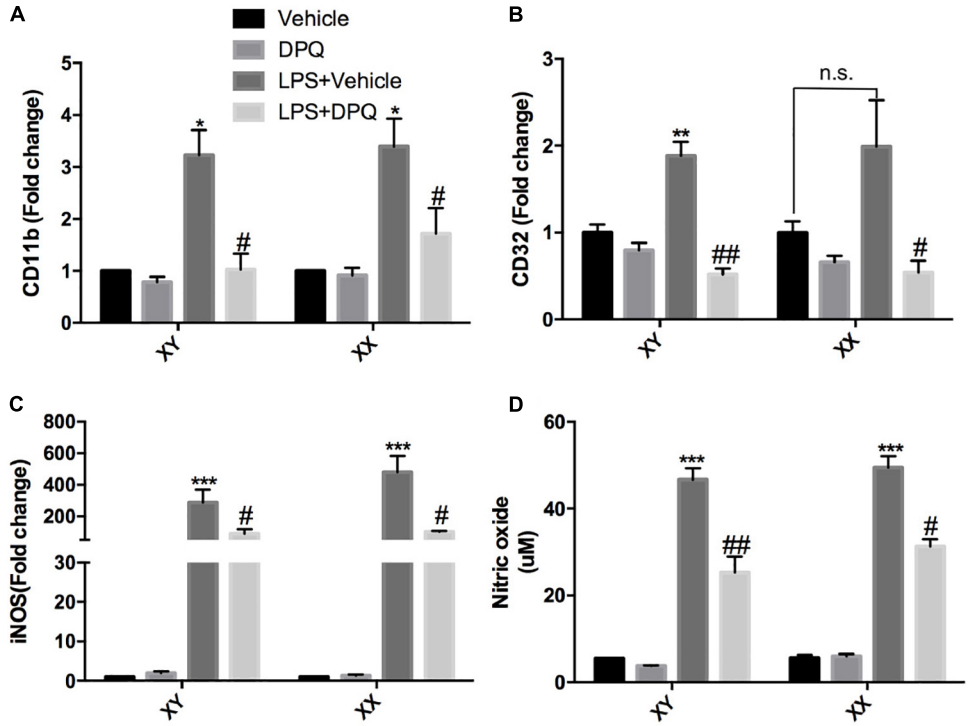

FIGURE 4 | PARP-1 inhibition alleviated microglial activation *in vitro.* Relative mRNA level of inflammatory factors in sex-segregated (XY, male; XX, female) primary microglia were detected via real-time PCR, including **(A)** CD11b, **(B)** CD32, and **(C)** iNOS. **(D)** NO production measured by Griess assay. Values are presented as mean ± SEM in each group of three to four independent experimental procedures. $^{*}P < 0.05$, $^{**}P < 0.01$, and $^{***}P < 0.001$ versus Vehicle groups, $\#P < 0.05$ and $\#\#P < 0.01$ versus LPS + Vehicle groups. n.s., no significance.

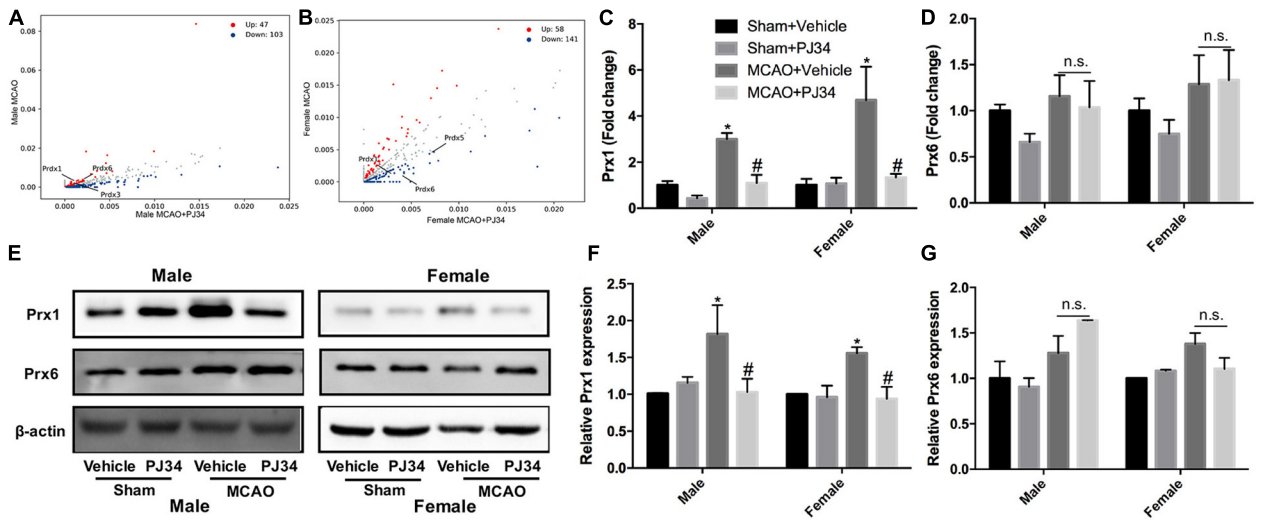

FIGURE 5 | PARP-1 suppression regulated peroxiredoxins in MCAO mice. Scatter plots assessing the variations in protein expression between vehicle and PJ34 treatment group in **(A)** males and **(B)** females. Relative expression of **(C)** Prx1 and **(D)** Prx6 mRNA level were detected via quantitative PCR. Values are presented as mean ± SEM in each group of three independent experimental procedures. $^{*}P < 0.05$ versus sham + Vehicle groups, $\#P < 0.05$ versus MCAO + Vehicle groups. **(E)** Representative western blotting results of Prx1 and Prx6 in both male and female MCAO mice. **(F)** Quantification of the western blotting result of Prx1. **(G)** Quantification of the western blotting result of Prx6. Values are presented as mean ± SEM for three mice in each group. $^{*}P < 0.05$ versus sham + Vehicle groups, $\#P < 0.05$ versus MCAO + Vehicle groups. n.s., no significance.

A substantial decrease of Prx1 was observed in both male and female MCAO mice (**Figure 5C**), whereas no evident alteration of Prx6 mRNA level was found in MCAO mice of both genders (**Figure 5D**). Consistently, Prx1 protein level in the ischemic cortex from either male or female mice was significantly reduced by PJ34, while Prx6 protein level was not affected (**Figures 5E–G**).

Exogenous Prx1 Reverses the Effects of PARP-1 Inhibition in the Experimental Stroke

To further confirm whether PARP-1 regulated microglial activation and aggravated post-stroke inflammation via Prx1, recombinant mouse Prx1 together with PJ34 were injected into the ischemic striatum, where microglia was abundantly clustered in both males and females. Quantitative PCR and western blotting were performed to evaluate the neuro-inflammation profiles. As shown in **Figure 6**, the exogenous recombinant Prx1 could block the inhibitory effects of PJ34 on post-stroke inflammation in the male MCAO mice,as the reduction of Iba-1, iNOS, and TNF-α mRNA levels induced by PARP-1 inhibition were reversed by Prx1. Consistently, reduction of mRNA level of Iba-1 and iNOS were also reversed by exogenous Prx1 in female MCAO mice, although TNF-α mRNA level was not significantly up-regulated (**Figures 6A–C**). Besides, Prx1 injection could also reverse the CD11b protein level reduction induced PJ34 in both males and females (**Figures 6D,E**). Collectively, these data showed that exogenous Prx1 rescued the inhibition of both microglial activation and neuro-inflammation induced by PARP-1 suppression.

DISCUSSION

This study has shown that delayed treatment of PARP-1 inhibitor at 48 h after ischemic stroke could prominently suppress microglial activation, and mitigate both post-stroke neuro-inflammation and neurological deficits. It is worthy to note that the regulatory effects of delayed PARP-1 inhibition on post-stroke inflammation are comparable in males and females. However, the extent of decline in inflammatory cytokines not completely consistent and improvement of neurological performance was more prominent in males. In addition, our study also demonstrated that Prx1 might be a critical mediator for the actions of PARP-1.

PARP-1, a major member of PARP family, plays an important role in a variety of biological functions, including DNA repair, genomic stability, and gene expression (Gibson et al., 2016). PARP-1 inhibitor has been approved for clinical treatments for several tumors, such as ovarian cancers (Lin and Kraus, 2017), microsatellite unstable cancers (Chan et al., 2019) and pancreatic cancers (Tuli et al., 2019), with satisfactory clinical effects and safety. Interestingly, the potential of PARP-1 inhibitor in non-tumor diseases has been put forward by some researchers and clinical physicians, especially in the scope of CNS diseases. In the brain, mild DNA damage activates PARP-1 to help DNA repair

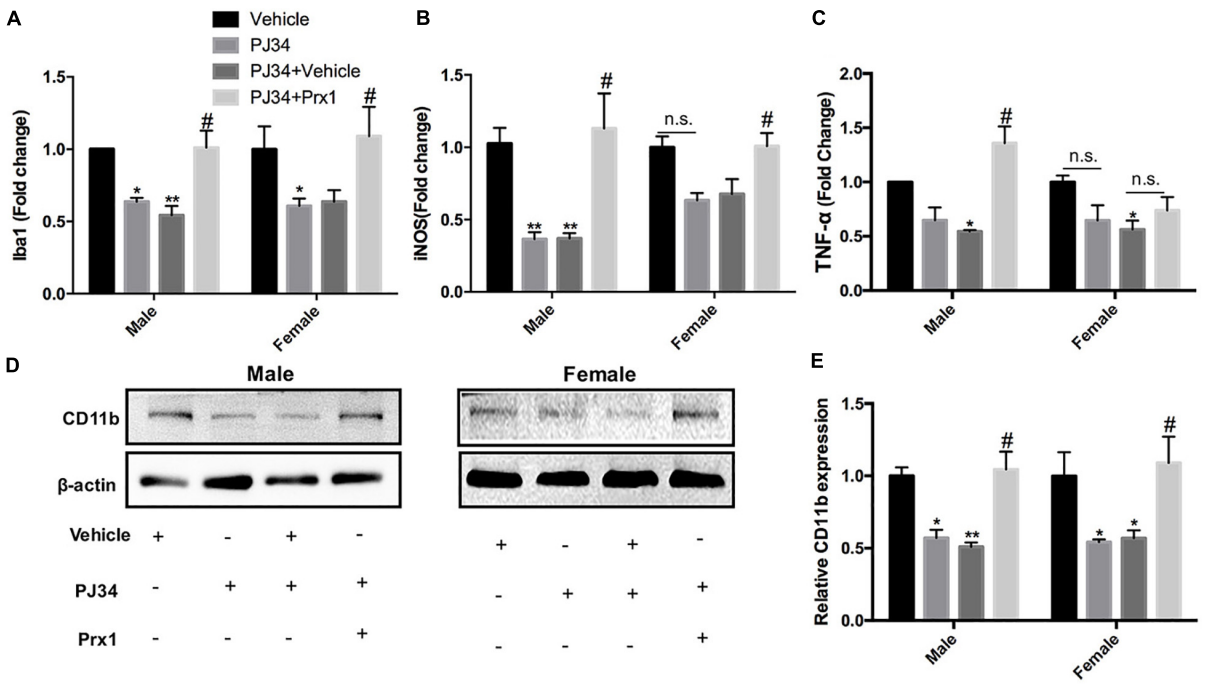

FIGURE 6 | Exogenous recombinant Prx1 reversed the effects of PARP-1 inhibition in the experimental stroke. Relative mRNA expression level in striatum in male and female groups ($n = 3$) were detected via quantitative PCR, including **(A)** Iba-1, **(B)** TNF-α, and **(C)** iNOS. Values are presented as mean ± SEM for three mice in each group. **(D,E)** CD11b protein level was detected via western blotting. $^{*}P < 0.05$ and $^{**}P < 0.01$ versus Vehicle groups, $\#P < 0.05$ versus PJ34 + Vehicle groups. n.s., no significance.

and cell survival. However, excessive PARP-1 activation results in an energy-consuming cellular process, which ultimately leads to neuronal cell death (Schreiber et al., 2006). In addition, PARP-1 has also been shown to modulate neuro-inflammation and adaptive immunity (Rosado et al., 2013). In the ischemic stroke, Koh et al. reported that PARP-1 inhibitor (3-AB, given at 15 min before MCAO) could reduce ischemic cell death and neuro-inflammatory response,with inflammatory cytokines including CD11b and IL-1β down-regulated in the 3-AB treatment group (Koh et al., 2004). Xu et al. (2016) found that PARP-1 inhibitor (PJ34, given immediately after MCAO and followed by one injection per day until brain harvest at 72 h after injury) could block post-stroke microglial activation and reduce MMP9 level. Overall, previous studies mainly focused on the effects of immediate PARP-1 inhibitor administration on post- stroke inflammation. However, few attention had been paid on whether delayed PARP-1 inhibitor treatment, especially after the acute phase of cell death, could also alleviate neuro-inflammation, which is of great significance. In this study, PARP-1 inhibitor PJ34 was given to male and female MCAO mice at 48 h after MCAO, and our results demonstrated that delayed delivery of PJ34 could significantly block post-stroke microglial activation, alleviate neuro-inflammation in male and female MCAO mice (**Figures 1**–**3**). *In vitro*, PJ34 was also found to inhibit LPS-induced primary microglial activation (**Figure 4**). Therefore, our findings indicated that delayed PARP-1 inhibition at 48 h could significantly alleviate neuro-inflammation, with a widen time window providing possibility of intervention.

It is widely acknowledged that the pathophysiology and functional outcomes of ischemic stroke are sexually dimorphic and age-dependent (Lang and McCullough, 2008; Shen et al., 2019). Tissue plasminogen activator (tPA) improves stroke outcomes for both sexes while females display more robust improvement in stroke outcome (Sohrabji et al., 2017). Despite greater age and higher rate of atrial fibrillation, females displayed comparable functional outcomes and greater years of optimal life after endovascular stroke thrombectomy compared with males (Sheth et al., 2019). PARP-1 was definitely over-activated in both males and females, and inhibition of PARP-1 was proven to dramatically reduce ischemia-induced PAR formation in both sexes (Yuan et al., 2009; Jog and Caricchio, 2013). Therefore, PARP-1 inhibitors hold promise in clinical treatment for ischemic stroke. However, it is controversial that whether gender dimorphism exists in the neuroprotective effects of PARP-1 inhibitor in stroke. Interfering PARP-1 signaling was reported to alleviate ischemic brain injury in males while aggravate brain injury in females (Yuan et al., 2009; Liu et al., 2011). In contrast, it was observed that PARP inhibition modulated microglial phenotypes, improved behavioral functions, and myelination during adulthood only in female mice following neonatal ischemia (Charriaut-Marlangue et al., 2018). On the contrary, the sex differences were not observed in some studies. In a primate study of stroke, the PARP inhibitor MP-124 showed comparable protective effects in both sexes (Matsuura et al., 2011). Likely, Du et al. (2004) showed that PARP inhibition was equally protective in sex-segregated primary cortical neurons exposed to nitrosative stress. In this study, we compared the innate gender-based proclivity in response to delayed PARP-1 inhibition in the experimental stroke. Our findings demonstrated that neuro-inflammation at 72 h after MCAO were comparably mitigated by delayed treatment of PARP-1 inhibitor PJ34 (**Figures 1**, **3**), and PARP-1 inhibition was also found to remarkably alleviate LPS-induced sex-segregated primary microglial activation *in vitro* (**Figure 4**). Our microarray assay results indicated that delayed PARP-1 inhibition could differently affect inflammatory pathways in male and female MCAO mice. Besides, inflammatory cytokines reduction induced by delayed PARP-1 inhibition were not completely consistent in males and females. For instance, more significant reduction of iNOS and MMP9 by PARP-1 inhibition were found in male MCAO mice (**Figures 1A,C**). It was widely accepted that iNOS and MMP9 play critical roles in damaging blood–brain barrier integrity and aggravating ischemic brain injury (Ransohoff, 2016; Li et al., 2018). These differences might to some extent account for the more significantly improved neurological performance in males compared to females in stroke (**Figures 1E,F**), however, the detailed mechanism of which still need our further investigation.

Much effort has been paid to explore the detailed mechanisms underlying the actions of PARP-1 in modulating cell apoptosis, necrosis, and inflammation after ischemic stroke. PARP-1 has been proven to act as a co-activator in the NF-κB-mediated transcription, which was a key modulator regulating the expression of several elements of inflammation such as cytokines, chemokines, adhesion molecules, and inflammatory mediator (Rosado et al., 2013). In this study, substantial decreases of iNOS and MMP9 by PARP-1 inhibition were only found in male MCAO mice (**Figures 1A,C**). However, our findings in parallel demonstrated that delayed PARP-1 inhibition mitigated inflammatory molecules including Iba-1, CD11b, and IL-1 β (**Figures 1A–D**) in MCAO mice of both genders. To screen, we conducted a protein mass spectrometry to explore potential molecular mechanisms underlying the effects of delayed PARP-1 inhibition on the post-stroke inflammation. Prxs are a family of antioxidant enzymes that catalyze the reduction of peroxides (Bell and Hardingham, 2011), and Prxs were markedly increased during ischemic stress (Nakamura and Shichita, 2019). PRX1 is abundant in microglia, PRX2 to 5 in neurons, and PRX6 in astrocytes (Nakamura and Shichita, 2019). Recent evidence proposed that extracellular Prxs could be a damage-associated molecular pattern molecules (DAMPs) to activate the Toll-like receptor (TLR) 2 and TLR4, resulting in aggravated post-ischemic inflammation (Shichita et al., 2012; Nakamura and Shichita, 2019). Based on the findings of proteomic analysis, we further demonstrated that Prx1 were significantly down-regulated after PJ34 treatment in both males and females with Prx6 not affected, using western blotting assay (**Figure 5**). Consistently, the microglial activation and inflammatory response were prominently suppressed (**Figures 3**, **4**). In addition, previous studies indicated that Prx1 could significantly induce the expression of TNF-α, IL-1β, and IL-6 via the Toll-like-receptor-4a-mediated NF-κB signaling pathway in stroke (Liu et al., 2016; Liu and Zhang, 2019). Prx1 level was also reported to be a biological marker for determining cerebral infarction onset (Richard et al., 2016). In this study, it was shown

that exogenous recombinant Prx1 injection reversed the anti-inflammatory effects of PARP-1 inhibition (**Figure 6**), which further validated our hypothesis that PARP-1 inhibition might block microglial activation and alleviate neuro-inflammation via down-regulating Prx1.

CONCLUSION

In conclusion, we for the first time investigated the effects of delayed PARP-1 inhibition on post-stroke inflammation in males versus females. Our findings revealed that delayed treatment of PARP-1 inhibitor could comparably suppress microglial activation and alleviate post-ischemic neuro-inflammation. We further proposed that Prx1 might be a critical factor involved in the actions of PARP-1 inhibitor in both males and females in the ischemic stroke. However, more significant reduction of iNOS and MMP9 induced by PARP-1 inhibition and better neurological functions were found in male MCAO mice, indicating gender differences of PARP-1 inhibitor treatment for stroke. Further investigations are needed to identify the detailed mechanisms of the sex-specific effects of PARP-1 inhibition in stroke.

DATA AVAILABILITY STATEMENT

The datasets generated for this study are available on request to the corresponding author.

ETHICS STATEMENT

All experiments involving animals were approved by the Animal care and Use Committee at Nanjing University.

AUTHOR CONTRIBUTIONS

YX and YC conceived and designed the study. JC, XL, SX, and ZW performed the experiments and analyzed the data. YC, JC, MZ, and XZ wrote, revised, and checked the data analysis. All authors revised and approved the final version of the manuscript.

FUNDING

This research was supported by the National Natural Science Foundation of China (81400971, 81630028, 81920108017, and 81971112), the Nanjing Outstanding Youth Foundation (JQX16024), the Key Research and Development Program of Jiangsu Province of China (BE2016610), and the Jiangsu Province Key Medical Discipline (ZDXKA2016020).

SUPPLEMENTARY MATERIAL

The Supplementary Material for this article can be found online at: https://www.frontiersin.org/articles/10.3389/fncel.2020.00077/full#supplementary-material

REFERENCES

Ahnstedt, H., and McCullough, L. D. (2019). The impact of sex and age on T cell immunity and ischemic stroke outcomes. *Cell. Immunol.* 345:103960. doi: 10.1016/j.cellimm.2019.103960

Amiri-Nikpour, M. R., Nazarbaghi, S., Hamdi-Holasou, M., and Rezaei, Y. (2015). An open-label evaluator-blinded clinical study of minocycline neuroprotection in ischemic stroke: gender-dependent effect. *Acta Neurol. Scand.* 131, 45–50. doi: 10.1111/ane.12296

Bai, P., and Canto, C. (2012). The role of PARP-1 and PARP-2 enzymes in metabolic regulation and disease. *Cell Metab.* 16, 290–295. doi: 10.1016/j.cmet.2012.06.016

Bell, K. F., and Hardingham, G. E. (2011). CNS peroxiredoxins and their regulation in health and disease. *Antioxid. Redox Signal.* 14, 1467–1477. doi: 10.1089/ars.2010.3567

Berger, N. A., Besson, V. C., Boulares, A. H., Burkle, A., Chiarugi, A., Clark, R. S., et al. (2018). Opportunities for the repurposing of PARP inhibitors for the therapy of non-oncological diseases. *Br. J. Pharmacol.* 175, 192–222. doi: 10.1111/bph.13748

Bosetti, F., Koenig, J. I., Ayata, C., Back, S. A., Becker, K., Broderick, J. P., et al. (2017). Translational stroke research: vision and opportunities. *Stroke* 48, 2632–2637. doi: 10.1161/STROKEAHA.117.017112

Chan, E. M., Shibue, T., McFarland, J. M., Gaeta, B., Ghandi, M., Dumont, N., et al. (2019). WRN helicase is a synthetic lethal target in microsatellite unstable cancers. *Nature* 568, 551–556. doi: 10.1038/s41586-019-1102-x

Charriaut-Marlangue, C., Leconte, C., Csaba, Z., Chafa, L., Pansiot, J., Talatizi, M., et al. (2018). Sex differences in the effects of PARP inhibition on microglial phenotypes following neonatal stroke. *Brain Behav. Immun.* 73, 375–389. doi: 10.1016/j.bbi.2018.05.022

Chen, J., Zhang, M., Zhang, X., Fan, L., Liu, P., Yu, L., et al. (2019). EZH2 inhibitor DZNep modulates microglial activation and protects against ischaemic brain injury after experimental stroke. *Eur. J. Pharmacol.* 857:172452. doi: 10.1016/j.ejphar.2019.172452

Chen, Y., Won, S. J., Xu, Y., and Swanson, R. A. (2014). Targeting microglial activation in stroke therapy: pharmacological tools and gender effects. *Curr. Med. Chem.* 21, 2146–2155. doi: 10.2174/09298673216661312282 03906

Cheon, S. Y., Kim, E. J., Kim, J. M., Kam, E. H., Ko, B. W., and Koo, B. N. (2017). Regulation of microglia and macrophage polarization via apoptosis signal-regulating kinase 1 silencing after ischemic/hypoxic injury. *Front. Mol. Neurosci.* 10:261. doi: 10.3389/fnmol.2017.00261

Cserep, C., Posfai, B., Lenart, N., Fekete, R., Laszlo, Z. I., and Lele, Z. (2019). Microglia monitor and protect neuronal function via specialized somatic purinergic junctions. *Science* 367, 528–537. doi: 10.1126/science.aax6752

Curtin, N. J., and Szabo, C. (2013). Therapeutic applications of PARP inhibitors: anticancer therapy and beyond. *Mol. Aspects Med.* 34, 1217–1256. doi: 10.1016/j.mam.2013.01.006

Deng, X. X., Li, S. S., and Sun, F. Y. (2019). Necrostatin-1 prevents necroptosis in brains after ischemic stroke via inhibition of RIPK1-mediated RIPK3/MLKL signaling. *Aging Dis.* 10, 807–817. doi: 10.14336/AD.2018.0728

Du, L., Bayir, H., Lai, Y., Zhang, X., Kochanek, P. M., Watkins, S. C., et al. (2004). Innate gender-based proclivity in response to cytotoxicity and programmed cell death pathway. *J. Biol. Chem.* 279, 38563–38570. doi: 10.1074/jbc.M405461200

Garcia-Bonilla, L., and Iadecola, C. (2012). Peroxiredoxin sets the brain on fire after stroke. *Nat. Med.* 18, 858–859. doi: 10.1038/nm.2797

George, P. M., and Steinberg, G. K. (2015). Novel stroke therapeutics: unraveling stroke pathophysiology and its impact on clinical treatments. *Neuron* 87, 297–309. doi: 10.1016/j.neuron.2015.05.041

Gibson, B. A., Zhang, Y., Jiang, H., Hussey, K. M., Shrimp, J. H., Lin, H., et al. (2016). Chemical genetic discovery of PARP targets reveals a role for PARP-1 in transcription elongation. *Science* 353, 45–50. doi: 10.1126/science.aaf7865

Haddad, M., Beray-Berthat, V., Coqueran, B., Plotkine, M., Marchand-Leroux, C., and Margaill, I. (2013). Combined therapy with PJ34, a poly(ADP-ribose)polymerase inhibitor, reduces tissue plasminogen activator-induced hemorrhagic transformations in cerebral ischemia in mice. *Fundam. Clin. Pharmacol.* 27, 393–401. doi: 10.1111/j.1472-8206.2012.01036.x

Hagberg, H., Wilson, M. A., Matsushita, H., Zhu, C., Lange, M., Gustavsson, M., et al. (2004). PARP-1 gene disruption in mice preferentially protects males from perinatal brain injury. *J. Neurochem.* 90, 1068–1075. doi: 10.1111/j.1471-4159.2004.02547.x

Jiang, M. Q., Zhao, Y. Y., Cao, W., Wei, Z. Z., Gu, X., Wei, L., et al. (2017). Long-term survival and regeneration of neuronal and vasculature cells inside the core region after ischemic stroke in adult mice. *Brain Pathol.* 27, 480–498. doi: 10.1111/bpa.12425

Jog, N. R., and Caricchio, R. (2013). Differential regulation of cell death programs in males and females by poly (ADP-Ribose) polymerase-1 and 17beta estradiol. *Cell Death Dis.* 4:e758. doi: 10.1038/cddis.2013.251

Kerr, N., Dietrich, D. W., Bramlett, H. M., and Raval, A. P. (2019). Sexually dimorphic microglia and ischemic stroke. *CNS Neurosci. Ther.* 25, 1308–1317. doi: 10.1111/cns.13267

Koh, S. H., Park, Y., Song, C. W., Kim, J. G., Kim, K., Kim, J., et al. (2004). The effect of PARP inhibitor on ischaemic cell death, its related inflammation and survival signals. *Eur. J. Neurosci.* 20, 1461–1472. doi: 10.1111/j.1460-9568.2004.03632.x

Lambertsen, K. L., Finsen, B., and Clausen, B. H. (2019). Post-stroke inflammation-target or tool for therapy? *Acta Neuropathol.* 137, 693–714. doi: 10.1007/s00401-018-1930-z

Lang, J. T., and McCullough, L. D. (2008). Pathways to ischemic neuronal cell death: are sex differences relevant? *J. Transl. Med.* 6:33. doi: 10.1186/1479-5876-6-33

Li, Y., Chen, L., Yao, S., Chen, J., Hu, W., Wang, M., et al. (2018). Association of polymorphisms of the matrix metalloproteinase 9 gene with ischaemic stroke in a southern Chinese population. *Cell. Physiol. Biochem.* 49, 2188–2199. doi: 10.1159/000493823

Lin, K. Y., and Kraus, W. L. (2017). PARP inhibitors for cancer therapy. *Cell* 169:183. doi: 10.1016/j.cell.2017.03.034

Liu, D. L., Zhao, L. X., Zhang, S., and Du, J. R. (2016). Peroxiredoxin 1-mediated activation of TLR4/NF-kappaB pathway contributes to neuroinflammatory injury in intracerebral hemorrhage. *Int. Immunopharmacol.* 41, 82–89. doi: 10.1016/j.intimp.2016.10.025

Liu, F., Lang, J., Li, J., Benashski, S. E., Siegel, M., Xu, Y., et al. (2011). Sex differences in the response to poly(ADP-ribose) polymerase-1 deletion and caspase inhibition after stroke. *Stroke* 42, 1090–1096. doi: 10.1161/STROKEAHA.110.594861

Liu, G. P., Xiang, L. X., Shao, T., Lin, A. F., and Shao, J. Z. (2018). Stimulatory function of peroxiredoxin 1 in activating adaptive humoral immunity in a zebrafish model. *Dev. Comp. Immunol.* 84, 353–360. doi: 10.1016/j.dci.2018.03.004

Liu, P. Y., Zhang, Z., Liu, Y., Tang, X. L., Shu, S., Bao, X. Y., et al. (2019). TMEM16A inhibition preserves blood-brain barrier integrity after ischemic stroke. *Front. Cell Neurosci.* 13:360. doi: 10.3389/fncel.2019.00360

Liu, Q., and Zhang, Y. (2019). PRDX1 enhances cerebral ischemia-reperfusion injury through activation of TLR4-regulated inflammation and apoptosis. *Biochem. Biophys. Res. Commun.* 519, 453–461. doi: 10.1016/j.bbrc.2019.08.077

Ma, Y., Liu, Y., Zhang, Z., and Yang, G. Y. (2019). Significance of complement system in ischemic stroke: a comprehensive review. *Aging Dis.* 10, 429–462. doi: 10.14336/AD.2019.0119

Matsuura, S., Egi, Y., Yuki, S., Horikawa, T., Satoh, H., and Akira, T. (2011). MP-124, a novel poly(ADP-ribose) polymerase-1 (PARP-1) inhibitor, ameliorates ischemic brain damage in a non-human primate model. *Brain Res.* 1410, 122–131. doi: 10.1016/j.brainres.2011.05.069

Meng, H., Zhao, H., Cao, X., Hao, J., Zhang, H., Liu, Y., et al. (2019). Double-negative T cells remarkably promote neuroinflammation after ischemic stroke. *Proc. Natl. Acad. Sci. U.S.A.* 116, 5558–5563. doi: 10.1073/pnas.1814394116

Nakamura, K., and Shichita, T. (2019). Cellular and molecular mechanisms of sterile inflammation in ischaemic stroke. *J. Biochem.* 165, 459–464. doi: 10.1093/jb/mvz017

Posynick, B. J., and Brown, C. J. (2019). Escape from X-chromosome inactivation: an evolutionary perspective. *Front. Cell Dev. Biol.* 7:241. doi: 10.3389/fcell.2019.00241

Ransohoff, R. M. (2016). A polarizing question: do M1 and M2 microglia exist? *Nat. Neurosci.* 19, 987–991. doi: 10.1038/nn.4338

Ray Chaudhuri, A., and Nussenzweig, A. (2017). The multifaceted roles of PARP1 in DNA repair and chromatin remodelling. *Nat. Rev. Mol. Cell Biol.* 18, 610–621. doi: 10.1038/nrm.2017.53

Richard, S., Lapierre, V., Girerd, N., Bonnerot, M., Burkhard, P. R., Lagerstedt, L., et al. (2016). Diagnostic performance of peroxiredoxin 1 to determine time-of-onset of acute cerebral infarction. *Sci. Rep.* 6:38300. doi: 10.1038/srep38300

Rosado, M. M., Bennici, E., Novelli, F., and Pioli, C. (2013). Beyond DNA repair, the immunological role of PARP-1 and its siblings. *Immunology* 139, 428–437. doi: 10.1111/imm.12099

Schreiber, V., Dantzer, F., Ame, J. C., and de Murcia, G. (2006). Poly(ADP-ribose): novel functions for an old molecule. *Nat. Rev. Mol. Cell Biol.* 7, 517–528. doi: 10.1038/nrm1963

Shao, A., Zhu, Z., Li, L., Zhang, S., and Zhang, J. (2019). Emerging therapeutic targets associated with the immune system in patients with intracerebral haemorrhage (ICH): from mechanisms to translation. *EBioMedicine* 45, 615–623. doi: 10.1016/j.ebiom.2019.06.012

Shen, F., Jiang, L., Han, F., Degos, V., Chen, S., and Su, H. (2019). Increased inflammatory response in old mice is associated with more severe neuronal injury at the acute stage of ischemic stroke. *Aging Dis.* 10, 12–22. doi: 10.14336/AD.2018.0205

Sheth, S. A., Lee, S., Warach, S. J., Gralla, J., Jahan, R., Goyal, M., et al. (2019). Sex differences in outcome after endovascular stroke therapy for acute ischemic stroke. *Stroke* 50, 2420–2427. doi: 10.1161/STROKEAHA.118.023867

Shichita, T., Hasegawa, E., Kimura, A., Morita, R., Sakaguchi, R., Takada, I., et al. (2012). Peroxiredoxin family proteins are key initiators of post-ischemic inflammation in the brain. *Nat. Med.* 18, 911–917. doi: 10.1038/nm.2749

Sohrabji, F., Park, M. J., and Mahnke, A. H. (2017). Sex differences in stroke therapies. *J. Neurosci. Res.* 95, 681–691. doi: 10.1002/jnr.23855

Tao, X., Yang, W., Zhu, S., Que, R., Liu, C., Fan, T., et al. (2019). Models of poststroke depression and assessments of core depressive symptoms in rodents: how to choose? *Exp. Neurol.* 322:113060. doi: 10.1016/j.expneurol.2019.113060

Teng, F., Beray-Berthat, V., Coqueran, B., Lesbats, C., Kuntz, M., Palmier, B., et al. (2013). Prevention of rt-PA induced blood-brain barrier component degradation by the poly(ADP-ribose)polymerase inhibitor PJ34 after ischemic stroke in mice. *Exp. Neurol.* 248, 416–428. doi: 10.1016/j.expneurol.2013.07.007

Tuli, R., Shiao, S. L., Nissen, N., Tighiouart, M., Kim, S., Osipov, A., et al. (2019). A phase 1 study of veliparib, a PARP-1/2 inhibitor, with gemcitabine and radiotherapy in locally advanced pancreatic cancer. *EBioMedicine* 40, 375–381. doi: 10.1016/j.ebiom.2018.12.060

Wang, Y. Q., Wang, P. Y., Wang, Y. T., Yang, G. F., Zhang, A., and Miao, Z. H. (2016). An update on poly(ADP-ribose)polymerase-1 (PARP-1) inhibitors: opportunities and challenges in cancer therapy. *J. Med. Chem.* 59, 9575–9598. doi: 10.1021/acs.jmedchem.6b00055

Waye, J. D. (2009). A balancing view: should large colon polyps be removed colonoscopically or surgically? *Am. J. Gastroenterol.* 104, 275–276. doi: 10.1038/ajg.2009.36

Xu, J., Wang, H., Won, S. J., Basu, J., Kapfhamer, D., and Swanson, R. A. (2016). Microglial activation induced by the alarmin S100B is regulated by poly(ADP-ribose) polymerase-1. *Glia* 64, 1869–1878. doi: 10.1002/glia.23026

Yang, C. S., Guo, A., Li, Y., Shi, K., Shi, F. D., and Li, M. (2019). Dl-3-n-butylphthalide reduces neurovascular inflammation and ischemic brain injury in mice. *Aging Dis.* 10, 964–976. doi: 10.14336/AD.2019.0608

Yuan, M., Siegel, C., Zeng, Z., Li, J., Liu, F., and McCullough, L. D. (2009). Sex differences in the response to activation of the poly (ADP-ribose) polymerase pathway after experimental stroke. *Exp. Neurol.* 217, 210–218. doi: 10.1016/j.expneurol.2009.02.012

Zha, S., Li, Z., Cao, Q., Wang, F., and Liu, F. (2018). PARP1 inhibitor (PJ34) improves the function of aging-induced endothelial progenitor cells by preserving intracellular NAD(+) levels and increasing SIRT1 activity. *Stem Cell Res. Ther.* 9:224. doi: 10.1186/s13287-018-0961-7

Zhang, Y., Guo, H., Cheng, B. C., Su, T., Fu, X. Q., Li, T., et al. (2018). Dingchuan tang essential oil inhibits the production of inflammatory mediators via suppressing the IRAK/NF-kappaB, IRAK/AP-1, and TBK1/IRF3 pathways in lipopolysaccharide-stimulated RAW264.7 cells. *Drug Des. Devel. Ther.* 12, 2731–2748. doi: 10.2147/DDDT.S160645

Zhu, S., Wei, X., Yang, X., Huang, Z., Chang, Z., Xie, F., et al. (2019). Plasma lipoprotein-associated phospholipase A2 and superoxide dismutase are independent predicators of cognitive impairment in cerebral small vessel disease patients: diagnosis and assessment. *Aging Dis.* 10, 834–846. doi: 10.14336/AD.2019.0304

Conflict of Interest: The authors declare that the research was conducted in the absence of any commercial or financial relationships that could be construed as a potential conflict of interest.

frontiers in Cellular Neuroscience

REVIEW
published: 03 April 2020
doi: 10.3389/fncel.2020.00068

Programmed Cell Deaths and Potential Crosstalk With Blood–Brain Barrier Dysfunction After Hemorrhagic Stroke

Yuanjian Fang[1†], Shiqi Gao[1†], Xiaoyu Wang[1], Yang Cao[1], Jianan Lu[1], Sheng Chen[1], Cameron Lenahan[2,3,4], John H. Zhang[2,4,5,6], Anwen Shao[1] and Jianmin Zhang[1,7,8*]*

[1]Department of Neurosurgery, The Second Affiliated Hospital, School of Medicine, Zhejiang University, Hangzhou, China, [2]Department of Physiology and Pharmacology, Loma Linda University School of Medicine, Loma Linda, CA, United States, [3]Burrell College of Osteopathic Medicine, Las Cruces, NM, United States, [4]Center for Neuroscience Research, Loma Linda University School of Medicine, Loma Linda, CA, United States, [5]Department of Anesthesiology, Loma Linda University School of Medicine, Loma Linda, CA, United States, [6]Department of Neurosurgery, Loma Linda University School of Medicine, Loma Linda, CA, United States, [7]Brain Research Institute, Zhejiang University, Hangzhou, China, [8]Collaborative Innovation Center for Brain Science, Zhejiang University, Hangzhou, China

OPEN ACCESS

Edited by:
Dennis Qing Wang, Zhujiang Hospital, Southern Medical University, China

Reviewed by:
Xiaoya Gao, Southern Medical University, China
Stefano Angiari, Trinity College Dublin, Ireland

***Correspondence:**
Anwen Shao
anwenshao@sina.com;
21118116@zju.edu.cn
Jianmin Zhang
zjm135@zju.edu.cn

[†]These authors have contributed equally to this work

Received: *23 December 2019*
Accepted: *06 March 2020*
Published: *03 April 2020*

Citation:
Fang Y, Gao S, Wang X, Cao Y, Lu J, Chen S, Lenahan C, Zhang JH, Shao A and Zhang J (2020) Programmed Cell Deaths and Potential Crosstalk With Blood–Brain Barrier Dysfunction After Hemorrhagic Stroke. Front. Cell. Neurosci. 14:68. doi: 10.3389/fncel.2020.00068

Hemorrhagic stroke is a life-threatening neurological disease characterized by high mortality and morbidity. Various pathophysiological responses are initiated after blood enters the interstitial space of the brain, compressing the brain tissue and thus causing cell death. Recently, three new programmed cell deaths (PCDs), necroptosis, pyroptosis, and ferroptosis, were also found to be important contributors in the pathophysiology of hemorrhagic stroke. Additionally, blood–brain barrier (BBB) dysfunction plays a crucial role in the pathophysiology of hemorrhagic stroke. The primary insult following BBB dysfunction may disrupt the tight junctions (TJs), transporters, transcytosis, and leukocyte adhesion molecule expression, which may lead to brain edema, ionic homeostasis disruption, altered signaling, and immune infiltration, consequently causing neuronal cell death. This review article summarizes recent advances in our knowledge of the mechanisms regarding these new PCDs and reviews their contributions in hemorrhagic stroke and potential crosstalk in BBB dysfunction. Numerous studies revealed that necroptosis, pyroptosis, and ferroptosis participate in cell death after subarachnoid hemorrhage (SAH) and intracerebral hemorrhage (ICH). Endothelial dysfunction caused by these three PCDs may be the critical factor during BBB damage. Also, several signaling pathways were involved in PCDs and BBB dysfunction. These new PCDs (necroptosis, pyroptosis, ferroptosis), as well as BBB dysfunction, each play a critical role after hemorrhagic stroke. A better understanding of the interrelationship among them might provide us with better therapeutic targets for the treatment of hemorrhagic stroke.

Keywords: programmed cell death, necroptosis, ferroptosis, pyroptosis, blood–brain barrier dysfunction, crosstalk

INTRODUCTION

Hemorrhagic stroke, including intracerebral hemorrhage (ICH) and subarachnoid hemorrhage (SAH), is an important public health concern with high morbidity and mortality worldwide (Scimemi, 2018; Fang et al., 2019). ICH and SAH have annual incidence rates of nearly 20 and 10 cases per 100,000, respectively, but with some regional variations (de Rooij et al., 2007; van Asch et al., 2010). Despite significant improvements in the prevention and clinical treatment of ICH and SAH, the global incidence, as well as related mortality and morbidity rates, has increased over the past several decades (Qureshi et al., 2009; Turan et al., 2016; Macdonald and Schweizer, 2017). As reported, the 5-year survival rate of patients with hemorrhagic stroke is less than 50%. Most survivors of hemorrhagic stroke have a reduced quality of life and may require more time and resources during hospitalization and rehabilitation (Gustavsson et al., 2011). Recently, numerous studies have focused on the pathological mechanisms after hemorrhagic stroke, with the intention of seeking potential therapeutic targets to guide treatment (Grysiewicz et al., 2008). However, because of the complexity of its mechanism and the limitations of translational studies, the benefits have been limited (Wilkinson et al., 2018). Hemorrhagic stroke occurs when a weakened vessel ruptures, allowing blood to traverse the broken blood–brain barrier (BBB) into the brain tissue, or fissures, which leads to a mass effect that increases the intracranial pressure and decreases the cerebral blood flow (Topkoru et al., 2017; Tao et al., 2019). Thus, the deficiency of ATP and increased blood toxic substances initiate a cascade of pathophysiological changes, such as depolarization, excitotoxicity, cell edema, inflammatory responses, oxidative stress, ionic homeostasis, and secondary BBB disruption (Zille et al., 2017; Fang et al., 2018; Marbacher et al., 2018; Shao A. et al., 2019; Shao Z. et al., 2019; Wan et al., 2019). These pathophysiological changes may lead to various forms of cell death, including apoptosis, necrosis, necroptosis, autosis, ferroptosis, pyroptosis, parthanatos, and cyclophilin D necrosis, which are also categorized under programmed cell deaths (PCDs; Fuchs and Steller, 2015; Sekerdag et al., 2018). Increasing efforts have been deployed to study these PCDs and their related pathways to discover potential therapeutic targets that will provide neuroprotection after hemorrhagic stroke (Leist and Jaattela, 2001).

Pathological changes in BBB function are widely implicated in the pathophysiological changes after hemorrhagic stroke (Daneman and Prat, 2015; Lublinsky et al., 2019; Ma et al., 2020). Recent studies have proposed that endothelial cells (ECs) do not work alone in the maintenance of the BBB and that astrocytes, pericytes, neurons, and microglia also contribute and are collectively known as the neurovascular unit (NVU). The death of these cells may directly or indirectly result in dysfunction of the BBB (Jiang et al., 2018). Additionally, BBB disruption may further aggravate brain edema, ionic homeostasis disruption, altered signaling, and immune infiltration, consequently causing cell death (Daneman and Prat, 2015).

Given the significant role of PCDs and BBB dysfunction in the pathophysiological mechanisms after hemorrhagic stroke, this review article focuses on the mechanism and recent studies of three PCDs (necroptosis, pyroptosis, and ferroptosis) after hemorrhagic stroke. In addition, we will also discuss, summarize, and hypothesize that the crosstalk between these PCDs and BBB dysfunction after hemorrhagic stroke may lead to the development of novel therapeutic approaches in the future.

THE MECHANISM OF NECROPTOSIS

Necroptosis is a cell death similar to necrosis in terms of morphological features, such as being triggered by death ligands or intracellular stimuli and being executed in a caspase-independent manner (Liu et al., 2018). Morphologically, necroptosis is distinguished from apoptosis by the presence of clusters of dying cells, which may be indicated by early destruction of membrane integrity, cell and organelle swelling, cytoplasmic granulation, chromatin fragmentation, and cell lysis (Zhang et al., 2017). Ligands, such as tumor necrosis factor (TNF), TNF-related apoptosis-inducing ligand, and the intracellular stimuli, such as DNA-dependent activator of interferon regulatory factors (which may act as a cytoplasmic viral RNA sensor) and protein kinase R, can initiate necroptosis (Linkermann and Green, 2014). Furthermore, necroptosis can also be triggered by interferons and Toll-like receptor signaling (Zhang et al., 2017). The receptor-interacting kinase 3 (RIPK3) and its substrate, the pseudokinase mixed lineage kinase domain-like protein (MLKL), execute the core component of necroptosis without caspase participation (Zhang et al., 2009; Sun et al., 2012). Generally, there are several signaling pathways involved in necroptosis, including TNFα, TNF receptor (TNFR1)-related signaling pathway, TRAIL, and other factors associated with the apoptosis signaling pathway, as well as the RIPK3 mitochondrial reactive oxygen species (ROS) metabolic pathway and the zVAD-mediated PKC/mitogen-activated protein kinase (MAPK)/AP1-related signaling pathway (Jin and El-Deiry, 2006; Vanden Berghe et al., 2007; Wu et al., 2011; Liu et al., 2018).

The first step of necroptosis is the formation of the necrosome (Zhang et al., 2017; **Figure 1**). Take the thoroughly studied TNFα–TNFR1-related signaling pathway as an example. TNF α activates TNFR1 through the extracellular domain and subsequently triggers the trimerization of TNFR1, which recruits several proteins to form complex I at the plasma membrane. Complex I comprised several components, such as TNFα receptor-associated death domain (interact with RIPK1), RIPK1 (core protein), TNFR-associated factor 2 (TRAF2), TRAF5, cellular inhibitor of apoptosis 1 (cIAP1), and cIAP2 (mediates the ubiquitination of RIPK1; Micheau and Tschopp, 2003). Ubiquitination of RIPK1 generates binding sites for TAB2/3 (transforming growth factor beta–activated kinase 1 (TAK1) and NEMO [the regulatory subunit of the IκB kinase (IKK) complex], which leads to further recruitment and activation of TAK1 and IKKα/β. Then, activated IKKα/β phosphorylated IκB and leads to nuclear factor κB release and MAPK activation, promoting cell survival (Bertrand et al., 2008; Hayden and Ghosh, 2014).

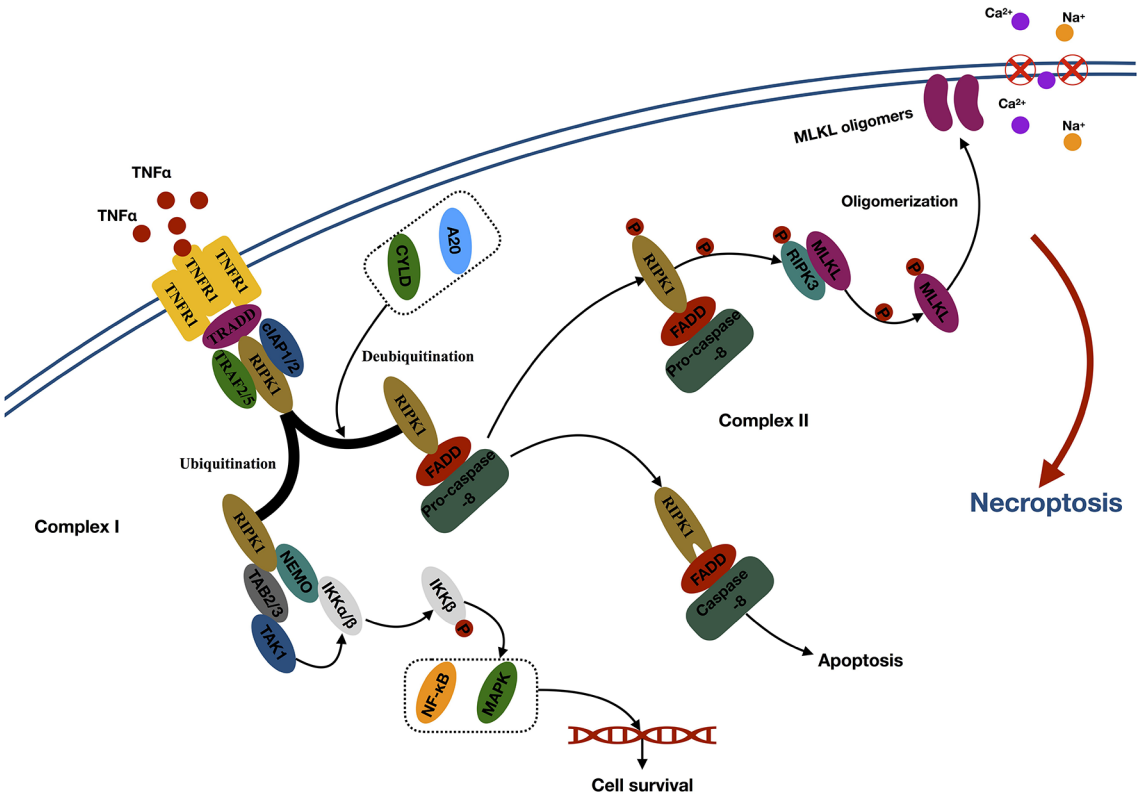

FIGURE 1 | Mechanisms of necroptosis. Abbreviations: TNFα, tumor necrosis factor; TNFR1, tumor necrosis factor receptor type 1; TRADD, TNFα receptor-associated death domain; TRAF2, TNFR-associated factor 2; cIAP1, cellular inhibitor of apoptosis 1; RIPK1, receptor-interacting kinase 1; CYLD, cylindromatosis; FADD, Fas-associated death domain; RIPK3, receptor-interacting kinase 3; MLKL, mixed lineage kinase domain-like protein; NEMO, NF-κB essential modulator; TAB2/3, TAK1-binding 2/3; TAK1, TGF-β–activated kinase 1; IKKα/β, IκB kinase α/β; NF-κb, nuclear factor κB; MAPK, mitogen-activated protein kinase.

Conversely, RIPK1 loses its default prosurvival function when it is deubiquitinated by the induction of deubiquitinases, such as cylindromatosis and A20 (Wertz et al., 2004; Moquin et al., 2013). Then, the deubiquitinated RIPK1 can bind to FAS-associated protein with a death domain and recruit procaspase 8 to form complex II within the cytoplasm. Apoptosis occurs when caspase 8 is activated. However, necroptosis occurs when caspase 8 is inhibited (Oberst et al., 2011). In the necrosome, RIPK1 can phosphorylate the RIPK3 to execute the following necroptosis (Zhang et al., 2009).

The second step of necroptosis is processing (**Figure 1**). The activated RIPK3 binds to and induces phosphorylation of cytoplasmic MLKL. Phosphorylation leads to the oligomerization of MLKL and membrane translocation of the MLKL oligomers, which disrupts the integrity and increases permeability of the membrane, therefore inducing internal flow of Ca^{2+} or Na^{+} ions, finally leading to cell death (Wang et al., 2014).

NECROPTOSIS IN HEMORRHAGIC STROKE

Although the phenomenon of necroptosis has been extensively investigated in the pathophysiological mechanisms of other diseases, there are relatively few studies regarding necroptosis and hemorrhagic stroke (**Table 1**). It is known that necroptosis can be blocked by a small, specific molecular compound, known as necrostatin 1 (nec-1), by targeting and binding with RIPK1 (Galluzzi et al., 2017). Numerous studies have attempted to inhibit necroptosis by using nec-1 to reduce cell death and improve neurological function, thereby indirectly demonstrating the existence of necroptosis in the pathophysiological development after hemorrhagic stroke (Laird et al., 2008; King et al., 2014; Majmundar et al., 2016). Administration of nec-1 and the irreversible pan-caspase inhibitor, z-VAD, in astrocytic cells revealed that only nec-1 could significantly reduce hemin-induced astrocytic death, suggesting that caspase-independent necroptosis may mediate astrocytic death after hemorrhagic injury in an *in vitro* model. In addition, the proinflammatory effect of hemin relied on the enhanced astrocytic necroptosis after ICH (Laird et al., 2008). Meanwhile, nec-1 presented the capacity to reduce hematoma volume and neurovascular injury, while improving neurological outcomes after ICH in mice (King et al., 2014; Majmundar et al., 2016). However, they did not reveal detailed information pertaining to the cell types and mechanisms of necroptosis in their studies.

It should be mentioned that nec-1 administration may also suppress the apoptotic and autophagic pathways after ICH and

TABLE 1 | Latest research of necroptosis in hemorrhagic stroke.

References	Stroke	Vitro/Vivo	Subjects	Related pathway	Conclusion
Laird et al. (2008)	ICH	Vitro	Mice primary astrocytes	/	Caspase-independent necroptosis mediates hemin toxicity in astrocytes
Chang et al. (2014)	ICH	Vivo	Mice	/	Nec-1 suppresses apoptosis and autophagy after ICH
King et al. (2014)	ICH	Vivo	Mice	/	Nec-1 reduces neurological injury after ICH
Su et al. (2015)	ICH	Vivo	Mice	RIPK1/RIPK3	Nec-1 ameliorates ICH-induced brain injury by inhibiting RIPK1/RIPK3 pathway after ICH
Xie et al. (2016)	SAH	Vitro/ Vivo	Rats/BV-2 microglial cells	SAP130/Mincle/Syk/IL-1β	Neuronal necroptosis product, SAP130, activates microglial Mincle and sequential inflammatory response after SAH
Majmundar et al. (2016)	ICH	Vivo	Mice	/	Nec-1 improved neurologic outcomes after ICH
Shen et al. (2017)	ICH	Vitro/Vivo	Rats/Primary neuron& microglia	TNFα/RIPK1/RIPK3/MLKL	Necroptosis is an important mechanism of neuron death in brain injury after ICH
Zille et al. (2017)	ICH	Vitro/Vivo	Mice and primary cultured neurons	RIPK1/RIPK3	Necroptosis involved in neuronal death mechanisms after ICH
Su et al. (2018)	ICH	Vitro	HT-22 cells	RIPK1/RIPK3	RIP1/RIP3 mediated hemin-induced neuron death, which can be reversed by nec-1
Chu et al. (2018)	ICH	Vitro/Vivo	Mice/Primary cultured neurons	IL-1R1/RIPK1/RIPK3	Inhibition of the interaction between IL-1R1 and the necrosome complex reduces neuron death and improves neurological functions after ICH
Chen et al. (2018)	SAH	Vivo	Rats	RIPK1/RIPK3/MLKL	Inhibition of RIPK3 attenuates early brain injury after SAH, possibly through alleviating necroptosis
Zhang et al. (2020)	ICH	Vitro/Vivo	Rats/AAV-293 cells	CHIP/RIPK1/RIPK3	E3 ligase CHIP inhibits neuron necroptosis and pathological inflammation following ICH
Yang et al. (2019)	SAH	Vivo	Rats	Nec-1 /CREB/BDNF	Inhibition of necroptosis by nec-1 rescues SAH-induced synaptic impairments in hippocampus
Lu et al. (2019)	ICH	Vitro/Vivo	Mice/HT-22 neuron cells	A20/RIPK1/RIPK3	Melatonin ameliorates microglial necroptosis by regulating A20 after ICH
Yuan et al. (2019)	SAH	Vitro/Vivo	Rats/Primary neurons& microglia	TNFα/RIPK1/RIPK3/MLKL	RIP3 induced neuron necroptosis involved in the pathological process after SAH
Chen et al. (2019)	SAH	Vivo	Rats	RIP1/RIP3/MLKL	Nec-1 attenuates brain swelling and BBB disruption and reduces necroptosis after SAH

exert a neuroprotective effect (Chang et al., 2014). Necrostatin 1 treatment increased Bcl-2 expression and decreased cleaved caspase 3 levels, as well as the beclin 1/Bcl-2 ratio at 24 and 72 h after ICH (Chang et al., 2014). Thus, the following study attempts to identify the interaction between the key pathway in necroptosis (RIPK1/RIPK3) and nec-1. It has been found that RIPK1 and RIPK3 were significantly decreased, with reduced necrotic cell death (no detailed cell type was shown), under the treatment of nec-1 in mice after ICH, further suggesting that nec-1 inhibited necroptosis after ICH (Su et al., 2015).

The RIPK1/RIPK3 pathway was shown to play an important role in hemin-induced cell death (Zille et al., 2017; Su et al., 2018). RIPK1 and RIPK3 mRNA levels and phospho-RIPK1 increased after the primary cortical neuron had been treated with hemin (Zille et al., 2017). Necrostatin 1 or RIPK3 siRNA dramatically attenuated hemin-induced cell death and ROS accumulation in the HT-22 neuron cell line (Su et al., 2018). Furthermore, the neuronal necroptosis can be diminished if mutations are present at the serine kinase phosphorylation site of RIPK1, further supporting the significance of RIPK1 phosphorylation in necroptosis (Shen et al., 2017).

Meanwhile, the RIPK1/RIPK3-mediated necroptosis pathway was also involved in the alterations of pathophysiology after SAH (Chen et al., 2018, 2019; Yuan et al., 2019). The RIPK3 protein level increased in the rat brain and peaked at 24 h after SAH. Inhibition of RIPK3 by genetic or pharmacological treatment attenuated the brain injury in rats after SAH and neuronal necroptosis induced by oxygen hemoglobin (OxyHb; Chen et al., 2018, 2019; Yuan et al., 2019). Besides, pretreatment of nec-1 in rats after SAH demonstrated that nec-1 could also prevent BBB dysfunction by reducing the degradation of TJ proteins (occludin, claudin-5, and ZO-1), by increasing active matrix metalloproteinase 9 (MMP-9), and by reducing neuroinflammation *via* reduction of proinflammatory cytokines, such as interleukin 1β (IL-1β), IL-6, and TNFα after SAH (Chen et al., 2019). These findings seemingly indicated that nec-1 attenuated astrocytic and endothelial cell necroptosis. Additionally, it has been reported that the neuroprotective effect of nec-1 was also connected with another pathway. Necrostatin 1 rescues SAH-induced synaptic impairments and neuronal death in the hippocampus of rats *via* the cAMP-responsive element-binding proteins (CREB)/brain-derived neurotrophic factor (BDNF) pathway (Yang et al., 2019). cAMP-responsive element-binding protein and BDNF play an important role in synaptic plasticity, which contributes to memory processing (Seoane et al., 2011). Necrostatin 1 can reverse the decreased protein level of CREB and BDNF in rats after SAH (Yang et al., 2019).

Recently, several upstream regulators of necroptosis were found in hemorrhagic stroke (Shen et al., 2017; Chu et al., 2018). Necroptosis of primary cultured neurons could be induced by supernatant medium derived from microglia treated with OxyHb, but could be countered by a TNFα inhibitor, indicating that the TNFα–TNFR1-related signaling pathway participates in this process (Shen et al., 2017). Besides, hemin triggers neuronal necroptosis through promotion of IL-1 receptor 1 (IL-1R1) and RIPK complex formation. Inhibition of IL-1R1 can prevent necrosome and RIPK1/RIPK3 pathway activation, suggesting that the IL-1R1/RIPK1/RIPK3 pathway was also an important signaling pathway involved in necroptosis (Chu et al., 2018).

Downstream in the RIPK1/RIPK3 pathway, there are several regulators of necroptosis found in hemorrhagic stroke, such as carboxyl terminus of Hsp70-interacting protein (CHIP) and A20 (Lu et al., 2019; Zhang et al., 2020). CHIP is an E3 ligase that mediates ubiquitylation and negatively regulates the protein level of RIPK1 and RIPk3 (Seo et al., 2016). The expression of CHIP increased in the perihematomal region in rats after ICH. Overexpression of CHIP exerts neuroprotective effects by regulating the RIPK1/RIPK3 necroptosis pathway in neurons and therefore attenuating ICH-associated cerebral inflammation (Zhang et al., 2020). Additionally, the deubiquitylating enzyme, A20, was shown to inhibit RIP3 activity and reduce microglial necroptosis after ICH, *in vitro* and *in vivo*. Moreover, the A20 was identified as a novel target of melatonin, which upregulates A20 activity and suppresses necroptosis following ICH (Lu et al., 2019). On the other hand, it was found that the neuronal necroptosis product, SAP130, activates microglial macrophage-inducible C-type lectin (Mincle) and the sequential inflammatory response by mediating Mincle/Syk/IL-1b signaling in the ipsilateral hemisphere that had been subjected to SAH (Xie et al., 2017).

In conclusion, necroptosis is initiated after hemorrhagic stroke or hemin treatment in different cell types, such as astrocytes, neurons, and microglia. Inhibition of necroptosis by administration of nec-1 appears to be a potential target for the treatment of hemorrhagic stroke. However, the detailed mechanisms of necroptosis should be further investigated, not only *in vivo* but also *in vitro*, with particular emphasis regarding ECs due to the numerous studies demonstrating that inhibition of necroptosis can protect the BBB after hemorrhagic stroke.

THE MECHANISM OF FERROPTOSIS

Ferroptosis is a form of cell death characterized by the accumulation of intracellular iron and lipid ROS. The primary morphologic manifestations of ferroptosis include cell volume shrinkage and increased mitochondrial membrane density (Yu et al., 2017). The ferroptosis can be roughly divided into two segments: the core pathway of ferroptosis and iron metabolism (Xie et al., 2016; **Figure 2**).

The core component of ferroptosis includes lipid ROS accumulation due to the inhibition of System X_c^- and glutathione peroxidase (GPX4). According to the different inhibition targets, the reducers can be divided into two classes. The first class includes erastin, sulfasalazine, DPI-sorafenib, and buthionine sulfoximine, which inhibits the depletion of System X_c^- and glutathione (GSH; Xie et al., 2016). The second class comprised Ras-selective lethal 3 compound (RSL3), as well as DPI family members, which inactivate GPX4 (Yang et al., 2014). System X_c^- is a membrane Na^+-dependent cysteine–glutamate exchange transporter (with a ratio of 1:1) that is composed of a light-chain

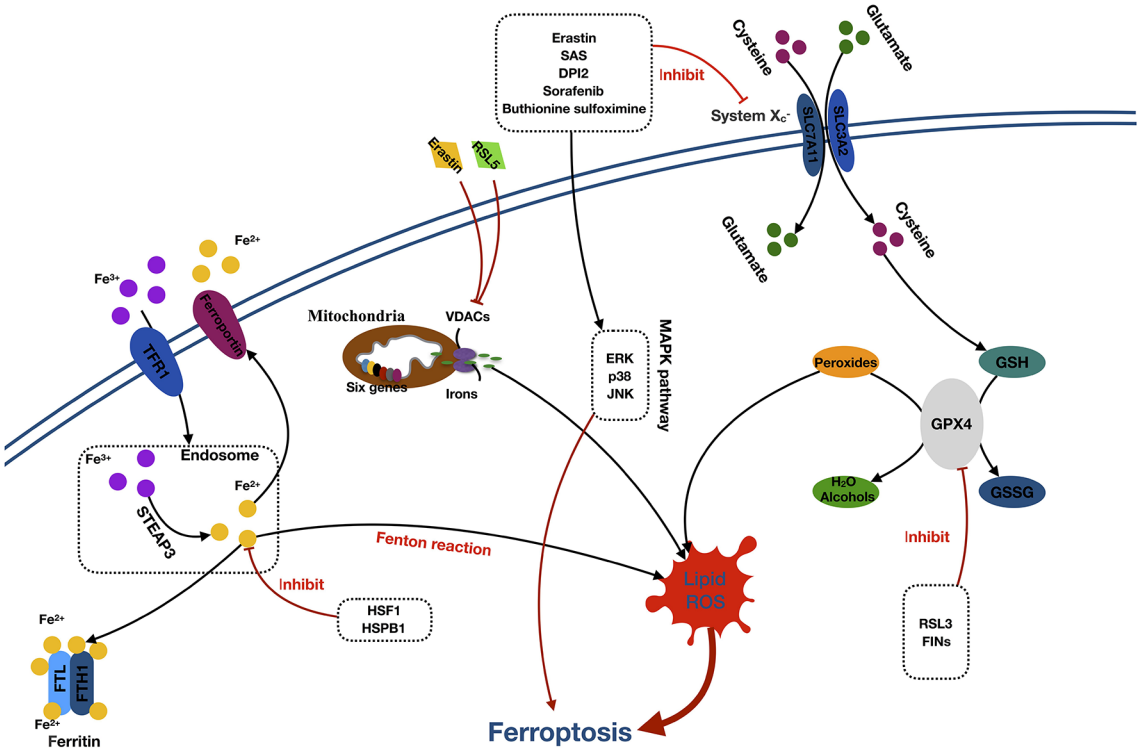

FIGURE 2 | Mechanisms of ferroptosis. Abbreviations: TFR1, transferrin receptor 1; STEAP3, six-transmembrane epithelial antigen of prostate 3; FTL, ferritin light chain; FTH1, ferritin heavy chain 1; HSF1, heat shock factor 1; HSPB1, (HSF1)-heat-shock protein B1; RSL5, Ras selective lethal 5; VDACs, voltage-dependent anion channels; SAS, sulfasalazine; DPI2, diphenyleneiodonium 2; ERK, extracellular signal–regulated kinase; JNK, c-jun–N-terminal kinase; MAPK pathway, mitogen-activated protein kinase pathway; SLC7A11, solute carrier family 7 member 11; SLC3A2, solute carrier family 3 member 2; GSH, glutathione; GPX4, glutathione peroxidase 4; GSSG, oxidized glutathione; RL3, ribonuclease 1; FINS, fasting serum insulin.

subunit (xCT, SLC7A11) and a heavy-chain subunit (CD98hc, SLC3A2). It is critical for maintaining redox homeostasis by reducing the intracellular cysteine that is required for the synthesis of GSH, a major antioxidant. When cells are cultured in glutamate, a substance causing neuronal hyperexcitability (Yang et al., 2019), the intracellular GSH content will decrease, and ferroptosis will be induced. Cells stimulated with class 1 ferroptosis inducers will usually have a significantly reduced GSH level (Yang and Stockwell, 2016). GSH peroxidase was a specific downstream site of GSH. GSH peroxidase uses two GSH molecules as electron donors to reduce H_2O_2, as well as other common small-molecule and complex lipid peroxides *via* decomposition of H_2O_2 into water or corresponding alcohols (Ursini et al., 1995). The class 2 ferroptosis inducers, such as RSL3 and FINs, directly inhibit GPX4 activity, contributing to the intracellular accumulation of lipid peroxides and subsequent ferroptosis (Yang et al., 2014).

The detailed role of iron in ferroptosis remains unclear. However, it was considered that the participation of iron is necessary for ferroptosis in oxidative reactions (Dixon et al., 2012; Gao et al., 2015). Free Fe^{3+} induces ferroptosis *via* importation into cells through the membrane protein transferrin receptor 1 and then stored in the endosome where Fe^{3+} is converted into Fe^{2+} by STEAP3. Subsequently, Fe^{2+} is transported by the divalent metal transporter 1 out of the endosome. The cytoplasmic Fe^{2+} is then transferred to three locations. Some is stored in ferritin, an iron storage protein complex, which includes a ferritin light chain and ferritin heavy chain 1. Some is transported out of the cell by the transmembrane protein, ferroportin. The rest is utilized in the Fenton reaction to create lipid ROS, which is an important source of ROS (Dixon and Stockwell, 2014; Xie et al., 2016; Wu et al., 2019). Moreover, erastin and RSL5 can alter the ion selectivity of the voltage-dependent anion channels, preventing the bidirectional movement of cations within the mitochondria, causing mitochondrial dysfunction and oxidant release (Yagoda et al., 2007; Yang and Stockwell, 2008).

Additionally, activation of the MAPK pathway and heat shock factor 1 (HSF1)–heat shock protein B1 (HSPB1) pathway also plays a significant role in ferroptosis. Inhibition of the MAPKs family, such as extracellular signal regulated kinase (ERK), p38, and c-Jun NH2-terminal kinase (JNK) can significantly attenuate the erastin-induced cell death, which indicates the potential role of MAPKs in ferroptosis (Yagoda et al., 2007; Yu et al., 2015). Furthermore, research has proven that HSF1 and HSPB1 can inhibit cell ferroptosis by decreasing the concentrations of iron and lipid ROS in cells (Sun et al., 2015).

FERROPTOSIS IN HEMORRHAGIC STROKE

Ferroptosis was first reported in cell death during tumor and embryonic development (Dixon et al., 2012; Jiang et al., 2015; Sun et al., 2015). However, few studies have reported this form of cell death in hemorrhagic stroke (**Table 2**). Morphologically, the mitochondria of ferroptotic neurons appeared shrunken, with decreased cytomembrane mitochondria at 3 and 6 days after ICH in mice. After several days, the swollen mitochondrial count appears to stabilize and is sustained until 28 days (Li et al., 2018). Interestingly, another study failed to find the shrunken mitochondria in primary neurons subjected to hemin stimulation (Zille et al., 2017). Regarding the molecular mechanism of ferroptosis, most studies attempt to confirm the presence of ferroptosis and the effects of ferroptosis inhibition *via* modulation of downstream pathways. To date, several ferroptosis inhibitors have been found. Accordingly, these inhibitors are primarily categorized as either antioxidants or iron chelators. The antioxidants include ferrostatin 1 (fer-1), liproxstatin 1 (lip-1), cycloheximide, N-acetylcysteine (NAC), Trolox, and U0126 (Dixon et al., 2012; Cao and Dixon, 2016; Zille et al., 2017), whereas the iron chelators include deferoxamine (DFO), ciclopirox (CPO), and dihydroxybenzoic acid (DHB; Okauchi et al., 2010; Karuppagounder et al., 2016).

It was found that the neuron death and iron deposition, induced by hemoglobin in organotypic hippocampal slice cultures and primary cortical neurons, can be attenuated by administration of fer-1, or other ferroptosis inhibitors (Li et al., 2017; Zille et al., 2017). Ferrostatin 1 prevents Hb-induced GPX4 deficits and lipid ROS accumulation and attenuates the injury volume and neurological deficits after ICH in mice (Li et al., 2017). The phospho-ERK1/2 level was significantly elevated at 6 and 24 h after ICH in mice and blocked by U0126 (an inhibitor of MAPK), suggesting the involvement of the MAPK/ERK pathway in the regulation of ferroptosis (Zille et al., 2017). Regarding the downstream production of ferroptosis, cyclooxygenase 2 (COX-2), an enzyme encoded by the PTGS-2 gene, was found to be significantly increased within the first 3 days after ICH in mice and can be inhibited by fer-1 (Li et al., 2017). By using spectrometric analysis, the following study also proved that COX-dependent lipid species participate in the facilitation of ferroptosis (Karuppagounder et al., 2018).

N-acetylcysteine is a clinically approved cysteine prodrug, which modulates redox reactions by mediating activity of the X_c^- transporter and the cysteine/glutamate ratio. Moreover, recent data suggest that NAC can inhibit ferroptosis *in vitro* and *in vivo* (Zille et al., 2017; Karuppagounder et al., 2018). N-acetylcysteine attenuates hemin-/hemoglobin-induced cell death in primary cortical neuronal cells and improved functional recovery after ICH in mice (Zille et al., 2017; Karuppagounder et al., 2018). In this study, arachidonate 5-lipoxygenase (ALOX5)–derived reactive lipid species was revealed to contribute significantly in hemin-induced ferroptosis. The NAC-mediated neuroprotective effect was executed by increasing GSH levels and subsequently neutralizing nuclear ALOX5-derived lipid species after ICH

TABLE 2 | Latest research of ferroptosis in hemorrhagic stroke.

References	Stroke	Vitro/Vivo	Subjects	Related pathway	Conclusion
Karuppagounder et al. (2016)	ICH	Vitro	Primary cortical neurons/HT22 cells	HIF-PHD/ATF4	Iron chelators prevent glutamate or hemin-induced ferroptosis in neurons by targeting the HIF-PHDs/ATF4 pathway
Li et al. (2017)	ICH	Vitro/Vivo	Mice/Organotypic hippocampal slice cultures	/	Ferrostatin-1 inhibits neuronal death and provides neuroprotection by preventing lipid ROS accumulation and reducing GPX4 activity after ICH.
Zille et al. (2017)	ICH	Vitro/Vivo	Primary cortical neurons/mice	MAPK/ERK	Inhibition of ferroptosis abrogated hemoglobin-induced cell death *via* inhibition of MAPK/ERK1 pathway.
Karuppagounder et al. (2018)	ICH	Vitro/Vivo	Primary cortical neurons/mice		N-acetylcysteine functions as a neuroprotective therapy by preventing ferroptosis-generated toxic lipids.
Li et al. (2018)	ICH	Vivo	Mice	/	Ferroptosis existed in injured striatum during the acute phase of ICH.
Alim et al., 2019	ICH	Vitro/Vivo	Primary cortical neurons&HT22cells /Mice	GPX4 /TFAP2c/SP1	Pharmacological selenium inhibited GPX4-dependent ferroptotic death.

(Karuppagounder et al., 2018). Additionally, this study also found that the COX-2–derived species, PGE2 and NAC, could synergize to prevent hemin-induced ferroptosis *in vitro* and improve functional recovery after ICH (Karuppagounder et al., 2018). However, this result seems to be in contrast of the detrimental effect of COX-2 after ICH, as mentioned in the previous study (Li et al., 2017).

A recent study revealed that iron chelators (DFO, CPO, DHB) inhibit glutamate- or hemin-induced ferroptosis in neurons by targeting the hypoxia-inducible factor prolyl hydroxylase domain enzymes (HIF-PHDs), a family of iron-dependent enzymes necessary for ATF4-dependent prodeath transcription. However, this process was identified independently to the inhibition of the Fenton reaction (Karuppagounder et al., 2016). ATF4 is a leucine zipper transcription factor that is activated in the ferroptosis-induced transcriptional responses found in neurons and cancer cells. Neurons with a germline deletion of ATF4 had resistance to the homocysteic acid–induced ferroptosis (Lange et al., 2008; Karuppagounder et al., 2016; Chen et al., 2017). This evidence suggests that the ATF4-dependent pathway may have an important role in ferroptosis after ICH.

The GPX4 homeostasis is a critical component of ferroptotic cell death after ICH. However, little is known about the expression levels of GPX4 and other selenoproteins after ferroptotic initiation. The latest study found an increased expression of several selenium-containing antioxidant enzymes, including GPX4, thioredoxin reductase 1, GPX3, and selenoprotein P *in vivo* and *in vitro* (Alim et al., 2019). The neuron-specific expression of GPX4 after ICH functions as a protective factor to avoid neuronal loss from ferroptosis-induced oxidative damage. However, it seems to be an insufficient response in preventing cell death as a result of ferroptotic insults (Karuppagounder et al., 2018; Alim et al., 2019). Interestingly, this study found that selenium augments the transcriptional response involving GPX4 *via* coordinated activation of the transcription factors, TFAP2c and Sp1, to protect the neurons from ferroptotic death and improve functional recovery after ICH in mice (Alim et al., 2019).

It should be mentioned that there have not been any studies that investigate the role of ferroptosis in the pathophysiology after SAH. Our laboratory has found that lip-1 can reduce the characteristic shrunken mitochondria in ipsilateral cortical neurons after SAH in mice. Liproxstatin 1 participated in attenuation of active lipid ROS by reducing the production of malondialdehyde and 4-hydroxynonenal (4-HNE) and by increasing the level of GSH and the activity GPX. Furthermore, lip-1 downregulated acyl-CoA synthetase long-chain family member 4 and COX-2, but also reduced the activation of microglia and inflammatory response (data unpublished).

In conclusion, ferroptosis has a critical role in the cell death of neurons. However, there have not been any studies conducted that focus on other cell types. After hemorrhagic stroke, the iron metabolic disorders and ROS accumulation both existed in the endothelium, microglia, and astrocytes. In addition, the BBB dysfunction and inflammation were also shown to be associated with the ferroptosis inhibitors (Zhang Z. et al., 2018; Zhang Y. H. et al., 2018). Ferroptosis may also occur in these cells after hemorrhagic stroke. Further studies should expand their research beyond the role of ferroptosis in neuronal death.

THE MECHANISM OF PYROPTOSIS

Pyroptosis is a proinflammatory form of cell death (Bergsbaken et al., 2009; Chen et al., 2018). Morphologically, pyroptotic cell death possesses features of both necrosis and apoptosis. The morphological changes include necrosis-like cell membrane rupture, pore formation, cellular swelling, proinflammatory intracellular content release, as well as apoptosis-like nuclear condensation and DNA fragmentation. In contrast to apoptosis, pyroptotic cells have an integral mitochondrion and "balloon-shaped" vesicle formation, but no cytochrome c release (Xu et al., 2018; Jia et al., 2019). Molecularly, pyroptosis is characteristic in gasdermin-mediated cell death (Shi et al., 2017). Normally, the gasdermin is activated by two caspase-dependent pathways, including canonical caspase 1 and the noncanonical caspase 4/5/11 pathway (Jia et al., 2019; **Figure 3**).

In the canonical caspase 1 pathway, inflammasomes (also called pyroptosomes) assemble in the cytosol after recognizing pathogen-associated molecular patterns and danger-associated molecular patterns released by dying cells and some proinflammatory cytokines (Lamkanfi and Dixit, 2014). Inflammasomes are multimeric protein complexes, which are composed of the nucleotide-binding oligomerization domain (NOD)-like receptor (NLR) family (NLRP1, NLRP3, NLRC4, NLRP6, and NLRP9), PYHIN protein families [absent in melanoma 2 (AIM2)], or pyrin proteins (Zheng et al., 2011; Sekerdag et al., 2018). Typically, an NLR consists of three parts: C-terminal leucine-rich repeats, which are responsible for ligand recognition and autoinhibition, a central NOD (NACHT), which activates the signaling complex, and an N-terminal caspase activation and recruitment domain (CARD) or pyrin domain (PYD), which mediates homotypic protein–protein interactions (Martinon et al., 2002; Aachoui et al., 2013). The AIM2 contains a DNA-binding HIN-200 domain and PYD. The pyrin protein consists of the PYD, a zinc finger domain (bBOX), a coiled coil domain, and/or a B30.2/SPRY domain (Jia et al., 2019). The signaling domains, such as the PYD and CARD, both recruit the apoptosis-associated speck-like protein containing a caspase recruitment domain (ASC). This subsequently activates pro–caspase 1 to generate active caspase 1 (Aachoui et al., 2013). Then, the activated caspase 1 cleaves the gasdermin D (GSDMD) and triggers oligomerization of the GSDMD-N domain in the cell, which finally forms the pores and releases cellular contents, such as IL-1α and HMGB1. Besides, the active caspase 1 is also responsible for processing and maturing IL-1β/18, which cause inflammation (Dinarello, 2011; Xu et al., 2018).

In the noncanonical caspase 4/5/11 pathway, caspase 4/5/11 was activated by a direct interaction with cytosolic lipopolysaccharide. Next, activated caspase 4/5/11 directly initiates the cleavage of GSDMD and triggers pyroptosis. Meanwhile, active caspase 4/5/11 can initiate pannexin 1 cleavage and K^+ efflux, indirectly facilitating the release of mature IL-1β (Kayagaki et al., 2011; Cheng et al., 2017).

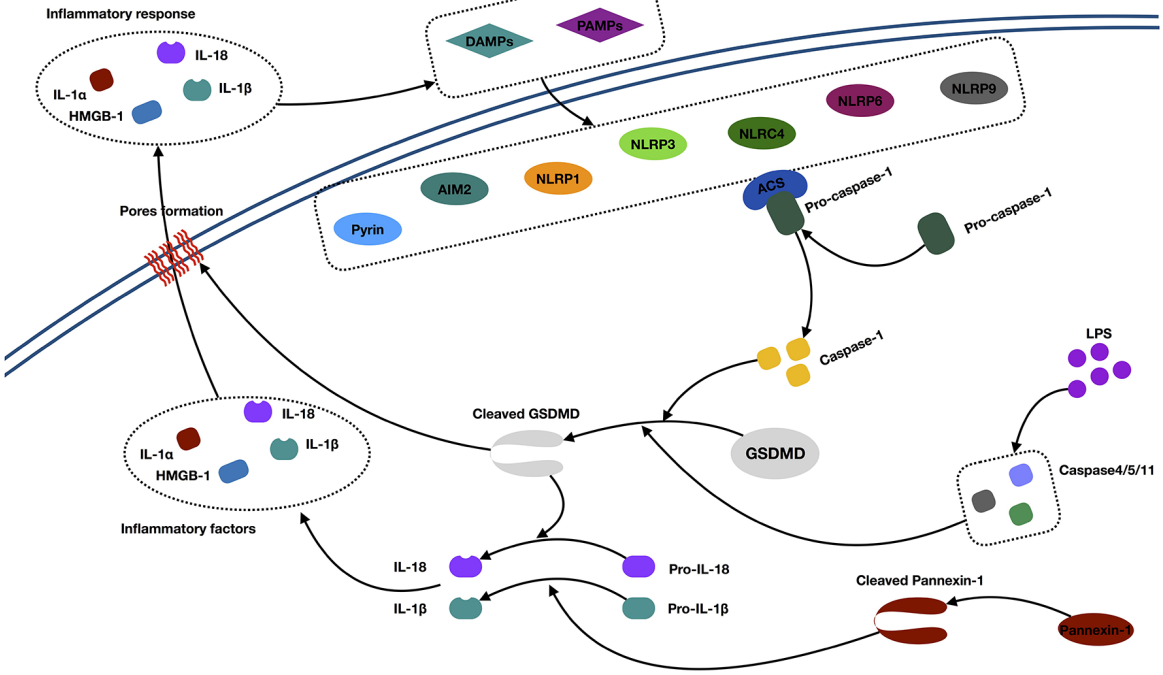

FIGURE 3 | Mechanisms of pyroptosis. Abbreviations: IL-1α/1β/18, interleukin 1α/1β/18; DAMPs, danger-associated molecular patterns; PAMPs, pathogen-associated molecular patterns; AIM2, absent in melanoma 2; NLRP, (NOD)-like receptor protein; ACS, andacyl-CoA synthetase; GSDMD, Gasdermin D; HMGB1, high-mobility group box 1; LPS, lipopolysaccharide.

PYROPTOSIS IN HEMORRHAGIC STROKE

Pyroptosis, unlike other types of PCDs, cannot be detected morphologically. Thus, the existing research is limited to the molecular level (**Table 3**). It was shown that the NLRP3 protein is upregulated after ICH and SAH and peaked at 24 h, along with elevation of inflammatory factors, IL-1β and IL-18 (Chen et al., 2013; Ma et al., 2014; Feng et al., 2015; Dong et al., 2016). Meanwhile, the significant upregulation of caspase 1 was detected at 3 h and peaked at 24–72 h after ICH (Ma et al., 2014; Feng et al., 2015). Inhibition of caspase 1 by Ac-YVAD-CMK could significantly decrease brain injury presentation, as evidenced by improved neurological functions, and amelioration of brain edema after ICH (Wu et al., 2010; Lin et al., 2018). The neuroprotection was associated with decreased expression of IL-1β, JNK, and MMP-9 and inhibition of ZO-1 degradation (Wu et al., 2010). The Ac-YVAD-CMK administration reduced M1-type microglia polarization and increased the number of M2-type cells around the hematoma (Lin et al., 2018). This characteristic polarization of microglia was also reported to reduce the poststroke neuroinflammatory damage in an ischemic stroke study (Xu et al., 2019).

The NLRP1 inflammasome is the first member that has been characterized among the NLR family. It has been reported to be primarily expressed in neurons and glial cells (Abulafia et al., 2009; Tan et al., 2014). The melanocortin 4 receptor (MC4R) is a seven-transmembrane G-protein–coupled receptor that could be activated by neuropeptide α-MSH, which exerts anti-inflammatory and neuroprotective effects after traumatic brain injury and cerebral ischemia (Forslin Aronsson et al., 2006; Yang et al., 2014). Treatment with the MC4R agonist, RO27-3225, successfully attenuated NLRP1-dependent neuron pyroptosis (including the cleaved caspase 1 and IL-1β level) after ICH in mice (Chen et al., 2019). Furthermore, RO27-3225 also reduced the expression of p-ASK1, JNK, and p-p38 mitogen-activated protein kinase (p38 MAPK) after ICH. This study presented a hypothesis that RO27-3225–mediated neuronal pyroptosis suppression may be regulated by the activation of MC4R and the inhibition of ASK1/JNK/p38 MAPK signaling pathways (Chen et al., 2019).

NLRP3 is another member of the NLR family reported in the central nervous system (CNS), with expression primarily located within the microglia and endothelium (Ma et al., 2014; Yang et al., 2014; Lin et al., 2018). Previous studies investigated several upstream regulators of NLRP3 involved in ICH pathophysiology. The ATP-gated transmembrane cation channel purinergic 2X7 receptor (P2X7R) is the key regulator in upstream activation of the NLRP3 inflammasome (Di Virgilio, 2007). P2X7R was activated after ICH and SAH *in vivo*. Inhibition of P2X7R activity can reduce NLRP3, IL-1β, and IL-18 from microglia (Chen et al., 2013; Feng et al., 2015). It was also postulated that peroxynitrite ($ONOO^-$) could be involved in the P2X7R-regulated NLRP3 inflammasome formation after ICH (Feng et al., 2015).

TABLE 3 | Latest research of pyroptosis in hemorrhagic stroke.

References	Stroke	Vitro/Vivo	Subjects	Related pathway	Conclusion
Wu et al. (2010)	ICH	Vivo	Mice	JNK/caspase-1/Il-1β	Caspase-1 inhibitor, Ac-YVAD-CMK, reduced brain injury *via* downregulation of IL-1β, JNK, MMP-9, and inhibition of ZO-1 degradation after ICH
Chen et al. (2013)	SAH	Vivo	Rats	P2X7R/NLRP3/IL-1β(18)	P2X7R/NLRP3 axis inhibition reduces neuroinflammation after SAH
Ma et al. (2014)	ICH	Vivo	Mice	ROS/NLRP3/caspase-1/Il-1β	ICH activated the NLRP3 inflammasome and the following inflammatory response, which may be stimulated by mitochondrial ROS.
Dong et al. (2016)	SAH	Vivo	Mice	NLRP3/Il-1β	Melatonin attenuates EBI following SAH, by inhibiting the NLRP3 inflammasome and following neuroinflammation
Feng et al. (2015)	ICH	Vivo	Rats	P2X7R/NLRP3/ IL-1β(18)	P2X7R/NLRP3 axis inhibition reduces neuroinflammation after ICH
Yang et al. (2015)	ICH	Vitro/Vivo	Mice/Primary neuron culture	miR-223/ NLRP3/Caspase-1/ IL-1β	miR-223-mediated NLRP3 participated inflammation through caspase-1 and IL-1β.
Weng et al. (2015)	ICH	Vitro/Vivo	Mice/N9 microglial cell lines	NMDAR1/NLRP3/IL-1β	Elevated NMDAR1 expression and NMDAR1 phosphorylation may subsequently activate NLRP3 and IL-1β after ICH
Lin et al. (2018)	ICH	Vivo	Mice	Caspase-1/IL-1β	AC-YVAD- CMK could reduce caspase-1 activation and inhibit IL-1β production and maturation
Chen et al. (2019)	ICH	Vivo	Mice	MC4R/ASK1/JNK/p38 MAPK	RO27-3225 improved neurological functions and inhibited NLRP1-dependent neuronal pyroptosis *via* mediating MC4R/ASK1/JNK/p38 MAPK signaling pathways after ICH

Another study found evidence that microRNA-223 was a potential negative regulator of NLRP3 formation by using TargetScan (a searching program for potential regulator microRNA; Yang et al., 2015). The NLRP3 mRNA has conserved miR-223 binding sites in its 3′ UTR, which could be used to regulate the expression of NLRP3. Inhibition of NLRP3 by miR-223 reduces erythrocyte lysis-induced microglial inflammation and neuronal injury after ICH in mice (Yang et al., 2015). It was also found that the miR-223 levels decreased after erythrocyte lysis stimulation was decreased in microglia and ICH in mice (Yang et al., 2015). Meanwhile, *N*-methyl-D-aspartic acid receptor 1 (NMDAR1) was also suggested to play an important role in NLRP3 regulation after ICH *in vivo* and *in vitro* (Weng et al., 2015). The expression and phosphorylation of NMDAR1 were significantly increased after ICH and in cultured microglial cells treated with hemin (Weng et al., 2015). Furthermore, they demonstrated that an NMDAR1 inhibitor (MK801) attenuated hemin-induced activation of microglia, subsequently leading to a decrease in NLRP3 and Il- 1β microglia production (Weng et al., 2015).

Although several studies have attempted to investigate the expression of inflammasomes and upstream regulators of canonical inflammasomes after ICH, few have explored the key protein, GSDMD, downstream of the inflammasome and the noncanonical inflammasome. As we know, pyroptosis is a GSDMD-related cell death process, where two inflammasome signaling pathways converge at the GSDMD and are executed following pore formation (Jia et al., 2019). In addition to the canonical-inflammasome activation, caspase 4/5/11 also participates in IL-1/IL-18 processing and cell death (Jia et al., 2019). We propose that future studies should investigate the role that GSDMD and caspase 4/5/11 signaling pathways have in hemorrhagic stroke.

MECHANISMS OF BBB DYSFUNCTION SECONDARY TO HEMORRHAGIC STROKE

The mechanism of BBB dysfunction after hemorrhagic is a complex process as shown in **Figure 4**. ICH and SAH are two categories of hemorrhagic stroke that occur in different intracerebral regions. ICH is mainly secondary to arteriolosclerosis induced by hypertension, coagulopathy, and vascular malformation rupture, whereas SAH is mainly caused by the rupture of an intracranial aneurysm (Gross et al., 2019; Zhang et al., 2019) Even with different etiologies, ICH and SAH are initially caused by vascular disruption in different intracerebral sites, which can be defined as the first phase of BBB disruption. This initial hemorrhage may result in early phases of cell death because of physical injury, brain edema, and increased intracranial pressure. At this stage, the death of cells comprising the NVU may significantly contribute to the induction of secondary BBB dysfunction (Hawkins and Davis, 2005; Knowland et al., 2014; Zhang et al., 2019). Currently, a normal BBB is no longer just a physical "barrier," but a dynamic and metabolic interface, based on the novel structural foundation known as the NVU (Tso and Macdonald, 2014; Zou et al., 2017). This structure includes components, such as ECs and their linking TJs, pericytes, astrocytic end-feet, neurons, and extracellular matrix (ECM) components (Tso and Macdonald, 2014; Erdo and Krajcsi, 2019). These components interact with each other to form a highly connected entirety, which has a critical function in regulating the homeostasis of water and electrolytes, immune cell trafficking, transporting necessary nutrients, and preventing the entry of compounds into the brain (Abbott et al., 2010; Hladky and Barrand, 2016; Erdo and Krajcsi, 2019).

After hemorrhagic stroke, the blood components initiate the process of cell excitotoxicity, cell edema, oxidative stress, and neuroinflammation, which further disrupt the BBB. These neurotoxic blood–derived factors include thrombin, fibrin, and erythrocyte components (Keep et al., 2014; Tso and Macdonald, 2014; Zhu et al., 2019). Thrombin is the cascade product of prothrombin during hemostasis after hemorrhagic stroke. The binding of thrombin to protease activated receptor 1 induces secondary BBB disruption through phosphorylating Src kinases and activating microglia (Möller et al., 2006; Liu et al., 2010). Fibrin cleaved from fibrinogen has been reported to play a potential role in neuroinflammation and microglial activation (Lim-Hing and Rincon, 2017). Iron, degraded from hemoglobin, is one of most important factors among various components for hemorrhagic stroke–induced BBB hyperpermeability (Hua et al., 2007; Gomes et al., 2014), which is supported by ICH/SAH studies revealing alleviated brain edema with administration of the iron chelator, deferoxamine (Lee et al., 2010; Okauchi et al., 2010; Yu et al., 2014), or a heme oxygenase (HO) inhibitor (Wagner et al., 2000; Han et al., 2018). HO plays a critical role in the degradation of heme and the release of free ferrous iron (Kamat et al., 2019). Importantly, iron has been shown to mediate BBB dysfunction mainly through generating ROS, which can directly induce degradation of the endothelium and activate signaling pathways (Mori et al., 2001; Fraser, 2011). Meanwhile, the influx of albumin accompanied by disequilibrium of water and ion homeostasis leads to cerebral edema (Lehmann et al., 2013; Di Napoli et al., 2018).

It is widely accepted that the inflammatory response occurs when resident microglia of the brain are activated within the early stages of hemorrhagic stroke. This is due to stimuli, such as neurotoxic factor accumulation and reduced blood flow, which then causes the release of proinflammatory cytokines (Ge et al., 2018; Chen et al., 2019). Among other CNS diseases, such as cerebral ischemia, Alzheimer disease, or multiple sclerosis, the mechanisms of leukocytic infiltration into the brain and the immune response with the complement system have been widely studied (Jiang et al., 2018; Sweeney et al., 2018; Ma et al., 2019; Shen et al., 2019). DL-3-n-Butylphthalide, a synthetic compound that has been approved for the treatment of ischemic stroke in China, has been shown to inhibit neurovascular inflammation *via* downregulation of intercellular adhesion molecule 1 (ICAM-1; Yang et al., 2019). Despite a slight lag, it was recently revealed that these cytokines may also upregulate adhesion molecules, including ICAM-1, vascular adhesion molecule 1, and vascular adhesion protein 1 after hemorrhagic stroke (Ma et al., 2011; Xu et al., 2015; Cheng et al., 2018; Gris et al., 2019). These

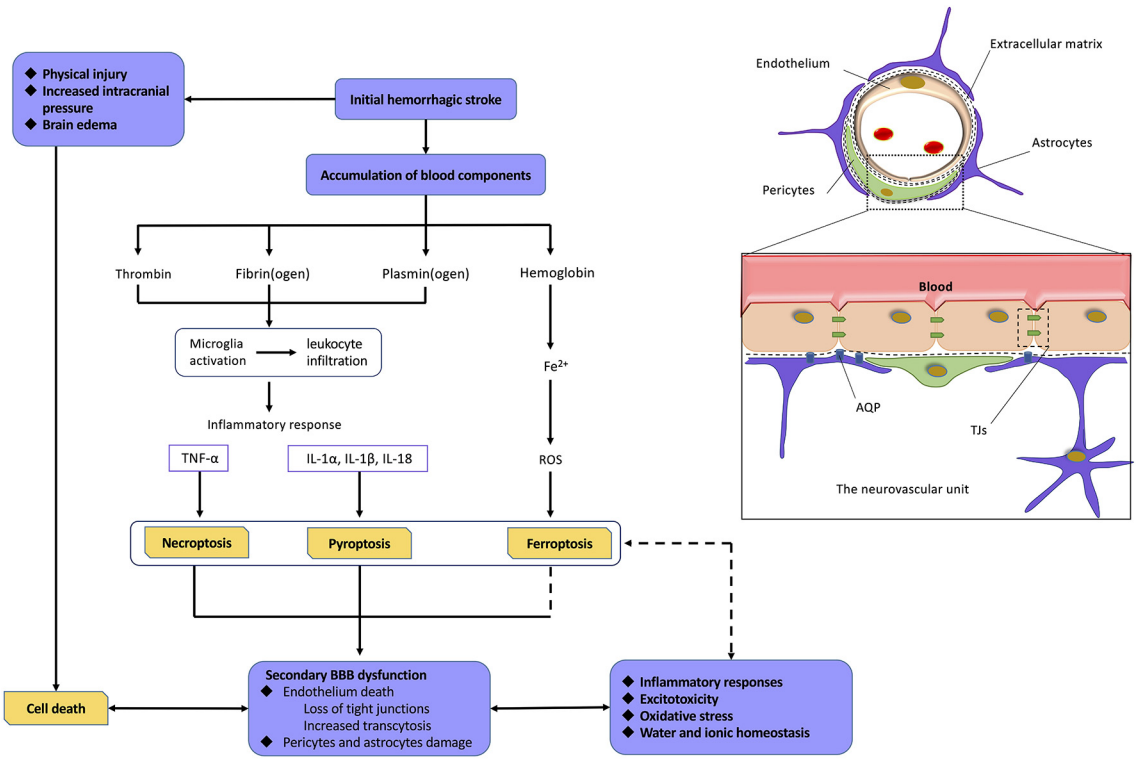

FIGURE 4 | Relationship among hemorrhagic stroke, programmed cell deaths, and blood–brain barrier (BBB) dysfunction. Normal neurovascular units (NVUs) are composed of intact endothelial cells (ECs), pericytes, astrocytic endfeet, and extracellular matrix (ECM) components. ECs, with their tight junctions (TJs), are the most important components. On the one hand, initial hemorrhagic stroke directly causes cell death in central nervous system (CNS) as a result of physical injury, intracranial pressure, and brain edema. On the other hand, abundant blood components can also mediate programmed cell deaths (PCDs) *via* proinflammatory response, reactive oxygen species (ROS), and so on. The death of cell, especially ECs, leads to severe damage on BBB. As a result, BBB dysfunction induces a variety of pathophysiological processes including inflammatory responses, excitotoxicity, oxidative stress, water, and ionic homeostasis, which finally mediate more extensive PCDs. Abbreviations: TNFα, tumor necrosis factor; IL-1α/1β/18, interleukin 1α/1β/18.

recruited leukocytes further accumulate and transmigrate across the endothelium, finally releasing an abundance of cytokines and chemokines (Cheng et al., 2018; Gris et al., 2019). Cytokines mediating various signaling pathways are an important part of the inflammatory processes after hemorrhagic stroke. For example, TNFα and IL-1β are both found to mediate cell function, including endothelial cell death, followed by BBB hyperpermeability (King et al., 2013; Yang et al., 2014; Liu et al., 2019). Chemokines, such as monocyte chemoattractant protein 1, not only can mediate leukocyte chemotaxis, but also can directly damage TJs. These both result in BBB dysfunction (Niwa et al., 2016; Yang et al., 2016). Meanwhile, more recent studies have focused on the immune response, with an emphasis on lymphocytic infiltration, as they contribute to brain recovery through hematoma resolution, neurogenesis, and axonal regeneration after ICH. Regulatory T cells were shown to mediate anti-inflammatory responses and improve neurological function in a chronic subdural hematoma rat model (Frost et al., 2019; Quan et al., 2019). These studies may provide emerging therapeutic targets for ICH (Shao A. et al., 2019). It should be noted that MMPs, which are primarily released by neutrophils, are also thoroughly studied potent proteinases and play a critical role in the increase of endothelial permeability *via* disruption of TJs, ECM degradation, and increased transcytosis of the endothelium (Abilleira et al., 2003; Qi et al., 2016; Liu et al., 2019). Recently, MMP-9 was also found to mediate endothelial permeability through the activity of von Willebrand factor and the initial recruitment of inflammatory leukocytes (Askenase and Sansing, 2016).

CROSSTALK BETWEEN BBB DYSFUNCTION AND PCDs IN HEMORRHAGIC STROKE

Cell death, which occurs over an extended period following hemorrhagic stroke, not only can be directly induced by physical injury, but also indirectly mediated by pathophysiological process associated with BBB dysfunction mentioned above (Keep et al., 2014). The death of NVU cells further exacerbates BBB damage. While the three PCDs (necroptosis, ferroptosis, and pyroptosis) have distinct morphological, biochemical, and genetic characteristics, they have been shown to mutually participate in BBB dysfunction. The endothelium remains the primary target of study because of their paramount significance

in the BBB (**Figure 4**; Zille et al., 2017; Chen et al., 2018, 2019; Zhao et al., 2018).

A significant amount of proinflammatory cytokines are increased during these three processes, such as TNFα, IL-1β, and IL-6 (Ge et al., 2018; Zhang Z. et al., 2018; Chen et al., 2019). As described above, upregulation of these cytokines will significantly induce microglial activation and increase BBB permeability, either directly or indirectly. To support this, several animal experiments have demonstrated this hyperpermeability of BBB *via* albumin extravasation or an Evans blue dye extravasation assay, and this pathological change can be reversed by specific inhibitors of necroptosis, ferroptosis, and pyroptosis (Chen et al., 2017; Ge et al., 2018; Zhang Z. et al., 2018; Yuan et al., 2019). More recently, research found that necroptosis occurred in the endothelium and is initiated by interactions between TNFα secreted by M1-type microglia and TNFR1 on the endothelium (Chen et al., 2019). The significant decrease in the levels of occludin and claudin-5 (major transmembrane TJs) and the increase in MMP-9 levels and activity can both be reversed by nec-1 after SAH (Chen et al., 2019). It implies that there is a high degree of correlation between necroptosis and BBB dysfunction after SAH. Similarly, pyroptosis of brain microvascular ECs was shown in a TBI model and was induced by GSDMD. BBB function and neurological outcomes improved when the process of pyroptosis was inhibited (Chen et al., 2018). According to the discovery above, it seems reasonable to speculate that ferroptosis also occurred in the endothelium after stroke events. In an ICH model, GPX4 reduced oxidative stress and thus inhibited ferroptosis to recover the function of the BBB (Zhang Z. et al., 2018). The inflammatory and innate immune responses are among the most important factors in BBB regulation. Recently, a series of experiments on aged mice revealed severe dysregulation of immunity and an excessive inflammatory response (Freitas et al., 2019; Shen et al., 2019; Zhang et al., 2019). As hemorrhagic stroke is a disease with an increased incidence in elderly populations, we should further investigate the effect of these changes on BBB dysfunction and PCDs.

Currently, research pertaining to ferroptosis and BBB dysfunction is very limited. However, according to the mechanisms of BBB dysfunction and ferroptosis discussed above, the role of ferroptosis on BBB damage warrants more attention. We have mentioned above with sufficient evidence that iron, when degraded from hemoglobin, has a critically important role in BBB hyperpermeability after hemorrhagic stroke, and decreasing iron content through various methods significantly reversed the brain edema (Wagner et al., 2000; Hua et al., 2007; Gomes et al., 2014; Yu et al., 2014). The key point of this problem lies in the poor understanding regarding the exact mechanism of iron overload-induced BBB hyperpermeability. Oxidative stress seems to be a promising candidate (Fraser, 2011). Interestingly, the mechanism of ferroptosis has not been fully clarified. However, iron and lipid peroxidation products have been demonstrated to be indispensable initiators of critical death signals (Yang and Stockwell, 2016; Stockwell et al., 2017). Moreover, studies had shown increased deleterious effects of lipid peroxidation products, such as HO-1, on free radical scavenging after ICH (Chang et al., 2014). Therefore, there are theoretical bases to prove the role of ferroptosis in BBB dysfunction.

In addition to the mechanisms of endothelial cell destruction being elucidated to some extent, these three PCDs may have some potential mechanisms relevant to other BBB structures and signaling pathways based on current research findings. Astrocytes are an important component of the BBB basic structure; they regulate electrolyte and water balance *via* an abundance of AQP-4 and gap junctions in the end-feet (Zlokovic, 2008). In the condition of depleted intracellular GSH, astrocytes undergo caspase-independent cell death. This process is highly relevant to the secretion of TNFα from human astrocytes and can be inhibited by nec-1 (Laird et al., 2008). It suggests that the studies regarding the exact mechanisms of necroptosis and nec-1 in astrocytes, as well as other BBB structures, strengthen the understanding of BBB dysfunction after hemorrhagic stroke.

Interestingly, there may also be some intersection between the three PCDs. Inducible GPX4 alleviates ferroptosis and pyroptosis in bacterial infection, whereas degradation of GSH enhances necroptosis and ferroptosis in human triple-negative breast cancer cells, suggesting a potential pathway involving pyroptosis and necroptosis (Zille et al., 2017; Zhu et al., 2019). Lastly, these three patterns of death may share common causes, which are not limited to oxidative stress. A logical plan of action would be to find shared targets of different PCDs to inhibit, therefore improving the efficacy of neurological recovery after hemorrhagic stroke.

CONCLUSION

A growing number of studies show that PCDs are involved in hemorrhagic stroke. This review article summarizes the role of necroptosis, ferroptosis, and pyroptosis after hemorrhagic stroke, as well as their relationship with BBB dysfunction. Although most consequences of BBB dysfunction are detrimental, one potential beneficial result is that the entire brain would benefit if a novel therapeutic target was uncovered. Further studies exploring the mechanisms of these three forms of cell death and the crosstalk with BBB dysfunction will assist in the search for promising interventional targets of hemorrhagic stroke. Furthermore, more studies should broaden their scope to include research on cell types other than neurons.

AUTHOR CONTRIBUTIONS

All the authors participated in analyzing and discussing the literature, commenting on, and approving the manuscript. AS and JZ supervised the research, led the discussion, wrote and revised the manuscript. All authors read and approved the final manuscript.

FUNDING

This work was funded by the China Postdoctoral Science Foundation (2017M612010), the National Natural Science Foundation of China (81701144) and Fundamental Research Funds for the Central Universities (2019QNA7038).

REFERENCES

Aachoui, Y., Sagulenko, V., Miao, E. A., and Stacey, K. J. (2013). Inflammasome-mediated pyroptotic and apoptotic cell death and defense against infection. *Curr. Opin. Microbiol.* 16, 319–326. doi: 10.1016/j.mib.2013.04.004

Abbott, N. J., Patabendige, A. A., Dolman, D. E., Yusof, S. R., and Begley, D. J. (2010). Structure and function of the blood-brain barrier. *Neurobiol. Dis.* 37, 13–25. doi: 10.1016/j.nbd.2009.07.030

Abilleira, S., Montaner, J., Molina, C. A., Monasterio, J., Castillo, J., and Alvarez-Sabin, J. (2003). Matrix metalloproteinase-9 concentration after spontaneous intracerebral hemorrhage. *J. Neurosurg.* 99, 65–70. doi: 10.3171/jns.2003.99.1.0065

Abulafia, D. P., de Rivero Vaccari, J. P., Lozano, J. D., Lotocki, G., Keane, R. W., and Dietrich, W. D. (2009). Inhibition of the inflammasome complex reduces the inflammatory response after thromboembolic stroke in mice. *J. Cereb. Blood Flow Metab.* 29, 534–544. doi: 10.1038/jcbfm.2008.143

Alim, I., Caulfield, J. T., Chen, Y., Swarup, V., Geschwind, D. H., Ivanova, E., et al. (2019). Selenium drives a transcriptional adaptive program to block ferroptosis and treat stroke. *Cell* 177, 1262.e25–1279.e25. doi: 10.1016/j.cell.2019.03.032

Askenase, M. H., and Sansing, L. H. (2016). Stages of the inflammatory response in pathology and tissue repair after intracerebral hemorrhage. *Semin. Neurol.* 36, 288–297. doi: 10.1055/s-0036-1582132

Bergsbaken, T., Fink, S. L., and Cookson, B. T. (2009). Pyroptosis: host cell death and inflammation. *Nat. Rev. Microbiol.* 7, 99–109. doi: 10.1038/nrmicro2070

Bertrand, M. J., Milutinovic, S., Dickson, K. M., Ho, W. C., Boudreault, A., Durkin, J., et al. (2008). cIAP1 and cIAP2 facilitate cancer cell survival by functioning as E3 ligases that promote RIP1 ubiquitination. *Mol. Cell* 30, 689–700. doi: 10.1016/j.molcel.2008.05.014

Cao, J. Y., and Dixon, S. J. (2016). Mechanisms of ferroptosis. *Cell. Mol. Life Sci.* 73, 2195–2209. doi: 10.1007/s00018-016-2194-1

Chang, C. F., Cho, S., and Wang, J. (2014). (−)-Epicatechin protects hemorrhagic brain *via* synergistic Nrf2 pathways. *Ann. Clin. Transl. Neurol.* 1, 258–271. doi: 10.1002/acn3.54

Chang, P., Dong, W., Zhang, M., Wang, Z., Wang, Y., Wang, T., et al. (2014). Anti-necroptosis chemical necrostatin-1 can also suppress apoptotic and autophagic pathway to exert neuroprotective effect in mice intracerebral hemorrhage model. *J. Mol. Neurosci.* 52, 242–249. doi: 10.1007/s12031-013-0132-3

Chen, A. Q., Fang, Z., Chen, X. L., Yang, S., Zhou, Y. F., Mao, L., et al. (2019). Microglia-derived TNF-α mediates endothelial necroptosis aggravating blood brain-barrier disruption after ischemic stroke. *Cell Death Dis.* 10:487. doi: 10.1038/s41419-019-1716-9

Chen, D., Fan, Z., Rauh, M., Buchfelder, M., Eyupoglu, I. Y., and Savaskan, N. (2017). ATF4 promotes angiogenesis and neuronal cell death and confers ferroptosis in a xCT-dependent manner. *Oncogene* 36, 5593–5608. doi: 10.1038/onc.2017.146

Chen, J., Jin, H., Xu, H., Peng, Y., Jie, L., Xu, D., et al. (2019). The neuroprotective effects of necrostatin-1 on subarachnoid hemorrhage in rats are possibly mediated by preventing blood-brain barrier disruption and RIP3-mediated necroptosis. *Cell Transplant.* 28, 1358–1372. doi: 10.1177/0963689719867285

Chen, S., Ma, Q., Krafft, P. R., Hu, Q., Rolland, W. II., Sherchan, P., et al. (2013). P2X7R/cryopyrin inflammasome axis inhibition reduces neuroinflammation after SAH. *Neurobiol. Dis.* 58, 296–307. doi: 10.1016/j.nbd.2013.06.011

Chen, S., Mei, S., Luo, Y., Wu, H., Zhang, J., and Zhu, J. (2018). Gasdermin family: a promising therapeutic target for stroke. *Transl. Stroke Res.* 9, 555–563. doi: 10.1007/s12975-018-0666-3

Chen, T., Pan, H., Li, J., Xu, H., Jin, H., Qian, C., et al. (2018). Inhibiting of RIPK3 attenuates early brain injury following subarachnoid hemorrhage: possibly through alleviating necroptosis. *Biomed. Pharmacother.* 107, 563–570. doi: 10.1016/j.biopha.2018.08.056

Chen, F., Su, X., Lin, Z., Lin, Y., Yu, L., Cai, J., et al. (2017). Necrostatin-1 attenuates early brain injury after subarachnoid hemorrhage in rats by inhibiting necroptosis. *Neuropsychiatr. Dis. Treat.* 13, 1771–1782. doi: 10.2147/NDT.S140801

Chen, S., Zuo, Y., Huang, L., Sherchan, P., Zhang, J., Yu, Z., et al. (2019). The MC4 receptor agonist RO27–3225 inhibits NLRP1-dependent neuronal pyroptosis *via* the ASK1/JNK/p38 MAPK pathway in a mouse model of intracerebral haemorrhage. *Br. J. Pharmacol.* 176, 1341–1356. doi: 10.1111/bph.14639

Cheng, K. T., Xiong, S., Ye, Z., Hong, Z., Di, A., Tsang, K. M., et al. (2017). Caspase-11-mediated endothelial pyroptosis underlies endotoxemia-induced lung injury. *J. Clin. Invest.* 127, 4124–4135. doi: 10.1172/jci94495

Cheng, Y., Zan, J., Song, Y., Yang, G., Shang, H., and Zhao, W. (2018). Evaluation of intestinal injury, inflammatory response and oxidative stress following intracerebral hemorrhage in mice. *Int. J. Mol. Med.* 42, 2120–2128. doi: 10.3892/ijmm.2018.3755

Chu, X., Wu, X., Feng, H., Zhao, H., Tan, Y., Wang, L., et al. (2018). Coupling between interleukin-1R1 and necrosome complex involves in hemin-induced neuronal necroptosis after intracranial hemorrhage. *Stroke* 49, 2473–2482. doi: 10.1161/strokeaha.117.019253

Daneman, R., and Prat, A. (2015). The blood-brain barrier. *Cold Spring Harb. Perspect. Biol.* 7:a020412. doi: 10.1101/cshperspect.a020412

de Rooij, N. K., Linn, F. H., van der Plas, J. A., Algra, A., and Rinkel, G. J. (2007). Incidence of subarachnoid haemorrhage: a systematic review with emphasis on region, age, gender, and time trends. *J. Neurol. Neurosurg. Psychiatry* 78, 1365–1372. doi: 10.1136/jnnp.2007.117655

Di Napoli, M., Slevin, M., Popa-Wagner, A., Singh, P., Lattanzi, S., and Divani, A. A. (2018). Monomeric C-reactive protein and cerebral hemorrhage: from bench to bedside. *Front. Immunol.* 9:1921. doi: 10.3389/fimmu.2018.01921

Di Virgilio, F. (2007). Liaisons dangereuses: $P2X_7$ and the inflammasome. *Trends Pharmacol. Sci.* 28, 465–472. doi: 10.1016/j.tips.2007.07.002

Dinarello, C. A. (2011). A clinical perspective of IL-1β as the gatekeeper of inflammation. *Eur. J. Immunol.* 41, 1203–1217. doi: 10.1002/eji.201141550

Dixon, S. J., Lemberg, K. M., Lamprecht, M. R., Skouta, R., Zaitsev, E. M., Gleason, C. E., et al. (2012). Ferroptosis: an iron-dependent form of nonapoptotic cell death. *Cell* 149, 1060–1072. doi: 10.1016/j.cell.2012.03.042

Dixon, S. J., and Stockwell, B. R. (2014). The role of iron and reactive oxygen species in cell death. *Nat. Chem. Biol.* 10, 9–17. doi: 10.1038/nchembio.1416

Dong, Y., Fan, C., Hu, W., Jiang, S., Ma, Z., Yan, X., et al. (2016). Melatonin attenuated early brain injury induced by subarachnoid hemorrhage *via* regulating NLRP3 inflammasome and apoptosis signaling. *J. Pineal Res.* 60, 253–262. doi: 10.1111/jpi.12300

Erdo, F., and Krajcsi, P. (2019). Age-related functional and expressional changes in efflux pathways at the blood-brain barrier. *Front. Aging Neurosci.* 11:196. doi: 10.3389/fnagi.2019.00196

Fang, Y., Chen, S., Reis, C., and Zhang, J. (2018). The role of autophagy in subarachnoid hemorrhage: an update. *Curr. Neuropharmacol.* 16, 1255–1266. doi: 10.2174/1570159x15666170406142631

Fang, Y., Shao, Y., Lu, J., Dong, X., Zhao, X., Zhang, J., et al. (2019). The effectiveness of lumbar cerebrospinal fluid drainage in aneurysmal subarachnoid hemorrhage with different bleeding amounts. *Neurosurg. Rev.* doi: 10.1007/s10143-019-01116-1 [Epub ahead of print].

Feng, L., Chen, Y., Ding, R., Fu, Z., Yang, S., Deng, X., et al. (2015). P2X7R blockade prevents NLRP3 inflammasome activation and brain injury in a rat model of intracerebral hemorrhage: involvement of peroxynitrite. *J. Neuroinflammation* 12:190. doi: 10.1186/s12974-015-0409-2

Forslin Aronsson, S., Spulber, S., Popescu, L. M., Winblad, B., Post, C., Oprica, M., et al. (2006). α-Melanocyte-stimulating hormone is neuroprotective in rat global cerebral ischemia. *Neuropeptides* 40, 65–75. doi: 10.1016/j.npep.2005.10.006

Fraser, P. A. (2011). The role of free radical generation in increasing cerebrovascular permeability. *Free Radic. Biol. Med.* 51, 967–977. doi: 10.1016/j.freeradbiomed.2011.06.003

Freitas, G. R. R., da Luz Fernandes, M., Agena, F., Jaluul, O., Silva, S. C., Lemos, F. B. C., et al. (2019). Aging and end stage renal disease cause a decrease in absolute circulating lymphocyte counts with a shift to a memory profile and diverge in treg population. *Aging Dis.* 10, 49–61. doi: 10.14336/ad.2018.0318

Frost, P. S., Barros-Aragão, F., da Silva, R. T., Venancio, A., Matias, I., Lyra E Silva, N. M., et al. (2019). Neonatal infection leads to increased susceptibility to Aβ oligomer-induced brain inflammation, synapse loss and cognitive impairment in mice. *Cell Death Dis.* 10:323. doi: 10.1038/s41419-019-1529-x

Fuchs, Y., and Steller, H. (2015). Live to die another way: modes of programmed cell death and the signals emanating from dying cells. *Nat. Rev. Mol. Cell Biol.* 16, 329–344. doi: 10.1038/nrm3999

Galluzzi, L., Kepp, O., Chan, F. K., and Kroemer, G. (2017). Necroptosis: mechanisms and relevance to disease. *Annu. Rev. Pathol.* 12, 103–130. doi: 10.1146/annurev-pathol-052016-100247

Gao, M., Monian, P., Quadri, N., Ramasamy, R., and Jiang, X. (2015). Glutaminolysis and transferrin regulate ferroptosis. *Mol. Cell* 59, 298–308. doi: 10.1016/j.molcel.2015.06.011

Ge, X., Li, W., Huang, S., Yin, Z., Xu, X., Chen, F., et al. (2018). The pathological role of NLRs and AIM2 inflammasome-mediated pyroptosis in damaged blood-brain barrier after traumatic brain injury. *Brain Res.* 1697, 10–20. doi: 10.1016/j.brainres.2018.06.008

Gomes, J. A., Selim, M., Cotleur, A., Hussain, M. S., Toth, G., Koffman, L., et al. (2014). Brain iron metabolism and brain injury following subarachnoid hemorrhage: iCeFISH-pilot (CSF iron in SAH). *Neurocrit. Care* 21, 285–293. doi: 10.1007/s12028-014-9977-8

Gris, T., Laplante, P., Thebault, P., Cayrol, R., Najjar, A., Joannette-Pilon, B., et al. (2019). Innate immunity activation in the early brain injury period following subarachnoid hemorrhage. *J. Neuroinflammation* 16:253. doi: 10.1186/s12974-019-1629-7

Gross, B. A., Jankowitz, B. T., and Friedlander, R. M. (2019). Cerebral intraparenchymal hemorrhage: a review. *JAMA* 321, 1295–1303. doi: 10.1001/jama.2019.2413

Grysiewicz, R. A., Thomas, K., and Pandey, D. K. (2008). Epidemiology of ischemic and hemorrhagic stroke: incidence, prevalence, mortality, and risk factors. *Neurol. Clin.* 26, 871–895. doi: 10.1016/j.ncl.2008.07.003

Gustavsson, A., Svensson, M., Jacobi, F., Allgulander, C., Alonso, J., Beghi, E., et al. (2011). Cost of disorders of the brain in Europe 2010. *Eur. Neuropsychopharmacol.* 21, 718–779. doi: 10.1016/j.euroneuro.2011.08.008

Han, Y.-W., Liu, X.-J., Zhao, Y., and Li, X.-M. (2018). Role of Oleanolic acid in maintaining BBB integrity by targeting p38MAPK/VEGF/Src signaling pathway in rat model of subarachnoid hemorrhage. *Eur. J. Pharmacol.* 839, 12–20. doi: 10.1016/j.ejphar.2018.09.018

Hawkins, B. T., and Davis, T. P. (2005). The blood-brain barrier/neurovascular unit in health and disease. *Pharmacol. Rev.* 57, 173–185. doi: 10.1124/pr.57.2.4

Hayden, M. S., and Ghosh, S. (2014). Regulation of NF-κB by TNF family cytokines. *Semin. Immunol.* 26, 253–266. doi: 10.1016/j.smim.2014.05.004

Hladky, S. B., and Barrand, M. A. (2016). Fluid and ion transfer across the blood-brain and blood-cerebrospinal fluid barriers; a comparative account of mechanisms and roles. *Fluids Barriers CNS* 13:19. doi: 10.1186/s12987-016-0040-3

Hua, Y., Keep, R. F., Hoff, J. T., and Xi, G. (2007). Brain injury after intracerebral hemorrhage: the role of thrombin and iron. *Stroke* 38, 759–762. doi: 10.1161/01.str.0000247868.97078.10

Jia, C., Chen, H., Zhang, J., Zhou, K., Zhuge, Y., Niu, C., et al. (2019). Role of pyroptosis in cardiovascular diseases. *Int. Immunopharmacol.* 67, 311–318. doi: 10.7150/ijbs.33568

Jiang, X., Andjelkovic, A. V., Zhu, L., Yang, T., Bennett, M. V. L., Chen, J., et al. (2018). Blood-brain barrier dysfunction and recovery after ischemic stroke. *Prog. Neurobiol.* 163–164, 144–171. doi: 10.1016/j.pneurobio.2017.10.001

Jiang, L., Kon, N., Li, T., Wang, S. J., Su, T., Hibshoosh, H., et al. (2015). Ferroptosis as a p53-mediated activity during tumour suppression. *Nature* 520, 57–62. doi: 10.1038/nature14344

Jin, Z., and El-Deiry, W. S. (2006). Distinct signaling pathways in TRAIL-versus tumor necrosis factor-induced apoptosis. *Mol. Cell. Biol.* 26, 8136–8148. doi: 10.1128/mcb.00257-06

Kamat, P. K., Ahmad, A. S., and Doré, S. (2019). Carbon monoxide attenuates vasospasm and improves neurobehavioral function after subarachnoid hemorrhage. *Arch. Biochem. Biophys.* 676:108117. doi: 10.1016/j.abb.2019.108117

Karuppagounder, S. S., Alim, I., Khim, S. J., Bourassa, M. W., Sleiman, S. F., John, R., et al. (2016). Therapeutic targeting of oxygen-sensing prolyl hydroxylases abrogates ATF4-dependent neuronal death and improves outcomes after brain hemorrhage in several rodent models. *Sci. Transl. Med.* 8:328ra29. doi: 10.1126/scitranslmed.aac6008

Karuppagounder, S. S., Alin, L., Chen, Y., Brand, D., Bourassa, M. W., Dietrich, K., et al. (2018). N-acetylcysteine targets 5 lipoxygenase-derived, toxic lipids and can synergize with prostaglandin E2 to inhibit ferroptosis and improve outcomes following hemorrhagic stroke in mice. *Ann. Neurol.* 84, 854–872. doi: 10.1002/ana.25356

Kayagaki, N., Warming, S., Lamkanfi, M., Vande Walle, L., Louie, S., Dong, J., et al. (2011). Non-canonical inflammasome activation targets caspase-11. *Nature* 479, 117–121. doi: 10.1038/nature10558

Keep, R. F., Zhou, N., Xiang, J., Andjelkovic, A. V., Hua, Y., and Xi, G. (2014). Vascular disruption and blood-brain barrier dysfunction in intracerebral hemorrhage. *Fluids Barriers CNS* 11:18. doi: 10.1186/2045-8118-11-18

King, M. D., Alleyne, C. H. Jr., and Dhandapani, K. M. (2013). TNF-alpha receptor antagonist, R-7050, improves neurological outcomes following intracerebral hemorrhage in mice. *Neurosci. Lett.* 542, 92–96. doi: 10.1016/j.neulet.2013.02.051

King, M. D., Whitaker-Lea, W. A., Campbell, J. M., Alleyne, C. H. Jr., and Dhandapani, K. M. (2014). Necrostatin-1 reduces neurovascular injury after intracerebral hemorrhage. *Int. J. Cell Biol.* 2014:495817. doi: 10.1155/2014/495817

Knowland, D., Arac, A., Sekiguchi, K. J., Hsu, M., Lutz, S. E., Perrino, J., et al. (2014). Stepwise recruitment of transcellular and paracellular pathways underlies blood-brain barrier breakdown in stroke. *Neuron* 82, 603–617. doi: 10.1016/j.neuron.2014.03.003

Laird, M. D., Wakade, C., Alleyne, C. H. Jr., and Dhandapani, K. M. (2008). Hemin-induced necroptosis involves glutathione depletion in mouse astrocytes. *Free Radic. Biol. Med.* 45, 1103–1114. doi: 10.1016/j.freeradbiomed.2008.07.003

Lamkanfi, M., and Dixit, V. M. (2014). Mechanisms and functions of inflammasomes. *Cell* 157, 1013–1022. doi: 10.1016/j.cell.2014.04.007

Lange, P. S., Chavez, J. C., Pinto, J. T., Coppola, G., Sun, C. W., Townes, T. M., et al. (2008). ATF4 is an oxidative stress-inducible, prodeath transcription factor in neurons *in vitro* and *in vivo*. *J. Exp. Med.* 205, 1227–1242. doi: 10.1084/jem.20071460

Lee, J.-Y., Keep, R. F., He, Y., Sagher, O., Hua, Y., and Xi, G. (2010). Hemoglobin and iron handling in brain after subarachnoid hemorrhage and the effect of deferoxamine on early brain injury. *J. Cereb. Blood Flow Metab.* 30, 1793–1803. doi: 10.1038/jcbfm.2010.137

Lehmann, L., Bendel, S., Uehlinger, D. E., Takala, J., Schafer, M., Reinert, M., et al. (2013). Randomized, double-blind trial of the effect of fluid composition on electrolyte, acid-base, and fluid homeostasis in patients early after subarachnoid hemorrhage. *Neurocrit. Care* 18, 5–12. doi: 10.1007/s12028-012-9764-3

Leist, M., and Jaattela, M. (2001). Four deaths and a funeral: from caspases to alternative mechanisms. *Nat. Rev. Mol. Cell Biol.* 2, 589–598. doi: 10.1038/35085008

Li, Q., Han, X., Lan, X., Gao, Y., Wan, J., Durham, F., et al. (2017). Inhibition of neuronal ferroptosis protects hemorrhagic brain. *JCI Insight* 2:e90777. doi: 10.1172/jci.insight.90777

Li, Q., Weiland, A., Chen, X., Lan, X., Han, X., Durham, F., et al. (2018). Ultrastructural characteristics of neuronal death and white matter injury in mouse brain tissues after intracerebral hemorrhage: coexistence of ferroptosis, autophagy, and necrosis. *Front. Neurol.* 9:581. doi: 10.3389/fneur.2018.00581

Lim-Hing, K., and Rincon, F. (2017). Secondary hematoma expansion and perihemorrhagic edema after intracerebral hemorrhage: from bench work to practical aspects. *Front. Neurol.* 8:74. doi: 10.3389/fneur.2017.00074

Lin, X., Ye, H., Siaw-Debrah, F., Pan, S., He, Z., Ni, H., et al. (2018). AC-YVAD-CMK inhibits pyroptosis and improves functional outcome after intracerebral hemorrhage. *Biomed. Res. Int.* 2018:3706047. doi: 10.1155/2018/3706047

Linkermann, A., and Green, D. R. (2014). Necroptosis. *N. Engl. J. Med.* 370, 455–465. doi: 10.1056/NEJMra1310050

Liu, D. Z., Ander, B. P., Xu, H., Shen, Y., Kaur, P., Deng, W., et al. (2010). Blood-brain barrier breakdown and repair by Src after thrombin-induced injury. *Ann. Neurol.* 67, 526–533. doi: 10.1002/ana.21924

Liu, Y., Luo, H., Wang, L., Li, C., Liu, L., Huang, L., et al. (2019). Increased serum matrix metalloproteinase-9 levels are associated with anti-jo1 but not anti-MDA5 in myositis patients. *Aging Dis.* 10, 746–755. doi: 10.14336/ad.2018.1120

Liu, Z., Wang, X., Jiang, K., Ji, X., Zhang, Y. A., and Chen, Z. (2019). TNFα-induced up-regulation of *Ascl2* affects the differentiation and proliferation of neural stem cells. *Aging Dis.* 10, 1207–1220. doi: 10.14336/ad.2018.1028

Liu, C., Zhang, K., Shen, H., Yao, X., Sun, Q., and Chen, G. (2018). Necroptosis: a novel manner of cell death, associated with stroke (Review). *Int. J. Mol. Med.* 41, 624–630. doi: 10.3892/ijmm.2017.3279

Lu, J., Sun, Z., Fang, Y., Zheng, J., Xu, S., Xu, W., et al. (2019). Melatonin suppresses microglial necroptosis by regulating deubiquitinating enzyme A20 after intracerebral hemorrhage. *Front. Immunol.* 10:1360. doi: 10.3389/fimmu.2019.01360

Lublinsky, S., Major, S., Kola, V., Horst, V., Santos, E., Platz, J., et al. (2019). Early blood-brain barrier dysfunction predicts neurological outcome following aneurysmal subarachnoid hemorrhage. *EBioMedicine* 43, 460–472. doi: 10.1016/j.ebiom.2019.04.054

Möller, T., Weinstein, J. R., and Hanisch, U.-K. (2006). Activation of microglial cells by thrombin: past, present, and future. *Semin. Thromb. Hemost.* 32, 69–76. doi: 10.1055/s-2006-939556

Ma, Q., Chen, S., Hu, Q., Feng, H., Zhang, J. H., and Tang, J. (2014). NLRP3 inflammasome contributes to inflammation after intracerebral hemorrhage. *Ann. Neurol.* 75, 209–319. doi: 10.1002/ana.24070

Ma, Y., Liu, Y., Zhang, Z., and Yang, G. Y. (2019). Significance of complement system in ischemic stroke: a comprehensive review. *Aging Dis.* 10, 429–462. doi: 10.14336/ad.2019.0119

Ma, Q., Manaenko, A., Khatibi, N. H., Chen, W., Zhang, J. H., and Tang, J. (2011). Vascular adhesion protein-1 inhibition provides antiinflammatory protection after an intracerebral hemorrhagic stroke in mice. *J. Cereb. Blood Flow Metab.* 31, 881–893. doi: 10.1038/jcbfm.2010.167

Ma, F., Zhang, X., and Yin, K. J. (2020). MicroRNAs in central nervous system diseases: a prospective role in regulating blood-brain barrier integrity. *Exp. Neurol.* 323:113094. doi: 10.1016/j.expneurol.2019.113094

Macdonald, R. L., and Schweizer, T. A. (2017). Spontaneous subarachnoid haemorrhage. *Lancet* 389, 655–666. doi: 0.1016/S0140-6736(16)30668-7

Majmundar, N., Kim, B., and Prestigiacomo, C. J. (2016). Necroptosis pathway in treatment of intracerebral hemorrhage: novel therapeutic target. *World Neurosurg.* 89, 716–717. doi: 10.1016/j.wneu.2016.03.071

Marbacher, S., Gruter, B., Schopf, S., Croci, D., Nevzati, E., D'Alonzo, D., et al. (2018). Systematic review of *in vivo* animal models of subarachnoid hemorrhage: species, standard parameters, and outcomes. *Transl. Stroke Res.* 10, 250–258. doi: 10.1007/s12975-018-0657-4

Martinon, F., Burns, K., and Tschopp, J. (2002). The inflammasome: a molecular platform triggering activation of inflammatory caspases and processing of proIL-β. *Mol. Cell* 10, 417–426. doi: 10.1016/s1097-2765(02)00599-3

Micheau, O., and Tschopp, J. (2003). Induction of TNF receptor I-mediated apoptosis *via* two sequential signaling complexes. *Cell* 114, 181–190. doi: 10.1016/s0092-8674(03)00521-x

Moquin, D. M., McQuade, T., and Chan, F. K. (2013). CYLD deubiquitinates RIP1 in the TNFα-induced necrosome to facilitate kinase activation and programmed necrosis. *PLoS One* 8:e76841. doi: 10.1371/journal.pone.0076841

Mori, T., Nagata, K., Town, T., Tan, J., Matsui, T., and Asano, T. (2001). Intracisternal increase of superoxide anion production in a canine subarachnoid hemorrhage model. *Stroke* 32, 636–642. doi: 10.1161/01.str.32.3.636

Niwa, A., Osuka, K., Nakura, T., Matsuo, N., Watabe, T., and Takayasu, M. (2016). Interleukin-6, MCP-1, IP-10, and MIG are sequentially expressed in cerebrospinal fluid after subarachnoid hemorrhage. *J. Neuroinflammation* 13:217. doi: 10.1186/s12974-016-0675-7

Oberst, A., Dillon, C. P., Weinlich, R., McCormick, L. L., Fitzgerald, P., Pop, C., et al. (2011). Catalytic activity of the caspase-8-FLIP$_L$ complex inhibits RIPK3-dependent necrosis. *Nature* 471, 363–367. doi: 10.1038/nature09852

Okauchi, M., Hua, Y., Keep, R. F., Morgenstern, L. B., Schallert, T., and Xi, G. (2010). Deferoxamine treatment for intracerebral hemorrhage in aged rats: therapeutic time window and optimal duration. *Stroke* 41, 375–382. doi: 10.1161/strokeaha.109.569830

Qi, Y. X., Zhang, X. H., Wang, Y. Q., Pang, Y. Z., Zhang, Z. B., Zhang, T. L., et al. (2016). Expression of MMP-1, -2, and -8 in longissimus dorsi muscle and their relationship with meat quality traits in cattle. *Genet. Mol. Res.* 15:15017593. doi: 10.4238/gmr.15017593

Quan, W., Zhang, Z., Li, P., Tian, Q., Huang, J., Qian, Y., et al. (2019). Role of regulatory T cells in atorvastatin induced absorption of chronic subdural hematoma in rats. *Aging Dis.* 10, 992–1002. doi: 10.14336/ad.2018.0926

Qureshi, A. I., Mendelow, A. D., and Hanley, D. F. (2009). Intracerebral haemorrhage. *Lancet* 373, 1632–1644. doi: 10.1016/S0140-6736(09)60371-8

Scimemi, A. (2018). Astrocytes and the warning signs of intracerebral hemorrhagic stroke. *Neural Plast.* 2018:7301623. doi: 10.1155/2018/7301623

Sekerdag, E., Solaroglu, I., and Gursoy-Ozdemir, Y. (2018). Cell death mechanisms in stroke and novel molecular and cellular treatment options. *Curr. Neuropharmacol.* 16, 1396–1415. doi: 10.2174/1570159x16666180302115544

Seo, J., Lee, E. W., Sung, H., Seong, D., Dondelinger, Y., Shin, J., et al. (2016). CHIP controls necroptosis through ubiquitylation- and lysosome-dependent degradation of RIPK3. *Nat. Cell Biol.* 18, 291–302. doi: 10.1038/ncb3314

Seoane, A., Tinsley, C. J., and Brown, M. W. (2011). Interfering with perirhinal brain-derived neurotrophic factor expression impairs recognition memory in rats. *Hippocampus* 21, 121–126. doi: 10.1002/hipo.20763

Shao, Z., Tu, S., and Shao, A. (2019). Pathophysiological mechanisms and potential therapeutic targets in intracerebral hemorrhage. *Front. Pharmacol.* 10:1079. doi: 10.3389/fphar.2019.01079

Shao, A., Zhu, Z., Li, L., Zhang, S., and Zhang, J. (2019). Emerging therapeutic targets associated with the immune system in patients with intracerebral haemorrhage (ICH): from mechanisms to translation. *EBioMedicine* 45, 615–623. doi: 10.1016/j.ebiom.2019.06.012

Shen, F., Jiang, L., Han, F., Degos, V., Chen, S., and Su, H. (2019). Increased inflammatory response in old mice is associated with more severe neuronal injury at the acute stage of ischemic stroke. *Aging Dis.* 10, 12–22. doi: 10.14336/AD.2018.0205

Shen, H., Liu, C., Zhang, D., Yao, X., Zhang, K., Li, H., et al. (2017). Role for RIP1 in mediating necroptosis in experimental intracerebral hemorrhage model both *in vivo* and *in vitro*. *Cell Death Dis.* 8:e2641. doi: 10.1038/cddis.2017.58

Shi, J., Gao, W., and Shao, F. (2017). Pyroptosis: gasdermin-mediated programmed necrotic cell death. *Trends Biochem. Sci.* 42, 245–254. doi: 10.1016/j.tibs.2016.10.004

Stockwell, B. R., Friedmann Angeli, J. P., Bayir, H., Bush, A. I., Conrad, M., Dixon, S. J., et al. (2017). Ferroptosis: a regulated cell death nexus linking metabolism, redox biology, and disease. *Cell* 171, 273–285. doi: 10.1016/j.cell.2017.09.021

Sun, X., Ou, Z., Xie, M., Kang, R., Fan, Y., Niu, X., et al. (2015). HSPB1 as a novel regulator of ferroptotic cancer cell death. *Oncogene* 34, 5617–5625. doi: 10.1038/onc.2015.32

Su, X., Wang, H., Kang, D., Zhu, J., Sun, Q., Li, T., et al. (2015). Necrostatin-1 ameliorates intracerebral hemorrhage-induced brain injury in mice through inhibiting RIP1/RIP3 pathway. *Neurochem. Res.* 40, 643–650. doi: 10.1007/s11064-014-1510-0

Su, X., Wang, H., Lin, Y., and Chen, F. (2018). RIP1 and RIP3 mediate hemin-induced cell death in HT22 hippocampal neuronal cells. *Neuropsychiatr. Dis. Treat.* 14, 3111–3119. doi: 10.2147/ndt.s181074

Sun, L., Wang, H., Wang, Z., He, S., Chen, S., Liao, D., et al. (2012). Mixed lineage kinase domain-like protein mediates necrosis signaling downstream of RIP3 kinase. *Cell* 148, 213–227. doi: 10.1016/j.cell.2011.11.031

Sweeney, M. D., Sagare, A. P., and Zlokovic, B. V. (2018). Blood-brain barrier breakdown in Alzheimer disease and other neurodegenerative disorders. *Nat. Rev. Neurol.* 14, 133–150. doi: 10.1038/nrneurol.2017.188

Tan, M. S., Tan, L., Jiang, T., Zhu, X. C., Wang, H. F., Jia, C. D., et al. (2014). Amyloid-β induces NLRP1-dependent neuronal pyroptosis in models of Alzheimer's disease. *Cell Death Dis.* 5:e1382. doi: 10.1038/cddis.2014.348

Tao, X., Yang, W., Zhu, S., Que, R., Liu, C., Fan, T., et al. (2019). Models of poststroke depression and assessments of core depressive symptoms in rodents: how to choose? *Exp. Neurol.* 322:113060. doi: 10.1016/j.expneurol.2019.113060

Topkoru, B., Egemen, E., Solaroglu, I., and Zhang, J. H. (2017). Early brain injury or vasospasm? an overview of common mechanisms. *Expert Rev. Cardiovasc. Ther.* 18, 1424–1429. doi: 10.2174/1389450117666160905112923

Tso, M. K., and Macdonald, R. L. (2014). Subarachnoid hemorrhage: a review of experimental studies on the microcirculation and the neurovascular unit. *Transl. Stroke Res.* 5, 174–189. doi: 10.1007/s12975-014-0323-4

Turan, N., Heider, R. A., Zaharieva, D., Ahmad, F. U., Barrow, D. L., and Pradilla, G. (2016). Sex differences in the formation of intracranial aneurysms and incidence and outcome of subarachnoid hemorrhage: review of experimental and human studies. *Transl. Stroke Res.* 7, 12–19. doi: 10.1007/s12975-015-0434-6

Ursini, F., Maiorino, M., Brigelius-Flohé, R., Aumann, K. D., Roveri, A., Schomburg, D., et al. (1995). Diversity of glutathione peroxidases. *Methods Enzymol.* 252, 38–53. doi: 10.1016/0076-6879(95)52007-4

van Asch, C. J., Luitse, M. J., Rinkel, G. J., van der Tweel, I., Algra, A., and Klijn, C. J. (2010). Incidence, case fatality, and functional outcome

of intracerebral haemorrhage over time, according to age, sex, and ethnic origin: a systematic review and meta-analysis. *Lancet Neurol.* 9, 167–176. doi: 10.1016/s1474-4422(09)70340-0

Vanden Berghe, T., Declercq, W., and Vandenabeele, P. (2007). NADPH oxidases: new players in TNF-induced necrotic cell death. *Mol. Cell* 26, 769–771. doi: 10.1016/j.molcel.2007.06.002

Wagner, K. R., Hua, Y., de Courten-Myers, G. M., Broderick, J. P., Nishimura, R. N., Lu, S. Y., et al. (2000). Tin-mesoporphyrin, a potent heme oxygenase inhibitor, for treatment of intracerebral hemorrhage: *in vivo* and *in vitro* studies. *Cell. Mol. Biol.* 46, 597–608.

Wan, J., Ren, H., and Wang, J. (2019). Iron toxicity, lipid peroxidation and ferroptosis after intracerebral haemorrhage. *Stroke Vasc. Neurol.* 4, 93–95. doi: 10.1136/svn-2018-000205

Wang, H., Sun, L., Su, L., Rizo, J., Liu, L., Wang, L. F., et al. (2014). Mixed lineage kinase domain-like protein MLKL causes necrotic membrane disruption upon phosphorylation by RIP3. *Mol. Cell* 54, 133–146. doi: 10.1016/j.molcel.2014.03.003

Weng, X., Tan, Y., Chu, X., Wu, X. F., Liu, R., Tian, Y., et al. (2015). N-methyl-D-aspartic acid receptor 1 (NMDAR1) aggravates secondary inflammatory damage induced by hemin-NLRP3 pathway after intracerebral hemorrhage. *Chin. J. Traumatol.* 18, 254–258. doi: 10.1016/j.cjtee.2015.11.010

Wertz, I. E., O'Rourke, K. M., Zhou, H., Eby, M., Aravind, L., Seshagiri, S., et al. (2004). De-ubiquitination and ubiquitin ligase domains of A20 downregulate NF-kappaB signalling. *Nature* 430, 694–699. doi: 10.1038/nature02794

Wilkinson, D. A., Pandey, A. S., Thompson, B. G., Keep, R. F., Hua, Y., and Xi, G. (2018). Injury mechanisms in acute intracerebral hemorrhage. *Neuropharmacology* 134, 240–248. doi: 10.1016/j.neuropharm.2017.09.033

Wu, B., Ma, Q., Khatibi, N., Chen, W., Sozen, T., Cheng, O., et al. (2010). Ac-YVAD-CMK decreases blood-brain barrier degradation by inhibiting caspase-1 activation of interleukin-1β in intracerebral hemorrhage mouse model. *Transl. Stroke Res.* 1, 57–64. doi: 10.1007/s12975-009-0002-z

Wu, Y., Song, J., Wang, Y., Wang, X., Culmsee, C., and Zhu, C. (2019). The potential role of ferroptosis in neonatal brain injury. *Front. Neurosci.* 13:115. doi: 10.3389/fnins.2019.00115

Wu, Y. T., Tan, H. L., Huang, Q., Sun, X. J., Zhu, X., and Shen, H. M. (2011). zVAD-induced necroptosis in L929 cells depends on autocrine production of TNFα mediated by the PKC-MAPKs-AP-1 pathway. *Cell Death Differ.* 18, 26–37. doi: 10.1038/cdd.2010.72

Xie, Y., Guo, H., Wang, L., Xu, L., Zhang, X., Yu, L., et al. (2017). Human albumin attenuates excessive innate immunity *via* inhibition of microglial Mincle/Syk signaling in subarachnoid hemorrhage. *Brain Behav. Immun.* 60, 346–360. doi: 10.1016/j.bbi.2016.11.004

Xie, Y., Hou, W., Song, X., Yu, Y., Huang, J., Sun, X., et al. (2016). Ferroptosis: process and function. *Cell Death Differ.* 23, 369–379. doi: 10.1038/cdd.2015.158

Xu, H., Testai, F. D., Valyi-Nagy, T., N Pavuluri, M., Zhai, F., Nanegrungsunk, D., et al. (2015). VAP-1 blockade prevents subarachnoid hemorrhage-associated cerebrovascular dilating dysfunction *via* repression of a neutrophil recruitment-related mechanism. *Brain Res.* 1603, 141–149. doi: 10.1016/j.brainres.2015.01.047

Xu, P., Zhang, X., Liu, Q., Xie, Y., Shi, X., Chen, J., et al. (2019). Microglial TREM-1 receptor mediates neuroinflammatory injury *via* interaction with SYK in experimental ischemic stroke. *Cell Death Dis.* 10:555. doi: 10.1038/s41419-019-1777-9

Xu, Y. J., Zheng, L., Hu, Y. W., and Wang, Q. (2018). Pyroptosis and its relationship to atherosclerosis. *Clin. Chim. Acta* 476, 28–37. doi: 10.1016/j.cca.2017.11.005

Yagoda, N., von Rechenberg, M., Zaganjor, E., Bauer, A. J., Yang, W. S., Fridman, D. J., et al. (2007). RAS-RAF-MEK-dependent oxidative cell death involving voltage-dependent anion channels. *Nature* 447, 864–868. doi: 10.1038/nature05859

Yang, C. S., Guo, A., Li, Y., Shi, K., Shi, F. D., and Li, M. (2019). Dl-3-n-butylphthalide reduces neurovascular inflammation and ischemic brain injury in mice. *Aging Dis.* 10, 964–976. doi: 10.14336/ad.2019.0608

Yang, Q., Huang, Z., Luo, Y., Zheng, F., Hu, Y., Liu, H., et al. (2019). Inhibition of Nwd1 activity attenuates neuronal hyperexcitability and GluN2B phosphorylation in the hippocampus. *EBioMedicine* 47, 470–483. doi: 10.1016/j.ebiom.2019.08.050

Yang, C., Li, T., Xue, H., Wang, L., Deng, L., Xie, Y., et al. (2019). Inhibition of necroptosis rescues SAH-induced synaptic impairments in hippocampus *via* CREB-BDNF pathway. *Front. Neurosci.* 12:990. doi: 10.3389/fnins.2018.00990

Yang, Z., Liu, Y., Yuan, F., Li, Z., Huang, S., Shen, H., et al. (2014). Sinomenine inhibits microglia activation and attenuates brain injury in intracerebral hemorrhage. *Mol. Immunol.* 60, 109–114. doi: 10.1016/j.molimm.2014.03.005

Yang, W. S., and Stockwell, B. R. (2008). Synthetic lethal screening identifies compounds activating iron-dependent, nonapoptotic cell death in oncogenic-RAS-harboring cancer cells. *Chem. Biol.* 15, 234–245. doi: 10.1016/j.chembiol.2008.02.010

Yang, W. S., and Stockwell, B. R. (2016). Ferroptosis: death by lipid peroxidation. *Trends Cell Biol.* 26, 165–176. doi: 10.1016/j.tcb.2015.10.014

Yang, W. S., SriRamaratnam, R., Welsch, M. E., Shimada, K., Skouta, R., Viswanathan, V. S., et al. (2014). Regulation of ferroptotic cancer cell death by GPX4. *Cell* 156, 317–331. doi: 10.1016/j.cell.2013.12.010

Yang, F., Wang, Z., Wei, X., Han, H., Meng, X., Zhang, Y., et al. (2014). NLRP3 deficiency ameliorates neurovascular damage in experimental ischemic stroke. *J. Cereb. Blood Flow Metab.* 34, 660–667. doi: 10.1038/jcbfm.2013.242

Yang, Z., Wang, J., Yu, Y., and Li, Z. (2016). Gene silencing of MCP-1 prevents microglial activation and inflammatory injury after intracerebral hemorrhage. *Int. Immunopharmacol.* 33, 18–23. doi: 10.1016/j.intimp.2016.01.016

Yang, Z., Zhong, L., Xian, R., and Yuan, B. (2015). MicroRNA-223 regulates inflammation and brain injury *via* feedback to NLRP3 inflammasome after intracerebral hemorrhage. *Mol. Immunol.* 65, 267–276. doi: 10.1016/j.molimm.2014.12.018

Yu, H., Guo, P., Xie, X., Wang, Y., and Chen, G. (2017). Ferroptosis, a new form of cell death, and its relationships with tumourous diseases. *J. Cell. Mol. Med.* 21, 648–657. doi: 10.1111/jcmm.13008

Yu, Y., Lin, Z., Yin, Y., and Zhao, J. (2014). The ferric iron chelator 2,2'-dipyridyl attenuates basilar artery vasospasm and improves neurological function after subarachnoid hemorrhage in rabbits. *Neurol. Sci.* 35, 1413–1419. doi: 10.1007/s10072-014-1730-8

Yu, Y., Xie, Y., Cao, L., Yang, L., Yang, M., Lotze, M. T., et al. (2015). The ferroptosis inducer erastin enhances sensitivity of acute myeloid leukemia cells to chemotherapeutic agents. *Mol. Cell. Oncol.* 2:e1054549. doi: 10.1080/23723556.2015.1054549

Yuan, S., Yu, Z., Zhang, Z., Zhang, J., Zhang, P., Li, X., et al. (2019). RIP3 participates in early brain injury after experimental subarachnoid hemorrhage in rats by inducing necroptosis. *Neurobiol. Dis.* 129, 144–158. doi: 10.1016/j.nbd.2019.05.004

Zhang, S., Hu, Z. W., Luo, H. Y., Mao, C. Y., Tang, M. B., Li, Y. S., et al. (2020). AAV/BBB-mediated gene transfer of CHIP attenuates brain injury following experimental intracerebral hemorrhage. *Transl. Stroke Res.* 11, 296–309. doi: 10.1007/s12975-019-00715-w

Zhang, C., Jiang, M., Wang, W. Q., Zhao, S. J., Yin, Y. X., Mi, Q. J., et al. (2019). Selective mGluR1 negative allosteric modulator reduces blood-brain barrier permeability and cerebral edema after experimental subarachnoid hemorrhage. *Transl. Stroke Res.* doi: 10.1007/s12975-019-00758-z [Epub ahead of print].

Zhang, D. W., Shao, J., Lin, J., Zhang, N., Lu, B. J., Lin, S. C., et al. (2009). RIP3, an energy metabolism regulator that switches TNF-induced cell death from apoptosis to necrosis. *Science* 325, 332–336. doi: 10.1126/science.1172308

Zhang, S., Tang, M. B., Luo, H. Y., Shi, C. H., and Xu, Y. M. (2017). Necroptosis in neurodegenerative diseases: a potential therapeutic target. *Cell Death Dis.* 8:e2905. doi: 10.1038/cddis.2017.286

Zhang, J., Wang, Y., Aili, A., Sun, X., Pang, X., Ge, Q., et al. (2019). Th1 biased progressive autoimmunity in aged aire-deficient mice accelerated thymic epithelial cell senescence. *Aging Dis.* 10, 497–509. doi: 10.14336/ad.2018.0608

Zhang, Y. H., Wang, D. W., Xu, S. F., Zhang, S., Fan, Y. G., Yang, Y. Y., et al. (2018). α-Lipoic acid improves abnormal behavior by mitigation of oxidative stress, inflammation, ferroptosis, and tauopathy in P301S Tau transgenic mice. *Redox Biol.* 14, 535–548. doi: 10.1016/j.redox.2017.11.001

Zhang, Z., Wu, Y., Yuan, S., Zhang, P., Zhang, J., Li, H., et al. (2018). Glutathione peroxidase 4 participates in secondary brain injury through mediating ferroptosis in a rat model of intracerebral hemorrhage. *Brain Res.* 1701, 112–125. doi: 10.1016/j.brainres.2018.09.012

Zhao, H., Chen, Y., and Feng, H. (2018). P2X7 receptor-associated programmed cell death in the pathophysiology of hemorrhagic stroke. *Curr. Neuropharmacol.* 16, 1282–1295. doi: 10.2174/1570159x16666180516094500

Zheng, Y., Gardner, S. E., and Clarke, M. C. (2011). Cell death, damage-associated molecular patterns, and sterile inflammation in cardiovascular disease. *Arterioscler. Thromb. Vasc. Biol.* 31, 2781–2786. doi: 10.1161/atvbaha.111.224907

Zhu, H., Santo, A., Jia, Z., and Robert Li, Y. (2019). GPx4 in bacterial infection and polymicrobial sepsis: involvement of ferroptosis and pyroptosis. *React. Oxyg. Species Apex* 7, 154–160. doi: 10.20455/ros.2019.835

Zhu, S., Wei, X., Yang, X., Huang, Z., Chang, Z., Xie, F., et al. (2019). Plasma lipoprotein-associated phospholipase A2 and superoxide dismutase are independent predicators of cognitive impairment in cerebral small vessel disease patients: diagnosis and assessment. *Aging Dis.* 10, 834–846. doi: 10.14336/ad.2019.0304

Zille, M., Karuppagounder, S. S., Chen, Y., Gough, P. J., Bertin, J., Finger, J., et al. (2017). Neuronal death after hemorrhagic stroke *in vitro* and *in vivo* shares features of ferroptosis and necroptosis. *Stroke* 48, 1033–1043. doi: 10.1161/strokeaha.116.015609

Zlokovic, B. V. (2008). The blood-brain barrier in health and chronic neurodegenerative disorders. *Neuron* 57, 178–201. doi: 10.1016/j.neuron.2008.01.003

Zou, J., Chen, Z., Wei, X., Chen, Z., Fu, Y., Yang, X., et al. (2017). Cystatin C as a potential therapeutic mediator against Parkinson's disease *via* VEGF-induced angiogenesis and enhanced neuronal autophagy in neurovascular units. *Cell Death Dis.* 8:e2854. doi: 10.1038/cddis.2017.240

Conflict of Interest: The authors declare that the research was conducted in the absence of any commercial or financial relationships that could be construed as a potential conflict of interest.

frontiers in Neuroscience

REVIEW
published: 15 April 2020
doi: 10.3389/fnins.2020.00326

Rhodopsin: A Potential Biomarker for Neurodegenerative Diseases

Cameron Lenahan[1,2†], Rajvee Sanghavi[1†], Lei Huang[2,3,4] and John H. Zhang[2,3,4,5]*

[1] Burrell College of Osteopathic Medicine, Las Cruces, NM, United States, [2] Center for Neuroscience Research, Loma Linda University School of Medicine, Loma Linda, CA, United States, [3] Department of Neurosurgery, Loma Linda University School of Medicine, Loma Linda, CA, United States, [4] Department of Physiology and Pharmacology, Loma Linda University School of Medicine, Loma Linda, CA, United States, [5] Department of Anesthesiology, Loma Linda University School of Medicine, Loma Linda, CA, United States

Retinal alterations have recently been associated with numerous neurodegenerative diseases. Rhodopsin is a G-protein coupled receptor found in the rod cells of the retina. As a biomarker associated with retinal thinning and degeneration, it bears potential in the early detection and monitoring of several neurodegenerative diseases. In this review article, we summarize the findings of correlations between rhodopsin and several neurodegenerative disorders as well as the potential of a novel technique, cSLO, in the quantification of rhodopsin.

Keywords: rhodopsin, amyotrophic lateral sclerosis, Parkinson's disease, Alzheimer's disease, Huntington's disease, confocal scanning laser ophthalmoscopy

OPEN ACCESS

Edited by:
Dennis Qing Wang, Southern Medical University, China

Reviewed by:
Yi Yang, University of New Mexico, United States
Fudong Liu, University of Texas Health Science Center at Houston, United States

***Correspondence:**
John H. Zhang
johnzhang3910@yahoo.com

† These authors have contributed equally to this work

Specialty section:
This article was submitted to Neurodegeneration, a section of the journal Frontiers in Neuroscience

Received: *12 January 2020*
Accepted: *19 March 2020*
Published: *15 April 2020*

Citation:
Lenahan C, Sanghavi R, Huang L and Zhang JH (2020) Rhodopsin: A Potential Biomarker for Neurodegenerative Diseases. Front. Neurosci. 14:326. doi: 10.3389/fnins.2020.00326

INTRODUCTION

Neurodegenerative disease is a major problem faced by an aging population around the world (Prince et al., 2013). As the population of elderly patients aged 65 and older will likely double between 2000 and 2030, the prevalence of age-related diseases is expected to substantially increase (Jedrziewski et al., 2007). These disorders are characterized by genetic mutations, which in turn upset protein homeostasis, leading to a variety of clinical manifestations. Current brain imaging techniques, such as magnetic resonance imaging, enable detection of cerebral atrophy or measure metabolic changes, which help to diagnose neurodegenerative pathologies (Schaller, 2008). However, certain pathologies seen on imaging are often detected only after the disease has progressed (Schaller, 2008). Moreover, current imaging, such as PET scans, would be difficult to implement for population-wide screening of preclinical signs due to the expense or necessity of radioactive isotopes (Colligris et al., 2018). While the molecular mechanisms of distinct neurodegenerative diseases may vary, there are also shared characteristics, such as neurite retraction and neuronal death (Bredesen, 2009). Given the nature of neuronal death, treatment for late stages of neurodegenerative diseases, such as Alzheimer's, have been ineffective, therefore requiring early diagnosis (Sheinerman and Umansky, 2013). Should screening become possible at earlier stages, clinicians can better intervene in the progression of these diseases. Retinal alterations have recently been associated with numerous neurodegenerative diseases (Helmer et al., 2013; Sivak, 2013; Tanito and Ohira, 2013; Hubers et al., 2016; Mukherjee et al., 2017; Sudharsan et al., 2017; Ahn et al., 2018; Satue et al., 2018; Chiquita et al., 2019; Cipollini et al., 2019; den Haan et al., 2019; Dhalla et al., 2019). Rhodopsin, a G-protein coupled receptor in the rod cells of the retina is a biomarker

Abbreviations: AD, Alzheimer's disease; ALS, amyotrophic lateral sclerosis; cSLO, confocal scanning laser ophthalmoscopy; HD, Huntington's disease; OCT, optical coherence tomography; PD, Parkinson's disease; RNFL, retinal nerve fiber layer; SLO, scanning laser ophthalmoscopy.

associated with retinal thinning and degeneration (Cideciyan et al., 2005; Xiong and Bellen, 2013), suggesting its potential in the early detection and progression monitoring of neurodegenerative diseases. In this review, we summarize physiological function of rhodopsin, research findings of correlations between rhodopsin with several neurodegenerative disorders, and a novel technique, cSLO, in rhodopsin quantification.

RHODOPSIN

Rhodopsin is a G-protein coupled receptor, and is the most abundant protein in the rod cells found in the retina (**Figure 1**). It functions as the primary photoreceptor molecule of vision, and contains two parts: an opsin molecule linked to a chromophore, 11-*cis*-retinal (Athanasiou et al., 2018). The opsin molecule is comprised of 348 amino acids, and has seven transmembrane domains (Athanasiou et al., 2018). Rhodopsin is synthesized in the rough endoplasmic reticulum of the inner segments of photoreceptors and subsequently undergoes posttranslational modifications in the Golgi before becoming functional (Murray et al., 2009). In **Figure 2**, an image adapted from an article by Pahlberg and Sampath, 2011 depicts the signaling pathway of rhodopsin. When light activates rhodopsin, phototransduction occurs, initiating the exchange of GDP for GTP on the G-protein, transducing ($G_t\alpha$), consequently increasing cGMP (or cG) hydrolysis through the PDE complex (Pahlberg and Sampath, 2011). If the cGMP concentration decreases, the cGMP-gated channels will close, preventing depolarization induced by the influx of Na^+ and Ca^{2+}. Therefore, activation of rhodopsin from photons of light is consequently followed by a small, graded hyperpolarization in membrane potential (Pahlberg and Sampath, 2011).

Rhodopsin's function as a photoreceptor also allows its participation in circadian rhythm. Degeneration of these photoreceptors may manifest as a gradual thinning of the outer nuclear layer, a reduction of electroretinogram amplitudes, and vision loss (Xiao et al., 2019). A recent study by Ni et al. (2017) found that rhodopsin receptors in drosophila functions as a circadian pacemaker in neurons. Other studies have found that disruptions of normal circadian rhythms can have significant effects on health, and potential mechanisms have been suggested to link circadian dysfunction and neurodegenerative diseases (Musiek and Holtzman, 2016).

Microbial rhodopsins have been discovered in various species throughout the animal kingdom, and have aided in our understanding of neuronal functions (Duebel et al., 2015). In these microbes, they play an important role in photosynthesis and phototaxis. Examples of microbial rhodopsins include Channelrhodopsin, bacteriorhodopsin, and archaerhodopsin (Zhang et al., 2011). Channelrhodopsins were first isolated from the alga *Chlamydomonas reinhardtii* by Nagel et al. (2002). These channelrhodopsins are light-gated cation channels that can induce neuronal depolarization in response to stimulation from light (Daadi et al., 2016). Channelrhodopsin and its variants have since been used in research to manipulate cell membrane potentials using light energy (Lin, 2011). The opsin component of these proteins have rapid kinetics and are structurally simplistic, allowing neuronal expression using optogenetics (Zhang et al., 2011). Therefore, rhodopsin has emerged as a biomarker, which may serve as the link between retinal thinning and neuronal pathology seen in neurodegenerative diseases.

RHODOPSIN AND RETINAL DEGENERATION

In recent years, retinal thinning has become heavily associated with neurodegenerative diseases of the brain (Helmer et al., 2013; Sivak, 2013). There have been correlations established between retinal thinning and Alzheimer's disease (Chiquita et al., 2019; Cipollini et al., 2019; den Haan et al., 2019), Parkinson's disease (Ahn et al., 2018; Satue et al., 2018), Huntington's disease (Dhalla et al., 2019), Amyotrophic lateral sclerosis (Hubers et al., 2016; Mukherjee et al., 2017), and a case has been reported of reduced retinal thickness after an occipital lobe infarction (Tanito and Ohira, 2013). Given this, it is important that we consider exploring biomarkers of the retina as possible routes of monitoring and diagnosing these debilitating neurodegenerative diseases. In recent years, more studies have explored the relationship between the two. Sudharsan et al. (2017) found that light-induced damage of the photoreceptors consequently led to a thinning of the outer nuclear layer, induction of Müller cell gliosis, focal loss of retinal pigment epithelial cell integrity, and an increased expression of endothelin receptor B in Müller cells. The retinal pigment epithelial layer is a monolayer of pigmented cells, known to contribute significantly, functioning as both a barrier and as an immunosuppressant in the eye (Touhami et al., 2018). Unsurprisingly, the relationship between the retinal pigment epithelial cells and photoreceptor cells is vitally necessary for sight (Sparrow et al., 2010). As previously described, Xiao et al. (2019) revealed that rhodopsin knockout mice had a reduction of electroretinogram amplitudes, vision loss, and gradual thinning of the outer nuclear layer of the retina. Correlations have already been established between rhodopsin and the conditions that are associated with retinal thinning, such as retinitis pigmentosa and age-related macular degeneration (Liu et al., 2015). More specifically, while changes in the retina may be early indicators for neurodegeneration, changes in rhodopsin have been shown to contribute to the early events of retinal degeneration (Di Pierdomenico et al., 2017), lending credibility to its potential as an even earlier biomarker for diagnosis.

RHODOPSIN AND ALZHEIMER'S DISEASE

Alzheimer's disease (AD) is a degenerative disease involving cortical atrophy, neuritic plaques, and neurofibrillary tangles (Hardy and Allsop, 1991), and is the most common dementia among the aging population (Reitz et al., 2011). Approximately 30 million people suffer from Alzheimer's disease, and this number is expected to triple over the next 20 years (Jahn, 2018). The pathophysiology of AD lies in the buildup of misfolded

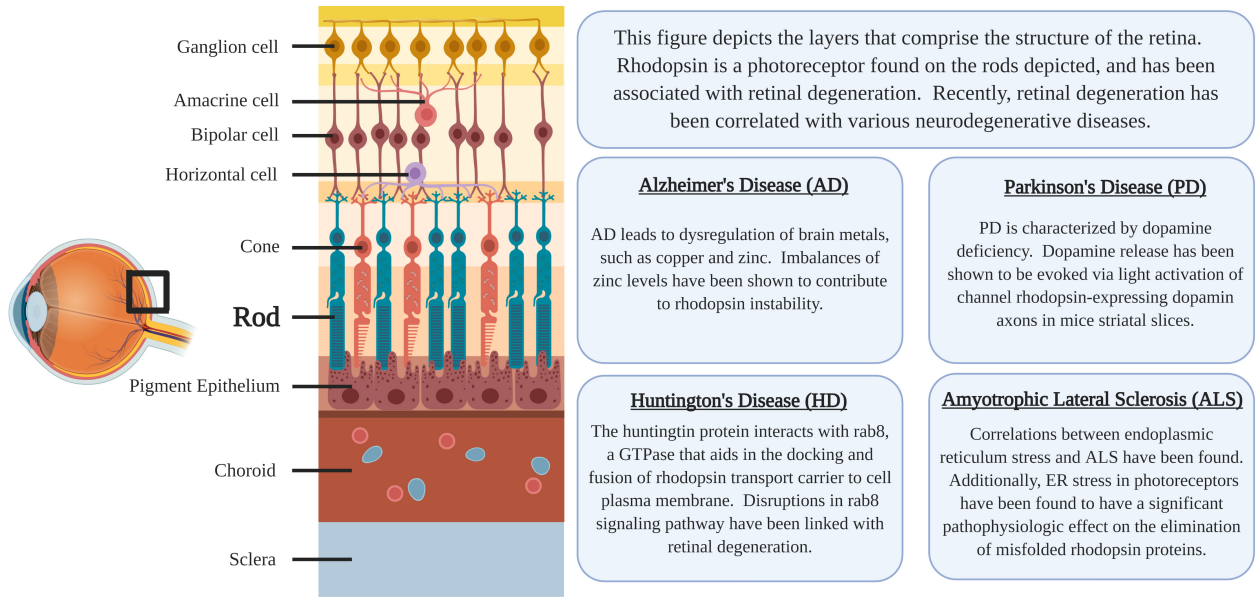

FIGURE 1 | The location of rhodopsin-expressing Rod cells within the retina and a summary of the associations regarding neurodegenerative diseases and rhodopsin pathology.

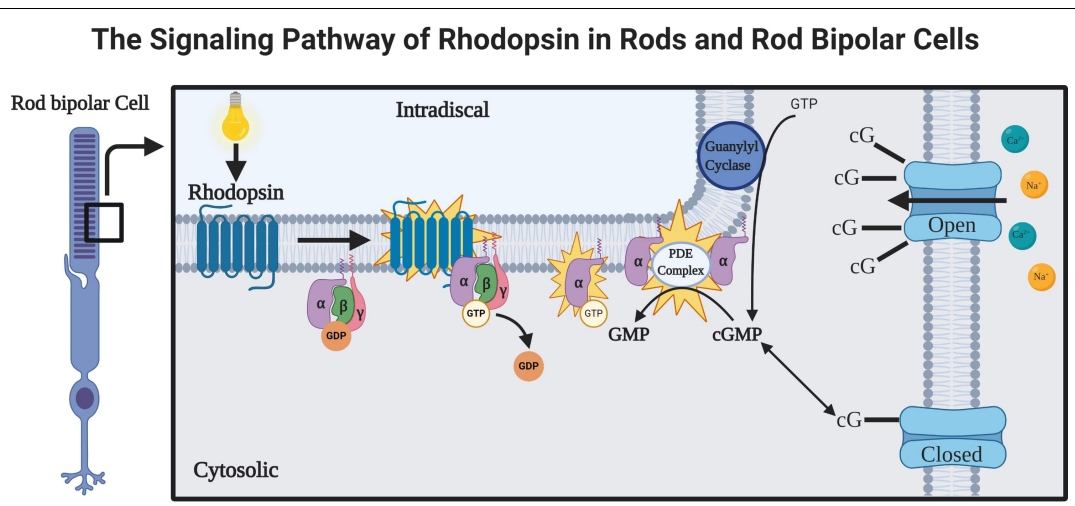

FIGURE 2 | The rhodopsin-mediated signal transduction cascade in rods and rod bipolar cells (adapted from Pahlberg and Sampath, 2011). As light is absorbed by rhodopsin, a G-protein-coupled receptor (GPCR), the activations of phototransduction in the photoreceptors initiate an exchange of GTP and GDP. The cGMP is hydrolyzed by a cGMP phosphodiesterase complex (PDE complex). This reduction in the concentration of cGMP will close the cGMP-gated channels, which function to depolarize the membrane potential of rod bipolar cells via influx of Na^+ and Ca^{2+} (Pahlberg and Sampath, 2011).

extracellular amyloid plaque and intracellular neurofibrillary tangles in the brain (Reitz et al., 2011). It is currently believed that toxic amyloid plaques serve as the earliest manifestation of the disease (Albert et al., 2011; McKhann et al., 2011; Sperling et al., 2011; Weller and Budson, 2018). More recently, Manifestations of AD have been discovered in many different parts of the eye, such as the pupil, lens, choroid, and optic nerve, although this research has been minimally used in the clinic (Javaid et al., 2016). A study conducted by Yoon et al. (2019) found microvascular retinal changes both in patients with the disease, as well as patients with mild cognitive impairment, a notable precursor to Alzheimer's disease. Amyloid deposits have also been found in the retina (Koronyo-Hamaoui et al., 2011). One study has found a correlation between the thinning of the retinal nerve fiber layer (RNFL) and retinal ganglion cell degeneration leading to the progression of Alzheimer's disease (Javaid et al., 2016). For example, Mutlu et al. conducted a cohort study, and found that the thinner RNFL was associated with a greater risk for developing AD, independent of cardiovascular risk factors. Furthermore, studies on post-mortem specimens revealed that

patients with AD had a substantial loss of retinal ganglion cells and thinner RNFL compared to those who did not have AD (Mutlu et al., 2018). These results suggest that retinal thinning occurs in the earlier stages of the disease, potentially enabling earlier diagnosis.

One study proposes a mechanism where rhodopsin misfolding ultimately contributes to retinal degeneration and the visual changes that are seen in both retinitis pigmentosa and Alzheimer's disease (Stojanovic et al., 2004). Surprisingly, recent research has suggested that the dysregulation of brain metals, such as copper and zinc, occurs in AD (Sensi et al., 2018). In addition, zinc supplementation positively affects neurotrophic signaling and activation of the brain-derived neurotrophic factor (BDNF)-TrkB axis (Hwang et al., 2005; Sensi et al., 2009; Corona et al., 2010). Conversely, zinc deficiency contributes to retinal neurodegeneration and night blindness (Ugarte and Osborne, 2001). Stojanovic et al. (2004) found that mutations leading to these visual changes involve a high-affinity transmembrane site of rhodopsin that coordinates zinc, showing that zinc plays an important role in rhodopsin stability. However, at excess concentrations, zinc actually reduces the thermal stability ability of rhodopsin to link with 11-*cis*-retinal (del Valle et al., 2003). Too much zinc also promotes the aggregation of amyloid and prions in addition to rhodopsin. Therefore, a delicate balance of zinc is crucial in maintaining adequate rhodopsin stability (Stojanovic et al., 2004).

A study by Reddy et al. (2017) described the effects of Alzheimer's on the retina, and found that the architectural disruption of the retina was associated by a loss of rhodopsin, increased gliosis, and retinal thinning.

RHODOPSIN AND PARKINSON'S DISEASE

Dopamine imbalance is involved in many neurodegenerative disorders, such as schizophrenia and Parkinson's disease (PD) (Birtwistle and Baldwin, 1998). PD is the second most common neurodegenerative disorder in the United States (Kowal et al., 2013), and is caused by a loss of dopaminergic neurons of the substantia nigra pars compacta (Miller and O'Callaghan, 2015). The symptoms of PD usually appear after approximately 80% of these neurons have been lost (Altintas et al., 2008). Histologic findings reveal accumulation of alpha-synuclein bound to ubiquitin, forming Lewy Body inclusions, which are involved in disease pathology (Schulz, 2007). It is characterized by tremor, cogwheel rigidity, akinesia/bradykinesia, postural instability, and shuffling gait (Miller and O'Callaghan, 2015). In PD, changes in visual function have been reported, such as decline in visual acuity, contrast sensitivity, color vision, motion perception, and bioelectrical activity (Archibald et al., 2009).

Ahn et al. (2018) studied retinas in individuals who were recently diagnosed with PD using optical coherence tomography (OCT). They propose that retinal thinning in the macular area occurs early during the course of PD and corresponds to disease severity. These retinal changes were observed in patients who had been diagnosed with PD 2 years prior, but had not started a medication regimen (Ahn et al., 2018). Their research reveals that retinal thinning may be connected with the loss of dopaminergic neurons. Retinal thinning in the inner plexiform and ganglion cell layers was discovered in these patients. However, the degree of thinning also corresponded to the subjects' scores on the Hoehn and Yahr scale, a measure of PD progression (Goetz et al., 2004). Retinal thinning in this area also correlated with decreased dopamine transporter activity in the left substantia nigra (Ahn et al., 2018). Most interesting, a recent study indicates that dopamine release was evoked via light activation of channel rhodopsin-expressing dopamine axons in mouse striatal slices (Brimblecombe et al., 2015). Therefore, it is reasonable to further explore the impact that rhodopsin concentrations may have in diagnosing this devastating disease, and further supports the hypothesis that rhodopsin may play a pivotal role in early diagnosis.

RHODOPSIN AND HUNTINGTON'S DISEASE

Huntington's disease (HD) is an autosomal dominant disorder caused by trinucleotide repeat expansion (CAG) in the huntingtin gene on chromosome 4 (Jordan and Wright, 2010). This leads to atrophy of the caudate and putamen, resulting in increased levels of dopamine and decreased levels of GABA and acetylcholine in the brain. It is characterized by chorea, athetosis, depression, and mental decline in later stages.

OCT imaging was also used to measure the thickness of the retinal layers using foveal scans in patients with Huntington's disease. Compared to healthy control patients, there was reduced thickness in the macular RNFL and ganglion cell layer in those with Huntington's disease, which also corresponded to disease progression markers (Gulmez Sevim et al., 2019). Another study revealed significant abnormalities in color vision in HD patients who had reduced thickness of the temporal portion of the RNFL (Kersten et al., 2015). Moreover, Knapp et al. (2018) followed a presymptomatic patient that had tested positive for the gene responsible for HD, and found rod dysfunction within both eyes. There are numerous proteins involved with rhodopsin trafficking, such as rab8. Disruptions in this rab8 signaling pathway have also been linked to retinal degeneration (Moritz et al., 2001). Rab8 is a GTPase that aids in the docking and fusion of rhodopsin transport carrier to the cell plasma membrane. They concluded that the huntingtin protein interacts with rab8, and is involved in linking cellular organelles to cytoskeletal components (Deretic, 2006), demonstrating a parallel mechanism between breakdown of cell trafficking in retinal degeneration and HD.

The aggregation of P23H, a mutated rhodopsin found in retinal cells and seen in retinitis pigmentosa, leads to the impairment of the ubiquitin proteasome system, an important protein degradation system (Bence et al., 2001). A mutated form of the huntingtin protein aggregates and impairs protein degradation in the same manner, according to Illing et al. (2002). Therefore, the aggregation of protein in Huntington's disease introduces the possibility that retinal degeneration may share a common mechanism with neurodegeneration of the retina.

While retinal thickness has been associated with HD, there have not been any confirmed studies regarding rhodopsin and HD. However, it is likely that HD would follow the same pathological patterns as the other neurodegenerative diseases. Future studies are necessary to determine any possible correlation with rhodopsin and Huntington's, and whether it has potential as an early diagnostic biomarker.

RHODOPSIN AND AMYOTROPHIC LATERAL SCLEROSIS

Amyotrophic lateral sclerosis (ALS) is the most common motor neuron disease in adults (Talbott et al., 2016). It is an unrelenting disease resulting in progressive paralysis, worsening until death is caused by respiratory failure (Al-Chalabi and Hardiman, 2013). The disease is distinct, in that it is characterized by upper and lower motor neuron involvement (Al-Chalabi and Hardiman, 2013). The most common gene mutations for ALS have been identified as C9orf72, SOD1, TARDBP, and FUS (Zou et al., 2017).

Several studies have found a positive correlation between retinal thinning and ALS patients (Hubers et al., 2016; Mukherjee et al., 2017; Rojas et al., 2019). However, loose connections may be made regarding ALS and rhodopsin, as one study has found a correlation between ER stress and ALS pathogenesis (Webster et al., 2017). Subsequently, ER stress in photoreceptors also has a significant pathophysiological effect on the elimination of misfolded rhodopsin proteins (Chiang et al., 2015). There is also a connection regarding the unfolded protein response inositol-requiring enzyme 1 (IRE1) signaling pathway. This pathway is strongly activated in misfolded rhodopsin-expressing photoreceptors, and significantly upregulated P23H rhodopsin degradation (Chiang et al., 2015). Similarly, ALS mice had increased IRE1 prior to symptom onset (Jaronen et al., 2014). While the evidence is not conclusive for a connection, it does provide sufficient evidence to warrant future inquiry.

RHODOPSIN AND STROKE

Hypertension and cerebrovascular changes, including stroke, increase the risk of cognitive impairment (Reitz et al., 2011). Ischemia occurs when blood supply has been restricted to an area due to blockage of blood vessels, resulting in dysregulation and cell death (Joachim et al., 2017). Likewise, retinal ischemia can result from a lack of perfusion due to a blockage of capillaries. Inflammation follows several hours after onset of ischemia, consequently leading to apoptosis (Osborne et al., 2004). Joachim et al. describes an animal model of retinal ischemia-ischemia reperfusion (I/R), in which pressure in the eye is temporarily increased through the infusion of liquid into the anterior chamber, leading to the compression of vasculature supplying the optic disc and loss of neuronal cells in the retina. They found that the thickness of the inner retinal layers is reduced first, and prolonged ischemia results in insult to the outer retinal layers, including the photoreceptors (Joachim et al., 2017).

Researchers propose that decreased contents of photoreceptor proteins represent an early stage of retinal degeneration. Retinal vein occlusion (RVO), the second most common retinal vascular disease after diabetic retinopathy, results from the compression of the retinal vein as a result of atherosclerosis or increased blood viscosity (Khayat et al., 2018). Coincidentally, individuals with RVO are also at a significantly greater risk of developing ischemic and hemorrhagic strokes (Chen et al., 2018). In one study, RVO was induced in pigs, which led to a reduction in proteins involved in vision, such as rhodopsin (Cehofski et al., 2018). This compromise in rhodopsin function suggests that neurotransmission is sensitive to ischemic insult. However, it is lacking specific research exploring the possible relationship between stroke and rhodopsin.

RHODOPSIN QUANTIFICATION AND SCANNING LASER OPHTHALMOSCOPY

Scientists at Florida International University have developed a novel technique, known as nano-second pulsed scanning laser ophthalmoscopy (SLO), which was established as an effective method of imaging rhodopsin (Liu et al., 2015). Other novel methods of rhodopsin imaging have also been proposed, such as the confocal laser ophthalmoscope (cSLO), which creates high-resolution spatial mapping of rhodopsin and retinal pigment epithelium distribution (Ehler et al., 2015). This proposed technique, using cSLO, is a novel, non-invasive *in vivo* method, and functions by analyzing the brightening of detected lipofuscin autofluorescence within small pixel clusters, creating images of ∼50-μm resolution (Ehler et al., 2015). Furthermore, to emphasize the clinical relevance of this technique, it was designed to be used with widely available clinical imaging devices (Ehler et al., 2015). It has recently been proposed that OCT may be used in various neurodegenerative diseases, due to its capability in measuring volumetric changes of the retina (Doustar et al., 2017). However, given the nature of neurodegenerative diseases, it is paramount that the diagnosis is established at the earliest possible time-point to provide the best prognosis to the patient. Therefore, cSLO warrants further research to determine the efficacy and correlation between rhodopsin concentrations and disease progression of neurodegenerative disorders.

CONCLUSION AND FUTURE DIRECTION

There are several limitations that should be addressed. For example, the unfolded protein response not only occurs neurodegenerative disorders, but is also activated as a part of the normal aging process, which is marked by an increase in oxidative stress and the pro-inflammatory state (Lenox et al., 2015). Jackson et al. hypothesized that aging results in disturbance of the visual cycle responsible for rhodopsin regeneration. Their investigation revealed that the transition point in the dark, at which the rod system is the primary contributor to vision, was delayed by nearly 2.5 min in elderly population compared to young adults, resulting in a slower rate of dark adaptation kinetics seen in older

adults (Jackson et al., 1999). This presents limitations in using rhodopsin as a biomarker, as more research is needed to discern reduction in rhodopsin as a biomarker for age-related changes versus disease pathology.

Currently, there are also limitations in specificity regarding rhodopsin and its potential use in diagnosis. Because of the lack of rhodopsin quantification in the studies described above, it would be difficult to identify one neurodegenerative disorder specifically, but may have potential, if used with other clinical presentations as a quick, non-invasive confirmatory test. Future studies should investigate and determine whether the rates of rhodopsin degeneration differ among neurodegenerative diseases.

With the substantial evidence suggesting a correlation between retinal thinning, rhodopsin levels, and progression of neurodegenerative diseases, there is a clearly defined need to explore whether this biomarker is more beneficial in the early detection and monitoring of these debilitating conditions. While there have not yet been any studies that attempt to correlate rhodopsin with Huntington's, or ALS, there are various genes and signaling pathways that suggest a possible relationship. Furthermore, rhodopsin has been associated with retinal degeneration, a recently discovered indicator of neurodegenerative diseases.

For each study that we found including rhodopsin with retinal thinning and degradation, it appears that the rhodopsin levels simultaneously decreased. Given that changes in rhodopsin levels are known to precede alterations of the retina, it is logical to suggest that research is warranted to determine whether the absence of rhodopsin is significant in diagnosing these neurodegenerative disorders. With the development of novel techniques, such as cSLO, which allows the quantification of rhodopsin, efforts should be made to determine whether rhodopsin might have an increased sensitivity for the diagnosis and monitoring of neurodegenerative diseases. Measuring rhodopsin levels will likely be a beneficial complementary biomarker used in conjunction with assessing retinal thickness via OCT.

AUTHOR CONTRIBUTIONS

CL and RS drafted the manuscript. LH assisted with revisions. CL, RS, LH, and JZ conceived of this study. All authors read and approved the final manuscript.

FUNDING

Funding supported by NIH R01NS103822 to JZ.

ACKNOWLEDGMENTS

Figures 1, **2** were created using Biorender.com.

REFERENCES

Ahn, J., Lee, J. Y., Kim, T. W., Yoon, E. J., Oh, S., Kim, Y. K., et al. (2018). Retinal thinning associates with nigral dopaminergic loss in de novo Parkinson disease. *Neurology* 91, e1003–e1012. doi: 10.1212/WNL.0000000000006157

Albert, M. S., DeKosky, S. T., Dickson, D., Dubois, B., Feldman, H. H., Fox, N. C., et al. (2011). The diagnosis of mild cognitive impairment due to Alzheimer's disease: recommendations from the National Institute on aging-Alzheimer's association workgroups on diagnostic guidelines for Alzheimer's disease. *Alzheimers Dement.* 7, 270–279. doi: 10.1016/j.jalz.2011.03.008

Al-Chalabi, A., and Hardiman, O. (2013). The epidemiology of ALS: a conspiracy of genes, environment and time. *Nat. Rev. Neurol.* 9, 617–628. doi: 10.1038/nrneurol.2013.203

Altintas, O., Iseri, P., Ozkan, B., and Caglar, Y. (2008). Correlation between retinal morphological and functional findings and clinical severity in Parkinson's disease. *Doc. Ophthalmol.* 116, 137–146. doi: 10.1007/s10633-007-9091-8

Archibald, N. K., Clarke, M. P., Mosimann, U. P., and Burn, D. J. (2009). The retina in Parkinson's disease. *Brain* 132(Pt 5), 1128–1145.

Athanasiou, D., Aguila, M., Bellingham, J., Li, W., McCulley, C., Reeves, P. J., et al. (2018). The molecular and cellular basis of rhodopsin retinitis pigmentosa reveals potential strategies for therapy. *Prog. Retin. Eye Res.* 62, 1–23. doi: 10.1016/j.preteyeres.2017.10.002

Bence, N. F., Sampat, R. M., and Kopito, R. R. (2001). Impairment of the ubiquitin-proteasome system by protein aggregation. *Science* 292, 1552–1555. doi: 10.1126/science.292.5521.1552

Birtwistle, J., and Baldwin, D. (1998). Role of dopamine in schizophrenia and Parkinson's disease. *Br. J. Nurs.* 7, 832–834.

Bredesen, D. E. (2009). Neurodegeneration in Alzheimer's disease: caspases and synaptic element interdependence. *Mol. Neurodegener.* 4:27. doi: 10.1186/1750-1326-4-27

Brimblecombe, K. R., Gracie, C. J., Platt, N. J., and Cragg, S. J. (2015). Gating of dopamine transmission by calcium and axonal N-, Q-, T- and L-type voltage-gated calcium channels differs between striatal domains. *J. Physiol.* 593, 929–946. doi: 10.1113/jphysiol.2014.285890

Cehofski, L. J., Kruse, A., Kirkeby, S., Alsing, A. N., Ellegaard Nielsen, J., Kojima, K., et al. (2018). IL-18 and S100A12 are upregulated in experimental central retinal vein occlusion. *Int. J. Mol. Sci.* 19:3328. doi: 10.3390/ijms19113328

Chen, Y. Y., Yen, Y. F., Lin, J. X., Feng, S. C., Wei, L. C., Lai, Y. J., et al. (2018). Risk of ischemic stroke, hemorrhagic stroke, and all-cause mortality in retinal vein occlusion: a nationwide population-based cohort study. *J. Ophthalmol.* 2018:8629429. doi: 10.1155/2018/8629429

Chiang, W. C., Kroeger, H., Sakami, S., Messah, C., Yasumura, D., Matthes, M. T., et al. (2015). Robust endoplasmic reticulum-associated degradation of rhodopsin precedes retinal degeneration. *Mol. Neurobiol.* 52, 679–695. doi: 10.1007/s12035-014-8881-8

Chiquita, S., Campos, E. J., Castelhano, J., Ribeiro, M., Sereno, J., Moreira, P. I., et al. (2019). Retinal thinning of inner sub-layers is associated with cortical atrophy in a mouse model of Alzheimer's disease: a longitudinal multimodal in vivo study. *Alzheimers Res. Ther.* 11:90. doi: 10.1186/s13195-019-0542-8

Cideciyan, A. V., Jacobson, S. G., Aleman, T. S., Gu, D., Pearce-Kelling, S. E., Sumaroka, A., et al. (2005). In vivo dynamics of retinal injury and repair in the rhodopsin mutant dog model of human retinitis pigmentosa. *Proc. Natl. Acad. Sci. U.S.A.* 102, 5233–5238. doi: 10.1073/pnas.0408892102

Cipollini, V., Abdolrahimzadeh, S., Troili, F., De Carolis, A., Calafiore, S., Scuderi, L., et al. (2019). Neurocognitive assessment and retinal thickness alterations in Alzheimer disease: is there a correlation? *J. Neuroophthalmol.* doi: 10.1097/WNO.0000000000000831 [Epub ahead of print]

Colligris, P., Perez de Lara, M. J., Colligris, B., and Pintor, J. (2018). Ocular manifestations of Alzheimer's and other neurodegenerative diseases: the prospect of the eye as a tool for the early diagnosis of Alzheimer's disease. *J. Ophthalmol.* 2018:8538573. doi: 10.1155/2018/8538573

Corona, C., Masciopinto, F., Silvestri, E., Viscovo, A. D., Lattanzio, R., Sorda, R. L., et al. (2010). Dietary zinc supplementation of 3xTg-AD mice increases BDNF levels and prevents cognitive deficits as well as mitochondrial dysfunction. *Cell Death Dis.* 1:e91. doi: 10.1038/cddis.2010.73

Daadi, M. M., Klausner, J. Q., Bajar, B., Goshen, I., Lee-Messer, C., Lee, S. Y., et al. (2016). Optogenetic stimulation of neural grafts enhances neurotransmission and downregulates the inflammatory response in experimental stroke model. *Cell Transplant.* 25, 1371–1380. doi: 10.3727/096368915X688533

del Valle, L. J., Ramon, E., Canavate, X., Dias, P., and Garriga, P. (2003). Zinc-induced decrease of the thermal stability and regeneration of rhodopsin. *J. Biol. Chem.* 278, 4719–4724. doi: 10.1074/jbc.m210760200

den Haan, J., Csinscik, L., Parker, T., Paterson, R. W., Slattery, C. F., Foulkes, A., et al. (2019). Retinal thickness as potential biomarker in posterior cortical atrophy and typical Alzheimer's disease. *Alzheimers Res. Ther.* 11:62. doi: 10.1186/s13195-019-0516-x

Deretic, D. (2006). A role for rhodopsin in a signal transduction cascade that regulates membrane trafficking and photoreceptor polarity. *Vision Res.* 46, 4427–4433. doi: 10.1016/j.visres.2006.07.028

Dhalla, A., Pallikadavath, S., and Hutchinson, C. V. (2019). Visual dysfunction in Huntington's disease: a systematic review. *J. Huntingtons Dis.* 8, 233–242. doi: 10.3233/JHD-180340

Di Pierdomenico, J., Garcia-Ayuso, D., Pinilla, I., Cuenca, N., Vidal-Sanz, M., Agudo-Barriuso, M., et al. (2017). Early events in retinal degeneration caused by rhodopsin mutation or pigment epithelium malfunction: differences and similarities. *Front. Neuroanat.* 11:14. doi: 10.3389/fnana.2017.00014

Doustar, J., Torbati, T., Black, K. L., Koronyo, Y., and Koronyo-Hamaoui, M. (2017). Optical coherence tomography in Alzheimer's disease and other neurodegenerative diseases. *Front. Neurol.* 8:701. doi: 10.3389/fneur.2017.00701

Duebel, J., Marazova, K., and Sahel, J. A. (2015). Optogenetics. *Curr. Opin. Ophthalmol.* 2015, 226–232.

Ehler, M., Dobrosotskaya, J., Cunningham, D., Wong, W. T., Chew, E. Y., Czaja, W., et al. (2015). Modeling photo-bleaching kinetics to create high resolution maps of rod rhodopsin in the human retina. *PLoS One* 10:e0131881. doi: 10.1371/journal.pone.0131881

Goetz, C. G., Poewe, W., Rascol, O., Sampaio, C., Stebbins, G. T., Counsell, C., et al. (2004). Movement disorder society task force report on the Hoehn and Yahr staging scale: status and recommendations. *Mov. Disord.* 19, 1020–1028. doi: 10.1002/mds.20213

Gulmez Sevim, D., Unlu, M., Gultekin, M., and Karaca, C. (2019). Retinal single-layer analysis with optical coherence tomography shows inner retinal layer thinning in Huntington's disease as a potential biomarker. *Int. Ophthalmol.* 39, 611–621. doi: 10.1007/s10792-018-0857-7

Hardy, J., and Allsop, D. (1991). Amyloid deposition as the central event in the aetiology of Alzheimer's disease. *Trends Pharmacol. Sci.* 12, 383–388. doi: 10.1016/0165-6147(91)90609-v

Helmer, C., Malet, F., Rougier, M. B., Schweitzer, C., Colin, J., Delyfer, M. N., et al. (2013). Is there a link between open-angle glaucoma and dementia? The three-city-alienor cohort. *Ann. Neurol.* 74, 171–179. doi: 10.1002/ana.23926

Hubers, A., Muller, H. P., Dreyhaupt, J., Bohm, K., Lauda, F., Tumani, H., et al. (2016). Retinal involvement in amyotrophic lateral sclerosis: a study with optical coherence tomography and diffusion tensor imaging. *J. Neural. Transm. (Vienna).* 123, 281–287. doi: 10.1007/s00702-015-1483-4

Hwang, J. J., Park, M. H., Choi, S. Y., and Koh, J. Y. (2005). Activation of the Trk signaling pathway by extracellular zinc. Role of metalloproteinases. *J. Biol. Chem.* 280, 11995–12001. doi: 10.1074/jbc.m403172200

Illing, M. E., Rajan, R. S., Bence, N. F., and Kopito, R. R. (2002). A rhodopsin mutant linked to autosomal dominant retinitis pigmentosa is prone to aggregate and interacts with the ubiquitin proteasome system. *J. Biol. Chem.* 277, 34150–34160. doi: 10.1074/jbc.m204955200

Jackson, G. R., Owsley, C., and McGwin, G. (1999). Aging and dark adaptation. *Vision Res.* 39, 3975–3982. doi: 10.1016/s0042-6989(99)00092-9

Jahn, H. (2018). Memory loss in Alzheimer's disease. *Dialogues Clin. Neurosci.* 2013, 445–454.

Jaronen, M., Goldsteins, G., and Koistinaho, J. (2014). ER stress and unfolded protein response in amyotrophic lateral sclerosis-a controversial role of protein disulphide isomerase. *Front. Cell Neurosci.* 8:402. doi: 10.3389/fncel.2014.00402

Javaid, F. Z., Brenton, J., Guo, L., and Cordeiro, M. F. (2016). Visual and ocular manifestations of Alzheimer's disease and their use as biomarkers for diagnosis and progression. *Front. Neurol.* 7:55. doi: 10.3389/fneur.2016.00055

Jedrziewski, M. K., Lee, V. M., and Trojanowski, J. Q. (2007). Physical activity and cognitive health. *Alzheimers Dement.* 3, 98–108. doi: 10.1016/j.jalz.2007.01.009

Joachim, S. C., Renner, M., Reinhard, J., Theiss, C., May, C., Lohmann, S., et al. (2017). Protective effects on the retina after ranibizumab treatment in an ischemia model. *PLoS One* 12:e0182407. doi: 10.1371/journal.pone.0182407

Jordan, B. D., and Wright, E. L. (2010). Xenon as an anesthetic agent. *AANA J.* 78, 387–392.

Kersten, H. M., Danesh-Meyer, H. V., Kilfoyle, D. H., and Roxburgh, R. H. (2015). Optical coherence tomography findings in Huntington's disease: a potential biomarker of disease progression. *J. Neurol.* 262, 2457–2465. doi: 10.1007/s00415-015-7869-2

Khayat, M., Williams, M., and Lois, N. (2018). Ischemic retinal vein occlusion: characterizing the more severe spectrum of retinal vein occlusion. *Surv. Ophthalmol.* 63, 816–850. doi: 10.1016/j.survophthal.2018.04.005

Knapp, J., VanNasdale, D. A., Ramsey, K., and Racine, J. (2018). Retinal dysfunction in a presymptomatic patient with Huntington's disease. *Doc. Ophthalmol.* 136, 213–221. doi: 10.1007/s10633-018-9632-3

Koronyo-Hamaoui, M., Koronyo, Y., Ljubimov, A. V., Miller, C. A., Ko, M. K., Black, K. L., et al. (2011). Identification of amyloid plaques in retinas from Alzheimer's patients and noninvasive in vivo optical imaging of retinal plaques in a mouse model. *Neuroimage* 54(Suppl. 1), S204–S217. doi: 10.1016/j.neuroimage.2010.06.020

Kowal, S. L., Dall, T. M., Chakrabarti, R., Storm, M. V., and Jain, A. (2013). The current and projected economic burden of Parkinson's disease in the United States. *Mov. Disord.* 28, 311–318. doi: 10.1002/mds.25292

Lenox, A. R., Bhootada, Y., Gorbatyuk, O., Fullard, R., and Gorbatyuk, M. (2015). Unfolded protein response is activated in aged retinas. *Neurosci. Lett.* 609, 30–35. doi: 10.1016/j.neulet.2015.10.019

Lin, J. Y. (2011). A user's guide to channelrhodopsin variants: features, limitations and future developments. *Exp. Physiol.* 96, 19–25. doi: 10.1113/expphysiol.2009.051961

Liu, T., Liu, X., Wen, R., Lam, B. L., and Jiao, S. (2015). In vivo imaging rhodopsin distribution in the photoreceptors with nano-second pulsed scanning laser ophthalmoscopy. *Quant. Imaging Med. Surg.* 5, 63–68. doi: 10.3978/j.issn.2223-4292.2014.11.06

McKhann, G. M., Knopman, D. S., Chertkow, H., Hyman, B. T., Jack, C. R. Jr., Kawas, C. H., et al. (2011). The diagnosis of dementia due to Alzheimer's disease: recommendations from the National Institute on aging-Alzheimer's association workgroups on diagnostic guidelines for Alzheimer's disease. *Alzheimers Dement.* 7, 263–269. doi: 10.1016/j.jalz.2011.03.005

Miller, D. B., and O'Callaghan, J. P. (2015). Biomarkers of Parkinson's disease: present and future. *Metabolism* 64(3 Suppl. 1), S40–S46. doi: 10.1016/j.metabol.2014.10.030

Moritz, O. L., Tam, B. M., Hurd, L. L., Peranen, J., Deretic, D., and Papermaster, D. S. (2001). Mutant rab8 impairs docking and fusion of rhodopsin-bearing post-Golgi membranes and causes cell death of transgenic Xenopus rods. *Mol. Biol. Cell* 12, 2341–2351. doi: 10.1091/mbc.12.8.2341

Mukherjee, N., McBurney-Lin, S., Kuo, A., Bedlack, R., and Tseng, H. (2017). Retinal thinning in amyotrophic lateral sclerosis patients without ophthalmic disease. *PLoS One* 12:e0185242. doi: 10.1371/journal.pone.0185242

Murray, A. R., Fliesler, S. J., and Al-Ubaidi, M. R. (2009). Rhodopsin: the functional significance of asn-linked glycosylation and other post-translational modifications. *Ophthalmic Genet.* 30, 109–120. doi: 10.1080/13816810902962405

Musiek, E. S., and Holtzman, D. M. (2016). Mechanisms linking circadian clocks, sleep, and neurodegeneration. *Science* 354, 1004–1008. doi: 10.1126/science.aah4968

Mutlu, U., Colijn, J. M., Ikram, M. A., Bonnemaijer, P. W. M., Licher, S., Wolters, F. J., et al. (2018). Association of retinal neurodegeneration on optical coherence tomography with dementia: a population-based study. *JAMA Neurol.* 75, 1256–1263. doi: 10.1001/jamaneurol.2018.1563

Nagel, G., Ollig, D., Fuhrmann, M., Kateriya, S., Musti, A. M., Bamberg, E., et al. (2002). Channelrhodopsin-1: a light-gated proton channel in green algae. *Science* 296, 2395–2398. doi: 10.1126/science.1072068

Ni, J. D., Baik, L. S., Holmes, T. C., and Montell, C. (2017). A rhodopsin in the brain functions in circadian photoentrainment in *Drosophila*. *Nature* 545, 340–344. doi: 10.1038/nature22325

Osborne, N. N., Casson, R. J., Wood, J. P., Chidlow, G., Graham, M., and Melena, J. (2004). Retinal ischemia: mechanisms of damage and potential therapeutic strategies. *Prog. Retin. Eye Res.* 23, 91–147. doi: 10.1016/j.preteyeres.2003.12.001

Pahlberg, J., and Sampath, A. P. (2011). Visual threshold is set by linear and nonlinear mechanisms in the retina that mitigate noise: how neural circuits in the retina improve the signal-to-noise ratio of the single-photon response. *Bioessays* 33, 438–447. doi: 10.1002/bies.201100014

Prince, M., Bryce, R., Albanese, E., Wimo, A., Ribeiro, W., and Ferri, C. P. (2013). The global prevalence of dementia: a systematic review and metaanalysis. *Alzheimers Dement.* 9, 63–75.e2. doi: 10.1016/j.jalz.2012.11.007

Reddy, G. B., Reddy, P. Y., and Surolia, A. (2017). Alzheimer's and Danish dementia peptides induce cataract and perturb retinal architecture in rats. *Biomol. Concepts* 8, 45–84. doi: 10.1515/bmc-2016-0025

Reitz, C., Brayne, C., and Mayeux, R. (2011). Epidemiology of Alzheimer disease. *Nat. Rev. Neurol.* 7, 137–152. doi: 10.1038/nrneurol.2011.2

Rojas, P., de Hoz, R., Ramirez, A. I, Ferreras, A., Salobrar-Garcia, E., Munoz-Blanco, J. L., et al. (2019). Changes in retinal OCT and their correlations with neurological disability in early ALS patients, a follow-up study. *Brain Sci.* 9:E337. doi: 10.3390/brainsci9120337

Satue, M., Obis, J., Alarcia, R., Orduna, E., Rodrigo, M. J., Vilades, E., et al. (2018). Retinal and choroidal changes in patients with Parkinson's disease detected by swept-source optical coherence tomography. *Curr. Eye Res.* 43, 109–115. doi: 10.1080/02713683.2017.1370116

Schaller, B. J. (2008). Strategies for molecular imaging dementia and neurodegenerative diseases. *Neuropsychiatr. Dis. Treat.* 4, 585–612.

Schulz, J. B. (2007). Mechanisms of neurodegeneration in idiopathic Parkinson's disease. *Parkinsonism Relat. Disord.* 13(Suppl. 3), S306–S308. doi: 10.1016/S1353-8020(08)70021-X

Sensi, S. L., Granzotto, A., Siotto, M., and Squitti, R. (2018). Copper and zinc dysregulation in Alzheimer's disease. *Trends Pharmacol. Sci.* 39, 1049–1063. doi: 10.1016/j.tips.2018.10.001

Sensi, S. L., Paoletti, P., Bush, A. I., and Sekler, I. (2009). Zinc in the physiology and pathology of the CNS. *Nat. Rev. Neurosci.* 10, 780–791. doi: 10.1038/nrn2734

Sheinerman, K. S., and Umansky, S. R. (2013). Early detection of neurodegenerative diseases: circulating brain-enriched microRNA. *Cell Cycle* 12, 1–2. doi: 10.4161/cc.23067

Sivak, J. M. (2013). The aging eye: common degenerative mechanisms between the Alzheimer's brain and retinal disease. *Invest. Ophthalmol. Vis. Sci.* 54, 871–880. doi: 10.1167/iovs.12-10827

Sparrow, J. R., Hicks, D., and Hamel, C. P. (2010). The retinal pigment epithelium in health and disease. *Curr. Mol. Med.* 10, 802–823.

Sperling, R. A., Aisen, P. S., Beckett, L. A., Bennett, D. A., Craft, S., Fagan, A. M., et al. (2011). Toward defining the preclinical stages of Alzheimer's disease: recommendations from the National Institute on Aging-Alzheimer's association workgroups on diagnostic guidelines for Alzheimer's disease. *Alzheimers Dement.* 7, 280–292. doi: 10.1016/j.jalz.2011.03.003

Stojanovic, A., Stitham, J., and Hwa, J. (2004). Critical role of transmembrane segment zinc binding in the structure and function of rhodopsin. *J. Biol. Chem.* 279, 35932–35941. doi: 10.1074/jbc.m403821200

Sudharsan, R., Simone, K. M., Anderson, N. P., Aguirre, G. D., and Beltran, W. A. (2017). Acute and protracted cell death in light-induced retinal degeneration in the canine model of rhodopsin autosomal dominant retinitis pigmentosa. *Invest. Ophthalmol. Vis. Sci.* 58, 270–281. doi: 10.1167/iovs.16-20749

Talbott, E. O., Malek, A. M., and Lacomis, D. (2016). The epidemiology of amyotrophic lateral sclerosis. *Handb. Clin. Neurol.* 138, 225–238. doi: 10.1016/B978-0-12-802973-2.00013-6

Tanito, M., and Ohira, A. (2013). Hemianopic inner retinal thinning after stroke. *Acta Ophthalmol.* 91, e237–e238. doi: 10.1111/aos.12039

Touhami, S., Beguier, F., Augustin, S., Charles-Messance, H., Vignaud, L., Nandrot, E. F., et al. (2018). Chronic exposure to tumor necrosis factor alpha induces retinal pigment epithelium cell dedifferentiation. *J. Neuroinflamm.* 15:85. doi: 10.1186/s12974-018-1106-8

Ugarte, M., and Osborne, N. N. (2001). Zinc in the retina. *Prog. Neurobiol.* 64, 219–249. doi: 10.1016/s0301-0082(00)00057-5

Webster, C. P., Smith, E. F., Shaw, P. J., and De Vos, K. J. (2017). Protein homeostasis in amyotrophic lateral sclerosis: therapeutic opportunities? *Front. Mol. Neurosci.* 10:123. doi: 10.3389/fnmol.2017.00123

Weller, J., and Budson, A. (2018). Current understanding of Alzheimer's disease diagnosis and treatment. *F1000Res.* 7:1161. doi: 10.12688/f1000research.14506.1

Xiao, J., Adil, M. Y., Chang, K., Yu, Z., Yang, L., Utheim, T. P., et al. (2019). Visual contrast sensitivity correlates to the retinal degeneration in rhodopsin knockout mice. *Invest. Ophthalmol. Vis. Sci.* 60, 4196–4204. doi: 10.1167/iovs.19-26966

Xiong, B., and Bellen, H. J. (2013). Rhodopsin homeostasis and retinal degeneration: lessons from the fly. *Trends Neurosci.* 36, 652–660. doi: 10.1016/j.tins.2013.08.003

Yoon, S. P., Grewal, D. S., Thompson, A. C., Polascik, B. W., Dunn, C., Burke, J. R., et al. (2019). Retinal microvascular and neurodegenerative changes in Alzheimer's disease and mild cognitive impairment compared with control participants. *Ophthalmol. Retina* 3, 489–499. doi: 10.1016/j.oret.2019.02.002

Zhang, F., Vierock, J., Yizhar, O., Fenno, L. E., Tsunoda, S., Kianianmomeni, A., et al. (2011). The microbial opsin family of optogenetic tools. *Cell* 147, 1446–1457. doi: 10.1016/j.cell.2011.12.004

Zou, Z. Y., Zhou, Z. R., Che, C. H., Liu, C. Y., He, R. L., and Huang, H. P. (2017). Genetic epidemiology of amyotrophic lateral sclerosis: a systematic review and meta-analysis. *J. Neurol. Neurosurg. Psychiatry* 88, 540–549.

Conflict of Interest: The authors declare that the research was conducted in the absence of any commercial or financial relationships that could be construed as a potential conflict of interest.

frontiers in Cellular Neuroscience

ORIGINAL RESEARCH
published: 30 April 2020
doi: 10.3389/fncel.2020.00088

Opposite Roles of δ- and μ-Opioid Receptors in BACE1 Regulation and Alzheimer's Injury

Yuan Xu[1,2,3], Feng Zhi[2,3], Gianfranco Balboni[4], Yilin Yang[2,3] and Ying Xia[1]**

[1] Shanghai Key Laboratory of Acupuncture Mechanism and Acupoint Function, Department of Aeronautics and Astronautics, Fudan University, Shanghai, China, [2] Modern Medical Research Center, The Third Affiliated Hospital of Soochow University, Changzhou, China, [3] Department of Neurosurgery, The First People's Hospital of Changzhou, Changzhou, China, [4] Department of Life and Environment Sciences, University of Cagliari, Cagliari, Italy

Alzheimer's disease (AD) is characterized by amyloid plaques and neurofibrillary tangles. Substantial evidence for AD pathogenesis suggests that β-site APP cleaving enzyme 1 (BACE1) and γ-secretase enzyme initiate the amyloidogenic pathway and produces toxic Aβ peptides that prone to aggregate in the brain. Therefore, the inhibition of BACE1 expression and function is an attractive strategy for AD therapy. In the present work, we made the first finding that activating δ-opioid receptors (DOR) with a specific DOR agonist significantly attenuated BACE1 expression and activity in the highly differentiated PC12 cells with mimicked AD injury, while the application of DOR inhibitor naltrindole reversed the UFP-512 effects, and even caused a major increase in BACE1 expression and activity as well as Aβ42 production in physiological conditions. Knocking-down DOR also enhanced BACE1 protein expression and its activity for APP processing, associating with a significant increase in Aβ42 production. In sharp contrast, activation of μ-opioid receptor (MOR) with DAMGO greatly promoted BACE1 expression and activity with an acceleration of APP cleavage, thus contributing to increased Aβ42 production. DADLE, a less selective DOR agonist that may bind to MOR, had no stable inhibitory effect on BACE1. Similar results were also found in APP mutant (APPswe) SH-SY5Y cell line, providing further validation of the DOR action on BACE1 regulation. Our novel data demonstrated entirely different roles of DOR and MOR in the regulation of BACE1 expression and activity with DOR being neuroprotective against AD injury. These findings provided a novel clue for new strategies of AD therapy via targeting endogenous opioid receptors.

Keywords: Alzheimer's disease, BACE1, Aβ peptides, δ-opioid receptor, μ-opioid receptor

OPEN ACCESS

Edited by:
Dennis Qing Wang, Southern Medical University, China

Reviewed by:
Anyang Sun, Shanghai University of Medicine & Health Sciences, China
Xiurong Zhao, University of Texas Health Science Center at Houston, United States

****Correspondence:***
Ying Xia
Y55738088@gmail.com
Yilin Yang
bigyang@vip.sina.com

Specialty section:
This article was submitted to Non-Neuronal Cells, a section of the journal Frontiers in Cellular Neuroscience

Received: *12 January 2020*
Accepted: *26 March 2020*
Published: *30 April 2020*

Citation:
Xu Y, Zhi F, Balboni G, Yang Y and Xia Y (2020) Opposite Roles of δ- and μ-Opioid Receptors in BACE1 Regulation and Alzheimer's Injury. Front. Cell. Neurosci. 14:88. doi: 10.3389/fncel.2020.00088

INTRODUCTION

Alzheimer's disease (AD) is characterized by a progressive loss of memory and cognition, which is the main cause of dementia and one of the great health problems of the 21st century. Indeed, dementia seriously affects almost 50 million people worldwide, and AD is the most well-known form of dementia, accounting for 50–75% of all cases (Cheignon et al., 2018). Two main pathological hallmarks of AD are amyloid plaques and neurofibrillary tangles. It has been widely accepted, though partially challenged now, that the deposition of Amyloid-β triggers

neuronal dysfunction and death in the brain, i.e., so-called the amyloid cascade hypothesis (Ballard et al., 2011). Amyloid-β peptides result from the sequential cleavage of APP, a type I integral membrane glycoprotein. There are two pathways lead to either non-amyloidogenic or amyloidogenic processing of this protein. In the non-amyloidogenic pathway, APP is cleaved by α-secretase and γ-secretase in its amyloid-β domain, producing soluble p3 peptides and the APP intracellular domain (AICD). The replacement of α-secretase with β-secretase (BACE1) changes the pathway to the amyloidogenic pathway, which releases amyloid-β peptides as well as the AICD fragment. The amyloid-β peptides with longer lengths such as Aβ42 are more prone to aggregation and more toxic (Canter et al., 2016).

Current medical management has a limited therapeutic effect on the quality of life for individuals with AD. Therefore, new treatments to prevent, delay, and cure AD are urgently needed. Several new approaches to treat AD have been proposed, most of them target Aβ. Among these, the development of specific inhibitors of BACE1 is an attractive prospect by fundamentally attenuating the production of Aβ in the first place (Scheltens et al., 2016).

Opioid receptors are widely distributed throughout the central nervous system, including the cortex and hippocampus, the major brain regions essential to cognition, learning and memory (Xia and Haddad, 1991, 2001; Erbs et al., 2015; Xia, 2015; Pellissier et al., 2018). Substantial data from our laboratory and other independent groups have demonstrated that δ-opioid receptor (DOR), rather than μ-opioid receptor (MOR), is an important neuroprotector in various injuries (He et al., 2013; Xia, 2015). DOR activation can stabilize brain ionic homeostasis (Chao et al., 2012; He et al., 2013; Lee et al., 2018) and inhibit hypoxic/ischemic neuroinflammation by regulating a PKC-dependent and a PKA-independent signaling pathway, increasing Nrf2 translocation and regulating PINK1-mediated mitochondrial homeostasis (Yang et al., 2009; He et al., 2013; Wang et al., 2014; Cao et al., 2015; Qiu et al., 2019; Xu et al., 2019). Since emerging evidence suggests that the pathogenesis of AD involves mitochondrial dysfunction, oxidative stress damage, calcium homeostasis and inflammation (Scheltens et al., 2016; Cheignon et al., 2018; Lee et al., 2018), we have proposed that opioid receptors may play a role in the pathology of AD, including regulations of the BACE1-mediated Aβ production with δ-opioid receptor (DOR) being neuroprotective.

However, a few studies seem to suggest that DOR contributes to the pathogenies of AD through promoting the APP processing. They argued that DOR activation enhanced β- and γ-secretase activities to mediate a specific processing of APP to Aβ, while DOR antagonism ameliorated Aβ pathology and Aβ-dependent behavioral deficits (Ni et al., 2006; Teng et al., 2010). In their work, a relatively non-specific opioid ligand, DADLE, was used as a DOR agonist in non-neuronal cell line (HEK293T cells). Since DADLE may bind to MOR and MOR may have a different role in certain neural functions (Lutz and Kieffer, 2013; Xia, 2015; Shrivastava et al., 2017; Wang et al., 2018) and since non-neuronal cells may react to AD stress in a different way, it is important to adopt more specific methodologies in neuron-like cells to yield more reliable conclusions in terms of the role of DOR in the pathology of AD.

In this study, we used a specific and potent DOR agonist and compared its effect with DADLE on the BACE1-mediated Aβ production and cell injury in highly differentiated PC12 cells. Moreover, we investigated the role of MOR activation in the BACE1-mediated Aβ production and cell injury in parallel. Our outcome data form the first evidence that DOR and MOR have entirely different roles in the BACE1 regulation and Aβ1–42 oligomer induced injury with DOR being neuroprotective.

MATERIALS AND METHODS

Chemicals and Reagents

Amyloid β1–42 peptide were purchased from Sigma-Aldrich (Cat: SCP0038, respectively, Bay St. Louis, MS, United States). UFP-512, a highly selective DOR agonist, was synthesized by our research partner (Aguila et al., 2007). Naltrindole hydrochloride, a DOR antagonist; DADLE, a DOR unspecific agonist; and DAMGO, a MOR agonist were all purchased from Tocris Bioscience (Cat: 0740, 3790, 1171, Bristol, United Kingdom). Cell Counting Kit-8 was from Beyotime, Co. (Cat: C0039, Shanghai, China). BACE1 Rabbit polyclonal antibody were purchased from Proteintech (Cat:12807-1-AP, Rosemont, IL, United States). Anti-β-actin antibody and APP rabbit antibody were purchased from Cell Signaling Technology (Cat: 4272, 76600S, Danvers, CO, United States). BACE1 Activity Kit were purchased from BioVision (Cat: K388-100, Milpitas, CA, United States). Human/Rat β Amyloid(42) ELISA Kit were obtained from Wako (Cat: 292-64501, Osaka, Japan).

Cell Cultures and Cell Treatments

An original highly differentiated rat PC-12 cell line was obtained from the Type Culture Collection of the Chinese Academy of Sciences, Shanghai, China. APP mutant (APPswe) SH-SY5Y cell were built by Fubio, Suzhou, China. The cells in the control group were incubated at 37°C in a humidified incubator with 5% CO_2. To mimic AD cell injury, PC-12 cells were exposed to 20 μM of Aβ1–42 oligomer for 48 h after cell attachment. UFP-512 (5 μM), a specific and potent DOR agonist, and naltrindole (1 μM), a DOR antagonist (Lutz and Kieffer, 2013; Scheltens et al., 2016; Xu et al., 2019), were applied to the culture medium in the subsequent experiments based on the preliminary results. Two concentrations of DADLE (1, 5 μM), a relatively non-specific DOR agonist and DAMGO (1 and 5 μM), a μ-opioid receptor (MOR) agonist (Ni et al., 2006; Lutz and Kieffer, 2013; Chen et al., 2014, 2019), were applied to the culture cells in the same way.

Cell Viability Assay

Cell viability was measured by CCK8 kit. Exponentially growing cells were plated at 5000 cells/well in a 96-well plate. A blank control was set with the well no cells but containing culture medium. After appropriate duration of drug treatments, the original medium was removed and 100 μl of fresh culture medium was added. 10 ul of CCK8 reagent per well was applied and the cells were incubated another 2 h for sufficient reaction.

The absorbance was measured at the wavelength of 450 nm using a microplate reader.

Fluorometric Secretase Activity Assay

BACE1 secretase assay kit was used to measure BACE1 activity according to the manufacturer's manual. In brief, the cell lysate fractions were extracted by BACE1 extraction buffer, and the samples were incubated with the secretase-specific substrate conjugated to a fluorescent reporter. An EDANS standard curve was set to evaluate the relative BACE1 activity. The wavelength at Ex/Em = 345/500 nm was detected in a kinetic mode for 10–60 min at 37°C on a multi-well spectrophotometer. The sample BACE1 activity was calculated as follows:

$$Sample\ BACE1\ Activty = \frac{B}{\Delta t \times V} \times D = mU/ml$$

Where: B is the EDNAS amount from Standard Curve(pmol)

Δt is the reaction time(min)
V is the sample volume added into the reaction well(μl)
D is the dilution factor.

Aβ42 Measurements

The Aβ42 levels were determined using a Human/Rat β Amyloid (42) ELISA kit. Following the manufacturer's instruction, the medium sheds and the cell lysates were collected and quantified. The samples and standards incubated in the wells for overnight at 4°C. Then the HRP conjugated antibody was added and TMB solution was used to start the HRP reaction at RT in the dark. After the reaction was terminated by stop solution, the absorbance was read at 450 nm with a multi-well microplate reader. Aβ42 concentrations were calculated based on the standard curve.

Western Blotting

Cells were lysed using the lysis buffer containing 0.5% 100 mM PMSF, 0.1% protease inhibitor, and 1% phosphatase inhibitor (KeyGEN Biotec, Cat: KGP2100, Nanjing, China). The protein concentration was determined by the BCA protein assay kit according to the manufacturer's protocols. Equal amounts of protein samples were diluted in a 5x loading buffer and run in 10–12.5% SDS-PAGE electrophoresis. Then proteins were transferred to hydrophobic polyvinylidenedifluorid (PVDF) membranes, and the membranes were blocked and incubated with certain mAbs. HRP conjugated secondary antibodies were used to detect the specific protein expression and it was visualized by chemiluminescence exposure using Western Lightening® Chemiluminescence Reagent Plus (Perkin-Elmer, Boston, MA, United States). Quantitation was performed by densitometry using the NIH Image program (Image J).

BACE1 mRNA Quantification

To measure the changes in the BACE1 mRNA content, total RNA from the cells was isolated using trizol reagent according to the manufacturer's instruction. In brief, the extracted RNA (1 μg) was used for the template in reversed transcription. RT-PCR was performed with the SYBR Select Master Mix (Applied Biosystems, Foster City, CA, United States). The primers designed are listed as follows:

BACE1 mRNA primers:
Sense 5′ AGACGCTCAACATCCTGGTG 3′
Anti-Sense 5′ CCTGGGTGTAGGGCACATAC 3′
Ribosomal mRNA primers:
Sense 5′ CAGAAGGACGTGAAGGATGG 3′
Anti-Sense 5′ CAGTGGTCTTGGTGTGCTGA 3′

The target mRNA levels were calculated depending on the Ct value of the target cDNA and the reference cDNA. The relative quantification of target mRNA were adjusted to the control.

siRNA Transfection

The siRNA oligonucleotides were synthesized by Genepharma, Co. (Shanghai, China). The sequences were designed as follows:

Negative control siRNA:
5′-UUC UCC GAA CGU GUC ACG UTT-3′
DOR siRNA (rat):
5′-GGC UGU GCU CUC CAU UGACUU-3′
DOR siRNA (human):
5′-GCCAAGCUGAUCAACAUCUTT-3′

PC12 cells and APPswe SH-SY5Y cells were transfected with DOR small interfering RNA (rat) constructs or DOR siRNA (human) respectively. The negative control were established following the manufacturer's instructions (Genepharma, Co., Shanghai, China). The siRNA compounds were diluted in Opti-MEM and then mixed at a 1:1 ratio with diluted Lipofectamine in Opti-MEM. The mixture was added directly to the culture medium for 20-min stabilization. After 6-h incubation, the medium containing siRNA was removed and the fresh medium was added. Successfully transfected PC12 cells were used for the follow-up experiments.

Statistical Analysis

All data are presented as means ± SEM and the independent experiments number performed for each measurement is at least three. Statistical analysis was processed with one-way ANOVA followed by Bonferroni's multiple comparison tests (Prism 5, GraphPad Software, La Jolla, CA, United States).

RESULTS

DOR Inhibition and MOR Activation Aggravated Aβ1–42 Oligomer Induced Cell Injury

Aβ oligomers have been well-linked to AD pathogenesis in animal models and human beings (Selkoe and Hardy, 2016; Jeong, 2017) and Aβ oligomer injury is now widely used to mimic AD injury in cell models (Geng et al., 2013; Balducci and Forloni, 2014; Morroni et al., 2016). In this work, we induced the AD injury by treating the highly differentiated PC12 cells with 20 μM Aβ1–42 oligomer (Aβ1–42 injury or AD injury). After Aβ1–42 oligomer exposure for 48 h, the cell viability showed a significant

reduction by 26.4% vs. the control group ($p < 0.01$, **Figure 1**). The cell injury was worsen with the increase in exposure time. At 72 h, the cell viability was reduced by 50% (vs. 100% of the control group, $p < 0.05$, **Figure 1**). Morphologically, the cell density was significantly reduced and the synapses of the PC12 cells was decreased to some extent.

Then, we applied DOR specific agonist UFP-512 (5 μM) and DOR inhibitor naltrindole (1 μM) to the PC12 cells to examine the effects of DOR on AD injury. The application of UFP-512 did not cause any significant change in the cell viability (**Figure 1B**) as well as the cell density (**Figure 1A**). However, the addition of DOR antagonist naltrindole greatly aggravated Aβ1–42 injury. The measurements at 48 h after the treatments showed a 25.1% decrease in the cell viability (from 73.6% in the group of Aβ1–42 oligomer alone to 48.5% in the group with Aβ1–42 oligomer plus naltrindole, $p < 0.05$, **Figure 1A**-right panel). After prolonging the exposure time to 72 h, the inhibition of DOR induced more severe cell damage. Under the condition of Aβ1–42 injury, either UFP-512 plus naltrindole or naltrindole alone caused much more cell injury compared to that of Aβ1–42 oligomer alone ($p < 0.01$, **Figure 1A**-right panel).

Furthermore, we examined the effects of DADLE, a much less selective DOR agonist than UFP-512, and MOR agonist DAMGO on cell viability. As **Figures 1A,C** depicted, DADLE did not significantly alter the cell injury induced by Aβ1–42 oligomer, similar as UFP-512. In contrast, the cell viability and cell density were progressively reduced with the duration of DAMGO treatments, with a decrease by 13.4% after 48 h and a decrease by 29.1% after 72 h vs. Aβ1–42 injury group ($p < 0.01$, **Figure 1B**).

The above results suggest that DOR and MOR have differential effects on AD injury in PC12 cells.

DOR Activation and MOR Activation Differentially Altered BACE1 Activity

The accumulation of Aβ triggers neuronal dysfunction and death in the brain (Scheltens et al., 2016), while the generation of Aβ involves APP cleavage by β secretase (BACE1). We therefore investigated if DOR inhibition or MOR activation caused any changes in BACE1 activity. As shown in **Figure 2A**, 30-min treatment of DOR agonist UFP-512 remarkably decreased BACE1 activity by 28.4% ($p < 0.05$, **Figure 2A**). At 48-h of UFP-512 treatment, however, there was no appreciable change in BACE1 activity as compared to the control group. Interestingly, DOR antagonist naltrindole, significantly enhanced BACE1 activity at both 30 min and 48 h of naltrindole exposure (111.3 vs. 100% of the control group at 30 min, $p < 0.01$, and 173.4 vs. 100% of the control group at 48 h, $p < 0.05$, **Figure 2A**). Even in the existence of UFP-512, naltrindole still increased BACE1 activity by 10.3% at 30 min and 81.1% at 48 h as compared to the control group ($p < 0.01$, **Figure 2A**).

Similarly, DADLE- and DAMGO-mediated alternations in BACE1 activity were evaluated using the BACE1 activity kit. We applied DADLE and DAMGO at 1 and 5 μM to the cells and lasted for 30 min or 48 h. The results showed that 1 μM DADLE did not cause a major impact on BACE1 activities, but 5 μM DADLE slightly enhanced BACE1 activity at both 30 min and 48 h after DADLE treatment (**Figure 2B**). In sharp contrast to DADLE, DAMGO significantly increased BACE1 activities in the concentrations of either 1 or 5 μM and at both 30 min and 48 h after DAMGO treatment ($p < 0.05$ vs. the control, **Figure 2B**).

Furthermore, we compared BACE1 activities after DOR vs. MOR activation in the AD cell model with Aβ1–42 oligomer treatment. As shown in **Figure 2C**, DOR activation with UFP-512 greatly reduced BACE1 activity by 30.2% after 30-min treatment ($p < 0.01$ vs. the control, "A" group) and 33.7% vs. after 48-h treatment ($p < 0.01$ vs. the control, "A" group) (**Figure 2C**), whereas the addition of DOR antagonist naltrindole reversed the changes. In the same condition, DADLE had no appreciable effect on the activity of BACE1 except for a slight decrease in BACE1 activity after 48-h treatment of 1 μM DADLE (+13.9%, $p < 0.05$, **Figure 2D**). In sharp contrast to the DOR agonists, MOR agonist DAMGO significantly increased the activity of BACE1 under AD stress (+30%, $p < 0.01$, **Figure 2D**) in the exactly same condition.

These data suggest that DOR and MOR regulate BACE1 activities in an opposite direction under both normal condition and AD injury.

DOR Inhibition and MOR Activation Induced BACE1 Upregulation Were Associated With an Increase in Aβ42 Production and Release

Since Aβ42 is more prone to aggregate in the brain, the initial deposition always begins from Aβ42, but not other Aβ product (Ni et al., 2006; Ballard et al., 2011). We therefore investigated whether the alterations in BACE1 activity after opioid receptor activation/inhibition lead to any change in the production of Aβ. Using a high sensitive ELISA kit to detect the C-terminal portion of Aβ42, we found that DOR activation with UFP-512 did not significantly change the Aβ42 production, but adding its antagonist naltrindole or applying naltrindole alone to the cell medium greatly increased the level of Aβ42, especially after 48-h treatment (from 100% of the control group to 181.4% of the "C + U + N" group in the cell lysate portion, $p < 0.01$, from 100% of the control group to 246.3% of the "C + N" group in the cell lysate portion, $p < 0.05$, from 100% of the control group to 154.4% of the "C + U + N" group in the medium shed portion, $p < 0.05$, from 100% of the control group to 179.6% of the "C + N" group in the medium shed portion, $p < 0.05$, **Figure 3A**).

With DADLE or DAMGO treatment, there was no appreciable change in Aβ42 production after 30-min treatments. The treatment with DADLE at 1 μM for 48 h led to a significant decrease in Aβ42 level in cell lysate, but not in the shed portion of Aβ42. The treatment with DAMGO, especially in a higher concentration (5 μM), remarkably increased Aβ42 production in both the cell lysate and medium shed ($p < 0.05$, **Figure 3B**).

To further validate the effects of DOR and MOR on Aβ production and release, we used SH-SY5Y cells with an APP mutant (APPswe), which thus harbors "Swedish" mutations, a characteristic of some AD cases. These cells possess endogenous DOR, BACE1 expression and activities. As shown in **Figure 3C**, the stimulation of DOR with its specific agonist UFP-512

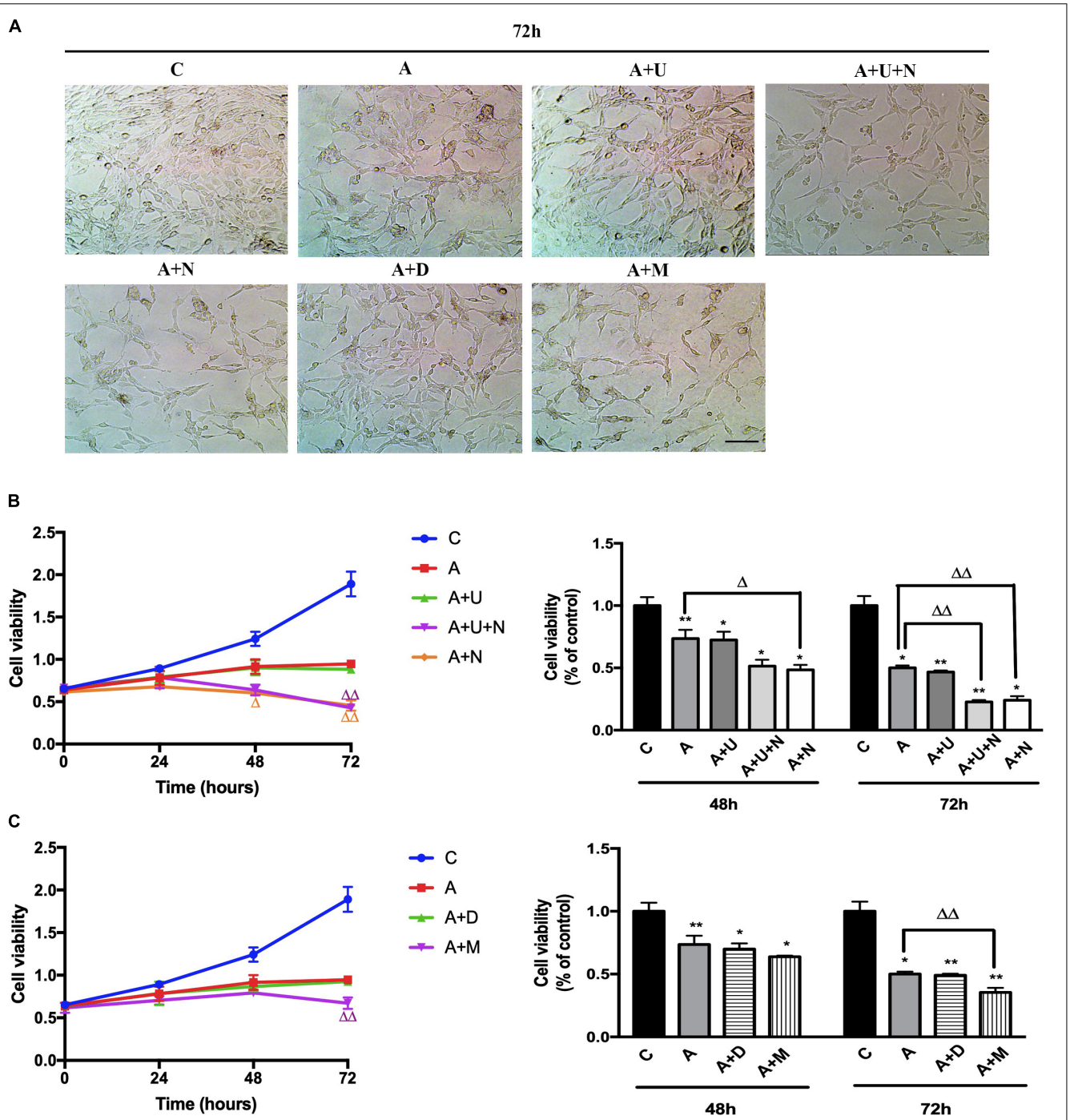

FIGURE 1 | DOR inhibition or MOR activation aggravated Aβ1–42 oligomer induced cell injury. The experiments were conducted on highly differentiated PC12 cells ($N = 3$ in each group). The cell viability were measured every 24 h using CCK8 kit. C: normal control. A: Aβ1–42 oligomer (20 μM) to mimic AD cell injury (Aβ1–42 injury or AD injury). A + U: DOR activation with UFP-512 in AD injury. A + U + N: A + U plus DOR inhibition with naltrindole. A + N: DOR inhibition with naltrindole in AD injury. A + D: DADLE (1 μM) treatment in AD injury. A + M: MOR activation with 1 μM DAMGO in AD injury. **(A)** DOR/MOR induced morphologic changes in PC12 cells. Note that Aβ1–42 oligomer induced cell injury and the administration of DOR antagonist naltrindole or MOR agonist DAMGO aggravated such injury. Morphologically, it was characterized by a reduction in cell density, decrease of synapses. Scale bar = 100 μm in panel **(A)** for all groups. **(B)** Cell viability and DOR-mediated alternations in cell proliferation under AD injury. $^{*}p < 0.05$, $^{**}p < 0.01$ vs. **(C)**; $^{\Delta}p < 0.05$, $^{\Delta\Delta}p < 0.01$ vs. **(A)**. Note that Aβ1–42 oligomer administration largely decreased the cell viability, and DOR inhibition further aggravated the cell injury. **(C)** Effects of DADLE and DAMGO on cell viability in Aβ1–42 injury. $^{*}p < 0.05$, $^{**}p < 0.01$ vs. **(C)**; $^{\Delta\Delta}p < 0.01$ vs. **(A)**. Note that MOR activation greatly aggravated the cell viability at 72 h after Aβ1–42 oligomer administration.

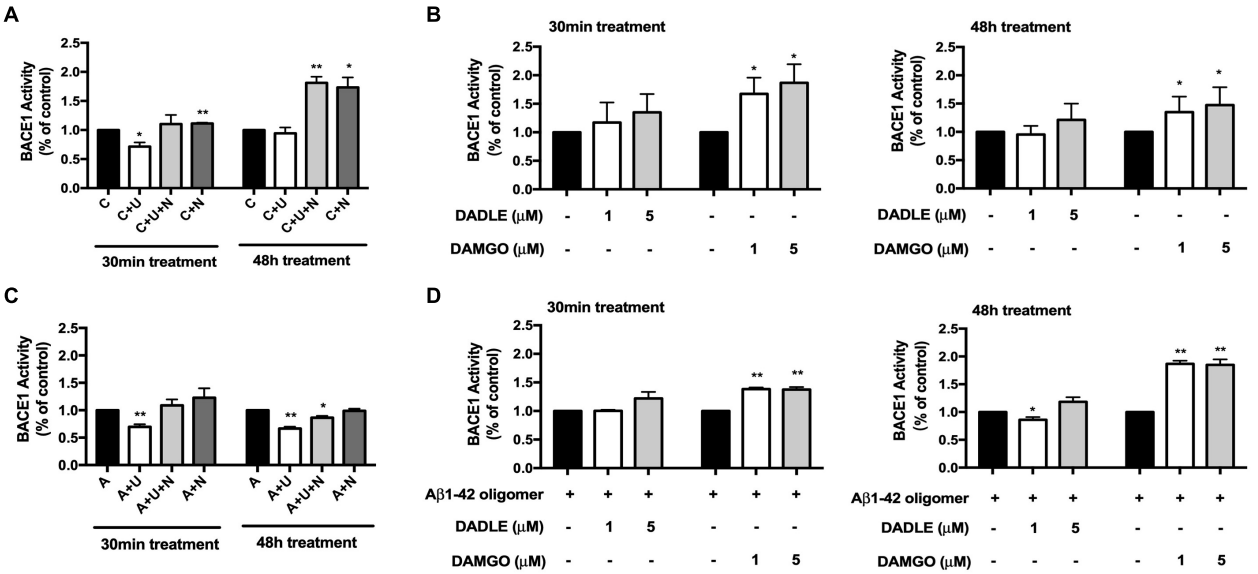

FIGURE 2 | DOR inhibition or MOR activation enhanced BACE1 activities in normal conditions, while DOR activation attenuated BACE1-mediated cleavage activities in Aβ1–42 injury. BACE1 activities were examined at 30 min and 48 h after the drug treatment ($N = 3$ in each group). C: control. C + U: DOR was activated by UFP-512. C + U + N: PC12 cells were treated with UFP-512 plus naltrindole at the same time under normal conditions. C + N: DOR was inhibited by naltrindole. A: PC12 cells were treated with 20 μM Aβ1–42 oligomer to mimic the AD injury. A + U: DOR was activated by UFP-512 under AD injury. A + U + N: PC12 cells were treated with UFP-512 plus naltrindole together under AD injury. A + N: DOR was inhibited by naltrindole under AD injury. **(A)** DOR-mediated regulation of BACE1 activities in the physiological condition. $^*p < 0.05$, $^{**}p < 0.01$ vs. **(C)**. Note that 30-min treatment with DOR agonist UFP-512 significantly decreased BACE1 activities, whereas the application of DOR antagonist naltrindole enhanced BACE1 activities at both 30 min and 48 h after the treatment. **(B)** Effects of DADLE and DAMGO on BACE1 activity in normal conditions. $^*p < 0.05$ vs. **(C)**. Note that DADLE did not induce any significant change in BACE1 activity, while MOR agonist DAMGO significantly upregulated BACE1 activities. **(C)** Effects of DOR agonist UFP-512 and antagonist naltrindole on BACE1 activity under AD injury. The PC12 cells were treated with 20 μM Aβ1–42 oligomer for 48 h to mimic AD injury. UFP-512 and naltrindole were simultaneously or separately applied to these cells for 48 h or at the last 30 min of Aβ1–42 oligomer exposure. $^*p < 0.05$, $^{**}p < 0.01$ vs. **(A)**. Note that DOR activation by UFP-512 significantly reduced BACE1 activities, whereas its inhibition with naltrindole reversed such effect. **(D)** Effects of MOR activation on BACE1 activity under AD injury. The cells with AD injury were exposed to DADLE or DAMGO at 1–5 μM. $^*p < 0.05$, $^{**}p < 0.01$ vs. **(A)**. Note that the BACE1 cleavage activity was significantly reduced by DADLE at 1 μM after 48-h treatment, but largely enhanced by the application of DAMGO at 1 or 5 μM.

for 48 h decreased the levels of Aβ42 in the lysate portion of APPswe SH-SY5Y cells ($p < 0.01$, **Figure 3C**), but not significantly altered the Aβ42 concentration in the medium shed. When exposing to a low concentration of DADLE (1 μM), these cells also showed a significant reduction of Aβ42 production ($p < 0.05$, **Figure 3C**). In contrast, MOR activation using DAMGO induced a gradual increase in Aβ42 in both the cell lysate and medium shed ($p < 0.05$, **Figure 3C**).

These results suggest that the changes in DOR and MOR activities alter both BACE1 activity and Aβ 42 production.

MOR Activation Increased BACE1 mRNA and Protein in Physiologic and AD Conditions, While DOR Activation Down-Regulated BACE1 Expression in AD Injury

Next, we asked if DOR and MOR modulate BACE1 expression at mRNA and/or protein levels. The total RNA were extracted from each treated group, specific BACE1 primers were used to quantify the relative concentrations of target mRNA. Under physiologic conditions, DOR activation led to an unappreciable effect on the level of BACE1 mRNA, while the inhibition of DOR by naltrindole tended to increase BACE1 mRNA level though not significant in our sample size (**Figure 4A**). On the other hand, MOR activation induced a significant increase in BACE1 mRNA (from 100% in the control group to 189.2% in the group treated with 1 μM DAMGO, $p < 0.05$, **Figure 4A**). Similar results were observed with the treatment of DAMGO in the group of Aβ1–42 oligomer injury. DADLE also tended to slightly increase BACE1 mRNA, though the change is not significant in our sample size. We then measured the BACE1 protein expression using Western blotting. In normal conditions, the results were consistent with those of BACE1 mRNA. The application of DOR agonist UFP-512 or DOR antagonist naltrindole caused unappreciable change in BACE1 protein levels, while DADLE caused a slight increase in the level of BACE1 protein under physiological conditions. The 48-h exposure to DAMGO led to a remarkable increase in BACE1 protein in the PC12 cells (from 100% in the control group to 162.7% in the group treated with 1 μM DAMGO, $p < 0.05$, **Figure 4B**). When the cells were exposed to the AD insult, i.e., 48-h treatment of Aβ1–42 oligomer, UFP-512, the specific DOR agonist, significantly decreased BACE1 protein level by 31.2% ($p < 0.05$, **Figure 4B**) whereas the addition of naltrindole reversed the effects induced by UFP-512. The

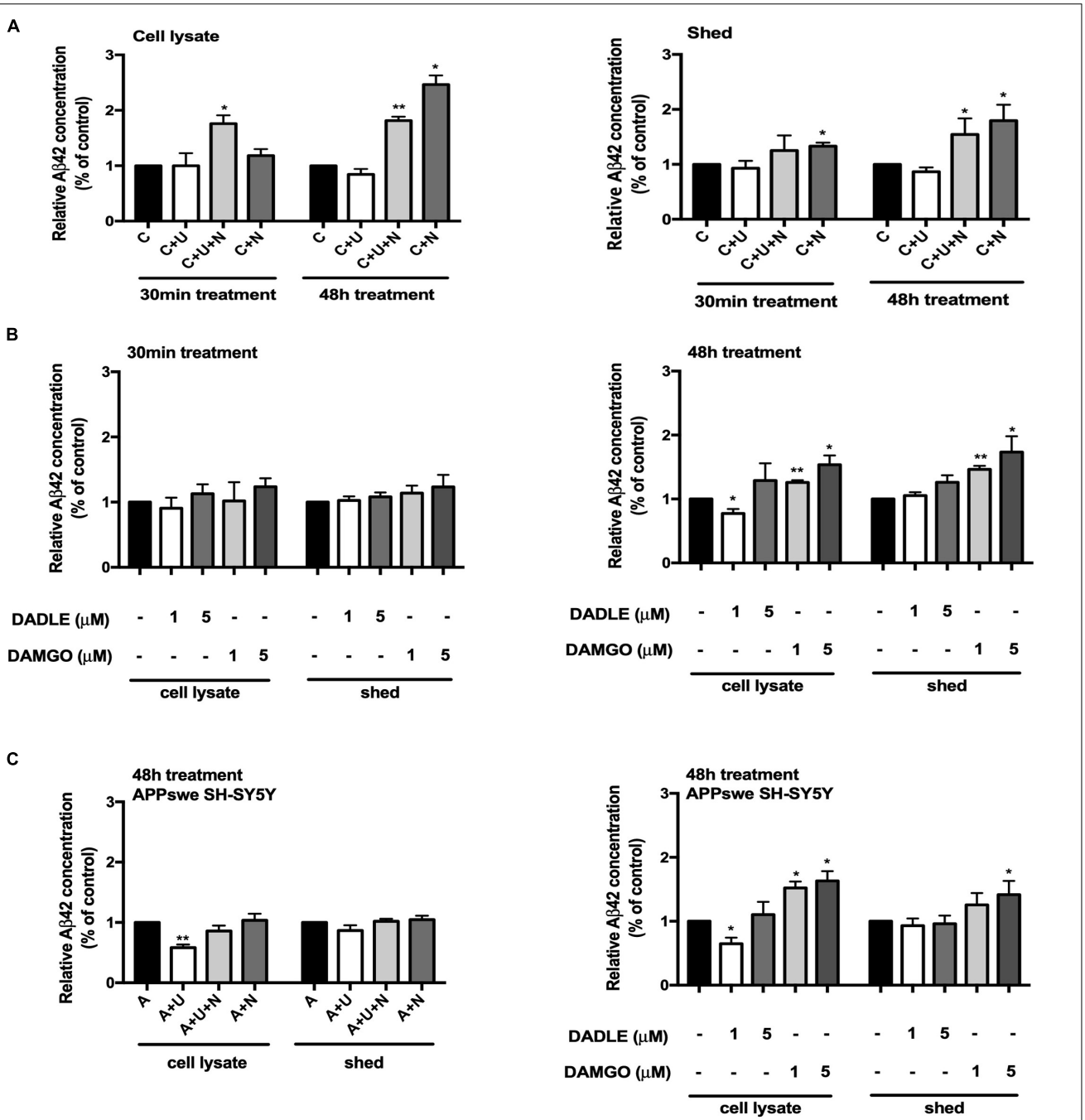

FIGURE 3 | DOR and MOR differently regulated Aβ42 production and release. Aβ42 concentrations were measured in the cell lysate and medium shed ($N = 3$ in each group). **(A)** Effects of DOR activation and inhibition on Aβ42 production and release in PC12 cell line. $^{*}p < 0.05$, $^{**}p < 0.01$ vs. **(C)**. Note that DOR antagonist naltrindole significantly increased the Aβ42 levels in both cell lysate and medium shed though UFP-512 did not induce any significant change. **(B)** DADLE- and DAMGO-induced changes in Aβ42 production and release in PC12 cell line. The PC12 cells were treated with DADLE or DAMGO at 1 and 5 μM. $^{*}p < 0.05$, $^{**}p < 0.01$ vs. **(C)**. Note that 30-min cell exposure to DADLE or DAMGO did not cause a significant change in the level of Aβ42 as well as its release. After prolonging the exposure time to 48 h, the Aβ42 production was slightly reduced by 1 μM DADLE treatment in the cell lysate portion, whereas the application of DAMGO remarkably increased the levels of Aβ42 in both cell lysate and medium shed. **(C)** The activation of DOR and MOR adversely regulated Aβ42 production in APPswe SH-SY5Y cell model. $^{*}p < 0.05$, $^{**}p < 0.01$ vs. **(A)**. Note that the 48-h exposure of UFP-512 to APPswe SH-SY5Y cells largely decreased Aβ42 production in cell lysate portion, but not in medium shed, while the addition of DOR antagonist naltrindole reversed such changes. Low concentration of DADLE also significantly attenuated Aβ42 production in APPswe SH-SY5Y cell model. In the contrast, DAMGO remarkably enhanced Aβ42 production and release with the concentration increased.

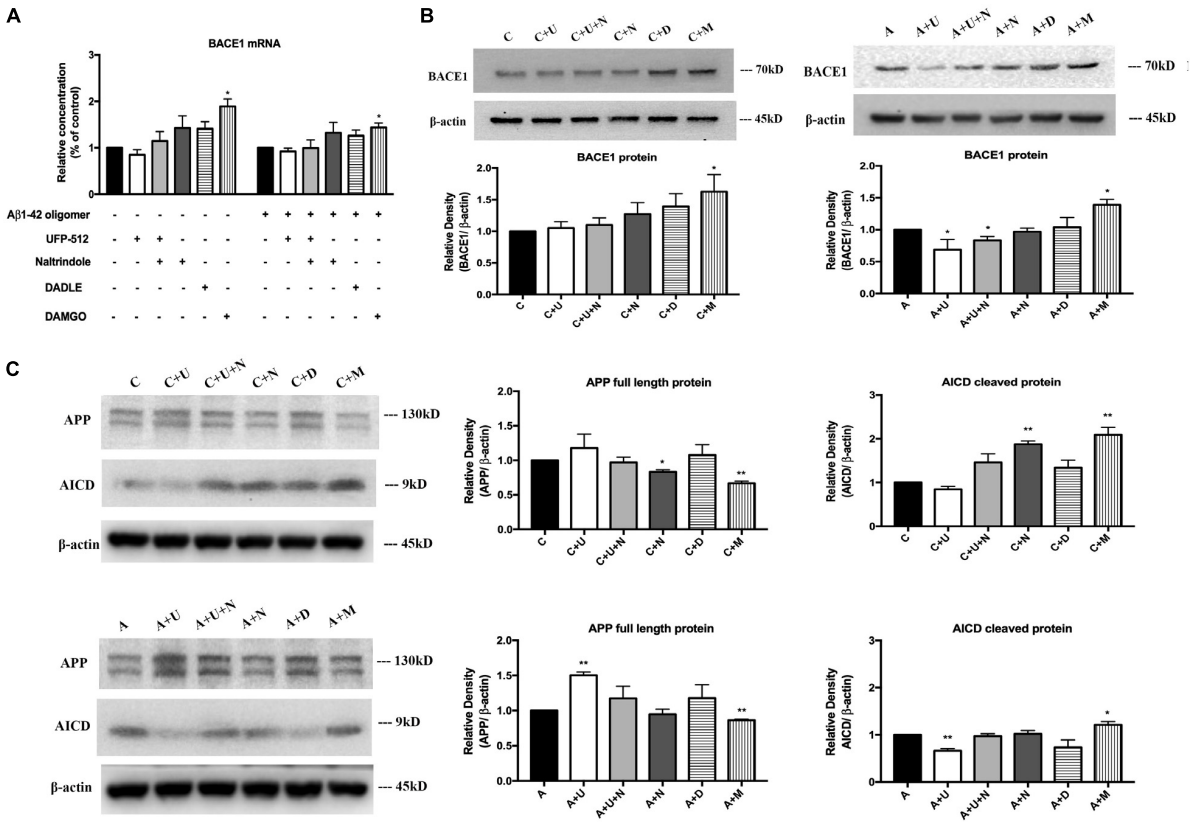

FIGURE 4 | DOR activation down-regulated, but MOR activation up-regulated BACE1 expression for APP processing. BACE1 mRNA and proteins were measured in the PC12 cells in the conditions of normal control and Aβ1–42 injury (48 h). APP processing was evaluated by measuring APP full length protein and AICD. $N = 3$ in each group. $^{*}p < 0.05$, $^{**}p < 0.01$ vs. **(C)** or **(A)**. **(A)** DAMGO-induced alternations in BACE1 mRNA in physiological condition and AD injury. **(B)** DAMGO-induced upregulation of BACE1 protein in both physiological condition and AD injury, while DOR activation specifically attenuated BACE1 expression under AD injury. **(C)** APP cleavage was associated with DOR activation and inhibition, while MOR activation significantly accelerated APP processing. Note that DOR activation had no significant effect on BACE1 mRNA expression though it tended to induce a slight reduction in both physiological and Aβ1–42 oligomer conditions. However, it significantly reduced the level of BACE1 protein in AD condition (Aβ1–42 oligomer exposure), which could be largely reversed by DOR antagonist naltrindole. In contrast, MOR activation with DAMGO significantly increased the expression of both BACE1 mRNA and protein in both physiological and Aβ1–42 oligomer conditions. Consistently, the APP cleavage was seriously interfered by DOR activation in Aβ1–42 oligomer conditions, while DAMGO accelerated APP processing in both physiological and Aβ1–42 oligomer conditions with a significant decrease in APP full length protein and a large increase in AICD, the APP cleavage product.

application of DAMGO largely enhanced BACE1 protein by 39.0% ($p < 0.05$, **Figure 4B**).

To further ascertain the effects of DOR and MOR on BACE1 regulation, we also evaluated the APP cleavage efficiency by measuring the APP full length protein and its cleavage product, AICD. We found that in physiological conditions, 48-h exposure to UFP-512 induced a slight increase in APP protein and a decrease in AICD, while the addition of DOR antagonist naltrindole reversed these change. Treating cells with naltrindole alone or treating cells with 5 μM DAMGO largely accelerated APP processing, with a significant conversion from APP full length protein to the cleavage form ($p < 0.01$, **Figure 4C**). Moreover, we tested the state of APP processing under AD injury and found that DOR activation with UFP-512 remarkably decreased the APP cleavage efficiency ($p < 0.01$, **Figure 4C**). In contrast, the DOR antagonist naltrindole abolished the effect of UFP-512 on APP processing. DAMGO kept promoting APP cleavage with a significant increase in AICD ($p < 0.05$, **Figure 4C**). DADLE showed an inappreciable effect on APP processing both under physiological and Aβ1–42 oligomer conditions.

Taken together, DOR activation reduced BACE1 activities and BACE1 protein especially under AD injury, while MOR activation induced an opposite effect and showed an increase in BACE1 activities as well as BACE1 protein and mRNA. The status of APP processing was differentially changed in response to DOR and MOR activation with a major alteration in BACE1 expression and activity.

DOR Knockdown Enhanced BACE1 Expression and Activities for APP Processing and Increased Aβ 42 Production

To further ascertain the inhibitory regulation of DOR in BACE1 expression and function, we knocked down DOR expression and

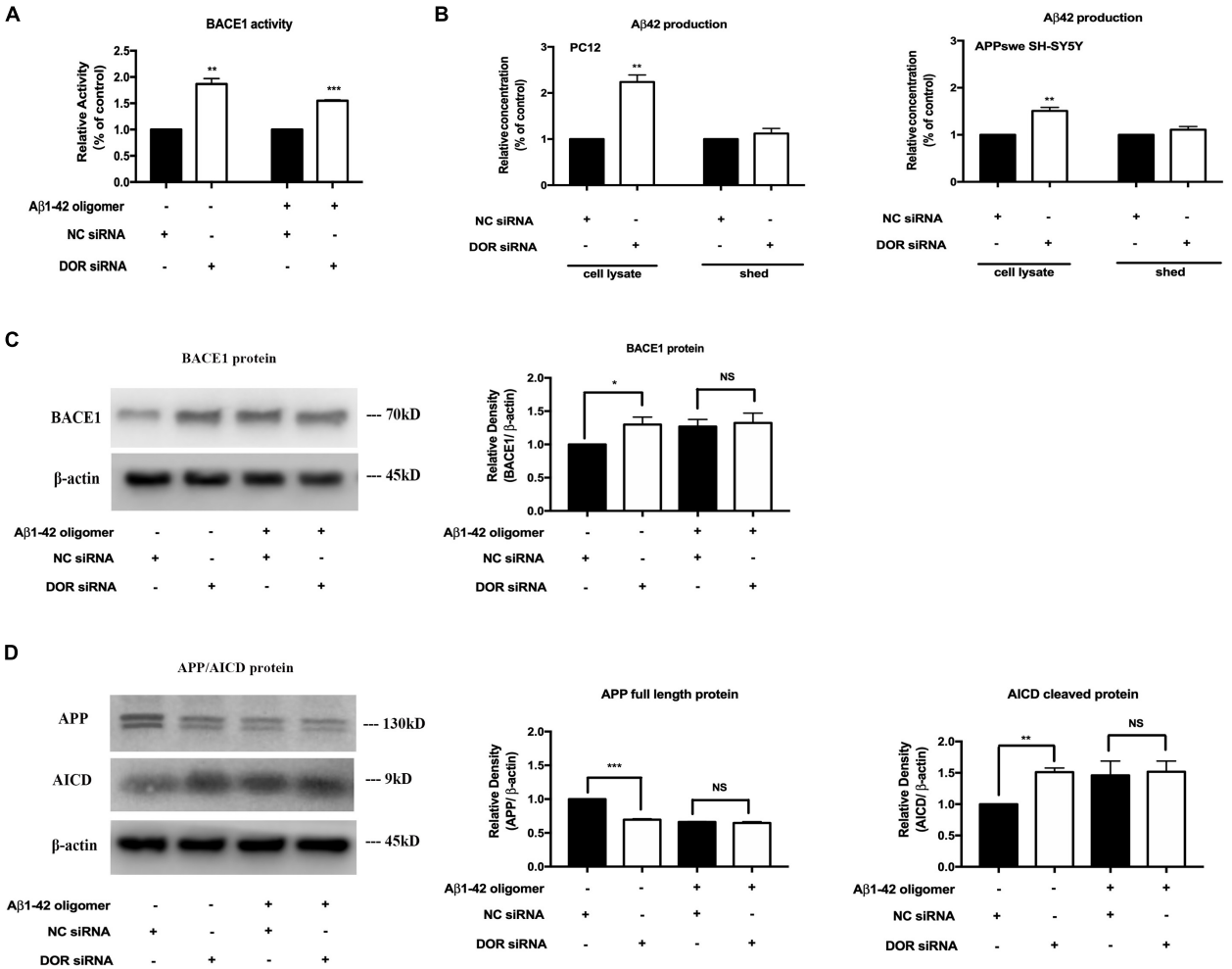

FIGURE 5 | Knocking-down DOR greatly enhanced BACE1 activity and expression for abnormal APP cleavage and contributed to the Aβ42 production. The PC12 cells transfected with DOR siRNA or negative control siRNA were cultured in the conditions of normal control and Aβ1–42 oligomer for 48 h. Similarly, APPswe SH-SY5Y cells were also transfected with human DOR siRNA or negative control siRNA for Aβ42 measurement. $N = 3$ in each group. NS: not significant, $^{*}p < 0.05$ vs. **(C)** or **(A)**; $^{**}p < 0.01$ vs. **(C)** or **(A)**; $^{***}p < 0.001$ vs. **(C)** or **(A)**. **(A)** BACE1 activity before and after DOR knockdown. Note that DOR knockdown significantly increased BACE1 activities in both normal and AD conditions. **(B)** DOR knockdown induced effects on Aβ42 production and release in PC12 and APPswe SH-SY5Y cell models. DOR knockdown caused a sharp increase in the Aβ42 level production in the cell lysate, but not in the medium shed in PC12 cells and the same was true in APPswe SH-SY5Y cell model. **(C)** BACE1 expression was largely increased by DOR knockdown in physiological condition but not under Aβ1–42 injury. Note that DOR knockdown up-regulated BACE1 protein in physiological condition, but did not further increase BACE1 protein in the cells exposed to Aβ1–42 olimoger that already had an increased BACE1 protein. **(D)** DOR knockdown was associated with a rise in APP processing. Note that along with an increase in BACE1 expression after DOR knockdown, the transfection with DOR siRNA also significantly increased APP cleavage in the physiological condition. Aβ1–42 olimoger caused a quick cleavage of APP, which was not further enhanced by DOR knockdown.

then examined the BACE1 expression and activities in the PC12 cells. The cells were transfected with DOR siRNA or negative control siRNA and were cultured in normal condition and that of Aβ1–42 injury. The results showed that the knockdown of DOR significantly increased BACE1 activities both under physiological and AD injury conditions (a significant increase by 86.6% vs. the control group, $p < 0.01$, a rise by 54.8% vs. "A" group after 48-h exposure, $p < 0.001$, **Figure 5A**). Consistently, the DOR knockdown-mediated enhancement of BACE1 activities was associated with a sharp increase in Aβ42 production by 123.9% in cell lysate ($p < 0.01$, **Figure 5B**), but not in medium shed. Moreover, we investigated the effects of DOR knockdown on Aβ42 production in APPswe SH-SY5Y cells. Similar results were obtained by measuring the Aβ42 level in the cell lysate and medium shed portion. DOR knockdown induced a 53.1% increase of Aβ42 production in the cell lysate portion ($p < 0.01$, **Figure 5B**), but did not significantly altered the concentration of Aβ42 in the medium shed.

Furthermore, we examined the BACE1 expression and APP cleavage state in the cells before and after DOR knockdown. We found that DOR knockdown remarkably up-regulated BACE1 expression and promoted APP cleavage in normoxic conditions

(**Figures 5C,D**). In the cells with Aβ1–42 injury, there was already a large increase in BACE1 protein level and an acceleration in APP processing. In such condition, DOR knockdown could not further enhance the level of BACE1 protein and enhance APP cleavage (**Figures 5C,D**).

All these results strongly demonstrated that DOR antagonism or knockdown promoted the destructive APP processing by up-regulating BACE1 expression and activities, suggesting an inhibitory role of DOR in the regulation of BACE1 expression and function.

DISCUSSION

WE made the following major findings in this work: (1) Specifically activating DOR attenuated BACE1 expression and its cleavage activity in the highly differentiated PC12 cells with mimicked AD injury, but not in physiological condition; (2) DOR antagonism induced a significant increase in BACE1 activity for APP cleavage, and contributing to Aβ42 production; (3) Knocking-down DOR increased BACE1 expression and activity for APP processing in physiological condition with an increase in Aβ42 production in both the PC12 cells and APPswe SH-SY5Y cell models, but could not further increase BACE1 expression and APP cleavage in the AD-injured cells that already had an increase in BACE1 expression and accelerated APP processing; and (4) MOR activation aggravated the mimicked AD injury with an upregulation of BACE1 expression and activity as well as APP process. Our data strongly demonstrate that DOR plays an inhibitory role in the regulation of BACE1 expression/activity under Aβ1–42 oligomer induced injury and the opposite is true for the same opioid receptor family member MOR, suggesting DOR is neuroprotective against AD injury.

There are three major classes of opioid receptors: DOR, MOR, and KOR (kappa-opioid receptor) (Xia and Haddad, 1991, 2001; Cai and Ratka, 2012; Xia, 2015). These receptors are differentially altered in the distinct areas of AD patients' brain in term of their expression (Mathieu-Kia et al., 2001; Xia and Haddad, 2001). Several previous reports suggest a relevance between opioid receptors and changes in AD pathology/behaviors, including alterations in cognition, hyperphosphorylated tau, Aβ production, and neuro-inflammation (Meilandt et al., 2008; Cai and Ratka, 2012). Although the specific roles of three opioid receptors in AD are not clear, a few studies (Ni et al., 2006; Teng et al., 2010) suggest that DOR is a "bad guy" favoring AD pathology. To confirm these observations for next mechanistic investigation, we conducted this work with more specific approaches on neuron-like cells.

Unexpectedly, our data draw a different conclusion, i.e., DOR is a "good guy" against AD injury. Having recognized the authenticity of the previous studies, we realized that the major difference between our results and those of others is the difference in methodologies and cell models. DADLE, a relatively non-specific DOR agonist, was used in previous work (Ni et al., 2006; Teng et al., 2010), which might activate MOR (Blurton et al., 1986; Balboni et al., 2002; Xia, 2015). In contrast to the previous work, the present study adopted a potent and specific DOR agonist UFP-512 in neuron-like cells with combinations of DOR antagonism and knockdown for the confirmation of DOR's effect. Indeed, our parallel comparison between DADLE and UFP-512 showed that the former did not induce the same neuroprotection as UFP-512, or even exacerbated the AD injury, which was very likely due to MOR activation, one of DADLE's dual actions. Moreover, the highly differentiated PC12 cells we used in the present study are of neuronal properties and their reactions to DOR signaling and AD injury are closer to the true actions of neurons. To further confirm our conclusions, we also used a stable APP mutant neuronal cell line, APPswe SH-SY5Y cell line that expresses endogenous DOR and BACE1. In sharp contrast, the cells used in the previous studies were HEK293T cells, non-neuronal cells.

Although numerous disrupted processes are interconnected in AD and drive the disease progresses, decades of research in genetic work on AD continue to suggest the accumulation of Aβ in the brain contributes to the loss of synapses, neurodegeneration and cell death (Canter et al., 2016). Since BACE1 is the rate-limiting enzyme in the amyloide cascade, it is of high significance to explore the linkage between opioid receptors and BACE1 regulation. Our novel data well-demonstrated that as compared to DOR, MOR has an entirely different role in the regulation of BACE1 and AD pathology. Its activation greatly enhanced BACE1 expression and activity, thus contributing to abnormal APP processing and increased Aβ42 production, aggravating AD-like injury. Meilandt et al. (2008) previously reported that the irreversible blockade of MOR with β-funaltrexamine ameliorated memory deficits induced by human amyloid precursor protein expressed in transgenic mice. Our results and their observation support each other in terms of MOR's role in AD pathology. Since DADLE is not a specific ligand for DOR (Blurton et al., 1986; Xia, 2015), its side action on MOR is likely the reason for DADLE-induced upregulation of BACE1 expression and activity as shown in the previous reports (Ni et al., 2006; Teng et al., 2010).

BACE1 is a critical target for AD because of its irreplaceable role in the generation of Aβ. However, BACE1 also functions as a housekeeping enzyme and is involved in several processes that are necessary for proper physiology of neuronal tissue (Yan and Vassar, 2014; Barao et al., 2016; Yan, 2017). For instance, BACE1 has been shown to play an important role in synaptic plasticity and development through cleavage of its substrates (Das and Yan, 2017). Germline BACE1 knockout mice have been reported to exhibit reduced survival rate, hypomyelination, seizures, and memory deficits (Laird et al., 2005; Hitt et al., 2010; Hu et al., 2010; Barao et al., 2016). Conditional BACE1 knockout mice showed disrupted organization of axonal pathway in the hippocampus, an important region for learning and memory (Ou-Yang et al., 2018). These results indicate the importance of proper expression and function of BACE1 in the survival and function of nerve cells. It is interesting, but not surprised to us, to note that DOR activation had a marked inhibitory effect on BACE1 expression and activity in the PC12 cells with mimicked AD injury, but not in those under physiological condition. In physiological condition, the cells have sufficient DOR signals to maintain an appropriate level of BACE1 expression and activity.

There is no need for additional DOR signals. The addition of limited amount of exogenous DOR agonist may not necessarily break the balance and alter BACE1 expression and function. In AD injury, however, the balance is disrupted by pathological changes with an over-production of Aβ peptides. Moreover, the redundant Aβ could be quickly degraded in the healthy cells under normal conditions, but not in AD pathogenic cells (Canter et al., 2016; Scheltens et al., 2016). The cells critically need a negative power to suppress such pathological alteration and restore normal functions. At this stage, an increase in DOR activity well meets the need of the injured cells and strengthens the inhibitory force for attenuating BACE1 expression and activity and reduces Aβ peptides. This may be the reason behind the phenomenon seen in this study.

The increased BACE1 expression and activity are one of the characteristic changes in the brain of AD patients (Scheltens et al., 2016; Koelsch, 2017). The overloading of BACE1 accelerates APP cleavage and induces an over-production of Aβ peptides. Based on our present data, there is a possibility that such pathological changes may directly or indirectly relevant to the impairment of DOR expression/function. This is because knocking down DOR alone could remarkably increase BACE1 expression and activity. Also, there is evidence showing that DOR density is largely decreased in the brain of AD patients (Mathieu-Kia et al., 2001). Therefore, we assume that restoring or strengthening DOR signaling is of great help for fighting against the pathology of AD. A strategy for DOR upregulation, either through increasing DOR expression or activity, might rebalance cellular ability to produce Aβ peptides by negatively regulating BACE1 expression and activity. Indeed, we have seen such outcomes after DOR activation in the AD-injured cells with increased BACE1 expression and activity.

The present results revealed that the concentration of Aβ42 was sharply increased by DOR knockdown in the cell lysate, but not in the shed medium of the cells. The experiments performed in APPswe SH-SY5Y showed the similar results, further validating our novel findings. It is difficult for us to explain this phenomenon at this stage. The regulatory mechanisms of Aβ42 production and transportation across the membrane are complicated and not well-understood yet. Multiple physiological and pathological factors may affect the process of Aβ42 transportation across the membrane. It is unknown if DOR knockdown, a major change in cell membrane, caused a structural change in cell membrane, dysfunction of membrane protein interaction and/or blockade of the pathway for intracellular Aβ42 movement. More studies are needed to clarify this issue.

In summary, this work made the first findings with reliable methodologies to clarify the myth about the roles of DOR vs. MOR in the pathology of AD. Specific activation of DOR by UFP-512 was neuroprotective by inhibiting BACE1 expression and activity, attenuating APP cleavage efficiency and reducing Aβ generation in AD condition, which was reversed by DOR antagonism. Interestingly, the same DOR activation did not significantly affect BACE1 expression and activity as well as Aβ production in physiological conditions. The unique role of DOR was further confirmed by the experiments with the reduction of DOR expression. DOR knockdown led to a major increase in BACE1 protein and activity, thus accelerating APP processing and increasing the cellular Aβ level in physiological condition, but did not further interfere the APP cleavage in Aβ oligomer injury. In sharp contrast, MOR activation greatly enhanced BACE1 activity/expression and contributed to AD pathology both in the physiological conditions and Aβ oligomer conditions. Our novel data suggest that DOR acts as an endogenous protector against AD injury by inhibiting BACE1 expression and activity, while the opposite is true for MOR, suggesting a possibility to develop a new strategy against AD by differentially targeting DOR and MOR.

DATA AVAILABILITY STATEMENT

The raw data supporting the conclusions of this article will be made available by the authors, without undue reservation, to any qualified researcher.

AUTHOR CONTRIBUTIONS

YXi initiated the project. YXu and YXi conceived and designed the experiments and wrote the manuscript. YXu performed the experiments. YXu and FZ analyzed the data. YXi, YY, and GB contributed reagents, materials, and analysis tools. YXi and YY supervised the conduct of the work. All authors read and approved the final manuscript.

FUNDING

This work was supported by the Science and Technology Commission of Shanghai Municipality (18401970100), the National Natural Science Foundation of China (81873361), Jiangsu Provincial Special Program of Medical Science (BL2014035), Changzhou Science and Technology Support Program (CE20155060 and CE20165048), Changzhou High-Level Medical Talents Training Project (2016CZBJ006), Changzhou Municipal Commissions of Health and Family Planning Major Scientific and Technological Project (ZD201620).

REFERENCES

Aguila, B., Coulbault, L., Boulouard, M., Leveille, F., Davis, A., Toth, G., et al. (2007). In vitro and in vivo pharmacological profile of UFP-512, a novel selective delta-opioid receptor agonist; correlations between desensitization and tolerance. *Br. J. Pharmacol.* 152, 1312–1324. doi: 10.1038/sj.bjp.0707497

Balboni, G., Salvadori, S., Guerrini, R., Negri, L., Giannini, E., Jinsmaa, Y., et al. (2002). Potent delta-opioid receptor agonists containing the Dmt-Tic pharmacophore. *J. Med. Chem.* 45, 5556–5563. doi: 10.1021/jm020336e

Balducci, C., and Forloni, G. (2014). In vivo application of beta amyloid oligomers: a simple tool to evaluate mechanisms of action and new therapeutic approaches. *Curr. Pharm. Des.* 20, 2491–2505. doi: 10.2174/13816128113199990497

Ballard, C., Gauthier, S., Corbett, A., Brayne, C., Aarsland, D., and Jones, E. (2011). Alzheimer's disease. *Lancet* 377, 1019–1031. doi: 10.1016/S0140-6736(10)61349-9

Barao, S., Moechars, D., Lichtenthaler, S. F., and De Strooper, B. (2016). BACE1 physiological functions may limit its use as therapeutic target for Alzheimer's Disease. *Trends Neurosci.* 39, 158–169. doi: 10.1016/j.tins.2016.01.003

Blurton, P. A., Broadhurst, A. M., Wood, M. D., and Wyllie, M. G. (1986). Is there a common, high-affinity opioid binding site in rat brain? *J. Recept. Res.* 6, 85–93. doi: 10.3109/10799898609073926

Cai, Z., and Ratka, A. (2012). Opioid system and Alzheimer's disease. *Neuromolecular Med.* 14, 91–111. doi: 10.1007/s12017-012-8180-3

Canter, R. G., Penney, J., and Tsai, L. H. (2016). The road to restoring neural circuits for the treatment of Alzheimer's disease. *Nature* 539, 187–196. doi: 10.1038/nature20412

Cao, S., Chao, D., Zhou, H., Balboni, G., and Xia, Y. (2015). A novel mechanism for cytoprotection against hypoxic injury: delta-opioid receptor-mediated increase in Nrf2 translocation. *Br. J. Pharmacol.* 172, 1869–1881. doi: 10.1111/bph.13031

Chao, D., He, X., Yang, Y., Bazzy-Asaad, A., Lazarus, L. H., Balboni, G., et al. (2012). DOR activation inhibits anoxic/ischemic Na+ influx through Na+ channels via PKC mechanisms in the cortex. *Exp. Neurol.* 236, 228–239. doi: 10.1016/j.expneurol.2012.05.006

Cheignon, C., Tomas, M., Bonnefont-Rousselot, D., Faller, P., Hureau, C., and Collin, F. (2018). Oxidative stress and the amyloid beta peptide in Alzheimer's disease. *Redox Biol.* 14, 450–464. doi: 10.1016/j.redox.2017.10.014

Chen, T., Li, J., Chao, D., Sandhu, H. K., Liao, X., Zhao, J., et al. (2014). delta-Opioid receptor activation reduces alpha-synuclein overexpression and oligomer formation induced by MPP(+) and/or hypoxia. *Exp. Neurol.* 255, 127–136. doi: 10.1016/j.expneurol.2014.02.022

Chen, T., Wang, Q., Chao, D., Xia, T. C., Sheng, S., Li, Z. R., et al. (2019). delta-Opioid receptor activation attenuates the oligomer formation induced by hypoxia and/or alpha-synuclein overexpression/mutation through dual signaling pathways. *Mol. Neurobiol.* 56, 3463–3475. doi: 10.1007/s12035-018-1316-1

Das, B., and Yan, R. (2017). Role of BACE1 in Alzheimer's synaptic function. *Transl. Neurodegener.* 6:23. doi: 10.1186/s40035-017-0093-5

Erbs, E., Faget, L., Scherrer, G., Matifas, A., Filliol, D., Vonesch, J. L., et al. (2015). A mu-delta opioid receptor brain atlas reveals neuronal co-occurrence in subcortical networks. *Brain Struct. Funct.* 220, 677–702. doi: 10.1007/s00429-014-0717-9

Geng, D., Kang, L., Su, Y., Jia, J., Ma, J., Li, S., et al. (2013). Protective effects of EphB2 on Abeta1-42 oligomer-induced neurotoxicity and synaptic NMDA receptor signaling in hippocampal neurons. *Neurochem. Int.* 63, 283–290. doi: 10.1016/j.neuint.2013.06.016

He, X., Sandhu, H. K., Yang, Y., Hua, F., Belser, N., Kim, D. H., et al. (2013). Neuroprotection against hypoxia/ischemia: delta-opioid receptor-mediated cellular/molecular events. *Cell Mol. Life Sci.* 70, 2291–2303. doi: 10.1007/s00018-012-1167-2

Hitt, B. D., Jaramillo, T. C., Chetkovich, D. M., and Vassar, R. (2010). BACE1-/- mice exhibit seizure activity that does not correlate with sodium channel level or axonal localization. *Mol. Neurodegener.* 5:31. doi: 10.1186/1750-1326-5-31

Hu, X., Zhou, X., He, W., Yang, J., Xiong, W., Wong, P., et al. (2010). BACE1 deficiency causes altered neuronal activity and neurodegeneration. *J. Neurosci.* 30, 8819–8829. doi: 10.1523/JNEUROSCI.1334-10.2010

Jeong, S. (2017). Molecular and cellular basis of neurodegeneration in Alzheimer's Disease. *Mol. Cells* 40, 613–620. doi: 10.14348/molcells.2017.0096

Koelsch, G. (2017). BACE1 function and inhibition: implications of intervention in the amyloid pathway of Alzheimer's Disease pathology. *Molecules* 22:1723. doi: 10.3390/molecules22101723

Laird, F. M., Cai, H., Savonenko, A. V., Farah, M. H., He, K., Melnikova, T., et al. (2005). BACE1, a major determinant of selective vulnerability of the brain to amyloid-beta amyloidogenesis, is essential for cognitive, emotional, and synaptic functions. *J. Neurosci.* 25, 11693–11709. doi: 10.1523/JNEUROSCI.2766-05.2005

Lee, J. Y., Liska, M. G., Crowley, M., Xu, K., Acosta, S. A., Borlongan, C. V., et al. (2018). Multifaceted effects of delta opioid receptors and DADLE in Diseases of the nervous system. *Curr. Drug Discov. Technol.* 15, 94–108. doi: 10.2174/1570163814666171010114403

Lutz, P. E., and Kieffer, B. L. (2013). Opioid receptors: distinct roles in mood disorders. *Trends Neurosci.* 36, 195–206. doi: 10.1016/j.tins.2012.11.002

Mathieu-Kia, A. M., Fan, L. Q., Kreek, M. J., Simon, E. J., and Hiller, J. M. (2001). Mu-, delta- and kappa-opioid receptor populations are differentially altered in distinct areas of postmortem brains of Alzheimer's disease patients. *Brain Res.* 893, 121–134. doi: 10.1016/s0006-8993(00)03302-3

Meilandt, W. J., Yu, G. Q., Chin, J., Roberson, E. D., Palop, J. J., Wu, T., et al. (2008). Enkephalin elevations contribute to neuronal and behavioral impairments in a transgenic mouse model of Alzheimer's disease. *J. Neurosci.* 28, 5007–5017. doi: 10.1523/JNEUROSCI.0590-08.2008

Morroni, F., Sita, G., Tarozzi, A., Rimondini, R., and Hrelia, P. (2016). Early effects of Abeta1-42 oligomers injection in mice: involvement of PI3K/Akt/GSK3 and MAPK/ERK1/2 pathways. *Behav Brain Res.* 314, 106–115. doi: 10.1016/j.bbr.2016.08.002

Ni, Y., Zhao, X., Bao, G., Zou, L., Teng, L., Wang, Z., et al. (2006). Activation of beta2-adrenergic receptor stimulates gamma-secretase activity and accelerates amyloid plaque formation. *Nat. Med.* 12, 1390–1396. doi: 10.1038/nm1485

Ou-Yang, M. H., Kurz, J. E., Nomura, T., Popovic, J., Rajapaksha, T. W., Dong, H., et al. (2018). Axonal organization defects in the hippocampus of adult conditional BACE1 knockout mice. *Sci. Transl Med.* 10:eaao5620. doi: 10.1126/scitranslmed.aao5620

Pellissier, L. P., Pujol, C. N., Becker, J. A. J., and Le Merrer, J. (2018). Delta opioid receptors: learning and motivation. *Handb. Exp. Pharmacol.* 247, 227–260. doi: 10.1007/164_2016_89

Qiu, J., Chao, D., Sheng, S., Khiati, D., Zhou, X., and Xia, Y. (2019). delta-opioid receptor-nrf-2-mediated inhibition of inflammatory cytokines in neonatal hypoxic-ischemic encephalopathy. *Mol. Neurobiol.* 56, 5229–5240. doi: 10.1007/s12035-018-1452-7

Scheltens, P., Blennow, K., Breteler, M. M., de Strooper, B., Frisoni, G. B., Salloway, S., et al. (2016). Alzheimer's disease. *Lancet* 388, 505–517. doi: 10.1016/S0140-6736(15)01124-1

Selkoe, D. J., and Hardy, J. (2016). The amyloid hypothesis of Alzheimer's disease at 25 years. *EMBO Mol. Med.* 8, 595–608. doi: 10.15252/emmm.201606210

Shrivastava, P., Cabrera, M. A., Chastain, L. G., Boyadjieva, N. I., Jabbar, S., Franklin, T., et al. (2017). Mu-opioid receptor and delta-opioid receptor differentially regulate microglial inflammatory response to control proopiomelanocortin neuronal apoptosis in the hypothalamus: effects of neonatal alcohol. *J. Neuroinflammation* 14:83. doi: 10.1186/s12974-017-0844-3

Teng, L., Zhao, J., Wang, F., Ma, L., and Pei, G. (2010). A GPCR/secretase complex regulates beta- and gamma-secretase specificity for Abeta production and contributes to AD pathogenesis. *Cell Res.* 20, 138–153. doi: 10.1038/cr.2010.3

Wang, D., Tawfik, V. L., Corder, G., Low, S. A., Francois, A., Basbaum, A. I., et al. (2018). Functional divergence of delta and mu opioid receptor organization in CNS pain circuits. *Neuron* 98, 90.e5–108.e5. doi: 10.1016/j.neuron.2018.03.002

Wang, Q., Chao, D., Chen, T., Sandhu, H., and Xia, Y. (2014). delta-Opioid receptors and inflammatory cytokines in hypoxia: differential regulation between glial and neuron-like cells. *Transl. Stroke Res.* 5, 476–483. doi: 10.1007/s12975-014-0342-1

Xia, Y. (ed.) (2015). *Neural Functions of the Delta-Opioid Recepto*. Switzerland: Springer Internatinal Publishing.

Xia, Y., and Haddad, G. G. (1991). Ontogeny and distribution of opioid receptors in the rat brainstem. *Brain Res.* 549, 181–193. doi: 10.1016/0006-8993(91)90457-7

Xia, Y., and Haddad, G. G. (2001). Major difference in the expression of delta- and mu-opioid receptors between turtle and rat brain. *J. Comp. Neurol.* 436, 202–210.

Xu, Y., Zhi, F., Peng, Y., Shao, N., Khiati, D., Balboni, G., et al. (2019). delta-opioid receptor activation attenuates hypoxia/MPP(+)-Induced Downregulation of

PINK1: a novel mechanism of neuroprotection against parkinsonian injury. *Mol. Neurobiol.* 56, 252–266. doi: 10.1007/s12035-018-1043-7

Yan, R. (2017). Physiological functions of the beta-site amyloid precursor protein cleaving enzyme 1 and 2. *Front. Mol. Neurosci.* 10:97. doi: 10.3389/fnmol.2017.00097

Yan, R., and Vassar, R. (2014). Targeting the beta secretase BACE1 for Alzheimer's disease therapy. *Lancet Neurol.* 13, 319–329. doi: 10.1016/S1474-4422(13)70276-X

Yang, Y., Xia, X., Zhang, Y., Wang, Q., Li, L., Luo, G., et al. (2009). delta-Opioid receptor activation attenuates oxidative injury in the ischemic rat brain. *BMC Biol.* 7:55. doi: 10.1186/1741-7007-7-55

Conflict of Interest: The authors declare that the research was conducted in the absence of any commercial or financial relationships that could be construed as a potential conflict of interest.

The handling Editor declared a past co-authorship with one of the authors YXi.

frontiers in Cellular Neuroscience

REVIEW
published: 03 June 2020
doi: 10.3389/fncel.2020.00139

G Protein-Coupled Receptors in the Mammalian Blood-Brain Barrier

Brock R. Pluimer[1,2,3], *Mark Colt*[1,2,3] *and Zhen Zhao*[1,2,3]*

[1]Center for Neurodegeneration and Regeneration, Zilkha Neurogenetic Institute, University of Southern California, Los Angeles, CA, United States, [2]Department of Physiology and Neuroscience, Keck School of Medicine, University of Southern California, Los Angeles, CA, United States, [3]Neuroscience Graduate Program, Keck School of Medicine, University of Southern California, Los Angeles, CA, United States

The mammalian neurovascular unit (NVU) is comprised of neurons, glia, and vascular cells. The NVU is the nexus between the cardiovascular and central nervous system (CNS). The central component of the NVU is the blood-brain barrier (BBB) which consists of a monolayer of tightly connected endothelial cells covered by pericytes and further surrounded by astrocytic endfeet. In addition to preventing the diffusion of toxic species into the CNS, the BBB endothelium serves as a dynamic regulatory system facilitating the transport of molecules from the bloodstream to the brain and vis versa. The structural integrity and transport functions of the BBB are maintained, in part, by an orchestra of membrane receptors and transporters including members of the superfamily of G protein-coupled receptors (GPCRs). Here, we provide an overview of GPCRs known to regulate mammalian BBB structure and function and discuss how dysregulation of these pathways plays a role in various neurodegenerative diseases.

Keywords: neurovascular unit, G-protein coupled receptors, blood-brain barrier, neurodegenerative disease, drug development

OPEN ACCESS

Edited by:
Eng-King Tan, National Neuroscience Institute (NNI), Singapore

Reviewed by:
Ethan Winkler, University of California, San Francisco, United States
Alla B. Salmina, Krasnoyarsk State Medical University named after Prof. V. F. Voino-Yasenetski, Russia

***Correspondence:**
Zhen Zhao
zzhao@usc.edu

***Specialty section**:*
This article was submitted to Non-Neuronal Cells, a section of the journal Frontiers in Cellular Neuroscience

Received: *06 February 2020*
Accepted: *22 April 2020*
Published: *03 June 2020*

Citation:
Pluimer BR, Colt M and Zhao Z (2020) G Protein-Coupled Receptors in the Mammalian Blood-Brain Barrier. Front. Cell. Neurosci. 14:139. doi: 10.3389/fncel.2020.00139

INTRODUCTION

The brain is the most complex mammalian organ. In humans, it consumes roughly 20% of the body's available metabolic energy (Iadecola, 2013; Sweeney et al., 2019). Despite these massive energy requirements, brain cells possess poor energy storage abilities relative to other cell types, so energy sources must be constantly supplied to maintain homeostasis. This immense challenge is overcome by the cerebrovascular system which delivers a constant supply of oxygen, glucose, and other nutrients precisely to brain cells *via* ∼400 miles of blood vessels (Sweeney et al., 2019). Given the sensitivity and indispensability of the central nervous system (CNS), the transfer of molecules between the cerebrovasculature and brain cells must be closely regulated. This is achieved through the coordinated activity of the neurovascular unit (NVU)—a multicellular mosaic comprised of neurons, glia, and vascular cells (Zlokovic, 2011; Zhao et al., 2015). Among its many roles, the NVU regulates the function and structural integrity of the blood-brain barrier (BBB; Sweeney et al., 2019).

The BBB consists of three cell types: endothelial cells separating the brain from the circulating blood, pericytes covering the endothelial wall, and astrocytic endfeet surrounding the pericytes. There are two major routes by which polar solutes cross the BBB—paracellular diffusion and transcytosis. Paracellular diffusion between endothelial cells is regulated by tight junction (TJ) proteins (e.g., claudin-5, occludin, and zonula occludens-1, ZO-1) and adhesion molecules (AM; e.g., vascular cell adhesion molecule, VCAM-1; junctional adhesion molecule, JAM-1),

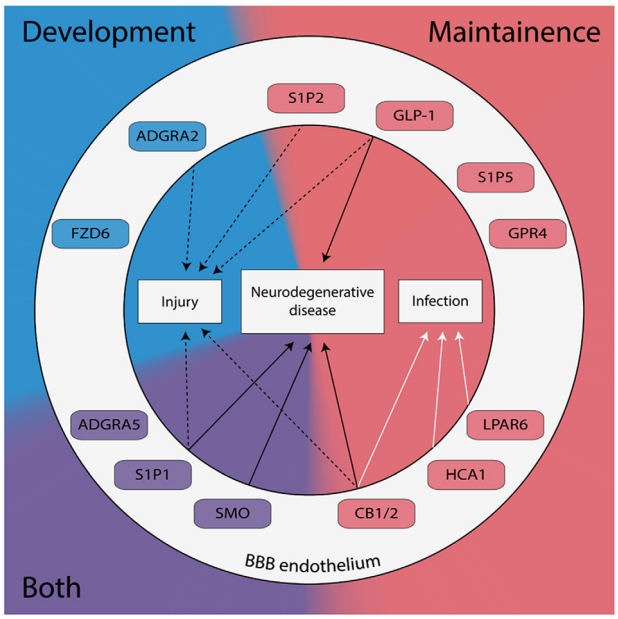

FIGURE 1 | G protein-coupled receptors (GPCRs) expressed in brain endothelial cells are known to regulate the blood-brain barrier (BBB) have been categorized by their role in development (blue), maintenance (red), or both (purple). GPCRs implicated in the pathogenesis of neurodegenerative diseases, neuronal injury, and/or neuronal infection are shown.

which seal the physical barriers between the endothelial cells. Transcytosis of molecules through the BBB endothelium is regulated by a large number of influx and efflux transporters, including glucose transporter 1 (GLUT1), P-glycoprotein (P-gp), and breast cancer resistance protein-1 (BRCP-1). Among hundreds of other membrane proteins, a collection of G protein-coupled receptors (GPCRs) are expressed in the BBB (**Figure 1**). Regulation of the BBB by GPCRs was first demonstrated in *Drosophila melanogaster* (Daneman and Barres, 2005).

GPCRs constitute the largest superfamily of membrane proteins in eukaryotes. Their capacity to bind a wide variety of ligands and diverse signaling profiles position them as ideal candidates for drug-targeted therapies (Stevens et al., 2013; Alexander et al., 2015; Roth et al., 2017). Accordingly, ∼20–30% of marketed drugs currently target GPCRs including opioid analgesics, anti-psychotics, and anti-histamines (Roth et al., 2017). The complex structure of GPCRs underlies their multifaceted pharmacological functionality. GPCRs consist of: (1) an extracellular region which contains the receptor's N-terminus and three extracellular loops; (2) seven hydrophobic transmembrane α-helices; and (3) an intracellular region which contains the C-terminus, three intracellular loops, and an amphipathic helix (Venkatakrishnan et al., 2013). Binding of ligands to the extracellular ligand-binding pocket causes the reorganization of contact residues between the transmembrane helices (Venkatakrishnan et al., 2013). This induces a conformational change of the intracellular region of the GPCR causing it to act as a guanine nucleotide exchange factor (GEF), exchanging GDP for GTP. The GTP-bound intracellular region then phosphorylates/activates downstream signaling effectors including heterotrimeric G proteins, kinases and arrestins. These signal transduction cascades can adjust BBB structure and function by modifying the expression of paracellular TJ and AM and plasma membrane-bound transporters (**Figure 2**). All five mammalian GPCR families classified by the International Union of Pharmacology are expressed in the BBB endothelium—Glutamate, Rhodopsin, Adhesion, Frizzled, and Secretin. Here, we review GPCRs from each of these families that are known to affect the BBB and contextualize their potential link to various neurodegenerative diseases.

RHODOPSIN FAMILY

Sphingosine 1-Phosphate Receptors

Of the >800 GPCRs expressed in humans, 719 belong to the Rhodopsin family (Alexander et al., 2015). In the context of BBB maintenance, the sphingosine 1-phosphate receptors ($S1P_{1-5}$) are among the most well-studied GPCRs. All members of the S1PR subfamily bind sphingosine 1-phosphate (S1P), a lysophospholipid that is highly concentrated in the blood and lymph plasma (Blaho and Hla, 2014). $S1P_1$ is highly expressed in cerebrovascular endothelium and astrocytes compared to other brain cells (Blaho and Hla, 2014; Vanlandewijck et al., 2018). Thirty years ago Hla and Maciag (1990) identified $S1P_1$ as an early gene regulator of endothelial cell differentiation. Since then, its role in cerebrovascular development and maintenance has been extensively studied (Blaho and Hla, 2014). Cannon et al. (2012) isolated rat brain capillaries and showed that $S1P_1$ activity regulates P-gp activity. In this study, treatment with either S1P or FTY720—a prodrug that is metabolized into a nonspecific S1PR agonist—similarly reduced P-gp activity as measured by NBD-CSA {[N-ε(4-nitrobenzofurazan-7-yl)-d-Lys8]-cyclosporin A} accumulation. It is important to note that FTY720 (also known as fingolimod) is currently a highly effective oral treatment for multiple sclerosis (MS; Chun and Hartung, 2010; Cannon et al., 2012). Highlighting the role of $S1P_1$ in this response, co-treatment with an $S1P_1$ selective antagonist (W146) caused P-gp activity to return to basal levels. Although FTY720 treatment did not affect the overall expression of P-gp or TJ permeability to sucrose in *ex vivo* preparations (Cannon et al., 2012), studies in endothelial specific $S1P_1$ knockout mice showed reduced membrane distribution of TJ proteins including claudin-5 and occludin (Yanagida et al., 2017), indicating $S1P_1$ agonists such as FTY720 may exert their therapeutic effects by regulating the distribution of TJ proteins and efflux pumps.

Other members of the S1PR subfamily are expressed throughout the NVU and are known to regulate BBB permeability and function. For example, $S1P_2$ is highly expressed in mouse pericytes, glia, fibroblasts, and endothelial cells (Vanlandewijck et al., 2018). Last year, Cao et al. (2019) demonstrated *in vivo* that antagonism of $S1P_2$ ameliorates oxidative stress-induced cerebrovascular endothelial barrier impairment likely by suppressing p38 mitogen-activated protein kinase (MAPK) and Erk1/2 signaling. In a permanent middle cerebral artery occlusion (pMCAO) model, they found that

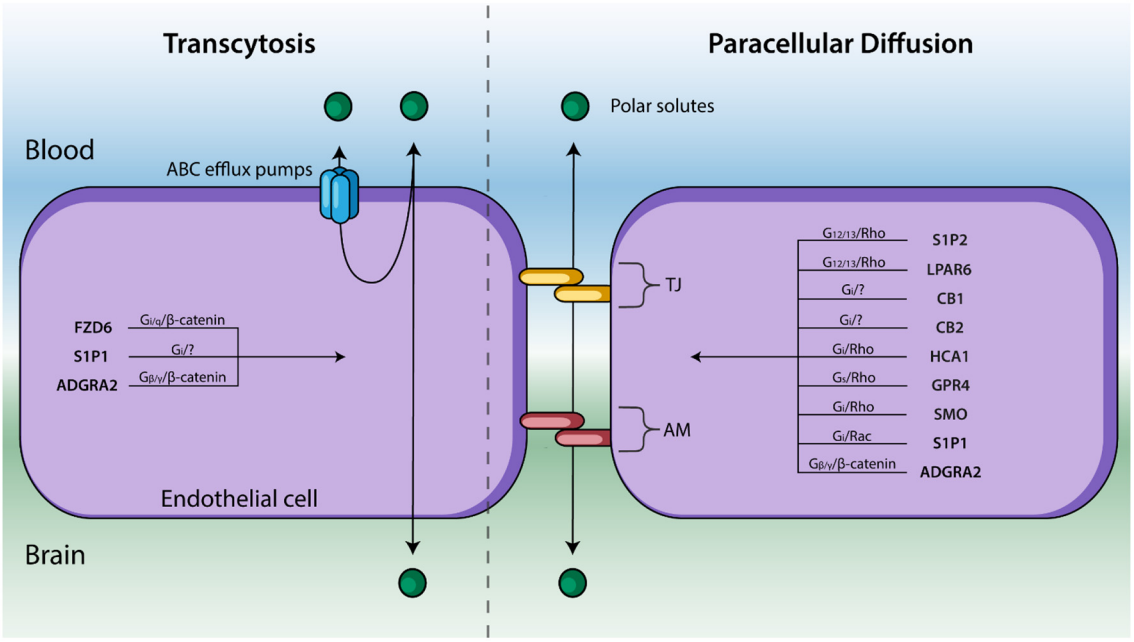

FIGURE 2 | Endothelial cells line cerebral capillaries and form the principal barrier regulating the entry of polar solutes across the BBB. Molecules cross between the blood and brain *via* paracellular diffusion regulated by tight junction (TJ) protein and adhesion molecules (AM) or *via* transcytosis (right). GPCRs are known to regulate these two processes—and their respective signal transduction pathways—are listed above. GPCRs that affect BBB permeability but have not been shown to regulate TJs, AM, nor transcytosis have been excluded.

treatment with an $S1P_2$ specific antagonist reduced BBB leakage after ischemia in mice and prevented depletion of BBB junctional proteins such as VE-cadherin, occludin, claudin-5, and platelet endothelial cell adhesion molecule (PECAM-1). Another S1PR family member, $S1P_5$, is enriched in BBB endothelium and oligodendrocytes (van Doorn et al., 2012; Vanlandewijck et al., 2018). van Doorn et al. (2012) elucidated its role in BBB maintenance. This group treated human brain endothelial cells (hCMEC/D3) with either FTY720P (the active, metabolized form of FTY720) or a selective $S1P_5$ agonist and evaluated the effects on barrier integrity using the electrical cell-substrate impedance sensing assay (ECIS). Treatment with the $S1P_5$ selective agonist improved BBB barrier functions *in vitro*, as indicated by measurements of transendothelial electrical resistance (TEER). Corroborating these findings, administration of a $S1P_5$-specific shRNA resulted in a compromised BBB as determined by ECIS and FITC-dextran staining. This treatment also reduced expression of claudin-5, VE-cadherin, GLUT-1, P-gp, and BCRP-1 expression as determined by qPCR, although the mechanism has not yet been defined (van Doorn et al., 2012).

Lysophosphatidic Acid Receptors

The lysophosphatidic acid receptors (LPAR) are closely related to the S1PR family; both bind lysophosphatidic acid (LPA). LPA was first shown to increase porcine brain endothelial cell permeability *in vitro* by Schulze et al. (2002). They found that while the administration of LPA did not alter the overall expression of TJ proteins, it did induce the recruitment of stress fibers and focal contacts to the TJs, thus destabilizing TJ structures, reducing barrier function, and increasing BBB permeability (Schulze et al., 2002). They hypothesized that modulation of the Rho pathway underlaid these changes, but experimental constraints at the time prevented exploration of this direction. This hypothesis has since been investigated by several groups. Masago et al. (2018) performed RT-PCR analysis of rat brain endothelial cells and found that, of the six LPARs, $LPAR_6$ is most highly expressed in BBB endothelium. The group further investigated the role of $LPAR_6$ in maintaining BBB integrity using *in vitro* and *in vivo* murine fulminant hepatic failure (FHF) models. FHF is known to cause excessive LPA buildup in the brain and is correlated with cerebral edema and a disrupted BBB. Using an *in vitro* BBB model with rat brain endothelial cells, they also revealed that treatment of LPA disrupted the structural integrity of TJ proteins, decreased TEER, and induced endothelial contraction. Transfection with $LPAR_6$-silencing siRNA blocked these effects, as did treatment with a Rho-associated protein kinase inhibitor. Also, recent work done by Kim et al. (2018) in cultured human brain microvascular endothelial cells indicates that $LPAR_1$ and $LPAR_3$ also regulate BBB permeability *via* Rho-mediated cytoskeletal changes. In total, these studies point to the LPA-$LPAR_s$-$G_{12/13}$-Rho pathway as a regulator of TJ stability and BBB permeability.

Psychoactive Compound Receptors

Exogenous psychoactive compounds such as tetrahydrocannabinol (THC), morphine, and lysergic acid

diethylamide (LSD) alter sensory and perceptual experiences by binding to distinct rhodopsin-like GPCRs within the CNS. Interestingly, reports show that the same GPCRs are expressed in BBB endothelium and mediate BBB structure and function. An extensive review from Vendel and de Lange (2014) highlights the cannabinoid receptors CB_1 and CB_2 as mediators of BBB integrity in both healthy, injured, and diseased states including MS and AD. Among the many experiments discussed in their review article is a study conducted by Ramirez et al. (2012), who showed that administration of a CB_2 selective agonist, O-1966, prevented LPS-induced loss of ZO-1, JAM-1 and claudin-5 in brain microvascular endothelial cells. Contrarily, a previous study conducted by Lu et al. (2008) found that pharmacological activation of CB_1 but not CB_2 restored TJ stability in an *in vitro* model of HIV-1 induced BBB disruption. So, evidence points to both CB_1 and CB_2 as regulators of BBB TJ proteins, but the exact underlying mechanism remains unclear (Vendel and de Lange, 2014). Investigating serotonergic GPCRs, Sharma and Dey found that pharmacological blocking of 5-hydroxytryptamine (5-HT) receptors with cyproheptadine increased rat BBB permeability caused by heat stress, as measured by Evans blue extravasation (Sharma and Dey, 1986).

Furthermore, Kousik et al. (2012) extensively reviewed preclinical and clinical data regarding the effects of several psychostimulants on BBB dysfunction. In brief, numerous *in vitro* and rodent BBB models demonstrate that treatment with psychostimulants such as methamphetamine, MDMA, cocaine, and nicotine can induce changes in TJ protein expression, as well as enzymatic pathways regulating BBB cytoskeleton organization (Kousik et al., 2012). But, whether these effects occur directly downstream of GPCRs expressed in the BBB or occur secondarily to neuronal signaling (Carhart-Harris et al., 2012; Nichols, 2016; Ly et al., 2018; Scott and Carhart-Harris, 2019) remains unclear. Indeed, significant resources should be allocated toward uncovering the cerebrovascular effects of these psychoactive compounds.

Hydroxycarboxylic Acid Receptors

Excessive lactic acid production *via* anaerobic glycolysis occurs after several cerebral ailments including ischemia and traumatic brain injury resulting in acidification of the brain. Hydroxycarboxylic acid receptor 1 (HCA1) is a lactate receptor and transporter responsible for regulating the effects of lactic acid and brain metabolism (Lauritzen et al., 2014; Morland et al., 2017). The function of HCA1 was originally identified in adipose tissue where its activation causes downregulation of cAMP and promotes the storage of energy-rich metabolites (Ahmed, 2011). In the CNS, HCA1 (also known as GPR81) is expressed in cerebral endothelial cells, astrocytes, and excitatory synapse membranes (Lauritzen et al., 2014). Pharmacological inhibition of HCA1 in N2A neuroblastomas is associated with reduced neuronal death in an *in vitro* middle cerebral artery occlusion murine model (Shen et al., 2015). Furthermore, Boitsova et al. (2018) generated an *in vitro* rat BMEC model of bacterial meningitis by treating the cells with lipopolysaccharide (LPS). LPS induced loss of HCA1 and TJ protein expression causing increased BBB permeability. These effects were attributed to PKC/RhoA-mediated cytoskeletal rearrangements.

Proton-Sensing Receptors

Ludwig et al. (2003) identified GPR4 as a pH-sensing GPCR. An acidic environment (pH ∼7.1) displaces the receptor's extracellular histidine residues and induces intracellular signaling through the G_s pathway causing cAMP accumulation (Ludwig et al., 2003). Other groups have suggested that GPR4 may also signal through G_q/PLC and G_{13}/Rho pathways to a lesser extent (Tobo et al., 2007; Chen et al., 2011). Single-cell RNA seq analysis and *in situ* hybridization have shown that GPR4 is enriched in mouse brain endothelium (Hosford et al., 2018; Vanlandewijck et al., 2018), and GPR4 knockout mice develop severe cerebrovascular abnormalities and hemorrhages as early as embryonic day E15 (Yang et al., 2007). Experiments performed by Chen et al. (2011) showed that GPR4 activates the cAMP/EPAC pathway in human umbilical vein endothelial cells (HUVECs) at physiological pH range and cAMP/EPAC pathway are known to regulate BBB integrity (Furihata et al., 2015; Lezoualc'h et al., 2016; Ramos and Antonetti, 2017). Therefore, the therapeutic potential of targeting GPR4 in neurodegenerative conditions associated with acidosis should be determined.

FRIZZLED FAMILY

Compared to other GPCR families, the Frizzled family signals unconventionally *via* three transduction pathways—the canonical Wnt pathway, the noncanonical planar cell polarity pathway, and the noncanonical Wnt/calcium pathway. In the canonical pathway, Frizzled receptors complex with low-density lipoprotein receptors (LRPs) which then bind Wnt ligands (Logan and Nusse, 2004; Daneman et al., 2009; Obermeier et al., 2013). Binding of Wnt to the FZD/LRP coreceptor complex induces the stabilization of β-catenin by inhibiting the Axin/APC/GSK-3 breakdown of β-catenin. Consequently, β-catenin accumulation and translocation into the nucleus activates the TCF/LEF-1 complex and regulates gene expression, including those involved in paracellular adhesion and transcytosis (Logan and Nusse, 2004; Daneman et al., 2009; Obermeier et al., 2013). Drugs targeting neuronal Frizzled GPCR pathways have been developed and tested extensively in a variety of neurodegeneration diseases (Kahn, 2014). The application of these drugs likely extends to neurodegenerative diseases of the BBB as well.

Daneman et al. (2009) showed that FZD_4, FZD_6, and FZD_8 are enriched in mouse endothelial cells with FZD_6 being most specifically expressed in the brain ECs. To investigate the role of Wnt/Frizzled/β-catenin in brain angiogenesis, this group used the Cre-Lox recombination to generate endothelial-specific depletion of β-catenin in the entire mouse body. Deficits in angiogenesis were observed only in the CNS of these mice, suggesting the ligands responsible for activating this pathway are exclusive to the developing mouse brain. Further elucidating these pathways, Daneman et al. (2009) determined that Wnt7a and Wnt7b ligands are responsible for angiogenesis in the

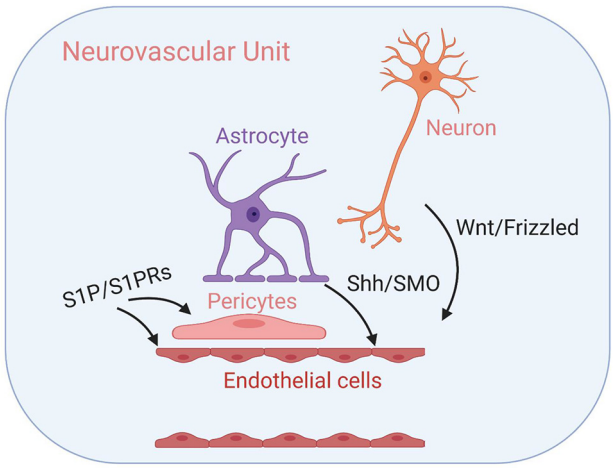

FIGURE 3 | GPCR-mediated intercellular communication within the neurovascular unit (NVU). Intercellular GPCR signaling governs central nervous system (CNS) angiogenesis, BBB formation, and the development of the NVU modules, including well-characterized Wnt/Frizzled signaling between neuronal cells and endothelial cells, Shh/SMO signaling between astrocytes and endothelial cells and sphingosine 1-phosphate (S1P)/S1PR signaling that influence both endothelial cells and pericytes. Their respective signal transduction pathways are listed above. See the main text for details.

forebrain and ventral neural tube, whereas Wnt1, Wnt3, Wnt3a and Wnt4 drive angiogenesis in the dorsal neural tube. Other studies have also revealed that Wnt7a may drive the expression of several BBB transporters including GLUT-1—the indispensable glucose uniporter at BBB (Deng et al., 2014; Winkler et al., 2015).

The GPCR Smoothed (SMO) is abundantly expressed throughout the NVU including the BBB endothelium (Alvarez et al., 2011; Vanlandewijck et al., 2018). SMO activates upon Sonic hedgehog (SHH) binding to Patched-1 (PTCH-1) which inhibits SMO when SHH is not present (Alvarez et al., 2011). In MS patients, dysregulated Hedgehog signaling induces BBB disruption leading to the uncontrolled entry of leukocytes into the CNS causing demyelination. Alvarez et al. (2011) confirmed that Hedgehog signaling *via* SMO regulates BBB integrity. Using human cells, they showed that SHH released from astrocytes binds to PTCH-1 on the BBB endothelium and thus activates SMO causing increased expression of occludin, JAM-1, and VE-cadherin (Alvarez et al., 2011). Treatment with either human recombinant SHH or an SMO specific agonist purmorphamine similarly increased BBB integrity as determined by TEER, whereas pharmacological disruption of SMO signaling resulted in decreased TJ expression.

ADHESION FAMILY

The Adhesion GPCRs (aGPCRs) are the largest family of orphan GPCRs (Alexander et al., 2015). That is, almost all receptors in this 33-member family currently lack an identified endogenous ligand. Adhesion GPCRs are characterized by their long N-terminal region containing various adhesion domains for integrins, cadherins, and selectins and a GPCR proteolytic motif (Paavola and Hall, 2012; Tang et al., 2012; Bassilana et al., 2019). This unique structure distinguishes the aGPCRs from the secretin family and allows for G protein independent signaling (Mizuno and Itoh, 2010). One of the most well-studied aGPCRs is ADGRF5, also known as GPR116, which is known to regulate BBB development and maintenance. ADGRF5 was identified as part of the endothelial core transcriptome in mice (Wallgard et al., 2008). Niaudet et al. (2015) verified that ADGRF5 is specifically, but not exclusively, expressed in mouse brain vascular endothelium. They then generated an ADGRF5 knockout mouse *via* the LacZ-based method, in which exon 4 to exon 21 of the ADGR5 locus was deleted (Niaudet et al., 2015). Twelve month old ADGRF5 deficient mice exhibited a faulty BBB as indicated by the accumulation of 1 kDa Alexa Fluor 555-cadaverine tracer in the brain parenchyma (Niaudet et al., 2015). They also observed increased astrocytic localization near blood vessels in 18-month old knockout mice *via* GFAP staining. However, ADGRF5 deletion did not disrupt vascular patterning nor perfusion, and the leaky BBB was not associated with significant alterations in transcytosis nor adhesion molecule expression, so the precise mechanism by which ADGRF5 regulates BBB permeability remains partly unclear. It has been proposed that ADGRF5 and $S1P_1$ may

TABLE 1 | Summary of exogenous agonists and antagonists targeting blood-brain barrier (BBB), G protein-coupled receptors (GPCRs) mentioned here.

GPCR	Agonist	Antagonist	References
CB_1	WIN-55, 212-2; CP55940; THC		Lu et al. (2008) and Vendel and de Lange (2014)
CB_2	WIN-55, 212-2; O-1966; CP55940; THC		Lu et al. (2008), Ramirez et al. (2012) and Vendel and de Lange (2014)
FZD_6	SAG1.3		Kozielewicz et al. (2020)
GLP-1	Exendin-4	Exendin-3	Fukuda et al. (2016)
GPR4		NE 52-QQ57	Hosford et al. (2018)
HCA1	Lactate; 3, 5-DHBA	3-OBA	Shen et al. (2015)
$5\text{-}HT_{1A}$		Cyproheptadine	Sharma and Dey (1986)
$5\text{-}HT_{2A}$		Cyproheptadine	Sharma and Dey (1986)
$LPAR_1$	Gintonin	Ki16425	Kim et al. (2018)
$LPAR_3$	Gintonin	Ki16425	Kim et al. (2018)
$LPAR_6$	Gintonin		Kim et al. (2018)
$S1P_1$	Fingolimod	W146	Cannon et al. (2012)
$S1P_2$	Fingolimod	JTE013	Cao et al. (2019)
$S1P_5$	Fingolimod; compound 18		Hanessian et al. (2007) and van Doorn et al. (2012)
SMO	Purmorphamine	Cyclopamine; SANT-1; Vismodegib	Alvarez et al. (2011) and Kahn (2014)

function in concert to regulate the BBB (Yanagida et al., 2017). A recent report suggests ADGRF5 may also function as a receptor for fibronectin type III domain-containing proteins (FNDC; Wuensch et al., 2019).

Several studies have identified ADGRA2, also known as GPR124, as a key endothelial regulator of brain-specific angiogenesis (Obermeier et al., 2013; Sweeney et al., 2019). Knockout of ADGRA2 in mice is associated with hemorrhages in the cerebrovasculature in the forebrain and ventral spinal cord and failure of vascular sprouts to grow into embryonic neuroectoderm (Daneman et al., 2009; Kuhnert et al., 2010; Cullen et al., 2011). Interestingly, both Wnt signaling mutants and ADGRA2 knockout mice exhibit reduced Glut-1 expression in the BBB (Daneman et al., 2009). The crosstalk between Wnt and ADGRA2 signaling has since been further explored by several groups. Posokhova et al. (2015) clarified the role of GPR124 in regulating the vascularization of the developing neural tube by showing that ADGRA2 serves as a WNT7A/WNT7B-specific coactivator of β-catenin signaling. Later, Cho et al. (2017) showed that Reck is an essential part of this signaling network as it complexes with ADGRA2 and then interacts with FZD and LRP to stabilize β-catenin and thus promote angiogenesis and barriergenesis. Chang et al. (2017) demonstrate that conditional knockout of ADGRA2 in endothelium induced BBB disruption and microvascular hemorrhage in mouse models of ischemia and glioblastoma. These effects corresponded with reduced Wnt/β-catenin signaling and decreased expression of claudin-5.

Given the unique structural properties of aGPCRs mentioned here, it is likely that many more members of this family are involved in BBB maintenance. The Adhesion GPCR Consortium, a multinational open laboratory network, is investigating such possibilities (Alexander et al., 2015; Krishnan et al., 2016).

SECRETIN FAMILY

The Secretin family contains 15 members and is descended from the Adhesion family (Nordström et al., 2008). The ligands for Secretin GPCRs are moderate length peptides (20–50 residues) possessing C-terminal α-helices that bind to a conserved binding groove in the disulfide-bonded N-terminal domain of the GPCR (Miller and Dong, 2013). Because the cognate ligands for this family are not as useful templates for lead compounds compared to the Rhodopsin family, Secretin GPCRs have been sparsely investigated for pharmacological treatments (Poyner and Hay, 2012). One notable exception to this trend are compounds targeting the glucagon receptors.

Glucagon Receptors

Glucagon-like peptide 1 (GLP-1) is a hormone that signals at the BBB through several GPCRs *via* adenylyl cyclase and cAMP (Drucker et al., 1987; Erbil et al., 2019). Piling evidence in animal models shows GLP-1 and structurally similar GLP-1 receptor (GLP-1R) agonists protect against neurodegenerative and neurovascular diseases including AD and Parkinson's disease (PD; Erbil et al., 2019). Fukuda et al. (2016) constructed an *in vitro* BBB model from rat brain endothelial cells and treated them with GLP-1. This treatment decreased the permeability of sodium fluorescein and increased TEER. These effects were lost when the cells were co-treated with either a GLP-1 receptor antagonist or a PKA inhibitor. Treatment of GLP-1 was also associated with increased expression of occludin and claudin-5 as determined by Western blot analysis. Furthermore, Fukuda et al. (2016) showed that treatment with GLP-1 improved BBB integrity in an *in vitro* model of hyperglycemia. Other studies have implicated GLP-1 analogs as BBB protectors after TBI and ischemia (Hakon et al., 2015; Gonçalves et al., 2016).

GLUTAMATE FAMILY

The glutamate GPCRs include γ-aminobutyric acid B-type receptors ($GABA_B$), calcium-sensing receptors (CaS), metabotropic glutamate (mGlu) receptors, taste receptors (TAS), and numerous orphan receptors. The Glutamate family is distinguished by: (1) a large extracellular domain containing the Venus flytrap module and a cysteine-rich domain, excluding $GABA_B$ receptors; and (2) dimerization of the receptors upon activation by the ligand (Chun et al., 2012). These subfamilies are expressed throughout the mammalian NVU but are not often studied in the context of regulating BBB permeability. Glutamate transport is undoubtedly crucial for BBB endothelium function, but it is facilitated by other protein classes. A subfamily of glutamate family orphans called the retinoic acid-inducible GPCRs ($GPRC5_{A-D}$, also known as $RAIG_{1-4}$) is likely to play a role in BBB development given that retinoic acid is known to induce BBB development, but to the best of our knowledge this subfamily has not been explicitly studied in this context (Mizee et al., 2013; Alexander et al., 2015).

DISCUSSION

GPCR-mediated regulation of the *Drosophila melanogaster* BBB has been well-documented (Daneman and Barres, 2005; Schwabe et al., 2005; Hatan et al., 2011; Hindle and Bainton, 2014). Here, we provide—to the best of our knowledge—the first review summarizing the role of GPCR signaling in regulating mammalian BBB maintenance and development in both healthy and diseased states. While, we have focused on GPCRs expressed in the BBB endothelium, it is important to note that several other GPCRs expressed throughout the NVU has either confirmed or hypothesized functions in regulating BBB structure and function—including rhodopsin-like prostanoid, leukotriene, and proteinase-activated receptors, calcium-sensing receptors of the glutamate family, and corticotropin-releasing factor receptors of the secretin family (Tu et al., 2007; Chiarini et al., 2009; Frankowski et al., 2015; Gelosa et al., 2017; Machida et al., 2017). See **Figure 3** for examples of GPCR-mediated intercellular communication within the NVU.

As human lifespan increases, neurodegenerative diseases will become increasingly prevalent (Gitler et al., 2017). Optimal treatments will need to be easily mass-produced, distributed, and administered e.g., oral drugs. Undeniably,

GPCR targeting offers an auspicious avenue for developing such treatments for diseases of the BBB and CNS broadly (Roth et al., 2017; Bassilana et al., 2019). Since total brain health directly reflects BBB health, by pharmacologically modulating BBB structure and function, researchers and clinicians can, directly and indirectly, treat a variety of NVU disorders through GPCR-dependent mechanisms. In addition to modulating CNS drug transport through the mechanisms described here, the functional selectivity of GPCRs allows for nuanced and varied manipulation of cellular systems that mirror the complexity of diseased states, allowing for more complete treatments. See **Table 1** for a summary of exogenous agonists and antagonists targeting the GPCRs discussed here; visit guidetopharmacology.org for a comprehensive summary. We look forward to a future where the potential of these proteins is fully realized.

AUTHOR CONTRIBUTIONS

BP wrote the manuscript. MC prepared the figures. MC and ZZ edited the manuscript.

FUNDING

This work was supported by National Institutes of Health (NIH) grants R01AG061288, R01NS110687, R03AG063287 and R21AG066090, and BrightFocus Foundation grant A2019218S to ZZ.

REFERENCES

Ahmed, K. (2011). Biological roles and therapeutic potential of hydroxy-carboxylic acid receptors. *Front. Endocrinol.* 2:51. doi: 10.3389/fendo.2011.00051

Alexander, S. P., Davenport, A. P., Kelly, E., Marrion, N., Peters, J. A., Benson, H. E., et al. (2015). The concise guide to PHARMACOLOGY 2015/16: G protein-coupled receptors: the concise guide to PHARMACOLOGY 2015/16: G protein-coupled receptors. *Br. J. Pharmacol.* 172, 5744–5869. doi: 10.1111/bph.13348

Alvarez, J. I., Dodelet-Devillers, A., Kebir, H., Ifergan, I., Fabre, P. J., Terouz, S., et al. (2011). The hedgehog pathway promotes blood-brain barrier integrity and CNS immune quiescence. *Science* 334, 1727–1731. doi: 10.1126/science.1206936

Bassilana, F., Nash, M., and Ludwig, M.-G. (2019). Adhesion G protein-coupled receptors: opportunities for drug discovery. *Nat. Rev. Drug Discov.* 18, 869–884. doi: 10.1038/s41573-019-0039-y

Blaho, V. A., and Hla, T. (2014). An update on the biology of sphingosine 1-phosphate receptors. *J. Lipid Res.* 55, 1596–1608. doi: 10.1194/jlr.r046300

Boitsova, E. B., Morgun, A. V., Osipova, E. D., Pozhilenkova, E. A., Martinova, G. P., Frolova, O. V., et al. (2018). The inhibitory effect of LPS on the expression of GPR81 lactate receptor in blood-brain barrier model *in vitro*. *J. Neuroinflammation* 15:196. doi: 10.1186/s12974-018-1233-2

Cannon, R. E., Peart, J. C., Hawkins, B. T., Campos, C. R., and Miller, D. S. (2012). Targeting blood-brain barrier sphingolipid signaling reduces basal P-glycoprotein activity and improves drug delivery to the brain. *Proc. Natl. Acad. Sci. U S A* 109, 15930–15935. doi: 10.1073/pnas.1203534109

Cao, C., Dai, L., Mu, J., Wang, X., Hong, Y., Zhu, C., et al. (2019). S1PR2 antagonist alleviates oxidative stress-enhanced brain endothelial permeability by attenuating p38 and Erk1/2-dependent cPLA2 phosphorylation. *Cell. Signal.* 53, 151–161. doi: 10.1016/j.cellsig.2018.09.019

Carhart-Harris, R. L., Erritzoe, D., Williams, T., Stone, J. M., Reed, L. J., Colasanti, A., et al. (2012). Neural correlates of the psychedelic state as determined by fMRI studies with psilocybin. *Proc. Natl. Acad. Sci. U S A* 109, 2138–2143. doi: 10.1073/pnas.1119598109

Chang, J., Mancuso, M. R., Maier, C., Liang, X., Yuki, K., Yang, L., et al. (2017). Gpr124 is essential for blood-brain barrier integrity in central nervous system disease. *Nat. Med.* 23, 450–460. doi: 10.1038/nm.4309

Chen, A., Dong, L., Leffler, N. R., Asch, A. S., Witte, O. N., and Yang, L. V. (2011). Activation of GPR4 by acidosis increases endothelial cell adhesion through the cAMP/Epac pathway. *PLoS One* 6:e27586. doi: 10.1371/journal.pone.0027586

Chiarini, A., Pra, I., Marconi, M., Chakravarthy, B., Whitfield, J., and Armato, U. (2009). Calcium-sensing receptor (CaSR) in human brains pathophysiology: roles in late-onset Alzheimers disease (LOAD). *Curr. Pharm. Biotechnol.* 10, 317–326. doi: 10.2174/138920109787847501

Cho, C., Smallwood, P. M., and Nathans, J. (2017). Reck and Gpr124 are essential receptor cofactors for Wnt7a/Wnt7b-specific signaling in mammalian CNS angiogenesis and blood-brain barrier regulation. *Neuron* 95, 1056.e5–1073.e5. doi: 10.1016/j.neuron.2017.07.031

Chun, J., and Hartung, H.-P. (2010). Mechanism of action of oral fingolimod (FTY720) in multiple sclerosis. *Clin. Neuropharmacol.* 33, 91–101. doi: 10.1097/wnf.0b013e3181cbf825

Chun, L., Zhang, W., and Liu, J. (2012). Structure and ligand recognition of class C GPCRs. *Acta Pharmacol. Sin.* 33, 312–323. doi: 10.1038/aps.2011.186

Cullen, M., Elzarrad, M. K., Seaman, S., Zudaire, E., Stevens, J., Yang, M. Y., et al. (2011). GPR124, an orphan G protein-coupled receptor, is required for CNS-specific vascularization and establishment of the blood-brain barrier. *Proc. Natl. Acad. Sci. U S A* 108, 5759–5764. doi: 10.1073/pnas.1017192108

Daneman, R., Agalliu, D., Zhou, L., Kuhnert, F., Kuo, C. J., and Barres, B. A. (2009). Wnt/β-catenin signaling is required for CNS, but not non-CNS, angiogenesis. *Proc. Natl. Acad. Sci. U S A* 106, 641–646. doi: 10.1073/pnas.0805165106

Daneman, R., and Barres, B. A. (2005). The blood-brain barrier— lessons from moody flies. *Cell* 123, 9–12. doi: 10.1016/j.cell.2005.09.017

Deng, D., Xu, C., Sun, P., Wu, J., Yan, C., Hu, M., et al. (2014). Crystal structure of the human glucose transporter GLUT1. *Nature* 510, 121–125. doi: 10.1038/nature13306

Drucker, D. J., Philippe, J., Mojsov, S., Chick, W. L., and Habener, J. F. (1987). Glucagon-like peptide I stimulates insulin gene expression and increases cyclic AMP levels in a rat islet cell line. *Proc. Natl. Acad. Sci. U S A* 84, 3434–3438. doi: 10.1073/pnas.84.10.3434

Erbil, D., Eren, C. Y., Demirel, C., Küçüker, M. U., Solaroğlu, I., and Eser, H. Y. (2019). GLP-1's role in neuroprotection: a systematic review. *Brain Inj.* 33, 734–819. doi: 10.1080/02699052.2019.1587000

Frankowski, J. C., DeMars, K. M., Ahmad, A. S., Hawkins, K. E., Yang, C., Leclerc, J. L., et al. (2015). Detrimental role of the EP1 prostanoid receptor in blood-brain barrier damage following experimental ischemic stroke. *Sci. Rep.* 5:17956. doi: 10.1038/srep17956

Fukuda, S., Nakagawa, S., Tatsumi, R., Morofuji, Y., Takeshita, T., Hayashi, K., et al. (2016). Glucagon-like peptide-1 strengthens the barrier integrity in primary cultures of rat brain endothelial cells under basal and hyperglycemia conditions. *J. Mol. Neurosci.* 59, 211–219. doi: 10.1007/s12031-015-0696-1

Furihata, T., Kawamatsu, S., Ito, R., Saito, K., Suzuki, S., Kishida, S., et al. (2015). Hydrocortisone enhances the barrier properties of HBMEC/ciβ, a brain microvascular endothelial cell line, through mesenchymal-to-endothelial transition-like effects. *Fluids Barriers CNS* 12:7. doi: 10.1186/s12987-015-0003-0

Gelosa, P., Colazzo, F., Tremoli, E., Sironi, L., and Castiglioni, L. (2017). Cysteinyl leukotrienes as potential pharmacological targets for cerebral diseases. *Mediators Inflamm.* 2017:3454212. doi: 10.1155/2017/3454212

Gitler, A. D., Dhillon, P., and Shorter, J. (2017). Neurodegenerative disease: models, mechanisms, and a new hope. *Dis. Model. Mech.* 10, 499–502. doi: 10.1242/dmm.030205

Gonçalves, A., Lin, C.-M., Muthusamy, A., Fontes-Ribeiro, C., Ambrósio, A. F., Abcouwer, S. F., et al. (2016). Protective effect of a GLP-1 analog on ischemia-reperfusion induced blood-retinal barrier breakdown and inflammation. *Invest. Ophthalmol. Vis. Sci.* 57, 2584–2592. doi: 10.1167/iovs.15-19006

Hakon, J., Ruscher, K., Romner, B., and Tomasevic, G. (2015). Preservation of the blood brain barrier and cortical neuronal tissue by liraglutide, a long acting glucagon-like-1 analogue, after experimental traumatic brain injury. *PLoS One* 10:e0120074. doi: 10.1371/journal.pone.0120074

Hanessian, S., Charron, G., Billich, A., and Guerini, D. (2007). Constrained azacyclic analogues of the immunomodulatory agent FTY720 as molecular probes for sphingosine 1-phosphate receptors. *Bioorg. Med. Chem. Lett.* 17, 491–494. doi: 10.1016/j.bmcl.2006.10.014

Hatan, M., Shinder, V., Israeli, D., Schnorrer, F., and Volk, T. (2011). The *Drosophila* blood brain barrier is maintained by GPCR-dependent dynamic actin structures. *J. Cell Biol.* 192, 307–319. doi: 10.1083/jcb.201007095

Hindle, S. J., and Bainton, R. J. (2014). Barrier mechanisms in the *Drosophila* blood-brain barrier. *Front. Neurosci.* 8:414. doi: 10.3389/fnins.2014.00414

Hla, T., and Maciag, T. (1990). An abundant transcript induced in differentiating human endothelial cells encodes a polypeptide with structural similarities to G-protein-coupled receptors. *J. Biol. Chem.* 265, 9308–9313.

Hosford, P. S., Mosienko, V., Kishi, K., Jurisic, G., Seuwen, K., Kinzel, B., et al. (2018). CNS distribution, signalling properties and central effects of G-protein coupled receptor 4. *Neuropharmacology* 138, 381–392. doi: 10.1016/j.neuropharm.2018.06.007

Iadecola, C. (2013). The pathobiology of vascular dementia. *Neuron* 80, 844–866. doi: 10.1016/j.neuron.2013.10.008

Kahn, M. (2014). Can we safely target the WNT pathway? *Nat. Rev. Drug Discov.* 13, 513–532. doi: 10.1038/nrd4233

Kim, D.-G., Jang, M., Choi, S.-H., Kim, H.-J., Jhun, H., Kim, H.-C., et al. (2018). Gintonin, a ginseng-derived exogenous lysophosphatidic acid receptor ligand, enhances blood-brain barrier permeability and brain delivery. *Int. J. Biol. Macromol.* 114, 1325–1337. doi: 10.1016/j.ijbiomac.2018.03.158

Kousik, S. M., Napier, T. C., and Carvey, P. M. (2012). The effects of psychostimulant drugs on blood brain barrier function and neuroinflammation. *Front. Pharmacol.* 3:121. doi: 10.3389/fphar.2012.00121

Kozielewicz, P., Turku, A., Bowin, C.-F., Petersen, J., Valnohova, J., Cañizal, M. C. A., et al. (2020). Structural insight into small molecule action on Frizzleds. *Nat. Commun.* 11:414. doi: 10.1038/s41467-019-14149-3

Krishnan, A., Nijmeijer, S., de Graaf, C., and Schiöth, H. B. (2016). "Classification, nomenclature and structural aspects of adhesion GPCRs," in *Adhesion G Protein-Coupled Receptors*, eds T. Langenhan and T. Schöneberg (Cham: Springer International Publishing), 15–41.

Kuhnert, F., Mancuso, M. R., Shamloo, A., Wang, H.-T., Choksi, V., Florek, M., et al. (2010). Essential regulation of CNS angiogenesis by the orphan G protein-coupled receptor GPR124. *Science* 330, 985–989. doi: 10.1126/science.1196554

Lauritzen, K. H., Morland, C., Puchades, M., Holm-Hansen, S., Hagelin, E. M., Lauritzen, F., et al. (2014). Lactate receptor sites link neurotransmission, neurovascular coupling and brain energy metabolism. *Cereb. Cortex* 24, 2784–2795. doi: 10.1093/cercor/bht136

Lezoualc'h, F., Fazal, L., Laudette, M., and Conte, C. (2016). Cyclic AMP sensor EPAC proteins and their role in cardiovascular function and disease. *Circ. Res.* 118, 881–897. doi: 10.1161/circresaha.115.306529

Logan, C. Y., and Nusse, R. (2004). The Wnt signaling pathway in development and disease. *Annu. Rev. Cell Dev. Biol.* 20, 781–810. doi: 10.1146/annurev.cellbio.20.010403.113126

Lu, T.-S., Avraham, H. K., Seng, S., Tachado, S. D., Koziel, H., Makriyannis, A., et al. (2008). Cannabinoids inhibit HIV-1 Gp120-mediated insults in brain microvascular endothelial cells. *J. Immunol.* 181, 6406–6416. doi: 10.4049/jimmunol.181.9.6406

Ludwig, M.-G., Vanek, M., Guerini, D., Gasser, J. A., Jones, C. E., Junker, U., et al. (2003). Proton-sensing G-protein-coupled receptors. *Nature* 425, 93–98. doi: 10.1038/nature01905

Ly, C., Greb, A. C., Cameron, L. P., Wong, J. M., Barragan, E. V., Wilson, P. C., et al. (2018). Psychedelics promote structural and functional neural plasticity. *Cell Rep.* 23, 3170–3182. doi: 10.1016/j.celrep.2018.05.022

Machida, T., Dohgu, S., Takata, F., Matsumoto, J., Kimura, I., Koga, M., et al. (2017). Role of thrombin-PAR1-PKCθ/δ axis in brain pericytes in thrombin-induced MMP-9 production and blood-brain barrier dysfunction *in vitro*. *Neuroscience* 350, 146–157. doi: 10.1016/j.neuroscience.2017.03.026

Masago, K., Kihara, Y., Yanagida, K., Hamano, F., Nakagawa, S., Niwa, M., et al. (2018). Lysophosphatidic acid receptor, LPA6, regulates endothelial blood-brain barrier function: implication for hepatic encephalopathy. *Biochem. Biophys. Res. Commun.* 501, 1048–1054. doi: 10.1016/j.bbrc.2018.05.106

Miller, L. J., and Dong, M. (2013). The orthosteric agonist-binding pocket in the prototypic class B G-protein-coupled secretin receptor. *Biochem. Soc. Trans.* 41, 154–158. doi: 10.1042/bst20120204

Mizee, M. R., Wooldrik, D., Lakeman, K. A. M., van het Hof, B., Drexhage, J. A. R., Geerts, D., et al. (2013). Retinoic acid induces blood-brain barrier development. *J. Neurosci.* 33, 1660–1671. doi: 10.1523/JNEUROSCI.1338-12.2013

Mizuno, N., and Itoh, H. (2010). "Signal transduction mediated through adhesion-GPCRs," in *Adhesion-GPCRs*, eds S. Yona and M. Stacey (Boston, MA: Springer US), 157–166.

Morland, C., Andersson, K. A., Haugen, Ø. P., Hadzic, A., Kleppa, L., Gille, A., et al. (2017). Exercise induces cerebral VEGF and angiogenesis *via* the lactate receptor HCAR1. *Nat. Commun.* 8:15557. doi: 10.1038/ncomms15557

Niaudet, C., Hofmann, J. J., Mäe, M. A., Jung, B., Gaengel, K., Vanlandewijck, M., et al. (2015). Gpr116 receptor regulates distinctive functions in pneumocytes and vascular endothelium. *PLoS One* 10:e0137949. doi: 10.1371/journal.pone.0137949

Nichols, D. E. (2016). Psychedelics. *Pharmacol. Rev.* 68, 264–355. doi: 10.1124/pr.115.011478

Nordström, K. J. V., Lagerstrom, M. C., Waller, L. M. J., Fredriksson, R., and Schioth, H. B. (2008). The secretin GPCRs descended from the family of adhesion GPCRs. *Mol. Biol. Evol.* 26, 71–84. doi: 10.1093/molbev/msn228

Obermeier, B., Daneman, R., and Ransohoff, R. M. (2013). Development, maintenance and disruption of the blood-brain barrier. *Nat. Med.* 19, 1584–1596. doi: 10.1038/nm.3407

Paavola, K. J., and Hall, R. A. (2012). Adhesion G protein-coupled receptors: signaling, pharmacology and mechanisms of activation. *Mol. Pharmacol.* 82, 777–783. doi: 10.1124/mol.112.080309

Posokhova, E., Shukla, A., Seaman, S., Volate, S., Hilton, M. B., Wu, B., et al. (2015). GPR124 functions as a WNT7-specific coactivator of canonical β-catenin signaling. *Cell Rep.* 10, 123–130. doi: 10.1016/j.celrep.2014.12.020

Poyner, D. R., and Hay, D. L. (2012). Secretin family (Class B) G protein-coupled receptors - from molecular to clinical perspectives: B GPCRs. *Br. J. Pharmacol.* 166, 1–3. doi: 10.1111/j.1476-5381.2011.01810.x

Ramirez, S. H., Hasko, J., Skuba, A., Fan, S., Dykstra, H., McCormick, R., et al. (2012). Activation of cannabinoid receptor 2 attenuates leukocyte-endothelial cell interactions and blood-brain barrier dysfunction under inflammatory conditions. *J. Neurosci.* 32, 4004–4016. doi: 10.1523/JNEUROSCI.4628-11.2012

Ramos, C. J., and Antonetti, D. A. (2017). The role of small GTPases and EPAC-Rap signaling in the regulation of the blood-brain and blood-retinal barriers. *Tissue Barriers* 5:e1339768. doi: 10.1080/21688370.2017.1339768

Roth, B., Irwin, J. J., and Shoichet, B. K. (2017). Discovery of new GPCR ligands to illuminate new biology. *Nat. Chem. Biol.* 13, 1143–1151. doi: 10.1038/nchembio.2490

Schulze, C., Smales, C., Rubin, L. L., and Staddon, J. M. (2002). Lysophosphatidic acid increases tight junction permeability in cultured brain endothelial cells. *J. Neurochem.* 68, 991–1000. doi: 10.1046/j.1471-4159.1997.68030991.x

Schwabe, T., Bainton, R. J., Fetter, R. D., Heberlein, U., and Gaul, U. (2005). GPCR signaling is required for blood-brain barrier formation in *Drosophila*. *Cell* 123, 133–144. doi: 10.1016/j.cell.2005.08.037

Scott, G., and Carhart-Harris, R. L. (2019). Psychedelics as a treatment for disorders of consciousness. *Neurosci. Conscious.* 2019:niz003. doi: 10.1093/nc/niz003

Sharma, H., and Dey, P. (1986). Probable involvement of 5-hydroxytryptamine in increased permeability of blood-brain barrier under heat stress in young rats. *Neuropharmacology* 25, 161–167. doi: 10.1016/0028-3908(86)90037-7

Shen, Z., Jiang, L., Yuan, Y., Deng, T., Zheng, Y.-R., Zhao, Y.-Y., et al. (2015). Inhibition of G protein-coupled receptor 81 (GPR81) protects against ischemic brain injury. *CNS Neurosci. Ther.* 21, 271–279. doi: 10.1111/cns.12362

Stevens, R. C., Cherezov, V., Katritch, V., Abagyan, R., Kuhn, P., Rosen, H., et al. (2013). The GPCR Network: a large-scale collaboration to determine human GPCR structure and function. *Nat. Rev. Drug Discov.* 12, 25–34. doi: 10.1038/nrd3859

Sweeney, M. D., Zhao, Z., Montagne, A., Nelson, A. R., and Zlokovic, B. V. (2019). Blood-brain barrier: from physiology to disease and back. *Physiol. Rev.* 99, 21–78. doi: 10.1152/physrev.00050.2017

Tang, X., Wang, Y., Li, D., Luo, J., and Liu, M. (2012). Orphan G protein-coupled receptors (GPCRs): biological functions and potential drug targets. *Acta Pharmacol. Sin.* 33, 363–371. doi: 10.1038/aps.2011.210

Tobo, M., Tomura, H., Mogi, C., Wang, J., Liu, J., Komachi, M., et al. (2007). Previously postulated "ligand-independent" signaling of GPR4 is mediated through proton-sensing mechanisms. *Cell. Signal.* 19, 1745–1753. doi: 10.1016/j.cellsig.2007.03.009

Tu, H., Kastin, A. J., and Pan, W. (2007). Corticotropin-releasing hormone receptor (CRHR)1 and CRHR2 are both trafficking and signaling receptors for urocortin. *Mol. Endocrinol.* 21, 700–711. doi: 10.1210/me.2005-0503

van Doorn, R., Lopes Pinheiro, M. A., Kooij, G., Lakeman, K., van het Hof, B., van der Pol, S. M., et al. (2012). Sphingosine 1-phosphate receptor 5 mediates the immune quiescence of the human brain endothelial barrier. *J. Neuroinflammation* 9:133. doi: 10.1186/1742-2094-9-133

Vanlandewijck, M., He, L., Mäe, M. A., Andrae, J., Ando, K., Del Gaudio, F., et al. (2018). A molecular atlas of cell types and zonation in the brain vasculature. *Nature* 554, 475–480. doi: 10.1038/nature25739

Vendel, E., and de Lange, E. C. M. (2014). Functions of the CB1 and CB2 receptors in neuroprotection at the level of the blood-brain barrier. *Neuromolecular Med.* 16, 620–642. doi: 10.1007/s12017-014-8314-x

Venkatakrishnan, A. J., Deupi, X., Lebon, G., Tate, C. G., Schertler, G. F., and Babu, M. M. (2013). Molecular signatures of G-protein-coupled receptors. *Nature* 494, 185–194. doi: 10.1038/nature11896

Wallgard, E., Larsson, E., He, L., Hellström, M., Armulik, A., Nisancioglu, M. H., et al. (2008). Identification of a core set of 58 gene transcripts with broad and specific expression in the microvasculature. *Arterioscler. Thromb. Vasc. Biol.* 28, 1469–1476. doi: 10.1161/atvbaha.108.165738

Winkler, E. A., Nishida, Y., Sagare, A. P., Rege, S. V., Bell, R. D., Perlmutter, D., et al. (2015). GLUT1 reductions exacerbate Alzheimer's disease vasculo-neuronal dysfunction and degeneration. *Nat. Neurosci.* 18, 521–530. doi: 10.1038/nn.3966

Wuensch, T., Wizenty, J., Quint, J., Spitz, W., Bosma, M., Becker, O., et al. (2019). Expression analysis of fibronectin type III domain-containing (FNDC) genes in inflammatory bowel disease and colorectal cancer. *Gastroenterol. Res. Pract.* 2019:3784172. doi: 10.1155/2019/3784172

Yanagida, K., Liu, C. H., Faraco, G., Galvani, S., Smith, H. K., Burg, N., et al. (2017). Size-selective opening of the blood-brain barrier by targeting endothelial sphingosine 1-phosphate receptor 1. *Proc. Natl. Acad. Sci. U S A* 114, 4531–4536. doi: 10.1073/pnas.1618659114

Yang, L. V., Radu, C. G., Roy, M., Lee, S., McLaughlin, J., Teitell, M. A., et al. (2007). Vascular abnormalities in mice deficient for the G protein-coupled receptor GPR4 that functions as a pH sensor. *Mol. Cell. Biol.* 27, 1334–1347. doi: 10.1128/mcb.01909-06

Zhao, Z., Nelson, A. R., Betsholtz, C., and Zlokovic, B. V. (2015). Establishment and dysfunction of the blood-brain barrier. *Cell* 163, 1064–1078. doi: 10.1016/j.cell.2015.10.067

Zlokovic, B. V. (2011). Neurovascular pathways to neurodegeneration in Alzheimer's disease and other disorders. *Nat. Rev. Neurosci.* 12, 723–738. doi: 10.1038/nrn3114

Conflict of Interest: The authors declare that the research was conducted in the absence of any commercial or financial relationships that could be construed as a potential conflict of interest.

frontiers in Aging Neuroscience

ORIGINAL RESEARCH
published: 05 June 2020
doi: 10.3389/fnagi.2020.00161

Dilated Perivascular Space in the Midbrain May Reflect Dopamine Neuronal Degeneration in Parkinson's Disease

Yanxuan Li[1], Zili Zhu[1], Jie Chen[1], Minming Zhang[2], Yunjun Yang[1] and Peiyu Huang[1,2]**

[1]*Department of Radiology, The First Affiliated Hospital of Wenzhou Medical University, Wenzhou, China,* [2]*Department of Radiology, The Second Affiliated Hospital, Zhejiang University School of Medicine, Hangzhou, China*

Background: The imbalance between the production and clearance of alpha-synuclein and its consequent accumulation plays a pivotal role in the pathogenesis of Parkinson's disease (PD). The diminished clearance of alpha-synuclein may be partly attributable to impaired interstitial fluid, which can be reflected by the extent of dilated perivascular space (dPVS). We studied the association between dPVS and dopamine neuronal degeneration.

Method: We screened 71 healthy controls (HCs) and 88 patients from the Parkinson Progression Markers Initiative (PPMI) database. The dPVS was evaluated in different brain regions on axial T2-weighted images, and dopamine transporter (DAT) imaging data was used to elucidate the extent of dopaminergic neuronal degeneration. Patients with PD were further divided into two groups (SN + PD and SN − PD groups) according to whether dPVS was observed in the substantia nigra (SN). DAT uptake values and clinical scales were compared between the patients with PD and HCs and against dPVS scores. We also investigated the correlation between baseline dPVS scores and longitudinal DAT changes.

Results: Relative to the HCs, patients with PD had more dPVS in the SN and basal ganglia (BG). PD patients with dPVS in the SN region exhibited greater expression of tau protein in cerebrospinal fluid ($P = 0.038$) and a trend towards decreased DAT binding ($P = 0.086$) relative to those without SN dPVS. No correlations were found between dPVS scores and DAT uptake values or between dPVS scores and longitudinal DAT changes.

Conclusion: The dPVS in the SN of patients with PD may reflect the degeneration of dopaminergic neurons.

Keywords: perivascular space, Parkinson's disease, dopamine transporter imaging, tau protein, midbrain, basal ganglia

OPEN ACCESS

Edited by:
Eng-King Tan,
National Neuroscience Institute (NNI), Singapore

Reviewed by:
Richard Camicioli,
University of Alberta, Canada
Uwe Walter,
University Hospital Rostock, Germany

****Correspondence:***
Yunjun Yang
yyjunjim@163.com
Peiyu Huang
huangpy@zju.edu.cn

Received: *15 February 2020*
Accepted: *11 May 2020*
Published: *05 June 2020*

Citation:
Li Y, Zhu Z, Chen J, Zhang M, Yang Y and Huang P (2020) Dilated Perivascular Space in the Midbrain May Reflect Dopamine Neuronal Degeneration in Parkinson's Disease. Front. Aging Neurosci. 12:161. doi: 10.3389/fnagi.2020.00161

INTRODUCTION

The second-most common neurodegenerative disease among older adults, Parkinson's disease (PD) manifests as various motor and non-motor symptoms primarily attributable to the excessive accumulation of toxic alpha-synuclein and a series of secondary alterations (de Lau and Breteler, 2006; Suchowersky et al., 2006; Narayanan et al., 2013; Chung et al., 2016; Huang et al., 2016; Sundaram et al., 2019; Li et al., 2020). Hence, the imbalance between the production and clearance of alpha-synuclein (Bobela et al., 2015; Abeliovich and Gitler, 2016) plays a pivotal role in PD development (Webb et al., 2003; Ebrahimi-Fakhari et al., 2011; Maiti et al., 2017).

Several studies have shown that diminished drainage mediated by the brain glymphatic system might contribute to the impaired extracellular clearance of soluble alpha-synuclein and aggravate PD pathology. Recently, Zou et al. (2019) ligated deep cervical lymph nodes in A53T mice at 18 weeks of age and thus blocked meningeal lymphatic drainage. Six weeks later, decreases in cerebrospinal fluid flow were observed along with depositions of alpha-synuclein and losses of astroglial aquaporin-4 (AQP-4) in the substantia nigra (SN). These findings strongly suggest that the dysfunction of the glymphatic system aggravates the accumulation of alpha-synuclein and further accelerates the loss of dopaminergic neurons and motor functionality thereby.

Imaging studies of the human brain also support this theory. Detectable with T2-weighted magnetic resonance (MR) images, perivascular spaces—an important component of the brain glymphatic system that functions as a conduit to remove soluble proteins and toxic metabolites from the brain (Aspelund et al., 2015; Mezey and Palkovits, 2015; Ramirez et al., 2015; Louveau et al., 2016)—dilate to restore drainage functionality following the stacking of metabolite wastes and cell debris therein (Mestre et al., 2017).

Prior research has found that dilated perivascular spaces (dPVS) in the basal ganglia (BG) might be related to cognitive decline and tremor in patients with PD (Park et al., 2019; Shibata et al., 2019; Wan et al., 2019). However, other research has failed to identify such associations (Kim et al., 2018), and their veracity thus remains uncertain. Importantly, whether dPVS in the midbrain (Elster and Richardson, 1991; Papayannis et al., 2003; Ferrer et al., 2017) are associated with the loss of dopaminergic neurons in the SN of patients with PD remains unclear.

The present study sought to ascertain whether dPVS is associated with the degeneration of the midbrain dopaminergic systems and the clinical symptoms of patients with PD. By analyzing the correlation between dPVS scores (evaluated on T2-weighted MR images) and dopamine transporter (DAT) uptake values obtained from both cross-sectional and longitudinal data, as well as the correlation between PVS scores and motor/non-motor scales, we explore the hypothesis that dPVS is related to dopamine neuron damage by diminishing DAT uptake and exacerbating clinical symptoms.

MATERIALS AND METHODS

Participants

Participant data were obtained from the Parkinson Progression Markers Initiative (PPMI) database[1]. The PPMI study was approved by the institutional review board of all participating sites and written informed consent was obtained from all participants before their registration in the study. Since data obtained from the DAT scans were most complete at the V04 and V06 time points, we used V04 as the baseline and V06 as the 1-year follow-up. A total of 96 patients with PD were included; both baseline and follow-up T1- and T2-weighted MR images, as well as DAT scan data, were available for all of them. Due to the T2 images of eight patients have been blurry, they were excluded from the study. Nighty-two healthy controls (HCs; age range, 52–70 years) with T1- and T2-weighted MR images and clinical scale records were collected from the PPMI database. Because the T1- or T2-weighted MR images of 21 HCs were blurred or of poor quality, they were excluded from the study (**Figure 1**). The MR images of all participants were obtained from multiple research centers using the ADNI MRI protocol, a detailed report of which is available from the ADNI website[2].

Assessment

Clinical evaluations and DAT results at baseline and 1-year follow-up were available for all 88 patients with PD; data concerning cerebral spinal fluid (CSF) markers [Aβ 42, total tau, phosphorylated tau 181P (p-Tau181P) and Alpha-synuclein] and systolic and diastolic blood pressure in the supine position were only collected in this population at baseline. Clinical scale scores and the expression of CSF markers, but not DAT results, were available for the 71 HCs. All examinations and assessments are reported in detail at http://www.ppmi-info.org/study-design. The motor symptoms of patients were assessed with Unified Parkinson's Disease Rating Scale Part III (UPDRS-III). The following clinical scales were further used in this study: Geriatric Depression Scale (GDS), Epworth Sleepiness Scale (ESS), and Montreal Cognitive Assessment (MoCA).

The mean of the bilateral DAT uptake values (Ave-DAT) was calculated for the caudate and putamen nuclei for further analysis. The dPVS were evaluated on axial T2-weighted images according to the Standards for Reporting Vascular Changes on Neuroimaging criteria (Wardlaw et al., 2013) by two trained neuroradiologists (YL and ZZ, with 4 and 2 years of experience, respectively) blinded to the patients' clinical information and the other evaluator's scoring. Briefly, the dPVS were defined as structures situated perpendicular to the surface of the brain in the direction of perforating vessels that evinced cerebrospinal fluid signals and presented sharp edges of less than 3 mm in diameter. Hence, they were round or ovoid on axial slices (in the BG) and linear on longitudinal slices [in the centrum semiovale (CSO)]. The dPVS corresponded to high signals on T2-weighted images and low signals on T1-weighted and FLAIR images. This method requires the differentiation of dPVS from lacunes, which

[1] www.ppmi-info.org/data
[2] http://adni.loni.usc.edu/methods/documents/mri-protocols/

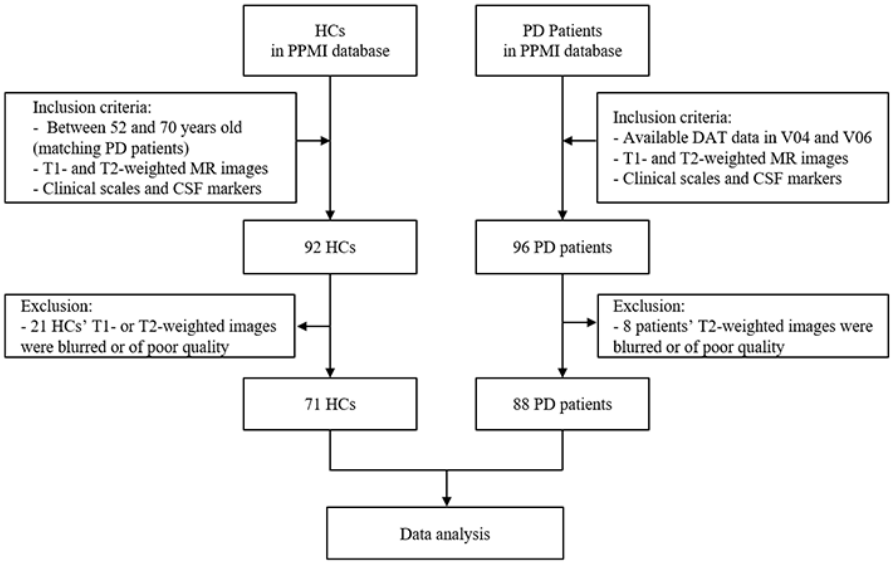

FIGURE 1 | Subject screening workflow.

are generally oval-shaped lesions of a diameter larger than 3 mm. The dPVS in the BG and CSO were assessed with a 4-point visual rating scale (0 = absent dPVS, 1 = less than 10 dPVS, 2 = 11–20 dPVS, 3 = 21–40 dPVS, 4 = more than 40 dPVS) according to the method described by Doubal et al. (2010). After reviewing all relevant slices, the dPVS were counted in the slice that featured the highest number of dPVS. Each hemisphere was assessed separately, and the hemisphere with a higher score was used. The evaluators also counted the number of dPVS in the midbrain and thalamus to ascertain the presence of dPVS in the SN. A dPVS that continued across multiple slices was counted only once. The presence of dPVS in the SN was confirmed if the dPVS was located in or connected to the SN. The boundaries of the regions of interest were defined by comparison to standard brain atlases. **Figure 2** illustrates a representative case of a patient with PD. The inter-rater reliability was good for the BG-PVS score (intraclass correlation coefficient = 0.75) and the number of midbrain PVS (intraclass correlation coefficient = 0.80). The PVS rating scale of the senior radiologist was used for the analysis.

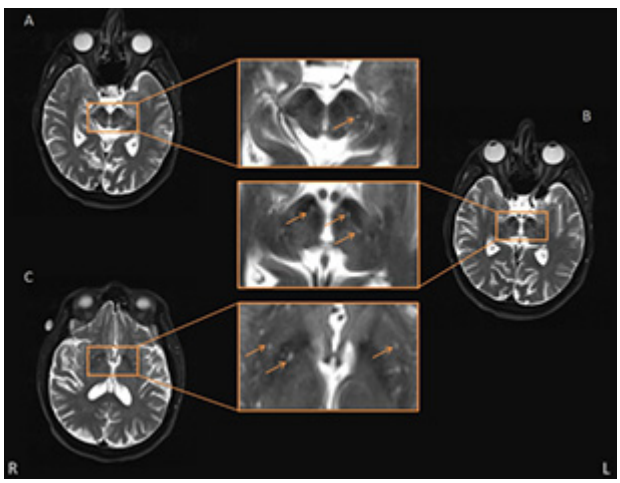

FIGURE 2 | Representative axial T2-weighted images showing basal ganglia (BG) and midbrain perivascular space (PVS). Some typical PVS are indicated by the orange arrow. Panels **(A,B)** are two consecutive layers showing PVS in the midbrain, in which the PVS in panel **(A)** is continuous to the rightmost PVS in panel **(B)**, and the PVS is shown passing through the SN. The other PVS in panel **(B)** were also deemed adjacent to SN. Panel **(C)** shows the axial slice which had the most PVS in the BG area.

Statistical Analysis

Demographic data, expression of CSF markers, imaging characteristics, and clinical scales were compared between the HCs and patients with PD. Two-sample *t*-tests were used for continuous data, while Wilcoxon Rank-Sum tests were used for categorical data. Because the loss of dopaminergic neurons in the SN of the midbrain is particularly important to the development of PD, we divided the 88 patients with PD into two groups according to the presence of dPVS in the SN region: 40 PD patients had dPVS in the SN region (SN + PD), and 48 PD patients did not (SN − PD). Baseline clinical scales, CSF markers, Ave-DAT values, and imaging characteristics were compared between the two groups. Subsequently, after controlling for age, sex, and level of education, we calculated the partial Pearson's correlation coefficients between baseline dPVS scores/numbers and Ave-DAT, clinical scales, and CSF markers. Finally, we examined the correlation between baseline dPVS scores and the rate of longitudinal changes of Ave-DAT and other clinical scales. To calculate the rate of change, we took the difference between the baseline and follow-up values divided by the absolute baseline value.

RESULTS

The demographic characteristics of the patients with PD are presented in **Table 1**. Age ($p = 0.298$), sex ($p = 0.830$), and years of education ($p = 0.064$) did not differ significantly between the HCs and patients with PD. There were significant differences in the dPVS of the SN ($p = 0.022$) and BG ($p < 0.001$) between patients with PD and HCs. Differences between the two populations were also found in p-Tau181P expression ($p = 0.002$), MoCA score ($p < 0.001$), and GDS score ($p = 0.002$).

There were no significant differences in age ($p = 0.558$), sex ($p = 0.356$), and years of education ($p = 0.265$) between the SN + PD and SN − PD groups; however, they differed significantly in their total expression of tau-protein ($p = 0.038$) and many midbrain dPVS ($p < 0.001$). While we found that the Ave-DAT (putamen) of the SN + PD group was lower than that of the SN − PD group, the corresponding p-value was only marginally significant ($p = 0.086$). Other statistical results were nonsignificant (**Table 1**).

No correlations were found between the dPVS scores and baseline CSF markers or between the dPVS scores and cognitive scales (**Tables 2**, **3**). Correlations between dPVS scores and longitudinal alterations were nonsignificant. The results remained nonsignificant after Bonferroni correction.

DISCUSSION

The present study found that PD patients had more dPVS in the BG and SN and lower expression of p-Tau181P relative to HCs. Further, although PD patients with SN dPVS were found to exhibit lower DAT uptake and higher levels of CSF tau, the difference in DAT uptake was only marginally significant. Correlation analyses and longitudinal observations showed no significant associations between dPVS, DAT, and clinical symptoms. These results suggest a mechanistic link between dPVS and SN degeneration.

We found that dPVS in the BG differed significantly between HCs and PD patients. Our findings are consistent with those of previous studies, suggesting that the appearance of these signs may reflect certain features of PD pathology rather than normal aging. Some studies have found that the appearance of dPVS in patients with PD is related to their clinical symptoms: Wan et al. (2019) found that dPVS in the BG correlated with tremor, and Schwartz et al. (2012) observed that characteristics of the small-vessel disease, including dPVS, might be associated with motor impairments in PD. However, such correlations were not stable. It is possible that brain alterations outside the BG area have imposed stronger influence over clinical symptoms, therefore, we found no significant correlation between BG dPVS and clinical symptoms.

We further observed PD patients have more dPVS near the SN relative to HCs, a result not previously reported in the literature. Additionally, PD patients with dPVS in the SN showed a trend towards decreased DAT uptake ($p = 0.086$) when compared to their counterparts without SN dPVS. This observation suggests a link between SN dPVS and dopaminergic neuronal degeneration. The mechanisms underlying such association might be complex (**Figure 3**): during brain aging, hypertension and the loss of AQP-4 water channels could impair the drainage of local interstitial fluid, and disrupt alpha-synuclein clearance (Peng et al., 2016; Lenck et al., 2018), for which the perivascular spaces function as an important pathway

TABLE 1 | Clinical and demographic data of participants and comparisons.

Parameters	SN + PD		SN − PD		HC		*p*-value	
	M	SEM	M	SEM	M	SEM	SN + PD vs. SN − PD	PD vs. HC
Sex(M/F)	32/15		24/17		44/27		0.356[#]	0.830[#]
Age	62.06	1.135	60.9	1.614	60.31	0.635	0.558	0.294
Years of education	15.6	0.39	14.9	0.487	16.1	0.312	0.265	0.064
Duration of PD	1.72	0.103	1.64	0.114	–	–	0.6	–
Ave-DAT (caudate)	1.694	0.684	1.821	0.059	–	–	0.173	–
Ave-DAT (putamen)	0.657	0.029	0.737	0.036	–	–	0.086	–
SN dPVS (+/−)	47		41		25/46		–	0.022[#]
Midbrain-dPVS number	3.6	0.275	0.88	0.189	1.86	0.291	<0.001	0.194
BG-dPVS score	1.87	0.078	1.76	0.076	1.35	0.07	0.294	<0.001
Thalamus-dPVS number	1.81	0.254	1.66	0.246	2.35	0.294	0.674	0.064
CSO-dPVS score	3.45	0.135	3.37	0.12	3.01	0.118	0.659	0.008
Systolic blood pressure (mmHg)	127.83	2.267	130.39	3.069	–	–	0.497	–
Diastolic blood pressure (mmHg)	75.15	1.281	76.83	1.853	–	–	0.449	–
Aβ 42 (pg/ml)	380.682	13.798	379.146	14.808	400.528	13.69	0.94	0.218
p-Tau181P (pg/ml)	15.16	1.298	14.341	1.315	19.989	1.39	0.66	0.002
Total tau (pg/ml)	47.791	2.924	40.098	2.191	48.524	2.342	0.038	0.15
Alpha-synuclein (pg/ml)	1,895.191	103.57	1,783.61	110.123	2,021.102	95.068	0.462	0.139
MoCA	26.68	0.45	26.61	0.392	28.14	0.138	0.907	<0.001
UPDRS-III	23.53	1.525	22.15	0.869	–	–	0.564	–
ESS	6.17	0.604	6.39	0.62	5.59	0.402	0.8	0.258
GDS	2.23	0.363	2.59	0.463	1.25	0.221	0.547	0.002

[#]Is for the Wilcoxon Rank-Sum test, the others were t-tests. Abbreviation: SN, substantia nigra; PD, Parkinson's disease; M/F, male/female; DAT, dopamine transporter; dPVS, dilated perivascular space; BG, basal ganglia; CSO, centrum semiovale; UPDRS-III, Unified Parkinson's Disease Rating Scale Part III; GDS, Geriatric Depression Scale; ESS, Epworth Sleepiness Scale; MoCA, Montreal Cognitive Assessment; p-Tau181P, phosphorylated tau 181P.

TABLE 2 | Correlations between midbrain or BG-d PVS number and indicators (baseline).

Parameters	Midbrain-dPVS number			BG-dPVS score		
	R	*P*-value[a]	*P*-value[b]	*R*	*P*-value[a]	*P*-value[b]
Ave-DAT (caudate)	0.09	0.41	1	−0.13	0.25	1
Ave-DAT (putamen)	0.1	0.36	1	−0.02	0.87	1
Systolic blood pressure (mmHg)	−0.148	0.177	1	0.145	0.159	1
Diastolic blood pressure (mmHg)	−0.154	0.186	1	0.016	0.882	1
Aβ 42 (pg/ml)	0.02	0.89	1	0.05	0.64	1
p-Tau181P (pg/ml)	0.05	0.67	1	0.03	0.78	1
Total tau (pg/ml)	0.09	0.43	1	−0.07	0.5	1
Alpha-synuclein (pg/ml)	−0.13	0.23	1	0.15	0.18	1
UPDRS-III	0.03	0.78	1	−0.03	0.76	1
MoCA	0.14	0.21	1	−0.05	0.65	1
ESS	−0.1	0.36	1	−0.03	0.8	1
GDS	−0.14	0.2	1	0.11	0.31	1

[a]*Unadjusted;* [b]*after Bonferroni correction. Abbreviation: dPVS, dilated perivascular space; BG, basal ganglia; DAT, dopamine transporter; UPDRS-III, Unified Parkinson's Disease Rating Scale Part III; GDS, Geriatric Depression Scale; ESS, Epworth Sleepiness Scale; MoCA, Montreal Cognitive Assessment; p-Tau181P, phosphorylated tau 181P.*

TABLE 3 | Correlations between altered midbrain or BG-d PVS number and indicators (longitudinal).

Parameters	Midbrain-dPVS number			BG-dPVS score		
	R	*P*-value[a]	*P*-value[b]	*R*	*P*-value[a]	*P*-value[b]
DAT ratio (caudate)	0.03	0.81	1	−0.03	0.82	1
DAT ratio (putamen)	−0.03	0.81	1	−0.16	0.15	1
Aβ 42 (pg/ml)	0.02	0.87	1	0.05	0.64	1
p-Tau181P (pg/ml)	0.05	0.67	1	0.03	0.78	1
Total tau (pg/ml)	0.09	0.43	1	−0.07	0.5	1
Alpha-synuclein (pg/ml)	−0.13	0.23	1	0.15	0.18	1
MoCA ratio	−0.11	0.32	1	0.09	0.41	1
UPDRS-III ratio	−0.06	0.59	1	−0.07	0.53	1
ESS ratio	−0.03	0.8	1	−0.01	0.9	1
GDS ratio	0.14	0.22	1	−0.08	0.08	1

[a]*Unadjusted;* [b]*after Bonferroni correction. Abbreviation: dPVS, dilated perivascular space; BG, basal ganglia; DAT, dopamine transporter; UPDRS-III, Unified Parkinson's Disease Rating Scale Part III; GDS, Geriatric Depression Scale; ESS, Epworth Sleepiness Scale; MoCA, Montreal Cognitive Assessment; p-Tau181P, phosphorylated tau 181P.*

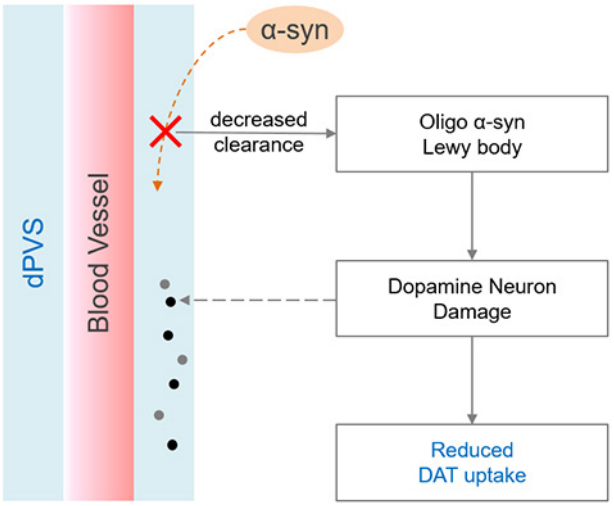

FIGURE 3 | Possible mechanisms linking dilated PVS (dPVS) and reduced dopamine transporter (DAT) uptake. On one hand, decreased alpha-synuclein clearance may accelerate the formation of Lewy body, and lead to dopamine neuron damage. On the other hand, dopamine neuron degeneration can produce excessive metabolic wastes, which may stack in the perivascular space and cause compensatory dilation.

(Zou et al., 2019). Accumulated alpha-synuclein may transform into oligo alpha-synuclein and Lewy bodies (Lashuel et al., 2013) that could damage dopaminergic neurons and reduce DAT uptake. Furthermore, multiple genetic and environmental factors might cause the degeneration of SN dopaminergic neurons, yielding excessive neuronal debris as well as other metabolic waste and cell fragments (Zou et al., 2019). Large molecules might consequently stack in the perivascular spaces, inducing compensatory dilation. Additionally, the loss of neurons and glial cells could also shrink local brain tissues, creating larger spaces between blood vessels and brain parenchyma—i.e., dPVS. Importantly, the aforementioned processes might interact with one another, creating a cycle that causes escalating damage to the SN.

We found that patients with SN dPVS exhibited more total tau expression than did those without SN dPVS, suggesting that PD patients with SN dPVS suffer from a higher degree of neuron degeneration. Tau is a microtubule-associated protein, which may be released into extracellular spaces during the course of several neurodegenerative diseases. Interestingly, Alpha-synuclein could accelerate tau phosphorylation, and their interaction may induce the fibrilization of both proteins. Tau pathologies may compromise axonal transport and cause the further aggregation of alpha-synuclein within the cell body (Giasson et al., 2003; Lei et al., 2010). Although the p-Tau181P is considered more harmful than total tau, elevated concentrations of the latter have also been found in Alzheimer's disease patients (Hampel et al., 2008). Despite these mechanistic links, several studies investigating the role of CSF tau in PD pathology yielded conflicting results (Loeffler et al., 2019). However, in agreement with previous results (Kang et al., 2013; Parnetti et al., 2014), the present study observed the CSF total tau concentration in HCs to exceed that of patients with PD. This phenomenon may be due to the interaction between tau proteins and alpha-synuclein, which may limit tau-protein release into the CSF. The role of CSF tau in PD pathogenesis thus requires further investigation.

To elucidate the causal relationship between dPVS and dopamine neuron degeneration, we performed a correlation analysis between baseline dPVS scores and follow-up Ave-DAT but found no significant correlation. However, this nonsignificant finding does not imply the lack of a causal relationship between dPVS scores and Ave-DAT. The degeneration may have been insufficient across the relatively short duration of follow-up to reflect the contribution of dPVS. The limited imaging resolution was also a major constraint in conducting analyses of dPVS. The state-of-art sub-millimeter isotropic T2 imaging method (Gao et al., 2014) may be used in the future to better facilitate dPVS quantification.

CONCLUSIONS

Our findings indicate that PD patients had more dPVS in the SN compared to HCs, a discrepancy may relate to the degeneration of dopaminergic neurons in the SN. However, because the decrease of DAT uptake was only marginally significant ($p = 0.086$), further study is warranted to confirm our findings and validate the potential value of dPVS as a marker for PD pathology.

DATA AVAILABILITY STATEMENT

The datasets analyzed for this study can be found in the PPMI data repository (http://www.ppmi-info.org/access-data-specimens/download-data/).

ETHICS STATEMENT

The studies involving human participants were reviewed and approved by the PPMI study, which was approved by the institutional review board of all participating sites. The patients/participants provided their written informed consent to participate in this study.

AUTHOR CONTRIBUTIONS

PH, MZ and YY direct the experiment's overall design and revised the manuscript. YL and ZZ evaluated the image data. YL and JC conceived the design details and analytic plan, then performed statistical analyses and drafted the manuscript.

FUNDING

This study was supported by the 13th Five-year Plan for National Key Research and Development Program of China (Grant No. 2016YFC1306600), the National Natural Science Foundation of China (Grant No. 81771820), the Natural Science Foundation of Zhejiang Province (Grant No. LSZ19H180001), and the Health Foundation for Creative Talents in Zhejiang Province (2016).

ACKNOWLEDGMENTS

Data used in this article were obtained from the Parkinson's Progression Markers Initiative (PPMI) database (www.ppmi-info.org/data). For detailed information on the study, visit www.ppmi-info.org. PPMI—a public-private partnership—is funded by the Michael J. Fox Foundation for Parkinson's Research and funding partners, including Abbvie, Avid, Biogen, Biolegend, Bristol-Meyers Squibb, GE Healthcare, Genetech, GSK, Lilly, Lundbeck, Merck, Meso Scale Discovery, Pfizer, Piramal, Roche, Sanofi Genzyme, Servier, Takeda, Teva, UCB, and Golub Capital.

REFERENCES

Abeliovich, A., and Gitler, A. D. (2016). Defects in trafficking bridge Parkinson's disease pathology and genetics. *Nature* 539, 207–216. doi: 10.1038/nature20414

Aspelund, A., Antila, S., Proulx, S. T., Karlsen, T. V., Karaman, S., Detmar, M., et al. (2015). A dural lymphatic vascular system that drains brain interstitial fluid and macromolecules. *J. Exp. Med.* 212, 991–999. doi: 10.1084/jem.20142290

Bobela, W., Aebischer, P., and Schneider, B. L. (2015). Alph-synuclein as a mediator in the interplay between aging and Parkinson's disease. *Biomolecules* 5, 2675–2700. doi: 10.3390/biom5042675

Chung, S. J., Lee, J. J., Ham, J. H., Lee, P. H., and Sohn, Y. H. (2016). Apathy and striatal dopamine defects in non-demented patients with Parkinson's disease. *Parkinsonism Relat. Disord.* 23, 62–65. doi: 10.1016/j.parkreldis.2015.12.003

de Lau, L. M. L., and Breteler, M. M. B. (2006). Epidemiology of Parkinson's disease. *Lancet Neurol.* 5, 525–535. doi: 10.1016/S1474-4422(06)70471-9

Doubal, F. N., MacLullich, A. M. J., Ferguson, K. J., Dennis, M. S., and Wardlaw, J. M. (2010). Enlarged perivascular spaces on MRI are a feature of cerebral small vessel disease. *Stroke* 41, 450–454. doi: 10.1161/strokeaha.109.564914

Ebrahimi-Fakhari, D., Cantuti-Castelvetri, I., Fan, Z., Rockenstein, E., Masliah, E., Hyman, B. T., et al. (2011). Distinct roles *in vivo* for the ubiquitin-proteasome system and the autophagy-lysosomal pathway in the degradation of α-synuclein. *J. Neurosci.* 31, 14508–14520. doi: 10.1523/jneurosci.1560-11.2011

Elster, A. D., and Richardson, D. N. (1991). Focal high signal on MR scans of the midbrain caused by enlarged perivascular spaces: MR-pathologic correlation. *AJR Am. J. Roentgenol.* 156, 157–160. doi: 10.2214/ajr.156.1.1898553

Ferrer, P., Montoya, J., and Garcia Ruiz, P. J. (2017). Teaching NeuroImages: a rare case of giant perivascular spaces in the midbrain manifesting as atypical parkinsonism. *Neurology* 89, e272–e273. doi: 10.1212/wnl.0000000000004706

Gao, K. C., Nair, G., Cortese, I. C. M., Koretsky, A., and Reich, D. S. (2014). Sub-millimeter imaging of brain-free water for rapid volume assessment in atrophic brains. *NeuroImage* 100, 370–378. doi: 10.1016/j.neuroimage.2014.06.014

Giasson, B. I., Forman, M. S., Higuchi, M., Golbe, L. I., Graves, C. L., Kotzbauer, P. T., et al. (2003). Initiation and synergistic fibrillization of tau and α-synuclein. *Science* 300, 636–640. doi: 10.1126/science.1082324

Hampel, H., Burger, K., Teipel, S. J., Bokde, A. L. W., Zetterberg, H., and Blennow, K. (2008). Core candidate neurochemical and imaging biomarkers of Alzheimer's disease. *Alzheimers Dement.* 4, 38–48. doi: 10.1016/j.jalz.2007.08.006

Huang, P., Lou, Y., Xuan, M., Gu, Q., Guan, X., Xu, X., et al. (2016). Cortical abnormalities in Parkinson's disease patients and relationship to depression: a surface-based morphometry study. *Psychiatry Res. Neuroimaging* 250, 24–28. doi: 10.1016/j.pscychresns.2016.03.002

Kang, J.-H., Irwin, D. J., Chen-Plotkin, A. S., Siderowf, A., Caspell, C., Coffey, C. S., et al. (2013). Association of cerebrospinal fluid β-amyloid 1–42, T-tau, P-tau181 and α-synuclein levels with clinical features of drug-naive patients with early Parkinson disease. *JAMA Neurol.* 70, 1277–1287. doi: 10.1001/jamaneurol.2013.3861

Kim, K. J., Bae, Y. J., Kim, J.-M., Kim, B. J., Oh, E. S., Yun, J. Y., et al. (2018). The prevalence of cerebral microbleeds in non-demented Parkinson's disease patients. *J. Korean Med. Sci.* 33:e289. doi: 10.3346/jkms.2018.33.e289

Lashuel, H. A., Overk, C. R., Oueslati, A., and Masliah, E. (2013). The many faces of α-synuclein: from structure and toxicity to therapeutic target. *Nat. Rev. Neurosci.* 14, 38–48. doi: 10.1038/nrn3406

Lei, P., Ayton, S., Finkelstein, D. I., Adlard, P. A., Masters, C. L., and Bush, A. I. (2010). Tau protein: relevance to Parkinson's disease. *Int. J. Biochem. Cell Biol.* 42, 1775–1778. doi: 10.1016/j.biocel.2010.07.016

Lenck, S., Radovanovic, I., Nicholson, P., Hodaie, M., Krings, T., and Mendes-Pereira, V. (2018). Idiopathic intracranial hypertension: the veno glymphatic connections. *Neurology* 91, 515–522. doi: 10.1212/WNL.0000000000006166

Li, Y., Huang, P., Guo, T., Guan, X., Gao, T., Sheng, W., et al. (2020). Brain structural correlates of depressive symptoms in Parkinson's disease patients at different disease stage. *Psychiatry Res. Neuroimaging* 296:111029. doi: 10.1016/j.pscychresns.2019.111029

Loeffler, D. A., Aasly, J. O., LeWitt, P. A., and Coffey, M. P. (2019). What have we learned from cerebrospinal fluid studies about biomarkers for detecting LRRK2 Parkinson's disease patients and healthy subjects with Parkinson's-associated LRRK2 mutations? *J. Parkinsons Dis.* 9, 467–488. doi: 10.3233/jpd-191630

Louveau, A., Smirnov, I., Keyes, T. J., Eccles, J. D., Rouhani, S. J., Peske, J. D., et al. (2016). Corrigendum: structural and functional features of central nervous system lymphatic vessels. *Nature* 533:278. doi: 10.1038/nature16999

Maiti, P., Manna, J., and Dunbar, G. L. (2017). Current understanding of the molecular mechanisms in Parkinson's disease: targets for potential treatments. *Transl. Neurodegener.* 6:28. doi: 10.1186/s40035-017-0099-z

Mestre, H., Kostrikov, S., Mehta, R. I., and Nedergaard, M. (2017). Perivascular spaces, glymphatic dysfunction and small vessel disease. *Clin. Sci.* 131, 2257–2274. doi: 10.1042/cs20160381

Mezey, E., and Palkovits, M. (2015). Neuroanatomy: forgotten findings of brain lymphatics. *Nature* 524:415. doi: 10.1038/524415b

Narayanan, N. S., Rodnitzky, R. L., and Uc, E. Y. (2013). Prefrontal dopamine signaling and cognitive symptoms of Parkinson's disease. *Rev. Neurosci.* 24, 267–278. doi: 10.1515/revneuro-2013-0004

Papayannis, C. E., Saidon, P., Rugilo, C. A., Hess, D., Rodriguez, G., Sica, R. E. P., et al. (2003). Expanding Virchow Robin spaces in the midbrain causing hydrocephalus. *AJNR Am. J. Neuroradiol.* 24, 1399–1403.

Park, Y. W., Shin, N.-Y., Chung, S. J., Kim, J., Lim, S. M., Lee, P. H., et al. (2019). Magnetic resonance imaging-visible perivascular spaces in basal ganglia predict cognitive decline in Parkinson's disease. *Mov. Disord.* 34, 1672–1679. doi: 10.1002/mds.27798

Parnetti, L., Farotti, L., Eusebi, P., Chiasserini, D., De Carlo, C., Giannandrea, D., et al. (2014). Differential role of CSF α-synuclein species, tau and Aβ42 in Parkinson's Disease. *Front. Aging Neurosci.* 6:53. doi: 10.3389/fnagi.2014.00053

Peng, W., Achariyar, T. M., Li, B., Liao, Y., Mestre, H., Hitomi, E., et al. (2016). Suppression of glymphatic fluid transport in a mouse model of Alzheimer's disease. *Neurobiol. Dis.* 93, 215–225. doi: 10.1016/j.nbd.2016.05.015

Ramirez, J., Berezuk, C., McNeely, A. A., Scott, C. J. M., Gao, F., and Black, S. E. (2015). Visible Virchow-Robin spaces on magnetic resonance imaging of Alzheimer's disease patients and normal elderly from the Sunnybrook Dementia Study. *J. Alzheimers Dis.* 43, 415–424. doi: 10.3233/JAD-132528

Schwartz, R. S., Halliday, G. M., Cordato, D. J., and Kril, J. J. (2012). Small-vessel disease in patients with Parkinson's disease: a clinicopathological study. *Mov. Disord.* 27, 1506–1512. doi: 10.1002/mds.25112

Shibata, K., Sugiura, M., Nishimura, Y., and Sakura, H. (2019). The effect of small vessel disease on motor and cognitive function in Parkinson's disease. *Clin. Neurol. Neurosurg.* 182, 58–62. doi: 10.1016/j.clineuro.2019.04.029

Suchowersky, O., Reich, S., Perlmutter, J., Zesiewicz, T., Gronseth, G., and Weiner, W. J. (2006). Practice Parameter: diagnosis and prognosis of new onset Parkinson disease (an evidence-based review): report of the Quality Standards Subcommittee of the American Academy of Neurology. *Neurology* 66, 968–975. doi: 10.1212/01.wnl.0000215437.80053.d0

Sundaram, S., Hughes, R. L., Peterson, E., Muller-Oehring, E. M., Bronte-Stewart, H. M., Poston, K. L., et al. (2019). Establishing a framework for neuropathological correlates and glymphatic system functioning in Parkinson's disease. *Neurosci. Biobehav. Rev.* 103, 305–315. doi: 10.1016/j.neubiorev.2019.05.016

Wan, Y., Hu, W., Gan, J., Song, L., Wu, N., Chen, Y., et al. (2019). Exploring the association between Cerebral small-vessel diseases and motor symptoms in Parkinson's disease. *Brain Behav.* 9:e01219. doi: 10.1002/brb3.1219

Wardlaw, J. M., Smith, E. E., Biessels, G. J., Cordonnier, C., Fazekas, F., Frayne, R., et al. (2013). Neuroimaging standards for research into small vessel disease and its contribution to ageing and neurodegeneration. *Lancet Neurol.* 12, 822–838. doi: 10.1016/S1474-4422(13)70124-8

Webb, J. L., Ravikumar, B., Atkins, J., Skepper, J. N., and Rubinsztein, D. C. (2003). α-synuclein is degraded by both autophagy and the proteasome. *J. Biol. Chem.* 278, 25009–25013. doi: 10.1074/jbc.m300227200

Zou, W., Pu, T., Feng, W., Lu, M., Zheng, Y., Du, R., et al. (2019). Blocking meningeal lymphatic drainage aggravates Parkinson's disease-like pathology in mice overexpressing mutated α-synuclein. *Transl. Neurodegener.* 8:7. doi: 10.1186/s40035-019-0147-y

Conflict of Interest: The authors declare that the research was conducted in the absence of any commercial or financial relationships that could be construed as a potential conflict of interest.

frontiers in Neuroscience

ORIGINAL RESEARCH
published: 05 June 2020
doi: 10.3389/fnins.2020.00403

Bloodletting Puncture at Hand Twelve *Jing*-Well Points Improves Neurological Recovery by Ameliorating Acute Traumatic Brain Injury-Induced Coagulopathy in Mice

Bo Li[1,2†], Xiu Zhou[1†], Tai-Long Yi[1†], Zhong-Wei Xu[3], Ding-Wei Peng[1], Yi Guo[2], Yong-Ming Guo[2], Yu-Lin Cao[4], Lei Zhu[5], Sai Zhang[1]* and Shi-Xiang Cheng[1]**

[1] Tianjin Key Laboratory of Neurotrauma Repair, Institute of Neurotrauma Repair of Characteristic Medical Center of Chinese People's Armed Police Force (PAP), Tianjin, China, [2] Acupuncture Research Center, Tianjin University of Traditional Chinese Medicine, Tianjin, China, [3] Central Laboratory of Logistics University of Chinese People's Armed Police Force (PAP), Tianjin, China, [4] Zhenxigu Medical Research Center, Beijing, China, [5] Department of Spine Surgery, Xi'an Honghui Hospital, Xi'an Jiaotong University, Xi'an, China

OPEN ACCESS

Edited by:
Dennis Qing Wang,
Zhujiang Hospital of Southern Medical University, China

Reviewed by:
Wanlin Yang,
Department of Neurology, Zhujiang Hospital of Southern Medical University, China
Audrey Lafrenaye,
Virginia Commonwealth University, United States

***Correspondence:**
Lei Zhu
zhulei_phd@126.com
Sai Zhang
zhangsai718@vip.126.com
Shi-Xiang Cheng
shixiangcheng@vip.126.com

† These authors have contributed equally to this work and share first authorship

Specialty section:
This article was submitted to Neurodegeneration, a section of the journal Frontiers in Neuroscience

Received: 10 December 2019
Accepted: 02 April 2020
Published: 05 June 2020

Citation:
Li B, Zhou X, Yi T-L, Xu Z-W, Peng D-W, Guo Y, Guo Y-M, Cao Y-L, Zhu L, Zhang S and Cheng S-X (2020) Bloodletting Puncture at Hand Twelve Jing-Well Points Improves Neurological Recovery by Ameliorating Acute Traumatic Brain Injury-Induced Coagulopathy in Mice. Front. Neurosci. 14:403. doi: 10.3389/fnins.2020.00403

Traumatic brain injury (TBI) contributes to hypocoagulopathy associated with prolonged bleeding and hemorrhagic progression. Bloodletting puncture therapy at hand twelve *Jing*-well points (BL-HTWP) has been applied as a first aid measure in various emergent neurological diseases, but the detailed mechanisms of the modulation between the central nervous system and systemic circulation after acute TBI in rodents remain unclear. To investigate whether BL-HTWP stimulation modulates hypocoagulable state and exerts neuroprotective effect, experimental TBI model of mice was produced by the controlled cortical impactor (CCI), and treatment with BL-HTWP was immediately made after CCI. Then, the effects of BL-HTWP on the neurological function, cerebral perfusion state, coagulable state, and cerebrovascular histopathology post-acute TBI were determined, respectively. Results showed that BL-HTWP treatment attenuated cerebral hypoperfusion and improve neurological recovery post-acute TBI. Furthermore, BL-HTWP stimulation reversed acute TBI-induced hypocoagulable state, reduced vasogenic edema and cytotoxic edema by regulating multiple hallmarks of coagulopathy in TBI. Therefore, we conclude for the first time that hypocoagulopathic state occurs after acute experimental TBI, and the neuroprotective effect of BL-HTWP relies on, at least in part, the modulation of hypocoagulable state. BL-HTWP therapy may be a promising strategy for acute severe TBI in the future.

Keywords: traumatic brain injury, coagulopathy, bloodletting puncture at hand twelve *Jing*-well points, controlled cortical impact, model, mouse

INTRODUCTION

Traumatic brain injury (TBI) is defined as an altered brain function or other evidence of brain pathology caused by an external force. In 2016, there were 27.08 million new cases of TBI, with age-standardized incidence rates of 369 per 100,000 populations (GBD 2016 Traumatic Brain Injury and Spinal Cord Injury Collaborators, 2019). In China alone, age-standardized incidence rates increased by 33.1% for TBI from 1990 to 2016, and China had more patients with TBI than most

other countries in the world, causing a huge burden to families and society (GBD 2016 Traumatic Brain Injury and Spinal Cord Injury Collaborators, 2019; Jiang et al., 2019). In most cases of TBI, the brain tissue may be damaged, the blood vessels can rupture and cause bleeding, or a combination of these injuries may occur (Silverberg et al., 2019). Therefore, developing the effective early diagnostic methods and treatment strategies in preventing the diverse and complex nature of the pathological processes activated by TBI poses a major challenge for neurological researchers (Cheng et al., 2018). However, the hypocoagulable state after acute TBI involves complex and multifactorial molecular mechanisms that are poorly understood.

Until now, it has been generally assumed that trauma-induced coagulopathy (TIC) is strongly associated with poorer outcomes and progression of intracranial injury after TBI (Zhang et al., 2015; Chang et al., 2016), and the number of patients with TBI and coagulopathy doubles within 24 h after injury (Greuters et al., 2011). Clinical studies have demonstrated that coagulopathy occurred in nearly two-thirds of severe TBI patients, resulting in hypocoagulopathy associated with prolonged bleeding and hemorrhagic progression after TBI (Harhangi et al., 2008; Laroche et al., 2012; Maegele et al., 2017). It has been shown that TIC contributes to immediate or progressive hemorrhagic contusions in various pathophysiological conditions, including tissue and/or vessel injury, blood–brain barrier disruption, endothelial activation, and inflammation. However, these pathological processes affect the prognosis of TBI. Whether it is possible to improve the prognosis of TBI by altering these pathological processes remains to be elucidated. Additionally, the degree to which these coagulation abnormalities affect neurorestoratology after TBI and whether they are modifiable risk factors for neurorestorative strategies are not known (McCully and Schreiber, 2013; Huang et al., 2018, 2019). Furthermore, coagulopathy is also a common occurrence after severe systemic trauma in the absence of TBI (Spahn et al., 2019), and whether systemic management approaches in these patients might also apply to patients with TBI is unclear. Given these limitations, there is an urgent need to deeply explore the TBI-induced coagulopathic processes and focus primarily on novel treatment of coagulopathy to best manage these TBI patients.

As a treatment of traditional Chinese medicine, acupuncture mechanically inserts fine needles into specific acupoints in the body to stimulate a desired physiologic response, and bloodletting puncture therapy has been applied as one of the first aid measures in various types of emergency for more than 3,000 years in ancient China (Cybularz et al., 2015). With the growing acceptance and application since its endorsement by the National Institutes of Health (NIH), acupuncture has been shown to be safe and effective across a variety of clinical settings (National Institutes of Health, 1998). In particular, bloodletting puncture at hand twelve *Jing*-well points (BL-HTWP), which is a main concept in traditional Chinese acupuncture theory, has been applied to treat various neurological diseases. Our previous study, as well as those from other groups have demonstrated that BL-HTWP could ameliorate blood–brain barrier dysfunction after acute severe TBI (Tu et al., 2016), alleviated cerebral edema in ischemic stroke (Yu et al., 2017), and improved consciousness disorders of acute carbon monoxide poisoning patients (Yue et al., 2015), suggesting that BL-HTWP might be a neuroprotective effect in the brain as a novel approach to treatment of TBI. Nevertheless, the mechanism of this neuroprotective effect is unclear. However, one of the possible mechanism is related to some special ways called meridians (Xu et al., 2014), which connect between the CNS and systemic circulation.

We hypothesized that stimulation of BL-HTWP modulates hypocoagulable state after acute TBI and may exert a neuroprotective effect. Hence, in the present study, the therapeutic efficacy of BL-HTWP against cerebral hypoperfusion, neurological deficits, blood–brain barrier disruption, and vasogenic/cytotoxic edema was evaluated in TBI mice, respectively, and the effects of BL-HTWP on multiple hallmarks of coagulopathy in TBI were investigated.

MATERIALS AND METHODS

Study Design of Experimental Animals

A total of 130 male C57BL/6J mice aged 10 weeks (weighing 20–25 g; Laboratory Animal Center of Academy of Military Medical Sciences, China) were used for this study. All animal procedures were approved by the Institutional Animal Care and Use Committee at the Characteristic Medical Center of PAP. Mice were randomly divided into three groups for assessment: sham-operated group served as uninjured control (Sham), controlled cortical impact (CCI) injury group, and bloodletting puncture at hand twelve *Jing*-well points group (BL-HTWP, abbreviated as BL). Both CCI and BL groups were subjected to CCI insults, and the sham animals underwent all identical surgical craniotomy procedures without receiving CCI.

All groups were sutured and disinfected after operation. The CCI and Sham groups had only the wound disinfected without any treatment. The study design is presented in **Figure 1A**, which consisted of four stages: (1) Cerebral blood perfusion (0, 1, 2, 4, 6 h), cerebral perfusion pressure (0, 2, 4, 6, 12, 18, 24 h), motor-evoked potential (6 h), and modified neurological severity score (12, 24, 48, 72 h) post-CCI were performed instantaneously (n = 12/group). (2) Six hours after CCI, blood samples were collected for the detection of conventional coagulation tests (n = 5/group) and thromboelastography (n = 5/group). (3) Six hours after CCI, mice were sacrificed for the measurement of the following parameters: histology, blood–brain barrier, immunofluorescence histochemistry, and brain water content (n = 4/group, respectively), and (4) Western blotting was detected at 6, 24, 48, and 72 h post-CCI (n = 4 for the Sham group; n = 12 for the CCI and BL groups, respectively).

Controlled Cortical Impact Injury (CCI)

The experimental TBI method used in this study was performed using a CCI protocol as described previously with minor modifications (Cheng et al., 2018). Briefly, mice were placed in the prone position and anesthetized with a continuous flow of isoflurane; then, the skull was exposed by a midline scalp incision.

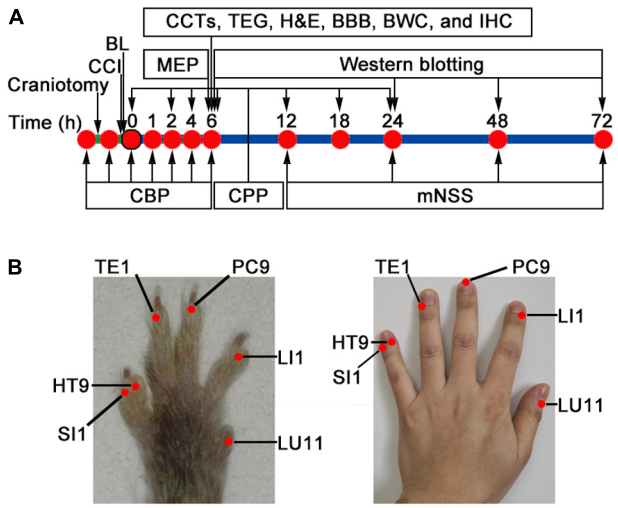

FIGURE 1 | Study design and bloodletting puncture at hand twelve *Jing*-well points (BL-HTWP) treatment in mice. **(A)** Schematic of workflow for experiments. CCI, controlled cortical impact injury; BL, BL-HTWP; CBP, cerebral blood perfusion; CPP, cerebral perfusion pressure; MEP, motor-evoked potential; mNSS, modified neurological severity score; CCTs, conventional coagulation tests; TEG, thromboelastography; BBB, brain-blood barrier permeability; and BWC, brain water content assay. **(B)** After CCI, mice received immediate treatment of BL-HTWP once. BL-HTWP was located at the tips of the mouse toes (*left*), corresponding to the human fingers (*right*), including *Shaoshang* (LU11), *Shangyang* (LI1), *Zhongchong* (PC9), *Guanchong* (TE1), *Shaochong* (HT9), and *Shaoze* (SI1).

A 4 mm diamter circular craniotomy was made over the right parietal cortex between bregma and lambda with the medial edge 0.5 mm lateral to the midline. TBI mice were then subjected to a CCI injury with an electric cortical contusion impactor device (eCCI-6.3; Custom Design & Fabrication, Richmond, VA, United States) generated at 5 m/s velocity, 1.5 mm impact depth, and a dwell time of 120 ms.

Bloodletting Puncture at Hand Twelve *Jing*-Well Points (BL-HTWP)

Treatment of BL-HTWP was performed according to previous studies in rats (Tu et al., 2016; Yu et al., 2017), and comparative anatomy was used for point selection, with reference to human anatomical acupoints (Yue et al., 2015) shown in **Figure 1B**. Briefly, a 21-gauge blood lancet (Hanaco Medical Co., Tianjin, China) was perpendicularly inserted into the skin to a depth of 1 mm in the distal ends of the bilateral acupoints for bloodletting immediately after CCI, with the sequence of LU11 (Shaoshang), LI1 (Shangyang), PC9 (Zhongchong), TE1 (Guanchong), HT9 (Shaochong), and SI1 (Shaoze). Each acupoint was squeezed three to five times to bleed about 5 μl before compressing with cotton balls. BL-HTWP was operated once during the experiment.

Cerebral Blood Perfusion (CBP)

CBP was assessed using a blood perfusion imager (PeriCam PSI System, Perimed AB, Stockholm, Sweden) based on laser speckle contrast imaging (LSCI) technology. Briefly, the skull of the anesthetized mouse was exposed by creating a midline skin incision, and the through-skull cerebral blood flow was detected with a speckle contrast. The dynamic and spatial distribution of CBP was then recorded from mice before/after craniotomy (**Figure 2A**), immediately following CCI (0 h), as well as at 1, 2, 4, and 6 h post-CCI by PSI scanning. The unit of CBP is expressed in PU (perfusion units, PU).

Cerebral Perfusion Pressure (CPP)

CPP is the difference between mean arterial pressure and intracranial pressure (MAP-ICP) and has become a commonly cited goal in the management of severe TBI. The MAP and ICP of CPP was then recorded from mice before/after craniotomy (**Figure 2A**), immediately following CCI (0 h), as well as at 2, 4, 6, 12, 18, and 24 h post-CCI by 1 Fr MILRO-TIP transducer (Millar, Houston, TX, United States). Mean arterial pressure was continuously monitored and recorded via the femoral arterial catheter at baseline following CCI. Heart rate was similarly monitored and recorded. Using medical ear–brain glue, the optical fiber probe with a diameter of 0.5 mm was fixed on the bone window opened during modeling to detect ICP.

Motor-Evoked Potential (MEP)

MEP is used to evaluate the motor nerve function after TBI, including the overall synchronization and integrity of the conduction pathway from the cortex to the muscle by recording the motor compound potential of the cortex in the contralateral target muscle. Measurements of the MEP for the hindlimbs were made using an evoked potential (EP) instrument Viking Quest (Thermo Nicolet Corporation, United States) after 6 h post-CCI. A needle electrode was inserted into the belly of the tibialis anterior muscle as an active electrode, and two needle recording electrodes were inserted into the tendon of the tibialis anterior muscle of both hindlimbs. The reference electrode was placed subcutaneously. The stimulus intensity was 20 V, the stimulation pulse width was 0.5 ms, and the stimulation frequency was 1 Hz. The ground wire was positioned at the tail. Amplitude (mV) was the peak-to-peak voltage, meaning the potential difference between the most positive and the most negative peaks, and latency (ms) was time between the start of the stimulus to the appearance of the initial response wave.

Modified Neurological Severity Score (mNSS)

mNSS is an independent set of scales, which was performed to evaluate the post-injury neurological functions of mice (n = 12/group) before and 12, 24, 48, and 72 h after CCI, which is a composite of motor, sensory, balance, and reflex tests with the maximum scores of 6, 2, 6, and 4 points, respectively (Wang et al., 2014). Thus, higher scores indicate more severe neurological dysfunction (13–18 = severe, 7–12 = moderate, and 1–6 = mild).

Preparation and Collection of Blood Samples

After 6 h of CCI, blood samples (∼1 ml/mice) were collected via direct left ventricle puncture. Blood for the laboratory analysis,

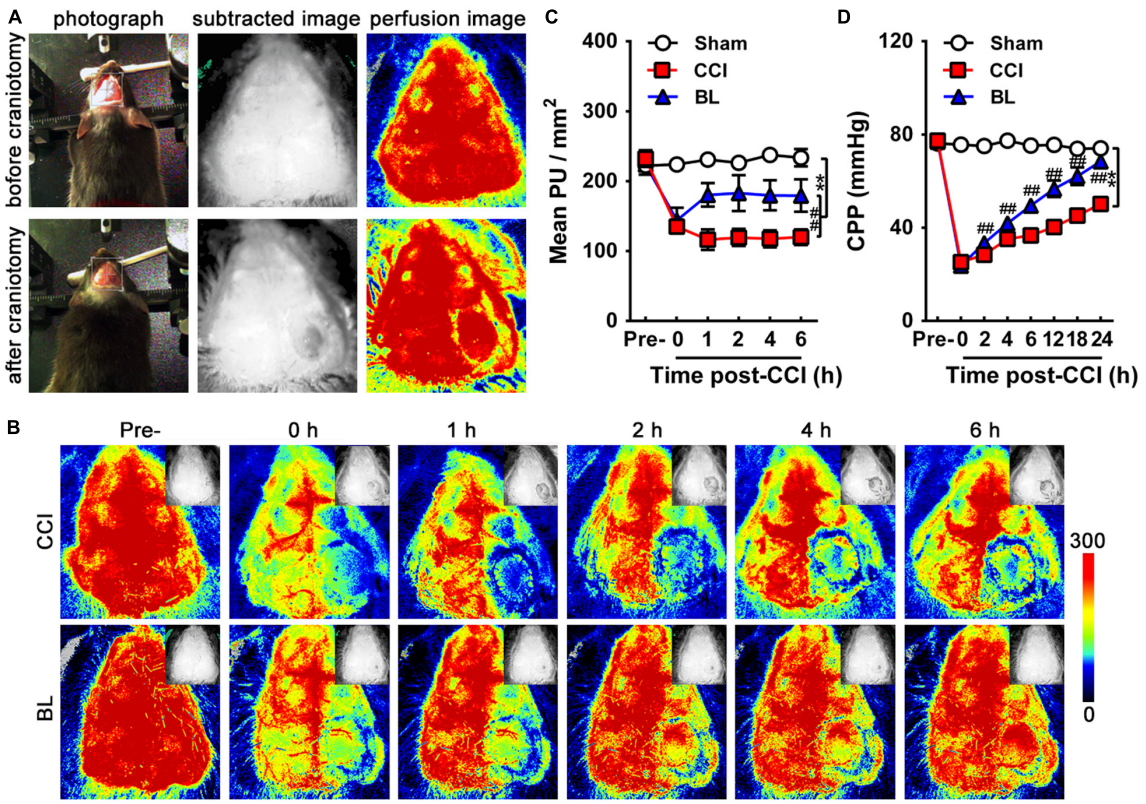

FIGURE 2 | Acute effects of BL-HTWP on cerebral blood perfusion (CBP) and cerebral perfusion pressure (CPP) after TBI. **(A)** CBP was assessed using a blood perfusion imager (PeriCam PSI System) based on laser speckle contrast imaging (LSCI) technology. The dynamic and spatial distribution of CBP was recorded before/after craniotomy, which was performed over the right parietal cortex (photograph, subtracted image, and perfusion image). **(B)** Representative LSCI images in mouse brain at pre-injury, 0, 1, 2, 4, and 6 h post-CCI. Images show areas of yellow-red as high blood perfusion and that of blue-black as low blood perfusion. **(C)** Statistical analysis of mean perfusion units (PU) per square millimeter. **(D)** CPP was assessed at pre-injury, 0, 2, 4, 6, 12, 18, and 24 h post-CCI. Quantitative analysis (n = 12) were conducted by one-way ANOVA. $^{**}p < 0.01$ vs. Sham, $^{\#\#}p < 0.01$ vs. CCI.

including CCTs and TEG assays, was collected in a vacuum tube containing 0.109 M (3.2%) of sodium citrate. The ratio of sodium citrate to whole blood is 9:1. The vacuum tube was inverted eight times to allow the blood to mix with sodium citrate to prevent clotting.

Conventional Coagulation Tests

Citrated plasma tubes were prepared after centrifugation at room temperature for 10 min at 3,000 × *g*. Then, CCTs – hematology parameters including prothrombin time (PT), activated partial thromboplastin time (aPTT), international normalized ratio (INR), plasma fibrinogen (FIB), thrombin time (TT), prothrombin time activity (PTA), platelet counts, and coagulation Factor VII and VIII levels—were measured with the STA-R evolution coagulation analyzer (Diagnostica Stago S.A.S, Asnières sur Seine, France) in accordance with the laboratory standard operating procedure.

Thromboelastography (TEG)

TEG assay was performed with non-activated citrated whole blood using a TEG 5000 System (Haemoscope Corporation, Niles, IL, United States) in accordance with the manufacturer' instructions. Six hours after CCI, samples were tested at room temperature until all of the following parameters were recorded: reaction time [R, minutes (time to first clot formation)], clotting time [K, minutes (time until the clot reaches a fixed strength)], angle [α, degrees (rate of clot formation)], and maximum amplitude [MA, millimeters (maximum strength of the platelet-fibrin clot)].

Histological Analysis

Six hours after CCI, mice were subjected to cardiac perfusion with 0.1 M PBS followed by fixation with 4% polyoxymethylene. The brains were removed and postfixed in 4% polyoxymethylene solution for 12 h, and tissues were frozen and embedded in Tissue-Tek OCT. Frozen tissues were cryosectioned at a thickness of 20 μm. The brain tissue sections with the edge of injury were taken, and 10 slices were taken every 1 mm. Representative sections from each mouse were stained with cresyl violet (CV) to assess the neurological damage, or stained by hematoxylin and eosin (*H&E*) to evaluate cerebrovascular histopathological changes. Coronal sections that spanned across the contusion areas were stained with CV (Sigma-Aldrich, St. Louis, MO, United States) as described

previously (Cheng et al., 2018). Slice was stained with standard H&E staining to determine the presence of morphological abnormalities and microbleedings post-CCI.

Permeability of Brain–Blood Barrier

After 5 h of CCI, mice were administered 200 μl of Evans blue (EB; 2% *w/v*; i.p.; Sigma-Aldrich, St. Louis, MO, United States), allowed to circulate for 1 h prior to sacrifice as described previously (Main et al., 2018). Mice were then perfused transcardially with saline to remove intravascular EB dye, and the right hemispheres were immediately removed and separated along the midline. Each sample was weighed, homogenized, and incubated at room temperature for 24 h. Then, the supernatant was collected, and absorbance was measured at 620 nm after centrifugation.

Brain Water Content

Cerebral edema was evaluated by water content of the brain tissue at 6 h post-CCI with the wet-to-dry weight ratio (Genet et al., 2017). Following sacrifice, the cerebellum and bilateral olfactory bulbs were discarded, and the brain tissue was separated into the left and right hemispheres along the midline. The right hemisphere was taken, the surface water was dried, and the brain tissue was placed on an electronic balance to weigh it and then dried for 24 h at 110°C in an oven, and re-weighed to obtain the dry weight. Brain water content was calculated: BWC = (wet weight - dry weight)/wet weight × 100%.

Immunofluorescence Histochemistry

Six hours after CCI, mice were subjected to cardiac perfusion with 0.1 M PBS followed by fixation with 4% polyoxymethylene. The brains were removed and postfixed in 4% polyoxymethylene solution for 12 h, and tissues were frozen and embedded in Tissue-Tek OCT. Frozen tissues were cryosectioned at a thickness of 20 μm. The brain tissue sections with the edge of injury were taken, and 10 slices were taken every 1 mm. Brain tissue sections were blocked with 10% bovine serum albumin (BSA) for 1 h, then incubated overnight at 4°C with primary antibodies: rabbit anti-neuronal nuclei (NeuN; ab104225; 1:500; Abcam), anti-glial fibrillary acidic protein (GFAP; #12389S; 1:200; Cell Signaling Technology), and anti-ionized calcium-binding adapter molecule 1 (Iba-1; 10904-1-AP; 1:400; Proteintech). After washing, slides were stained with the appropriate secondary antibodies for 30 min in darkness at 37°C. DAPI was then used to stain the nuclei. Under 400 times fluorescence microscope (Leica DMI400B; Germany), the hippocampus on the injured side was taken as the observation area, four fields from the peritraumatic area in each section were imaged, and the percentage of NeuN + -, GFAP + -, and Iba-1 + - cells were counted using Image J software. Finally, the average number of positive cells in the four sections was calculated as the number of positive cells in the tissue section. All analyses were performed in a blinded manner.

Western Blotting

Western blotting analysis was performed to detect the protein expression levels of tight junction proteins (Occludin and ZO-1), water channel protein aquaporin 4 (AQP4), inflammatory-related hallmarks including interleukin-6 (IL-6), IL-1β, intercellular adhesion molecule 1 (ICAM-1), and hypoxia-inducible factor-1α (HIF-1α), and trophic factors such as brain-derived neurotrophic factor (BDNF) and vascular endothelial growth factor (VEGF), respectively. Mice were sacrificed, and their brains were rapidly removed at 6, 24, 48, and 72 h post-CCI. For protein extraction, injured brain tissues (10 mg) were isolated and lysed in 4% SDS buffer then homogenized on ice. The proteins were recovered by centrifugation at 13,000 rpm for 15 min at 4°C. Protein samples of each group were separated by 10% polyacrylamide gel electrophoresis and transferred onto nitrocellulose membranes, which were blocked by 10% non-fat milk and incubated at a dilution of 1:1,000 overnight at 4°C with the primary antibodies as follows: Occludin (ab167161; Abcam), ZO-1 (21773-1-AP; Proteintech), AQP4 (ab46182; Abcam), IL-6 (BS6419; Bioworld), IL-1β (BS6067; Bioworld), ICAM-1 (BS7138; Bioworld), HIF-1α (ab179483; Abcam), BDNF (BS6533; Bioworld), VEGF (BS6496; Bioworld), and GAPDH (MB001; Bioworld). After washing, membranes were incubated at room temperature for 2 h with secondary antibody (IgG at 1:10,000 dilutions; KPL). Protein was developed with ECL reagent and visualized using an Amersham Imager 600 (GH Healthcare, Pittsburgh, PA, United States). The density of bands was determined by Scion Image 4.0 software. GAPDH was used as internal control. All analyses were performed in a blinded manner.

Statistical Analysis

All data were presented as means ± standard deviation (SD). SPSS 16.0 (IBM, Armonk, NY, United States) was used for analysis. Statistical analyses were performed using one-way analysis of variance (ANOVA) followed by *post hoc* comparison. All tests were two-tailed, and a value of $p < 0.05$ was considered to be statistically significant.

RESULTS

BL-HTWP Attenuates Cerebral Hypoperfusion Post-acute TBI

To evaluate the acute effects of the BL-HTWP on cerebral blood perfusion (CBP) after TBI, TBI was induced by controlled cortical impact (CCI) leading to cortical lesions with reduced CBP. We showed representative high-resolution CBP images with dynamic changes at pre-injury, immediately following CCI (0 h), as well as 1, 2, 4, and 6 h post-CCI in **Figure 2B**. As shown in **Figure 2C**, the mean CBP values determined before CCI were similar among the Sham, CCI, and BL mice. Immediately after CCI, a dramatic decrease in CBP occurred in the CCI and BL groups (134.9 ± 7.7 and 143.90 ± 18.1 PU/mm^2) compared to that of the Sham mice (223.8 ± 8.9 PU/mm^2, all $p < 0.01$). The severe reduction in CBP for the CCI group did not significantly improve within 6 h, but cerebral perfusion for the BL-HTWP group was partly recovered after 1 h and consistently remained higher at 2, 4, and 6 h compared to that in CCI mice (BL vs. CCI, 1 h, 180.4 ± 16.8 vs. 116.3 ± 14.7; 2 h, 183.0 ± 25.6 vs.

119.5 ± 12.1; 4 h, 179.8 ± 21.6 vs. 117.7 ± 12. h, 179.5 ± 23.0 vs. 120.0 ± 11.1 PU/mm^2; all $p < 0.01$). Additionally, CPP in both the CCI and BL groups immediately declined at 0 h post-CCI (25.25 ± 1.87, 23.77 ± 2.96 mmHg) compared with the Sham mice (75.71 ± 1.72 mmHg; all $p < 0.01$). After 24 h, the CPP of mice in the CCI and BL groups increased in varying degrees, but that of BL group consistently remained higher compared to that in CCI mice (all $p < 0.01$) (**Figure 2D**). These results suggested that BL-HTWP treatment promoted CBP and CPP restoration and their maintenance to attenuate cerebral hypoperfusion after acute TBI.

BL-HTWP Improves Neurological Recovery Post-acute TBI

To gain further insight into the efficacy of BL-HTWP in neurological recovery after TBI, motor-evoked potential (MEP) and mNSS tests were performed at 6 h (MEP) (**Figure 3A**), as well as 12, 24, 28, and 72 h (mNSS) post-TBI. Compared with the Sham group, CCI mice had significantly prolonged latency (7.13 ± 1.10 vs. 5.20 ± 0.12 ms, $p < 0.01$) in the left hindlimb and that (5.78 ± 0.58 vs. 5.18 ± 0.13 ms, $p < 0.05$) in the right hindlimb on the bilateral motor cortex stimulation at 6 h post-TBI (**Figure 3B**). Also, CCI mice had sharply deduced amplitude (1.20 ± 0.26 vs. 2.39 ± 0.09 mV, $p < 0.01$) in the left hindlimb, but not significantly changed in the right hindlimb. In the BL group, however, the latency in both hindlimbs (left, 5.12 ± 0.20 ms; right, 5.14 ± 0.19 ms, $p < 0.001$ or 0.05) was decreased, and the amplitude in the left hindlimb (2.04 ± 0.79 mV, $p < 0.01$) was increased after BL-HTWP in comparison with the values of the CCI group. Additionally, in contrast to the Sham group, significant neurological deficits were detected in the CCI and BL groups at 12, 24, 48, and 72 h post-TBI (all $p < 0.01$) (**Figure 3C**). However, the mNSS scores were found to be sharply reduced in BL mice, compared to those in CCI group at 12 h ($p < 0.05$) and 24 h ($p < 0.01$) after TBI. Altogether, these results confirmed that BL-HTWP ameliorated electrophysiological deficit and improved neurological recovery.

BL-HTW Preverses Acute TBI-Induced Hypocoagulable State and Increases the Level of Procoagulant

Because normal hemostasis depends on a balance between bleeding and thrombosis, this balance can be altered following TBI, leading to coagulopathy. So, we questioned whether BL-HTWP treatment is associated with TBI-induced coagulopathy. We first examined the coagulatory state at 6 h post-TBI using conventional coagulation tests (CCTs). PT reflects tissue factor and exogenous coagulation function. APTT mainly reflects the

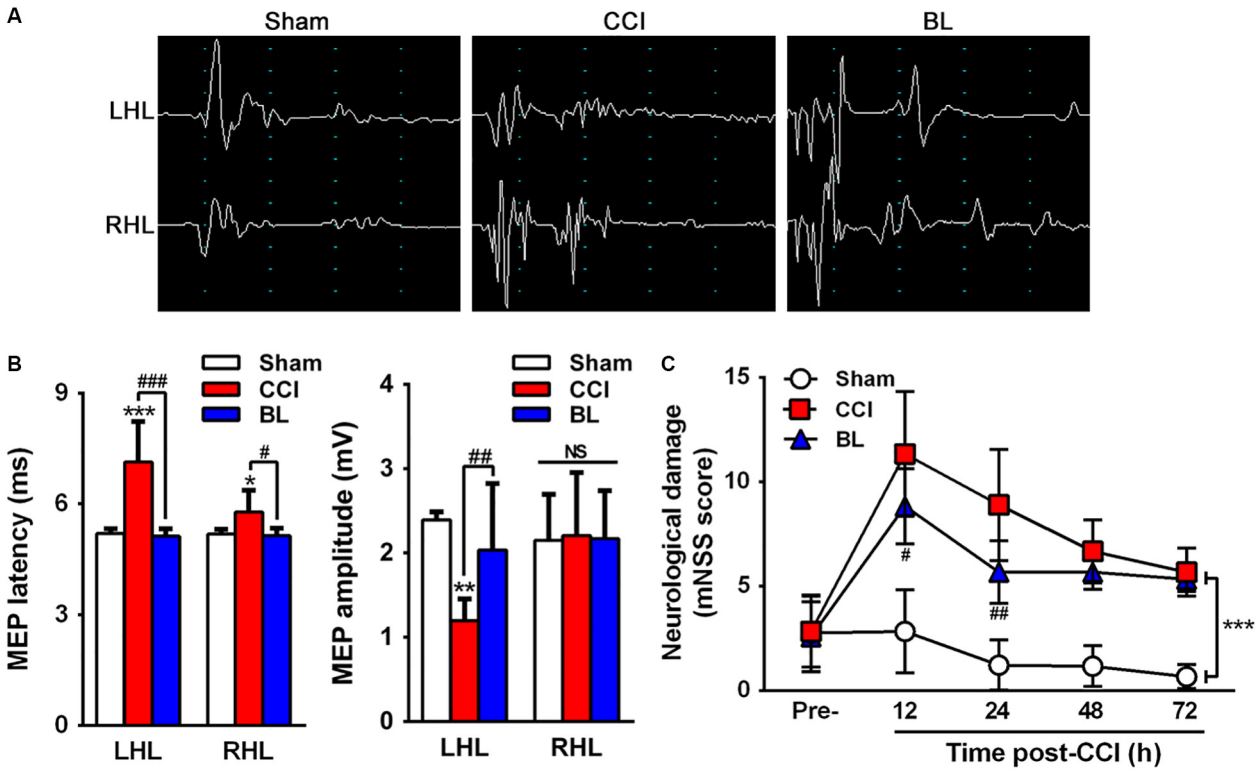

FIGURE 3 | Efficacy of BL-HTWP in neurologic recovery post-TBI. **(A)** Representative images of motor-evoked potential (MEP). LHL, left hindlimb (CCI-contralateral limb); RHL, right hindlimb (CCI-ipsilateral limb). **(B)** Alterations of MEP amplitude and latency in the mice of Sham, CCI, and BL at 6 h after CCI. **(C)** Modified neurological severity (mNSS) score was determined at pre-injury, 12, 24, 48, and 72 h after CCI. Quantitative analysis ($n = 12$) was conducted by one-way ANOVA. $^*p < 0.05$, $^{**}p < 0.01$ vs. Sham; $^{\#}p < 0.05$, $^{\#\#}p < 0.01$, $^{\#\#\#}p < 0.001$ vs. CCI. NS indicates $p > 0.05$.

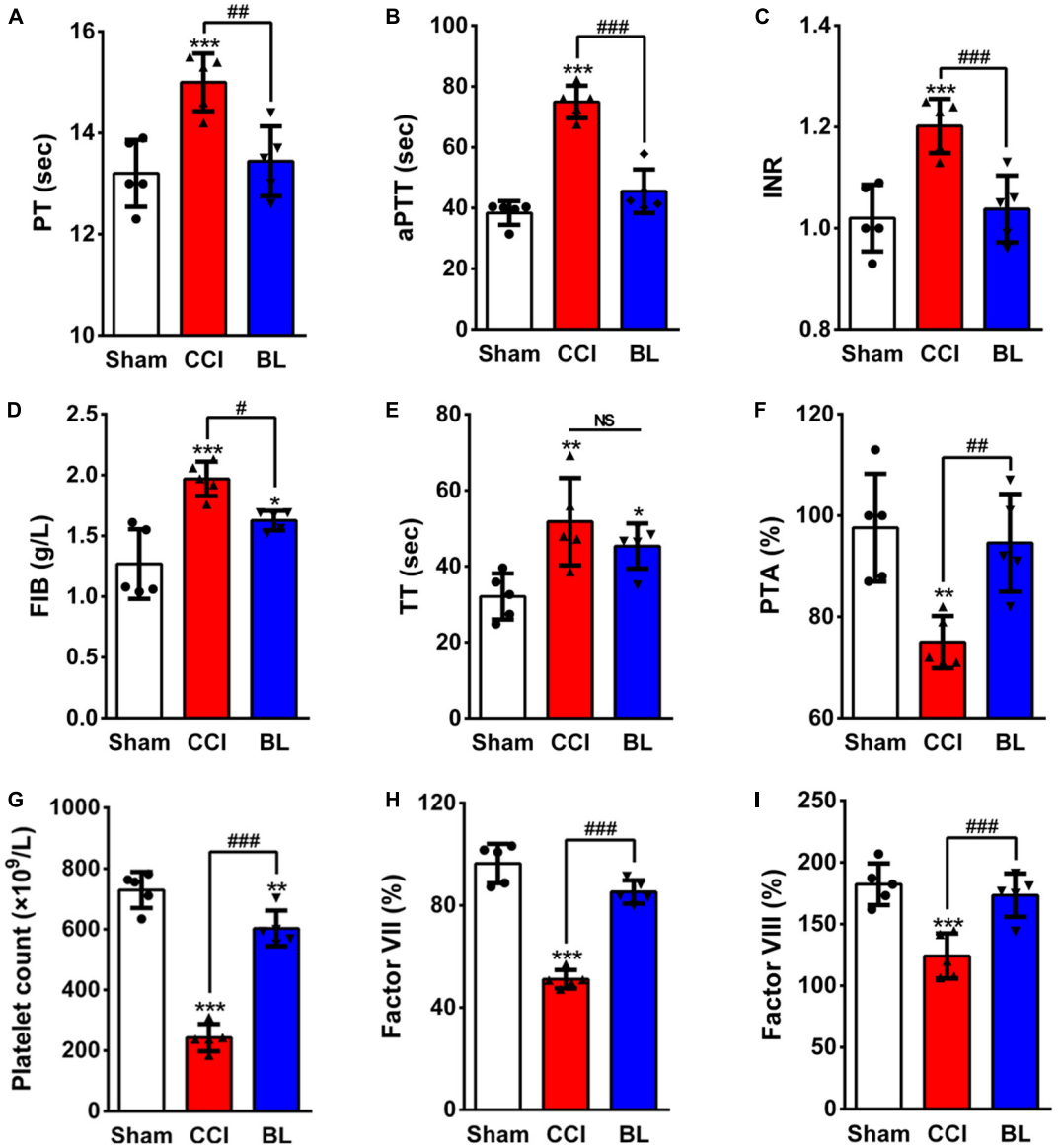

FIGURE 4 | Effects of BL-HTWP on conventional coagulation tests (CCTs) after TBI. At 6 h post-CCI, mice blood samples were assayed for coagulation by the CCT method with prothrombin time (PT, **A**), activated partial thromboplastin time (aPTT, **B**), international normalized ratio (INR, **C**), plasma fibrinogen (FIB, **D**), thrombin time (TT, **E**), prothrombin time activity (PTA, **F**), platelet count **(G)**, Factor VII **(H)**, and Factor VIII **(I)**. Quantitative analysis ($n = 5$) were conducted by one-way ANOVA. $^{*}p < 0.05$, $^{**}p < 0.01$, $^{***}p < 0.001$ vs. Sham; $^{\#}p < 0.05$, $^{\#\#}p < 0.01$, $^{\#\#\#}p < 0.001$ vs. CCI. NS indicates $p > 0.05$.

function of endogenous blood coagulation. The combination of PLT and FIB reflects the ability of thrombosis. When PT and aPTT increased and PLT and FIB decreased, it indicates high DIC risk. Among the most valuable parameters examined in the CCTs assays, the PT and aPTT (15.00 ± 0.57 s, 74.90 ± 5.32 s), INR and TT (1.20 ± 0.05, 51.76 ± 11.51 s), and the FIB values (1.97 ± 0.14 g/L) of the CCI mice were much higher than in the Sham group (PT 13.20 ± 0.66 s, aPTT 38.34 ± 3.90 s, INR 1.02 ± 0.07, TT 32.06 ± 6.05 s, and FIB 1.27 ± 0.29 g/L; $p < 0.001$ or 0.01, respectively) (**Figures 4A–E**). However, they were sharply lower in the BL mice (PT 13.44 ± 0.69 s, aPTT 45.50 ± 7.17 s, INR 1.04 ± 0.07, and FIB 1.63 ± 0.08 g/L) compared with the CCI group ($p < 0.001$, 0.01, or 0.05). There was no significant difference between the BL group and the CCI group in the TT values (45.35 ± 5.96 s vs. 51.76 ± 11.51 s; $p > 0.05$). Additionally, there was significant shorter PTA in CCI mice (75.00 ± 5.15%) than in the Sham controls (97.60 ± 10.64%; $p < 0.01$) (**Figure 4F**), but BL significantly prolonged the PTA (94.60 ± 9.66%) compared with the CCI group ($p < 0.01$). Furthermore, BL-HTWP better preserved the platelet counts (603 vs. 243 × 10^9/L; $p < 0.001$) (**Figure 4G**) and significantly increased in Factor VII (85% vs. 51%; $p < 0.001$) (**Figure 4H**) and Factor VIII (173% vs. 124%; $p < 0.001$) (**Figure 4I**) compared with that of the CCI group, and Factor VII and VIII levels had

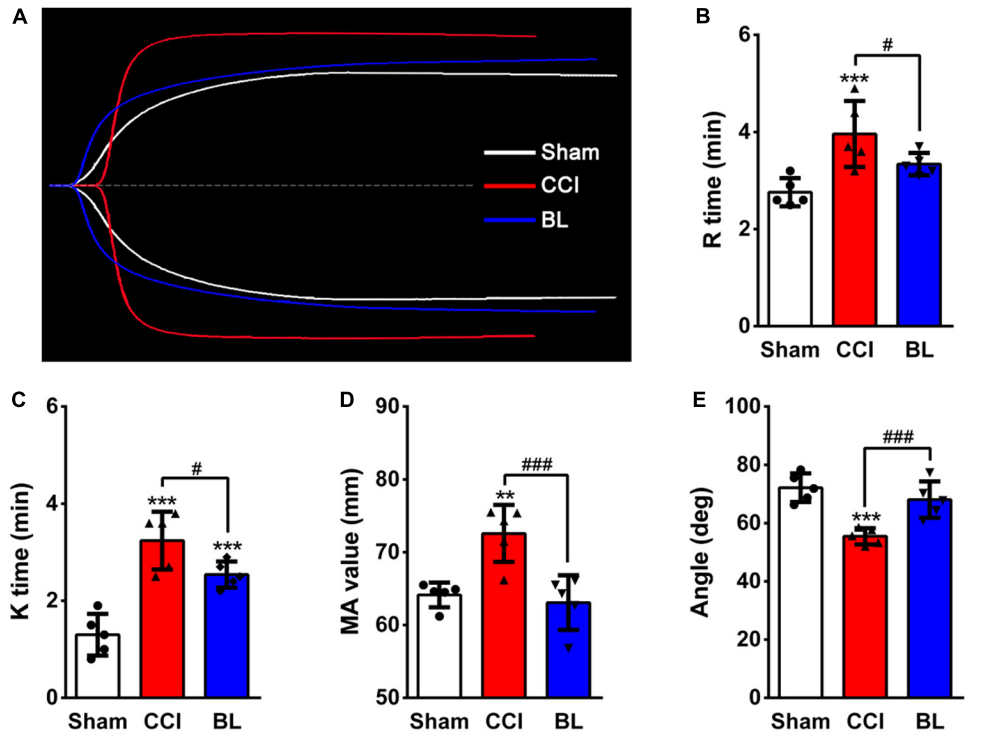

FIGURE 5 | Effects of BL-HTWP on thromboelastography (TEG) values after TBI. **(A)** Representative TEG tracings from the Sham (white line), CCI (red line), and BL (blue line) group. Impact of TEG after bloodletting puncture at HTWP (BL) on R time **(B)**, K time **(C)**, α-angle **(D)**, and MA value **(E)** in mice at 6 h post-CCI. Quantitative analysis (n = 5) were conducted by one-way ANOVA. $^{**}p < 0.01$, $^{***}p < 0.001$ vs. Sham; $^{\#}p < 0.05$, $^{\#\#\#}p < 0.001$ vs. CCI.

no statistical difference compared to those of the Sham mice (all $p > 0.05$).

In addition to CCTs, thromboelastography (TEG) assays were also performed. Representative TEG tracings from the groups are also shown in **Figure 5A**. Among the parameters examined in the TEG assays, the R time, K time, and MA value of the CCI groups (3.96 ± 0.68 min, 3.24 ± 0.59 min, 72.58 mm) were significantly higher compared with the Sham control (2.76 ± 0.29 min, 1.30 ± 0.43 min, 64.14 ± 1.69 mm; $p < 0.001$ or 0.01) (**Figures 5B–D**), but the α angle of the CCI group (55.46 ± 2.81°) was sharply lower than that of the Sham group (72.16 ± 4.90°; $p < 0.001$) (**Figure 5E**). However, the BL mice showed a shorter R (3.34 ± 0.23 min), K (2.54 ± 0.27 min), MA value (63.08 ± 3.74 mm), and a longer α angle (68.06 ± 6.26°) compared with that of the CCI group ($p < 0.001$ or 0.05). Taken together, these results demonstrated that TBI induced a hypocoagulable state with prolonged bleeding at 6 h post-CCI; however, treatment of blood with BL-HTWP resulted in a shorter PT, aPTT, INR, FIB, a lower R, K, MA value, a greater PTA, and a larger angle than CCI alone, indicating that BL-HTWP could reverse acute TBI-induced hypocoagulability.

BL-HTWP Promotes BBB Integrity to Reduce Vasogenic Edema

Coagulation abnormalities increased risk for potentially dangerous bleeding and worse outcome after TBI. In this regard, we explored whether BL-HTWP treatment could attenuate progression of intracranial hemorrhagic lesions by reversing hypocoagulability at 6 h after TBI. As expected, BL mice showed smaller cortical lesion sizes than those of CCI animals, and representative examples of cresyl violet-staining sections are shown in **Figure 6A**. *H&E* examination also confirmed the presence of tissue loss and intracranial hemorrhage at the area surrounding the cortical lesion of the CCI mice, but BL-treated mice displayed smaller hemorrhagic areas (**Figure 6B**).

After TBI, disruption of cerebral blood vessels – mainly in a blood–brain barrier (BBB) breakdown – results in the progression of hemorrhagic lesions, which underlies brain edema formation. So, the effects of BL-HTWP on BBB permeability and brain edema were observed. Levels of EB extravasation of the injured hemisphere were significantly higher in the CCI group (7.5 ± 1.1 μg/g) compared with those in the Sham control (2.6 ± 0.3 μg/g, $p < 0.01$). However, the extravasation demonstrated lower values in the BL group (4.8 ± 0.8 μg/g) than those in the CCI mice ($p < 0.01$) (**Figure 6C**). Additionally, CCI mice developed obvious brain edema (78.8 ± 0.5%) compared with the Sham group (76.1 ± 0.8%, $p < 0.05$), whereas the value in the BL mice was lower (76.3 ± 1.0%) than those of the CCI group ($p < 0.01$), and similar to that of the Sham animals ($p > 0.05$) (**Figure 6D**). Overall, these results suggested that BL-HTWP ameliorated TBI-induced cerebrovascular histopathology including disruption of BBB and vasogenic cerebral edema formation.

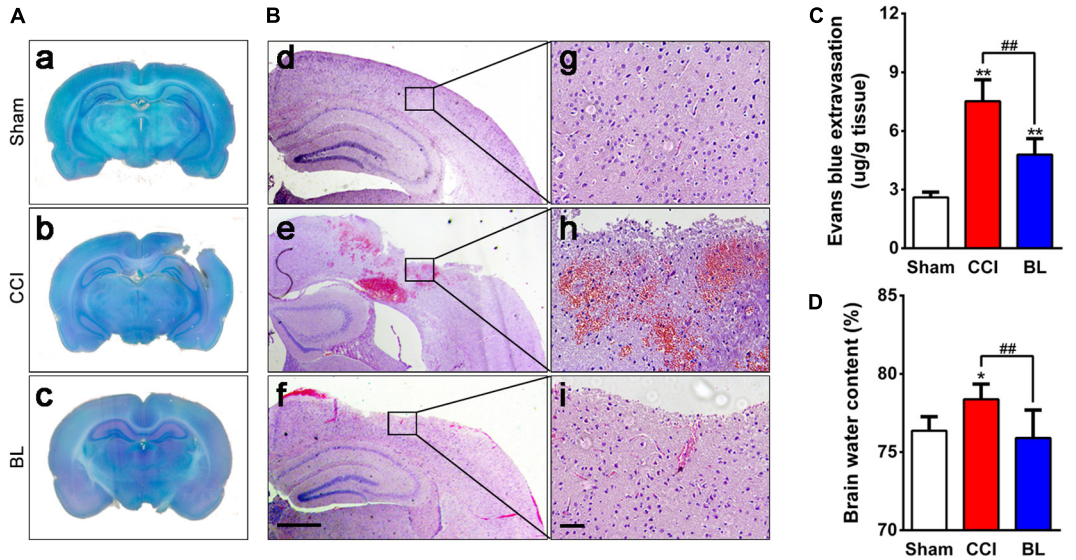

FIGURE 6 | Effects of BL-HTWP on neurological damage and cerebrovascular histopathological changes post-TBI. Brain tissues were collected at 6 h after TBI. **(A)** Lesion assessment was performed on cresyl violet-staining brain sections. **(B)** Microbleedings were observed with hematoxylin and eosin (H&E) staining. (d–f) Representative images of contusion areas visualized with H&E staining. Scale bar, 250 μm. (g–i) Magnification of images shown in (d–f). Scale bar, 50 μm. **(C)** Blood–brain barrier permeability was measured by assessing the extravasation of Evans blue (EB) dye. **(D)** Cerebral edema was evaluated by water content of the brain tissue with the wet-to-dry weight ratio. Quantitative analysis (n = 4) were conducted by one-way ANOVA. $^{*}p < 0.05$, $^{**}p < 0.01$ vs. Sham; $^{\#\#}p < 0.01$ vs. CCI.

BL-HTWP Reduces the Damage of Gliovascular Unit

In order to evaluate the damage of gliovascular unit generated in the perilesional area of mice after TBI, brain sections were immunostained for NeuN (**Figure 7A**), GFAP (**Figure 7B**), and Iba-1 (**Figure 7C**), which are specific markers of neurons, astrocytes, and microglia, respectively. As shown in **Figure 7D**, NeuN-positive neurons accounted for approximately 80% in the Sham mice, but this percentage was dramatically decreased at 6 h after TBI, with only approximately 39% of cells expressing NeuN ($p < 0.001$). However, the percentage of NeuN^{+}-cells in the BL group was higher (∼52%) than those in the CCI group ($p < 0.01$).

Additionally, In the Sham brains, GFAP and Iba-1 immunoreactivity were relatively weak in the Sham brains. At 6 h post-TBI, the percentage of GFAP^{+}- and Iba-1^{+}-cells (18.06 ± 4.20% and 17.78 ± 2.33%) were sharply upregulated in the perilesional area compared with those of the Sham group (4.44 ± 0.85% and 6.32 ± 0.92%, all $p < 0.001$). In contrast, fewer GFAP^{+}-cells (7.85 ± 0.82%, $p < 0.001$) and Iba-1^{+}-cells (11.43 ± 2.96%, $p < 0.01$) were found in the BL group than in the CCI mice.

BL-HTWP Regulates Multiple Hallmarks of Coagulopathy in TBI

To identify biochemical alterations induced by TBI and further explore the underlying mechanisms of protective action of BL-HTWP, a time course experiment was performed to evaluate the changes of multiple protein expression levels related to blood–brain barrier integrity, inflammation, and trophic factors at 6, 24, 48, and 72 h after TBI with Western blotting analysis (**Figure 8A**).

Expression States of Occludin, ZO-1, and AQP4

As shown in **Figures 8Ba–c**, levels of Occludin and ZO-1 were found to be significantly lower in the CCI than in the Sham group at different time points ($p < 0.001$ or 0.01), while levels of those were dramatically increased in the BL compared with those in the CCI group ($p < 0.001$) except for the Occludin levels at 24 h post-TBI. Levels of AQP4, on the other hand, were significantly higher in both the CCI and BL groups than in the Sham group over a broad period (all $p < 0.001$), but BL mice showed lower levels of AQP4 at 6 h ($p < 0.05$) and 24–72 h (all $p < 0.01$) than those of the CCI mice.

Expression States of IL-6, IL-1β, and ICAM-1

As shown in **Figures 8Bd–f**, IL-6, IL-1β, and ICAM-1 levels were strongly elevated in CCI mice above Sham ($p < 0.001$ or 0.01) except for the IL-6 levels at 24 h post-TBI. In contrast, levels of those proteins were dramatically decreased in the BL compared with those in the CCI group ($p < 0.001$).

Expression States of BDNF, VEGF, and HIF-1α

As shown in **Figures 8Bg–h**, levels of BDNF and VEGF levels were reduced spontaneously at 6, 24, 48, and 72 h post-TBI. On the contrary, the expression levels of BDNF and VEGF were always maintained as the higher states in the BL mice than those in the CCI groups (all $p < 0.001$). Interestingly, the level of HIF-1α sharply increased at 6 h and decreased from 24 to 72 h compared with the Sham mice (all $p < 0.001$). However, the elevated levels of HIF-1α were reversed by the administration of BL immediately after TBI, and this low level was maintained over a broad period compared with the CCI group (all $p < 0.001$) (**Figure 8Bi**).

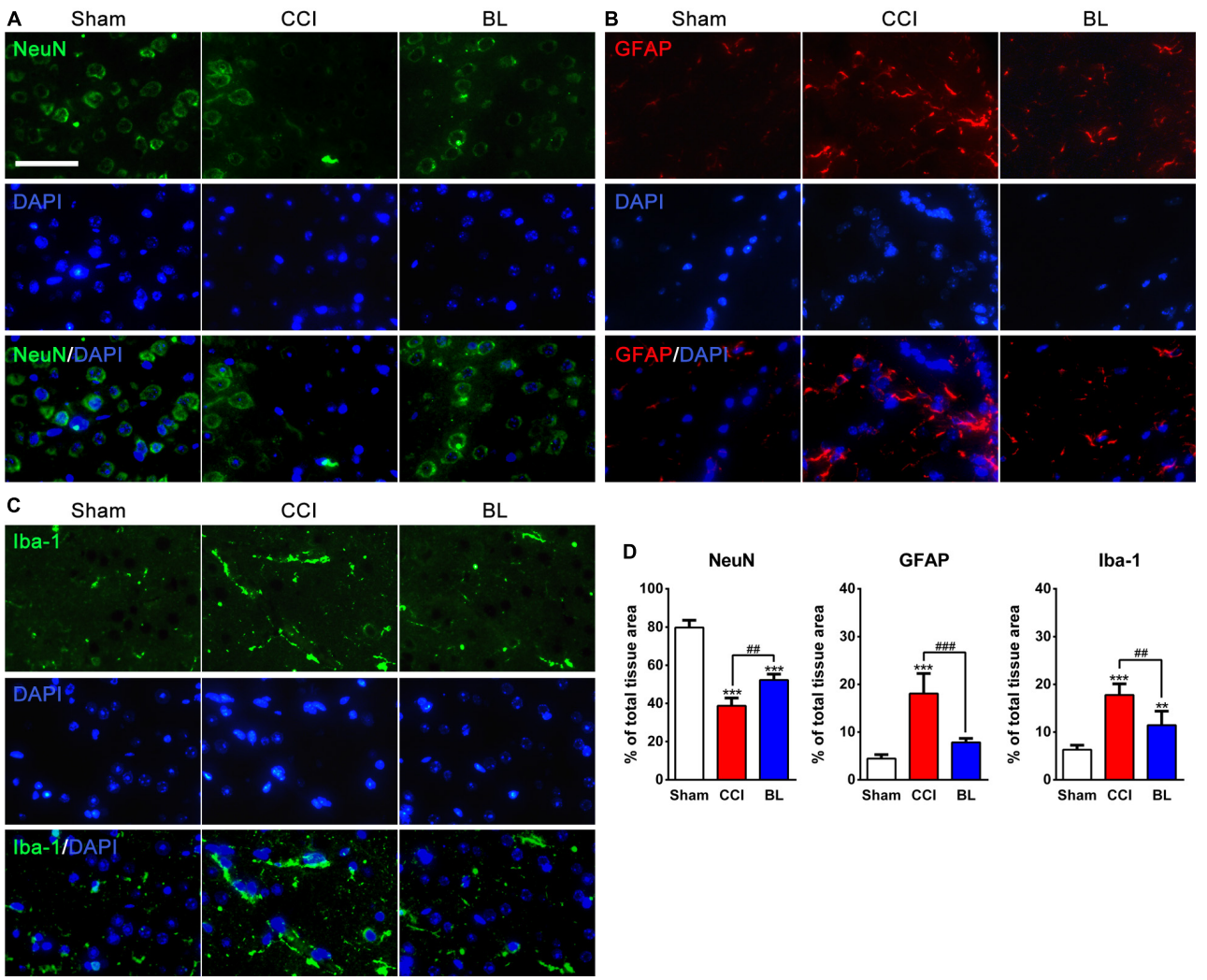

FIGURE 7 | Neuroprotective effects of BL-HTWP against neural death and activation of microglia and astrocytes post-TBI. Brain tissues were collected at 6 h after TBI, and the presence of neural death and microglia or astrocyte activation was visualized by immunofluorescence in the perilesional brain area of mice. **(A–C)** Representative images (green: NeuN or Iba-1, red: GFAP, blue: DAPI). Scale bar, 50 μm. **(D)** Quantification of percentage of $NeuN^+$-, $GFAP^+$-, and Iba-1^+-cells of total tissue area, respectively. Quantitative analysis ($n = 4$) was conducted by one-way ANOVA. $^{**}p < 0.01$, $^{***}p < 0.001$ vs. Sham; $^{\#\#}p < 0.01$, $^{\#\#\#}p < 0.001$ vs. CCI.

Overall, these data indicated that BL-HTWP might play a vital role in mediating the upregulation of tight-junction molecules to protect the BBB integrity, downregulation of pro-inflammatory cytokines to attenuate neuroinflammation, or modulation of trophic factors to promote neuroprotection.

DISCUSSION

In the present study, we demonstrated for the first time that BL-HTWP, a treatment of traditional Chinese medicine, attenuated cerebral hypoperfusion, electrophysiological and neurological deficits in mice after acute TBI. These functions may be associated with amelioration of intracranial hemorrhagic lesions and cerebral edema caused by reversing acute TBI-induced hypocoagulable state. We further revealed that the anti-edematous effect of BL-HTWP may be through alleviating BBB breakdown (vasogenic edema) and attenuating activation of glial cells (cytotoxic edema), indicating that it was necessary for mediating the upregulation of tight-junction molecules to protect the BBB integrity, downregulation of pro-inflammatory cytokines to attenuate neuroinflammation, or modulation of trophic factors to promote neuroprotection.

By all accounts to date, normal hemostasis depends on an intricate balance between bleeding and thrombosis formation, and this balance can be altered after trauma. Conversely, coagulopathic bleeding is extremely difficult to control, resulting in diffuse bleeding involving uninjured sites.

Recently, various studies have highlighted the importance of coagulopathy in isolated TBI subsequently displaying hemorrhagic progression and ongoing intracranial hemorrhage. More than 60% of patients with severe head injury have

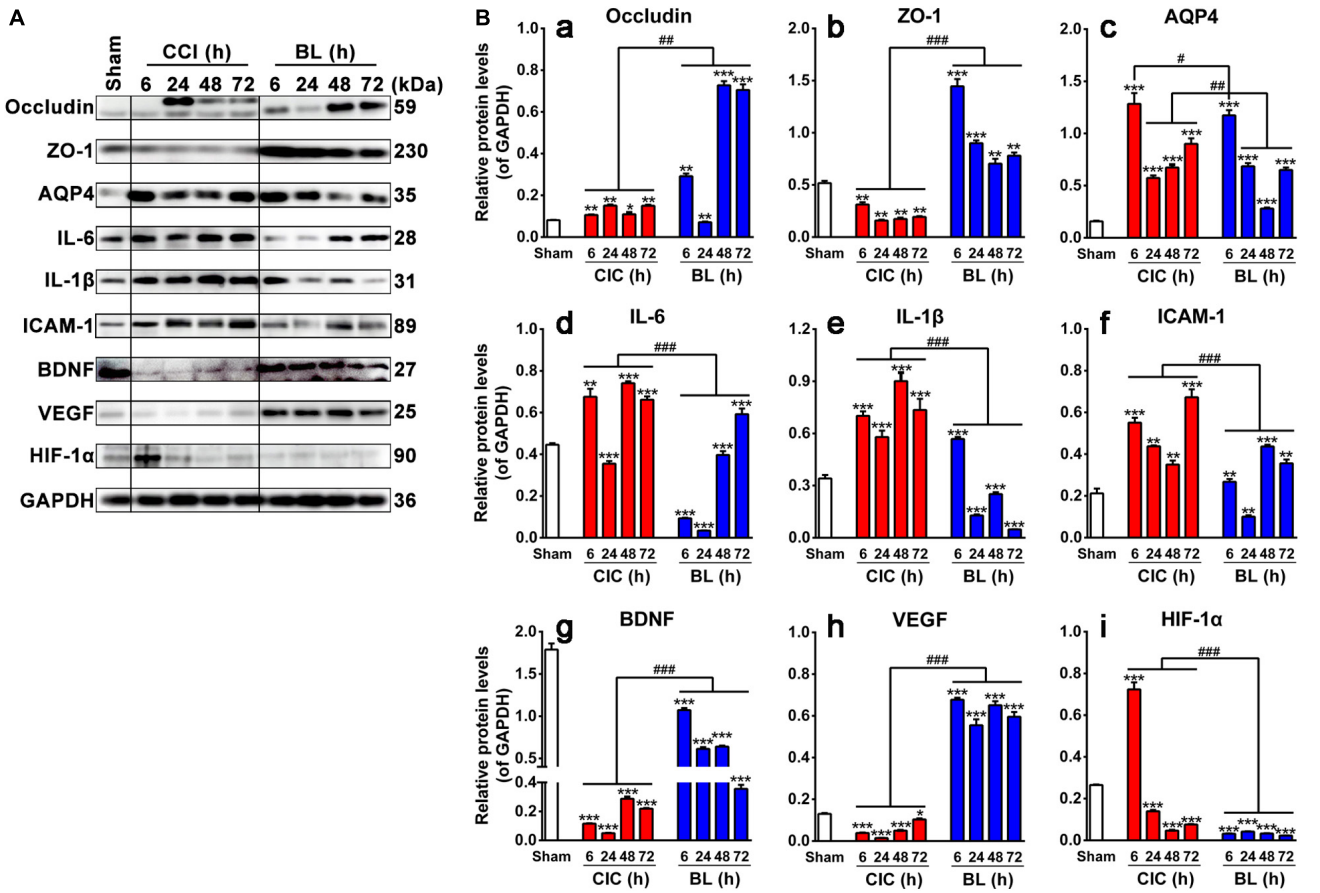

FIGURE 8 | Effects of BL-HTWP on blood–brain barrier, inflammation, and neurogenesis-related hallmarks post-TBI. **(A)** Representative Western blot results for the protein expression at 6, 24, 48, and 72 h after TBI. **(B)** Quantification of relative protein levels of Occludin (a), ZO-1 (b), AQP4 (c), IL-6 (d), IL-1β (e), ICAM-1 (f), BDNF (g), VEGF (h), and HIF-1α (i), respectively. Quantitative analysis (n = 4 for Sham group; n = 12 for CCI and BL groups, respectively) were conducted by one-way ANOVA. $^{*}p < 0.05$, $^{**}p < 0.01$, $^{***}p < 0.001$ vs. Sham; $^{\#}p < 0.05$, $^{\#\#}p < 0.01$, $^{\#\#\#}p < 0.001$ vs. CCI.

coagulopathy. Approximately 50% of patients with coagulopathy after TBI exhibit progressive bleeding injury and persistent intracranial hemorrhage within 48 h (Tong et al., 2012; Castellino et al., 2014; Juratli et al., 2014; Yuan et al., 2016; Jenkins et al., 2018; Zhang et al., 2018). Coagulopathy presented a power predictor of outcome and prognosis in TBI, contributing to higher risk of mortality and unfavorable outcome than in TBI without coagulopathy. An evidence-based study of 1,718 sample sizes found that patients with coagulopathy after TBI can have a mortality rate of up to 45.1% (Epstein et al., 2014; Talving et al., 2009). Early correction of coagulation disorders after TBI is independently related to the survival of patients (Epstein et al., 2015). The most common choice for the treatment of coagulation disorders associated with TBI is the transfusions of blood components, including red blood cell transfusions, fresh frozen plasma and platelet-concentrate transfusions (Baharoglu et al., 2016; Boutin et al., 2016; Chang et al., 2017). Besides, there is the treatment of coagulation factor concentrates, such as prothrombin complex concentrate, fibrinogen, recombinant Factor VIIa (Brown et al., 2010; Rourke et al., 2012; Yanamadala et al., 2014), and some drug treatments including hemostatic agents, tranexamic acid, and desmopressin (CRASH-2 Trial Collaborators et al., 2010; Roberts et al., 2013; Naidech et al., 2014; Myles Paul et al., 2017). The above treatments have made some progress in alleviating hypercoagulable state and preventing progressive hemorrhage, but there is no consensus on the strategy for the use of blood transfusion therapy (Washington et al., 2011). The treatment of coagulation factor concentrates and drug therapy also has potential risks (Shen et al., 2015). The reason might be due to the complexity of the cascade system of blood coagulation mechanism. It is difficult to balance the whole system by simply regulating one of a link. Nevertheless, a much complex series of events associated with coagulopathy occurs either simultaneously or sequentially after TBI, and the clinical coagulopathic bleeding course has been considered to reflect rapid progression from a state of hypercoagulability to hypocoagulability (Maegele et al., 2017). Intravascular coagulation can occur within 6 h after TBI, which is characterized by activation of the coagulation cascade system, resulting in fibrin deposition and intravascular microthrombosis, potential disturbance of cerebral microcirculation, and increased consumption of coagulation, leading to further platelet depletion

(Chauny et al., 2016). On the other hand, microvessels serve as a circulation platform for initiating and amplifying coagulation, which usually occurs on the surface of activated platelets and locates at the injured site, resulting in non-focal and diffuse clotting. Previous studies have also shown that TBI, itself, does not cause early coagulation disorders, but it must be combined with low perfusion to cause coagulation disorders, and the destruction of the integrity of the cerebrovascular microvascular wall caused by impact will quickly activate the coagulation cascade (Maegele et al., 2017).

As the most commonly used assessment of coagulation abnormalities, conventional coagulation tests (CCTs) and Thromboelastography (TEG) can facilitate prediction of outcome after TBI (Gonzalez et al., 2014; Joseph et al., 2014). Several studies had used the prothrombin time (PT), activated partial thromboplastin time (aPTT), international normalized ratio (INR), or other values for CCTs (MacLeod et al., 2003; Hoyt et al., 2008), as well as reaction time (R time, which means aggregation time of fiber factor), clotting time (K time, which means the time of fibrin formation), maximum thrombus amplitude (MA, reflect the binding ability of platelets to fibrin), and alpha angle values (α values, reflect the rate of fibrinogen coagulation) for TEG to describe coagulopathy after TBI (Davis et al., 2013; Castellino et al., 2014). As expected, the results of our study found decreased coagulation activity at 6 h following isolated TBI, prolonged PT, aPTT, INR, TT, increased FIB, as well as decreased PTA. Furthermore, the increased R, K, and MA values, as well as decreased α angle, also indicate hypocoagulable tendencies. In contrast, BL mice received immediate treatment of BL-HTWP showing recovery of hypocoagulopathy induced by TBI, which was demonstrated by CCTs or TEG variables, such as decreased PT, aPTT, INR, TT, R, K, and MA values, as well as elevated PTA and α angle at 6 h after TBI, suggesting that BL-HTWP could reverse acute TBI-induced hypocoagulable state. Taking current studies into consideration, we further tried to decipher the underlying mechanisms of this anti-hypocoagulopathic effect of BL-HTWP after acute TBI.

After severe trauma and blood loss, the organism is faced with the competing interests of both limiting further blood loss and limiting microvascular thrombosis to maintain end-organ perfusion in a low-flow state (Chang et al., 2016). However, coagulopathy induced by isolated TBI is likely different from that of other trauma owing to, at least in part, the existence of intact blood–brain barrier (BBB), which may play a key role in the response to vessel injury and coagulation. The release of tissue factors (TF) caused by BBB destruction is also considered to be one of the main causes of blood coagulation disorder after TBI and runs through the process of TBI. Within minutes of TBI, due to the destruction of the BBB, a large number of TF enters the peripheral blood and widely binds with VII factors to trigger exogenous coagulation (Hoffman and Monroe, 2009; Genet et al., 2013; Salehi et al., 2017). With the further destruction of the blood–brain barrier after secondary injury, a large number of platelets are consumed, resulting in intracranial hemorrhage and systemic DIC (Castellino et al., 2014; Atefi et al., 2016; Leeper et al., 2019). The human brain contains ∼644 km of blood vessels, which supply neural cells with oxygen, energy, and nutrients from the brain to the systemic circulation (Zlokovic, 2008). BBB is a continuous endothelial membrane within brain microvessels, and endothelial cells are connected by tight junctions, which involve all kinds of proteins such as Occludin and ZO-1 (Sweeney et al., 2018). Loss of BBB integrity following TBI increases vascular permeability and contributes to reduced cerebral blood and elevated vasogenic cerebral edema (Unterberg et al., 2004; Marmarou et al., 2006), and the latter is thought be a result of AQP protein dysfunction, which regulates the balance between preventing and facilitating water movement (Filippidis et al., 2016). In this study, we found that BL-HTWP treatment promoted cerebral blood perfusion restoration and improved performance in the MEP and mNSS tests after acute TBI. We also found this treatment reduced formation of gaps in tight junctions (Occludin and ZO-1) and expression of AQP4 and showed a protective effect on BBB integrity after TBI, implying that BL-HTWP plays a role in inhibition of vasogenic cerebral edema and may reduce the risk of cerebral hemorrhage by protecting the BBB by slowing the release of TF and thus retaining more coagulation factors.

A growing body of evidence has demonstrated that brain tissue/vessel injury, and even hypoperfusion, activated inflammation pathways triggered by endothelium activation after TBI and aggravated coagulopathy then occurred with extensive cross-talk between coagulation and inflammation pathways (Sillesen et al., 2014; Di Battista et al., 2016; Foley and Conway, 2016). Thrombin can act on microglia, cause cytoskeleton rearrangement of microglia, stimulate their proliferation and activation, and increase the synthesis of proinflammatory mediators such as IL-1β and IL-6 (Nimmerjahn et al., 2005; Schachtrup et al., 2010; Lee and Suk, 2017). Furthermore, these proinflammatory cytokines could lead to the upregulation of intercellular adhesion molecule-1 (ICAM-1) – a marker of endothelial damage – which mediated leukocyte transendothelial migration as part of a cascade of molecular interactions and associated with prolonged inflammation (Svetlov et al., 2012; Glushakova et al., 2014; Vignoli et al., 2018). Fibrinogen may affect the process of neuronal repair after trauma. It has been shown that fibrinogen inhibits neurite growth by activating the epidermal growth factor receptor in neurons and which promotes astroglial scar formation by acting as a potential carrier of transforming growth factor-β (Schachtrup et al., 2007; Schachtrup et al., 2010). Above these factors may cause the damage of the gliovascular unit and aggravate the cross-talk between coagulation and inflammation (Wolburg et al., 2009). In this study, we found larger numbers of $GFAP^+$–astrocyte and Iba-1^+–microglia, and higher levels of IL-6, IL-1β, and ICAM-1 in the peritraumatic areas of brain tissue after TBI than those of the sham control, which was in accord with previous studies. In contrast, fewer $GFAP^+$- and Iba-1^+-cells and lower levels of proinflammatory cytokines were mentioned above in the BL group than in the CCI mice, further suggesting that the function of BL-HTWP is associated with anti-inflammatory effect, which acts at least partly through the inhibition of coagulation.

In parallel, it has been generally assumed that molecular events post-TBI could be counterbalanced by two central processes that are involved in endogenous repair: trophic support and immunomodulation that mediate neuroinflammation (Tovar-y-Romo et al., 2016). Laboratory and clinical studies have demonstrated that trophic factors such as BDNF and VEGF are closely associated with the maintenance of normal function of the nervous system. Increased BDNF level can reduce excitotoxicity, microglial activation, and neuroinflammation (Jiang et al., 2011; Baydyuk et al., 2015). Additionally, the role of VEGF as an endogenous factor of recovery after CNS damage is proven in stroke, where ischemia induces the stabilization of HIF-1α as a transcriptional activator of VEGF (Lopez-Hernandez et al., 2012). In this study, we found low levels of BDNF and VEGF at different time points after TBI, whereas BL-HTWP significantly increased their expression levels. Intriguingly, the level of HIF-1α quickly increased at 6 h and then decreased rapidly from 24 to 72 h after TBI, but this low level was maintained over a broad period in the BL group, which showed an asynchronous state with VEGF level. These results suggested that BL-HTWP indirectly upregulates the VEGF expression via other upstream activators rather than HIF-1α. Further studies delineating the mechanism of these observed effects are warranted.

BL-HTWP has been applied as one of the first aid measures in various types of emergency for more than 3,000 years in China. Previous studies have found that it can improve the state of consciousness and increase systolic blood pressure in patients with severe craniocerebral trauma (Zhang et al., 2016). Other studies have shown that it reduces PT and aPTT time in patients with blood coagulation caused by stroke (Zhang et al., 2003). The molecular mechanism of BL-HTWP restoring the balance of coagulation system is not clear, but it may be related to maintaining cerebral microcirculation perfusion and protecting the structure and function of BBB (Li et al., 2017, 2019; Yu et al., 2017). To date, studies have shown that stimulating specific body surface sites can cause specific nuclei to secrete a variety of neurotransmitters; for example, a study activated the mesencephalic aqueduct to secrete orexin by stimulating Neiguan (PC6), which is located in the median nerve (Chen et al., 2018). Another study activated endorphin receptors in the hypothalamic arcuate nucleus by stimulating Shenmen (HT7), which is located at the distribution of the ulnar nerve in the wrist flexor tendon (Chang et al., 2019). Interestingly, we can see that the neurotransmitters activated by stimulating different acupoints are not exactly the same, which may be linked to the anatomical structure of the body surface where the acupoints are located. The position of the hand twelve *Jing-well* points is unique, all located at the end of the fingertips, and the fingertips have very rich sensory nerve endings and capillary network. From this, we can speculate that when using BL-HTWP treatment, first, the pain stimulus signal was uploaded to the nerve center after being amplified several times and activated certain specific nucleus to secrete certain types of neurotransmitters. To some extent, it plays a role in regulating vasoconstriction and stabilizing blood pressure. The second is to stimulate the vascular wall of the capillary network at the fingertips of the hand by bloodletting. The coagulation reaction is initiated locally and amplified through the cascade effect of the coagulation system, and then the coagulation disorder of the whole body is adjusted in a hedging manner. It is also worth noting that BL-HTWP is a treatment consisting of multiple stimuli. According to our analysis, there are at least three factors: bleeding, pain stimulation, and acupoint specificity. Studies have shown that no matter which of the above factors is excluded, although the amplitude of cerebral blood flow can be increased to a certain extent, its effect is significantly weakened than before (Zhou and Tp, 1998; Zhou et al., 1999). This also shows that BL-HTWP is a systematic regulation method, which may result in coordinated regulation of multiple targets.

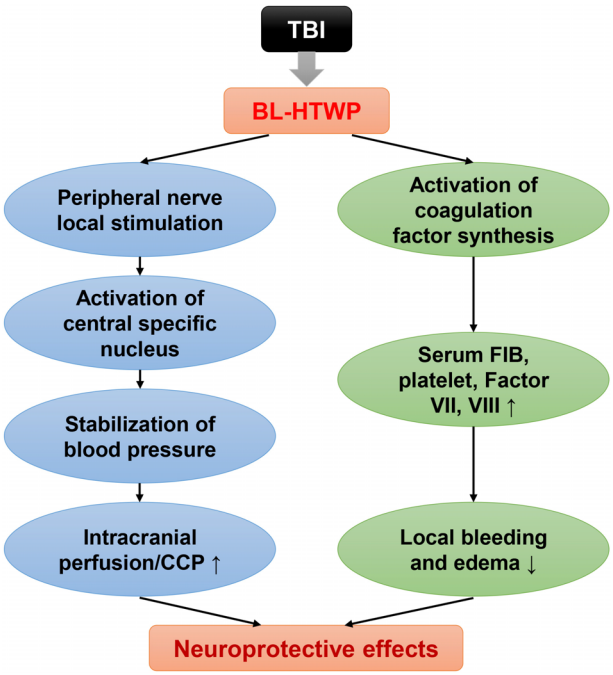

FIGURE 9 | Mechanisms of neuroprotective effects of BL-HTWP post-TBI.

Taken together, these results demonstrated that coagulopathy is closely involved in the pathologic process of tissue/vessel injury, BBB disruption, and inflammatory response after acute TBI in mice. We conclude that bloodletting puncture at hand twelve *Jing*-well points improve neurological function after TBI in two ways (**Figure 9**). First, local stimulation of peripheral nerves after acupuncture causes central specific nucleus activation, which stabilizes or increases blood pressure and increases intracranial blood perfusion. Second, blood loss after bloodletting puncture causes the level of procoagulant factor synthesis, ameliorating local brain tissue hemorrhage and brain edema.

DATA AVAILABILITY STATEMENT

The datasets generated for this study are available on request to the corresponding author.

ETHICS STATEMENT

The animal study was reviewed and approved by the Institutional Animal Care and Use Committee at Characteristic Medical Center of Chinese People's Armed.

AUTHOR CONTRIBUTIONS

S-XC, BL, LZ, and SZ conceived and designed the experiments. BL, XZ, and T-LY conducted the experiments. Z-WX, YG, Y-MG, D-WP and Y-LC helped with the eperiments. S-XC and BL analyzed the data. BL and S-XC wrote the manuscript. All authors discussed and commented on the manuscript.

FUNDING

This study was funded by the National Natural Science Foundation Major Program of China (81891003), National High-Tech R&D Program of China (2016YFC1101502), Science and Technology Program of Tianjin (15ZXLCSY00040), Technology Research Projects of PAL (AWS15J001), and Key Project of Natural Science Foundation for University of Anhui Province of China (KJ2018ZD027).

SUPPLEMENTARY MATERIAL

The Supplementary Material for this article can be found online at: https://www.frontiersin.org/articles/10.3389/fnins.2020.00403/full#supplementary-material

REFERENCES

Atefi, G., Aisiku, O., Shapiro, N., Hauser, C., Dalle, L. J., Flaumenhaft, R., et al. (2016). Complement activation in trauma patients alters platelet function. *Shock* 46(3 Suppl. 1), 83–88. doi: 10.1097/SHK.0000000000000675

Baharoglu, M. I., Cordonnier, C., Al-Shahi, S. R., de Gans, K., Koopman, M. M., Brand, A., et al. (2016). Platelet transfusion versus standard care after acute stroke due to spontaneous cerebral haemorrhage associated with antiplatelet therapy (PATCH): a randomised, open-label, phase 3 trial. *Lancet* 387, 2605–2613. doi: 10.1016/S0140-6736(16)30392-30390

Baydyuk, M., Wu, X. S., He, L., and Wu, L. G. (2015). Brain-derived neurotrophic factor inhibits calcium channel activation, exocytosis, and endocytosis at a central nerve terminal. *J. Neurosci.* 35, 4676–4682.

Boutin, A., Chasse, M., Shemilt, M., Lauzier, F., Moore, L., Zarychanski, R., et al. (2016). Red blood cell transfusion in patients with traumatic brain injury: a systematic review and meta-analysis. *Transfus Med Rev.* 30, 15–24. doi: 10.1016/j.tmrv.2015.08.004

Brown, C. V., Foulkrod, K. H., Lopez, D., Villareal, J., and Foarde, K. (2010). Recombinant factor VIIa for the correction of coagulopathy before emergent craniotomy in blunt trauma patients. *J. Trauma* 68, 348–352. doi: 10.1097/TA.0b013e3181bbfb6b

Castellino, F. J., Chapman, M. P., Donahue, D. L., Thomas, S., Moore, E. E., Wohlauer, M. V., et al. (2014). Traumatic brain injury causes platelet adenosine diphosphate and arachidonic acid receptor inhibition independent of hemorrhagic shock in humans and rats. *J. Trauma Acute Care Surg.* 76, 1169–1176. doi: 10.1097/TA.0000000000000216

Chang, R., Cardenas, J. C., Wade, C. E., and Holcomb, J. B. (2016). Advances in the understanding of trauma-induced coagulopathy. *Blood* 128, 1043–1049. doi: 10.1182/blood-2016-01-636423

Chang, R., Folkerson, L. E., Sloan, D., Tomasek, J. S., Kitagawa, R. S., Choi, H. A., et al. (2017). Early plasma transfusion is associated with improved survival after isolated traumatic brain injury in patients with multifocal intracranial hemorrhage. *Surgery* 161, 538–545. doi: 10.1016/j.surg.2016.08.023

Chang, S., Kim, D. H., Jang, E. Y., Yoon, S. S., Gwak, Y. S., Yi, Y. J., et al. (2019). Acupuncture attenuates alcohol dependence through activation of endorphinergic input to the nucleus accumbens from the arcuate nucleus. *Sci. Adv.* 5:x1342. doi: 10.1126/sciadv.aax1342

Chauny, J.-M., Marquis, M., Bernard, F., Williamson, D., Albert, M., Laroche, M., et al. (2016). Risk of delayed intracranial hemorrhage in anticoagulated patients with mild traumatic brain injury: systematic review and meta-analysis. *J. Emerg. Med.* 51, 519–528. doi: 10.1016/j.jemermed.2016.05.045

Chen, Y. H., Lee, H. J., Lee, M. T., Wu, Y. T., Lee, Y. H., Hwang, L. L., et al. (2018). Median nerve stimulation induces analgesia via orexin-initiated endocannabinoid disinhibition in the periaqueductal gray. *Proc. Natl. Acad. Sci. U.S.A.* 115, E10720–E10729. doi: 10.1073/pnas.1807991115

Cheng, S. X., Xu, Z. W., Yi, T. L., Yu, Z. Q., Yang, X. S., Jin, X. H., et al. (2018). iTRAQ-based quantitative proteomics reveals the new evidence base for traumatic brain injury treated with targeted temperature management. *Neurotherapeutics* 15, 216–232. doi: 10.1007/s13311-017-0591-2

CRASH-2 Trial Collaborators, Shakur, H., Roberts, I., Bautista, R., Caballero, J., Coats, T., Dewan, Y., et al. (2010). Effects of tranexamic acid on death, vascular occlusive events, and blood transfusion in trauma patients with significant haemorrhage (CRASH-2): a randomised, placebo-controlled trial. *Lancet* 376, 23–32. doi: 10.1016/S0140-6736(10)60835-5

Cybularz, P. A., Brothers, K., Singh, G. M., Feingold, J. L., Lewis, M. E., and Niesley, M. L. (2015). The Safety of acupuncture in patients with cancer therapy-related thrombocytopenia. *Med. Acupunct.* 27, 224–229. doi: 10.1089/acu.2015.1099

Davis, P. K., Musunuru, H., Walsh, M., Cassady, R., Yount, R., Losiniecki, A., et al. (2013). Platelet dysfunction is an early marker for traumatic brain injury-induced coagulopathy. *Neurocrit. Care* 18, 201–208. doi: 10.1007/s12028-012-9745-6

Di Battista, A. P., Rhind, S. G., Hutchison, M. G., Hassan, S., Shiu, M. Y., Inaba, K., et al. (2016). Inflammatory cytokine and chemokine profiles are associated with patient outcome and the hyperadrenergic state following acute brain injury. *J. Neuroinflamm.* 13:40. doi: 10.1186/s12974-016-0500-503

Epstein, D. S., Mitra, B., Cameron, P. A., Fitzgerald, M., and Rosenfeld, J. V. (2015). Acute traumatic coagulopathy in the setting of isolated traumatic brain injury: definition, incidence and outcomes. *Br. J. Neurosurg.* 29, 118–122. doi: 10.3109/02688697.2014.950632

Epstein, D. S., Mitra, B., O'Reilly, G., Rosenfeld, J. V., and Cameron, P. A. (2014). Acute traumatic coagulopathy in the setting of isolated traumatic brain injury: a systematic review and meta-analysis. *Injury* 45, 819–824. doi: 10.1016/j.injury.2014.01.011

Filippidis, A. S., Carozza, R. B., and Rekate, H. L. (2016). Aquaporins in brain edema and neuropathological conditions. *Int. J. Mol. Sci.* 18:55. doi: 10.3390/ijms18010055

Foley, J. H., and Conway, E. M. (2016). Cross talk pathways between coagulation and inflammation. *Circ. Res.* 118, 1392–1408. doi: 10.1161/CIRCRESAHA.116.306853

GBD 2016 Traumatic Brain Injury and Spinal Cord Injury Collaborators (2019). Global, regional, and national burden of neurological disorders, 1990–2016: a systematic analysis for the global burden of disease study 2016. *Lancet Neurol.* 18, 459–480. doi: 10.1016/S1474-4422(18)30499-X

Genet, G. F., Bentzer, P., Ostrowski, S. R., and Johansson, P. I. (2017). Resuscitation with pooled and pathogen-reduced plasma attenuates the increase in brain water content following traumatic brain injury and hemorrhagic shock in rats. *J. Neurotrauma* 34, 1054–1062. doi: 10.1089/neu.2016.4574

Genet, G. F., Johansson, P. I., Meyer, M. A., Solbeck, S., Sorensen, A. M., Larsen, C. F., et al. (2013). Trauma-induced coagulopathy: standard coagulation tests, biomarkers of coagulopathy, and endothelial damage in patients with traumatic brain injury. *J. Neurotrauma* 30, 301–306. doi: 10.1089/neu.2012.2612

Glushakova, O. Y., Johnson, D., and Hayes, R. L. (2014). Delayed increases in microvascular pathology after experimental traumatic brain injury are associated with prolonged inflammation, blood-brain barrier disruption, and

progressive white matter damage. *J. Neurotrauma* 31, 1180–1193. doi: 10.1089/neu.2013.3080

Gonzalez, E., Moore, E. E., Moore, H. B., Chapman, M. P., Silliman, C. C., and Banerjee, A. (2014). Trauma-induced coagulopathy: an institution's 35 year perspective on practice and research. *Scand. J. Surg.* 103, 89–103. doi: 10.1177/1457496914531927

Greuters, S., van den Berg, A., Franschman, G., Viersen, V. A., Beishuizen, A., Peerdeman, S. M., et al. (2011). Acute and delayed mild coagulopathy are related to outcome in patients with isolated traumatic brain injury. *Crit. Care* 15:R2. doi: 10.1186/cc9399

Harhangi, B. S., Kompanje, E. J., Leebeek, F. W., and Maas, A. I. (2008). Coagulation disorders after traumatic brain injury. *Acta Neurochir.* 150, 165–175. doi: 10.1007/s00701-007-1475-1478

Hoffman, M., and Monroe, D. M. (2009). Tissue factor in brain is not saturated with factor VIIa. *Stroke* 40, 2882–2884. doi: 10.1161/STROKEAHA.109.555433

Hoyt, D. B., Dutton, R. P., Hauser, C. J., Hess, J. R., Holcomb, J. B., Kluger, Y., et al. (2008). Management of coagulopathy in the patients with multiple injuries: results from an international survey of clinical practice. *J. Trauma* 65, 764–765. doi: 10.1097/TA.0b013e318185fa9f

Huang, H. Y., Sharma, H. S., Chen, L., Saberi, H. S., and Mao, G. S. (2019). 2018 yearbook of neurorestoratology. *J. Neurorestoratol.* 7, 8–17. doi: 10.26599/JNR.2019.9040003

Huang, H. Y., Skaper, S., Mao, G. S., Jeon, S. R., Chen, L., and Dimitrijevic, M. L. (2018). 2017 yearbook of neurorestoratology. *J. Neurorestoratol.* 6, 67–73. doi: 10.2147/JN.S132589

Jenkins, D. R., Craner, M. J., Esiri, M. M., and DeLuca, G. C. (2018). Contribution of fibrinogen to inflammation and neuronal density in human traumatic brain injury. *J. Neurotrauma* 35, 2259–2271. doi: 10.1089/neu.2017.5291

Jiang, J. Y., Gao, G. Y., Feng, J. F., Huang, X. J., et al. (2019). Traumatic brain injury in China. *Lancet Neurol.* 18, 286–295. doi: 10.1016/S1474-4422(18)30469-1

Jiang, Y., Wei, N., Lu, T., Zhu, J., Xu, G., and Liu, X. (2011). Intranasal brain-derived neurotrophic factor protects brain from ischemic insult via modulating local inflammation in rats. *Neuroscience* 172, 398–405. doi: 10.1016/j.neuroscience.2010.10.054

Joseph, B., Aziz, H., Zangbar, B., Kulvatunyou, N., Pandit, V., O'Keeffe, T., et al. (2014). Acquired coagulopathy of traumatic brain injury defined by routine laboratory tests: which laboratory values matter? *J. Trauma Acute Care Surg.* 76, 121–125. doi: 10.1097/TA.0b013e3182a9cc95

Juratli, T. A., Zang, B., Litz, R. J., Sitoci, K. H., Aschenbrenner, U., Gottschlich, B., et al. (2014). Early hemorrhagic progression of traumatic brain contusions: frequency, correlation with coagulation disorders, and patient outcome: a prospective study. *J. Neurotrauma* 31, 1521–1527. doi: 10.1089/neu.2013.3241

Laroche, M., Kutcher, M. E., Huang, M. C., Cohen, M. J., and Manley, G. T. (2012). Coagulopathy after traumatic brain injury. *Neurosurgery* 70, 1334–1345. doi: 10.1227/NEU.0b013e31824d179b

Lee, S. H., and Suk, K. (2017). Emerging roles of protein kinases in microglia-mediated neuroinflammation. *Biochem. Pharmacol.* 146, 1–9. doi: 10.1016/j.bcp.2017.06.137

Leeper, C. M., Strotmeyer, S. J., Neal, M. D., and Gaines, B. A. (2019). Window of opportunity to mitigate trauma-induced coagulopathy. *Ann. Surg.* 270, 528–534. doi: 10.1097/SLA.0000000000003464

Li, X., Chen, C., Yang, X., Wang, J., Zhao, M.-L., Sun, H.-T., et al. (2017). Acupuncture improved neurological recovery after traumatic brain injury by activating BDNF/TrkB pathway. *Evid. Based Complement Alternat. Med.* 2017:8460145. doi: 10.1155/2017/8460145

Li, B., Tian, J. P., Zhang, S., Guo, Y., Tu, Y., Yi, T. L., et al. (2019). Effect of bloodletting acupuncture at twelve jing-well points of hand on microcirculatory disturbance in mice with traumatic brain injury. *Chin. Acupunct. Moxibust.* 39, 1075–1080. doi: 10.13703/j.0255-2930.2019.10.012

Lopez-Hernandez, B., Posadas, I., Podlesniy, P., Abad, M. A., Trullas, R., and Cena, V. (2012). HIF-1alpha is neuroprotective during the early phases of mild hypoxia in rat cortical neurons. *Exp. Neurol.* 233, 543–554. doi: 10.1016/j.expneurol.2011.11.040

MacLeod, J. B., Lynn, M., McKenney, M. G., Cohn, S. M., and Murtha, M. (2003). Early coagulopathy predicts mortality in trauma. *J. Trauma* 55, 39–44. doi: 10.1097/01.TA.0000075338.21177.EF

Maegele, M., Schöchl, H., Menovsky, T., Maréchal, H., Marklund, N., Buki, A., et al. (2017). Coagulopathy and haemorrhagic progression in traumatic brain injury: advances in mechanisms, diagnosis, and management. *Lancet Neurol.* 16, 630–647. doi: 10.1016/S1474-4422(17)30197-7

Main, B. S., Villapol, S., Sloley, S. S., Rodriguez, O. C., and Burns, M. P. (2018). Apolipoprotein E4 impairs spontaneous blood brain barrier repair following traumatic brain injury. *Mol. Neurodegener.* 13:17. doi: 10.1186/s13024-018-0249-5

Marmarou, A., Signoretti, S., Fatouros, P. P., Portella, G., Aygok, G. A., and Bullock, M. R. (2006). Predominance of cellular edema in traumatic brain swelling in patients with severe head injuries. *J. Neurosurg.* 104, 720–730. doi: 10.3171/jns.2006.104.5.720

McCully, S. P., and Schreiber, M. A. (2013). Traumatic brain injury and its effect on coagulopathy. *Semin. Thromb. Hemost.* 39, 896–901. doi: 10.1055/s-0033-1357484

Myles Paul, S., Smith Julian, A., Forbes, A., and Silbert, B. (2017). Tranexamic acid in patients undergoing coronary-artery surgery. *N. Engl. J. Med.* 376, 136–148. doi: 10.1056/NEJMoa1606424

Naidech, A. M., Maas, M. B., Levasseur-Franklin, K. E., Liotta, E. M., Guth, J. C., Berman, M., et al. (2014). Desmopressin improves platelet activity in acute intracerebral hemorrhage. *Stroke* 45, 2451–2453. doi: 10.1161/STROKEAHA.114.006061

National Institutes of Health (1998). NIH consensus conference. Acupuncture. *JAMA* 280, 1518–1524. doi: 10.1001/jama.280.17.1518

Nimmerjahn, A., Kirchhoff, F., and Helmchen, F. (2005). Resting microglial cells are highly dynamic surveillants of brain parenchyma in vivo. *Science* 308, 1314–1318. doi: 10.1126/science.1110647

Roberts, I., Shakur, H., Coats, T., Hunt, B., Balogun, E., Barnetson, L., et al. (2013). The CRASH-2 trial: a randomised controlled trial and economic evaluation of the effects of tranexamic acid on death, vascular occlusive events and transfusion requirement in bleeding trauma patients. *Health Technol. Assess.* 17, 1–79. doi: 10.3310/hta17100

Rourke, C., Curry, N., Khan, S., Taylor, R., Raza, I., Davenport, R., et al. (2012). Fibrinogen levels during trauma hemorrhage, response to replacement therapy, and association with patient outcomes. *J. Thromb. Haemost.* 10, 1342–1351. doi: 10.1111/j.1538-7836.2012.04752.x

Salehi, A., Zhang, J. H., and Obenaus, A. (2017). Response of the cerebral vasculature following traumatic brain injury. *J. Cereb. Blood Flow Metab.* 37, 2320–2339. doi: 10.1177/0271678X17701460

Schachtrup, C., Lu, P., Jones, L. L., Lu, J., and Sachs, B. D. (2007). Fibrinogen inhibits neurite outgrowth via beta 3 integrin-mediated phosphorylation of the EGF receptor. *Proc. Natl. Acad. Sci. U.S.A.* 104, 11814–11819. doi: 10.1073/pnas.0704045104

Schachtrup, C., Ryu, J. K., Helmrick, M. J., Vagena, E., Galanakis, D. K., Degen, J. L., et al. (2010). Fibrinogen triggers astrocyte scar formation by promoting the availability of active TGF-beta after vascular damage. *J. Neurosci.* 30, 5843–5854. doi: 10.1523/JNEUROSCI.0137-10.2010

Shen, X., Dutcher, S. K., Palmer, J., Liu, X., Kiptanui, Z., Khokhar, B., et al. (2015). A systematic review of the benefits and risks of anticoagulation following traumatic brain injury. *J. Head Trauma Rehabil.* 30, E29–E37. doi: 10.1097/HTR.0000000000000077

Sillesen, M., Rasmussen, L. S., Jin, G., Jepsen, C. H., Imam, A., Johansson, P., et al. (2014). Assessment of coagulopathy, endothelial injury, and inflammation after traumatic brain injury and hemorrhage in a porcine model. *J. Trauma Acute Care Surg.* 76, 12–19. doi: 10.1097/TA.0b013e3182aaa675

Silverberg, N. D., Duhaime, A. C., and Iaccarino, M. A. (2019). Mild Traumatic Brain Injury in 2019-2020. *JAMA* [Epub ahead of print], doi: 10.1001/jama.2019.18134

Spahn, D. R., Bouillon, B., Cerny, V., Duranteau, J., Filipescu, D., Hunt, B. J., et al. (2019). The European guideline on management of major bleeding and coagulopathy following trauma: fifth edition. *Crit. Care* 23:98. doi: 10.1186/s13054-019-2347-2343

Svetlov, S. I., Prima, V., Glushakova, O., Svetlov, A., Kirk, D. R., Gutierrez, H., et al. (2012). Neuro-glial and systemic mechanisms of pathological responses in rat models of primary blast overpressure compared to "composite" blast. *Front. Neurol.* 3:15. doi: 10.3389/fneur.2012.00015

Sweeney, M. D., Sagare, A. P., and Zlokovic, B. V. (2018). Blood-brain barrier breakdown in Alzheimer disease and other neurodegenerative disorders. *Nat. Rev. Neurol.* 14, 133–150. doi: 10.1038/nrneurol.2017.188

Talving, P., Benfield, R., Hadjizacharia, P., Inaba, K., Chan, L. S., and Demetriades, D. (2009). Coagulopathy in severe traumatic brain injury: a prospective study. *J. Trauma* 66, 61–62. doi: 10.1097/TA.0b013e318190c3c0

Tong, W. S., Zheng, P., Zeng, J. S., Guo, Y. J., Yang, W. J., Li, G. Y., et al. (2012). Prognosis analysis and risk factors related to progressive intracranial haemorrhage in patients with acute traumatic brain injury. *Brain Inj.* 26, 1136–1142. doi: 10.3109/02699052.2012.666437

Tovar-y-Romo, L. B., Penagos-Puig, A., and Ramirez-Jarquin, J. O. (2016). Endogenous recovery after brain damage: molecular mechanisms that balance neuronal life/death fate. *J. Neurochem.* 136, 13–27. doi: 10.1111/jnc.13362

Tu, Y., Miao, X. M., Yi, T. L., Chen, X. Y., Sun, H. T., Cheng, S. X., et al. (2016). Neuroprotective effects of bloodletting at Jing points combined with mild induced hypothermia in acute severe traumatic brain injury. *Neural Regen. Res.* 11, 931–936. doi: 10.4103/1673-5374.184491

Unterberg, A. W., Stover, J., Kress, B., and Kiening, K. L. (2004). Edema and brain trauma. *Neuroscience* 129, 1021–1029. doi: 10.1016/j.neuroscience.2004.06.046

Vignoli, A., Marchetti, M., and Falanga, A. (2018). Acute promyelocytic leukemia cell adhesion to vascular endothelium is reduced by heparins. *Ann. Hematol.* 97, 1555–1562. doi: 10.1007/s00277-018-3343-3344

Wang, N., Zhang, Y., Wu, L., Wang, Y., Cao, Y., He, L., et al. (2014). Puerarin protected the brain from cerebral ischemia injury via astrocyte apoptosis inhibition. *Neuropharmacology* 79, 282–289. doi: 10.1016/j.neuropharm.2013.12.004

Washington, C. W., Schuerer, D. J., and Grubb, R. J. (2011). Platelet transfusion: an unnecessary risk for mild traumatic brain injury patients on antiplatelet therapy. *J. Trauma* 71, 358–363. doi: 10.1097/TA.0b013e318220ad7e

Wolburg, H., Noell, S., Mack, A., Wolburg-Buchholz, K., and Fallier-Becker, P. (2009). Brain endothelial cells and the glio-vascular complex. *Cell Tissue Res.* 335, 75–96. doi: 10.1007/s00441-008-0658-659

Xu, X., Zheng, C., Zhang, M., Wang, W., and Huang, G. (2014). A randomized controlled trial of acupuncture to treat functional constipation: design and protocol. *BMC Complement. Altern. Med.* 14:423. doi: 10.1186/1472-6882-14-423

Yanamadala, V., Walcott, B. P., Fecci, P. E., Rozman, P., Kumar, J. I., Nahed, B. V., et al. (2014). Reversal of warfarin associated coagulopathy with 4-factor prothrombin complex concentrate in traumatic brain injury and intracranial hemorrhage. *J. Clin. Neurosci.* 21, 1881–1884. doi: 10.1016/j.jocn.2014.05.001

Yu, N., Wang, Z., Chen, Y., Yang, J., Lu, X., and Guo, Y. (2017). The ameliorative effect of bloodletting puncture at hand twelve Jing-well points on cerebral edema induced by permanent middle cerebral ischemia via protecting the tight junctions of the blood-brain barrier. *BMC Complement. Altern Med.* 17:470. doi: 10.1186/s12906-017-1979-6

Yuan, Q., Sun, Y. R., Wu, X., Yu, J., Li, Z. Q., Du, Z. Y., et al. (2016). Coagulopathy in traumatic brain injury and its correlation with progressive hemorrhagic injury: a systematic review and meta-analysis. *J. Neurotrauma* 33, 1279–1291. doi: 10.1089/neu.2015.4205

Yue, Y., Pan, X., Zhang, S., Jin, J., and Wang, W. (2015). A randomized controlled trial of puncturing and bloodletting at twelve hand jing points to treat acute carbon monoxide poisoning as adjunct to first aid treatment: a study protocol. *Evid. Based Complement. Alternat. Med.* 2015:827305. doi: 10.1155/2015/827305

Zhang, D., Gong, S., Jin, H., Wang, J., and Hou, L. (2015). Coagulation parameters and risk of progressive hemorrhagic injury after traumatic brain injury: a systematic review and meta-analysis. *Biomed. Res Int.* 2015:261825. doi: 10.1155/2015/261825

Zhang, J., Jiang, Y.-J., and Lu, H.-X. (2003). Clinical study on the effect of pricking blood therapy on the blood coagulation system in the patient of cerebral infarction at restoration stage. *Chin. Acupunct. Moxibust.* 023, 44–47.

Zhang, J., Yi, G., and Geng, L. (2016). Clinical evaluation of treating severe traumatic brain injury by pricking blood on 12 hand well acupoints and nasal feeding coix seed with mild hypothermia. *World Chin. Med.* 3, 514–518.

Zhang, J., Zhang, F., and Dong, J. (2018). Coagulopathy induced by traumatic brain injury: systemic manifestation of a localized injury. *Blood* 131, 2001–2006. doi: 10.1182/blood-2017-11-784108

Zhou, G.-P., Tangping, X., and Zhetian, W. (1999). Effect of pricking "twelve-well points" induced painful stimulation on rabbit rheoencephalogram. *Acupunct. Res.* 02, 108–110.

Zhou, G.-P., and Tp, X. (1998). Comparison of effects of the twelve jing points of hands and Quchi(LI 11) blood letting on rheoencephalogram in rabbits of cerebral ischemia. *Acupunct. Res.* 23, 268–270.

Zlokovic, B. V. (2008). The blood-brain barrier in health and chronic neurodegenerative disorders. *Neuron* 57, 178–201. doi: 10.1016/j.neuron.2008.01.003

Conflict of Interest: The authors declare that the research was conducted in the absence of any commercial or financial relationships that could be construed as a potential conflict of interest.

frontiers in Neuroscience

HYPOTHESIS AND THEORY
published: 09 June 2020
doi: 10.3389/fnins.2020.00581

Persistent Neurovascular Unit Dysfunction: Pathophysiological Substrate and Trigger for Late-Onset Neurodegeneration After Traumatic Brain Injury

*Yunxiang Zhou[1], Qiang Chen[1], Yali Wang[1], Haijian Wu[2], Weilin Xu[2], Yuanbo Pan[2], Shiqi Gao[2], Xiao Dong[2], John H. Zhang[3,4] and Anwen Shao[2]**

[1] Department of Surgical Oncology, The Second Affiliated Hospital, School of Medicine, Zhejiang University, Hangzhou, China, [2] Department of Neurosurgery, The Second Affiliated Hospital, School of Medicine, Zhejiang University, Hangzhou, China, [3] Department of Physiology and Pharmacology, Basic Sciences, School of Medicine, Loma Linda University, Loma Linda, CA, United States, [4] Department of Anesthesiology, Neurosurgery and Neurology, School of Medicine, Loma Linda University, Loma Linda, CA, United States

OPEN ACCESS

Edited by:
Eng-King Tan,
National Neuroscience Institute (NNI), Singapore

Reviewed by:
Ye Xiong,
Henry Ford Health System, United States
Zezong Gu,
University of Missouri, United States

***Correspondence:**
Anwen Shao
21118116@zju.edu.cn;
anwenshao@sina.com

Specialty section:
This article was submitted to Neurodegeneration, a section of the journal Frontiers in Neuroscience

Received: 03 February 2020
Accepted: 12 May 2020
Published: 09 June 2020

Citation:
Zhou Y, Chen Q, Wang Y, Wu H, Xu W, Pan Y, Gao S, Dong X, Zhang JH and Shao A (2020) Persistent Neurovascular Unit Dysfunction: Pathophysiological Substrate and Trigger for Late-Onset Neurodegeneration After Traumatic Brain Injury. Front. Neurosci. 14:581. doi: 10.3389/fnins.2020.00581

Traumatic brain injury (TBI) represents one of the major causes of death worldwide and leads to persisting neurological deficits in many of the survivors. One of the most significant long-term sequelae deriving from TBI is neurodegenerative disease, which is a group of incurable diseases that impose a heavy socio-economic burden. However, mechanisms underlying the increased susceptibility of TBI to neurodegenerative disease remain elusive. The neurovascular unit (NVU) is a functional unit composed of neurons, neuroglia, vascular cells, and the basal lamina matrix. The key role of NVU dysfunction in many central nervous system diseases has been revealed. Studies have proved the presence of prolonged structural and functional abnormalities of the NVU after TBI. Moreover, growing evidence suggests impaired NVU function is also implicated in neurodegenerative diseases. Therefore, we propose the Neurovascular Unit Dysfunction (NVUD) Hypothesis, in which the persistent NVU dysfunction is thought to underlie the development of post-TBI neurodegeneration. We deduce NVUD Hypothesis through relational inference and supporting evidence, and suggest continued NVU abnormalities following TBI serve as the pathophysiological substrate and trigger yielding chronic neuroinflammation, proteinopathies and oxidative stress, consequently leading to the progression of neurodegenerative diseases. The NVUD Hypothesis may provide potential treatment and prevention strategies for TBI and late-onset neurodegenerative diseases.

Keywords: traumatic brain injury, neurodegenerative disease, neurovascular unit, hypothesis, neuroinflammation, proteinopathy, oxidative stress, blood–brain barrier

INTRODUCTION

Traumatic brain injury (TBI) represents one of the major causes of mortality and disability worldwide, with a global burden of approximately US$ 400 billion annually (GBD 2016; Maas et al., 2017; de la Tremblaye et al., 2018; GBD 2016 Traumatic Brain Injury and Spinal Cord Injury Collaborators, 2019). Patients surviving the TBI usually suffer from various long-term neurological and neuropsychiatric sequelae, which include (but not limited to) neurodegenerative diseases (Cruz-Haces et al., 2017) and sleep disturbances (Castriotta et al., 2007; Barshikar and Bell, 2017). Actually, TBI-induced neurodegenerative disease was first introduced in the 19th century in professional boxers who repeatedly suffered head trauma (Martland, 1928). From then on, accumulating evidence has suggested that TBI is a significant risk factor for a variety of neurodegenerative diseases such as Alzheimer's disease (AD) (Mortimer et al., 1991; Fleminger et al., 2003; Hayes et al., 2017; LoBue et al., 2019), Parkinson's disease (PD) (Goldman et al., 2006; Jafari et al., 2013), and amyotrophic lateral sclerosis (ALS) (Chen et al., 2007; Franz et al., 2019). Notably, sleep deprivation itself is an important predisposing factor for the development of neurodegenerative diseases (Boespflug and Iliff, 2018; Shokri-Kojori et al., 2018; Cordone et al., 2019).

Neurodegenerative diseases are declared a group of chronic diseases burdening the global aging society (de Lau and Breteler, 2006; Li et al., 2013). Alzheimer's disease is considered the most common neurodegenerative disorders, followed by PD. In 2015, the former incurred worldwide losses totaling US$ 818 billion, an increase of 35% over the previous five years (Fotuhi et al., 2009; Masters et al., 2015; Ascherio and Schwarzschild, 2016; Wimo et al., 2017). Although symptomatic and etiological treatments targeting patients with AD or PD may help alleviate some of the physical or mental symptoms of these incurable, age-related diseases, no treatment strategies have been proved sufficiently effective thus far (Ascherio and Schwarzschild, 2016; Kumar et al., 2016; Mendiola-Precoma et al., 2016; Orimo, 2017). Another neurodegenerative disease, ALS, although relatively less frequent, has a high fatality rate and a median survival of only 14 months from the time of diagnosis (Luna et al., 2019). Therefore, considering the huge medical and social burden of neurodegenerative diseases and the increased incidence in patients with prior TBI, exploring the underlying mechanisms of causality between TBI and post-TBI neurodegenerative diseases is of great significance.

Abbreviations: Aβ, amyloid β peptide; AD, Alzheimer's disease; ALS, amyotrophic lateral sclerosis; AQP4, aquaporin-4; BBB, blood–brain barrier; CNS, central nervous system; DTI, diffusion tensor imaging; ECM, extracellular matrix; fMRI, functional magnetic resonance imaging; HD, Huntington disease; HTT, Huntingtin gene; ICAM-1, intracellular adhesion molecule-1; IL, interleukin; iNOS, inducible nitric oxide synthase; JAK, Janus kinase; MCP, monocyte chemoattractant protein; MMP, matrix metalloprotein; MRS, magnetic resonance spectroscopy; MSNs, medium spiny neurons; NFκB, nuclear factor-κB; NVU, neurovascular unit, NVUD, Neurovascular Unit Dysfunction; PD, Parkinson's disease, PET, positron emission tomography; RNS, reactive nitrogen species, ROS, reactive oxygen species; SPECT, Single Photon Emission Computed Tomography, STAT1, signal transducers and activators of transcription 1 SWI, susceptibility weight imaging; TBI, traumatic brain injury; TGF-β, transforming growth factor-β, TJ, tight junction; TNF, tumor necrosis factor.

The neurovascular unit (NVU; **Figure 1**) was originally introduced as a conceptual framework for cerebrovascular diseases, especially ischemic stroke, and has recently been identified as a key player in many other central nervous system (CNS) diseases, including TBI, whose primary and secondary pathologic processes can lead to persistent structural or metabolic abnormalities of the NVU (Zhang et al., 2005; Lok et al., 2015; Perez et al., 2017). Recently, more and more lines of evidence have proved that NVU dysfunction is also related to neurodegenerative diseases (Cai et al., 2017b). Thus, NVU dysfunction participates in both TBI and neurodegenerative diseases, and it may be a candidate mechanism underlying the TBI-induced neurodegenerative diseases. To understand the underlying mechanisms further, we propose the Neurovascular Unit Dysfunction (NVUD) Hypothesis, in which persistent NVU dysfunction accounts for the pathophysiological substrate and trigger condition for post-TBI neurodegeneration. In the present study, we elaborate on the functions of the components of the NVU and their significant roles in the pathophysiology of TBI. We also present scientific evidence supporting the involvement of NVU dysfunction in neurodegenerative disorders and attempt to summarize precise mechanisms linking acute TBI to chronic effects on neurodegeneration. Consequently, we suggest the reasonability of the NVUD Hypothesis and illuminate its value and limitations.

THE COMPONENTS OF THE NVU PLAY CRITICAL ROLES IN THE HOMEOSTASIS OF THE CNS

The paradigm of the NVU nowadays encompasses neurons, neuroglia (astrocytes, microglia, and oligodendrocytes), vascular cells (pericytes, endothelial cells, and vascular smooth muscle cells), and the basal lamina matrix of brain vasculature (Lo and Rosenberg, 2009; Cai et al., 2017a). Among these components, neurons may constitute the most pivotal cells for neurological function and have been studied by a great deal of previous work (Cai et al., 2017b). In this section, we mainly focus on the components other than neurons, which also play critical roles in the homeostasis of the CNS and closely interact with neurons.

Glial Components in the NVU

Brain-resident glial cells, which are comprised of astrocytes (astroglia), oligodendrocytes and microglia, exert various functions to maintain CNS homeostasis (Sofroniew and Vinters, 2010; Yang and Wang, 2015). Specifically, astrocytes, the most abundant brain-resident glial cells (Yang and Wang, 2015), stretch out their endfeet to the microvessels to regulate cerebral blood flow and form a functional barrier named glia limitans (Abbott et al., 2006). Through the glia limitans, astrocytes separate neurons from the blood vessels, meninges and perivascular spaces (Sofroniew, 2015). In addition to structural support for neurons, astrocytes also functionally favor neurons in a number of ways (Zhou et al., 2020), including regulating the neurotransmitter glutamate (Rothstein et al., 1996; Anderson and Swanson, 2000; Zou et al., 2010), releasing neurotrophic factors

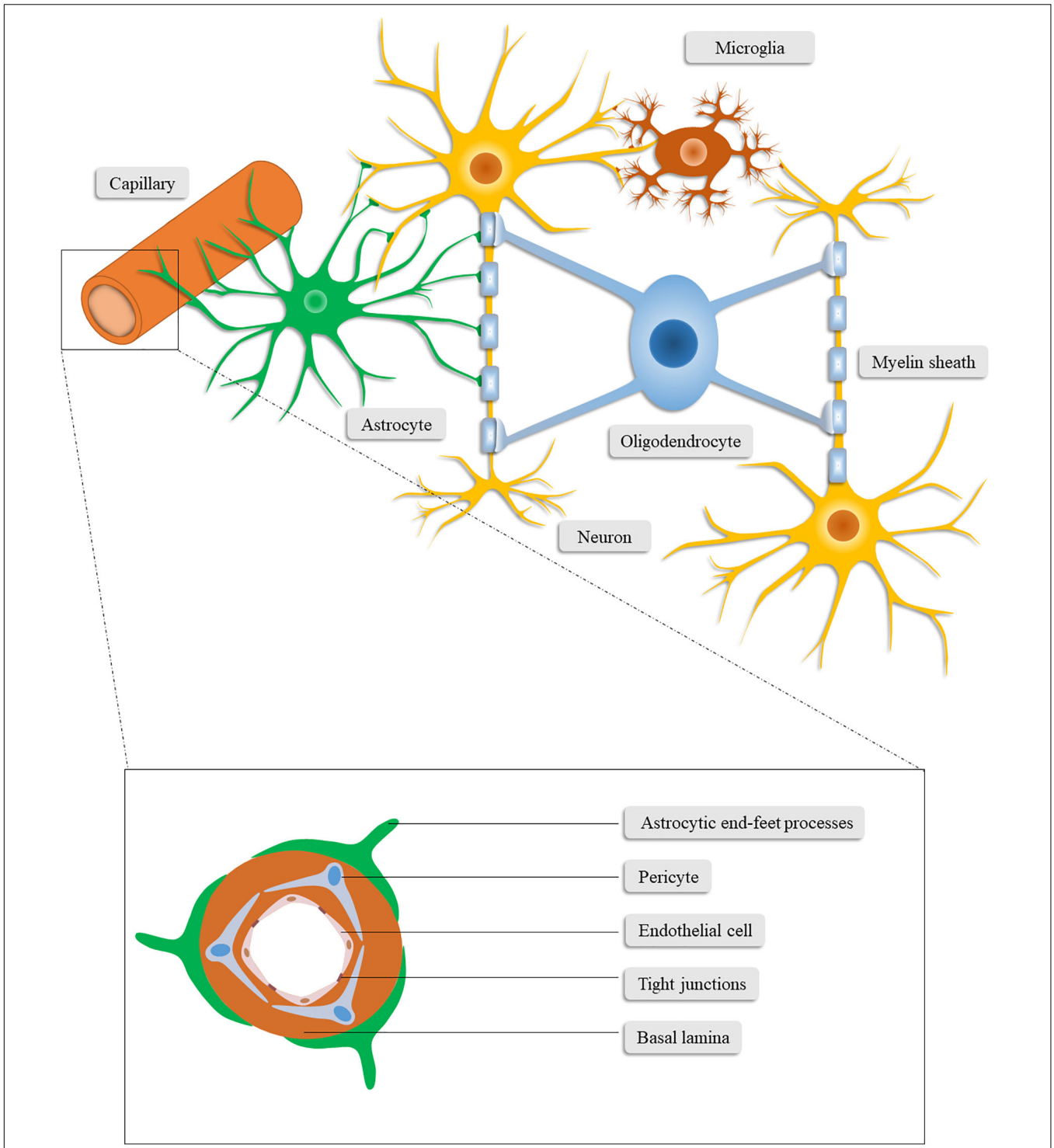

FIGURE 1 | Schematic illustration of the neurovascular unit. The neurovascular unit consists of neurons, neuroglia (astrocytes, microglia, and oligodendrocytes), vascular cells (pericytes, endothelial cells, and vascular smooth muscle cells) and the basal lamina matrix of brain vasculature.

and gliotransmitters (Ye et al., 2003; Kardos et al., 2017; Perez et al., 2017), synthesizing glutamine, cholesterol, glutathione, and thrombospondin (Dringen et al., 2000; Slemmer et al., 2008; Colangelo et al., 2012), converting glucose into lactate (Magistretti and Pellerin, 1999; Danbolt, 2001; Magistretti, 2006), and controlling water homeostasis and neuronal activation (Lang et al., 1998; Walz, 2000; Kofuji and Newman, 2004; Jayakumar and Norenberg, 2010). Furthermore, the concentration of

extracellular ions (Colangelo et al., 2012) and the glymphatic system (Jessen et al., 2015) are regulated by astrocytes.

Microglia are immunocompetent cells in the CNS that are easily activated and have the function of recognizing and phagocytizing pathogens, debris and dead cells. They form the first line of defense system of the CNS and conduct phagocytosis-mediated cleanup during senescence or pathological processes (Hu et al., 2014). Conversely, microglia are also involved in the secretion of neurotoxins, such as nitric oxide and pro-inflammatory cytokines, which further deteriorate the cerebral microenvironment in pathological conditions (Hailer, 2008).

Oligodendrocytes, another type of brain-resident glial cell, produce lipid-enriched myelin that wraps axons and accelerates nerve impulses (Plemel et al., 2014). Taken together, glial cells can affect the outcome of patients with CNS disorders given the multifunctional roles of glial cells in the CNS.

Microvascular Components in the NVU

Vascular cells involved in the NVU include pericytes, endothelial cells, and vascular smooth muscle cells. As vascular wall cells embedded in the microvascular basement membrane, pericytes are centrally positioned between endothelial cells, astrocytes and neurons (Sweeney et al., 2016). Pericytes are involved in signal transduction and communication with neighboring cells, through which they regulate blood–brain barrier (BBB) permeability, angiogenesis, neurotoxic metabolism and clearance, neuroinflammation, capillary hemodynamic response, and stem cell activity, demonstrating their vital role in the CNS during health and disease (Sweeney et al., 2016).

Similar to pericytes, endothelial cells are physiologically versatile cells that are involved in the maintenance of vascular homeostasis, regulation of cerebral vasoconstriction and vasodilatation, angiogenesis, and secretion of anti-coagulation factors. Expressing multiple substrate-specific transport systems, endothelial cells also play a vital role in controlling the exchange of CNS with peripheral substances and regulating the transport of ions and nutrients (Cai et al., 2017b). Endothelial cells are highly connected through tight junctions (TJs) which restricts the paracellular diffusion of substances from blood to the CNS (Tso and Macdonald, 2014). These continuously interconnected endothelial cells, together with pericytes, the basal lamina matrix and the astrocytic end-foot processes, constitute the BBB (Najjar et al., 2017). The integrity of the BBB is critical to the homeostasis and immunoprotection of the CNS (Najjar et al., 2017). Of the microvascular components in the NVU, endothelial cells are the main component of the BBB (Cai et al., 2017b) while pericytes primarily maintain the integrity of the BBB (Armulik et al., 2010; Bell et al., 2010; Daneman et al., 2010).

The Extracellular Matrix

The extracellular matrix (ECM) of the basal lamina functions as an anchor for the endothelium through cell-matrix interactions between laminin (or other matrix proteins) and the endothelial integrin receptors. Through these interactions, numerous intracellular signaling pathways can be stimulated (Hynes, 1992; Tilling et al., 2002). The TJs are thought to constitute the primary impediment of paracellular diffusion, therefore, given the involvement of matrix proteins in the regulation of expression of endothelial TJs, the basal lamina proteins are likely to maintain the diffusion as well (Tilling et al., 1998). The ECM and TJs are fundamental to the permeability of the BBB and the degradation of these proteins under pathological circumstances can potently exacerbate BBB dysfunction (Rascher et al., 2002). Additionally, matrix metalloproteinases (MMPs), particularly MMP-9, are capable of degrading the ECM and TJs, which enhances the permeability of the BBB and leads to vasogenic edema (Fujimoto et al., 2008; Halliday et al., 2013).

NVU DYSFUNCTION IN THE PATHOPHYSIOLOGY OF TBI

While numerous causes of trauma exist, TBI is consistently related to both primary and secondary damage mechanisms (Logsdon et al., 2015). During TBI, mechanical force directly leads to instant damage, which includes neuronal damage and vascular disruption, followed by the secondary injury mediated by succeeding pathophysiological processes such as oxidative stress, neuroinflammation, BBB dysfunction, and apoptosis (Abdul-Muneer et al., 2015; Chen X. et al., 2018; Khaksari et al., 2018; Main et al., 2018; Sevenich, 2018). All these primary and secondary pathologic processes contribute to the structural and/or metabolic abnormalities of the NVU, resulting in long-term neurological deficits in the patients (Zhang et al., 2005; Perez et al., 2017).

Oxidative Stress

Oxidative stress gives rise to progressive neuropathology during TBI and contributes primarily to secondary injury (Abdul-Muneer et al., 2015; Anthonymuthu et al., 2018). Oxidative stress is considered physiological and biochemical stress or insult deriving mainly from reactive oxygen species (ROS) and reactive nitrogen species (RNS) (Abdul-Muneer et al., 2015). The enhanced production of ROS and RNS following TBI is due to excessive excitotoxicity and insufficient endogenous antioxidant systems. These reactive species result in increased oxidative stress and parallel the production of super-oxidized cellular and vascular structures, oxidized protein, cleaved DNA, and impaired mitochondrial electron transport chain, which can induce more ROS and RNS, thus triggering a vicious circle (Cornelius et al., 2013).

Oxidative stress and elevated toxic proteins can act on astrocytes to induce astrocyte-secreted pro-inflammatory factors, such as interleukin (IL)-6, monocyte chemoattractant protein (MCP)-1, and MMP-9, leading to the BBB compromise and neuroinflammation (Salminen et al., 2011). Oxidative stress is a major contributor to endothelial impairment. Enriched with mitochondria for the normal performance of ATP-dependent active transporters, endothelial cells can thus malfunction under increased oxidative stress and impaired mitochondrial functions (Cai et al., 2017b). Furthermore, oxidative stress and energy depletion induce the dysfunction of cellular ion channels that leads to the depolarization of neurons and the aggregation of excitatory neurotransmitters (e.g., glutamate),

which further aggravate neuronal depolarization and the increase of toxic calcium levels (Weilinger et al., 2013). Moreover, enhanced oxidative stress and the subsequent biochemical cascade are adequate to induce early or late apoptosis, immediate cell necrosis and delayed neurodegeneration post TBI (Abdul-Muneer et al., 2015).

Neuroinflammation

Neuroinflammation is a hallmark of different CNS pathologies (Sevenich, 2018). Following the initial injury, the changed microenvironment and released intracellular components from damaged cells trigger the activation and recruitment of local glial cells (Corps et al., 2015; Gyoneva and Ransohoff, 2015; Sharma et al., 2015). Both microglia and astrocytes react within 24 h and peak around day 3–7 post TBI (Fujita et al., 1998; Di Giovanni et al., 2005; Susarla et al., 2014). The activation and proliferation of glia release signaling factors and induce a robust, sterile immune reaction that consists of brain-resident and peripherally recruited inflammatory cells (Corps et al., 2015; Gyoneva and Ransohoff, 2015; Sharma et al., 2015). In addition to danger signals released by damaged cells, mitochondrial stress, glutamate excitotoxicity, and vascular injury have also been identified as inflammatory triggers of neuroinflammation (Simon et al., 2017). This immune reaction is supposed to exert a neuroprotective role and promote wound healing, but it can become neurodestructive and aggravate neuronal damage under certain circumstances (Murakami et al., 2011; Gyoneva and Ransohoff, 2015; Kumar et al., 2017). For instance, resident glia and infiltrating immune cells up-regulate the expression of tumor necrosis factor (TNF)-α, IL-6, and IL-1β rapidly to cope with injury, among which, however, TNF-α is correlated with BBB disruption and brain edema, and can act together with IL-1β to drive astrocyte dysfunction and resultant glutamate excitotoxicity (Ziebell and Morganti-Kossmann, 2010; Viviani et al., 2014; Simon et al., 2017). Notably, many mediators activated after TBI may exhibit pleiotropic effects in a context-dependent manner. In this regard, the conceptual framework of NVU may also help understand the shifting profiles of TBI pathophysiology over time (Lok et al., 2015).

As the inflammatory response progresses, the glial progenitor cells around the damaged tissue form a glial scar, which isolates the injured areas and inhibits the spread of inflammatory cells (Sofroniew, 2009; Karimi-Abdolrezaee and Billakanti, 2012; Burda and Sofroniew, 2014; Peng et al., 2014; Sofroniew, 2015). Nonetheless, the glial scar highly expresses inhibitory components for axonal regeneration and acts as both a physical and chemical barrier to axon elongation. The glial scar is therefore considered the main obstacle for axonal regeneration and the restoration of neuronal connectivity, which makes it a likely cause of the long-term sequelae in TBI patients (Voskuhl et al., 2009; Jeong et al., 2012; Cregg et al., 2014; Sharma et al., 2015).

Blood–Brain Barrier Dysfunction

The BBB functions as a key homeostatic site between the CNS and other major systems in the body (Zhao et al., 2015). As the core feature of TBI, BBB dysfunction may indicate the severity of the injury as well as the length of recovery from TBI (Neuwelt et al., 2008; Main et al., 2018). The disruption of BBB integrity can result from the initial injury or arise secondarily from the succeeding pathological processes, including extensive inflammation, metabolic disturbances, and astrocytic dysfunction (Shlosberg et al., 2010; Badaut and Bix, 2014; Corps et al., 2015; Johnson et al., 2018). Following the brain injury, several pro-inflammatory pathways such as the IL-1β/nuclear factor-κ-gene binding (NF-κB) signaling pathway (Petty and Lo, 2002; Suzuki et al., 2010) and the Janus kinase/signal transducers and activators of transcription 1 (JAK/STAT1) signaling pathway (Gong et al., 2018) have been demonstrated to induce the upregulation of MMPs and the consequential degradation of the ECM and TJs. Moreover, upregulated NF-κB, as a transcription factor, also induces the transcription of pro-inflammatory genes and enzymes, including intracellular adhesion molecule-1 (ICAM-1) and inducible nitric oxide synthase (iNOS; Kumar et al., 2004). The former has been shown to increase BBB permeability through facilitating transendothelial leukocyte migration (Najjar et al., 2017) while the latter has been identified to be excitotoxic and neurotoxic as well as activate MMPs via nitric oxide (Ji et al., 2017; Chen H. et al., 2018). In addition, neuroinflammation and energy depletion result in the impairments of ionic transport, transporters, and mitochondrial oxidative metabolism of endothelial cells, which all exacerbate the breakdown of the BBB (Ott et al., 2007). Moreover, the BBB compromise can, in turn, aggravate the inflammatory response due to the enhanced influx of serum elements, proinflammatory molecules, and infiltrating leukocytes. It can also lead to cerebral hemorrhage, brain edema, and hypoxia (Shlosberg et al., 2010; Badaut and Bix, 2014; Corps et al., 2015; Johnson et al., 2018).

As described above, TJ-interconnected endothelial cells and pericytes are the main constituents that primarily contribute to the maintenance of the BBB (Armulik et al., 2010; Bell et al., 2010; Daneman et al., 2010; Cai et al., 2017b). The impairment of crosstalk between them ultimately leads to BBB dysfunction after TBI onset (Bhowmick et al., 2019). Astrocytes also hold a critical role in BBB function and cerebral water homeostasis (Burda et al., 2016) as astrocytic end-foot processes ensheathe the BBB and densely express perivascular aquaporin-4 (AQP4) channels (Louveau et al., 2017; Sweeney et al., 2018). In addition, BBB permeability can be altered by astrocyte-derived factors (Michinaga and Koyama, 2019). Moreover, other cell types involved in the NVU have also been shown to affect BBB homeostasis after TBI. For example, studies have indicated that oligodendrocyte precursor cells protect BBB against disruption via the transforming growth factor-β (TGF-β) signaling pathway (Seo et al., 2014). The activation, proliferation and phenotypic transformation of microglia indirectly have an impact on BBB function considering their involvement in the inflammatory response, especially the pro-inflammatory role (such as iNOS-expressing) of M1-like phenotype (Ladwig et al., 2017). These glial cells and microvascular cells have a functional interaction with each other in a paracrine manner (Abdul-Muneer et al., 2015). Therefore, the coordinated response of all

components within the NVU is the determinant of BBB integrity (Lok et al., 2015).

Persistent NVU Abnormalities and Imaging/Serum/CSF Biomarkers

Growing evidence has demonstrated these post-TBI NVU abnormalities may persist for months or years, especially in patients with a history of moderate-to-severe TBI (Hayes et al., 2017; LoBue et al., 2019). Reports regarding long-term brain changes after milder injuries have been mixed, and the results were often complicated by factors concerned with the number and severity/complications of injuries, genetic risk, and mental states and behavior (Hayes et al., 2017; LoBue et al., 2019). Diffuse axonal injury has been found in TBI of any severity and post-mortem studies reported widespread axonal pathology could continue for a sufficient length of time (weeks to months, even years) after mild-to-severe TBI in humans (Blumbergs et al., 1989; Johnson et al., 2013a,b; Shetty et al., 2014; Logsdon et al., 2015). A continuum of microglia activation across a wide range of TBI conditions was also observed in animal models (Nagamoto-Combs et al., 2007; Nagamoto-Combs et al., 2010) and human autopsy (form different cause) (Gentleman et al., 2004; Johnson et al., 2013a), even up to 18 years after TBI, and this was related to the consistently ongoing white matter degeneration (Johnson et al., 2013a). However, the functional impact of these microglia is still an enigma, as controversy remains regarding whether they exhibit a pro-inflammatory or pro-regenerative phenotype (Ramlackhansingh et al., 2011; Johnson et al., 2013a; Russo and McGavern, 2016; Scott et al., 2018; Tagge et al., 2018). Evidence of prolonged reactive astrogliosis after even mild injuries was revealed by brain tissue from animal models (Smith et al., 1997) and humans (Goldstein et al., 2012; Shively et al., 2017; Tagge et al., 2018) as well. Likewise, microvascular injury could be detected in the autopsy of long-term survivors from different types of TBI (Hay et al., 2015; Tagge et al., 2018). These continued NVU dysfunctions could bring about chronic pathological processes such as oxidative stress, chronic neuroinflammation, and proteinopathy, which were also reported to be identified years post TBI and could, in turn, aggravate the NVU dysfunction (Johnson et al., 2012; Simon et al., 2017; LoBue et al., 2019). Although chronic oxidative stress has not yet been observed following a single mild human TBI, it appears that oxidative stress after concussion and its associated pathophysiological processes may worsen or prolong symptoms (Hoffer et al., 2013; Cruz-Haces et al., 2017).

Currently, technological advances in clinical TBI neuroimaging make it possible to study NVU dysfunction and ensuing pathological processes *in vivo*, and findings by neuroimaging studies support the persistent abnormalities as well (LoBue et al., 2019). For example, microglia activation and related chronic neuroinflammation in moderate to severe TBI survivors can be assessed up to 17 years after trauma by positron emission tomography (PET) imaging technology binding to translocator protein, which is expressed by mitochondria of activated microglia (Folkersma et al., 2011; Ramlackhansingh et al., 2011). Moreover, significant increased binding to translocator protein can be identified by PET technology decades after the history of repetitive mild TBI in retired athletes compared to healthy controls (Coughlin et al., 2015). Similarly, selective PET techniques with ligands for neurodegenerative proteins [e.g., amyloid-β peptide (Aβ) and tau protein] can image the deposition of proteinopathy, showing increased binding in moderate-severe TBI victims/retired athletes versus control cases (Hong et al., 2014; Barrio et al., 2015; Scott et al., 2016). Advanced magnetic resonance imaging (MRI) modalities, such as diffusion tensor imaging (DTI, particularly in white matter pathology visualization), magnetic resonance spectroscopy (MRS, particularly in metabolic change assessment), susceptibility weight imaging (SWI, particularly in microscopic bleeding detection), and functional magnetic resonance imaging (fMRI, particularly in neurocognitive function examination) have emerged to allow the discovery of injury biomarkers and the detection of brain changes in patients with even mild TBI over time (Baugh et al., 2012; Xiong et al., 2014; Pavlovic et al., 2019). Additionally, Single Photon Emission Computed Tomography (SPECT) scan also has significance, as being a promising tool for detecting regional functional changes in the brain of patients sustaining TBI (Baugh et al., 2012).

Continued presence of some serum/plasma and CSF biomarkers is also able to persist many years post TBI, which depends on the type and extent of injury, thereby holding great promise for assessing the duration and degree of pathological processes (Williams et al., 2018; LoBue et al., 2019). Proteins including Aβ, tau, α-synuclein, and nuclear transactive response DNA-binding protein 43 (TDP-43) are critically implicated in the pathogenesis of several different neurodegenerative diseases, and have been utilized as neurobiological markers to monitor neuronal damage following TBI, moreover, different marker binding fingerprints may function as predictors for a particular late-onset neurodegenerative disease (Williams et al., 2018). A growing body of literature data has suggested that neurofilament light in the blood and/or CSF also serves as a biomarker indicating neuronal injury after TBI (Shahim et al., 2017; Bernick et al., 2018). Besides, glial fibrillary acidic protein, ubiquitin C-terminal hydrolase L1, S100β, and neuron-specific enolase have shown immense value as reliable blood/CSF markers in predicting poor outcome and evaluating microstructural injuries undetected by computed tomography (Bohmer et al., 2011; Mondello et al., 2016; Papa et al., 2016; Welch et al., 2016). Additionally, chronically elevated expression of serum cytokines may reflect chronic immune activation after TBI (Simon et al., 2017).

PATIENTS WITH TBI HAVE INCREASED SUSCEPTIBILITY TO NEURODEGENERATIVE DISEASES

Accumulating evidence provides support for an association between the risk of developing neurodegenerative disease and a prior TBI event. Previous studies have reported an increased risk of AD among TBI victims (Roberts et al., 1991; Fleminger et al., 2003). Similarly, 1.5–3.8 times higher incidence of PD has

been reported in post-TBI cases (Goldman et al., 2006; Jafari et al., 2013). Traumatic brain injury, particularly of repeated TBI, is also considered a predisposing factor for ALS (Chen et al., 2007; Pupillo et al., 2018; Franz et al., 2019). Additionally, age at trauma has been suggested to be a determinant of the TBI victims' susceptibility to ALS (Seals et al., 2016; Pupillo et al., 2018). Notably, although vulnerability to neurodegenerative diseases has been indicated in patients with TBI of any severity, this increased susceptibility is more common in survivors sustaining moderate-to-severe TBI (Hayes et al., 2017; Graham and Sharp, 2019; LoBue et al., 2019), and these patients have a 1.8-fold increase in neurodegenerative disease risk compared with those with mild TBI (Raj et al., 2017).

Unfortunately, mechanisms underlying this risk remain elusive thus far (LoBue et al., 2019). Early after the initial injury, TBI can induce the production of pathological proteins, whose neurotoxicity contributes directly to persistent abnormalities of brain structure and function, with these proteinopathies lasting for months or years (Goldstein et al., 2012; Johnson et al., 2012, 2013a; Hay et al., 2015; Williams et al., 2018). Intriguingly, post-TBI proteinopathies have similarities to multiple neurodegenerative diseases (Smith et al., 2013; Graham and Sharp, 2019). For instance, pathological accumulation of Aβ and neurofibrillary tangles comprising hyperphosphorylated neuronal tau brings about the development of AD (Zenaro et al., 2017), similarly, α-synuclein is linked to PD (Kalia and Lang, 2016). Furthermore, TDP-43 is considered the primary disease-related protein in ALS, and TDP-43 proteinopathy also features in other neurodegenerative disorders such as AD, PD, and Huntington's disease (HD; Johnson et al., 2011). However, TDP-43 proteinopathy after TBI is more obscure and several controversial areas remain (Graham and Sharp, 2019). The study by Wiesner et al. (2018) addressed that brain trauma could boost ALS-related TDP-43 pathology, whereas the extent was modulated by ALS-related gene mutations, and the process was indicated to reversible and incapable of triggering ALS progression and neuronal vulnerability. Moreover, a single TBI does not appear to induce TDP-43 proteinopathy in humans (Johnson et al., 2011). In addition to proteinopathies, chronic neuroinflammation and persistent oxidative stress may represent other candidates for the increased susceptibility. Neuroinflammation is a hallmark of CNS disorders, including TBI and neurodegenerative diseases (Heneka et al., 2015; Russo and McGavern, 2016; Sevenich, 2018). Oxidative stress gives rise to progressive neuropathology and contributes primarily to the secondary injury post TBI (Abdul-Muneer et al., 2015; Anthonymuthu et al., 2018), concurrently being involved in the pathogenesis of neurodegenerative diseases (Cruz-Haces et al., 2017).

Taken collectively, proteinopathies, persistent oxidative stress, and chronic neuroinflammation may be the pivotal intermediary pathological processes between early and delayed post-TBI changes (LoBue et al., 2019). Herein we present that there is a pathological correlation between TBI and post-TBI neurodegenerative diseases, and we speculate it is the aforementioned persistent NVU dysfunction following TBI that accounts for the pathophysiological substrate and trigger condition for this pathological correlation. Readers seeking an in-depth discussion regarding the supporting evidence and internal mechanisms for this hypothesis should consult the section "Supporting Evidence and Precise Mechanisms." But before that, as we have elucidated the bond between NVU dysfunction and TBI pathophysiology, however, is NVU dysfunction involved in the pathophysiology of neurodegenerative diseases?

IS NVU DYSFUNCTION INVOLVED IN THE PATHOPHYSIOLOGY OF NEURODEGENERATIVE DISEASES?

More and more lines of evidence favor the perspective that not only the neuronal degeneration and loss, but also aberrant neuroglia and vascular cells contribute to the pathogenesis of neurodegenerative diseases (Cai et al., 2017b). In this section, we describe several roles of NVU components involved in the pathophysiology of AD, PD, and ALS.

Alzheimer's Disease

A growing number of studies from post-mortem brain tissue reveal the existence of neurovascular dysfunction in patients with AD, including brain capillary leakage, degeneration of BBB-related cells (e.g., endothelial cells and pericytes), brain infiltration of peripheral cells, abnormal angiogenesis and molecular changes (Sweeney et al., 2018).

Blood–Brain Barrier disruption is considered the key pathway of AD onset (Cai et al., 2017b). This is firstly reflected in its impact on the aggregation of pathological protein. The dysfunction of NVU leads to aberrant cerebral blood flow regulation and impaired BBB transport, resulting in faulty Aβ clearance and increased Aβ production in soluble and fibrillary forms, which are the most neurotoxic and vasculotoxic forms (Benarroch, 2007). Accumulation of Aβ can subsequently induce oxidative stress, neuroinflammation and cell apoptosis, aggravating BBB impairment (Benarroch, 2007). Tau protein is associated with BBB compromise as well, as BBB dysfunction is in concert with the phenomenon that the major hippocampal blood vessels are surrounded by tau protein (Blair et al., 2015). In addition to pathological protein aggregation, AD is also pathologically characterized by chronic inflammation with the involvement of resident microglia and infiltrating peripheral immune cells (Heneka et al., 2015). A dysfunctional BBB is convenient for migrating immune cells to infiltrate the CNS. In this context, when the requisite adhesion molecules are expressed, circulating leukocytes migrate into the brain parenchyma through activated brain endothelial cells and then interact with NVU components to further affect their structural integrity and function (Zenaro et al., 2017).

Parkinson's Disease

In PD pathogenesis, BBB dysfunction is not as important as it is in AD, but the effects of neuronal and glial cell damage are more crucial. Dopaminergic neuronal loss and Lewy bodies

and Lowy neurites containing α-synuclein are the hallmarks of PD (Kalia and Lang, 2016). Dopaminergic neurons are characterized as highly metabolic and thus have abundant amounts of mitochondria, the DNA of which is easily damaged by ROS and DNA repair can meanwhile be reduced in the absence of energy support (Liang et al., 2007; Gredilla et al., 2010). In addition, the metabolic process of dopamine itself will produce a large amount of accumulated ROS under pathological conditions (Cai et al., 2017b). Therefore, oxidative stress and energy depletion can easily give rise to dopaminergic neuronal loss as well as α-synuclein aggregation, which further forms Lewy bodies and Lowy neurites.

Besides neuronal loss, glial components in the NVU also play a pivotal role in PD onset. Equipped with unmyelinated axons, dopaminergic neurons interact most closely with astrocytes (Rodriguez et al., 2014; Rodriguez et al., 2015). In normal physiological conditions, astrocytes provide both structural and functional support for dopaminergic neurons in multifactorial ways (see section "Glial Components in the NVU" for the detailed mechanisms) while dysfunctional astrocytes secrete various cytokines, chemokines, and excitotoxins, which contribute to a series of pathological processes (Salminen et al., 2011; Zhou et al., 2020). Furthermore, microglia–astrocyte interactions can further propel disease progression (Chen et al., 2019).

Amyotrophic Lateral Sclerosis

Amyotrophic lateral sclerosis is resulting from a complex combination of genetic predispositions and environmental insults. ALS-linked genes include *FUS*, *TARDBP* (the one encoding TDP-43), *SOD1*, *C9orf72*, among others (Sleigh et al., 2020). Based on the function of these genes, impaired cytoskeletal dynamics and axonal transport have emerged as a key role in ALS (Sleigh et al., 2020). Besides, dysfunctions of other NVU components are also involved in the pathogenesis of ALS. Both astrocytes and microglia have been argued to serve as central players in the pathogenesis. In the early stage of disease preceding the emergence of neuronal death and clinical symptoms, incompetent astrocytes due to astrodegeneration and astrocytic atrophy break the glutamate homeostasis and elicit glutamate excitotoxicity. Microglia are also induced to secrete neurotoxic factors, while in the later stage of disease, reactive astrogliosis and activated microglia may further promote neuronal damage and death (Verkhratsky et al., 2014). Additionally, the involvement of microvascular components in ALS pathology has also been suggested and microvascular compromise appears to precede the neuronal lesions and even the neuroinflammation (Guo and Lo, 2009).

THE NEUROVASCULAR UNIT DYSFUNCTION HYPOTHESIS AND ITS LIMITATIONS

Definition and Relational Reasoning

The NVUD Hypothesis underscores the core role of NVU dysfunction in the development of post-TBI neurodegenerative diseases, which is concluded with relational reasoning from the following: (1) The NVU comprises neurons, neuroglial cells, vascular cells, and the basal lamina matrix of brain vasculature, playing critical roles in the homeostasis of the CNS, (2) all of the primary and secondary pathologic processes during TBI contribute to the persisting NVU dysfunction, including neuronal death, neuroglial dysfunction, and BBB compromise, (3) patients with TBI have an increased risk for developing neurodegenerative diseases, based on epidemiology and mutual pathological processes, and (4) NVU dysfunction is also involved in the pathophysiology of neurodegenerative diseases.

Additionally, we have mentioned in the previous sections that the persistent NVU abnormalities after TBI are related to the number and severity of injuries, and there is a dose–response relationship between TBI and later neurodegenerative disease. This similarity may further strengthen the reasonability of our assumption that continued NVU dysfunction serves as the pathophysiological substrate to trigger the development of post-TBI neurodegeneration.

Consistent with our relational inference, increasing supporting evidence obtained by animal models and human postmortem studies has suggested NVU dysfunction an important causative factor for post-TBI neurodegeneration (**Figure 2**; Graham and Sharp, 2019; LoBue et al., 2019). These evidences also explain the induction of chronic neuroinflammation, persistent oxidative stress, and neurodegenerative protein aggregation after the initial injury.

Supporting Evidence and Precise Mechanisms

Prolonged injured axons are considered a source of pathological proteins (Johnson et al., 2013b). Following TBI, the shear forces applied to the cytoskeleton result in damaged microstructure and impaired axonal transport (Maxwell et al., 2003; Tagge et al., 2018), which is also involved in AD (Johnson et al., 2013b) and ALS (Sleigh et al., 2020) pathogenesis. Impaired axonal transport can lead to the co-accumulation of amyloid precursor protein (APP) and AAP-cleaving enzymes in axonal varicosities within just hours of trauma and thus, forming abundant Aβ in the varicosities (Chen et al., 2004; Uryu et al., 2007; Chen et al., 2009; Tran et al., 2011). In the case where damaged axons eventually break down, these intraneuronal Aβ can aggregate in the parenchyma to form plaques (Chen et al., 2004; Johnson et al., 2013b). Shear forces also induce the dissociation of tau from microtubules, which is subsequently processed into a highly pathogenic tau form contributing to mitochondrial damage, neuronal apoptosis, and abnormal long-term potentiation (Kondo et al., 2015; Tagge et al., 2018). Besides, injured axons yield an extensive release of glutamate as well, coupled with cytokine stimulation, distorted glutamate receptor trafficking, and impaired glutamate clearance due to loss of astrocytic functional glutamate transporters, which together contribute to the dysregulation of glutamate homeostasis (Baker et al., 1993; Piao et al., 2019; Zhang et al., 2019). This dysregulation is adequate

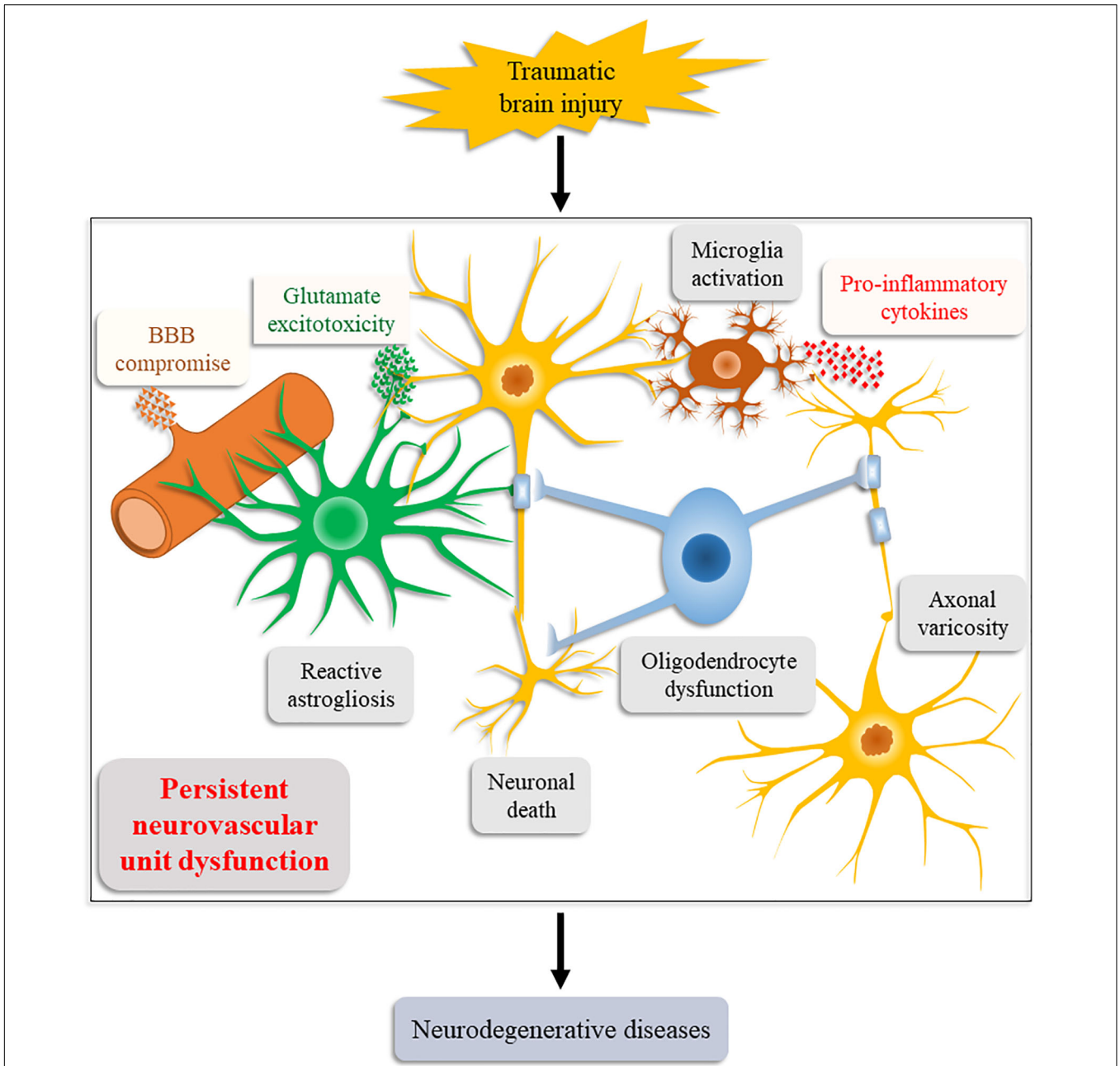

FIGURE 2 | Schematic illustration of the Neurovascular Unit Dysfunction (NVUD) Hypothesis. During TBI, primary and secondary pathologic processes lead to persistent structural and/or functional abnormalities of the neurovascular unit, such as neuronal death, neuroglial dysfunction, and BBB compromise, which propel the progression of neurodegenerative diseases post TBI.

to incur neuroexcitotoxicity as well as resultant oxidative stress and mitochondrial dysfunction post TBI (Cornelius et al., 2013; Abdul-Muneer et al., 2015), which are strictly implicated in the PD pathogenesis including dopaminergic neuronal loss and α-synuclein aggregation (Liang et al., 2007; Gredilla et al., 2010; Cai et al., 2017b). Indeed, oxidative stress potentially plays a key role in protein carbonylation and pathological protein accumulation (Cruz-Haces et al., 2017). Notably, TBI is suggested to form a transmissible self-propagating proteinopathy (Zanier et al., 2018; Graham and Sharp, 2019). Altogether, the possibility of persistent axonopathy and transmissible proteinopathy provide a potential mechanism for long-term and extensive neurodegeneration in the brain, thereby propelling progression of neurodegenerative diseases (Johnson et al., 2012, 2013b; Zanier et al., 2018; Graham and Sharp, 2019).

Continued BBB dysfunction and neuroglial dysfunction following TBI are also implicated as triggers of post-TBI

neurodegeneration, and the underlying mechanisms include, certainly, astrocyte dysfunction-induced impaired glutamate clearance as mentioned above. Perennial BBB alterations recruit brain-resident neuroglia and infiltrating leukocytes to form chronic neuroinflammation (Shetty et al., 2014; Hay et al., 2015), which is also a pathological characteristic of neurodegenerative diseases (Heneka et al., 2015; Sevenich, 2018). Similar to oxidative stress, neuroinflammation is indicated to elicit the abnormal accumulation of pathological proteins (LoBue et al., 2019), which may further exacerbate vascular lesion as the perivascular location of proteinopathies has been observed in autopsies of TBI victims (McKee et al., 2012; Tagge et al., 2018). The glymphatic system is a recently discovered brain-wide waste clearance pathway that utilizes astrocytic AQP4 channels to promote efficient elimination of interstitial solutes, including pathological proteins, from the CNS (Iliff et al., 2012; Jessen et al., 2015). In the acute phase following TBI, reactive astrogliosis is associated with alterations in AQP4 channel distribution and polarization, which are in line with the injury severity and persist for 14–28 days and 28 days in mild TBI and moderate TBI, respectively, resulting in decreased glymphatic influx and increased metabolic waste accumulation (Ren et al., 2013; Rasmussen et al., 2018; Sullan et al., 2018). Besides, decreased glymphatic function is also critically attributed to reactive astrogliosis-induced glial scars (Jessen et al., 2015). Furthermore, the glymphatic system functions primarily during sleep and is largely suppressed during waking state, whereas sleep deprivation constitutes one of the most frequently reported chronic complications following TBI (Jessen et al., 2015; Rasmussen et al., 2018; Sullan et al., 2018). As a result, the function of glymphatic pathway can be down to about 40% and maintained for at least 1 month after TBI (Iliff et al., 2014; Jessen et al., 2015). Therefore, both chronic impairment of BBB transport (Benarroch, 2007; Hay et al., 2015) and glymphatic pathway function (Iliff et al., 2014; Sullan et al., 2018) can induce impaired protein clearance, contributing to the succedent accumulation of neurotoxic and vasculotoxic proteins as well as the onset of post-TBI neurodegeneration.

Neurovascular Unit Dysfunction Hypothesis as a Promising Theoretical Basis for Treatment

Neurovascular Unit Dysfunction abnormalities and ensuing pathological processes evolving over time have cast a spotlight on positive TBI interventions, which may be beneficial over an extended time frame (Ramlackhansingh et al., 2011). In the past, neuronal damage had been considered the main cause of functional impairment in brain injury or neurodegenerative diseases, and almost all the therapeutic strategies were targeted at repairing neuronal injury and rescuing neurons (Cai et al., 2017b). However, in most cases, saving neurons alone seemed to be insufficient for treating brain injuries or diseases (Lok et al., 2015). We have previously reviewed the advance of a variety of stem cells in TBI treatment. Although some preclinical studies and small trials showed a good therapeutic effect, practical value of clinic application has not reached a general success (Zhou et al., 2019). Analogously, stem cell therapies in other CNS diseases, including neurodegenerative diseases and stroke, have not generated substantial clinical improvements (Wang et al., 2017). The NVUD Hypothesis may provide new insights into the treatment strategies for TBI and potential prevention for later neurodegeneration, namely integrated restoration of all neural, neuroglial and vascular connectivity. Indeed, it is increasingly recognized that cell-cell crosstalk within the NVU components is absolutely required for remodeling and repair in acute brain injury and neurodegeneration (Lok et al., 2015). To date, several candidate agents have been found to promote the restoration of NVU integrity in TBI models, such as sonic hedgehog, and troxerutin cerebroprotein hydrolysate (Zhao et al., 2018; Wu et al., 2020), more preclinical and clinical studies are warranted.

Limitations of NVUD Hypothesis

There are some aspects that NVUD Hypothesis cannot explain. For instance, studies have revealed that cell-cell signaling within the NVU is crucial in the pathogenesis of HD and that TDP-43 pathology may feature in HD (Gu et al., 2005; Shin et al., 2005; Gu et al., 2007; Faideau et al., 2010; Johnson et al., 2011; Jansen et al., 2017). However, the increased incidence of HD in TBI victims has been rarely reported. Moreover, despite universal occurred NVU dysfunction, only a subgroup of TBI victims develop late-onset neurodegenerative diseases, indicating other factors should be taken into consideration, such as genetic susceptibility (e.g., *APOE* genotyping) (Baugh et al., 2012; Goldstein et al., 2012; Shively et al., 2017; LoBue et al., 2019). Furthermore, aging not only increases the NVU's vulnerability to neurodegeneration, but also attenuates its self-repair capabilities (Cai et al., 2017b; Wang et al., 2017). Thus, the crosstalk between NVUD Hypothesis and aging merits further explanation. The NVUD Hypothesis also needs further refinement. Although the NVU paradigm in this study focuses on the components surrounding the cerebral capillaries, critical roles of vascular components and perivascular nerve fibers connecting with larger blood vessels in CNS diseases have also been proposed (Zhang et al., 2012). These groups of structures may need to be incorporated into an expanded NVUD paradigm, which will revise the NVUD Hypothesis.

CONCLUSION

In the present study, we propose the NVUD Hypothesis and discuss the reasonability. We also present its value as a promising theoretical basis for treatment and illustrate the limitations of this theory. The NVUD Hypothesis emphasizes that persistent NVU dysfunction functions as the pathophysiological substrate and trigger for late-onset neurodegeneration after TBI. Specifically, continued NVU abnormalities following TBI incur the chronic neuroinflammation, persistent oxidative stress, and neurodegenerative proteins aggregation, which in turn exacerbate NVU dysfunction and thus, forming a

vicious circle and consequently leading to the progression of neurodegenerative diseases.

AUTHOR CONTRIBUTIONS

YZ and AS conceptualized the research project. YZ, YW, HW, SG, and YP wrote the manuscript and made the original figures. QC, AS, WX, JZ, and XD critically revised the texts and figures. AS supervised the research and led the discussion. All authors read and approved the final manuscript.

FUNDING

This work was funded by China Postdoctoral Science Foundation (2017M612010), National Natural Science Foundation of China (81701144), and Zhejiang Province Natural Science Foundation (LQ17H090003).

REFERENCES

Abbott, N. J., Ronnback, L., and Hansson, E. (2006). Astrocyte-endothelial interactions at the blood-brain barrier. *Nat. Rev. Neurosci.* 7, 41–53. doi: 10.1038/nrn1824

Abdul-Muneer, P. M., Chandra, N., and Haorah, J. (2015). Interactions of oxidative stress and neurovascular inflammation in the pathogenesis of traumatic brain injury. *Mol. Neurobiol.* 51, 966–979. doi: 10.1007/s12035-014-8752-3

Anderson, C. M., and Swanson, R. A. (2000). Astrocyte glutamate transport: review of properties, regulation, and physiological functions. *Glia* 32, 1–14. doi: 10.1002/1098-1136(200010)32:1<1::aid-glia10>3.0.co;2-w

Anthonymuthu, T. S., Kenny, E. M., Lamade, A. M., Kagan, V. E., and Bayir, H. (2018). Oxidized phospholipid signaling in traumatic brain injury. *Free Rad. Biol. Med.* 124, 493–503. doi: 10.1016/j.freeradbiomed.2018.06.031

Armulik, A., Genove, G., Mae, M., Nisancioglu, M. H., Wallgard, E., Niaudet, C., et al. (2010). Pericytes regulate the blood-brain barrier. *Nature* 468, 557–561.

Ascherio, A., and Schwarzschild, M. A. (2016). The epidemiology of Parkinson's disease: risk factors and prevention. *Lancet Neurol.* 15, 1257–1272. doi: 10.1016/s1474-4422(16)30230-7

Badaut, J., and Bix, G. J. (2014). Vascular neural network phenotypic transformation after traumatic injury: potential role in long-term sequelae. *Transl. Stroke Res.* 5, 394–406. doi: 10.1007/s12975-013-0304-z

Baker, A. J., Moulton, R. J., MacMillan, V. H., and Shedden, P. M. (1993). Excitatory amino acids in cerebrospinal fluid following traumatic brain injury in humans. *J. Neurosurg.* 79, 369–372. doi: 10.3171/jns.1993.79.3.0369

Barrio, J. R., Small, G. W., Wong, K. P., Huang, S. C., Liu, J., Merrill, D. A., et al. (2015). In vivo characterization of chronic traumatic encephalopathy using [F-18]FDDNP PET brain imaging. *Proc. Natl. Acad. Sci. U.S.A.* 112, E2039–E2047.

Barshikar, S., and Bell, K. R. (2017). Sleep disturbance after TBI. *Curr. Neurol. Neurosci. Rep.* 17:87.

Baugh, C. M., Stamm, J. M., Riley, D. O., Gavett, B. E., Shenton, M. E., Lin, A., et al. (2012). Chronic traumatic encephalopathy: neurodegeneration following repetitive concussive and subconcussive brain trauma. *Brain Imag. Behav.* 6, 244–254. doi: 10.1007/s11682-012-9164-5

Bell, R. D., Winkler, E. A., Sagare, A. P., Singh, I., LaRue, B., Deane, R., et al. (2010). Pericytes control key neurovascular functions and neuronal phenotype in the adult brain and during brain aging. *Neuron* 68, 409–427. doi: 10.1016/j.neuron.2010.09.043

Benarroch, E. E. (2007). Neurovascular unit dysfunction: a vascular component of Alzheimer disease? *Neurology* 68, 1730–1732. doi: 10.1212/01.wnl.0000264502.92649.ab

Bernick, C., Zetterberg, H., Shan, G., Banks, S., and Blennow, K. (2018). Longitudinal performance of plasma neurofilament light and tau in professional fighters: the professional fighters brain health study. *J. Neurotr.* 35, 2351–2356. doi: 10.1089/neu.2017.5553

Bhowmick, S., D'Mello, V., Caruso, D., Wallerstein, A., and Abdul-Muneer, P. M. (2019). Impairment of pericyte-endothelium crosstalk leads to blood-brain barrier dysfunction following traumatic brain injury. *Exp. Neurol.* 317, 260–270. doi: 10.1016/j.expneurol.2019.03.014

Blair, L. J., Frauen, H. D., Zhang, B., Nordhues, B. A., Bijan, S., Lin, Y. C., et al. (2015). Tau depletion prevents progressive blood-brain barrier damage in a mouse model of tauopathy. *Acta Neuropathol. Commun.* 3:8.

Blumbergs, P. C., Jones, N. R., and North, J. B. (1989). Diffuse axonal injury in head trauma. *J. Neurol. Neurosurg. Psychiatry* 52, 838–841.

Boespflug, E. L., and Iliff, J. J. (2018). The emerging relationship between interstitial fluid-cerebrospinal fluid exchange, amyloid-beta, and sleep. *Biol. Psychiatry* 83, 328–336. doi: 10.1016/j.biopsych.2017.11.031

Bohmer, A. E., Oses, J. P., Schmidt, A. P., Peron, C. S., Krebs, C. L., Oppitz, P. P., et al. (2011). Neuron-specific enolase, S100B, and glial fibrillary acidic protein levels as outcome predictors in patients with severe traumatic brain injury. *Neurosurgery* 68, 1624–1630.

Burda, J. E., Bernstein, A. M., and Sofroniew, M. V. (2016). Astrocyte roles in traumatic brain injury. *Exp. Neurol.* 275(Pt 3), 305–315. doi: 10.1016/j.expneurol.2015.03.020

Burda, J. E., and Sofroniew, M. V. (2014). Reactive gliosis and the multicellular response to CNS damage and Disease. *Neuron* 81, 229–248. doi: 10.1016/j.neuron.2013.12.034

Cai, W., Liu, H., Zhao, J., Chen, L. Y., Chen, J., Lu, Z., et al. (2017a). Pericytes in brain injury and repair after ischemic stroke. *Transl. Stroke Res.* 8, 107–121. doi: 10.1007/s12975-016-0504-4

Cai, W., Zhang, K., Li, P., Zhu, L., Xu, J., Yang, B., et al. (2017b). Dysfunction of the neurovascular unit in ischemic stroke and neurodegenerative diseases: an aging effect. *Ageing Res. Rev.* 34, 77–87. doi: 10.1016/j.arr.2016.09.006

Chen, H., Guan, B., Chen, X., Chen, X., Li, C., Qiu, J., et al. (2018). Baicalin attenuates blood-brain barrier disruption and hemorrhagic transformation and improves neurological outcome in ischemic stroke rats with delayed t-PA treatment: involvement of ONOO(-)-MMP-9 pathway. *Transl. Stroke Res.* 9, 515–529. doi: 10.1007/s12975-017-0598-3

Chen, X., Pan, Z., Fang, Z., Lin, W., Wu, S., Yang, F., et al. (2018). Omega-3 polyunsaturated fatty acid attenuates traumatic brain injury-induced neuronal apoptosis by inducing autophagy through the upregulation of SIRT1-mediated deacetylation of Beclin-1. *J. Neuroinflamm.* 15:310.

Castriotta, R. J., Wilde, M. C., Lai, J. M., Atanasov, S., Masel, B. E., and Kuna, S. T. (2007). Prevalence and consequences of sleep disorders in traumatic brain injury. *J. Clin. Sleep Med.* 3, 349–356. doi: 10.5664/jcsm.26855

Chen, H., Richard, M., Sandler, D. P., Umbach, D. M., and Kamel, F. (2007). Head injury and amyotrophic lateral sclerosis. *Am. J. Epidemiol.* 166, 810–816.

Chen, X. H., Johnson, V. E., Uryu, K., Trojanowski, J. Q., and Smith, D. H. (2009). A lack of amyloid beta plaques despite persistent accumulation of amyloid beta in axons of long-term survivors of traumatic brain injury. *Brain Pathol.* 19, 214–223. doi: 10.1111/j.1750-3639.2008.00176.x

Chen, X. H., Siman, R., Iwata, A., Meaney, D. F., Trojanowski, J. Q., and Smith, D. H. (2004). Long-term accumulation of amyloid-beta, beta-secretase, presenilin-1, and caspase-3 in damaged axons following brain trauma. *Am. J. Pathol.* 165, 357–371. doi: 10.1016/s0002-9440(10)63303-2

Chen, Z., Zhong, D., and Li, G. (2019). The role of microglia in viral encephalitis: a review. *J. Neuroinflamm.* 16:76.

Colangelo, A. M., Cirillo, G., Lavitrano, M. L., Alberghina, L., and Papa, M. (2012). Targeting reactive astrogliosis by novel biotechnological strategies. *Biotechnol. Adv.* 30, 261–271. doi: 10.1016/j.biotechadv.2011.06.016

Cordone, S., Annarumma, L., Rossini, P. M., and De Gennaro, L. (2019). Sleep and beta-Amyloid deposition in Alzheimer Disease: insights on mechanisms and possible innovative treatments. *Front. Pharmacol.* 10:695. doi: 10.3389/fphar.2019.00695

Cornelius, C., Crupi, R., Calabrese, V., Graziano, A., Milone, P., Pennisi, G., et al. (2013). Traumatic brain injury: oxidative stress and neuroprotection. *Antioxid. Redox Signal.* 19, 836–853.

Corps, K. N., Roth, T. L., and McGavern, D. B. (2015). Inflammation and neuroprotection in traumatic brain injury. *JAMA Neurol.* 72, 355–362.

Coughlin, J. M., Wang, Y., Munro, C. A., Ma, S., Yue, C., Chen, S., et al. (2015). Neuroinflammation and brain atrophy in former NFL players: an in vivo multimodal imaging pilot study. *Neurobiol. Dis.* 74, 58–65. doi: 10.1016/j.nbd.2014.10.019

Cregg, J. M., DePaul, M. A., Filous, A. R., Lang, B. T., Tran, A., and Silver, J. (2014). Functional regeneration beyond the glial scar. *Exp. Neurol.* 253, 197–207. doi: 10.1016/j.expneurol.2013.12.024

Cruz-Haces, M., Tang, J., Acosta, G., Fernandez, J., and Shi, R. (2017). Pathological correlations between traumatic brain injury and chronic neurodegenerative diseases. *Transl. Neurodegen.* 6:20.

Danbolt, N. C. (2001). Glutamate uptake. *Prog. Neurobiol.* 65, 1–15.

Daneman, R., Zhou, L., Kebede, A. A., and Barres, B. A. (2010). Pericytes are required for blood-brain barrier integrity during embryogenesis. *Nature* 468, 562–566. doi: 10.1038/nature09513

de la Tremblaye, P. B., O'Neil, D. A., LaPorte, M. J., Cheng, J. P., Beitchman, J. A., Thomas, T. C., et al. (2018). Elucidating opportunities and pitfalls in the treatment of experimental traumatic brain injury to optimize and facilitate clinical translation. *Neurosci. Biobehav. Rev.* 85, 160–175. doi: 10.1016/j.neubiorev.2017.05.022

de Lau, L. M. L., and Breteler, M. M. B. (2006). Epidemiology of Parkinson's disease. *Lancet Neurol.* 5, 525–535.

Di Giovanni, S., Movsesyan, V., Ahmed, F., Cernak, I., Schinelli, S., Stoica, B., et al. (2005). Cell cycle inhibition provides neuroprotection and reduces glial proliferation and scar formation after traumatic brain injury. *Proc. Natl. Acad. Sci. U.S.A.* 102, 8333–8338. doi: 10.1073/pnas.0500989102

Dringen, R., Gutterer, J. M., and Hirrlinger, J. (2000). Glutathione metabolism in brain metabolic interaction between astrocytes and neurons in the defense against reactive oxygen species. *Eur. J. Biochem.* 267, 4912–4916. doi: 10.1046/j.1432-1327.2000.01597.x

Faideau, M., Kim, J., Cormier, K., Gilmore, R., Welch, M., Auregan, G., et al. (2010). In vivo expression of polyglutamine-expanded huntingtin by mouse striatal astrocytes impairs glutamate transport: a correlation with Huntington's disease subjects. *Hum. Mol. Genet.* 19, 3053–3067. doi: 10.1093/hmg/ddq212

Fleminger, S., Oliver, D. L., Lovestone, S., Rabe-Hesketh, S., and Giora, A. (2003). Head injury as a risk factor for Alzheimer's disease: the evidence 10 years on, a partial replication. *J. Neurol. Neurosurg. Psychiatry* 74, 857–862. doi: 10.1136/jnnp.74.7.857

Folkersma, H., Boellaard, R., Yaqub, M., Kloet, R. W., Windhorst, A. D., Lammertsma, A. A., et al. (2011). Widespread and prolonged increase in (R)-(11)C-PK11195 binding after traumatic brain injury. *J. Nuclear Med.* 52, 1235–1239. doi: 10.2967/jnumed.110.084061

Fotuhi, M., Hachinski, V., and Whitehouse, P. J. (2009). Changing perspectives regarding late-life dementia. *Nat. Rev. Neurol.* 5, 649–658. doi: 10.1038/nrneurol.2009.175

Franz, C. K., Joshi, D., Daley, E. L., Grant, R. A., Dalamagkas, K., Leung, A., et al. (2019). Impact of traumatic brain injury on amyotrophic lateral sclerosis: from bedside to bench. *J. Neurophysiol.* 122, 1174–1185. doi: 10.1152/jn.00572.2018

Fujimoto, M., Takagi, Y., Aoki, T., Hayase, M., Marumo, T., Gomi, M., et al. (2008). Tissue inhibitor of metalloproteinases protect blood-brain barrier disruption in focal cerebral ischemia. *J. Cereb. Blood Flow Metab.* 28, 1674–1685. doi: 10.1038/jcbfm.2008.59

Fujita, T., Yoshimine, T., Maruno, M., and Hayakawa, T. (1998). Cellular dynamics of macrophages and microglial cells in reaction to stab wounds in rat cerebral cortex. *Acta Neurochir.* 140, 275–279. doi: 10.1007/s007010050095

GBD 2016 Traumatic Brain Injury and Spinal Cord Injury Collaborators (2019). Global, regional, and national burden of traumatic brain injury and spinal cord injury, 1990-2016: a systematic analysis for the Global burden of disease study 2016. *Lancet Neurol.* 18, 56–87.

Gentleman, S. M., Leclercq, P. D., Moyes, L., Graham, D. I., Smith, C., Griffin, W. S., et al. (2004). Long-term intracerebral inflammatory response after traumatic brain injury. *Forensic Sci. Int.* 146, 97–104. doi: 10.1016/j.forsciint.2004.06.027

Goldman, S. M., Tanner, C. M., Oakes, D., Bhudhikanok, G. S., Gupta, A., and Langston, J. W. (2006). Head injury and Parkinson's disease risk in twins. *Ann. Neurol.* 60, 65–72. doi: 10.1002/ana.20882

Goldstein, L. E., Fisher, A. M., Tagge, C. A., Zhang, X. L., Velisek, L., Sullivan, J. A., et al. (2012). Chronic traumatic encephalopathy in blast-exposed military veterans and a blast neurotrauma mouse model. *Sci. Transl. Med.* 4:134ra60.

Gong, L., Manaenko, A., Fan, R., Huang, L., Enkhjargal, B., McBride, D., et al. (2018). Osteopontin attenuates inflammation via JAK2/STAT1 pathway in hyperglycemic rats after intracerebral hemorrhage. *Neuropharmacology* 138, 160–169. doi: 10.1016/j.neuropharm.2018.06.009

Graham, N. S., and Sharp, D. J. (2019). Understanding neurodegeneration after traumatic brain injury: from mechanisms to clinical trials in dementia. *J. Neurol. Neurosurg. Psychiatry* 90, 1221–1233. doi: 10.1136/jnnp-2017-317557

Gredilla, R., Bohr, V. A., and Stevnsner, T. (2010). Mitochondrial DNA repair and association with aging–an update. *Exp. Gerontol.* 45, 478–488. doi: 10.1016/j.exger.2010.01.017

Gu, X., Andre, V. M., Cepeda, C., Li, S. H., Li, X. J., Levine, M. S., et al. (2007). Pathological cell-cell interactions are necessary for striatal pathogenesis in a conditional mouse model of Huntington's disease. *Mol. Neurodegen.* 2:8. doi: 10.1186/1750-1326-2-8

Gu, X., Li, C., Wei, W., Lo, V., Gong, S., Li, S. H., et al. (2005). Pathological cell-cell interactions elicited by a neuropathogenic form of mutant Huntingtin contribute to cortical pathogenesis in HD mice. *Neuron* 46, 433–444. doi: 10.1016/j.neuron.2005.03.025

Guo, S., and Lo, E. H. (2009). Dysfunctional cell-cell signaling in the neurovascular unit as a paradigm for central nervous system disease. *Stroke* 40, S4–S7.

Gyoneva, S., and Ransohoff, R. M. (2015). Inflammatory reaction after traumatic brain injury: therapeutic potential of targeting cell-cell communication by chemokines. *Trends Pharmacol. Sci.* 36, 471–480. doi: 10.1016/j.tips.2015.04.003

Hailer, N. P. (2008). Immunosuppression after traumatic or ischemic CNS damage: it is neuroprotective and illuminates the role of microglial cells. *Prog. Neurobiol.* 84, 211–233. doi: 10.1016/j.pneurobio.2007.12.001

Halliday, M. R., Pomara, N., Sagare, A. P., Mack, W. J., Frangione, B., and Zlokovic, B. V. (2013). Relationship between cyclophilin a levels and matrix metalloproteinase 9 activity in cerebrospinal fluid of cognitively normal apolipoprotein e4 carriers and blood-brain barrier breakdown. *JAMA Neurol.* 70, 1198–1200.

Hay, J. R., Johnson, V. E., Young, A. M., Smith, D. H., and Stewart, W. (2015). Blood-brain barrier disruption is an early event that may persist for many years after traumatic brain injury in humans. *J. Neuropathol. Exp. Neurol.* 74, 1147–1157. doi: 10.1093/jnen/74.12.1147

Hayes, J. P., Logue, M. W., Sadeh, N., Spielberg, J. M., Verfaellie, M., Hayes, S. M., et al. (2017). Mild traumatic brain injury is associated with reduced cortical thickness in those at risk for Alzheimer's disease. *Brain* 140, 813–825.

Heneka, M. T., Carson, M. J., El Khoury, J., Landreth, G. E., Brosseron, F., Feinstein, D. L., et al. (2015). Neuroinflammation in Alzheimer's disease. *Lancet Neurol.* 14, 388–405.

Hoffer, M. E., Balaban, C., Slade, M. D., Tsao, J. W., and Hoffer, B. (2013). Amelioration of acute sequelae of blast induced mild traumatic brain injury by N-acetyl cysteine: a double-blind, placebo controlled study. *PLoS One* 8:e54163. doi: 10.1371/journal.pone.054163

Hong, Y. T., Veenith, T., Dewar, D., Outtrim, J. G., Mani, V., Williams, C., et al. (2014). Amyloid imaging with carbon 11-labeled Pittsburgh compound B for traumatic brain injury. *JAMA Neurol.* 71, 23–31.

Hu, X., Liou, A. K., Leak, R. K., Xu, M., An, C., Suenaga, J., et al. (2014). Neurobiology of microglial action in CNS injuries: receptor-mediated signaling mechanisms and functional roles. *Prog. Neurobiol.* 119-120, 60–84. doi: 10.1016/j.pneurobio.2014.06.002

Hynes, R. O. (1992). Integrins: versatility, modulation, and signaling in cell adhesion. *Cell* 69, 11–25. doi: 10.1016/0092-8674(92)90115-s

Iliff, J. J., Chen, M. J., Plog, B. A., Zeppenfeld, D. M., Soltero, M., Yang, L., et al. (2014). Impairment of glymphatic pathway function promotes tau pathology after traumatic brain injury. *J. Neurosci.* 34, 16180–16193. doi: 10.1523/jneurosci.3020-14.2014

Iliff, J. J., Wang, M., Liao, Y., Plogg, B. A., Peng, W., Gundersen, G. A., et al. (2012). A paravascular pathway facilitates CSF flow through the brain parenchyma and

the clearance of interstitial solutes, including amyloid beta. *Sci. Transl. Med.* 4:147ra111. doi: 10.1126/scitranslmed.3003748

Jafari, S., Etminan, M., Aminzadeh, F., and Samii, A. (2013). Head injury and risk of Parkinson disease: a systematic review and meta-analysis. *Mov. Disord.* 28, 1222–1229. doi: 10.1002/mds.25458

Jansen, A. H., van Hal, M., Op den Kelder, I. C., Meier, R. T., de Ruiter, A. A., Schut, M. H., et al. (2017). Frequency of nuclear mutant huntingtin inclusion formation in neurons and glia is cell-type-specific. *Glia* 65, 50–61. doi: 10.1002/glia.23050

Jayakumar, A. R., and Norenberg, M. D. (2010). The Na–K–Cl Co-transporter in astrocyte swelling. *Metab. Brain Dis.* 25, 31–38. doi: 10.1007/s11011-010-9180-3

Jeong, S. R., Kwon, M. J., Lee, H. G., Joe, E. H., Lee, J. H., Kim, S. S., et al. (2012). Hepatocyte growth factor reduces astrocytic scar formation and promotes axonal growth beyond glial scars after spinal cord injury. *Exp. Neurol.* 233, 312–322. doi: 10.1016/j.expneurol.2011.10.021

Jessen, N. A., Munk, A. S., Lundgaard, I., and Nedergaard, M. (2015). The glymphatic system: a beginner's guide. *Neurochem. Res.* 40, 2583–2599.

Ji, B., Zhou, F., Han, L., Yang, J., Fan, H., Li, S., et al. (2017). Sodium tanshinone IIA sulfonate enhances effectiveness Rt-PA treatment in acute ischemic stroke patients associated with ameliorating blood-brain barrier damage. *Transl. Stroke Res.* 8, 334–340. doi: 10.1007/s12975-017-0526-6

Johnson, V. E., Stewart, J. E., Begbie, F. D., Trojanowski, J. Q., Smith, D. H., and Stewart, W. (2013a). Inflammation and white matter degeneration persist for years after a single traumatic brain injury. *Brain* 136, 28–42. doi: 10.1093/brain/aws322

Johnson, V. E., Stewart, W., and Smith, D. H. (2013b). Axonal pathology in traumatic brain injury. *Exp. Neurol.* 246, 35–43. doi: 10.1016/j.expneurol.2012.01.013

Johnson, V. E., Stewart, W., and Smith, D. H. (2012). Widespread tau and amyloid-beta pathology many years after a single traumatic brain injury in humans. *Brain Pathol.* 22, 142–149. doi: 10.1111/j.1750-3639.2011.00513.x

Johnson, V. E., Stewart, W., Trojanowski, J. Q., and Smith, D. H. (2011). Acute and chronically increased immunoreactivity to phosphorylation-independent but not pathological TDP-43 after a single traumatic brain injury in humans. *Acta Neuropathol.* 122, 715–726. doi: 10.1007/s00401-011-0909-9

Johnson, V. E., Weber, M. T., Xiao, R., Cullen, D. K., Meaney, D. F., Stewart, W., et al. (2018). Mechanical disruption of the blood-brain barrier following experimental concussion. *Acta Neuropathol.* 135, 711–726. doi: 10.1007/s00401-018-1824-0

Kalia, L. V., and Lang, A. E. (2016). Parkinson disease in 2015: evolving basic, pathological and clinical concepts in PD. *Nat. Rev. Neurol.* 12, 65–66. doi: 10.1038/nrneurol.2015.249

Kardos, J., Heja, L., Jemnitz, K., Kovacs, R., and Palkovits, M. (2017). The nature of early astroglial protection-Fast activation and signaling. *Prog. Neurobiol.* 153, 86–99. doi: 10.1016/j.pneurobio.2017.03.005

Karimi-Abdolrezaee, S., and Billakanti, R. (2012). Reactive astrogliosis after spinal cord injury-beneficial and detrimental effects. *Mol. Neurobiol.* 46, 251–264. doi: 10.1007/s12035-012-8287-4

Khaksari, M., Soltani, Z., and Shahrokhi, N. (2018). Effects of female sex steroids administration on pathophysiologic mechanisms in traumatic brain injury. *Transl. Stroke Res.* 9, 393–416. doi: 10.1007/s12975-017-0588-5

Kofuji, P., and Newman, E. A. (2004). Potassium buffering in the central nervous system. *Neuroscience* 129, 1045–1056.

Kondo, A., Shahpasand, K., Mannix, R., Qiu, J., Moncaster, J., Chen, C. H., et al. (2015). Antibody against early driver of neurodegeneration cis P-tau blocks brain injury and tauopathy. *Nature* 523, 431–436. doi: 10.1038/nature14658

Kumar, A., Nisha, C. M., Silakari, C., Sharma, I., Anusha, K., Gupta, N., et al. (2016). Current and novel therapeutic molecules and targets in Alzheimer's disease. *J. Form. Med. Assoc.* 115, 3–10.

Kumar, A., Stoica, B. A., Loane, D. J., Yang, M., Abulwerdi, G., Khan, N., et al. (2017). Microglial-derived microparticles mediate neuroinflammation after traumatic brain injury. *J. Neuroinflamm.* 14:47.

Kumar, A., Takada, Y., Boriek, A. M., and Aggarwal, B. B. (2004). Nuclear factor-kappaB: its role in health and disease. *J. Mol. Med.* 82, 434–448.

Ladwig, A., Walter, H. L., Hucklenbroich, J., Willuweit, A., Langen, K. J., Fink, G. R., et al. (2017). Osteopontin augments M2 microglia response and separates M1- and M2-polarized microglial activation in permanent focal cerebral ischemia. *Med. Inflamm.* 2017:7189421.

Lang, F., Busch, G. L., Ritter, M., Völkl, H., Waldegger, S., Gulbins, E., et al. (1998). Functional significance of cell volume regulatory mechanisms. *Physiol. Rev.* 78, 247–306. doi: 10.1152/physrev.1998.78.1.247

Li, C., Ebrahimi, A., and Schluesener, H. (2013). Drug pipeline in neurodegeneration based on transgenic mice models of Alzheimer's disease. *Ageing Res. Rev.* 12, 116–140. doi: 10.1016/j.arr.2012.09.002

Liang, C. L., Wang, T. T., Luby-Phelps, K., and German, D. C. (2007). Mitochondria mass is low in mouse substantia nigra dopamine neurons: implications for Parkinson's disease. *Exp. Neurol.* 203, 370–380. doi: 10.1016/j.expneurol.2006.08.015

Lo, E. H., and Rosenberg, G. A. (2009). The neurovascular unit in health and disease: introduction. *Stroke* 40, S2–S3.

LoBue, C., Munro, C., Schaffert, J., Didehbani, N., Hart, J., Batjer, H., et al. (2019). Traumatic brain injury and risk of long-term brain changes, accumulation of pathological markers, and developing dementia: a review. *J. Alzheimer Dis.* 70, 629–654. doi: 10.3233/jad-190028

Logsdon, A. F., Lucke-Wold, B. P., Turner, R. C., Huber, J. D., Rosen, C. L., and Simpkins, J. W. (2015). Role of microvascular disruption in brain damage from traumatic brain injury. *Comprehens. Physiol.* 5, 1147–1160. doi: 10.1002/cphy.c140057

Lok, J., Wang, X. S., Xing, C. H., Maki, T. K., Wu, L. M., Guo, S. Z., et al. (2015). Targeting the neurovascular unit in brain trauma. *CNS Neurosci. Therap.* 21, 304–308. doi: 10.1111/cns.12359

Louveau, A., Plog, B. A., Antila, S., Alitalo, K., Nedergaard, M., and Kipnis, J. (2017). Understanding the functions and relationships of the glymphatic system and meningeal lymphatics. *J. Clin. Invest.* 127, 3210–3219. doi: 10.1172/jci90603

Luna, J., Diagana, M., Ait Aissa, L., Tazir, M., Ali Pacha, L., Kacem, I., et al. (2019). Clinical features and prognosis of amyotrophic lateral sclerosis in Africa: the TROPALS study. *J. Neurol. Neurosurg. Psychiatry* 90, 20–29.

Maas, A. I. R., Menon, D. K., Adelson, P. D., Andelic, N., Bell, M. J., Belli, A., et al. (2017). Traumatic brain injury: integrated approaches to improve prevention, clinical care, and research. *Lancet Neurol.* 16, 987–1048.

Magistretti, P. J. (2006). Neuron-glia metabolic coupling and plasticity. *J. Exp. Biol.* 209, 2304–2311. doi: 10.1242/jeb.02208

Magistretti, P. J., and Pellerin, L. (1999). Cellular mechanisms of brain energy metabolism and their relevance to functional brain imaging. *Philos. Trans. R. Soc. Lond. B Biol. Sci.* 354, 1155–1163. doi: 10.1098/rstb.1999.0471

Main, B. S., Villapol, S., Sloley, S. S., Barton, D. J., Parsadanian, M., Agbaegbu, C., et al. (2018). Apolipoprotein E4 impairs spontaneous blood brain barrier repair following traumatic brain injury. *Mol. Neurodegen.* 13:17.

Martland, H. S. (1928). Punch drunk. *J. Am. Med. Assoc.* 91, 1103–1107.

Masters, C. L., Bateman, R., Blennow, K., Rowe, C. C., Sperling, R. A., and Cummings, J. L. (2015). Alzheimer's disease. *Nat. Rev. Dis. Prim.* 1:15056.

Maxwell, W. L., Domleo, A., McColl, G., Jafari, S. S., and Graham, D. I. (2003). Post-acute alterations in the axonal cytoskeleton after traumatic axonal injury. *J. Neurotrauma* 20, 151–168. doi: 10.1089/08977150360547071

McKee, A. C., Stein, T. D., Nowinski, C. J., Stern, R. A., Daneshvar, D. H., Alvarez, V. E., et al. (2012). The spectrum of disease in chronic traumatic encephalopathy. *Brain* 136, 43–64.

Mendiola-Precoma, J., Berumen, L. C., Padilla, K., and Garcia-Alcocer, G. (2016). Therapies for prevention and treatment of Alzheimer's Disease. *Biomed. Res. Intern.* 2016:2589276.

Michinaga, S., and Koyama, Y. (2019). Dual roles of astrocyte-derived factors in regulation of blood-brain barrier function after brain damage. *Intern. J. Mol. Sci.* 20:E571.

Mondello, S., Kobeissy, F., Vestri, A., Hayes, R. L., Kochanek, P. M., and Berger, R. P. (2016). Serum concentrations of ubiquitin C-terminal hydrolase-L1 and glial fibrillary acidic protein after pediatric traumatic brain injury. *Sci. Rep.* 6:28203.

Mortimer, J. A., Van Duijn, C. M., Chandra, V., Fratiglioni, L., Graves, A. B., Heyman, A., et al. (1991). Head trauma as a risk factor for alzheimer's disease: A collaborativere-analysis of case-control studies. *Int. J. Epidemiol.* 20, S28–S35.

Murakami, K., Koide, M., Dumont, T. M., Russell, S. R., Tranmer, B. I., and Wellman, G. C. (2011). Subarachnoid hemorrhage induces gliosis and increased

expression of the pro-inflammatory cytokine high mobility group box 1 protein. *Transl. Stroke Res.* 2, 72–79. doi: 10.1007/s12975-010-0052-2

Nagamoto-Combs, K., McNeal, D. W., Morecraft, R. J., and Combs, C. K. (2007). Prolonged microgliosis in the rhesus monkey central nervous system after traumatic brain injury. *J. Neurotrauma* 24, 1719–1742. doi: 10.1089/neu.2007.0377

Nagamoto-Combs, K., Morecraft, R. J., Darling, W. G., and Combs, C. K. (2010). Long-term gliosis and molecular changes in the cervical spinal cord of the rhesus monkey after traumatic brain injury. *J. Neurotrauma* 27, 565–585. doi: 10.1089/neu.2009.0966

Najjar, S., Pahlajani, S., De Sanctis, V., Stern, J. N. H., Najjar, A., and Chong, D. (2017). Neurovascular unit dysfunction and blood-brain barrier hyperpermeability contribute to schizophrenia neurobiology: a theoretical integration of clinical and experimental evidence. *Front. Psychiatry* 8:83. doi: 10.3389/fpsyt.2017.00083

Neuwelt, E., Abbott, N. J., Abrey, L., Banks, W. A., Blakley, B., Davis, T., et al. (2008). Strategies to advance translational research into brain barriers. *Lancet Neurol.* 7, 84–96. doi: 10.1016/s1474-4422(07)70326-5

Orimo, S. (2017). New development of diagnosis and treatment for Parkinson's disease. *Clin. Neurol.* 57, 259–273.

Ott, M., Gogvadze, V., Orrenius, S., and Zhivotovsky, B. (2007). Mitochondria, oxidative stress and cell death. *Apoptosis* 12, 913–922. doi: 10.1007/s10495-007-0756-2

Papa, L., Mittal, M. K., Ramirez, J., Ramia, M., Kirby, S., Silvestri, S., et al. (2016). In children and youth with mild and moderate traumatic brain injury, glial fibrillary acidic protein out-performs s100beta in detecting traumatic intracranial lesions on computed tomography. *J. Neurotrauma* 33, 58–64. doi: 10.1089/neu.2015.3869

Pavlovic, D., Pekic, S., Stojanovic, M., and Popovic, V. (2019). Traumatic brain injury: neuropathological, neurocognitive and neurobehavioral sequelae. *Pituitary* 22, 270–282. doi: 10.1007/s11102-019-00957-9

Peng, L., Parpura, V., and Verkhratsky, A. (2014). Editorial neuroglia as a central element of neurological diseases: an underappreciated target for therapeutic intervention. *Curr. Neuropharmacol.* 12, 303–307. doi: 10.2174/1570159x12999140829152550

Perez, E. J., Tapanes, S. A., Loris, Z. B., Balu, D. T., Sick, T. J., Coyle, J. T., et al. (2017). Enhanced astrocytic d-serine underlies synaptic damage after traumatic brain injury. *J. Clin. Invest.* 127, 3114–3125. doi: 10.1172/jci92300

Petty, M. A., and Lo, E. H. (2002). Junctional complexes of the blood-brain barrier: permeability changes in neuroinflammation. *Prog. Neurobiol.* 68, 311–323. doi: 10.1016/s0301-0082(02)00128-4

Piao, C. S., Holloway, A. L., Hong-Routson, S., and Wainwright, M. S. (2019). Depression following traumatic brain injury in mice is associated with down-regulation of hippocampal astrocyte glutamate transporters by thrombin. *J. Cereb. Blood Flow Metab.* 39, 58–73. doi: 10.1177/0271678x17742792

Plemel, J. R., Keough, M. B., Duncan, G. J., Sparling, J. S., Yong, V. W., Stys, P. K., et al. (2014). Remyelination after spinal cord injury: is it a target for repair? *Prog. Neurobiol.* 117, 54–72.

Pupillo, E., Poloni, M., Bianchi, E., Giussani, G., Logroscino, G., Zoccolella, S., et al. (2018). Trauma and amyotrophic lateral sclerosis: a european population-based case-control study from the EURALS consortium. *Amyotrop. Later. Scler. Frontotemp. Degen.* 19, 118–125. doi: 10.1080/21678421.2017.1386687

Raj, R., Kaprio, J., Korja, M., Mikkonen, E. D., Jousilahti, P., and Siironen, J. (2017). Risk of hospitalization with neurodegenerative disease after moderate-to-severe traumatic brain injury in the working-age population: a retrospective cohort study using the Finnish national health registries. *PLoS Med.* 14:e1002316. doi: 10.1371/journal.pone.01002316

Ramlackhansingh, A. F., Brooks, D. J., Greenwood, R. J., Bose, S. K., Turkheimer, F. E., Kinnunen, K. M., et al. (2011). Inflammation after trauma: microglial activation and traumatic brain injury. *Ann. Neurol.* 70, 374–383. doi: 10.1002/ana.22455

Rascher, G., Fischmann, A., Kroger, S., Duffner, F., Grote, E. H., and Wolburg, H. (2002). Extracellular matrix and the blood-brain barrier in glioblastoma multiforme: spatial segregation of tenascin and agrin. *Acta Neuropathol.* 104, 85–91. doi: 10.1007/s00401-002-0524-x

Rasmussen, M. K., Mestre, H., and Nedergaard, M. (2018). The glymphatic pathway in neurological disorders. *Lancet Neurol.* 17, 1016–1024. doi: 10.1016/s1474-4422(18)30318-1

Ren, Z., Iliff, J. J., Yang, L., Yang, J., Chen, X., Chen, M. J., et al. (2013). 'Hit & Run' model of closed-skull traumatic brain injury (TBI) reveals complex patterns of post-traumatic AQP4 dysregulation. *J. Cereb. Blood Flow Metab.* 33, 834–845.

Roberts, G. W., Gentleman, S. M., Lynch, A., and Graham, D. I. (1991). beta A4 amyloid protein deposition in brain after head trauma. *Lancet* 338, 1422–1423. doi: 10.1016/0140-6736(91)92724-g

Rodriguez, M., Morales, I., Rodriguez-Sabate, C., Sanchez, A., Castro, R., Brito, J. M., et al. (2014). The degeneration and replacement of dopamine cells in Parkinson's disease: the role of aging. *Front. Neuroanat.* 8:80. doi: 10.3389/fphar.2019.0080

Rodriguez, M., Rodriguez-Sabate, C., Morales, I., Sanchez, A., and Sabate, M. (2015). Parkinson's disease as a result of aging. *Aging Cell* 14, 293–308.

Rothstein, J. D., Dykes-Hoberg, M., Pardo, C. A., Bristol, L. A., Jin, L., Kuncl, R. W., et al. (1996). Knockout of glutamate transporters reveals a major role for astroglial transport in excitotoxicity and clearance of glutamate. *Neuron* 16, 675–686. doi: 10.1016/s0896-6273(00)80086-0

Russo, M. V., and McGavern, D. B. (2016). Inflammatory neuroprotection following traumatic brain injury. *Science* 353, 783–785. doi: 10.1126/science.aaf6260

Salminen, A., Ojala, J., Kaarniranta, K., Haapasalo, A., Hiltunen, M., and Soininen, H. (2011). Astrocytes in the aging brain express characteristics of senescence-associated secretory phenotype. *Eur. J. Neurosci.* 34, 3–11. doi: 10.1111/j.1460-9568.2011.07738.x

Scott, G., Ramlackhansingh, A. F., Edison, P., Hellyer, P., Cole, J., Veronese, M., et al. (2016). Amyloid pathology and axonal injury after brain trauma. *Neurology* 86, 821–828. doi: 10.1212/wnl.0000000000002413

Scott, G., Zetterberg, H., Jolly, A., Cole, J. H., De Simoni, S., Jenkins, P. O., et al. (2018). Minocycline reduces chronic microglial activation after brain trauma but increases neurodegeneration. *Brain* 141, 459–471. doi: 10.1093/brain/awx339

Seals, R. M., Hansen, J., Gredal, O., and Weisskopf, M. G. (2016). Physical trauma and amyotrophic lateral sclerosis: a population-based study using danish national registries. *Am. J. Epidemiol.* 183, 294–301. doi: 10.1093/aje/kwv169

Seo, J. H., Maki, T., Maeda, M., Miyamoto, N., Liang, A. C., Hayakawa, K., et al. (2014). Oligodendrocyte precursor cells support blood-brain barrier integrity via TGF-beta signaling. *PLoS One* 9:e103174. doi: 10.1371/journal.pone.0103174

Sevenich, L. (2018). Brain-resident microglia and blood-borne macrophages orchestrate central nervous system inflammation in neurodegenerative disorders and brain cancer. *Front. Immunol.* 9:697.

Shahim, P., Zetterberg, H., Tegner, Y., and Blennow, K. (2017). Serum neurofilament light as a biomarker for mild traumatic brain injury in contact sports. *Neurology* 88, 1788–1794. doi: 10.1212/wnl.0000000000003912

Sharma, K., Zhang, G., and Li, S. (2015). *Chapter 11 - Astrogliosis and Axonal Regeneration*. Oxford: Academic Press.

Shetty, A. K., Mishra, V., Kodali, M., and Hattiangady, B. (2014). Blood brain barrier dysfunction and delayed neurological deficits in mild traumatic brain injury induced by blast shock waves. *Front. Cell. Neurosci.* 8:232. doi: 10.3389/fphar.2019.00232

Shin, J. Y., Fang, Z. H., Yu, Z. X., Wang, C. E., Li, S. H., and Li, X. J. (2005). Expression of mutant huntingtin in glial cells contributes to neuronal excitotoxicity. *J. Cell Biol.* 171, 1001–1012. doi: 10.1083/jcb.200508072

Shively, S. B., Edgerton, S. L., Iacono, D., Purohit, D. P., Qu, B. X., Haroutunian, V., et al. (2017). Localized cortical chronic traumatic encephalopathy pathology after single, severe axonal injury in human brain. *Acta Neuropathol.* 133, 353–366. doi: 10.1007/s00401-016-1649-7

Shlosberg, D., Benifla, M., Kaufer, D., and Friedman, A. (2010). Blood-brain barrier breakdown as a therapeutic target in traumatic brain injury. *Nat. Rev. Neurol.* 6, 393–403. doi: 10.1038/nrneurol.2010.74

Shokri-Kojori, E., Wang, G. J., Wiers, C. E., Demiral, S. B., Guo, M., Kim, S. W., et al. (2018). beta-Amyloid accumulation in the human brain after one night of sleep deprivation. *Proc. Natl. Acad. Sci. U.S.A.* 115, 4483–4488. doi: 10.1073/pnas.1721694115

Simon, D. W., McGeachy, M. J., Bayir, H., Clark, R. S., Loane, D. J., and Kochanek, P. M. (2017). The far-reaching scope of neuroinflammation after traumatic brain injury. *Nat. Rev. Neurol.* 13, 171–191. doi: 10.1038/nrneurol.2017.13

Sleigh, J. N., Tosolini, A. P., Gordon, D., Devoy, A., Fratta, P., Fisher, E. M. C., et al. (2020). Mice carrying ALS mutant TDP-43, but not mutant FUS, display in vivo defects in axonal transport of signaling endosomes. *Cell Rep.* 30, 3655–3662.

Slemmer, J. E., Shacka, J. J., Sweeney, M. I., and Weber, J. T. (2008). Antioxidants and free radical scavengers for the treatment of stroke, traumatic brain injury and aging. *Curr. Med. Chem.* 15, 404–414. doi: 10.2174/092986708783497337

Smith, D. H., Chen, X. H., Pierce, J. E., Wolf, J. A., Trojanowski, J. Q., Graham, D. I., et al. (1997). Progressive atrophy and neuron death for one year following brain trauma in the rat. *J. Neurotrauma* 14, 715–727. doi: 10.1089/neu.1997.14.715

Smith, D. H., Johnson, V. E., and Stewart, W. (2013). Chronic neuropathologies of single and repetitive TBI: substrates of dementia? *Nat. Rev. Neurol.* 9, 211–221. doi: 10.1038/nrneurol.2013.29

Sofroniew, M. V. (2009). dissection of reactive astrogliosis and glial scar formation. *Trends Neurosci.* 32, 638–647. doi: 10.1016/j.tins.2009.08.002

Sofroniew, M. V. (2015). Astrocyte barriers to neurotoxic inflammation. *Nat. Rev. Neurosci.* 16, 249–263. doi: 10.1038/nrn3898

Sofroniew, M. V., and Vinters, H. V. (2010). Astrocytes: biology and pathology. *Acta Neuropathol.* 119, 7–35. doi: 10.1007/s00401-009-0619-8

Sullan, M. J., Asken, B. M., Jaffee, M. S., DeKosky, S. T., and Bauer, R. M. (2018). Glymphatic system disruption as a mediator of brain trauma and chronic traumatic encephalopathy. *Neurosci. Biobehav. Rev.* 84, 316–324. doi: 10.1016/j.neubiorev.2017.08.016

Susarla, B. T., Villapol, S., Yi, J. H., Geller, H. M., and Symes, A. J. (2014). Temporal patterns of cortical proliferation of glial cell populations after traumatic brain injury in mice. *ASN Neuro* 6, 159–170.

Suzuki, H., Ayer, R., Sugawara, T., Chen, W., Sozen, T., Hasegawa, Y., et al. (2010). Protective effects of recombinant osteopontin on early brain injury after subarachnoid hemorrhage in rats. *Crit. Care Med.* 38, 612–618. doi: 10.1097/ccm.0b013e3181c027ae

Sweeney, M. D., Ayyadurai, S., and Zlokovic, B. V. (2016). Pericytes of the neurovascular unit: key functions and signaling pathways. *Nat. Neurosci.* 19, 771–783. doi: 10.1038/nn.4288

Sweeney, M. D., Sagare, A. P., and Zlokovic, B. V. (2018). Blood-brain barrier breakdown in Alzheimer disease and other neurodegenerative disorders. *Nat. Rev. Neurol.* 14, 133–150. doi: 10.1038/nrneurol.2017.188

Tagge, C. A., Fisher, A. M., Minaeva, O. V., Gaudreau-Balderrama, A., Moncaster, J. A., Zhang, X. L., et al. (2018). Concussion, microvascular injury, and early tauopathy in young athletes after impact head injury and an impact concussion mouse model. *Brain* 141, 422–458. doi: 10.1093/brain/awx350

Tilling, T., Engelbertz, C., Decker, S., Korte, D., Huwel, S., and Galla, H. J. (2002). Expression and adhesive properties of basement membrane proteins in cerebral capillary endothelial cell cultures. *Cell Tissue Res.* 310, 19–29. doi: 10.1007/s00441-002-0604-1

Tilling, T., Korte, D., Hoheisel, D., and Galla, H. J. (1998). Basement membrane proteins influence brain capillary endothelial barrier function in vitro. *J. Neurochem.* 71, 1151–1157. doi: 10.1046/j.1471-4159.1998.71031151.x

Tran, H. T., LaFerla, F. M., Holtzman, D. M., and Brody, D. L. (2011). Controlled cortical impact traumatic brain injury in 3xTg-AD mice causes acute intra-axonal amyloid-beta accumulation and independently accelerates the development of tau abnormalities. *J. Neurosci.* 31, 9513–9525. doi: 10.1523/jneurosci.0858-11.2011

Tso, M. K., and Macdonald, R. L. (2014). Subarachnoid hemorrhage: a review of experimental studies on the microcirculation and the neurovascular unit. *Transl. Stroke Res.* 5, 174–189. doi: 10.1007/s12975-014-0323-4

Uryu, K., Chen, X. H., Martinez, D., Browne, K. D., Johnson, V. E., Graham, D. I., et al. (2007). Multiple proteins implicated in neurodegenerative diseases accumulate in axons after brain trauma in humans. *Exp. Neurol.* 208, 185–192. doi: 10.1016/j.expneurol.2007.06.018

Verkhratsky, A., Parpura, V., Pekna, M., Pekny, M., and Sofroniew, M. (2014). Glia in the pathogenesis of neurodegenerative diseases. *Biochem. Soc. Trans.* 42, 1291–1301. doi: 10.1042/bst20140107

Viviani, B., Boraso, M., Marchetti, N., and Marinovich, M. (2014). Perspectives on neuroinflammation and excitotoxicity: a neurotoxic conspiracy? *Neurotoxicology* 43, 10–20. doi: 10.1016/j.neuro.2014.03.004

Voskuhl, R. R., Peterson, R. S., Song, B., Ao, Y., Morales, L. B., Tiwari-Woodruff, S., et al. (2009). Reactive astrocytes form scar-like perivascular barriers to leukocytes during adaptive immune inflammation of the CNS. *J. Neurosci.* 29, 11511–11522. doi: 10.1523/jneurosci.1514-09.2009

Walz, W. (2000). Role of astrocytes in the clearance of excess extracellular potassium. *Neurochem. Int.* 36, 291–300. doi: 10.1016/s0197-0186(99)00137-0

Wang, Y., Ji, X., Leak, R. K., Chen, F., and Cao, G. (2017). Stem cell therapies in age-related neurodegenerative diseases and stroke. *Ageing Res. Rev.* 34, 39–50. doi: 10.1016/j.arr.2016.11.002

Weilinger, N. L., Maslieieva, V., Bialecki, J., Sridharan, S. S., Tang, P. L., and Thompson, R. J. (2013). Ionotropic receptors and ion channels in ischemic neuronal death and dysfunction. *Acta Pharmacol. Sin.* 34, 39–48. doi: 10.1038/aps.2012.95

Welch, R. D., Ayaz, S. I., Lewis, L. M., Unden, J., Chen, J. Y., Mika, V. H., et al. (2016). Ability of serum glial fibrillary acidic protein, Ubiquitin C-terminal hydrolase-L1, and S100B to differentiate normal and abnormal head computed tomography findings in patients with suspected mild or moderate traumatic brain injury. *J. Neurotrauma* 33, 203–214. doi: 10.1089/neu.2015.4149

Wiesner, D., Tar, L., Linkus, B., Chandrasekar, A., Olde Heuvel, F., Dupuis, L., et al. (2018). Reversible induction of TDP-43 granules in cortical neurons after traumatic injury. *Exp. Neurol.* 299, 15–25. doi: 10.1016/j.expneurol.2017.09.011

Williams, S. M., Peltz, C., Yaffe, K., Schulz, P., and Sierks, M. R. (2018). CNS disease-related protein variants as blood-based biomarkers in traumatic brain injury. *Neurology* 91, 702–709. doi: 10.1212/wnl.0000000000006322

Wimo, A., Guerchet, M., Ali, G.-C., Wu, Y.-T., Prina, A. M., Winblad, B., et al. (2017). The worldwide costs of dementia 2015 and comparisons with 2010. *Alzheimer Dement.* 13, 1–7. doi: 10.1016/j.jalz.2016.07.150

Wu, J., He, J., Tian, X., Zhong, J., Li, H., and Sun, X. (2020). Activation of the hedgehog pathway promotes recovery of neurological function after traumatic brain injury by protecting the neurovascular unit. *Transl. Stroke Res.* doi: 10.1007/s12975-019-00771-2 [Epub ahead of print].

Xiong, K. L., Zhu, Y. S., and Zhang, W. G. (2014). Diffusion tensor imaging and magnetic resonance spectroscopy in traumatic brain injury: a review of recent literature. *Brain Imag. Behav.* 8, 487–496. doi: 10.1007/s11682-013-9288-2

Yang, Z., and Wang, K. K. (2015). Glial fibrillary acidic protein: from intermediate filament assembly and gliosis to neurobiomarker. *Trends Neurosci.* 38, 364–374. doi: 10.1016/j.tins.2015.04.003

Ye, Z. C., Wyeth, M. S., Baltan-Tekkok, S., and Ransom, B. R. (2003). hemichannels in astrocytes: a novel mechanism of glutamate release. *J. Neurosci.* 23, 3588–3596. doi: 10.1523/jneurosci.23-09-03588.2003

Zanier, E. R., Bertani, I., Sammali, E., Pischiutta, F., Chiaravalloti, M. A., Vegliante, G., et al. (2018). Induction of a transmissible tau pathology by traumatic brain injury. *Brain* 141, 2685–2699.

Zenaro, E., Piacentino, G., and Constantin, G. (2017). The blood-brain barrier in Alzheimer's disease. *Neurobiol. Dis.* 107, 41–56.

Zhang, D., Xiao, M., Wang, L., and Jia, W. (2019). Blood-based glutamate scavengers reverse traumatic brain injury-induced synaptic plasticity disruption by decreasing glutamate level in hippocampus interstitial fluid, but not cerebral spinal fluid, in vivo. *Neurotox. Res.* 35, 360–372. doi: 10.1007/s12640-018-9961-8

Zhang, J. H., Badaut, J., Tang, J., Obenaus, A., Hartman, R., and Pearce, W. J. (2012). The vascular neural network–a new paradigm in stroke pathophysiology. *Nat. Rev. Neurol.* 8, 711–716. doi: 10.1038/nrneurol.2012.210

Zhang, X., Chen, Y., Jenkins, L. W., Kochanek, P. M., and Clark, R. S. (2005). Bench-to-bedside review: apoptosis/programmed cell death triggered by traumatic brain injury. *Crit. Care* 9, 66–75.

Zhao, H., Liu, Y., Zeng, J., Li, D., and Huang, Y. (2018). *Troxerutin cerebroprotein* hydrolysate injection ameliorates neurovascular injury induced by traumatic brain injury - via endothelial nitric oxide synthase pathway regulation. *Int. J. Neurosci.* 128, 1118–1127. doi: 10.1080/00207454.2018.1486828

Zhao, Z., Nelson, A. R., Betsholtz, C., and Zlokovic, B. V. (2015). Establishment and dysfunction of the blood-brain barrier. *Cell* 163, 1064–1078. doi: 10.1016/j.cell.2015.10.067

Zhou, Y., Shao, A., Xu, W., Wu, H., and Deng, Y. (2019). Advance of stem cell treatment for traumatic brain injury. *Front. Cell. Neurosci.* 13:301. doi: 10.3389/fphar.2019.00301

Zhou, Y., Shao, A., Yao, Y., Tu, S., Deng, Y., and Zhang, J. (2020). Dual roles of astrocytes in plasticity and reconstruction after traumatic brain injury. *Cell Commun. Signal.* 18:62.

Ziebell, J. M., and Morganti-Kossmann, M. C. (2010). Involvement of pro- and anti-inflammatory cytokines and chemokines in the pathophysiology of traumatic brain injury. *Neurotherapeutics* 7, 22–30. doi: 10.1016/j.nurt.2009.10.016

Zou, J., Wang, Y. X., Dou, F. F., Lu, H. Z., Ma, Z. W., Lu, P. H., et al. (2010). Glutamine synthetase down-regulation reduces astrocyte protection against glutamate excitotoxicity to neurons. *Neurochem. Int.* 56, 577–584. doi: 10.1016/j.neuint.2009.12.021

Conflict of Interest: The authors declare that the research was conducted in the absence of any commercial or financial relationships that could be construed as a potential conflict of interest.

frontiers in Neuroscience

ORIGINAL RESEARCH
published: 09 July 2020
doi: 10.3389/fnins.2020.00723

Neuroprotection Against Parkinson's Disease Through the Activation of Akt/GSK3β Signaling Pathway by Tovophyllin A

Yanjun Huang[1†], Lirong Sun[1†], Shuzhen Zhu[2], Liu Xu[1], Shuhu Liu[1], Chunhua Yuan[1], Yanwu Guo[3] and Xuemin Wang[1*]*

[1] Key Laboratory of Mental Health of the Ministry of Education, Guangdong-Hong Kong-Macao Greater Bay Area Center for Brain Science and Brain-Inspired Intelligence, Guangdong Province Key Laboratory of Psychiatric Disorders, Department of Neurobiology, School of Basic Medical Sciences, Southern Medical University, Guangzhou, China, [2] Department of Neurology, Zhujiang Hospital, Southern Medical University, Guangzhou, China, [3] Department of Neurosurgery, Zhujiang Hospital, Southern Medical University, Guangzhou, China

OPEN ACCESS

Edited by:
Eng-King Tan,
National Neuroscience Institute (NNI), Singapore

Reviewed by:
Wanlin Yang,
Zhujiang Hospital, Southern Medical University, China
Xiaoli Tang,
Brown University, United States
Penghua Wang,
University of Connecticut Health Center, United States

***Correspondence:**
Lirong Sun
sunlr0807@smu.edu.cn
Xuemin Wang
xmwang@smu.edu.cn

[†] These authors have contributed equally to this work

Specialty section:
This article was submitted to Neurodegeneration, a section of the journal Frontiers in Neuroscience

Received: 26 February 2020
Accepted: 17 June 2020
Published: 09 July 2020

Citation:
Huang Y, Sun L, Zhu S, Xu L, Liu S, Yuan C, Guo Y and Wang X (2020) Neuroprotection Against Parkinson's Disease Through the Activation of Akt/GSK3β Signaling Pathway by Tovophyllin A. Front. Neurosci. 14:723. doi: 10.3389/fnins.2020.00723

Parkinson's disease (PD) is one of the most prevalent and life-threatening neurodegenerative disease and mainly characterized by lack of sufficient dopaminergic neurons in the substantia nigra pars compacta (SNc). Although current treatments help to alleviate clinical symptoms, effective therapies preventing neuronal loss remain scarce. Tovophyllin A (TA), one of the xanthones extracted from *Garcinia mangostana* L. (GM), has recently been reported to play a beneficial role in the therapy of neurodegenerative diseases. In our research, we explored whether TA has protective effects on dopaminergic neurons in PD models. We found that TA significantly reduced apoptotic cell death in primary cortical neurons treated with 1-methyl-4-phenyl pyridinium (MPP^+) or paraquat (PQ) in the *in vitro* PD model. In an *in vivo* acute PD model induced by 1-methyl4-phenyl-1,2,3,5-tetrahydropyridine (MPTP) treatment, TA also attenuated the resulting behavioral dysfunctions and dopaminergic neuron loss. In the collected brain tissues, TA increased the phosphorylation of Akt and GSK-3β, which may be related to TA-mediated dopaminergic neuronal protective effects. In summary, our results illustrated that TA is a powerful cytoprotective agent for dopaminergic neurons in the MPTP-induced PD model, suggesting TA as a possible therapeutic candidate for PD.

Keywords: Tovophyllin A, Parkinson's disease, apoptosis, Akt, GSK3β

INTRODUCTION

Parkinson's disease (PD), a long-term and complex movement disorder, is hallmarked by the classical motor features, including slowness of movement, resting tremors, stiffness, and postural instability (Dauer and Przedborski, 2003; Dexter and Jenner, 2013; Kalia and Lang, 2015). In recent years, non-motor symptoms have also been highly concerned, such as olfactory impairments, sleep disorders, autonomic dysfunctions, and emotional disturbances (Kalia and Lang, 2015). The major pathology of PD is characterized by the gradual and massive loss of dopaminergic neurons in the substantial nigra pars compacta (SNc), resulting in a reduction in dopamine (DA) levels (Martinez et al., 2017). Although the precise pathogenic mechanism of the neurodegeneration in PD is not yet fully understood, various factors that alone or together, such as oxidative stress (OS), neuroinflammation and mitochondrial toxins,

have been implicated to the progressive impairments of dopaminergic neurons (Moon and Paek, 2015; Morris and Berk, 2015; Hu et al., 2019). It is widely accepted that energy deficits caused by mitochondrial dysregulation and oxidative stress induced by high levels of unstable radicals could mightily contributed to neurodegenerative diseases (Iarkov et al., 2020).

1-methyl4-phenyl-1,2,3,5-tetrahydropyridine (MPTP) and 1-methyl-4-phenyl pyridinium (MPP^+) are well-known neurotoxins. MPP^+, the active metabolite of MPTP, is transported into dopaminergic neurons by the dopamine transporter (DAT). It is then isolated into synaptosomal vesicles or enriched in the mitochondria, where it promotes the production of free radicals (Jackson-Lewis and Przedborski, 2007; Motyl et al., 2018). As dopaminergic neurons are highly sensitive to these compounds, MPP^+ and MPTP are widely used to establish diverse PD models, both *in vitro* and *in vivo* (Cui et al., 2013; Jantas et al., 2014; Zhao et al., 2016). When response to the toxicology of MPP^+ and MPTP, necrotic and apoptotic mechanisms of cell death occurred.

Current pharmacological therapeutics such as dopamine precursor, L-DOPA and DA receptor agonists could ameliorate clinical symptoms, and the classical surgical treatment called deep brain stimulation (DBS) can also improve the symptoms, however, all these approaches rarely alleviate dopaminergic neuronal loss (Rizek et al., 2016; Iarkov et al., 2020). Thus, identifying new neuroprotectants that reduce neuronal loss is of great significance for the treatment of PD.

Glycogen synthase kinase-3β (GSK-3β) is tightly related to the loss of dopaminergic neurons in PD models and MPP^+-caused neuronal death (Golpich et al., 2015; Chen et al., 2017; Yue et al., 2017). It can be inactivated by Akt and other kinases by phosphorylating of the single serine residue (Ser9), which is located in the regulatory N-terminal domain (Frame and Cohen, 2001; Beaulieu, 2007). Akt is a key player in the phosphoinositide 3-kinase (PI3K)/protein kinase B (Akt/PKB) signaling pathway which is essential for protecting neurons from oxidative stress (Lu et al., 2011). Activation of this pathway is considered to improve cell survival and protect from the apoptosis (Dudek et al., 1997). As a result, the cascade of PI3K/Akt/ GSK-3β is considered to serve a critical role in the pathogenesis of PD.

Garcinia mangostana L. (GM, Guttiferae family), also recognized as mangosteen, is native to the Southeast Asia countries. Seeds and pericarps of this tropical fruit have been used for a long time in traditional medicinal actions in these regions (Ovalle-Magallanes et al., 2017). The major phytoconstituent contents in the species are isoprenylated xanthones, a group of heterocyclic metabolites with a xanthene-9-one framework. Xanthones have a number of biological effects including anti-oxidation (Pedraza-Chaverri et al., 2008), anti-tumor (Hafeez et al., 2014), anti-nociception (Fidanboylu et al., 2011), anti-inflammation (Jang et al., 2012; Wang et al., 2016; Tousian Shandiz et al., 2017), neuroprotection (Wang et al., 2012), and anti-obesity (Liu et al., 2015). Tovophyllin A (TA), one of the xanthones mainly extracted from the mangosteen pericarp, has been displayed to protect mitochondrial functions and against oxidative stress (Ibrahim et al., 2018).

However, the neuroprotection of TA and its potential mechanisms in PD models remain to be further explored. In this research, we showed the neuroprotection of TA against MPP^+/PQ-induced cytotoxicity in primary neurons and investigated its potential therapeutic effect in a mouse PD model. The results indicated that TA modulated the pathway of Akt/GSK-3β, which may contribute to TA-induced dopaminergic neuron protection.

MATERIALS AND METHODS

General Experimental Procedures

NMR and HRESIMS spectra were recorded by a Bruker ADVANCE-600 (600 MHZ) Instrument (Bruker Biospin, Zurich, Switzerland) and UPLC-QTOF-MS (Waters Ltd., Milford, MA, United States) in positive ion mode, respectively. Silica gel (80–100 and 200–300 mesh) obtained from Qingdao Haiyang Chemical Co., Ltd., Qingdao, China, and Sephadex LH-20 was purchased from Pharmacia Fine Chemical Co., Ltd., Uppsala, Sweden. The $HSGF_{254}$ (Yantai Jiangyou Silica Gel Co., Ltd., Yantai, China) was used for thin-layer chromatography (TLC). Spots were visualized by spraying with 10% sulphuric acid in ethanol (*v*/*v*) followed by heating the silica gel plates. All reagents used were analytical-grade and purchased from the Tianjin Fuyu Fine Chemical Industry Co., Ltd. (Tianjin, China).

Plant Material

Fresh *G. mangostana* L. from Thailand were obtained from Guangzhou fruit market in January 2017. A dry voucher specimen (#20170316GM) has been deposited in the herbarium of the School of Basic Medical Science, Southern Medical University, China.

Extraction and Isolation of TA

Tovophyllin A (**Figure 1**) was extracted and purified from the pericarp of *G. mangostana* L. In brief, air-dried fruit pericarp (1 kg) was ground and extracted with 95% ethanol (10 L × 3) at room temperature for 24 h. The mixture was evaporated under a vacuum to produce a crude extract (188 g). The crude extract was

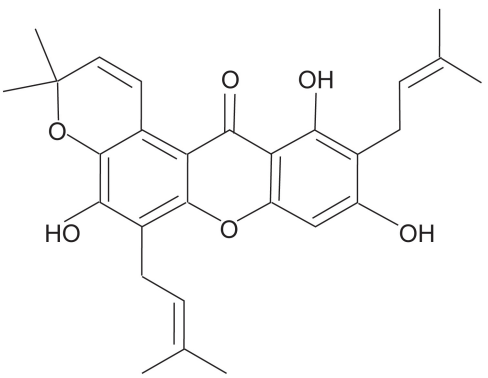

FIGURE 1 | Chemical structure of Tovophyllin A.

fractionated between methylene chloride and water to produce a methylene chloride fraction (5.4 g). The methylene chloride soluble fraction was dissolved in methylene chloride/ethyl acetate (3:1) and applied to a silica gel column (5 × 920 mm, 200–300 mesh). The sample was eluted with petroleum ether (1 L), dichloromethane (1 L), and dichloromethane: methanol (100:1; 2 L) to obtain impure TA. It was then purified using RP_{18} column chromatography eluted with a MeOH : H_2O gradient to give TA (18 mg) as a yellow powder. TA purity was shown to be >98% based on HPLC.

Spectral Data of TA

Tovophyllin A: yellow powder; $C_{28}H_{30}O_6$; ^{1}H NMR ($CDCl_3$, 600 MHz): δ_H 6.35 (s, H-4), 13.77 (s, 1-OH), 3.47 (d, J = 7.2 Hz, H-1′), 5.27 (tq, J = 7.2, 1.2 Hz, H-2′), 1.85 (s, H-4′), 1.87 (s, H-5′), 3.57 (d, J = 7.2 Hz, H-1″), 5.29 (tq, J = 7.2, 1.2 Hz, H-2″), 1.68 (s, H-4″), 1.78 (s, H-5″), 8.00 (d, J = 10.2 Hz, H-1‴), 5.78 (d, J = 10.2 Hz, H-2‴), 1.49 (s, H-4‴), 1.49 (s, H-5‴); ^{13}C NMR ($CDCl_3$,150 MHz): δ_C 160.4 (C-1), 108.2 (C-2), 161.6 (C-3), 93.4 (C-4), 155.3 (C-4a), 151.0 (C-4b), 115.2 (C-5), 148.6 (C-6), 135.9 (C-7),117.2 (C-8), 108.4 (C-8a), 103.7 (C-8b), 182.9 (C-9), 21.4 (C-1′), 121.0 (C-2′), 136.5 (C-3′), 25.8 (C-4′), 17.9 (C-5′), 22.6 (C-1″), 121.1 (C-2″), 132.6 (C-3″), 25.9 (C-4″), 17.9 (C-5″), 121.5 (C-1‴), 131.3 (C-2‴), 76.8 (C-3‴), 27.4 (C-4‴), 27.4 (C-5‴); HRESIMS *m/z* 485.1940 $(M + Na)^+$ ($C_{28}H_{30}O_6Na$, calcd for 485.1935), HRESIMS *m/z* 461.1975 $(M-H)^-$ ($C_{28}H_{29}O_6$, calcd for 461.1970). The structure of this compound was assigned by NMR and validated by comparing with the literature and spectroscopic and physical data (Ibrahim et al., 2018).

Chemicals and Antibodies

1-methyl4-phenyl-1,2,3,5-tetrahydropyridine (MPTP), 1-methyl-4-phenyl pyridium (MPP^+), paraquat (PQ), and 3-(4,5-Dimethylthiazol-2-yl)-2,5-diphenyltetrazolium bromide (MTT) were obtained from Sigma-Aldrich (St. Louis, MO, United States). Anti-tyrosine hydroxylase (TH) antibody (#ab112) was obtained from Abcam (Cambridge, United Kingdom). Antibodies against phospho-Ser473-Akt (#9271S), total Akt (#9272S), phospho-Ser9-GSK3β (#9336S), total GSK3β (#9315S) were purchased from Cell Signaling Technology (Danvers, MA, United States). Anti-GAPDH (#60004-1-Ig) was purchased from ProteinTech Group (Rosemont, IL, United States). Secondary antibodies conjugated to Alexa 488 were purchased from Invitrogen (Carlsbad, CA, United States).

Cultures of Primary Cortical Neurons

As previously described (Qin et al., 2015), primary cortical neurons were obtained from D0 C57BL/6 mice and cultured in neurobasal medium supplemented with 2% B27 and 25 μM glutamate on poly-L-lysine-coated plates in a 5% CO_2 incubator at 37°C. Every 3 days, half of the culture medium was changed with fresh medium without glutamate.

Analysis of Cell Viability by MTT Assay

Cell viability was evaluated by the colorimetric MTT assay. Briefly, primary neurons were treated with different concentrations of TA, and then exposed to 100 μM MPP^+ or PQ. After 24 h, MTT was added directly to the cells, which were incubated at 37°C for another 4 h. After removing the medium, 500 μl of DMSO was added to each well. Hundred microliters of the supernatant was transferred into a 96-well plate which were shaken on a microplate shaker to make sure that the MTT formazan crystals were completely dissolved. The absorbance was measured at 570 nm by a spectrophotometer. All values were normalized by subtracting the blank value measured with only DMSO. The absorbance value of the experimental groups was expressed as a percentage of the control group which was set as 100% viability.

Experimental Animals and MPTP Administration

Male C57BL/6 mice were obtained from the Animal Center of Southern Medical University (Guangzhou, Guangdong Province, China). The animals (8–10 weeks old, 25–28 g) were raised in SPF conditions (temperature: 22 ± 1°C) under a 12/12 h light-dark cycle with lights on 8:00 a.m. Food and water were available *ad libitum*. MPTP solution in saline was freshly prepared and injected intraperitoneally (i.p.) in four separate doses in 2 h intervals within a single day, in a total dose of 40 mg/kg of body weight (bw). Behavioral tests were performed 7 days after the treatment, then the mice were sacrificed for the collection of the brain tissues. All experimental procedures in this research were approved by the animal ethical committee of Southern Medical University.

Open Field Test

The open field test was performed by using a rectangular chamber (40 cm × 40 cm × 30 cm) which is made of polyvinyl chloride (PVC). Each mouse was put in the peripheral zone and allowed to explore the open field arena freely for 5 min. The behavioral responses were recorded using software EthoVision 7.0 (Noldus). At the end of each trial, 70% ethanol was used to clean the open field arena before placing the next animal. Data was recorded and analyzed in a blinded fashion.

Rotarod Test

Before MPTP treatment, the mice were trained on the rotarod three times with 20-min intervals between trials every day for three consecutive days (nine trials in total). Each mouse was trained by gradually increasing the speed of rotation on each day: 5–10 rpm (accelerated at 1 rpm/5 s) on day 1, 11–15 rpm (accelerated at 1 rpm/5 s) on day 2, and 16–20 rpm (accelerated at 1 rpm/5 s) on day 3. The rod was rotated manually (nonautomated). Seven days after the MPTP injections, the mice were re-evaluated with a constant acceleration from 4 to 40 rpm over 300 s. The average latency to fall from the rod of each mouse was measured and calculated.

Immunofluorescence Staining

Mice were perfused transcardially with 4% paraformaldehyde (PFA) in phosphate buffer (pH 7.4) and the brains were post-fixed overnight at 4°C. After the cryoprotection in 30% sucrose

solution over 3 days, coronal slices at a thickness of 40 μm were obtained from the frozen tissues using a sliding blade microtome and then collected on microscope slides. Immunofluorescence staining method was performed according to the previously reported (Luo et al., 2018). The SNc region of brain sections was permeabilized in PBS with 0.3% Triton X-100 for 30 min and blocked in PBS with 5% normal goat serum for 2 h at room temperature. Sections were incubated with specific primary antibodies (1:200 dilution for anti-TH) at 4°C overnight. After washing with PBS, slides were incubated in the solution containing Alexa Fluor 488-conjugated secondary antibody for 2 h at room temperature. The nuclei were stained with 4′,6-diamidino-2-phenylindole (DAPI) and the brain tissues were imaged under confocal microscopy.

Quantitative Analysis of TH-Positive Cells in the SNc

To investigate the loss of neurons in the SNc, serial section analysis of the total number of TH-positive neurons were shown by immunofluorescence staining. Four to six mice were used per group. The number of TH-positive neurons with obviously visible processes and nuclei was calculated on four sections for each subject by an investigator blind to group allocation. The serial sections were cut at 40 μm.

Western Blot

The protein concentration of each sample was determined using BCA Protein Assay Kit (Pierce). Samples (20–40 μg) were separated by 10% SDS-polyacrylamide gels and transferred to polyvinylidene difluoride (PVDF) membranes. The protein levels were determined using the following primary antibodies: anti-TH (1:200), phospho-Ser473-Akt (1:1000), total Akt (1:1000), phospho-Ser9-GSK3β (1:1000), total GSK3β (1:1000), and anti-GAPDH (1:10,000), overnight at 4°C, followed by 1 h incubation with the proper horseradish peroxidase-conjugated secondary antibodies (1:4000). Proteins were visualized using the enhanced chemiluminescence (ECL) reagent and densitometric analysis was performed using the ImageJ software. Densitometric analysis is displayed as relative optical density.

Statistical Analyses

All values are presented as mean ± SEM. Statistical analysis was performed using one-way ANOVAs followed by *post hoc* Bonferroni test for multiple comparisons. $p < 0.05$ or $p < 0.01$ was considered statistically significant. Each experiment was performed at least three times.

RESULTS

TA Significantly Protected Primary Cultured Cortical Neurons Against MPP^+-Induced or PQ-Induced Neurotoxicity

The timeline for the evaluation of TA was shown in **Figure 2A**. First, we examined the neurotoxicity of MPP^+ and PQ in primary cultured neurons. As depicted in **Figures 2B,C**, MPP^+ and PQ caused significant reductions of cell viability in a dose-dependent manner compared with control group. As a result, 100 μM MPP^+ or PQ was used for subsequent experiments.

The protective effects of TA on MPP^+-toxicity and PQ-toxicity in primary cultured neurons were investigated by MTT assay. Briefly, cells were co-treated with TA of different concentrations and 100 μM MPP^+ or PQ for 24 h. As shown in **Figure 2D**, the MPP^+-treated group showed significantly decreased cell viability compared to control group. Interestingly, TA treatment protected neurons from cell death caused by MPP^+, especially at the concentrations of 1 and 2.5 μM. Similarly, as shown in the **Figure 2E**, TA also exerted protective effects in PQ-treated cells. The results suggest that TA protects primary cortical neurons from MPP^+ and PQ cytotoxicity.

TA Ameliorated MPTP-Induced Behavioral Deficits

To evaluate the TA-mediated protective effect against MPTP-induced neurotoxicity in the *in vivo* model, as outlined in **Figure 3A**, we first detected whether TA could improve the motor dysfunctions in MPTP-treated mice by open field and rotarod tests. As shown in **Figure 3B**, the total distance in the open field test traveled by MPTP-treated cohort 7 days post-injection was remarkably reduced compared with that of the saline group (MPTP vs control, $p < 0.001$), validating MPTP-induced locomotive impairments. These impairments were reduced when pre-treated with TA (5 mg/kg) as the distance increased obviously (TA + MPTP vs MPTP, $p < 0.001$) and had no significance compared to the control cohort (TA + MPTP vs control, $p > 0.05$).

In the rotarod test, as shown in **Figure 3C**, the latency to falling of the rotarod for the MPTP cohort decreased dramatically compared with that of control cohort 7 days post-administration of MPTP (MPTP vs control, $p < 0.001$), affirming the motor impairments in MPTP-treated mice. Compared with the MPTP-treated cohort, the latency to fall in the TA pre-treatment cohort increased remarkably (TA + MPTP vs MPTP, $p < 0.05$). In addition, the latency to fall in the TA pre-treatment cohort was comparable with that of the control cohort (TA + MPTP vs control, $p > 0.05$). Thus, pre-treatment of TA has shown to rescue motor deficits resulted from MPTP toxicity *in vivo*.

TA Alleviated MPTP-Induced Dopaminergic Neuronal Loss *in vivo*

Next, we investigated the survival of dopaminergic neurons in mice after MPTP administration. Tyrosine hydroxylase (TH), as a particular biomarker for midbrain dopaminergic neurons, was detected by western blot analysis and immunofluorescence staining in the substantia nigra pars compacta (SNc). As shown in **Figures 4A,B**, the level of TH dramatically decreased in the midbrain tissues and striatum 7 days after MPTP treatment, while TA obviously alleviated the TH reduction in MPTP-treated mice. In **Figure 4C**, TH in the SNc was detected by immunofluorescence staining to visualize the number of dopaminergic neurons. MPTP

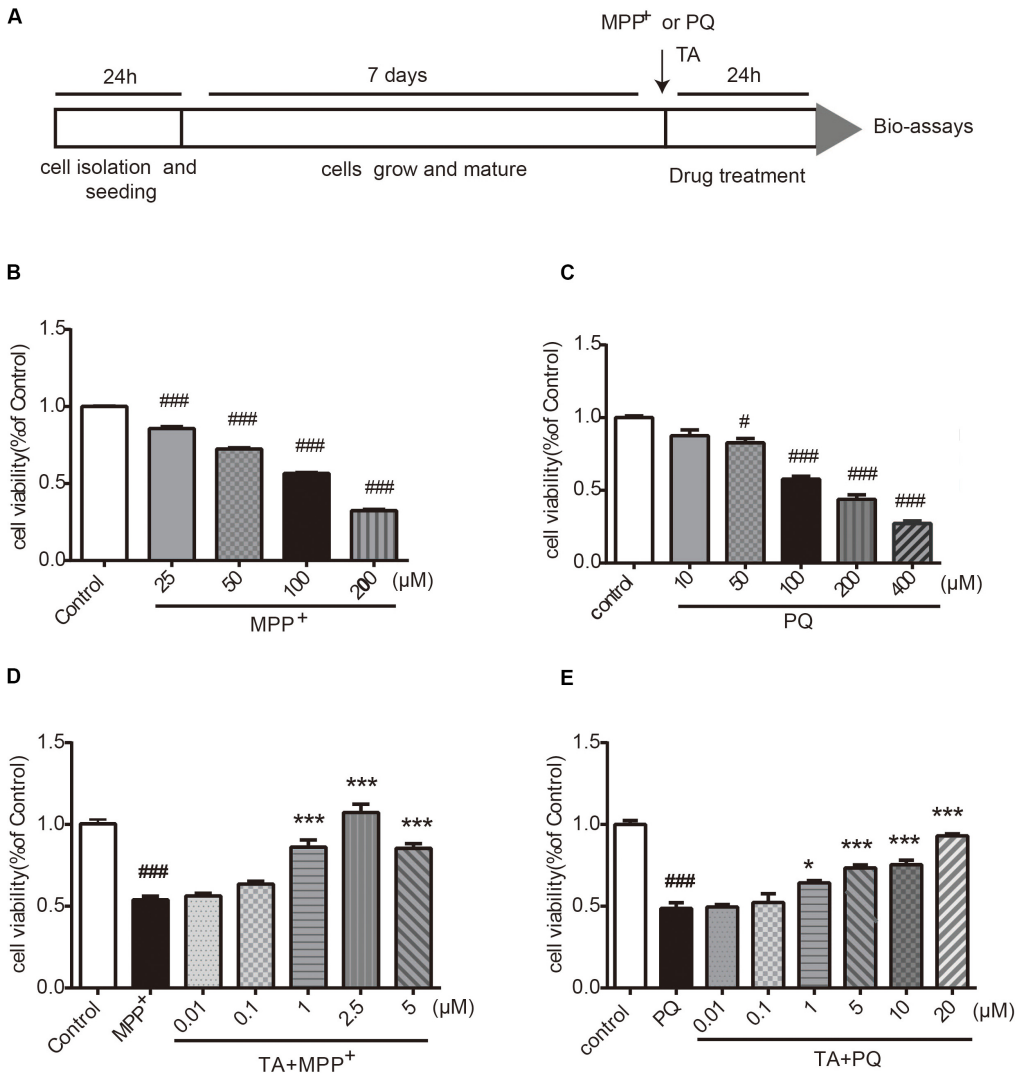

FIGURE 2 | The effects of TA on MPP^+ and PQ-induced cell death in primary cultured cortical neurons. **(A)** Timeline for the cell viability assay. **(B,C)** Dose-dependent decrease in cell viability with different doses of MPP^+/PQ or saline in cortical neurons. **(D,E)** TA protected neurons against MPP^+/PQ-induced neurotoxicity. Data are expressed as percentage of control ($n = 6$). One-way ANOVA followed by *post hoc* Bonferroni test: $^{\#}p < 0.05$, $^{\#\#\#}p < 0.001$ compared with the control group; $^{*}p < 0.05$, $^{***}p < 0.001$ compared with the MPP^+ group or the PQ group. All values are expressed as mean ± SEM.

caused the number of dopaminergic neurons decrease in SNc, whereas TA powerfully improved the survival of these neurons in MPTP-treated mice. Our results illustrated that TA treatment can effectively preserve the expression of TH in midbrain and dramatically improve the survival of dopaminergic neurons against neurotoxicity induced by MPTP.

TA Activated the Akt Pro-survival Pathway in MPTP Treated Mice

The PI3K / Akt/PKB signaling pathway is of great importance in cell survival, proliferation and differentiation (Babichev et al., 2016; Zhang et al., 2016). Akt phosphorylate alters the activity of its downstream substrate GSK-3β, which has been shown to result in DA neuronal reduction caused by MPTP and other insults. Thus, we evaluated whether TA promotes neuron survival by regulating of the Akt/GSK-3β signaling pathway. As shown in **Figure 5A**, MPTP administration decreased the phosphorylation level of Akt in the midbrain, while having no effect on total Akt. TA treatment, however, alleviated the inhibitory effect on the phosphorylation of Akt at Ser473 caused by MPTP and reversed the pAkt/Akt ratio significantly (**Figure 5A**). Similarly, MPTP administration induced activation of GSK3β, and TA treatment abolished the MPTP-induced activation of GSK-3β at Ser9 (**Figure 5B**). Next, we further investigated the changes in the Akt/GSK3β pathway in the striatum. As shown in **Figures 5C,D**, results found were consistent with western blot data. These findings indicate that the DA neuroprotective effects of TA may through the regulation of the Akt/GSK-3β pathway.

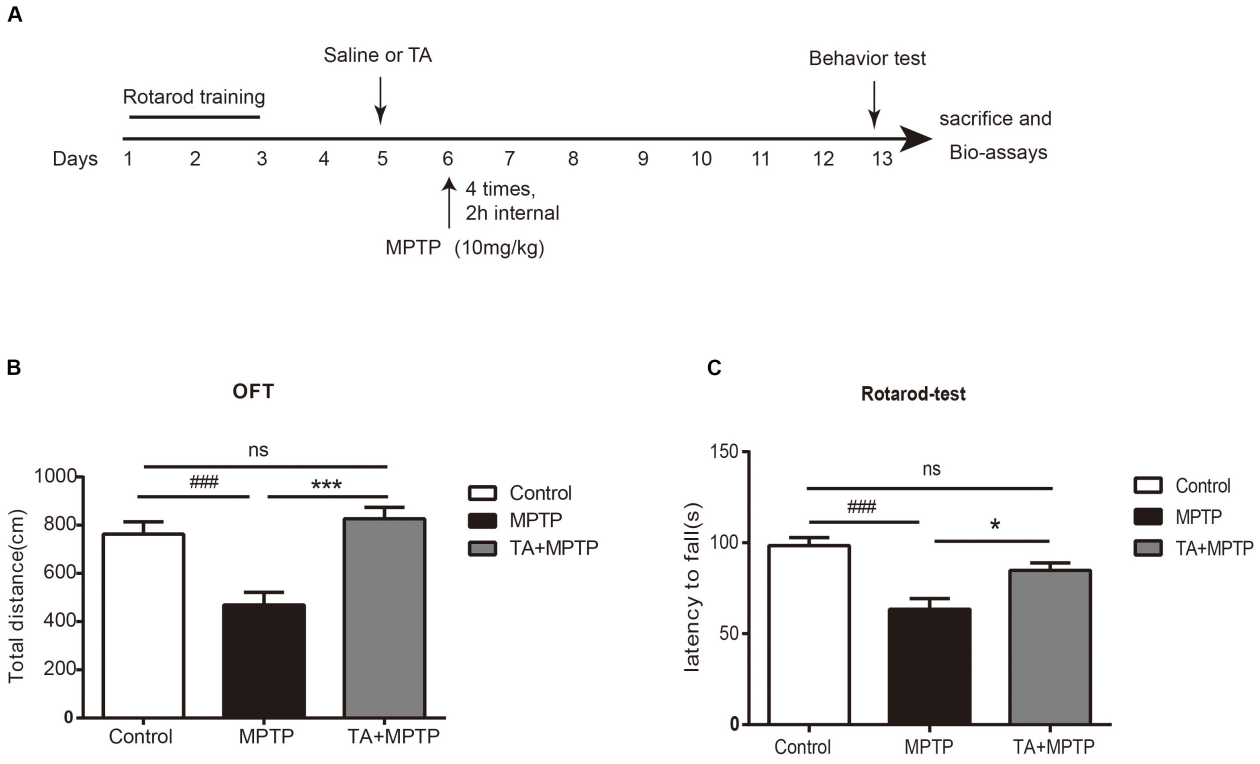

FIGURE 3 | TA ameliorated MPTP-induced behavioral deficits. **(A)** Timeline of experiments *in vivo*. **(B)** Total distance traveled by different cohorts, namely control, MPTP and TA+MPTP, in the open field test. **(C)** The latency to fall of various cohorts assessed by rotarod test. One-way ANOVA followed by *post hoc* Bonferroni test: $^{###}p < 0.001$ compared with the control group; $^{*}p < 0.05$, $^{***}p < 0.001$ compared with the MPTP group ($n \geq 8$). Data are shown as mean ± SEM.

DISCUSSION

Parkinson's disease is a frequent type neurodegenerative disease with uncertain precise underlying mechanisms and no clinically effective treatment available (Li et al., 2019). Since the progressive loss of dopaminergic neurons in the SNc is the most signature pathological features, identifying effective neuroprotectants is an important direction for the research in novel therapies (Iarkov et al., 2020). In this study, our present data demonstrated (1) TA significantly increased cell viability in neurotoxin (MPP^+ or PQ)-injured primary cortical neurons, consistent with previous findings by Jaisin et al. (2018); (2) MPTP-induced behavioral impairments and DA neuronal loss were significantly attenuated by co-treatment with TA *in vivo*; (3) TA administration activated Akt and increased GSK-3β phosphorylation level in the striatum and midbrain of MPTP-treated mice. These data provide clear evidence that TA is an effective neuroprotectant against MPP^+/MPTP lesions on DA neurons, which may be through the regulation of the Akt/GSK-3β signal pathway.

Garcinia mangostana L. has abundant pool of xanthones that present a variety of pharmacological activities (Ibrahim et al., 2018). The diversity of actions existed in mangosteen xanthones indicate that lots of signaling pathways involved in different pathologies have been targeted by these compounds, and allows them to become precious sources for developing new medicines for the treatment of chronic and degenerative diseases (Ovalle-Magallanes et al., 2017). For instance, α-mangostin, a major compound of the GM pericarps, was shown to prevent the fibril formation and dissociate Aβ aggregation, which is beneficial to attenuating Aβ oligomers-induced neurotoxicity in Alzheimer's disease (Wang et al., 2012). Moreover, α-mangostin can also alleviate the aggregation of α-synuclein and loss of TH in rotenone-treated SH-SY5Y cells, suggesting potential neuroprotective effects of α-mangostin against PD-related neuronal injury (Hao et al., 2017). In addition, similar to antioxidants, xanthones protect cells from lead-induced damages in the kidney by decreasing oxidative stress, downregulating inflammation factors and inhibiting apoptosis (Rana et al., 2020). TA, which is specially derived from GM pericarps, has recently been reported to serve a protective effect in acetaminophen-induced hepatic damage by activating Nrf2 and down regulating NF-κB pathways (Ibrahim et al., 2018). The etiopathogenesis of aging-related neurodegenerative disease is correlated with various processes, including neuroinflammation, oxidative stress, and abnormal dopaminergic system function (Motyl et al., 2018). Overproduction of reactive oxygen species (ROS) during oxidative stress and the disturbance of antioxidant defense have been considered as crucial causative factors in PD (Guo et al., 2018). In the study, we investigated whether TA had neuroprotective effects on PD models both *in vitro* and *in vivo*. We found that TA directly protected primary cultured neurons against MPP+ and PQ insults (**Figure 2**). Moreover, TA

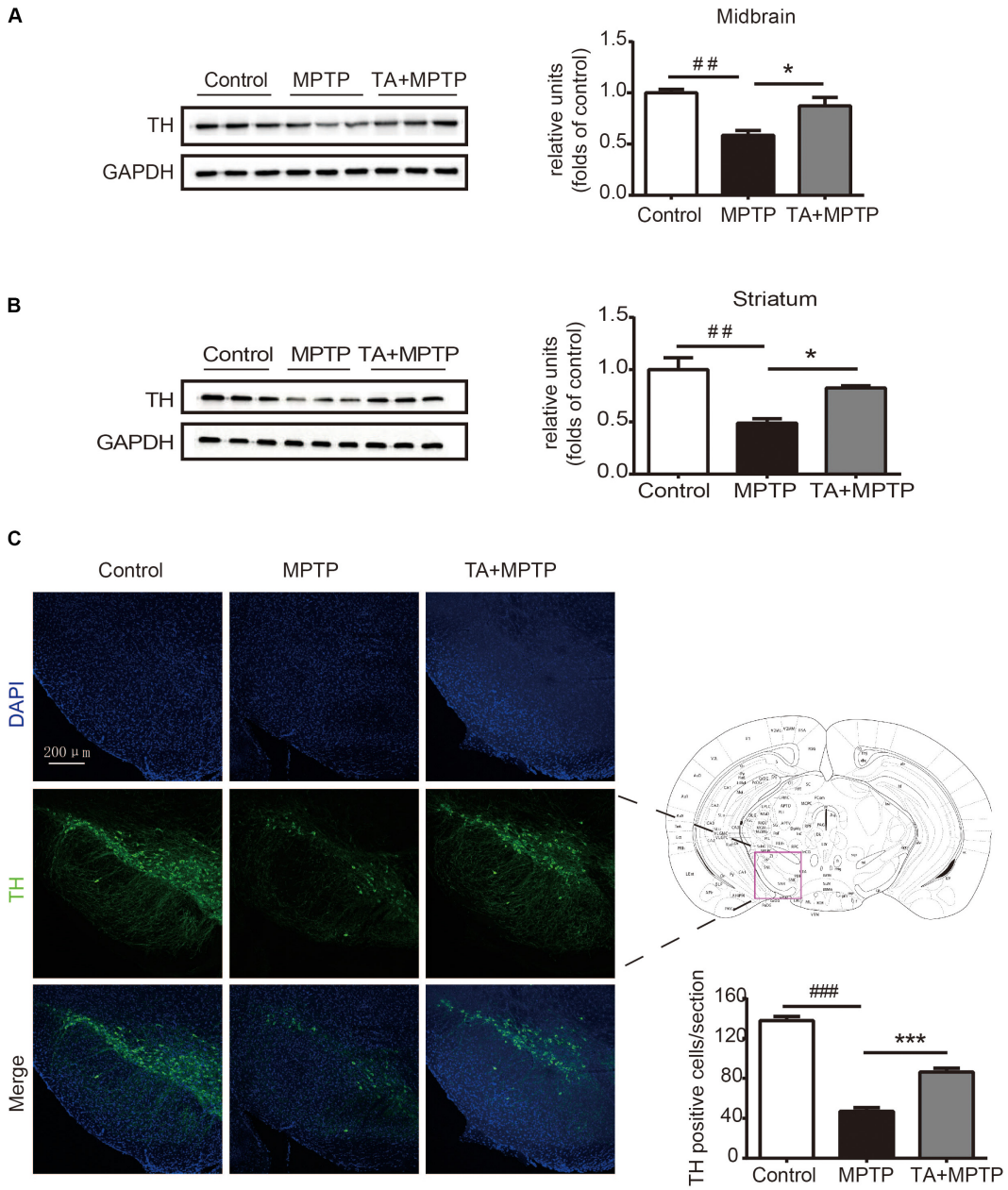

FIGURE 4 | TA treatment attenuated MPTP-induced decrease in tyrosine hydroxylase (TH) expression in mice. **(A,B)** Western blot analysis of the level of TH in the mouse midbrain and striatum. The relative optical density of TH was normalized by the internal loading control GAPDH. **(C)** Immunofluorescence staining with anti-TH antibody in the substantia nigra pars compacta (SNc). Scale bar: 200 μm. One-way ANOVA followed by *post hoc* Bonferroni test: $^{\#\#}p < 0.01$, $^{\#\#\#}p < 0.001$ compared with the control group; $^{*}p < 0.05$, $^{***}p < 0.001$ compared with the MPTP group ($n \geq 3$). Data are shown as mean ± SEM.

administration remarkably alleviated MPTP-induced behavioral dysfunctions and DA neuron loss (**Figures 3**, **4**), suggesting that TA may be a promising therapeutic approach in PD.

The PI3K/Akt cascade is a pro-survival pathway of great significance for the development of the nervous system. Akt is mainly activated by PI3K, and this pathway promotes cell survival and cytoprotection by phosphorylating various enzymes, including antioxidant proteins and pro-apoptotic regulators, as well as some transcription factors (Nakano et al., 2017; Yue et al., 2017). Inhibition of this cascade is correlated with neurodegeneration, particularly in PD (Hu et al., 2018). GSK-3 is involved in an array of progresses, such as metabolism, gene expression, proliferation and cell survival. Activities of the two isomers, GSK-3α and GSK-3β, are dependent on phosphorylation at specific sites (Golpich et al., 2015). GSK-3β, phosphorylated at Ser9, which is considered to be tightly associated with the

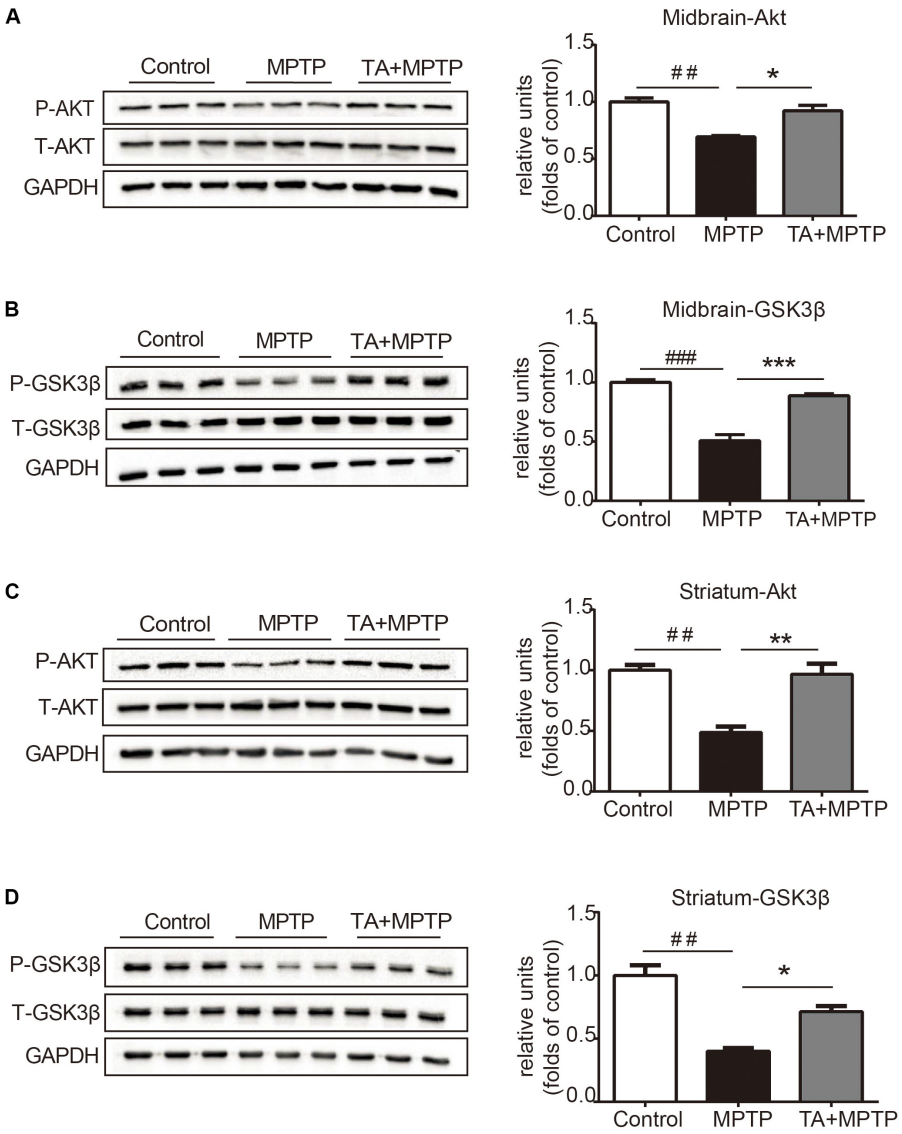

FIGURE 5 | TA activated Akt and attenuated MPTP-induced GSK-3β activation. **(A,B)** Protein levels of p-Akt, Akt, p-GSK3β, GSK3β, and GAPDH were determined by western blot analysis in the midbrain. **(C,D)** Protein levels of p-Akt, Akt, p-GSK3β, GSK3β, and GAPDH were determined by western blot analysis in the striatum. One-way ANOVA followed by *post hoc* Bonferroni test: $^{\#\#}p < 0.01$, $^{\#\#\#}p < 0.001$ compared with the control group; $^{*}p < 0.05$, $^{**}p < 0.01$, $^{***}p < 0.001$ compared with the MPTP group ($n \geq 3$). The data are presented as mean ± SEM.

pathogenesis of PD, has been proven to play a crucial role in neuronal apoptosis both in PD mouse model and postmortem brains of PD patients (Duka et al., 2009; Nagao and Hayashi, 2009). Akt inhibits GSK-3β function via phosphorylation at serine residue (Ser9 of GSK-3β) and thereby reduces apoptosis (Golpich et al., 2015; Norwitz et al., 2019). In our study, we found that MPTP decreased Akt activity and increased of GSK-3β function, consistent with previous studies (Hu et al., 2018). Remarkably, TA pre-treatment abolished MPTP-induced changes and increased p-Akt/Akt ratio while decreasing GSK-3β activity in mice. This likely contributed to TA-mediated DA neuronal protection and the resulting improvement in behavioral performances. In order to meet the higher level of energy consumption, the brain is enriched abundant mitochondria. The central nervous system, especially dopaminergic neurons, is susceptible to oxidative damage (Guo et al., 2018). As an important xanthone, TA might also have other important pharmacological properties, such as antioxidative, anti-bacterial, anti-inflammatory abilities. Its neuroprotection role might be achieved by ameliorating the vulnerability to oxidative attack, activating the MAPK pathway and attenuating the expression of inflammatory genes, such as TNF-α, IL-6, and INF-γ(Tousian Shandiz et al., 2017). Our study provides important evidences on the ability of TA to modulate the Akt/GSK-3β pathway in the mouse PD model. However, the relationship between neuroprotection against PD and the activation of Akt/GSK-3β by

TA is to be confirmed using Akt/GSK-3β inhibitors. Moreover, whether α-mangostin and TA could synergistically protect dopaminergic neurons against neurodegeneration in PD, and the exact mechanism underlying TA-mediated regulation of the Akt/GSK-3β signaling pathway must be further investigated.

CONCLUSION

In summary, our study demonstrated that TA has significant neuroprotective effects both in MPP^+/PQ-injured primary cortical neurons and MPTP-induced PD mouse model. Collectively, TA may be a potent pharmacological candidate for preventing dopaminergic neuronal death and neurodegeneration in PD.

DATA AVAILABILITY STATEMENT

All datasets generated for this study are included in the article/supplementary material.

ETHICS STATEMENT

The animal study was reviewed and approved by the animal ethical committee of Southern Medical University.

AUTHOR CONTRIBUTIONS

XW designed the experiments. LS extracted and isolated TA. YH, SZ, and LX performed the cell viability assays, behavioral tests, and the biochemical analysis. SL, CY, and YG analyzed the data. YH and LS wrote the manuscript with help from XW. All authors read and approved the final manuscript.

FUNDING

This study was supported by grants from the National Natural Science Foundation of China (81971234), the Program for Changjiang Scholars and the Innovative Research Team in University (IRT_16R37), and the Science and Technology Program of Guangdong (2018B0303340010).

REFERENCES

Babichev, Y., Kabaroff, L., Datti, A., Uehling, D., Isaac, M., Al-Awar, R., et al. (2016). PI3K/AKT/mTOR inhibition in combination with doxorubicin is an effective therapy for leiomyosarcoma. *J. Transl. Med.* 14:67. doi: 10.1186/s12967-016-0814-z

Beaulieu, J. M. (2007). Not only lithium: regulation of glycogen synthase kinase-3 by antipsychotics and serotonergic drugs. *Int. J. Neuropsychopharmacol.* 10, 3–6. doi: 10.1017/S1461145706006857

Chen, L., Cheng, L., Wei, X., Yuan, Z., Wu, Y., Wang, S., et al. (2017). Tetramethylpyrazine analogue CXC195 protects against dopaminergic neuronal apoptosis via activation of PI3K/Akt/GSK3beta signaling pathway in 6-OHDA-induced parkinson's disease mice. *Neurochem. Res.* 42, 1141–1150. doi: 10.1007/s11064-016-2148-x

Cui, W., Zhang, Z., Li, W., Hu, S., Mak, S., Zhang, H., et al. (2013). The anti-cancer agent SU4312 unexpectedly protects against MPP(+) -induced neurotoxicity via selective and direct inhibition of neuronal NOS. *Br. J. Pharmacol.* 168, 1201–1214. doi: 10.1111/bph.12004

Dauer, W., and Przedborski, S. (2003). Parkinson's disease: mechanisms and models. *Neuron* 39, 889–909. doi: 10.1016/s0896-6273(03)00568-3

Dexter, D. T., and Jenner, P. (2013). Parkinson disease: from pathology to molecular disease mechanisms. *Free Radic. Biol. Med.* 62, 132–144. doi: 10.1016/j.freeradbiomed.2013.01.018

Dudek, H., Datta, S. R., Franke, T. F., Birnbaum, M. J., Yao, R., Cooper, G. M., et al. (1997). Regulation of neuronal survival by the serine-threonine protein kinase Akt. *Science* 275, 661–665. doi: 10.1126/science.275.5300.661

Duka, T., Duka, V., Joyce, J. N., and Sidhu, A. (2009). Alpha-Synuclein contributes to GSK-3beta-catalyzed Tau phosphorylation in Parkinson's disease models. *FASEB J.* 23, 2820–2830. doi: 10.1096/fj.08-120410

Fidanboylu, M., Griffiths, L. A., and Flatters, S. J. (2011). Global inhibition of reactive oxygen species (ROS) inhibits paclitaxel-induced painful peripheral neuropathy. *PLoS One* 6:e25212. doi: 10.1371/journal.pone.0025212

Frame, S., and Cohen, P. (2001). GSK3 takes centre stage more than 20 years after its discovery. *Biochem. J.* 359(Pt 1), 1–16. doi: 10.1042/0264-6021:3590001

Golpich, M., Amini, E., Hemmati, F., Ibrahim, N. M., Rahmani, B., Mohamed, Z., et al. (2015). Glycogen synthase kinase-3 beta (GSK-3beta) signaling: implications for Parkinson's disease. *Pharmacol. Res.* 97, 16–26. doi: 10.1016/j.phrs.2015.03.010

Guo, J. D., Zhao, X., Li, Y., Li, G. R., and Liu, X. L. (2018). Damage to dopaminergic neurons by oxidative stress in Parkinson's disease (Review). *Int. J. Mol. Med.* 41, 1817–1825. doi: 10.3892/ijmm.2018.3406

Hafeez, B. B., Mustafa, A., Fischer, J. W., Singh, A., Zhong, W., Shekhani, M. O., et al. (2014). alpha-Mangostin: a dietary antioxidant derived from the pericarp of Garcinia mangostana L. inhibits pancreatic tumor growth in xenograft mouse model. *Antioxid. Redox. Signal* 21, 682–699. doi: 10.1089/ars.2013.5212

Hao, X. M., Li, L. D., Duan, C. L., and Li, Y. J. (2017). Neuroprotective effect of alpha-mangostin on mitochondrial dysfunction and alpha-synuclein aggregation in rotenone-induced model of Parkinson's disease in differentiated SH-SY5Y cells. *J. Asian. Nat. Prod. Res.* 19, 833–845. doi: 10.1080/10286020.2017.1339349

Hu, D., Sun, X., Liao, X., Zhang, X., Zarabi, S., Schimmer, A., et al. (2019). Alpha-synuclein suppresses mitochondrial protease ClpP to trigger mitochondrial oxidative damage and neurotoxicity. *Acta Neuropathol.* 137, 939–960. doi: 10.1007/s00401-019-01993-2

Hu, S., Mak, S., Zuo, X., Li, H., Wang, Y., and Han, Y. (2018). Neuroprotection against MPP(+)-induced cytotoxicity through the activation of PI3-K/Akt/GSK3beta/MEF2D signaling pathway by rhynchophylline, the major tetracyclic oxindole alkaloid isolated from uncaria rhynchophylla. *Front. Pharmacol.* 9:768. doi: 10.3389/fphar.2018.00768

Iarkov, A., Barreto, G. E., Grizzell, J. A., and Echeverria, V. (2020). Strategies for the treatment of parkinson's disease: beyond dopamine. *Front. Aging Neurosci.* 12:4. doi: 10.3389/fnagi.2020.00004

Ibrahim, S. R. M., El-Agamy, D. S., Abdallah, H. M., Ahmed, N., Elkablawy, M. A., and Mohamed, G. A. (2018). Protective activity of tovophyllin A, a xanthone isolated from Garcinia mangostana pericarps, against acetaminophen-induced liver damage: role of Nrf2 activation. *Food Funct.* 9, 3291–3300. doi: 10.1039/c8fo00378e

Jackson-Lewis, V., and Przedborski, S. (2007). Protocol for the MPTP mouse model of Parkinson's disease. *Nat. Protoc.* 2, 141–151. doi: 10.1038/nprot.2006.342

Jaisin, Y., Ratanachamnong, P., Kuanpradit, C., Khumpum, W., and Suksamrarn, S. (2018). Protective effects of gamma-mangostin on 6-OHDA-induced toxicity in SH-SY5Y cells. *Neurosci. Lett.* 665, 229–235. doi: 10.1016/j.neulet.2017.11.059

Jang, H. Y., Kwon, O. K., Oh, S. R., Lee, H. K., Ahn, K. S., and Chin, Y. W. (2012). Mangosteen xanthones mitigate ovalbumin-induced airway inflammation in a mouse model of asthma. *Food Chem. Toxicol.* 50, 4042–4050. doi: 10.1016/j.fct.2012.08.037

Jantas, D., Greda, A., Golda, S., Korostynski, M., Grygier, B., Roman, A., et al. (2014). Neuroprotective effects of metabotropic glutamate receptor group II and III activators against MPP(+)-induced cell death in human neuroblastoma SH-SY5Y cells: the impact of cell differentiation state. *Neuropharmacology* 83, 36–53. doi: 10.1016/j.neuropharm.2014.03.019

Kalia, L. V., and Lang, A. E. (2015). Parkinson's disease. *Lancet* 386, 896–912. doi: 10.1016/S0140-6736(14)61393-3

Li, K., Li, J., Zheng, J., and Qin, S. (2019). Reactive astrocytes in neurodegenerative diseases. *Aging Dis.* 10, 664–675. doi: 10.14336/AD.2018.0720

Liu, Q. Y., Wang, Y. T., and Lin, L. G. (2015). New insights into the anti-obesity activity of xanthones from Garcinia mangostana. *Food Funct.* 6, 383–393. doi: 10.1039/c4fo00758a

Lu, S., Lu, C., Han, Q., Li, J., Du, Z., Liao, L., et al. (2011). Adipose-derived mesenchymal stem cells protect PC12 cells from glutamate excitotoxicity-induced apoptosis by upregulation of XIAP through PI3-K/Akt activation. *Toxicology* 279, 189–195. doi: 10.1016/j.tox.2010.10.011

Luo, D., Zhao, J., Cheng, Y., Lee, S. M., and Rong, J. (2018). N-propargyl caffeamide (PACA) ameliorates dopaminergic neuronal loss and motor dysfunctions in MPTP mouse model of parkinson's disease and in mpp(+)-induced neurons via promoting the conversion of proNGF to NGF. *Mol. Neurobiol.* 55, 2258–2267. doi: 10.1007/s12035-017-0486-6

Martinez, B. A., Petersen, D. A., Gaeta, A. L., Stanley, S. P., Caldwell, G. A., and Caldwell, K. A. (2017). Dysregulation of the mitochondrial unfolded protein response induces non-apoptotic dopaminergic neurodegeneration in *C. elegans* models of Parkinson's Disease. *J. Neurosci.* 37, 11085–11100. doi: 10.1523/JNEUROSCI.1294-17.2017

Moon, H. E., and Paek, S. H. (2015). Mitochondrial dysfunction in Parkinson's Disease. *Exp. Neurobiol.* 24, 103–116. doi: 10.5607/en.2015.24.2.103

Morris, G., and Berk, M. (2015). The many roads to mitochondrial dysfunction in neuroimmune and neuropsychiatric disorders. *BMC Med.* 13:68. doi: 10.1186/s12916-015-0310-y

Motyl, J., Przykaza, L., Boguszewski, P. M., Kosson, P., and Strosznajder, J. B. (2018). Pramipexole and Fingolimod exert neuroprotection in a mouse model of Parkinson's disease by activation of sphingosine kinase 1 and Akt kinase. *Neuropharmacology* 135, 139–150. doi: 10.1016/j.neuropharm.2018.02.023

Nagao, M., and Hayashi, H. (2009). Glycogen synthase kinase-3beta is associated with Parkinson's disease. *Neurosci. Lett.* 449, 103–107. doi: 10.1016/j.neulet.2008.10.104

Nakano, N., Matsuda, S., Ichimura, M., Minami, A., Ogino, M., Murai, T., et al. (2017). PI3K/AKT signaling mediated by G proteincoupled receptors is involved in neurodegenerative Parkinson's disease (Review). *Int. J. Mol. Med.* 39, 253–260. doi: 10.3892/ijmm.2016.2833

Norwitz, N. G., Mota, A. S., Norwitz, S. G., and Clarke, K. (2019). Multi-loop model of alzheimer disease: an integrated perspective on the Wnt/GSK3beta, alpha-Synuclein, and Type 3 diabetes hypotheses. *Front. Aging Neurosci.* 11:184. doi: 10.3389/fnagi.2019.00184

Ovalle-Magallanes, B., Eugenio-Perez, D., and Pedraza-Chaverri, J. (2017). Medicinal properties of mangosteen (*Garcinia mangostana* L.): a comprehensive update. *Food Chem. Toxicol.* 109(Pt 1), 102–122. doi: 10.1016/j.fct.2017.08.021

Pedraza-Chaverri, J., Cardenas-Rodriguez, N., Orozco-Ibarra, M., and Perez-Rojas, J. M. (2008). Medicinal properties of mangosteen (*Garcinia mangostana*). *Food Chem. Toxicol.* 46, 3227–3239. doi: 10.1016/j.fct.2008.07.024

Qin, X., Wu, Q., Lin, L., Sun, A., Liu, S., Li, X., et al. (2015). Soluble epoxide hydrolase deficiency or inhibition attenuates MPTP-induced parkinsonism. *Mol. Neurobiol.* 52, 187–195. doi: 10.1007/s12035-014-8833-3

Rana, M. N., Tangpong, J., and Rahman, M. A. (2020). Xanthones protects lead-induced chronic kidney disease (CKD) via activating Nrf-2 and modulating NF-kB, MAPK pathway. *Biochem. Biophys. Rep.* 21:100718. doi: 10.1016/j.bbrep.2019.100718

Rizek, P., Kumar, N., and Jog, M. S. (2016). An update on the diagnosis and treatment of Parkinson disease. *CMAJ* 188, 1157–1165. doi: 10.1503/cmaj.151179

Tousian Shandiz, H., Razavi, B. M., and Hosseinzadeh, H. (2017). Review of *Garcinia mangostana* and its xanthones in metabolic syndrome and related complications. *Phytother. Res.* 31, 1173–1182. doi: 10.1002/ptr.5862

Wang, M., Xie, Y., Zhong, Y., Cen, J., Wang, L., Liu, Y., et al. (2016). Amelioration of experimental autoimmune encephalomyelitis by isogarcinol extracted from *Garcinia mangostana* L. Mangosteen. *J. Agric. Food Chem.* 64, 9012–9021. doi: 10.1021/acs.jafc.6b04145

Wang, Y., Xia, Z., Xu, J. R., Wang, Y. X., Hou, L. N., Qiu, Y., et al. (2012). Alpha-mangostin, a polyphenolic xanthone derivative from mangosteen, attenuates beta-amyloid oligomers-induced neurotoxicity by inhibiting amyloid aggregation. *Neuropharmacology* 62, 871–881. doi: 10.1016/j.neuropharm.2011.09.016

Yue, P., Gao, L., Wang, X., Ding, X., and Teng, J. (2017). Intranasal administration of GDNF protects against neural apoptosis in a rat model of parkinson's disease through PI3K/Akt/GSK3beta pathway. *Neurochem. Res.* 42, 1366–1374. doi: 10.1007/s11064-017-2184-1

Zhang, Y., Liu, S., Wang, L., Wu, Y., Hao, J., Wang, Z., et al. (2016). A novel PI3K/AKT signaling axis mediates Nectin-4-induced gallbladder cancer cell proliferation, metastasis and tumor growth. *Cancer Lett.* 375, 179–189. doi: 10.1016/j.canlet.2016.02.049

Zhao, Q., Ye, J., Wei, N., Fong, C., and Dong, X. (2016). Protection against MPP(+)-induced neurotoxicity in SH-SY5Y cells by tormentic acid via the activation of PI3-K/Akt/GSK3beta pathway. *Neurochem. Int.* 97, 117–123. doi: 10.1016/j.neuint.2016.03.010

Conflict of Interest: The authors declare that the research was conducted in the absence of any commercial or financial relationships that could be construed as a potential conflict of interest.

The reviewer WY declared a shared affiliation with one of the authors, SZ, to the handling editor.

frontiers in Neuroscience

REVIEW
published: 06 August 2020
doi: 10.3389/fnins.2020.00764

Blood-Brain Barrier: More Contributor to Disruption of Central Nervous System Homeostasis Than Victim in Neurological Disorders

Minjia Xiao[1,2], Zhi Jie Xiao[1], Binbin Yang[1], Ziwei Lan[1] and Fang Fang[1]*

[1] Department of Neurology, Second Xiangya Hospital, Central South University, Changsha, China, [2] Department of Critical Care Medicine, The First Affiliated Hospital, College of Medicine, Zhejiang University, Hangzhou, China

The blood-brain barrier (BBB) is a dynamic but solid shield in the cerebral microvascular system. It plays a pivotal role in maintaining central nervous system (CNS) homeostasis by regulating the exchange of materials between the circulation and the brain and protects the neural tissue from neurotoxic components as well as pathogens. Here, we discuss the development of the BBB in physiological conditions and then focus on the role of the BBB in cerebrovascular disease, including acute ischemic stroke and intracerebral hemorrhage, and neurodegenerative disorders, such as Alzheimer's disease (AD), Parkinson's disease (PD), and multiple sclerosis (MS). Finally, we summarize recent advancements in the development of therapies targeting the BBB and outline future directions and outstanding questions in the field. We propose that BBB dysfunction not only results from, but is causal in the pathogenesis of neurological disorders; the BBB is more a contributor to the disruption of CNS homeostasis than a victim in neurological disorders.

Keywords: blood-brain barrier, acute ischemic stroke, intracerebral hemorrhage, Alzheimer's disease, Parkinson's disease, multiple sclerosis

OPEN ACCESS

Edited by:
Eng-King Tan,
National Neuroscience Institute (NNI), Singapore

Reviewed by:
Malgorzata Burek,
Julius Maximilian University of Würzburg, Germany
Fabien Gosselet,
Artois University, France

****Correspondence:***
Zhi Jie Xiao
xiaominjia@csu.edu.cn

Specialty section:
This article was submitted to Neurodegeneration, a section of the journal Frontiers in Neuroscience

Received: *04 March 2020*
Accepted: *29 June 2020*
Published: *06 August 2020*

Citation:
Xiao M, Xiao ZJ, Yang B, Lan Z and Fang F (2020) Blood-Brain Barrier: More Contributor to Disruption of Central Nervous System Homeostasis Than Victim in Neurological Disorders. Front. Neurosci. 14:764. doi: 10.3389/fnins.2020.00764

INTRODUCTION

The neurovascular unit (NVU) is a functional complex critical to the stability of the CNS microenvironment and is composed of endothelial cells (ECs), glial cells, pericytes (PCs), neurons, and the extracellular matrix (ECM). Communication between the individual NVU components is key for its correct function. The blood-brain barrier (BBB) is considered the core structure of the NVU (Saint-Pol et al., 2020). It is established by tightly sealed ECs located at the luminal surface of the brain's vascular tree (Sweeney et al., 2019b). The presence of cell surface proteins, ion channels, efflux pumps, enzymes, specific receptors, and transporters on pericytes (PCs), vascular smooth muscle cells (VSMCs), and ECs maintain BBB integrity (Sweeney et al., 2019b) and allow bidirectional regulation of substances by transcellular or paracellular transport (Haseloff et al., 2015; Xiaoyan et al., 2018).

Under normal conditions, ECs in the CNS microvasculature have fewer endocytic vesicles than those in the endothelia of the peripheral capillaries and only ensure the supply of basic nutrients, including oxygen and glucose, to the neurons (Persidsky et al., 2006). Thus, decreased transcytosis across the BBB restricts permeability and impedes the delivery of therapeutic agents, which is of great importance for restoring CNS homeostasis under pathological conditions

(Liebner et al., 2018). Additionally, ECs also bidirectionally communicate with surrounding cells to maintain the dynamic nature of the BBB.

Blood-brain barrier dysfunction is a pathophysiological hallmark in the pathogenesis of multiple CNS diseases (Cummins, 2011). Extensive evidence implicates it in cerebrovascular, neurodegenerative, and neuroinflammatory diseases. Here, we first illustrate the physiological structure of the BBB and then discuss the development of junctional complex perturbations in pathological conditions, including cerebrovascular disease and neurodegenerative disorders. Finally, we summarize recent advancements in therapeutics targeting brain-barrier function. We emphasize the significance of the BBB in neurological disorders and put forward crucial questions to be answered in the future.

THE BLOOD-BRAIN BARRIER ESTABLISHMENT

Angiogenesis and Barriergenesis

Prior to BBB development, neuroectodermal neural progenitor cells secrete vascular endothelial growth factor (VEGF) to guide angioblasts from the perineural vascular plexus across the neuroectoderm to initiate angiogenesis (Potente et al., 2011; Obermeier et al., 2013). Meanwhile, neural progenitor cells also release Wnt ligands and activate the Wnt/β-catenin signaling pathway, which induces expression of genes indispensable for angiogenesis and BBB barriergenesis (Stenman et al., 2008). Orphan G-protein-coupled receptor 124 (Gpr124), a coactivator of the Wnt/β-catenin pathway, also impacts angiogenesis (Zhao et al., 2015a). During angiogenesis, nascent vascular ECs secrete platelet-derived growth factor-BB (PDGF-BB) and recruit PCs via the PDGF-receptor (PDGFR) (Sweeney et al., 2016, 2019b). PCs work synergistically with vascular ECs, deliver basement membrane (BM) proteins, and regulate integration of the BBB through interaction with the astrocyte end-feet that encircle vessels (Daneman et al., 2009; Armulik et al., 2010). The Sonic hedgehog (Hh) signaling pathway is crucial for EC polarity. Sonic hedgehog (SHH) released by astrocytes combines with Hh expressed by ECs to promote the expressions of tight junction (TJ) proteins and junctional adhesion molecules (JAMs). The SHH signaling pathway also suppresses the expression of proinflammatory factors and intercellular adhesion molecule-1 (ICAM-1), thereby inhibiting infiltration of leukocytes (Alvarez et al., 2011; Langen et al., 2019; Sweeney et al., 2019b).

Anatomical Structure

Endothelial cells in the CNS are distinct from those other tissues due to the following properties: possession of continuous intercellular TJs, lack of fenestration and pinocytosis, and low expression of leukocyte adhesion molecules (Obermeier et al., 2013; Langen et al., 2019). The BBB formed by the ECs is a dynamic but impassable wall, restricting the exchange of paracellular or transcellular substances and abrogating the infiltration of leukocytes.

Tight junction proteins, JAMs, adherens junctions (AJs), and gap junctions are responsible for restricting substance movement by prohibiting the paracellular pathway (Saint-Pol et al., 2020). On the other hand, enzymes and influx/efflux pumps maintain the dynamic nature of the barrier, limiting non-specific transport while also allowing specific transport (Saint-Pol et al., 2020).

Junctional molecules at the BBB are divided into four categories: TJ (with TJ proteins and TJ-associated proteins), AJ, JAM, and gap junctions (Chow and Gu, 2015; Tietz and Engelhardt, 2015; Sweeney et al., 2019b). They communicate with the cellular actin cytoskeleton via membrane-associated guanylate kinases (MAGUK), such as zonula occludens-1 (ZO-1), ZO-2, and ZO-3 (Bazzoni and Dejana, 2004; Zlokovic, 2008). TJ proteins are closest to the apical membrane and seal the BBB, thus acting as potential therapeutic targets. On the other hand, AJs, composed mainly of VE-cadherin and platelet endothelial cell adhesion molecule-1 (PECAM-1), are closest to the basolateral membrane (Sweeney et al., 2019b). JAMs consist of proteins, including JAM-A, JAM-B, and JAM-C, and endothelial cell adhesion molecules (ESAMs), and regulate transmigration of leukocytes across the BBB (Garrido-Urbani et al., 2014; Sweeney et al., 2019b). Gap junction proteins include connexin-37, connexin-40, and connexin-43 and act as a sort of "hemichannel" to facilitate communication between adjacent ECs (Sweeney et al., 2019b).

Claudin-1 is a non-specific claudin in vessels, overexpression of which has been reported to reduce the disease burden in

Abbreviations: Aβ, amyloid β-peptide; ABC, active efflux-ATP-binding cassette; AD, Alzheimer's disease; aHSCT, autologous hemopoietic stem-cell transplantation; AIS, acute ischemic stroke; AJs, adherence junctions; Ang-1, angiopoietin-1; APOE, apolipoprotein E; APP, β-amyloid precursor protein; AQP-4, aquaporin-4; ATP, adenosine triphosphate; BBB, blood-brain barrier; BDNF, brain-derived neurotrophic factor; BM, basement membrane; BMPs, bone morphogenetic proteins; CBF, cerebral blood flow; CCL2, (C-C motif) ligand 2; CCR5, chemokine receptor type 5; CMT, solute carrier-mediated transport; CNS, central nervous system; CSF, cerebrospinal fluid; CSF, cerebrospinal fluid; CypA, cytokine cyclophilin A; DMTs, disease-modifying treatments; ECM, extracellular matrix; ECs, endothelial cells; ESAM, endothelial cell adhesion molecule; FUS, focused ultrasound; GDNF, glial cell-derived neurotrophic factor; GLUT1, glucose transporter-1; Glut1-DS, glucose transporter-1 deficiency syndrome; GWAS, Genome Wide Association Study; HDL, high-density lipoprotein; Hh, Hedgehog; HT, hemorrhagic transformation; ICAM-1, adhesion molecule-1; ICAM-1, intercellular adhesion molecule-1; ICH, intracerebral hemorrhage; IL-1β, interleukin 1β; JAMs, junctional adhesion molecules; LBs, Lewy bodies; LRP, lipoprotein receptor–related protein; LRRK2, leucine-rich repeat kinase 2; MAGUK, membrane-associated guanylate kinases; McAb, monoclonal antibody; MCI, mild cognitive impairment; MLC, myosin light chain; MMP-9, matrix metalloproteinase-9; MS, multiple sclerosis; NF-κB, nuclear factor-κB; NGF, neurotrophin nerve growth factor; NOS, nitric oxide synthase; NVU, neurovascular unit; OGD, oxygen-glucose deprivation; OPC, oligodendrocyte precursor cells; PAR-4, protease-activated receptor-4; PCs, pericytes; PD, Parkinson's disease; PDGF-BB, platelet-derived growth factor BB; *P*-gp, *P*-glycoprotein; PDGFRβ, platelet-derived growth factor-receptor-β; PECAM-1, platelet endothelial cell adhesion molecule-1; PICALM, phosphatidylinositol-binding clathrin assembly; PML, progressive multifocal leukoencephalopathy; PPAR-γ Peroxisome proliferator-activated receptor γ; RA, retinoic acid; RAGE, receptor for advanced glycation end products; RhoK, Rho kinase; RMT, receptor-mediated transport; ROS, reactive oxygen species; rt-PA, recombinant tissue plasminogen activator; S1P, sphingosine 1-phosphate; SGLT, sodium-dependent glucose transporters; SHH, Sonic hedgehog; Smad, Sma- and Mad-related protein; SN, substantia nigra; TGF-β1, Transforming growth factor-β1; TJ, tight junction; TNF-α, tumor necrosis factor α; tPA, tissue-type plasminogen activator; Tregs, regulatory T cells; VCAM, vascular cell adhesion molecules; VEGF, vascular endothelial growth factor; VSMC, vascular smooth muscle cell; ZO, zonula occludens.

the chronic phase of a mouse model of multiple sclerosis (MS) (Pfeiffer et al., 2011). However, it has also been shown that claudin-1 overexpression decreased the level of claudin-5 and induced a proinflammatory phenotype in ECs in chronic stroke (Sladojevic et al., 2019). This suggests that claudin-1 overexpression compensated for BBB dysfunction only in the acute phase of injury. In addition to this, genetic polymorphisms in claudin-1 have been shown to contribute to small vessel vascular dementia (Srinivasan et al., 2017). Claudin-3 is involved in BBB induction and maintenance through signaling via the Wnt/β-catenin pathway (Polakis, 2008), while claudin-5 restricts the entrance of molecules up to 800 Da (Morita et al., 1999). Genetically modified mice lacking claudin-5 demonstrated leakage of intravascular tracers less than 800 Da in size despite having an intact BBB; 95% of pharmaceuticals are within this size range, implying that modulation of claudin-5 could be a potential target for drug delivery (Tsukita et al., 2003; Haseloff et al., 2015). Castro Dias et al. (2019) found that mice lacking claudin-12 still maintained an intact BBB as claudin-12 appears to be more important for cardiovascular functions (Castro Dias et al., 2019). It has also been shown to be involved in paracellular Ca^{2+} permeation in enterocytes (Saitou et al., 1997). To date, the exact function of claudin-12 in the CNS remains unknown and needs further investigation. Conversely, occludin is specifically expressed by the cells of the BBB rather than in non-neuronal tissues (Daneman et al., 2010a). Consequently, occludin knockout mice show morphologically normal TJs despite development of brain calcification (Fujita et al., 2008). LSR/angulin-1 are significant for maintenance of BBB characteristics, so loss of LSR results in leakage of small molecules (Ikenouchi et al., 2005; Sohet et al., 2015).

Cadherins and PECAM-1 are examples of proteins that make up AJs. VE-cadherin is important for AJ assembly and BBB regulation (Li et al., 2018). In conditions of oxygen-glucose deprivation (OGD), VE-cadherin internalization induces BBB hyperpermeability via the RhoA/ROCK2 pathway (Chen J. et al., 2019). VE-cadherin phosphorylation under pathological conditions results in uncoupling of ECs and increased vascular permeability; thus, it may also serve as a novel target in moderating BBB dysfunction (Li et al., 2018).

ZO-1 is indispensable for assembly of junction complexes between ECs. Both downregulation and phosphorylation of ZO-1 results in impaired BBB integrity (Chen W. et al., 2019). Connexin is a hemichannel protein expressed by ECs. It opens at low extracellular concentrations of Ca^{2+} or under OGD and perturbs transport across the BBB (Tachikawa et al., 2020). Knockout of Connexin-43/30 in astrocytes (ACs) results in end-feet edema and loss of aquaporin-4 (AQP-4) expression (Ezan et al., 2012).

JAM-A is a unique protein in that it has diverging functions under physiological and pathological conditions. During homeostasis, it moderates paracellular transport, and during inflammatory conditions, it is redistributed to the apical surface of ECs and serves as an adhesion molecule, regulating leukocyte migration (Stamatovic et al., 2012). It has been shown that JAM-A antagonists can modulate leukocyte infiltration in ischemia/reperfusion (I/R) injury, thereby making JAM-A a potential therapeutic target (Sladojevic et al., 2014). Mice void of JAM-B show extensive vacuolation in the brain parenchyma along with neurodegeneration (Schottlaender et al., 2020). Moreover, bi-allelic JAM2 variants result in brain calcification, which could be attributed to dysfunction of solute transport (Schottlaender et al., 2020).

ECs attach to the BM via the binding of integrins to ECM ligands and stimulate multiple pathways, including growth factors, growth factor receptors, or transactivation of growth factor receptors. They have Na^+-K^+-Cl^- cotransporters and Na^+/H^+ exchangers at the luminal side and Na^+/K^+-ATPases at the abluminal side (Baeten and Akassoglou, 2011).

Anatomically, PCs share a common BM and interdigitate with ECs, forming peg-and-socket contacts in regions lacking a BM via *N*-cadherin and connexins (Winkler et al., 2011); they have multiple functions, including adjusting vascular stability (Armulik et al., 2011), managing capillary diameter to regulate cerebral blood flow (CBF) (Hall et al., 2014), and phagocytosing toxins (Sagare et al., 2013) to ensure BBB stability (Winkler et al., 2011). PC coverage of ECs is mediated through release of PDGF-β and activation of PDGFR by ECs. $Pdgfrb^{-/-}$ mice manifest with a low pericyte coverage rate, aberrant capillary dilation, and increased BBB permeability (Daneman et al., 2010b).

Astrocytes are the most abundant glial cells in the CNS (Liu and Chopp, 2016). Their functions include balancing the extracellular potassium concentration, regulation of neurotransmitter delivery, excretion of growth factors, and metabolic support to neurons (Gee and Keller, 2005). Secretion of SHH, retinoic acid (RA) and angiopoietin-1 (Ang-1) by ACs is crucial to sustain EC impermeability (Alvarez et al., 2011; Gurnik et al., 2016). In turn, ECs can regulate differentiation of ACs via production of bone morphogenetic proteins (BMPs) and activating the Smad signaling pathway in progenitors (Imura et al., 2008).

ECs, ACs, and PCs all secrete ECM and form the BM. Multiple structural proteins (for instance, collagen type 4 and laminin), cell adhesion molecules, and extracellular matrix proteins make up the BM (Carvey et al., 2009). The BM interacts with surrounding cells to control vascularization and coordinate signaling between components of the NVU (Obermeier et al., 2013).

Transport System

The BBB transport system can be classified into the following categories: carrier-mediated transport (CMT), receptor-mediated transport (RMT), efflux transporters, and ion transporters (Sweeney et al., 2019b) (**Figure 1**). Corresponding transporters to these can also be found on PCs. Each transport system is discussed in turn, and then, we elaborate several common transporters involved in undermentioned diseases.

Carrier-mediated transport is responsible for transport of solutes, including carbohydrates, amino acids, and so on. Glucose transporter type 1 (GLUT1) is critically important in providing the CNS with energy. Therefore, GLUT1 dysfunction contributes to a variety of CNS diseases, termed GLUT1-deficiency syndromes (Glut1-DS), such as drug-resistant epileptic seizures, psychomotor retardation, ataxia, and microcephaly

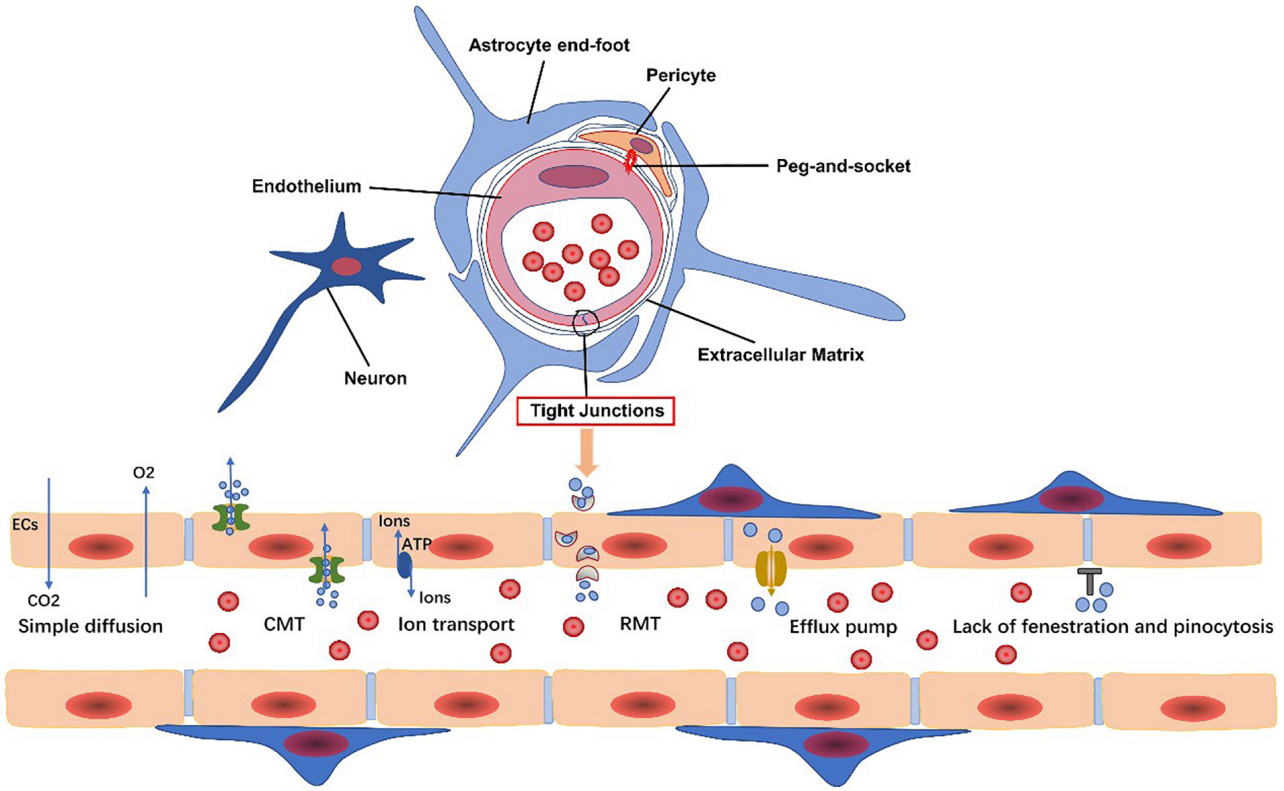

FIGURE 1 | Endothelial cells, pericytes, the extracellular matrix, glial cells, and neurons are all basic components of the neurovascular unit. The blood-brain barrier (BBB) is composed of specialized endothelial cells. The transport system of the BBB includes carrier-mediated transport (CMT), receptor-mediated transport (RMT), efflux transporters, and ion transport. Gases, such as oxygen and carbon dioxide, and small lipophilic molecules less than 400 Da in size can freely diffuse across the BBB.

(Galochkina et al., 2019; Koch and Weber, 2019). It also plays a role in AD pathogenesis as discussed below.

The main efflux pumps are the ATP-binding cassette (ABC) transporters. ABC transporters utilize ATP and pump out xenobiotics or endogenous metabolites to maintain EC homeostasis (Chow and Gu, 2015; De Rosa et al., 2015; Miller, 2015). ABCB1 (also known as *P*-glycoprotein, *P*-gp), ABCG2, and ABCC1 are all efflux transporters involved in the elimination of amyloid-β (Aβ), and so inhibition of these influences the Aβ level in the brain (Shubbar and Penny, 2020). In addition to AD, *P*-gp is involved in pathogenesis of stroke, epilepsy, and MS through upregulation or downregulation of expression influencing the inflammatory response (Huang et al., 2019).

Low-density lipoprotein receptor–related protein (LRP) is a lipoprotein receptor. It efficiently mediates clearance of Aβ, particularly Aβ42, via an LRP1/apolipoprotein E (APOE) isoform-specific mechanism (Ma et al., 2018). Both *P*-gp and LRP are regulated by phosphatidylinositol-binding clathrin assembly protein (PICALM) and PICALM deficiency diminishes transcytosis and clearance of Aβ (Zhao et al., 2015a; Storck et al., 2018). Conversely, the receptor for advanced glycation end products (RAGE) interacts with Aβ and mediates its transport across the BBB, thus inducing the release of proinflammatory cytokines (Deane et al., 2003).

Na^+-K^+-ATPases, Na^+-K^+-$2Cl^-$ cotransporters (NKCC1), Na^+-H^+ exchangers (sodium pump), and Na^+-Ca^{2+} exchangers are vital transporters for ionic equilibrium. Na^+-K^+-ATPase and NKCC1 function to maintain balance of sodium-potassium concentrations in the brain to guarantee stable physiological activity of neurons. The Na^+-H^+ exchanger is key for regulating normal pH of ECs, and the Na^+-Ca^{2+} exchanger maintains a low level of intracellular Ca^{2+} in ECs (Sweeney et al., 2019b). Dysfunction of ion transporters contributes to ionic imbalance, resulting in release of inflammatory mediators.

CEREBROVASCULAR DISEASE

Acute Ischemic Stroke

Acute ischemic stroke (AIS) is primarily caused by transient or permanent reduction in CBF induced by an embolus or thrombosis blocking regional arteries (except in cases of lacunar infarction) (Dirnagl et al., 1999); it induces a series of pathological events, including BBB disruption, vasogenic edema, hemorrhagic transformation (HT), and neuronal injury (Sifat et al., 2017). Intravenous tissue-type plasminogen activator (tPA) is an effective treatment for AIS if administered within a specific therapeutic time window (Powers et al., 2015).

However, BBB impairment restricts the application of this thrombolytic treatment; tPA passes through the impaired BBB and activates matrix metalloproteinase-9 (MMP-9) within the parenchyma, inducing ECM degradation and further altering BBB permeability. Consequently, BBB disruption aggravates cerebral edema, elevates risk of fatal HT, and intensifies the neuroinflammatory reaction after AIS (Khatri et al., 2012; Cheng et al., 2014). Therefore, BBB disruption is critical in AIS and contributes to subsequent brain damage.

Stroke is composed of two successive phases, ischemia and reperfusion, based on the paracellular penetrative state (Sandoval and Witt, 2008). In the ischemic phase, CBF is reduced, resulting in a deficient supply of glucose and oxygen (Sandoval and Witt, 2008). Glucose and oxygen are essential to maintain an adequate supply of adenosine triphosphate (ATP) to guarantee physiological cellular function and maintain normal ion gradients (Abdullahi et al., 2018). Following the onset of ischemia, oxidative phosphorylation is discontinued, followed by an ATP shortage (Hata et al., 2000). EC ion transporters are unable to function with inactivation of Na^+-K^+-ATPases and Ca^{2+}-ATPases due to lack of energy. Increased activity of other ion transporters, such as Na^+-H^+ exchangers, NKCC1, and the calcium-activated potassium channel, KCa3.1, elevates intracellular Na^+ levels and causes cytotoxic edema (Khatri et al., 2012; Xiaoyan et al., 2018). Na^+ accumulation also leads to membrane depolarization and Na^+-Ca^{2+} exchanger dysfunction, resulting in Ca^{2+} efflux and calcium overload (Abdullahi et al., 2018). This promotes the release of excitatory neurotransmitters and reactive oxygen species (ROS), which induce inflammatory cascades and destroy the BBB (Janardhan and Qureshi, 2004; Adibhatla and Hatcher, 2008). KCa3.1 blockade is capable of reversing cerebral edema within 3 h of AIS (Chen et al., 2015). Similarly, inhibition of NKCC1 can alleviate brain edema and neurological impairment (O'Donnell et al., 2004). Sodium-dependent glucose transporters (SGLTs) and GLUT1 both play a role in glucose transportation under pathological and physiological conditions, respectively. The function of SGLTs are dependent on the NKCC1-mediated sodium gradient, which contributes to sodium accumulation in ECs during stroke. Inhibition of SGLTs has been shown to reduce edema and improve poststroke outcome (Vemula et al., 2009). Interestingly, another study has shown that SGLTs are also present in neurons but not BBB ECs under physiological conditions (Yu et al., 2010; Patching, 2017). In any event, BBB ion transporters provide a hopeful therapeutic target.

In the reperfusion phase, CBF starts to recover, which is beneficial for neuronal survival but increases the risk of HT. BBB injury is a core pathophysiological mechanism in reperfusion damage (Vemula et al., 2009), and increased BBB permeability further increases HT risk (Sandoval and Witt, 2008). BBB dysfunction can be characterized into three stages: stage 1 includes the effects of oxidative stress on the BBB and associated ECM degeneration, whereas stages 2 and 3 are associated with vasogenic edema and angiogenesis. Alterations in BBB TJs during phase 1 induce the changes seen in stages 2 and 3 (Heo et al., 2005; Khatri et al., 2012). Activation of proteinases, such as MMPs, and tPA, are the most important contributors to BBB breakdown and are stimulated by either hypoxia-inducible factor-1α (HIF-1α)-dependent mechanisms or cytokines, such as tumor necrosis factor-α (TNF-α) and interleukin 1β (IL-1β) (Yang and Rosenberg, 2011). MMPs, particularly MMP-2 and MMP-9 have been shown to degrade TJ proteins (Yang and Rosenberg, 2011; Liu et al., 2012). MMP-9, derived from neutrophils, degrades claudin-5 and the BM following ischemia, resulting in brain edema, neurological deficits and increased HT risk (McColl et al., 2008). In experimental stroke mice, elevated levels of α2-antiplasmin enhanced the expression of MMP-9, exacerbating BBB breakdown and ischemic injury (Singh et al., 2018). In addition to MMPs, caveolin-1 mediates the translocation and downregulation of claudin-5, exacerbating BBB leakage (Liang et al., 2015). Furthermore, exudation of inflammatory cells also aggravates BBB breakdown (Sifat et al., 2017), accompanied by reduced expression of occluding (Liang et al., 2015), ZO-1 (Jiao et al., 2011), and VE-cadherin (Wacker et al., 2012; Weinl et al., 2015). For example, microglia secrete cytokines to stimulate upregulation of intercellular adhesion molecule-1 (ICAM-1), *P*-selectin and *E*-selectin on the surface of ECs, mediating the infiltration of neutrophils (Wang and Doerschuk, 2002). Rho kinase (RhoK) mediates the phosphorylation of occludin and claudin-5, increasing BBB permeability (Yamamoto et al., 2008). C-C motif ligand 2 (CCL2), also known as monocyte chemoattractant protein-1 (MCP-1) elevates expression of caveolin-1, resulting in phosphorylation of occludin and ZO-1, and thus, exacerbating BBB leakage. In summary, ischemia and hypoxia induce BBB dysfunction, which then facilitates inflammatory cascades that further induce decompose BBB dysfunction. Thus, the BBB is not only influenced by AIS but also contributes to AIS pathology (**Figure 2**).

In recent years, research has focused on exploring advanced therapies to alleviate BBB damage. Chemokine receptor type 5 (CCR5) stimulates regulatory T cells (Tregs) strengthens BBB immunoregulatory function and ameliorates inflammatory cascades, thus representing a potential treatment target (Li et al., 2017). Circular RNA DLGAP4 (circDLGAP4) can bind to miR-143, maintaining BBB integrity and diminishing infarct volume in AIS patients (Bai et al., 2018). miR-98 protects EC stability and strengthens BBB integrity through modifying activation of small Rho GTPases, rearranging the actin cytoskeleton, and redistributing TJ proteins. It also limits the recruitment of inflammatory cells by reducing expression of the proinflammatory cytokines, CCL2 and CCL5 (Bernstein et al., 2019). Transplantation of mesenchymal stem cells (MSCs) is a prominent research focus as they can promote neurogenesis and angiogenesis in the BBB (Dabrowska et al., 2019). Integrin α5β1 mediates leukocyte infiltration and subsequent BBB dysfunction; the integrin α5β1 inhibitor, ATN-161, can preserve claudin-5 and collagen-IV expression and reduce MMP-9 transcription, thus protecting BBB integrity (Edwards et al., 2019). Perlecan, a major heparan sulfate proteoglycan component of the BM, can maintain and repair the injured BBB by reinforcing the BM (Nakamura et al., 2019). Furthermore, release of microvesicles by ECs can upregulate ZO-1 and claudin-5 expression, thereby

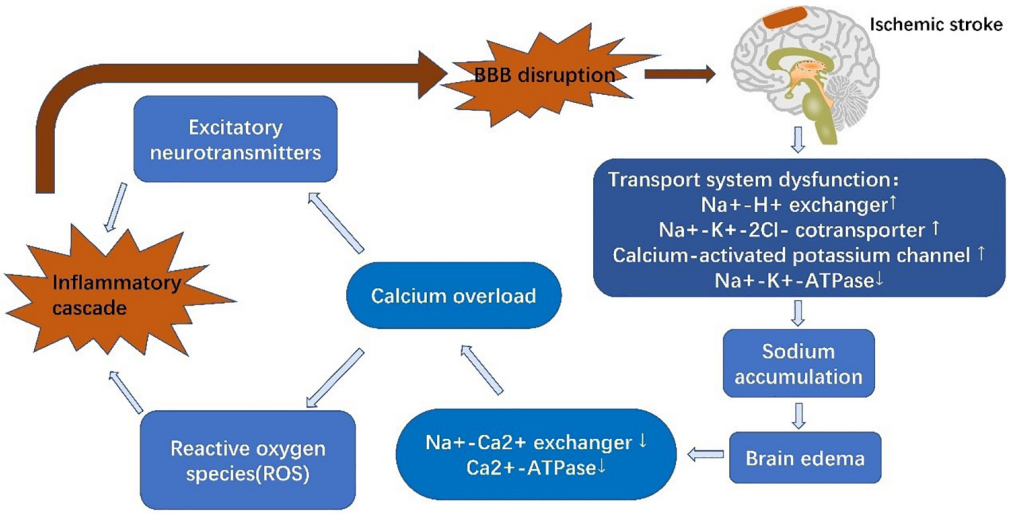

FIGURE 2 | Schematic diagram of blood-brain barrier alterations in acute ischemic stroke. Reduced levels of glucose and oxygen result in dysfunction of EC ion transporters, inducing calcium overload and triggering inflammatory cascades. These inflammatory cascades further degrade tight junctions, thus aggravating brain edema and increasing infarct size.

ameliorating BBB disruption and reducing infarct volume (Pan et al., 2016). Cystatin C is also capable of reducing the expression of caveolin-1, restricting the activity of MMP-9 and elevating occludin expression in mice that have undergone middle cerebral artery occlusion (MCAO) (Yang et al., 2019). It has been shown that deficiency of vitamin D hormone (VDH) reduces occludin and claudin-5 expression and correlates with poor prognosis in stroke (Balden et al., 2012; Stessman and Peeples, 2018). Therefore, sufficient supplementation of VDH appears to be advantageous to maintaining BBB integrity (Sayeed et al., 2019). Nanoparticles are an efficient method for transporting pharmacological compounds across the BBB. For instance, Bao et al. (2018) designed edaravone-loaded ceria nanoparticles that cleared ROS produced by AIS and effectively protected the BBB with minimal side-effects. Combination treatment with recombinant tissue plasminogen activator (rt-PA) and minocycline or rt-PA and cilostazol has been shown to protect TJ proteins from secondary degradation following thrombolysis (Ishiguro et al., 2010; Fan et al., 2013). Moreover, type 5 NADPH oxidase (NOX5) induces ROS; thus, applying a NOX5 inhibitor together with reperfusion treatment (thrombolysis or thrombectomy) has been shown to reduce ROS generation and ameliorate BBB injury (Casas et al., 2019). CO-releasing molecule (CORM)-3 decreases the level of TNF-α, and IL-1β, upregulates expression of PDGFR-β and ZO-1 and inhibits activity of MMP-9, thus alleviating BBB disruption in transient-MCAO mice (Wang et al., 2018).

Intracerebral Hemorrhage

Intracerebral hemorrhage (ICH) is a leakage of blood components from damaged vessels and into the brain parenchyma (Qureshi et al., 2009). The pathophysiology of ICH includes two phases; hematomas induce the initial mechanical compression damage, which leads to mitochondrial dysfunction and membrane depolarization. Cells affected by this damage induce secondary injury, which is characterized by excitotoxicity and oxidative stress caused by cellular dysfunction and the presence of blood components (Qureshi et al., 2009; Shi et al., 2019). Perihematomal edema (PHE) is evident in both stages although the relevant pathogenesis is different.

PHE develops immediately after ICH onset (Venkatasubramanian et al., 2011), which leads to rapid deterioration in the patient and subsequent poor prognosis (Mayer et al., 1994). It can be divided into three phases: phase 1 includes osmotic edema caused by the initial damage, and phases 2 and 3 are characterized by vasogenic edema resulting from secondary damage (Urday et al., 2015).

The osmotic edema phase, phase 1, occurs within the first hours of ICH onset and is composed of clot retraction and cytotoxic edema (Xi et al., 2002). Clot retraction occurs due to a secondary coagulation cascade, which extrudes serum proteins and prompts interstitial accumulation of ions and water. The cytotoxic edema can mainly be ascribed to dysfunction of cellular ionic pumps (such as Na^+-K^+-ATPase and NKCC1), resulting in sodium influx and edema formation (Urday et al., 2015). Phase 2, including the first 2 days in ICH, encompasses a further coagulation cascade and stimulation of thrombin. Thrombin combines with protease-activated receptor-4 (PAR-4) and stimulates microglia (Bodmer et al., 2012), which then release cytokines including TNF and IL-1β; TNF has been shown to be a pivotal factor in downregulation of the TJ proteins (Xi et al., 2002; Aslam et al., 2012). However, thrombin also induces PAR-1 and phosphorylates myosin light chain (MLC) in ECs, strengthening their contractility and increasing intercellular gaps (Simard et al., 2010; Urday et al., 2015). Moreover, thrombin facilitates leukocyte infiltration, followed by ROS production and increased ICAM expression in ECs, which further enhances leukocyte exudation (Bijli et al., 2007). The complement cascade also

contributes to PHE development. Recruitment of chemokines results in generation of membrane attack complexes (MACs) that promote dissolution of red blood cells (RBCs) and edema induced by blood components (Bodmer et al., 2012; Urday et al., 2015). Phase 3, following from phase 2, also contributes to BBB disruption. RBCs are degraded into hemoglobin (Hb) and iron by MACs. Hb activates the Toll-like receptor-2/4 (TLR2/TLR4) heterodimer, which promotes oxidative stress and mediates further BBB disruption (Urday et al., 2015). MMP-9, as a downstream factor activated by ROS, is key to iron-mediated edema. As previously discussed, it degrades TJ proteins and the basal lamina to aggravate BBB leakage (Florczak-Rzepka et al., 2012). Conventional treatment for ICH includes respiratory support, management of both blood and intracranial pressures, anti-coagulation therapy, and surgical evacuation (Qureshi et al., 2009). The BBB serves as a trigger point for inflammatory cascades and, thus, participates in the whole ICH disease course. Considering this central role, advanced treatments have recently been developed that aim to modulate this immunoreaction to reduce secondary BBB injury of BBB (**Figure 3**).

Statins can alleviate PHE in ICH through anti-inflammatory mechanisms. Siddiqui et al. (2017) analyzed the use of statins in ICH patients and found that patients taking statins had better clinical outcomes. Likewise, celecoxib can inhibit inflammation and reduce brain edema through lowering prostaglandin E2 expression (Chu et al., 2004; Lee et al., 2013). The colony-stimulating factor 1 receptor inhibitor, PLX3397 depletes microglia, inhibits leukocyte infiltration and decreases the level of pro-inflammatory mediators, thereby eliminating BBB breakdown and brain edema (Li et al., 2016). Transforming growth factor-β1 (TGF-β1) has also been shown to improve ICH prognosis through modulation of microglial phenotype and inhibition microglial-derived neuroinflammation (Taylor et al., 2017). LRP-1 is able to obliterate hemoglobin, blocking subsequent damage and, thus, stabilizing the BBB in mice (Wang et al., 2016). Fingolimod, an immunomodulatory compound, has also been shown to protect the BBB and improve clinical sequelae through reducing MMP-9 expression, inhibiting infiltration of immune cells and secretion of inflammatory mediators (Rolland et al., 2013; Li et al., 2015). The peroxisome proliferator-activated receptor γ (PPAR-γ) agonist, pioglitazone, is in phase II clinical trials to evaluate the safety of its application to promoting erythrocyte phagocytosis by microglia, which alleviates inflammation and protects the BBB *in vivo* (NCT00827892) (Fu et al., 2015). In addition, a randomized pilot phase II clinical trial of minocycline is also (NCT01805895) (Fu et al., 2015) assessing its BBB protection ability via reducing microglial infiltration and downregulating pro-inflammatory cytokine expression (Wu et al., 2010).

NEURODEGENERATIVE DISEASE

Alzheimer's Disease

Alzheimer's disease is characterized by deposition of misfolded Aβ and tau proteins in the CNS parenchyma (Hardy and Selkoe, 2002), leading to BBB breakdown and cognitive impairment (Montagne et al., 2015; Jevtic et al., 2017). Autopsy studies on patients with confirmed AD showed that more than half of these patients had evident vascular alterations (Sweeney et al., 2019a). Hereditary susceptibility combined with environmental factors, such as pollutants and diet, evoke a series of vascular changes. In fact, BBB disruption, as a contributor to the pathophysiological process, exists before the formation of typical vascular pathology. There is two-hit vascular hypothesis (Nelson et al., 2016), in which vascular dysfunction plays a leading role in the initial

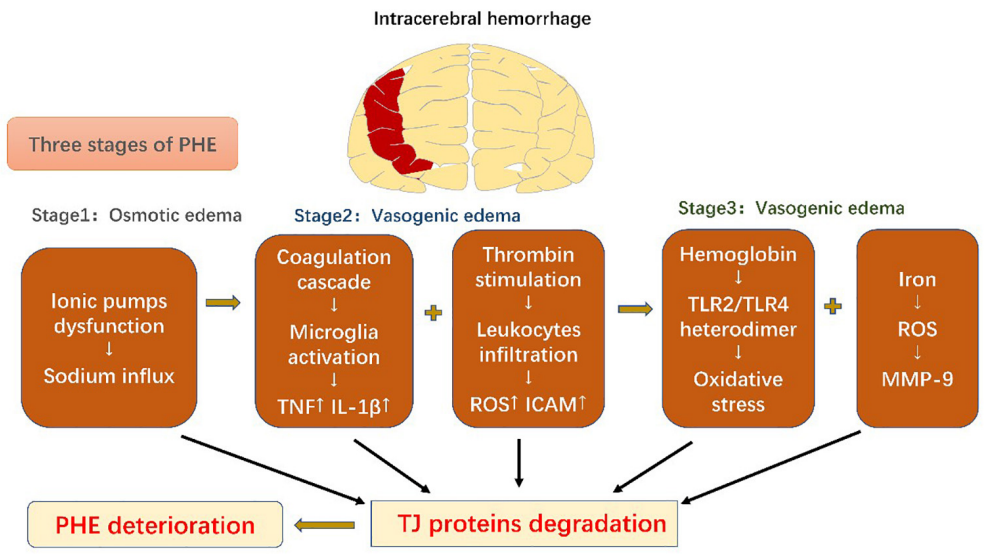

FIGURE 3 | Schematic diagram of blood-brain barrier changes in intracerebral hemorrhage. Perihematomal edema secondary to intracerebral hemorrhage can be divided into three phases. All the pathophysiological events result in degradation of tight-junction proteins, which exacerbate perihematomal edema and result in poor prognosis.

stages, resulting in ischemia-hypoxia and EC injury, and then facilitates deposition of neurotoxic substances in the CNS during the second stage.

APOE genetic variants, among the greatest genetic risk factors for sporadic AD, have been shown to cause BBB disruption and degeneration of PCs (Verghese et al., 2011; Halliday et al., 2016). In APOE4 carriers with normal cognition or mild cognitive impairment (MCI), a prelude to AD, dynamic contrast-enhanced magnetic resonance imaging evidenced BBB leakage prior to tissue loss, indicating that BBB disruption is independent of Aβ and tau deposition (Ishii and Iadecola, 2020; Montagne et al., 2020). In addition, secreted PDGFRβ (sPDGFRβ), a biomarker of PC injury, is elevated in the cerebrospinal fluid (CSF) of APOE4 carriers (Ishii and Iadecola, 2020; Montagne et al., 2020) and has been shown to be independent of pathological changes in AD (Montagne et al., 2020). Of all APOE isoforms, APOE4 increases AD susceptibility dramatically compared with APOE3, and APOE2 reduces AD risk (Verghese et al., 2011). APOE4 activates cytokine cyclophilin A (CypA), nuclear factor-κB (NF-κB) and MMP-9 in both PCs and ECs, degrading TJ and BM proteins, downregulating GLUT1 expression and upregulating expression of RAGE (Montagne et al., 2017). RAGE binds peptides and mediates influx of Aβ (Candela et al., 2010), thus damaging PCs and the BBB (Bell et al., 2012; Halliday et al., 2016). The impact of APOE4 on ECs and PCs is independent of Aβ or tau elevation (Ishii and Iadecola, 2020). Furthermore, increased APOE burden reduces Aβ transport, resulting in its accumulation in the brain and accelerating the course of the disease (Gosselet, 2012). Therefore, BBB dysfunction can independently trigger subsequent disorders and exacerbate cognitive impairment.

Moreover, evidence indicates that VSMCs and ECs can produce Aβ peptides in the adult brain (Kitazume et al., 2010; Schweinzer et al., 2011). The BBB is also an underlying source of Aβ peptides, which downregulate ZO-1, occludin, and claudin-5 and increase the permeability of ECs through interaction with RAGE, activation of MMPs and stimulation of oxidative stress pathways (Carrano et al., 2011; Kook et al., 2012). In addition, it has been shown that Aβ peptides promote angiogenesis and redistribution of TJs, impairing BBB integrity and allowing Aβ leakage (Biron et al., 2011).

The ABC superfamily is important for lipoprotein metabolism and Aβ efflux (Kim et al., 2008; Miller, 2015). *P*-gp and ABCG2 not only facilitate transport of Aβ across the BBB via LRP1 binding (Cirrito et al., 2005; Storck et al., 2018), but also restrict Aβ influx (Candela et al., 2010). ABCA1 mediates the transfer of cholesterol to APOE, high-density lipoprotein (HDL), and APOA-I and modifies the cleavage of amyloid precursor protein (APP) as well as clearance of Aβ across the BBB (Saint-Pol et al., 2013; Kuntz et al., 2015; Dal Magro et al., 2019). ABCA7 is the only ABC transporter implicated by AD Genome Wide Association Studies (GWAS) (Hollingworth et al., 2011). Absence of ABCA7 expression reduces the level of ABCA1 and APOE secretion with a concurrent reduction in cholesterol exchange (particularly that of HDL and ApoA-I) and Aβ efflux (Lamartiniere et al., 2018).

LRP-1 is the main transporter of Aβ with dysfunction increasing Aβ levels and promoting AD (Jaeger et al., 2009). *P*-gp, located on the luminal side of ECs, limits the transport of multiple products (Schinkel et al., 1994), including Aβ. *P*-gp deficiency contributes to LRP1 dysfunction and increases Aβ levels (Cirrito et al., 2005). A recent experiment involved in the BBB model *in vitro* indicated that a ketogenic diet could enhance expressions of LRP1, *P*-gp, and PICALM and, thus, promote Aβ efflux across the BBB (Versele et al., 2020). PICALM has been shown to promote binding of LRP1 to Aβ as well. It promotes Aβ endocytosis and Aβ-LRP1 transcytosis by transferring the protein complex to Rab5 and Rab11 (Zhao et al., 2015b). Furthermore, PICALM gene mutations have also been implicated in AD (Tian et al., 2013; Zhao et al., 2015a) (**Figure 4**).

Therapeutic BBB modulation has shown promising results in AD treatment. FPS-ZM1, an innoxious RAGE suppressant, inhibits RAGE activation and reduces entry of Aβ within the brain, thereby suppressing neuroinflammation (Deane et al., 2012). Van Skike et al. (2018) found that inhibiting the mammalian/mechanistic target of the rapamycin (mTOR) pathway can maintain BBB integrity and restore cognitive function. Bana et al. (2014) also succeeded in constructing a nanodevice to alter Aβ morphology and treat AD, which needs further clinical trials.

Parkinson's Disease

Parkinson's disease (PD) is a neurodegenerative disease characterized by tremors, limb rigidity, and hypokinesis (Calne and Sandler, 1970). The main pathological hallmark of PD is the progressive death of dopaminergic neurons in the substantia nigra (SN) and deposition of Lewy bodies (LBs), fibrillar aggregates composed of α-synuclein (α-syn), leucine-rich repeat kinase 2 (LRRK2), and other proteins (Lang and Lozano, 1998; Wakabayashi et al., 2013). PD occurrence is influenced by hereditary susceptibility, environmental toxins (such as rotenone and pesticides), age-related neurodegeneration, and interactions between these factors.

BBB lesions, including a thickened BM and degraded PCs, have been observed in PD (Farkas et al., 2000). Additionally, prominent BBB leakage has been shown in the striatum of PD patients with deposition of fibrin and hemosiderin forecasting its vulnerability (Gray and Woulfe, 2015). Positive correlations have also been found between parenchymal iron levels, resulting from BBB leakage, and brain pathology in PD patients (Götz et al., 2004). In addition to iron, extravasation of red blood cells that act as a source of α-syn might also contribute to PD pathology (Sweeney et al., 2018). Degradation of TJ proteins cause BBB injury and enhanced transcytosis. A recent study showed that misfolded α-syn could downregulate ZO-1 and occludin expression, indicating that α-syn is neurotoxic to the BBB (Kuan et al., 2016). Degradation of ECs also generates BBB breakdown and initiates neurodegenerative pathology. In addition, decreased expression of GLUT-1 and ABCG2 were evident in PD mouse models, and P-gp expression was increased (Vautier et al., 2009a; Sarkar et al., 2014). However, another study has found a reduction in *P*-gp expression although this could be attributed to the methods of establishing the models

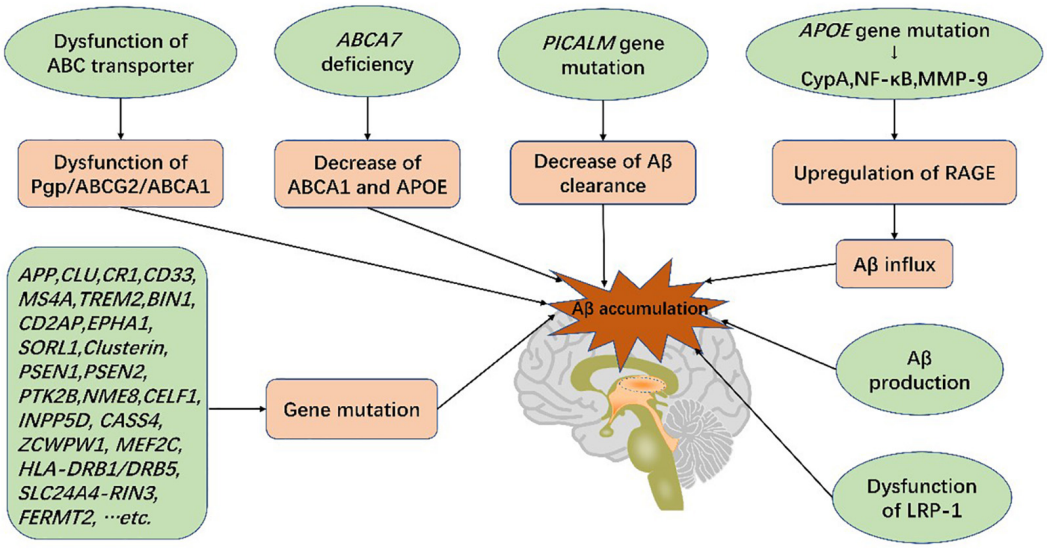

FIGURE 4 | Genetic mutations and Aβ production in the blood-brain barrier increase the risk of AD. Genetic mutations, such as ABCA7, PICALM, and APOE, lead to dysfunction of BBB transport systems, resulting in Aβ deposition in the brain. Aβ accumulation gives rise to blood-brain barrier breakdown and cognitive impairment, characteristic of Alzheimer's disease.

(Huang et al., 2016; Pan and Nicolazzo, 2018). *P*-gp dysfunction also plays an important role in PD pathogenesis due to decreased clearance of neurotoxic substances (Kortekaas et al., 2005), leading to their accumulation in the BBB, similarly to its role in AD pathogenesis. Thus, P-gp could be a promising therapeutic target in PD as well. Despite clearly thickened BM and decreased *P*-gp function in PD (Pan and Nicolazzo, 2018), the specific pathological mechanisms remain unclear. Neuroinflammation likely also plays a crucial role in this process with α-syn transport or iron deposition initiating the inflammatory reaction. It has been shown that metabolic iron disorders induce oxidative stress and free radical production, resulting in the induction of neurotoxic cascades (Crichton et al., 2011; Weinreb et al., 2013). Activated microglia secrete inflammatory factors, upregulate EC expression of adhesion molecules and recruit leukocytes, and amplify inflammatory cascades, ultimately resulting in neuronal (Reale et al., 2009). Inflammatory cytokines also downregulate ZO-1 and occludin, thus increasing BBB permeability (Wong et al., 2004). The inflammatory mediators MMP-3 and nuclear factor erythroid 2–related factor 2 (NRF2) have been show to stimulate α-Syn production, induce aggregation of amyloidogenic compounds and induce the release of inflammatory cytokines, mediating death of dopaminergic neurons (Rivera et al., 2019; Sivandzade et al., 2019). Interestingly, knockout of TNF-α expression in PD model mice attenuated BBB leakage (Zhao et al., 2007).

Furthermore, CSF from PD patients contains elevated levels of angiogenesis factors (Janelidze et al., 2015). Aberrant angiogenesis results in generation of immature vasculature and loose intercellular junctions, which has been connected with dopaminergic neuronal loss through leakage of neurotoxic substances (Desai et al., 2007). To summarize, BBB injury leads to substantial leakage of peripheral substances, thus expediting development of neurodegenerative disorders.

There are now multiple advanced treatments and newfound targets for PD. Milk fat globule-epidermal growth factor-VIII (MFG-E8) can promote neurogenesis and restore impaired neurocytes in PD (Cheyuo et al., 2019). Statins exert neuroprotective effects in PD models through anti-inflammatory and anti-oxidation mechanisms, providing a promising treatment option (Roy and Pahan, 2011; Wood et al., 2014). Glutathione is an antioxidative agent and demonstrates beneficial effects in PD by protecting dopaminergic neurons (Smeyne and Smeyne, 2013). Anti-complement agents that regulate immunoreactivity through inhibition of complement pathways have been effective in PD models but require further verification in clinical trials (Carpanini et al., 2019). Increased expression of hepcidin accelerates iron transport and metabolism, thus providing an additional potential therapy (Qian and Ke, 2019). Iron-chelation therapy is beneficial for adjusting iron homeostasis (Weinreb et al., 2013). Glial cell-derived neurotrophic factor (GDNF), nerve growth factor (NGF), and brain-derived neurotrophic factor (BDNF) are all beneficial for neural revival and regeneration, thus transporting these factors across the BBB could be an option for PD treatment (Allen et al., 2013). Several options are available for improved delivery of therapeutics across the BBB, including using micro- or nanotechnology to bind therapeutic agents or delivery of small hydrophobic agents with liposomal targeting (Torres-Ortega et al., 2019; Wang et al., 2019). Focused ultrasound (FUS) to open specific BBB regions and facilitate entry of therapeutic compounds is currently in phase 1 trials for PD treatment (NCT03608553) (Zlokovic, 2008).

Multiple Sclerosis

Multiple sclerosis (MS) is characterized by remitting-relapsing demyelination and axon loss. It is a chronic and progressive CNS inflammatory disorder, which ultimately evolves over time into neurodegeneration (Hemmer et al., 2002). The use of gadolinium enhancement in MRI has allowed measurement of BBB breakdown in MS (Miller et al., 1998), which is deemed as a trigger point for disease onset; the presence of immunocytes in the immune-privileged brain parenchyma via BBB breakdown induces the autoimmune disease in a hereditarily susceptible population (Daneman, 2012).

Energy metabolism dysfunction and endocrine disorders have been shown to initiate MS through crosstalk with immune cells (Procaccini et al., 2014; De Rosa et al., 2015). In addition, viral infection and environmental toxins in hereditarily susceptible individuals have also been shown to reduce immune tolerance and stimulate release of proinflammatory factors, such as IL-6 and NF-κB. As previously mentioned, these proinflammatory factors promote alternation of TJs and damage BBB integrity (Weksler et al., 2005) as well as facilitate leukocyte transmigration (Sheikh et al., 2020). *P*-gp expression is also increased and enhances migration of $CD4^+$ and $CD8^+$ T cells to further amplify neuroinflammation (Kooij et al., 2014). Silencing of P-gp expression significantly reduces $CD8^+$ T cell trafficking into the CNS (Kooij et al., 2014). Under inflammatory conditions, EC expression of selectins and their corresponding ligands are also elevated, promoting leukocyte binding; this mediates further interaction between integrins and their ligands, thus strengthening the adherence of leukocytes (Wilson et al., 2010). Further to this, cytokines and chemokines upregulate endothelial adhesion receptors, including PECAM1, *E*-selectin, VCAM, and ICAM-1 and augment subsequent leukocyte infiltration (Ricci et al., 2009). PECAM-1 facilitates leukocyte adherence and directs para-endothelial infiltration, thereby contributing to increased inflammation (Ricci et al., 2009; Losy, 2013). VCAM upregulates the expression of integrin α-4 in ECs, reducing the level of TJ proteins (Haarmann et al., 2015). Integrin α-4 is also indispensable for CD8 + T lymphocyte recruitment (Ifergan et al., 2011). ICAM-1 plays a crucial role in inflammation through phosphorylation of TJ proteins and restructuring of the cytoskeleton, thus promoting increased BBB permeability (Huber et al., 2001). Both VCAM and ICAM mediate trans-endothelial infiltration of leukocytes (Hernández-Pedro et al., 2013). $CD4^+$ T cells identify myelin sheath proteins and macrophages, and upregulate the release of pro-inflammatory factors (including IFN-γ, TNF-α, nitric oxide and free radicals), thus leading to demyelination (Hernández-Pedro et al., 2013). Neutrophils, monocytes, and microglia infiltrate the brain parenchyma and release extracellular glutamate, generating excitotoxity and accelerating BBB dysfunction (Macrez et al., 2016). Furthermore, fibrinogen leakage from the BBB prompts release of ROS by microglia (Davalos et al., 2012). Accumulation of leukocytes in the parenchyma induces further release of ROS, resulting in demyelination and breakdown of TJ proteins (Van der Goes et al., 2001; Hendriks et al., 2005). Demyelinated lesions further induce secretion of free radicals, magnifying the inflammatory reaction (Bagasra et al., 1995). As a result, the excessive oxidative stress downregulates occludin and ZO-1, thus further promoting TJ disruption (Ortiz et al., 2014).

Other members of the NVU also disrupt BBB integrity. In pathological circumstances, the AQP4-mediated polarization of ACs becomes misregulated, resulting in retraction of end-feet from the glia limitans (Wolburg-Buchholz et al., 2009; Spencer et al., 2018). Moreover, AC-expressed VEGF-A activates the downstream factor, *e*-nitrogen oxide (eNOS), which disrupts EC expression of claudin-5 and occludin and disrupts the BBB (Argaw et al., 2012). Oligodendrocyte precursor cells (OPCs) also accumulate in MS lesions, interrupting AC end-feet contacts and TJ integrity as well as impairing lesion repair and altering BBB permeability (Niu et al., 2019). To summarize, immune system abnormalities induce alterations in BBB TJs, which facilitates trans-endothelial migration of leukocytes and ultimately leads to neurodegeneration (Sheikh et al., 2020).

Disease-modifying therapies (DMTs) are a basic therapy for MS with multiple advanced drugs developed and clinically tested. Ozanimod, a sphingosine 1-phosphate (S1P) receptor modulator, was approved for MS treatment in March 2020 (Lamb, 2020). Siponimod is undergoing a phase-3 trial (NCT01185821) due to its beneficial effects on relapsing-remitting MS (Kappos et al., 2016). Ibudilast is currently in phase-2 trials due to its capability of crossing the BBB and restricting the shift in macrophage phenotype, thus benefiting progressive MS (NCT01982942) (Fox et al., 2018). Immunoablation and autologous hemopoietic stem-cell transplantation (aHSCT) has passed a phase 2 single-arm trial, which aims to provide long-term control of aggressive MS (NCT01099930) (Atkins et al., 2016). Minocycline has also been verified in clinical trials to lower the risk of clinically isolated syndromes progressing into MS (NCT00666887) (Metz et al., 2017). As previously stated, application of nanomaterials is an efficient way to deliver agents across the BBB (Furtado et al., 2018). Fingolimod reduces monocyte migration and reverses BBB dysfunction through targeting ACs (van Doorn et al., 2012). However, a recent large comparative study found that patients treated with fingolimod have a higher risk of cancer due to increased tumorigenicity from immunosuppression; use of rituximab and natalizumab in MS do not elevate invasive cancer risk (Alping et al., 2020). Natalizumab, a monoclonal antibody (McAb) mainly used in treatment of relapsing-remitting MS, can prevent leukocyte adherence and blocks integrin α-4 on ECs, thereby protecting the BBB (Haarmann et al., 2015). However, as an efficient inflammatory suppressant, it also inhibits immune surveillance and leads to progressive multifocal leukoencephalopathy (PML), an infectious disease caused by John Cunningham virus (Prezioso et al., 2020), which unfortunately restricts its clinical application.

CONCLUSION

In summary, BBB disruption plays a central role in the pathophysiology of cerebrovascular and neurodegenerative disease. Dysfunction in energy metabolism and leakage

of blood components catalyze CNS inflammation in cerebrovascular disease. Conversely, in neurodegenerative disease, endogenous inflammation is stimulated when genetically susceptible individuals develop endocrine disorders or are exposed to environmental factors, such as pollutants and exogenous infection. Despite diverging induction mechanisms, inflammation is a common characteristic of these CNS diseases. In general, disruption of the homeostatic CNS microenvironment triggers BBB reconstruction, resulting in leukocyte infiltration and leakage of neurotoxic substances that augment further neuroinflammation, which, in turn, exacerbates BBB permeability. Therefore, preservation of the BBB is a crucial therapeutic target. Recent investments mainly focus on the following two aspects: modulation of the inflammatory cascade modulation (including NOS, ROS, cytokines and chemokines) and BBB reinforcement. In this review, we have first correlated pro-inflammatory mediators with changes in the corresponding BBB-expressed molecules and listed several recent advanced treatments targeting the BBB and the inflammatory response. Existing therapies are also being applied to limit severe BBB dysfunction and the inflammation cascade. Further studies should concentrate on limiting the initial inflammation prior to BBB remodeling and on consolidating BBB integrity by directly promoting the synthesis of relevant TJ proteins; this may significantly improve treatment efficacy. In a word, BBB dysfunction is more of a contributor to CNS pathology than a victim in neurological disorders, and so more attention should be paid to its significant function in maintaining CNS homeostasis.

AUTHOR CONTRIBUTIONS

MX: study concept, study design, manuscript preparation, and editing. ZX: literature research and manuscript revision. BY: manuscript revision. ZL: literature research and management. FF: figure design. All authors contributed to the article and approved the submitted version.

REFERENCES

Abdullahi, W., Tripathi, D., and Ronaldson, P. T. (2018). Blood-brain barrier dysfunction in ischemic stroke: targeting tight junctions and transporters for vascular protection. *Am. J. Physiol. Cell Physiol.* 315, C343–C356. doi: 10.1152/ajpcell.00095.2018

Adibhatla, R. M., and Hatcher, J. F. (2008). Tissue plasminogen activator (tPA) and matrix metalloproteinases in the pathogenesis of stroke: therapeutic strategies. *CNS Neurol. Disord. Drug Targets* 7, 243–253. doi: 10.2174/187152708784936608

Allen, S. J., Watson, J. J., Shoemark, D. K., Barua, N. U., and Patel, N. K. (2013). GDNF, NGF and BDNF as therapeutic options for neurodegeneration. *Pharmacol. Ther.* 138, 155–175. doi: 10.1016/j.pharmthera.2013.01.004

Alping, P., Askling, J., Burman, J., Fink, K., Fogdell-Hahn, A., Gunnarsson, M., et al. (2020). Cancer risk for fingolimod, natalizumab, and rituximab in multiple sclerosis patients. *Ann. Neurol.* 87, 688–699. doi: 10.1002/ana.25701

Alvarez, J. I., Dodelet-Devillers, A., Kebir, H., Ifergan, I., Fabre, P. J., Terouz, S., et al. (2011). The Hedgehog pathway promotes blood-brain barrier integrity and CNS immune quiescence. *Science* 334, 1727–1731. doi: 10.1126/science.1206936

Argaw, A. T., Asp, L., Zhang, J., Navrazhina, K., Pham, T., Mariani, J. N., et al. (2012). Astrocyte-derived VEGF-A drives blood-brain barrier disruption in CNS inflammatory disease. *J. Clin. Invest.* 122, 2454–2468. doi: 10.1172/JCI60842

Armulik, A., Genové, G., and Betsholtz, C. (2011). Pericytes: developmental, physiological, and pathological perspectives, problems, and promises. *Dev. Cell* 21, 193–215. doi: 10.1016/j.devcel.2011.07.001

Armulik, A., Genové, G., Mäe, M., Nisancioglu, M. H., Wallgard, E., Niaudet, C., et al. (2010). Pericytes regulate the blood-brain barrier. *Nature* 468, 557–561. doi: 10.1038/nature09522

Aslam, M., Ahmad, N., Srivastava, R., and Hemmer, B. (2012). TNF-alpha induced NFκB signaling and p65 (RelA) overexpression repress Cldn5 promoter in mouse brain endothelial cells. *Cytokine* 57, 269–275. doi: 10.1016/j.cyto.2011.10.016

Atkins, H. L., Bowman, M., Allan, D., Anstee, G., Arnold, D. L., Bar-Or, A., et al. (2016). Immunoablation and autologous haemopoietic stem-cell transplantation for aggressive multiple sclerosis: a multicentre single-group phase 2 trial. *Lancet* 388, 576–585. doi: 10.1016/s0140-6736(16)30169-6

Baeten, K. M., and Akassoglou, K. (2011). Extracellular matrix and matrix receptors in blood-brain barrier formation and stroke. *Dev. Neurobiol.* 71, 1018–1039. doi: 10.1002/dneu.20954

Bagasra, O., Michaels, F. H., Zheng, Y. M., Bobroski, L. E., Spitsin, S. V., Fu, Z. F., et al. (1995). Activation of the inducible form of nitric oxide synthase in the brains of patients with multiple sclerosis. *Proc. Natl. Acad. Sci. U.S.A.* 92, 12041–12045. doi: 10.1073/pnas.92.26.12041

Bai, Y., Zhang, Y., Han, B., Yang, L., Chen, X., Huang, R., et al. (2018). Circular RNA DLGAP4 ameliorates ischemic stroke outcomes by targeting miR-143 to regulate endothelial-mesenchymal transition associated with blood-brain barrier integrity. *J. Neurosci.* 38, 32–50. doi: 10.1523/JNEUROSCI.1348-17.2017

Balden, R., Selvamani, A., and Sohrabji, F. (2012). Vitamin D deficiency exacerbates experimental stroke injury and dysregulates ischemia-induced inflammation in adult rats. *Endocrinology* 153, 2420–2435. doi: 10.1210/en.2011-1783

Bana, L., Minniti, S., Salvati, E., Sesana, S., Zambelli, V., Cagnotto, A., et al. (2014). Liposomes bi-functionalized with phosphatidic acid and an ApoE-derived peptide affect Abeta aggregation features and cross the blood-brain-barrier: implications for therapy of Alzheimer disease. *Nanomedicine* 10, 1583–1590. doi: 10.1016/j.nano.2013.12.001

Bao, Q., Hu, P., Xu, Y., Cheng, T., Wei, C., Pan, L., et al. (2018). Simultaneous blood–brain barrier crossing and protection for stroke treatment based on edaravone-loaded ceria nanoparticles. *ACS Nano* 12, 6794–6805. doi: 10.1021/acsnano.8b01994

Bazzoni, G., and Dejana, E. (2004). Endothelial cell-to-cell junctions: molecular organization and role in vascular homeostasis. *Physiol. Rev.* 84, 869–901. doi: 10.1152/physrev.00035.2003

Bell, R. D., Winkler, E. A., Singh, I., Sagare, A. P., Deane, R., Wu, Z., et al. (2012). Apolipoprotein E controls cerebrovascular integrity via cyclophilin A. *Nature* 485, 512–516. doi: 10.1038/nature11087

Bernstein, D. L., Zuluaga-Ramirez, V., Gajghate, S., Reichenbach, N. L., Polyak, B., Persidsky, Y., et al. (2019). miR-98 reduces endothelial dysfunction by protecting blood–brain barrier (BBB) and improves neurological outcomes in mouse ischemia/reperfusion stroke model. *J. Cereb. Blood Flow Metab.* 1–13. doi: 10.1177/0271678x19882264

Bijli, K. M., Minhajuddin, M., Fazal, F., O'Reilly, M. A., Platanias, L. C., and Rahman, A. (2007). c-Src interacts with and phosphorylates RelA/p65 to promote thrombin-induced ICAM-1 expression in endothelial cells. *Am. J. Physiol. Lung Cell. Mol. Physiol.* 292, L396–L404. doi: 10.1152/ajplung.00163.2006

Biron, K. E., Dickstein, D. L., Gopaul, R., and Jefferies, W. A. (2011). Amyloid triggers extensive cerebral angiogenesis causing blood brain barrier permeability and hypervascularity in Alzheimer's disease. *PLoS One* 6:e23789. doi: 10.1371/journal.pone.0023789

Bodmer, D., Vaughan, K. A., Zacharia, B. E., Hickman, Z. L., and Connolly, E. S. (2012). The molecular mechanisms that promote edema after intracerebral hemorrhage. *Transl. Stroke Res.* 3(Suppl. 1), 52–61. doi: 10.1007/s12975-012-0162-0

Calne, D. B., and Sandler, M. (1970). L-Dopa and Parkinsonism. *Nature* 226, 21–24. doi: 10.1038/226021a0

Candela, P., Gosselet, F., Saint-Pol, J., Sevin, E., Boucau, M. C., Boulanger, E., et al. (2010). Apical-to-basolateral transport of amyloid-β peptides through blood-brain barrier cells is mediated by the receptor for advanced glycation end-products and is restricted by P-glycoprotein. *J. Alzheimers Dis.* 22, 849–859. doi: 10.3233/jad-2010-100462

Carpanini, S. M., Torvell, M., and Morgan, B. P. (2019). Therapeutic inhibition of the complement system in diseases of the central nervous system. *Front. Immunol.* 10:362. doi: 10.3389/fimmu.2019.00362

Carrano, A., Hoozemans, J. J., van der Vies, S. M., Rozemuller, A. J., van Horssen, J., and de Vries, H. E. (2011). Amyloid Beta induces oxidative stress-mediated blood-brain barrier changes in capillary amyloid angiopathy. *Antioxid. Redox Signal.* 15, 1167–1178. doi: 10.1089/ars.2011.3895

Carvey, P. M., Hendey, B., and Monahan, A. J. (2009). The blood-brain barrier in neurodegenerative disease: a rhetorical perspective. *J. Neurochem.* 111, 291–314. doi: 10.1111/j.1471-4159.2009.06319.x

Casas, A. I., Kleikers, P. W., Geuss, E., Langhauser, F., Adler, T., Busch, D. H., et al. (2019). Calcium-dependent blood-brain barrier breakdown by NOX5 limits postreperfusion benefit in stroke. *J. Clin. Invest.* 129, 1772–1778. doi: 10.1172/jci124283ds1

Castro Dias, M., Coisne, C., Baden, P., Enzmann, G., Garrett, L., Becker, L., et al. (2019). Claudin-12 is not required for blood-brain barrier tight junction function. *Fluids Barriers CNS* 16:30. doi: 10.1186/s12987-019-0150-9

Chen, J., Sun, L., Ding, G. B., Chen, L., Jiang, L., Wang, J., et al. (2019). Oxygen-glucose deprivation/reoxygenation induces human brain microvascular endothelial cell hyperpermeability Via VE-cadherin internalization: roles of RhoA/ROCK2. *J. Mol. Neurosci.* 69, 49–59. doi: 10.1007/s12031-019-01326-8

Chen, W., Ju, X. Z., Lu, Y., Ding, X. W., Miao, C. H., and Chen, J. W. (2019). Propofol improved hypoxia-impaired integrity of blood-brain barrier via modulating the expression and phosphorylation of zonula occludens-1. *CNS Neurosci Ther* 25, 704–713. doi: 10.1111/cns.13101

Chen, Y. J., Wallace, B. K., Yuen, N., Jenkins, D. P., Wulff, H., and O'Donnell, M. E. (2015). Blood-brain barrier KCa3.1 channels: evidence for a role in brain Na uptake and edema in ischemic stroke. *Stroke* 46, 237–244. doi: 10.1161/STROKEAHA.114.007445

Cheng, Y., Xi, G., Jin, H., Keep, R. F., Feng, J., and Hua, Y. (2014). Thrombin-induced cerebral hemorrhage: role of protease-activated receptor-1. *Transl. Stroke Res.* 5, 472–475. doi: 10.1007/s12975-013-0288-8

Cheyuo, C., Aziz, M., and Wang, P. (2019). Neurogenesis in neurodegenerative diseases: role of MFG-E8. *Front. Neurosci.* 13:569. doi: 10.3389/fnins.2019.00569

Chow, B. W., and Gu, C. (2015). The molecular constituents of the blood-brain barrier. *Trends Neurosci.* 38, 598–608. doi: 10.1016/j.tins.2015.08.003

Chu, K., Jeong, S. W., Jung, K. H., Han, S. Y., Lee, S. T., Kim, M., et al. (2004). Celecoxib induces functional recovery after intracerebral hemorrhage with reduction of brain edema and perihematomal cell death. *J. Cereb. Blood Flow Metab.* 24, 926–933. doi: 10.1097/01.wcb.0000130866.25040.7d

Cirrito, J. R., Deane, R., Fagan, A. M., Spinner, M. L., Parsadanian, M., Finn, M. B., et al. (2005). P-glycoprotein deficiency at the blood-brain barrier increases amyloid-beta deposition in an Alzheimer disease mouse model. *J. Clin. Invest.* 115, 3285–3290. doi: 10.1172/JCI25247

Crichton, R. R., Dexter, D. T., and Ward, R. J. (2011). Brain iron metabolism and its perturbation in neurological diseases. *J. Neural Transm.* 118, 301–314. doi: 10.1007/s00702-010-0470-z

Cummins, P. M. (2011). Occludin: one Protein. Many Forms. *Mol. Cell. Biol.* 32, 242–250. doi: 10.1128/mcb.06029-11

Dabrowska, S., Andrzejewska, A., Lukomska, B., and Janowski, M. (2019). Neuroinflammation as a target for treatment of stroke using mesenchymal stem cells and extracellular vesicles. *J. Neuroinflammation* 16:178. doi: 10.1186/s12974-019-1571-8

Dal Magro, R., Simonelli, S., Cox, A., Formicola, B., Corti, R., Cassina, V., et al. (2019). The extent of human apolipoprotein A-I Lipidation strongly affects the beta-amyloid efflux across the blood-brain barrier *in vitro*. *Front. Neurosci.* 13:419. doi: 10.3389/fnins.2019.00419

Daneman, R. (2012). The blood-brain barrier in health and disease. *Ann. Neurol.* 72, 648–672. doi: 10.1002/ana.23648

Daneman, R., Agalliu, D., Zhou, L., Kuhnert, F., Kuo, C. J., and Barres, B. A. (2009). Correction for Daneman et al., Wnt/ -catenin signaling is required for CNS, but not non-CNS, angiogenesis. *Proc. Natl. Acad. Sci. U.S.A.* 106, 6422–6422. doi: 10.1073/pnas.0805165106

O'Donnell, M. E., Tran, L., Lam, T. I., Liu, X. B., and Anderson, S. E. (2004). Bumetanide inhibition of the blood-brain barrier Na-K-Cl cotransporter reduces edema formation in the rat middle cerebral artery occlusion model of stroke. *J. Cereb. Blood Flow Metab.* 24, 1046–1056. doi: 10.1097/01.Wcb.0000130867.32663.90

Daneman, R., Zhou, L., Agalliu, D., Cahoy, J. D., Kaushal, A., and Barres, B. A. (2010a). The mouse blood-brain barrier transcriptome: a new resource for understanding the development and function of brain endothelial cells. *PLoS One* 5:e13741. doi: 10.1371/journal.pone.0013741

Daneman, R., Zhou, L., Kebede, A. A., and Barres, B. A. (2010b). Pericytes are required for blood-brain barrier integrity during embryogenesis. *Nature* 468, 562–566. doi: 10.1038/nature09513

Florczak-Rzepka, M., Grond-Ginsbach, C., Montaner, J., and Steiner, T. (2012). Matrix metalloproteinases in human spontaneous intracerebral hemorrhage: an update. *Cerebrovasc. Dis.* 34, 249–262. doi: 10.1159/000341686

Davalos, D., Ryu, J. K., Merlini, M., Baeten, K. M., Le Moan, N., Petersen, M. A., et al. (2012). Fibrinogen-induced perivascular microglial clustering is required for the development of axonal damage in neuroinflammation. *Nat. Commun.* 3:1227. doi: 10.1038/ncomms2230

De Rosa, V., Galgani, M., Porcellini, A., Colamatteo, A., Santopaolo, M., Zuchegna, C., et al. (2015). Glycolysis controls the induction of human regulatory T cells by modulating the expression of FOXP3 exon 2 splicing variants. *Nat. Immunol.* 16, 1174–1184. doi: 10.1038/ni.3269

Deane, R., Du Yan, S., Submamaryan, R. K., LaRue, B., Jovanovic, S., Hogg, E., et al. (2003). RAGE mediates amyloid-beta peptide transport across the blood-brain barrier and accumulation in brain. *Nat. Med.* 9, 907–913. doi: 10.1038/nm890

Deane, R., Singh, I., Sagare, A. P., Bell, R. D., Ross, N. T., LaRue, B., et al. (2012). A multimodal RAGE-specific inhibitor reduces amyloid beta-mediated brain disorder in a mouse model of Alzheimer disease. *J. Clin. Invest.* 122, 1377–1392. doi: 10.1172/JCI58642

Desai, B. S., Monahan, A. J., Carvey, P. M., and Hendey, B. (2007). Blood–Brain Barrier Pathology in Alzheimer's and Parkinson's Disease: implications for Drug Therapy. *Cell Transplant.* 16, 285–299. doi: 10.3727/000000007783464731

Dirnagl, U., Iadecola, C., and Moskowitz, M. A. (1999). Pathobiology of ischaemic stroke: an integrated view. *Trends Neurosci.* 22, 391–397. doi: 10.1016/s0166-2236(99)01401-0

Edwards, D. N., Salmeron, K., Lukins, D. E., Trout, A. L., Fraser, J. F., and Bix, G. J. (2019). Integrin alpha5beta1 inhibition by ATN-161 reduces neuroinflammation and is neuroprotective in ischemic stroke. *J. Cereb. Blood Flow Metab.* 40, 1695–1708. doi: 10.1177/0271678X19880161

Ezan, P., Andre, P., Cisternino, S., Saubamea, B., Boulay, A. C., Doutremer, S., et al. (2012). Deletion of astroglial connexins weakens the blood-brain barrier. *J. Cereb. Blood Flow Metab.* 32, 1457–1467. doi: 10.1038/jcbfm.2012.45

Fan, X., Lo, E. H., and Wang, X. (2013). Effects of minocycline plus tissue plasminogen activator combination therapy after focal embolic stroke in type 1 diabetic rats. *Stroke* 44, 745–752. doi: 10.1161/STROKEAHA.111.000309

Farkas, E., De Jong, G. I., de Vos, R. A., Jansen Steur, E. N., and Luiten, P. G. (2000). Pathological features of cerebral cortical capillaries are doubled in Alzheimer's disease and Parkinson's disease. *Acta Neuropathol.* 100, 395–402. doi: 10.1007/s004010000195

Fox, R. J., Coffey, C. S., Conwit, R., Cudkowicz, M. E., Gleason, T., Goodman, A., et al. (2018). Phase 2 trial of ibudilast in progressive multiple sclerosis. *N. Engl. J. Med.* 379, 846–855. doi: 10.1056/NEJMoa1803583

Fu, Y., Liu, Q., Anrather, J., and Shi, F.-D. (2015). Immune interventions in stroke. *Nat. Rev. Neurol.* 11, 524–535. doi: 10.1038/nrneurol.2015.144

Fujita, H., Sugimoto, K., Inatomi, S., Maeda, T., Osanai, M., Uchiyama, Y., et al. (2008). Tight junction proteins claudin-2 and -12 are critical for vitamin D-dependent Ca2+ absorption between enterocytes. *Mol. Biol. Cell* 19, 1912–1921. doi: 10.1091/mbc.E07-09-0973

Furtado, D., Björnmalm, M., Ayton, S., Bush, A. I., Kempe, K., and Caruso, F. (2018). Overcoming the blood-brain barrier: the role of nanomaterials in treating neurological diseases. *Adv. Mater.* 30:e1801362. doi: 10.1002/adma.201801362

Galochkina, T., Ng Fuk Chong, M., Challali, L., Abbar, S., and Etchebest, C. (2019). New insights into GluT1 mechanics during glucose transfer. *Sci. Rep.* 9:998. doi: 10.1038/s41598-018-37367-z

Garrido-Urbani, S., Bradfield, P. F., and Imhof, B. A. (2014). Tight junction dynamics: the role of junctional adhesion molecules (JAMs). *Cell Tissue Res.* 355, 701–715. doi: 10.1007/s00441-014-1820-1

Gee, J. R., and Keller, J. N. (2005). Astrocytes: regulation of brain homeostasis via apolipoprotein E. *Int. J. Biochem. Cell Biol.* 37, 1145–1150. doi: 10.1016/j.biocel.2004.10.004

Gosselet, F. (2012). How ApoE regulates blood-brain barrier integrity. *Med. Sci.* 28, 920–923. doi: 10.1051/medsci/20122811006

Götz, M. E., Double, K., Gerlach, M., Youdim, M. B., and Riederer, P. (2004). The relevance of iron in the pathogenesis of Parkinson's disease. *Ann. N. Y. Acad. Sci.* 1012, 193–208. doi: 10.1196/annals.1306.017

Gray, M. T., and Woulfe, J. M. (2015). Striatal blood-brain barrier permeability in Parkinson's disease. *J. Cereb. Blood Flow Metab.* 35, 747–750. doi: 10.1038/jcbfm.2015.32

Gurnik, S., Devraj, K., Macas, J., Yamaji, M., Starke, J., Scholz, A., et al. (2016). Angiopoietin-2-induced blood-brain barrier compromise and increased stroke size are rescued by VE-PTP-dependent restoration of Tie2 signaling. *Acta Neuropathol.* 131, 753–773. doi: 10.1007/s00401-016-1551-3

Haarmann, A., Nowak, E., Deiß, A., van der Pol, S., Monoranu, C. M., Kooij, G., et al. (2015). Soluble VCAM-1 impairs human brain endothelial barrier integrity via integrin alpha-4-transduced outside-in signalling. *Acta Neuropathol.* 129, 639–652. doi: 10.1007/s00401-015-1417-0

Hall, C. N., Reynell, C., Gesslein, B., Hamilton, N. B., Mishra, A., Sutherland, B. A., et al. (2014). Capillary pericytes regulate cerebral blood flow in health and disease. *Nature* 508, 55–60. doi: 10.1038/nature13165

Halliday, M. R., Rege, S. V., Ma, Q., Zhao, Z., Miller, C. A., Winkler, E. A., et al. (2016). Accelerated pericyte degeneration and blood-brain barrier breakdown in apolipoprotein E4 carriers with Alzheimer's disease. *J. Cereb. Blood Flow Metab.* 36, 216–227. doi: 10.1038/jcbfm.2015.44

Hardy, J., and Selkoe, D. J. (2002). The amyloid hypothesis of Alzheimer's disease: progress and problems on the road to therapeutics. *Science* 297, 353–356. doi: 10.1126/science.1072994

Haseloff, R. F., Dithmer, S., Winkler, L., Wolburg, H., and Blasig, I. E. (2015). Transmembrane proteins of the tight junctions at the blood–brain barrier: Structural and functional aspects. *Semin. Cell Dev. Biol.* 38, 16–25. doi: 10.1016/j.semcdb.2014.11.004

Hata, R., Maeda, K., Hermann, D., Mies, G., and Hossmann, K. A. (2000). Evolution of brain infarction after transient focal cerebral ischemia in mice. *J. Cereb. Blood Flow Metab.* 20, 937–946. doi: 10.1097/00004647-200006000-00006

Hemmer, B., Archelos, J. J., and Hartung, H. P. (2002). New concepts in the immunopathogenesis of multiple sclerosis. *Nat. Rev. Neurosci.* 3, 291–301. doi: 10.1038/nrn784

Hendriks, J. J., Teunissen, C. E., de Vries, H. E., and Dijkstra, C. D. (2005). Macrophages and neurodegeneration. *Brain Res. Brain Res. Rev.* 48, 185–195. doi: 10.1016/j.brainresrev.2004.12.008

Heo, J. H., Han, S. W., and Lee, S. K. (2005). Free radicals as triggers of brain edema formation after stroke. *Free Radic. Biol. Med.* 39, 51–70. doi: 10.1016/j.freeradbiomed.2005.03.035

Hernández-Pedro, N. Y., Espinosa-Ramirez, G., de la Cruz, V. P., Pineda, B., and Sotelo, J. (2013). Initial immunopathogenesis of multiple sclerosis: innate immune response. *Clin. Dev. Immunol.* 2013:413465. doi: 10.1155/2013/413465

Hollingworth, P., Harold, D., Sims, R., Gerrish, A., Lambert, J. C., Carrasquillo, M. M., et al. (2011). Common variants at ABCA7, MS4A6A/MS4A4E, EPHA1, CD33 and CD2AP are associated with Alzheimer's disease. *Nat. Genet.* 43, 429–435. doi: 10.1038/ng.803

Huang, L., Deng, M., He, Y., Lu, S., Ma, R., and Fang, Y. (2016). β-asarone and levodopa co-administration increase striatal dopamine level in 6-hydroxydopamine induced rats by modulating P-glycoprotein and tight junction proteins at the blood-brain barrier and promoting levodopa into the brain. *Clin. Exp. Pharmacol. Physiol.* 43, 634–643. doi: 10.1111/1440-1681.12570

Huang, L., Li, B., Li, X., Liu, G., Liu, R., Guo, J., et al. (2019). Significance and mechanisms of P-glycoprotein in central nervous system diseases. *Curr. Drug Targets* 20, 1141–1155.doi: 10.2174/1389450120666190308144448

Huber, J. D., Egleton, R. D., and Davis, T. P. (2001). Molecular physiology and pathophysiology of tight junctions in the blood-brain barrier. *Trends Neurosci.* 24, 719–725. doi: 10.1016/s0166-2236(00)02004-x

Ifergan, I., Kebir, H., Alvarez, J. I., Marceau, G., Bernard, M., Bourbonnière, L., et al. (2011). Central nervous system recruitment of effector memory CD8+ T lymphocytes during neuroinflammation is dependent on 4 integrin. *Brain* 134, 3560–3577. doi: 10.1093/brain/awr268

Ikenouchi, J., Furuse, M., Furuse, K., Sasaki, H., Tsukita, S., and Tsukita, S. (2005). Tricellulin constitutes a novel barrier at tricellular contacts of epithelial cells. *J. Cell Biol.* 171, 939–945. doi: 10.1083/jcb.200510043

Imura, T., Tane, K., Toyoda, N., and Fushiki, S. (2008). Endothelial cell-derived bone morphogenetic proteins regulate glial differentiation of cortical progenitors. *Eur. J. Neurosci.* 27, 1596–1606. doi: 10.1111/j.1460-9568.2008.06134.x

Ishiguro, M., Mishiro, K., Fujiwara, Y., Chen, H., Izuta, H., Tsuruma, K., et al. (2010). Phosphodiesterase-III inhibitor prevents hemorrhagic transformation induced by focal cerebral ischemia in mice treated with tPA. *PLoS One* 5:e15178. doi: 10.1371/journal.pone.0015178

Ishii, M., and Iadecola, C. (2020). Risk factor for Alzheimer's disease breaks the blood–brain barrier. *Nature* 581, 31–32. doi: 10.1038/d41586-020-01152-8

Jaeger, L. B., Dohgu, S., Hwang, M. C., Farr, S. A., Murphy, M. P., Fleegal-DeMotta, M. A., et al. (2009). Testing the neurovascular hypothesis of Alzheimer's disease: LRP-1 antisense reduces blood-brain barrier clearance, increases brain levels of amyloid-beta protein, and impairs cognition. *J. Alzheimers Dis.* 17, 553–570. doi: 10.3233/JAD-2009-1074

Janardhan, V., and Qureshi, A. I. (2004). Mechanisms of ischemic brain injury. *Curr. Cardiol. Rep.* 6, 117–123. doi: 10.1007/s11886-004-0009-8

Janelidze, S., Lindqvist, D., Francardo, V., Hall, S., Zetterberg, H., Blennow, K., et al. (2015). Increased CSF biomarkers of angiogenesis in Parkinson disease. *Neurology* 85, 1834–1842. doi: 10.1212/WNL.0000000000002151

Jevtic, S., Sengar, A. S., Salter, M. W., and McLaurin, J. (2017). The role of the immune system in Alzheimer disease: etiology and treatment. *Ageing Res. Rev.* 40, 84–94. doi: 10.1016/j.arr.2017.08.005

Jiao, H., Wang, Z., Liu, Y., Wang, P., and Xue, Y. (2011). Specific role of tight junction proteins claudin-5, occludin, and ZO-1 of the blood-brain barrier in a focal cerebral ischemic insult. *J. Mol. Neurosci.* 44, 130–139. doi: 10.1007/s12031-011-9496-4

Kappos, L., Li, D. K., Stüve, O., Hartung, H. P., Freedman, M. S., Hemmer, B., et al. (2016). Safety and Efficacy of Siponimod (BAF312) in patients with relapsing-remitting multiple sclerosis. *JAMA Neurol.* 73, 1089–1098. doi: 10.1001/jamaneurol.2016.1451

Khatri, R., McKinney, A. M., Swenson, B., and Janardhan, V. (2012). Blood-brain barrier, reperfusion injury, and hemorrhagic transformation in acute ischemic stroke. *Neurology* 79(13 Suppl. 1), S52–S57. doi: 10.1212/WNL.0b013e3182697e70

Kim, W. S., Weickert, C. S., and Garner, B. (2008). Role of ATP-binding cassette transporters in brain lipid transport and neurological disease. *J. Neurochem.* 104, 1145–1166. doi: 10.1111/j.1471-4159.2007.05099.x

Kitazume, S., Tachida, Y., Kato, M., Yamaguchi, Y., Honda, T., Hashimoto, Y., et al. (2010). Brain endothelial cells produce amyloid {beta} from amyloid precursor protein 770 and preferentially secrete the O-glycosylated form. *J. Biol. Chem.* 285, 40097–40103. doi: 10.1074/jbc.M110.144626

Koch, H., and Weber, Y. G. (2019). The glucose transporter type 1 (Glut1) syndromes. *Epilepsy Behav.* 91, 90–93. doi: 10.1016/j.yebeh.2018.06.010

Kooij, G., Kroon, J., Paul, D., Reijerkerk, A., Geerts, D., van der Pol, S. M., et al. (2014). P-glycoprotein regulates trafficking of CD8+ T cells to the brain parenchyma. *Acta Neuropathol.* 127, 699–711. doi: 10.1007/s00401-014-1244-8

Kook, S. Y., Hong, H. S., Moon, M., Ha, C. M., Chang, S., and Mook-Jung, I. (2012). Aβ1-42-RAGE interaction disrupts tight junctions of the blood-brain barrier via Ca^2+-calcineurin signaling. *J. Neurosci.* 32, 8845–8854. doi: 10.1523/jneurosci.6102-11.2012

Kortekaas, R., Leenders, K. L., van Oostrom, J. C., Vaalburg, W., Bart, J., Willemsen, A. T., et al. (2005). Blood-brain barrier dysfunction in parkinsonian midbrain in vivo. *Ann. Neurol.* 57, 176–179. doi: 10.1002/ana.20369

Kuan, W. L., Bennett, N., He, X., Skepper, J. N., Martynyuk, N., Wijeyekoon, R., et al. (2016). α-Synuclein pre-formed fibrils impair tight junction protein expression without affecting cerebral endothelial cell function. *Exp. Neurol.* 285, 72–81. doi: 10.1016/j.expneurol.2016.09.003

Kuntz, M., Candela, P., Saint-Pol, J., Lamartiniere, Y., Boucau, M. C., Sevin, E., et al. (2015). Bexarotene promotes cholesterol efflux and restricts apical-to-basolateral transport of amyloid-beta peptides in an *in vitro* model of the human blood-brain barrier. *J. Alzheimers Dis.* 48, 849–862. doi: 10.3233/JAD-150469

Lamartiniere, Y., Boucau, M. C., Dehouck, L., Krohn, M., Pahnke, J., Candela, P., et al. (2018). ABCA7 downregulation modifies cellular cholesterol homeostasis and decreases amyloid-beta peptide efflux in an *in vitro* model of the blood-brain barrier. *J. Alzheimers Dis.* 64, 1195–1211. doi: 10.3233/JAD-170883

Lamb, Y. N. (2020). Ozanimod: first approval. *Drugs*. 80, 841–848. doi: 10.1007/s40265-020-01319-7

Lang, A. E., and Lozano, A. M. (1998). Parkinson's disease. First of two parts. *N. Engl. J. Med.* 339, 1044–1053. doi: 10.1056/NEJM199810083391506

Langen, U. H., Ayloo, S., and Gu, C. (2019). Development and cell biology of the blood-brain barrier. *Annu. Rev. Cell Dev. Biol.* 35, 12.11–12.23. doi: 10.1146/annurev-cellbio-100617062608

Lee, S. H., Park, H. K., Ryu, W. S., Lee, J. S., Bae, H. J., Han, M. K., et al. (2013). Effects of celecoxib on hematoma and edema volumes in primary intracerebral hemorrhage: a multicenter randomized controlled trial. *Eur. J. Neurol.* 20, 1161–1169. doi: 10.1111/ene.12140

Li, M., Li, Z., Ren, H., Jin, W. N., Wood, K., Liu, Q., et al. (2016). Colony stimulating factor 1 receptor inhibition eliminates microglia and attenuates brain injury after intracerebral hemorrhage. *J. Cereb. Blood Flow Metab.* 37, 2383–2395. doi: 10.1177/0271678x16666551

Li, P., Wang, L., Zhou, Y., Gan, Y., Zhu, W., Xia, Y., et al. (2017). C-C chemokine receptor type 5 (CCR5)-mediated docking of transferred tregs protects against early blood-brain barrier disruption after stroke. *J. Am. Heart Assoc.* 6:e006387. doi: 10.1161/JAHA.117.006387

Li, W., Chen, Z., Chin, I., Chen, Z., and Dai, H. (2018). The Role of VE-cadherin in blood-brain barrier integrity under central nervous system pathological conditions. *Curr. Neuropharmacol.* 16, 1375–1384. doi: 10.2174/1570159X16666180222164809

Li, Y. J., Chang, G. Q., Liu, Y., Gong, Y., Yang, C., Wood, K., et al. (2015). Fingolimod alters inflammatory mediators and vascular permeability in intracerebral hemorrhage. *Neurosci. Bull.* 31, 755–762. doi: 10.1007/s12264-015-1532-2

Liang, J., Qi, Z., Liu, W., Wang, P., Shi, W., Dong, W., et al. (2015). Normobaric hyperoxia slows blood-brain barrier damage and expands the therapeutic time window for tissue-type plasminogen activator treatment in cerebral ischemia. *Stroke* 46, 1344–1351. doi: 10.1161/STROKEAHA.114.008599

Liebner, S., Dijkhuizen, R. M., Reiss, Y., Plate, K. H., Agalliu, D., and Constantin, G. (2018). Functional morphology of the blood-brain barrier in health and disease. *Acta Neuropathol.* 135, 311–336. doi: 10.1007/s00401-018-1815-1

Liu, J., Jin, X., Liu, K. J., and Liu, W. (2012). Matrix metalloproteinase-2-mediated occludin degradation and caveolin-1-mediated claudin-5 redistribution contribute to blood-brain barrier damage in early ischemic stroke stage. *J. Neurosci.* 32, 3044–3057. doi: 10.1523/JNEUROSCI.6409-11.2012

Liu, Z., and Chopp, M. (2016). Astrocytes, therapeutic targets for neuroprotection and neurorestoration in ischemic stroke. *Prog. Neurobiol.* 144, 103–120. doi: 10.1016/j.pneurobio.2015.09.008

Losy, J. (2013). Is MS an inflammatory or primary degenerative disease? *J. Neural Transm.* 120, 1459–1462. doi: 10.1007/s00702-013-1079-9

Ma, Q., Zhao, Z., Sagare, A. P., Wu, Y., Wang, M., Owens, N. C., et al. (2018). Blood-brain barrier-associated pericytes internalize and clear aggregated amyloid-beta42 by LRP1-dependent apolipoprotein E isoform-specific mechanism. *Mol. Neurodegener.* 13:57. doi: 10.1186/s13024-018-0286-0

Macrez, R., Stys, P. K., Vivien, D., Lipton, S. A., and Docagne, F. (2016). Mechanisms of glutamate toxicity in multiple sclerosis: biomarker and therapeutic opportunities. *Lancet Neurol.* 15, 1089–1102. doi: 10.1016/s1474-4422(16)30165-x

Mayer, S. A., Sacco, R. L., Shi, T., and Mohr, J. P. (1994). Neurologic deterioration in noncomatose patients with supratentorial intracerebral hemorrhage. *Neurology* 44, 1379–1384. doi: 10.1212/wnl.44.8.1379

McColl, B. W., Rothwell, N. J., and Allan, S. M. (2008). systemic inflammation alters the kinetics of cerebrovascular tight junction disruption after experimental stroke in mice. *J. Neurosci.* 28, 9451–9462. doi: 10.1523/jneurosci.2674-08.2008

Metz, L. M., Li, D. K. B., Traboulsee, A. L., Duquette, P., Eliasziw, M., Cerchiaro, G., et al. (2017). Trial of minocycline in a clinically isolated syndrome of multiple sclerosis. *N. Engl. J. Med.* 376, 2122–2133. doi: 10.1056/NEJMoa1608889

Miller, D. H., Grossman, R. I., Reingold, S. C., and McFarland, H. F. (1998). The role of magnetic resonance techniques in understanding and managing multiple sclerosis. *Brain* 121, 3–24. doi: 10.1093/brain/121.1.3

Miller, D. S. (2015). Regulation of ABC transporters blood-brain barrier: the good, the bad, and the ugly. *Adv. Cancer Res.* 125, 43–70. doi: 10.1016/bs.acr.2014.10.002

Montagne, A., Barnes, S. R., Sweeney, M. D., Halliday, M. R., Sagare, A. P., Zhao, Z., et al. (2015). Blood-brain barrier breakdown in the aging human hippocampus. *Neuron* 85, 296–302. doi: 10.1016/j.neuron.2014.12.032

Montagne, A., Nation, D. A., Sagare, A. P., Barisano, G., Sweeney, M. D., Chakhoyan, A., et al. (2020). APOE4 leads to blood–brain barrier dysfunction predicting cognitive decline. *Nature*. 581, 71–76. doi: 10.1038/s41586-020-2247-3

Montagne, A., Zhao, Z., and Zlokovic, B. V. (2017). Alzheimer's disease: A matter of blood-brain barrier dysfunction? *J. Exp. Med.* 214, 3151–3169. doi: 10.1084/jem.20171406

Morita, K., Sasaki, H., Furuse, M., and Tsukita, S. (1999). Endothelial claudin: claudin-5/TMVCF constitutes tight junction strands in endothelial cells. *J. Cell Biol.* 147, 185–194. doi: 10.1083/jcb.147.1.185

Nakamura, K., Ikeuchi, T., Nara, K., Rhodes, C. S., Zhang, P., Chiba, Y., et al. (2019). Perlecan regulates pericyte dynamics in the maintenance and repair of the blood-brain barrier. *J. Cell Biol.* 218, 3506–3525. doi: 10.1083/jcb.201807178

Nelson, A. R., Sweeney, M. D., Sagare, A. P., and Zlokovic, B. V. (2016). Neurovascular dysfunction and neurodegeneration in dementia and Alzheimer's disease. *Biochim. Biophys. Acta* 1862, 887–900. doi: 10.1016/j.bbadis.2015.12.016

Niu, J., Tsai, H. H., Hoi, K. K., Huang, N., Yu, G., Kim, K., et al. (2019). Aberrant oligodendroglial-vascular interactions disrupt the blood-brain barrier, triggering CNS inflammation. *Nat. Neurosci.* 22, 709–718. doi: 10.1038/s41593-019-0369-4

Obermeier, B., Daneman, R., and Ransohoff, R. M. (2013). Development, maintenance and disruption of the blood-brain barrier. *Nat. Med.* 19, 1584–1596. doi: 10.1038/nm.3407

Ortiz, G. G., Pacheco-Moisés, F. P., Macías-Islas, M. Á., Flores-Alvarado, L. J., and Mireles-Ramírez, M. A. (2014). Role of the blood-brain barrier in multiple sclerosis. *Arch. Med. Res.* 45, 687–697. doi: 10.1016/j.arcmed.2014.11.013

Pan, Q., He, C., Liu, H., Liao, X., Dai, B., Chen, Y., et al. (2016). Microvascular endothelial cells-derived microvesicles imply in ischemic stroke by modulating astrocyte and blood brain barrier function and cerebral blood flow. *Mol. Brain* 9:63. doi: 10.1186/s13041-016-0243-1

Pan, Y., and Nicolazzo, J. A. (2018). Impact of aging, Alzheimer's disease and Parkinson's disease on the blood-brain barrier transport of therapeutics. *Adv. Drug Deliv. Rev.* 135, 62–74. doi: 10.1016/j.addr.2018.04.009

Patching, S. G. (2017). Glucose transporters at the blood-brain barrier: function, regulation and gateways for drug delivery. *Mol. Neurobiol.* 54, 1046–1077. doi: 10.1007/s12035-015-9672-6

Persidsky, Y., Ramirez, S. H., Haorah, J., and Kanmogne, G. D. (2006). Blood–brain barrier: structural components and function under physiologic and pathologic conditions. *J. Neuroimmune Pharmacol.* 1, 223–236. doi: 10.1007/s11481-006-9025-3

Pfeiffer, F., Schafer, J., Lyck, R., Makrides, V., Brunner, S., Schaeren-Wiemers, N., et al. (2011). Claudin-1 induced sealing of blood-brain barrier tight junctions ameliorates chronic experimental autoimmune encephalomyelitis. *Acta Neuropathol.* 122, 601–614. doi: 10.1007/s00401-011-0883-2

Polakis, P. (2008). Formation of the blood-brain barrier: Wnt signaling seals the deal. *J. Cell Biol.* 183, 371–373. doi: 10.1083/jcb.200810040

Potente, M., Gerhardt, H., and Carmeliet, P. (2011). Basic and therapeutic aspects of angiogenesis. *Cell* 146, 873–887. doi: 10.1016/j.cell.2011.08.039

Powers, W. J., Derdeyn, C. P., Biller, J., Coffey, C. S., Hoh, B. L., Jauch, E. C., et al. (2015). 2015 American Heart Association/American Stroke Association Focused Update of the 2013 Guidelines for the Early Management of Patients With Acute Ischemic Stroke Regarding Endovascular Treatment. *Stroke* 46, 3020–3035. doi: 10.1161/str.0000000000000074

Prezioso, C., Zingaropoli, M. A., Iannetta, M., Rodio, D. M., Altieri, M., Conte, A., et al. (2020). Which is the best PML risk stratification strategy in natalizumab-treated patients affected by multiple sclerosis? *Mult. Scler. Relat. Disord.* 41:102008. doi: 10.1016/j.msard.2020.102008

Procaccini, C., Pucino, V., De Rosa, V., Marone, G., and Matarese, G. (2014). Neuro-endocrine networks controlling immune system in health and disease. *Front. Immunol.* 5:143. doi: 10.3389/fimmu.2014.00143

Qian, Z. M., and Ke, Y. (2019). Hepcidin and its therapeutic potential in neurodegenerative disorders. *Med. Res. Rev.* 40, 1–21. doi: 10.1002/med.21631

Qureshi, A. I., Mendelow, A. D., and Hanley, D. F. (2009). Intracerebral haemorrhage. *Lancet* 373, 1632–1644. doi: 10.1016/S0140-6736(09)60371-8

Reale, M., Iarlori, C., Thomas, A., Gambi, D., Perfetti, B., Di Nicola, M., et al. (2009). Peripheral cytokines profile in Parkinson's disease. *Brain Behav. Immun.* 23, 55–63. doi: 10.1016/j.bbi.2008.07.003

Ricci, G., Volpi, L., Pasquali, L., Petrozzi, L., and Siciliano, G. (2009). Astrocyte-neuron interactions in neurological disorders. *J. Biol. Phys.* 35, 317–336. doi: 10.1007/s10867-009-9157-9

Rivera, S., García-González, L., Khrestchatisky, M., and Baranger, K. (2019). Metalloproteinases and their tissue inhibitors in Alzheimer's disease and other neurodegenerative disorders. *Cell. Mol. Life Sci.* 76, 3167–3191. doi: 10.1007/s00018-019-03178-2

Rolland, W. B., Lekic, T., Krafft, P. R., Hasegawa, Y., Altay, O., Hartman, R., et al. (2013). Fingolimod reduces cerebral lymphocyte infiltration in experimental models of rodent intracerebral hemorrhage. *Exp. Neurol.* 241, 45–55. doi: 10.1016/j.expneurol.2012.12.009

Roy, A., and Pahan, K. (2011). Prospects of statins in Parkinson disease. *Neuroscientist* 17, 244–255. doi: 10.1177/1073858410385006

Sagare, A. P., Bell, R. D., Zhao, Z., Ma, Q., Winkler, E. A., Ramanathan, A., et al. (2013). Pericyte loss influences Alzheimer-like neurodegeneration in mice. *Nat. Commun.* 4:2932. doi: 10.1038/ncomms3932

Saint-Pol, J., Candela, P., Boucau, M. C., Fenart, L., and Gosselet, F. (2013). Oxysterols decrease apical-to-basolateral transport of Ass peptides via an ABCB1-mediated process in an *in vitro* Blood-brain barrier model constituted of bovine brain capillary endothelial cells. *Brain Res.* 1517, 1–15. doi: 10.1016/j.brainres.2013.04.008

Saint-Pol, J., Gosselet, F., Duban-Deweer, S., Pottiez, G., and Karamanos, Y. (2020). Targeting and crossing the blood-brain barrier with extracellular vesicles. *Cells* 9:E851. doi: 10.3390/cells9040851

Saitou, M., Ando-Akatsuka, Y., Itoh, M., Furuse, M., Inazawa, J., Fujimoto, K., et al. (1997). Mammalian occludin in epithelial cells: its expression and subcellular distribution. *Eur. J. Cell Biol.* 73, 222–231.

Sandoval, K. E., and Witt, K. A. (2008). Blood-brain barrier tight junction permeability and ischemic stroke. *Neurobiol. Dis.* 32, 200–219. doi: 10.1016/j.nbd.2008.08.005

Sarkar, S., Chigurupati, S., Raymick, J., Mann, D., Bowyer, J. F., Schmitt, T., et al. (2014). Neuroprotective effect of the chemical chaperone, trehalose in a chronic MPTP-induced Parkinson's disease mouse model. *Neurotoxicology* 44, 250–262. doi: 10.1016/j.neuro.2014.07.006

Sayeed, I., Turan, N., Stein, D. G., and Wali, B. (2019). Vitamin D deficiency increases blood-brain barrier dysfunction after ischemic stroke in male rats. *Exp. Neurol.* 312, 63–71. doi: 10.1016/j.expneurol.2018.11.005

Schinkel, A. H., Smit, J. J., van Tellingen, O., Beijnen, J. H., Wagenaar, E., van Deemter, L., et al. (1994). Disruption of the mouse mdr1a P-glycoprotein gene leads to a deficiency in the blood-brain barrier and to increased sensitivity to drugs. *Cell* 77, 491–502. doi: 10.1016/0092-8674(94)90212-7

Schottlaender, L. V., Abeti, R., Jaunmuktane, Z., Macmillan, C., Chelban, V., O'Callaghan, B., et al. (2020). Bi-allelic JAM2 variants lead to early-onset recessive primary familial brain calcification. *Am. J. Hum. Genet.* 106, 412–421. doi: 10.1016/j.ajhg.2020.02.007

Schweinzer, C., Kober, A., Lang, I., Etschmaier, K., Scholler, M., Kresse, A., et al. (2011). Processing of endogenous AβPP in blood-brain barrier endothelial cells is modulated by liver-X receptor agonists and altered cellular cholesterol homeostasis. *J. Alzheimers Dis.* 27, 341–360. doi: 10.3233/jad-2011-110854

Sheikh, M. H., Henson, S. M., Loiola, R. A., Mercurio, S., Colamatteo, A., Maniscalco, G. T., et al. (2020). Immuno-metabolic impact of the multiple sclerosis patients' sera on endothelial cells of the blood-brain barrier. *J. Neuroinflammation* 17:153. doi: 10.1186/s12974-020-01810-8

Shi, K., Tian, D., Li, Z., Ducruet, A. F., Lawton, M. T., and Shi, F. D. (2019). Global brain inflammation in stroke. *Lancet Neurol.* 18, 1058–1066. doi: 10.1016/s1474-4422(19)30078-x

Shubbar, M. H., and Penny, J. I. (2020). Therapeutic drugs modulate ATP-Binding cassette transporter-mediated transport of amyloid beta(1–42) in brain microvascular endothelial cells. *Eur. J. Pharmacol.* 874:173009. doi: 10.1016/j.ejphar.2020.173009

Siddiqui, F. M., Langefeld, C. D., Moomaw, C. J., Comeau, M. E., Sekar, P., Rosand, J., et al. (2017). Use of statins and outcomes in intracerebral hemorrhage patients. *Stroke* 48, 2098–2104. doi: 10.1161/STROKEAHA.117.017358

Sifat, A. E., Vaidya, B., and Abbruscato, T. J. (2017). Blood-brain barrier protection as a therapeutic strategy for acute ischemic stroke. *AAPS J.* 19, 957–972. doi: 10.1208/s12248-017-0091-7

Simard, J. M., Kahle, K. T., and Gerzanich, V. (2010). Molecular mechanisms of microvascular failure in central nervous system injury—synergistic roles of NKCC1 and SUR1/TRPM4. *J. Neurosurg.* 113, 622–629. doi: 10.3171/2009.11.jns081052

Singh, S., Houng, A. K., and Reed, G. L. (2018). Matrix metalloproteinase-9 mediates the deleterious effects of alpha2-antiplasmin on blood-brain barrier breakdown and ischemic brain injury in experimental stroke. *Neuroscience* 376, 40–47. doi: 10.1016/j.neuroscience.2017.12.021

Sivandzade, F., Bhalerao, A., and Cucullo, L. (2019). Cerebrovascular and neurological disorders: protective role of NRF2. *Int. J. Mol. Sci.* 20:3433. doi: 10.3390/ijms20143433

Sladojevic, N., Stamatovic, S. M., Johnson, A. M., Choi, J., Hu, A., Dithmer, S., et al. (2019). Claudin-1-dependent destabilization of the blood–brain barrier in chronic stroke. *J. Neurosci.* 39, 743–757. doi: 10.1523/jneurosci.1432-18.2018

Sladojevic, N., Stamatovic, S. M., Keep, R. F., Grailer, J. J., Sarma, J. V., Ward, P. A., et al. (2014). Inhibition of junctional adhesion molecule-A/LFA interaction attenuates leukocyte trafficking and inflammation in brain ischemia/reperfusion injury. *Neurobiol. Dis.* 67, 57–70. doi: 10.1016/j.nbd.2014.03.010

Smeyne, M., and Smeyne, R. J. (2013). Glutathione metabolism and Parkinson's disease. *Free Radic. Biol. Med.* 62, 13–25. doi: 10.1016/j.freeradbiomed.2013.05.001

Sohet, F., Lin, C., Munji, R. N., Lee, S. Y., Ruderisch, N., Soung, A., et al. (2015). LSR/angulin-1 is a tricellular tight junction protein involved in blood-brain barrier formation. *J. Cell Biol.* 208, 703–711. doi: 10.1083/jcb.201410131

Spencer, J. I., Bell, J. S., and DeLuca, G. C. (2018). Vascular pathology in multiple sclerosis: reframing pathogenesis around the blood-brain barrier. *J. Neurol. Neurosurg. Psychiatry* 89, 42–52. doi: 10.1136/jnnp-2017-316011

Srinivasan, V., Braidy, N., Xu, Y. H., Xie, P., Kancherla, K., Chandramohan, S., et al. (2017). Association of genetic polymorphisms of claudin-1 with small vessel vascular dementia. *Clin. Exp. Pharmacol. Physiol.* 44, 623–630. doi: 10.1111/1440-1681.12747

Stamatovic, S. M., Sladojevic, N., Keep, R. F., and Andjelkovic, A. V. (2012). Relocalization of junctional adhesion molecule a during inflammatory stimulation of brain endothelial cells. *Mol. Cell Biol.* 32, 3414–3427. doi: 10.1128/MCB.06678-11

Stenman, J. M., Rajagopal, J., Carroll, T. J., Ishibashi, M., McMahon, J., and McMahon, A. P. (2008). Canonical Wnt signaling regulates organ-specific assembly and differentiation of CNS vasculature. *Science* 322, 1247–1250. doi: 10.1126/science.1164594

Stessman, L., and Peeples, E. S. (2018). Vitamin D and its role in neonatal hypoxic-ischemic brain injury. *Neonatology* 113, 305–312. doi: 10.1159/000486819

Storck, S. E., Hartz, A. M. S., Bernard, J., Wolf, A., Kachlmeier, A., Mahringer, A., et al. (2018). The concerted amyloid-beta clearance of LRP1 and ABCB1/P-gp across the blood-brain barrier is linked by PICALM. *Brain Behav. Immun.* 73, 21–33. doi: 10.1016/j.bbi.2018.07.017

Sweeney, M. D., Ayyadurai, S., and Zlokovic, B. V. (2016). Pericytes of the neurovascular unit: key functions and signaling pathways. *Nat. Neurosci.* 19, 771–783. doi: 10.1038/nn.4288

Sweeney, M. D., Montagne, A., Sagare, A. P., Nation, D. A., Schneider, L. S., Chui, H. C., et al. (2019a). Vascular dysfunction-The disregarded partner of Alzheimer's disease. *Alzheimers Dement.* 15, 158–167. doi: 10.1016/j.jalz.2018.07.222

Sweeney, M. D., Zhao, Z., Montagne, A., Nelson, A. R., and Zlokovic, B. V. (2019b). Blood-brain barrier: from physiology to disease and back. *Physiol. Rev.* 99, 21–78. doi: 10.1152/physrev.00050.2017

Sweeney, M. D., Sagare, A. P., and Zlokovic, B. V. (2018). Blood-brain barrier breakdown in Alzheimer disease and other neurodegenerative disorders. *Nat. Rev. Neurol.* 14, 133–150. doi: 10.1038/nrneurol.2017.188

Tachikawa, M., Murakami, K., Akaogi, R., Akanuma, S.-I., Terasaki, T., and Hosoya, K.-I. (2020). Polarized hemichannel opening of pannexin 1/connexin 43 contributes to dysregulation of transport function in blood-brain barrier endothelial cells. *Neurochem. Int.* 132:104600. doi: 10.1016/j.neuint.2019.104600

Taylor, R. A., Chang, C. F., Goods, B. A., Hammond, M. D., Mac Grory, B., Ai, Y., et al. (2017). TGF-beta1 modulates microglial phenotype and promotes recovery after intracerebral hemorrhage. *J. Clin. Invest.* 127, 280–292. doi: 10.1172/JCI88647

Tian, Y., Chang, J. C., Fan, E. Y., Flajolet, M., and Greengard, P. (2013). Adaptor complex AP2/PICALM, through interaction with LC3, targets Alzheimer's APP-CTF for terminal degradation via autophagy. *Proc. Natl. Acad. Sci. U.S.A.* 110, 17071–17076. doi: 10.1073/pnas.1315110110

Tietz, S., and Engelhardt, B. (2015). Brain barriers: crosstalk between complex tight junctions and adherens junctions. *J. Cell Biol.* 209, 493–506. doi: 10.1083/jcb.201412147

Torres-Ortega, P. V., Saludas, L., Hanafy, A. S., Garbayo, E., and Blanco-Prieto, M. J. (2019). Micro- and nanotechnology approaches to improve Parkinson's disease therapy. *J. Control. Release* 295, 201–213. doi: 10.1016/j.jconrel.2018.12.036

Tsukita, S., Furuse, M., Hashimoto, N., Sasaki, H., Seo, Y., Gotoh, S., et al. (2003). Size-selective loosening of the blood-brain barrier in claudin-5–deficient mice. *J. Cell Biol.* 161, 653–660. doi: 10.1083/jcb.200302070

Urday, S., Kimberly, W. T., Beslow, L. A., Vortmeyer, A. O., Selim, M. H., Rosand, J., et al. (2015). Targeting secondary injury in intracerebral haemorrhage—perihaematomal oedema. *Nat. Rev. Neurol.* 11, 111–122. doi: 10.1038/nrneurol.2014.264

Van der Goes, A., Wouters, D., Van Der Pol, S. M., Huizinga, R., Ronken, E., Adamson, P., et al. (2001). Reactive oxygen species enhance the migration of monocytes across the blood-brain barrier *in vitro*. *FASEB J.* 15, 1852–1854. doi: 10.1096/fj.00-0881fje

van Doorn, R., Nijland, P. G., Dekker, N., Witte, M. E., Lopes-Pinheiro, M. A., van het Hof, B., et al. (2012). Fingolimod attenuates ceramide-induced blood-brain barrier dysfunction in multiple sclerosis by targeting reactive astrocytes. *Acta Neuropathol.* 124, 397–410. doi: 10.1007/s00401-012-1014-4

Van Skike, C. E., Jahrling, J. B., Olson, A. B., Sayre, N. L., Hussong, S. A., Ungvari, Z., et al. (2018). Inhibition of mTOR protects the blood-brain barrier in models of Alzheimer's disease and vascular cognitive impairment. *Am. J. Physiol. Heart Circ. Physiol.* 314, H693–H703. doi: 10.1152/ajpheart.00570.2017

Vautier, S., Milane, A., Fernandez, C., Chacun, H., Lacomblez, L., and Farinotti, R. (2009a). Role of two efflux proteins, ABCB1 and ABCG2 in blood-brain barrier transport of bromocriptine in a murine model of MPTP-induced dopaminergic degeneration. *J. Pharm. Pharm. Sci.* 12, 199–208. doi: 10.18433/j3b596

Vemula, S., Roder, K. E., Yang, T., Bhat, G. J., Thekkumkara, T. J., and Abbruscato, T. J. (2009). A functional role for sodium-dependent glucose transport across the blood-brain barrier during oxygen glucose deprivation. *J. Pharmacol. Exp. Ther.* 328, 487–495. doi: 10.1124/jpet.108.146589

Venkatasubramanian, C., Mlynash, M., Finley-Caulfield, A., Eyngorn, I., Kalimuthu, R., Snider, R. W., et al. (2011). Natural history of perihematomal edema after intracerebral hemorrhage measured by serial magnetic resonance imaging. *Stroke* 42, 73–80. doi: 10.1161/strokeaha.110.590646

Verghese, P. B., Castellano, J. M., and Holtzman, D. M. (2011). Apolipoprotein E in Alzheimer's disease and other neurological disorders. *Lancet Neurol.* 10, 241–252. doi: 10.1016/s1474-4422(10)70325-2

Versele, R., Corsi, M., Fuso, A., Sevin, E., Businaro, R., Gosselet, F., et al. (2020). Ketone bodies promote amyloid-beta1-40 clearance in a Human *in Vitro* Blood-brain barrier model. *Int. J. Mol. Sci.* 21:934. doi: 10.3390/ijms21030934

Wacker, B. K., Freie, A. B., Perfater, J. L., and Gidday, J. M. (2012). Junctional protein regulation by sphingosine kinase 2 contributes to blood-brain barrier protection in hypoxic preconditioning-induced cerebral ischemic tolerance. *J. Cereb. Blood Flow Metab.* 32, 1014–1023. doi: 10.1038/jcbfm.2012.3

Wakabayashi, K., Tanji, K., Odagiri, S., Miki, Y., Mori, F., and Takahashi, H. (2013). The Lewy body in Parkinson's disease and related neurodegenerative disorders. *Mol. Neurobiol.* 47, 495–508. doi: 10.1007/s12035-012-8280-y

Wang, G., Manaenko, A., Shao, A., Ou, Y., Yang, P., Budbazar, E., et al. (2016). Low-density lipoprotein receptor-related protein-1 facilitates heme scavenging after intracerebral hemorrhage in mice. *J. Cereb. Blood Flow Metab.* 37, 1299–1310. doi: 10.1177/0271678x16654494

Wang, J., Zhang, D., Fu, X., Yu, L., Lu, Z., Gao, Y., et al. (2018). Carbon monoxide-releasing molecule-3 protects against ischemic stroke by suppressing neuroinflammation and alleviating blood-brain barrier disruption. *J. Neuroinflammation* 15:188. doi: 10.1186/s12974-018-1226-1

Wang, Q., and Doerschuk, C. M. (2002). The signaling pathways induced by neutrophil-endothelial cell adhesion. *Antioxid. Redox Signal.* 4, 39–47. doi: 10.1089/152308602753625843

Wang, Z. Y., Sreenivasmurthy, S. G., Song, J. X., Liu, J. Y., and Li, M. (2019). Strategies for brain-targeting liposomal delivery of small hydrophobic molecules in the treatment of neurodegenerative diseases. *Drug Discov. Today* 24, 595–605. doi: 10.1016/j.drudis.2018.11.001

Weinl, C., Castaneda Vega, S., Riehle, H., Stritt, C., Calaminus, C., Wolburg, H., et al. (2015). Endothelial depletion of murine SRF/MRTF provokes intracerebral hemorrhagic stroke. *Proc. Natl. Acad. Sci. U.S.A.* 112, 9914–9919. doi: 10.1073/pnas.1509047112

Weinreb, O., Mandel, S., Youdim, M. B. H., and Amit, T. (2013). Targeting dysregulation of brain iron homeostasis in Parkinson's disease by iron chelators. *Free Radic. Biol. Med.* 62, 52–64. doi: 10.1016/j.freeradbiomed.2013.01.017

Weksler, B. B., Subileau, E. A., Perrière, N., Charneau, P., Holloway, K., Leveque, M., et al. (2005). Blood-brain barrier-specific properties of a human adult brain endothelial cell line. *FASEB J.* 19, 1872–1874. doi: 10.1096/fj.04-3458fje

Wilson, E. H., Weninger, W., and Hunter, C. A. (2010). Trafficking of immune cells in the central nervous system. *J. Clin. Investig.* 120, 1368–1379. doi: 10.1172/jci41911

Winkler, E. A., Bell, R. D., and Zlokovic, B. V. (2011). Central nervous system pericytes in health and disease. *Nat. Neurosci.* 14, 1398–1405. doi: 10.1038/nn.2946

Wolburg-Buchholz, K., Mack, A. F., Steiner, E., Pfeiffer, F., Engelhardt, B., and Wolburg, H. (2009). Loss of astrocyte polarity marks blood-brain barrier impairment during experimental autoimmune encephalomyelitis. *Acta Neuropathol.* 118, 219–233. doi: 10.1007/s00401-009-0558-4

Wong, D., Dorovini-Zis, K., and Vincent, S. R. (2004). Cytokines, nitric oxide, and cGMP modulate the permeability of an *in vitro* model of the human blood-brain barrier. *Exp. Neurol.* 190, 446–455. doi: 10.1016/j.expneurol.2004.08.008

Wood, W. G., Müller, W. E., and Eckert, G. P. (2014). Statins and neuroprotection: basic pharmacology needed. *Mol. Neurobiol.* 50, 214–220. doi: 10.1007/s12035-014-8647-3

Wu, J., Yang, S., Hua, Y., Liu, W., Keep, R. F., and Xi, G. (2010). Minocycline attenuates brain edema, brain atrophy and neurological deficits after intracerebral hemorrhage. *Acta Neurochir. Suppl.* 106, 147–150. doi: 10.1007/978-3-211-98811-4_26

Xi, G., Keep, R. F., and Hoff, J. T. (2002). Pathophysiology of brain edema formation. *Neurosurg. Clin. N. Am.* 13, 371–383. doi: 10.1016/s1042-3680(02)00007-4

Xiaoyan, J., Anuska, V. A., Ling, Z., Yang, T., Bennett, M. V. L., Chen, J., et al. (2018). Blood-brain barrier dysfunction and recovery after ischemic stroke. *Prog. Neurobiol.* 16, 144–171. doi: 10.1016/j.pneurobio.2017.10.001

Yamamoto, M., Ramirez, S. H., Sato, S., Kiyota, T., Cerny, R. L., Kaibuchi, K., et al. (2008). Phosphorylation of Claudin-5 and Occludin by Rho Kinase in Brain Endothelial Cells. *Am. J. Pathol.* 172, 521–533. doi: 10.2353/ajpath.2008.070076

Yang, B., Xu, J., Chang, L., Miao, Z., Heang, D., Pu, Y., et al. (2019). Cystatin C improves blood-brain barrier integrity after ischemic brain injury in mice. *J. Neurochem.* 153, 413–425. doi: 10.1111/jnc.14894

Yang, Y., and Rosenberg, G. A. (2011). Blood–brain barrier breakdown in acute and chronic cerebrovascular disease. *Stroke* 42, 3323–3328. doi: 10.1161/strokeaha.110.608257

Yu, A. S., Hirayama, B. A., Timbol, G., Liu, J., Basarah, E., Kepe, V., et al. (2010). Functional expression of SGLTs in rat brain. *Am. J. Physiol. Cell Physiol.* 299, C1277–C1284. doi: 10.1152/ajpcell.00296.2010

Zhao, C., Ling, Z., Newman, M. B., Bhatia, A., and Carvey, P. M. (2007). TNF-alpha knockout and minocycline treatment attenuates blood-brain barrier leakage in MPTP-treated mice. *Neurobiol. Dis.* 26, 36–46. doi: 10.1016/j.nbd.2006.11.012

Zhao, Z., Nelson, A. R., Betsholtz, C., and Zlokovic, B. V. (2015a). Establishment and Dysfunction of the Blood-Brain Barrier. *Cell* 163, 1064–1078. doi: 10.1016/j.cell.2015.10.067

Zhao, Z., Sagare, A. P., Ma, Q., Halliday, M. R., Kong, P., Kisler, K., et al. (2015b). Central role for PICALM in amyloid-β blood-brain barrier transcytosis and clearance. *Nat. Neurosci.* 18, 978–987. doi: 10.1038/nn.4025

Zlokovic, B. V. (2008). The blood-brain barrier in health and chronic neurodegenerative disorders. *Neuron* 57, 178–201. doi: 10.1016/j.neuron.2008.01.003

Conflict of Interest: The authors declare that the research was conducted in the absence of any commercial or financial relationships that could be construed as a potential conflict of interest.

frontiers in Cellular Neuroscience

ORIGINAL RESEARCH
published: 30 October 2020
doi: 10.3389/fncel.2020.581861

The Effect of IDO on Neural Progenitor Cell Survival Under Oxygen Glucose Deprivation

Jixian Wang[1], Brian Wang[2], Lei Jiang[2], Kaijing Zhou[2], Guo-Yuan Yang[3,4] and Kunlin Jin[2]**

[1]Department of Rehabilitation, Ruijin Hospital, Shanghai Jiao Tong University School of Medicine, Shanghai, China, [2]Department of Pharmacology and Neuroscience, University of North Texas Health Science Center Fort Worth, Fort Worth, TX, United States, [3]Med-X Research Institute and School of Biomedical Engineering, Shanghai Jiao Tong University School of Medicine, Shanghai, China, [4]Department of Neurology, Ruijin Hospital, Shanghai Jiao Tong University School of Medicine, Shanghai, China*

Objective: Indoleamine 2,3-dioxygenase (IDO) activity plays an important role in many neurological disorders in the central nervous system, which may be associated with immunomodulation or anti-inflammatory activity. However, the action of IDO in the ischemic condition is still poorly understood. The purpose of the present study is to explore the expression and action of IDO in stem cell culture under oxygen and glucose deprivation.

Methods: Neural progenitor cells were obtained from the human embryonic stem cell line BG01. These cells underwent oxygen and glucose deprivation. We examined the IDO expression at 3 and 8 h of oxygen and glucose deprivation and then examined neuronal progenitor cell viability in the normal and oxygen and glucose deprivation condition using the [3-(4,5-dimethylthiazol-2-yl)-2,5-diphenyltetrazolium bromide] assay. In addition, we studied the effect of IDO inhibition and the expression of TNF-α, IGF-1, VEGF, IL-6, FGFβ, TGFβ, EGF, and Leptin to explore the mechanism of IDO under the oxygen and glucose deprivation.

Results: IDO expression in neural progenitor cells increased under oxygen and glucose deprivation, which is closely associated with cell death ($p < 0.05$). Inhibiting IDO did not affect cell survival in normal neural progenitor cells. However, inhibiting IDO could attenuate cell viability under oxygen and glucose deprivation ($p < 0.05$). Further study demonstrated that IDO expression was closely associated to the growth factor's leptin expression.

Conclusions: Our results demonstrated that an increase of IDO under oxygen and glucose deprivation was associated with cell death, suggesting that inhibiting IDO could be a target for neuroprotection.

Keywords: IDO, neural progenitor cells, oxygen glucose deprivation, cell viability, leptin

Abbreviations: EGF, epidermal growth factor; 1-MT, 1-Methyltryptophan; FGF-β, fibroblast growth factor; IDO, indoleamine 2,3-dioxygenase; IGF-1, insulin-like growth factor 1; IL-6, interleukin-6; MTT, [3-(4,5-dimethylthiazol-2-yl)-2,5-diphenyltetrazolium bromide; NPCs, neural progenitor cells; OGD, oxygen glucose deprivation; TGF-β, transforming growth factor; TNF-α, tumor necrosis factor α; VEGF, vascular endothelial growth factor.

OPEN ACCESS

Edited by:
Dennis Qing Wang, Southern Medical University, China

Reviewed by:
Raghavan Pillai Raju, Augusta University, United States
Shan Ping Yu, Emory University, United States

****Correspondence:***
Guo-Yuan Yang
gyyang0626@163.com
Kunlin Jin
kunlin.jin@unthsc.edu

Specialty section:
This article was submitted to Non-Neuronal Cells, a section of the journal Frontiers in Cellular Neuroscience

Received: *17 July 2020*
Accepted: *24 August 2020*
Published: *30 October 2020*

Citation:
Wang J, Wang B, Jiang L, Zhou K, Yang G-Y and Jin K (2020) The Effect of IDO on Neural Progenitor Cell Survival Under Oxygen Glucose Deprivation. Front. Cell. Neurosci. 14:581861. doi: 10.3389/fncel.2020.581861

INTRODUCTION

Ischemic stroke is one of the leading causes of death and adult disability worldwide, which leads to massive cell death and complex pathological changes (Tang et al., 2016; Naghavi et al., 2017; Wang et al., 2017). With the recent improvement of acute ischemic stroke management, tPA induced thrombolysis and intravascular thrombectomy are likely to provide insights to develop therapeutic strategies that may benefit stroke patients (Yang et al., 2019). However, stroke morbidity and mortality are still high. To understand the mechanisms of stroke occurrence and development is extremely critical to reduce the imminent danger of stroke. Increased evidence indicated immunomodulation and inflammation is crucial in the physiopathological development of stroke (Jayaraj et al., 2019). Our previous studies demonstrated that during an ischemic stroke attack, resident microglia/macrophages were activated, which could increase cytokines such as IL-1β, IL-6, TNFα, chemokines CXC, CC, CX3C, and XC, and adhesion molecules, calcium-independent integrins, and calcium-dependent cadherins expression in the ischemic region as well as system blood circulation (Ma et al., 2017). In addition, activated macrophages/microglia also triggered the immune system cascade through activating regulatory T cells, T cells, B cells, and the complement system (Wang et al., 2015). However, we do not know how these inflammatory or immune responses reflect the progression of these events during ischemic brain injury. A recent study in a mouse model of middle cerebral artery occlusion demonstrated that the macrophages/microglia could enhance indoleamine 2,3-dioxygenase 1 (IDO1)-dependent neurotoxic kynurenine metabolism during ischemic pathogenesis, which was closely related to the post-stroke depression (Koo et al., 2018). However, the role of IDO in the cell death under oxygen and glucose deprivation is largely unknown.

The kynurenine pathway is initiated by the oxidative metabolism of tryptophan. It has been studied since the early 20th century. No specific neurobiological activity was founded for kynurenine and its catabolic products. In 1978, a study showed that several tryptophan metabolites could produce convulsions when injected directly into the brain (Lapin, 1978). In the 1980s, there was interest in the biological function of an initial enzyme IDO in the kynurenine pathway, which could convert tryptophan to kynurenine. Pfefferkorn (1984) observed that IDO was activated by interferon in the immune response to infection, inhibiting the harmful effects of infectious mediators. However, the mechanism of the anti-infective effect was caused by the depletion of tryptophan or by the accumulation of kynurenine and its downstream metabolites was still controversial (Badawy, 2017). IDO is a heme-containing enzyme expressed in a number of tissues and cells (Yamazaki et al., 1985). IDO is an important molecule of the immune system and plays a part in the natural defense against various pathogens (Yoshida and Hayaishi, 1978; Yoshida et al., 1979). IDO has a function in the response to the inflammatory response and has an immunosuppressive function to limit T cell function (Munn and Mellor, 2013). IDO not only plays a key role in suppressing the anti-tumor immune response in the body (Prendergast et al., 2014), but is also involved in many neurological diseases such as atherosclerosis (Cole et al., 2015), Huntington's disease (Perkins and Stone, 1983), Alzheimer's disease, multiple sclerosis (Fiala et al., 1998; Guillemin et al., 2003), and psychiatric disorders (Savitz et al., 2015; Erhardt et al., 2017). However, the effect of IDO on these neurological disorders is still debatable or just beginning to receive a small degree of attention (Schwarcz and Stone, 2017). The function of IDO during cerebral ischemia has not been well studied both *in vivo* and *in vitro*. In the present study, we examined the IDO expression in neural progenitor cells during oxygen and glucose deprivation to explore the function of IDO in the neuronal death process. We further studied the relationship between IDO expression and the inflammatory response.

MATERIALS AND METHODS

Research protocol was approved by the Institutional Animal Care and Use Committee (IACUC) of Shanghai Jiao Tong University, Shanghai, China. The experiments were performed under the ARRIVE guideline.

Cell Culture and Identification

Neural stem/progenitor cells (NPCs) derived from the human embryonic stem cells (*h*ESC) line BG01 were obtained from Aruna Biomedical (Athens, GA, USA). Cells were seeded on 0.01% polyornithine (Sigma–Aldrich, St. Louis, MO, USA) and 20 μg/ml laminin (Stemgent Inc., Cambridge, MA, USA) coated dishes and cultured in a medium, consisting of a neurobasal medium with a B27 supplement containing 2 mmol/l L-glutamine (both from Gibco Life Sciences, Grand Island, USA), 50 μg/ml Pen/Strep (Invitrogen, Carlsbad, CA, USA), 10 ng/ml leukemia inhibitory factor (Thermo Fisher Scientific, Waltham, MA, USA), and 20 ng/ml fibroblast growth factor-2 (R&D Systems, Minneapolis, MN, USA; Jin et al., 2010). Cells were cultured in a humidified incubator at 37°C with 5% CO_2. They were propagated in the medium and, on reaching 90% to 100% confluence, were triturated to detach them from the dish.

Immunofluorescent Staining

Cells were treated with 100% methanol (chilled at −20°C) for 5 min. Then cells were washed with ice-cold PBS. The cells were incubated with 1% BSA in PBS for 60 min to block any unspecific binding of the antibodies. Then the cells were incubated in the primary antibodies Nestin (1:200 dilution, Millipore) and SOX2 (1:100 dilution, GeneTex, Zeeland, MI, USA), respectively at 4°C overnight, followed by incubation with secondary antibodies (Life Technologies) for 1 h at room temperature. The results were observed under confocal microscopy (Zeiss, Thornwood, NY, USA). The photomicrographs were taken for cell identification.

Oxygen-Glucose Deprivation (OGD)

The procedure of oxygen-glucose deprivation (OGD) and reoxygenation was as follows: NPCs were seeded on 0.01% polyornithine (Sigma–Aldrich) and 20 μg/ml laminin (Stemgent) coated dishes and cultured. Cells were transferred

from the original media to the deoxygenated glucose-free neurobasal medium. The OGD and reoxygenation experiment was performed using a specialized sealed chamber, which contained an anaerobic gas mixture (95% N_2 and 5% CO_2) at 37°C. NPCs cultured in the NPC culture medium without OGD were used as a negative control. After 3 or 8 h treatment, these cells were removed from the chamber; and the medium in the cultures was replaced with the maintenance medium. In the 8-h OGD groups, cells were then allowed to recover for 24 h in a regular incubator.

Western Blot Analysis

Cells were collected and lysed in RIPA (Millipore, Burlington, USA) supplemented with a cocktail (Sigma–Aldrich, St. Louis, MO, USA), 1 mmol/l PMSF (Thermo), and a phosphatase inhibitor (Thermo). For Western blots analysis, denatured samples containing the same amount of proteins (30 μg) were loaded onto the resolving gel (EpiZyme, Shanghai, China) for electrophoresis. Proteins were then transferred onto a nitrocellulose membrane (Whatman, Piscataway, NJ, USA). The membrane was blocked with blocking buffer (EpiZyme) and then incubated with primary antibodies at the following dilution IDO (1:200 dilution, LifeSpan Biosciences, Seattle, WA, USA) at 4°C overnight, respectively. The membrane was washed, incubated with the appropriate HRP-conjugated secondary antibody for 1 h, and then reacted with enhanced chemiluminescence substrate (Pierce, Rockford, IL, USA). The results were recorded by the Quantity One image software (Bio-Rad, Hercules, CA, USA) and relative intensity was calculated using the ImageJ software (NIH, USA).

MTT Assay

Cell survival assays were performed using an MTT kit (Sigma–Aldrich, St. Louis, MO, USA). The MTT solution was added to each well and incubated at 37°C for 4 h. After incubation, MTT solvent was added into each well. The plate was wrapped in foil and shaken on an orbital shaker for 15 min. Occasionally, pipetting of the liquid was required to fully dissolve the MTT formazan. Absorbance was measured at 590 nm using a microplate reader (Thermo Fisher Scientific, Waltham, MA, USA).

ELISA Assay

To assess the release of angiogenesis-related cytokines in *h*ESC derived NPCs after OGD, and 1-MT treatment, the amount of released TNF-α, IGF-1, VEGF, IL-6, FGF-β, TGF-β, EGF, and Leptin was measured by using a human angiogenesis ELISA kit (Signosis Inc., Santa Clara, CA, USA). The supernatant was collected from each sample. A hundred microliter sample was added into the well and incubated, for 1 h at room temperature with gentle shaking. Each well was washed by adding 200 μl of 1× assay wash buffer three times. A total

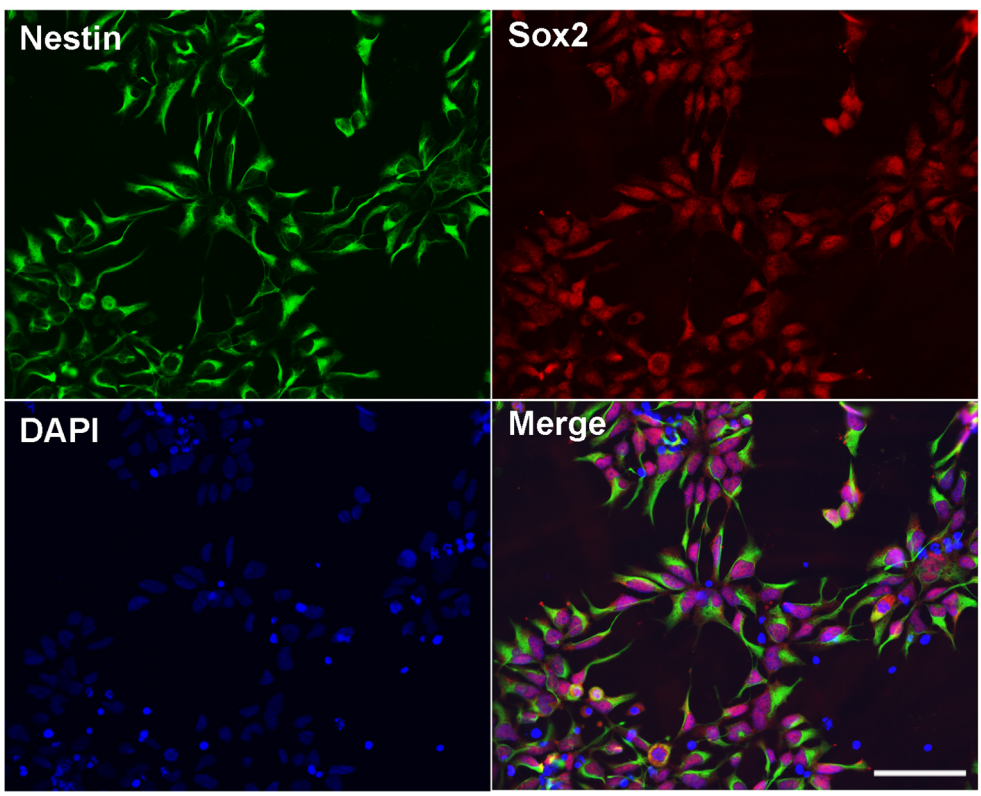

FIGURE 1 | Identification of human embryonic stem cells (*h*ESC)-derived neural progenitor cells (NPCs). Immunostaining images of *h*ESC-derived NPCs showed anti-Nestin (green), Sox2 (red), and DAPI (blue). Scale bar = 50 μm.

of 100 μl of diluted biotin-labeled antibody mixture and 100 μl of diluted streptavidin-HRP conjugate were in turn added to each well and incubated respectively for 1.5 h at room temperature with gentle shaking. A total of 100 μl of substrate was added to each well and incubated for 30 min. A total of 50 μl of stop solution was added to each well. The optical density was determined by a microplate reader at 450 nm within 30 min.

Statistical Analysis

Quantitative data were presented as mean ± SD and compared by one-way and two-way analysis of variance (ANOVA) with repeated measures, followed by *post hoc* multiple comparison tests (Fisher PLSD or Student's paired *t*-test with the Bonferroni correction) using the SPSS software (v18.0, SPSS Inc., Chicago, IL, USA). A probability value of less than 0.05 was considered to represent statistical significance.

RESULTS

NPC Identification and Culture

*h*ESC line BG01-derived NPCs were cultured and maintained in a medium. The morphology of the NPCs were characterized by a double immunostaining with anti-Nestin and anti-Sox2. We found that more than 99% of cells expressed both Nestin and Sox2 (**Figure 1**), which indicated that these cells showed the NPC morphology and could be appropriately used in the subsequent experiments.

IDO Expression Increased in the NPCs After OGD

To examine the expression of IDO in the NPCs during oxygen and glucose deprivation, we performed an NPCs OGD model. Western blot results showed that IDO expression was significantly increased in NPCs after 3 and 8 h of OGD compared to the NPCs that were in a normal condition (**Figure 2**, $p < 0.05$). There was the potential that IDO expression would increase with time.

Inhibition of IDO Attenuated NPC Viability

1-MT is an inhibitor of IDO. To explore the effect of IDO on the viability of NPCs, 1-MT was used to inhibit IDO expression. As is shown in the **Figure 3A**, some of the NPCs began to die after 8 h of OGD. 1-MT treatment further exacerbated the damage of the NPCs. Using the MTT method, we found that 1-MT had no effect on the survival in normal NPCs (**Figure 3B**, left, $p > 0.05$). However, 1-MT significantly reduced the viability of NPCs after 8 h of OGD at 62.5–500 μg/ml concentrations (**Figure 3B**, middle, $p < 0.05$ to $p < 0.001$). Moreover, 1-MT had the same effect on the viability of NPCs after 8 h of OGD and 24 h reperfusion (**Figure 3B**, left, $p < 0.01$).

IDO Inhibition Reduced Cytokine Expression

To further explore the molecular mechanism of IDO, ELISA was applied to detect cytokine expression in OGD-treated NPCs. As shown in **Figure 4**, we found that after 8 h of OGD, IGF-1, FGF-β, TGF-β, and Leptin expression in NPCs were significantly increased compared to the normal NPCs ($p < 0.01$). However, only Leptin was significantly decreased after 8 h of OGD with 1-MT treatment ($p < 0.05$). This phenomenon was also observed in the group of 8 h of OGD and 24 h reperfusion with 1-MT treatment ($p < 0.05$).

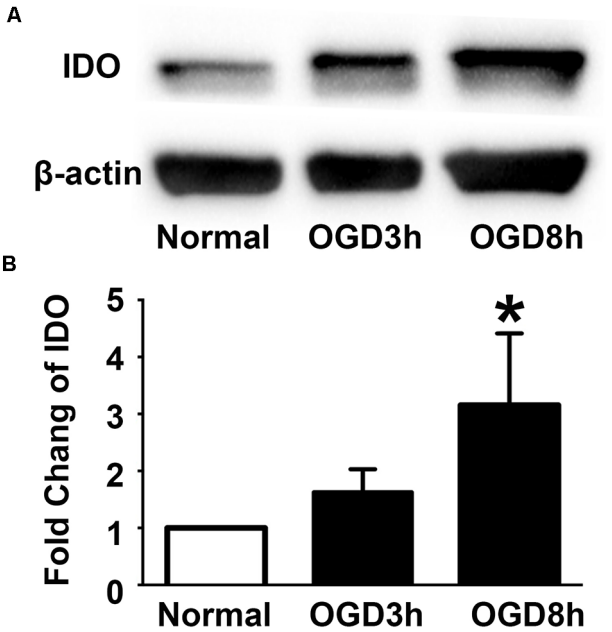

FIGURE 2 | Indoleamine 2,3-dioxygenase (IDO) expression increased in the NPCs after oxygen glucose deprivation (OGD). **(A)** Western blot results showed that the expression of IDO after 3 and 8 h of OGD in *h*ESC-derived NPCs. β-actin was an internal control. **(B)** The bar graph represented the semi-quantification of IDO expression. $N = 5$ per group, $^*p < 0.05$, compared to the control.

DISCUSSION

Although IDO plays an important role in many neurological diseases such as Huntington's disease, Alzheimer's disease, multiple sclerosis, and psychiatric disorders, the effect of IDO in the ischemic neuronal injury is largely unknown. In the present study, we used an OGD-treated NPC-cultured model *in vitro* which demonstrated that: (1) the expression of IDO in NPCs increased under the OGD condition, which was closely related to cell survival; (2) the inhibition of IDO could attenuate NPC viability; and (3) increased IDO is closely associated to growth factors TNFα, FGFβ, and Leptin expression. Our results suggested that inhibiting IDO could be a potential approach for neuroprotection in future studies *in vivo*.

After the discovery of IDO, the kynurenine pathway and its roles in the nervous and immune systems development was evaluated. IDO was involved not only in primarily peripheral afflictions including arthritis and atherosclerosis but also in central inflammation and immune function in Alzheimer's disease, multiple sclerosis, and Huntington's disease. These

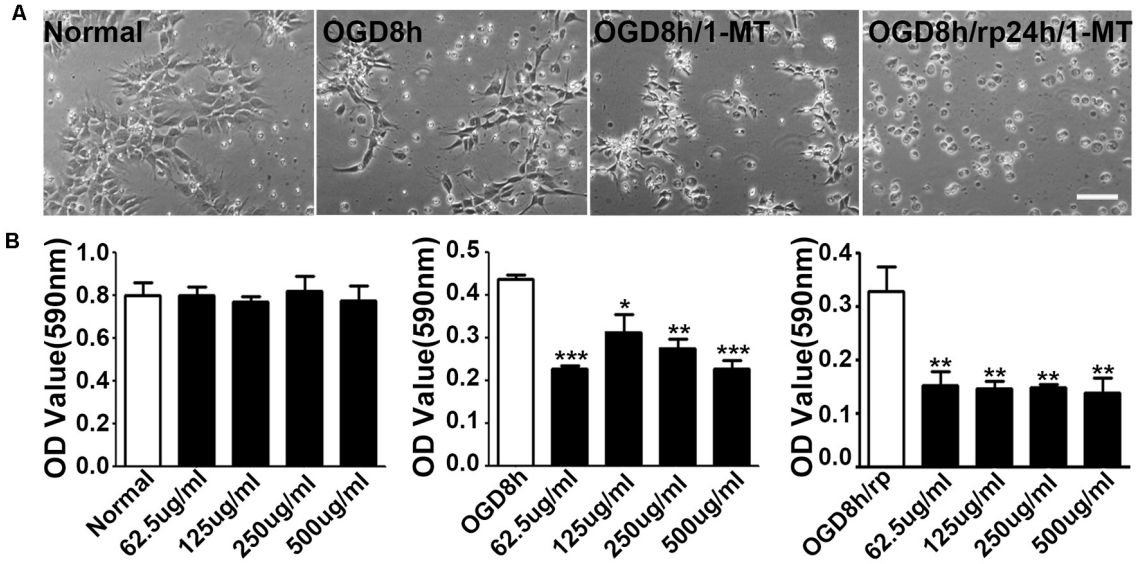

FIGURE 3 | Inhibition of IDO attenuated NPC viability. **(A)** Photomicrographs taken with a phase contract microscope showed neuroepithelial (NEP) morphological changes after 8-h OGD, 8-h OGD plus 1-MT treatment, and 8-h OGD followed by 24-h reperfusion plus 1-MT treatment. Scale bar = 50 μm. **(B)** Bar graphs presented the MTT results: the effect of 1-DL-MT at 62.5, 125, 250, and 500 μg/ml on NEP cells under normal condition (left), after 8-h OGD (middle), and 8-h OGD plus 24-h reperfusion (right). $N = 5$ per group, $^{*}p < 0.05$, $^{**}p < 0.01$, $^{***}p < 0.01$, compared to the controls.

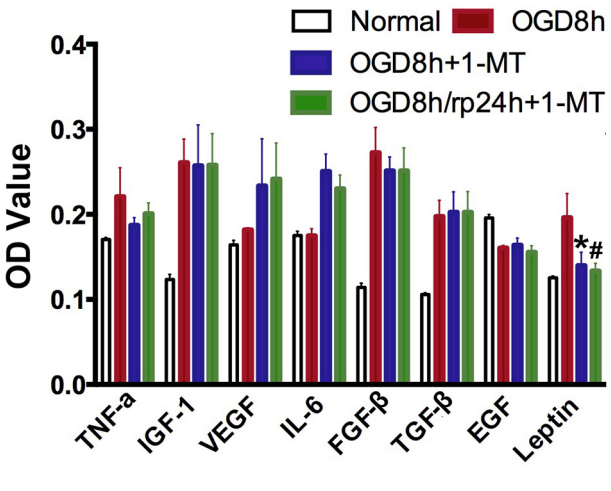

FIGURE 4 | IDO inhibition reduced cytokine expression. Bar graphs presented that TNF-α, IGF-1, VEGF, IL-6, FGFβ, TGFβ, EGF, and Leptin expression in the OGD by ELISA assay. $N = 5$ per group, $^{*}p < 0.05$, OGD 8 h vs. OGD 8 h + 1-MT group; $^{\#}p < 0.05$, OGD 8 h vs. OGD 8 h/rp 24 h + 1-MT.

interactions could contribute to a physiologic and pathogenic role to the immune system activity with potentially common targets. IDO could be activated in astrocytes, microglia, and even in the neurons (Guillemin et al., 2003, 2005). However, if IDO was expressed in NPCs it was not well understood. An interesting topic of increasing attention is the link between kynurenines and stem cell biology. Human and mouse mesenchymal stem cells (MSCs) and neural stem cells (NSCs) expressed the kynurenine pathway (Croitoru-Lamoury et al., 2011). Pluripotent progenitor cells had IDO-dependent immunomodulatory properties, implicating kynurenine, and possibly its downstream metabolites (Jacobs et al., 2013). Numerous studies demonstrated that MSC transplantation had neuroprotection and neuronal repair function, which was a new clinical approach for repairing injured tissue. The function of MSCs could modulate immunological responses *via* T cell suppression, through IDO and toll-like receptor (TLR) signaling pathways (Lyakisheva et al., 2002; Aggarwal and Pittenger, 2005). In this study, we chose NPCs to explore the effect of IDO in brain neurons because NPCs were an important component during injured brain tissue repair. We found that, similar to the MSCs, IDO expression increased in NPCs during OGD, which is related to the cell viability. Increased IDO could attenuate NPC death during OGD, suggesting that IDO plays a neuroprotection role in the cell survival process.

In studies of the role of kynurenines in the brain, the most useful information was commonly collected from *in vivo* models or acutely prepared tissue slices, while freshly dissociated cells *in vitro*, for example, neurons, astrocytes and microglia also provided relevant information (Guillemin et al., 2007). In a mouse middle cerebral artery occlusion model, Koo et al. (2018) found that microglial IDO expression, QUIN production, and reactive oxidative species (ROS) were prominently increased in the accumbens nucleus, hippocampus, and hypothalamus, and found that these increases were related to mouse depressive-like behaviors. They demonstrated that adjunctive antidepressant aripiprazole ameliorated depressive behavior and cognitive impairment in the ischemic mice *via* downregulation of IDO1, HAAO, QUIN, and ROS. The

action of IDO could be sustained for at least 9 weeks. This *in vivo* study provided evidence that the IDO1-dependent neurotoxic kynurenine metabolism represented a potential therapeutic target for the treatment of post-stroke dementia. However, our result was different from their study. We found that the over-expression of IDO could enhance cell viability while inhibiting IDO action could attenuate NPC survival. We believe that the effect of IDO in the early phase or the later phase of ischemia could be different. In the early stage, IDO may be involved in the acute inflammatory response while in the later stage it may promote anti-inflammation and immune-regulation. The action of IDO in the long term of neurological diseases could also be different with acute cerebral vascular disease. In addition, an argument against a special role of NMDA receptor inhibition could not be duplicated for the action of kynurenic acid in several experiments *in vitro* and *in vivo* (Hilmas et al., 2001; Beggiato et al., 2013), suggesting that IDO was involved in several signal pathways. Nevertheless, the effect of IDO on ischemic neurons and the brain should to be further studied.

Growing evidence indicated that IDO, TGF-β1, and PGE2 may represent relevant mediators of NK cell functional inhibition (Di Nicola et al., 2002; Meisel et al., 2004; Aggarwal and Pittenger, 2005). Quantitative real-time PCR confirmed that TNF-α could significantly upregulate HGF mRNA (English et al., 2007). Another study neutralized HGF and TGF-β1 and found that HGF worked in synergy with TGF-β1 to resist T cell recognition (Di Nicola et al., 2002). All this suggested that IDO and TGF-β1 together regulate the immune effect of NPCs. We found that increased IDO is closely associated to the cytokine TNF-α, and growth factors FGF-β and Leptin, but not IGF-1, VEGF, IL-6, TGF-β, and EGF expression. This finding indicated that IDO is not an exclusive mechanism for NPC protection especially in the early stage of ischemia.

In conclusion, our study demonstrated that IDO expression increased in NPCs during OGD, which is associated with NPC viability. IDO may represent a potential valuable target for the treatment of injured NPCs.

DATA AVAILABILITY STATEMENT

The raw data supporting the conclusions of this article will be made available by the authors, without undue reservation.

ETHICS STATEMENT

The animal study was reviewed and approved by the Institutional Animal Care and Use Committee (IACUC) of Shanghai Jiao Tong University.

AUTHOR CONTRIBUTIONS

JW and KJ designed the experiment. JW performed all experiments, analyzed the data, and drafted the manuscript. BW, LJ, and KZ performed the Western blot and ELISA experiment. G-YY was responsible for supervising all the experimental designs, experimental performance, and finalizing the manuscript. All authors critically reviewed the manuscript. All authors contributed to the article and approved the submitted version.

FUNDING

This work was supported by the National Natural Science Foundation of China (NSFC) projects (81802232, JW; 81771251, G-YY), major projects of the Shanghai Education Commission's scientific research and innovation program (2019-01-07-00-02-E00064, G-YY), and the K. C. Wong Education Foundation (G-YY).

REFERENCES

Aggarwal, S., and Pittenger, M. F. (2005). Human mesenchymal stem cells modulate allogeneic immune cell responses. *Blood* 105, 1815–1822. doi: 10.1182/blood-2004-04-1559

Badawy, A. A.-B. (2017). Kynurenine pathway of tryptophan metabolism: regulatory and functional aspects. *Int. J. Tryptophan Res.* 10:1178646917691938. doi: 10.1177/1178646917691938

Beggiato, S., Antonelli, T., Tomasini, M. C., Tanganelli, S., Fuxe, K., Schwarcz, R., et al. (2013). Kynurenic acid, by targeting alpha7 nicotinic acetylcholine receptors, modulates extracellular GABA levels in the rat striatum *in vivo*. *Eur. J. Neurosci.* 37, 1470–1477. doi: 10.1111/ejn.12160

Cole, J. E., Astola, N., Cribbs, A. P., Goddard, M. E., Park, I., Green, P., et al. (2015). Indoleamine 2,3-dioxygenase-1 is protective in atherosclerosis and its metabolites provide new opportunities for drug development. *Proc. Natl. Acad. Sci. U S A* 112, 13033–13038. doi: 10.1073/pnas.1517820112

Croitoru-Lamoury, J., Lamoury, F. M., Caristo, M., Suzuki, K., Walker, D., Takikawa, O., et al. (2011). Interferon-gamma regulates the proliferation and differentiation of mesenchymal stem cells *via* activation of indoleamine 2,3 dioxygenase (IDO). *PLoS One* 6:e14698. doi: 10.1371/journal.pone.0014698

Di Nicola, M., Carlo-Stella, C., Magni, M., Milanesi, M., Longoni, P. D., Matteucci, P., et al. (2002). Human bone marrow stromal cells suppress T-lymphocyte proliferation induced by cellular or nonspecific mitogenic stimuli. *Blood* 99, 3838–3843. doi: 10.1182/blood.v99.10.3838

English, K., Barry, F. P., Field-Corbett, C. P., and Mahon, B. P. (2007). IFN-gamma and TNF-alpha differentially regulate immunomodulation by murine mesenchymal stem cells. *Immunol. Lett.* 110, 91–100. doi: 10.1016/j.imlet.2007.04.001

Erhardt, S., Schwieler, L., Imbeault, S., and Engberg, G. (2017). The kynurenine pathway in schizophrenia and bipolar disorder. *Neuropharmacology* 112, 297–306. doi: 10.1016/j.neuropharm.2016.05.020

Fiala, M., Zhang, L., Gan, X., Sherry, B., Taub, D., Graves, M. C., et al. (1998). Amyloid-beta induces chemokine secretion and monocyte migration across a human blood—brain barrier model. *Mol. Med.* 4, 480–489. doi: 10.1007/BF03401753

Guillemin, G. J., Brew, B. J., Noonan, C. E., Takikawa, O., and Cullen, K. M. (2005). Indoleamine 2,3 dioxygenase and quinolinic acid immunoreactivity in Alzheimer's disease hippocampus. *Neuropathol. Appl. Neurobiol.* 31, 395–404. doi: 10.1111/j.1365-2990.2005.00655.x

Guillemin, G. J., Croitoru-Lamoury, J., Dormont, D., Armati, P. J., and Brew, B. J. (2003). Quinolinic acid upregulates chemokine production and chemokine receptor expression in astrocytes. *Glia* 41, 371–381. doi: 10.1002/glia.10175

Guillemin, G. J., Cullen, K. M., Lim, C. K., Smythe, G. A., Garner, B., Kapoor, V., et al. (2007). Characterization of the kynurenine pathway in human neurons. *J. Neurosci.* 27, 12884–12892. doi: 10.1523/JNEUROSCI.4101-07.2007

Hilmas, C., Pereira, E. F., Alkondon, M., Rassoulpour, A., Schwarcz, R., and Albuquerque, E. X. (2001). The brain metabolite kynurenic acid inhibits alpha7 nicotinic receptor activity and increases non-alpha7 nicotinic receptor expression: physiopathological implications. *J. Neurosci.* 21, 7463–7473. doi: 10.1523/JNEUROSCI.21-19-07463.2001

Jacobs, S. A., Pinxteren, J., Roobrouck, V. D., Luyckx, A., van't Hof, W., Deans, R., et al. (2013). Human multipotent adult progenitor cells are nonimmunogenic and exert potent immunomodulatory effects on alloreactive T-cell responses. *Cell Transpl.* 22, 1915–1928. doi: 10.3727/096368912X657369

Jayaraj, R. L., Azimullah, S., Beiram, R., Jalal, F. Y., and Rosenberg, G. A. (2019). Neuroinflammation: friend and foe for ischemic stroke. *J. Neuroinflammation* 16:142. doi: 10.1186/s12974-019-1516-2

Jin, K., Mao, X., Xie, L., Galvan, V., Lai, B., Wang, Y., et al. (2010). Transplantation of human neural precursor cells in Matrigel scaffolding improves outcome from focal cerebral ischemia after delayed postischemic treatment in rats. *J. Cereb. Blood Flow Metab.* 30, 534–544. doi: 10.1038/jcbfm.2009.219

Koo, Y. S., Kim, H., Park, J. H., Kim, M. J., Shin, Y. I., Choi, B. T., et al. (2018). Indoleamine 2,3-dioxygenase-dependent neurotoxic kynurenine metabolism contributes to poststroke depression induced in mice by ischemic stroke along with spatial restraint stress. *Oxid. Med. Cell. Longev.* 2018:2413841. doi: 10.1155/2018/2413841

Lapin, I. P. (1978). Stimulant and convulsive effects of kynurenines injected into brain ventricles in mice. *J. Neural Transm.* 42, 37–43. doi: 10.1007/BF01262727

Lyakisheva, A., Felda, O., Ganser, A., Schmidt, R. E., and Schubert, J. (2002). Paroxysmal nocturnal hemoglobinuria: differential gene expression of EGR-1 and TAXREB107. *Exp. Hematol.* 30, 18–25. doi: 10.1016/s0301-472x(01)00763-9

Ma, Y., Wang, J., Wang, Y., and Yang, G. Y. (2017). The biphasic function of microglia in ischemic stroke. *Prog. Neurobiol.* 157, 247–272. doi: 10.1016/j.pneurobio.2016.01.005

Meisel, R., Zibert, A., Laryea, M., Gobel, U., Daubener, W., and Dilloo, D. (2004). Human bone marrow stromal cells inhibit allogeneic T-cell responses by indoleamine 2,3-dioxygenase-mediated tryptophan degradation. *Blood* 103, 4619–4621. doi: 10.1182/blood-2003-11-3909

Munn, D. H., and Mellor, A. L. (2013). Indoleamine 2,3 dioxygenase and metabolic control of immune responses. *Trends Immunol.* 34, 137–143. doi: 10.1016/j.it.2012.10.001

Naghavi, M., Abajobir, A. A., Abbafati, C., Abbas, K. M., Abd-Allah, F., Abera, S. F., et al. (2017). Global, regional, and national age-sex specific mortality for 264 causes of death, 1980–2016: a systematic analysis for the global burden of disease study 2016. *Lancet* 390, 1151–1210. doi: 10.1016/S0140-6736(17)32152-9

Perkins, M. N., and Stone, T. W. (1983). Pharmacology and regional variations of quinolinic acid-evoked excitations in the rat central nervous system. *J. Pharmacol. Exp. Ther.* 226, 551–557.

Pfefferkorn, E. R. (1984). Interferon gamma blocks the growth of Toxoplasma gondii in human fibroblasts by inducing the host cells to degrade tryptophan. *Proc. Natl. Acad. Sci. U S A* 81, 908–912. doi: 10.1073/pnas.81.3.908

Prendergast, G. C., Smith, C., Thomas, S., Mandik-Nayak, L., Laury-Kleintop, L., Metz, R., et al. (2014). Indoleamine 2,3-dioxygenase pathways of pathogenic inflammation and immune escape in cancer. *Cancer Immunol. Immunother.* 63, 721–735. doi: 10.1007/s00262-014-1549-4

Savitz, J., Dantzer, R., Meier, T. B., Wurfel, B. E., Victor, T. A., McIntosh, S. A., et al. (2015). Activation of the kynurenine pathway is associated with striatal volume in major depressive disorder. *Psychoneuroendocrinology* 62, 54–58. doi: 10.1016/j.psyneuen.2015.07.609

Schwarcz, R., and Stone, T. W. (2017). The kynurenine pathway and the brain: Challenges, controversies and promises. *Neuropharmacology* 112, 237–247. doi: 10.1016/j.neuropharm.2016.08.003

Tang, Y., Wang, L., Wang, J., Lin, X., Wang, Y., Jin, K., et al. (2016). Ischemia-induced Angiogenesis is attenuated in aged rats. *Aging Dis.* 7, 326–335. doi: 10.14336/AD.2015.1125

Wang, W., Jiang, B., Sun, H., Ru, X., Sun, D., Wang, L., et al. (2017). Prevalence, incidence, and mortality of stroke in china: results from a nationwide population-based survey of 480 687 adults. *Circulation* 135, 759–771. doi: 10.1161/CIRCULATIONAHA.116.025250

Wang, J., Xie, L., Yang, C., Ren, C., Zhou, K., Wang, B., et al. (2015). Activated regulatory T cell regulates neural stem cell proliferation in the subventricular zone of normal and ischemic mouse brain through interleukin 10. *Front Cell. Neurosci.* 9:361. doi: 10.3389/fncel.2015.00361

Yamazaki, F., Kuroiwa, T., Takikawa, O., and Kido, R. (1985). Human indolylamine 2,3-dioxygenase. Its tissue distribution and characterization of the placental enzyme. *Biochem. J.* 230, 635–638. doi: 10.1042/bj2300635

Yang, C.-S., Guo, A., Li, Y., Shi, K., Shi, F.-D., and Li, M. (2019). Dl-3-n-butylphthalide reduces neurovascular inflammation and ischemic brain injury in mice. *Aging Dis.* 10, 964–976. doi: 10.14336/AD.2019.0608

Yoshida, R., and Hayaishi, O. (1978). Induction of pulmonary indoleamine 2,3-dioxygenase by intraperitoneal injection of bacterial lipopolysaccharide. *Proc. Natl. Acad. Sci. U S A* 75, 3998–4000. doi: 10.1073/pnas.75.8.3998

Yoshida, R., Urade, Y., Tokuda, M., and Hayaishi, O. (1979). Induction of indoleamine 2,3-dioxygenase in mouse lung during virus infection. *Proc. Natl. Acad. Sci. U S A* 76, 4084–4086. doi: 10.1073/pnas.76.8.4084

Conflict of Interest: The authors declare that the research was conducted in the absence of any commercial or financial relationships that could be construed as a potential conflict of interest.

The handling editor declared a past co-authorship with one of the authors KJ.

frontiers in Cellular Neuroscience

REVIEW
published: 18 January 2021
doi: 10.3389/fncel.2020.618986

Microvascular Alterations in Alzheimer's Disease

Joe Steinman[1], *Hong-Shuo Sun*[1,2] *and Zhong-Ping Feng*[1]*

[1] Department of Physiology, University of Toronto, Toronto, ON, Canada, [2] Department of Surgery, University of Toronto, Toronto, ON, Canada

Alzheimer's disease (AD) is a neurodegenerative disorder associated with continual decline in cognition and ability to perform routine functions such as remembering familiar places or understanding speech. For decades, amyloid beta (Aβ) was viewed as the driver of AD, triggering neurodegenerative processes such as inflammation and formation of neurofibrillary tangles (NFTs). This approach has not yielded therapeutics that cure the disease or significant improvements in long-term cognition through removal of plaques and Aβ oligomers. Some researchers propose alternate mechanisms that drive AD or act in conjunction with amyloid to promote neurodegeneration. This review summarizes the status of AD research and examines research directions including and beyond Aβ, such as tau, inflammation, and protein clearance mechanisms. The effect of aging on microvasculature is highlighted, including its contribution to reduced blood flow that impairs cognition. Microvascular alterations observed in AD are outlined, emphasizing imaging studies of capillary malfunction. The review concludes with a discussion of two therapies to protect tissue without directly targeting Aβ for removal: (1) administration of growth factors to promote vascular recovery in AD; (2) inhibiting activity of a calcium-permeable ion channels to reduce microglial activation and restore cerebral vascular function.

Keywords: Alzheimer's disease, amyloid hypotheses, vasculature, microvasculature, TRPM2, angiogeneis, growth factors, imaging

OPEN ACCESS

Edited by:
Eng-King Tan,
National Neuroscience Institute (NNI), Singapore

Reviewed by:
Luan Pereira Diniz,
Federal University of Rio de Janeiro, Brazil
Daniel Erny,
University of Freiburg Medical Center, Germany

***Correspondence:**
Zhong-Ping Feng
zp.feng@utoronto.ca

Specialty section:
This article was submitted to Non-Neuronal Cells, a section of the journal Frontiers in Cellular Neuroscience

Received: *19 October 2020*
Accepted: *17 December 2020*
Published: *18 January 2021*

Citation:
Steinman J, Sun HS and Feng ZP (2021) Microvascular Alterations in Alzheimer's Disease. Front. Cell. Neurosci. 14:618986. doi: 10.3389/fncel.2020.618986

PREFACE

Many drugs developed to treat Alzheimer's disease (AD) have been designed on the assumption that amyloid beta (Aβ) drives the disease. This approach has not yielded FDA-approved drugs, with approved medications such as cholinesterase inhibitors or memantine (glutamate blocker) only treating symptoms of AD. Proponents of the Amyloid Hypothesis (AH) feel that anti-Aβ therapies may have been administered too late in the disease process, and that the AH remains valid. To others, disease mechanisms beyond Aβ accumulation must be targeted.

Movement beyond traditional interpretations of the AH requires understanding the myriad of processes altered in AD. This influences research direction and treatment development. This review summarizes the status of AD research, and includes the examination and discussion of multiple mechanisms underlying AD pathology. Alternative hypotheses of AD beyond the AH, such as abnormal tau and inflammation, are detailed. Microvascular alterations in aging and AD are discussed, and their role assessed in reducing blood flow and impairing Aβ clearance from tissue. Techniques and methods for imaging microvasculature in AD are outlined, with results from studies highlighting the role of capillary imaging and mathematical analysis in understanding vascular contributions to AD. The review concludes by discussing potential therapies that promote vascular recovery and protection against Aβ toxicity without targeting Aβ.

INTRODUCTION: AN OVERVIEW

AD is associated with decline in episodic memory, impaired concentration or attention, disorientation, and loss of verbal fluency (Vandenberghe and Tournoy, 2005; Ferris and Farlow, 2013). Examples of factors contributing to loss of cognition include age-related capillary reductions and blood brain barrier (BBB) leakage (Farkas and Luiten, 2001; Zlokovic, 2005), release of pro-inflammatory cytokines from microglia that induce neuron death (Floden et al., 2005; Wang et al., 2015), plaque-induced neural network disruption (Knowles et al., 1999; Kuchibhotla et al., 2008), and toxic soluble Aβ oligomers that cause synaptic dysfunction (Smith and Strittmatter, 2017).

The AH proposes that extracellular Aβ deposition initiates neurodegenerative processes, such as neurofibrillary tangle (NFT) formation, leading to cognitive impairment (Hardy and Higgins, 1992; Makin, 2018). It was initially believed that elimination of plaques via targeting Aβ would improve cognition. This was supported by promising results in transgenic PDAPP mice overexpressing mutant human APP, where immunization with Aβ prevented plaque development and neurite damage (Schenk et al., 1999).

Current treatments, such as cholinesterase inhibitors, temporarily improve symptoms such as memory loss and reasoning capacity, without altering Aβ deposition or tau pathology (Govindpani et al., 2019; Madav et al., 2019). By passage of 3 months, the effect of these treatments is reduced due to tolerance development in patients (Madav et al., 2019).

One possibility for developing AD treatments is targeting multiple therapeutic sites in addition to, or separately from, Aβ (Selkoe, 2019). This could enable use of approved medications developed to treat other conditions. For example, a recent study that applied etodolac (a nonsteroidal anti-inflammatory) to an *in vitro* AD cell culture model found enhanced BBB integrity and reduced cell death in response to neurotoxins (thrombin) administered into the endothelial cell barrier (Shin et al., 2019).

Targeting multiple therapeutic sites in addition to Aβ requires understanding the complexity of AD pathology and numerous changes that occur possibly independent of Aβ. For example, BBB dysfunction may occur prior to Aβ deposition in individuals possessing the apolipoprotein E4 gene (ApoE4), where the ApoE4 gene is known to render susceptibility to AD (Montagne et al., 2020). Tau, a microtubule associated protein linked to synaptic loss and dysfunction, is more closely related to cognitive impairment than amyloid (Bejanin et al., 2017). Susceptibility to AD may be dependent on gender, with women twice as likely as men to contact AD. This is possibly due to metabolic alterations during menopause (Ferretti et al., 2018). Microglia, central nervous system (CNS) immune cells, may operate protectively by surrounding amyloid deposits, compacting fibrils into a less toxic form and preventing plaque growth. They may also harm neurons through release of inflammatory mediators (Hansen et al., 2018). This dual role highlights the complexity of the tissue response to AD.

Often overlooked in Alzheimer's research is the microvasculature, which is commonly viewed as secondary to neuronal death and inflammation. Recent microscopy studies suggest a critical role of the microvasculature in disease progression. Cruz Hernández et al. (2019) demonstrated via vascular and neutrophil imaging with 2-photon microscopy in AD mice and mathematical blood flow modeling (in mouse, human, and synthetic microvascular networks) that capillary flow blockage via neutrophils reduces cerebral blood flow (CBF). CBF was restored through antibody targeting of neutrophils, which improved short-term memory function up to 16-months of age in APP/PS1 mice (Bracko et al., 2020). Nortley et al. (2019) demonstrated capillary compression by pericytes induced by amyloid-triggered release of endothelin could lead to widespread reductions in blood flow. These findings suggest the microvasculature could contribute to damage of brain cells and synapses (Nortley et al., 2019).

Consideration of aspects of the disease beyond amyloid are necessary for the development of therapies. The following section discusses the AH and presents alternatives. Microvascular changes and their contributions to AD follow. The review concludes by discussing two therapies that do not target Aβ directly: (1) vascular endothelial growth factor (VEGF) administration to improve vascular survival (Religa et al., 2013); (2) inhibiting the calcium-permeable ion channel transient receptor potential melastatin 2 (TRPM2) to protect against Aβ toxicity (Ostapchenko et al., 2015).

ALZHEIMER'S RESEARCH: THE AMYLOID HYPOTHESIS

Alzheimer's Research: A General Summary

Although the AH influenced and directed drug development for many years, there has been a shift in opinion toward exploring alternatives. Up to 2019, ∼22% of clinical trials tested amyloid therapies, while significant research efforts are focused on a range of targets such as neurotransmitters and tau (Liu et al., 2019).

Promising results have been obtained with anti-Aβ strategies. Aducanumab, a human monoclonal antibody directed against Aβ, reduced soluble and insoluble parenchymal Aβ in Tg2576 AD mice, while reducing Aβ in humans and slowing clinical decline (Sevigny et al., 2016). However, Aducanumab provided insufficient relief from functional and cognitive decline in two Phase 3 clinical trials, though subsequent analyses indicated reduced rate of behavioral and cognitive decline (Walsh and Selkoe, 2020). Another antibody, BAN2401 cleared amyloid plaques and slowed cognitive decline in a Phase 2b study (Walsh and Selkoe, 2020).

Despite the promise of these anti-Aβ therapeutics, it is unclear whether removal of amyloid by itself would "cure" AD. For example, widespread inflammation may be initiated by Aβ deposition, limiting the benefits of amyloid removal if inflammation is not simultaneously reduced. Aging reduces capillary density and blood flow, which may contribute to cognitive deficits alongside amyloid. According to the Mitochondrial Cascade Hypothesis, genetically, and environmentally determined decline in mitochondrial function triggers AD pathology (Swerdlow et al., 2014). In this instance, Aβ removal may only marginally improve AD (Swerdlow et al.,

2014). Some researchers contend neural network function is a better predictor of disease progression when compared with plaques (Kosik, 2013). These disparate views indicate a lack of consensus in treating or detecting AD and could be attributable to the wide variety of mechanisms which initiate AD and aid its progression. Genetic risks associated with AD may be related to APP production and processing, as well as other processes such as the immune system and neuroinflammation (Bertram and Tanzi, 2019). A single intervention targeting Aβ removal may therefore be unable to significantly reverse disease progression.

The Amyloid Hypothesis

APP is a transmembrane protein processed by enzymes β- and γ-secretase in the amyloidogenic pathway (Stakos et al., 2020). The length of the Aβ peptide produced by this cleavage is 38–42 amino acids, depending on the position where γ-secretase cleaves APP. It is largely the 42-amino acid peptide that aggregates into soluble oligomers, ultimately coalescing into extracellular plaques.

According to the AH, overproduction of APP or failure of clearance mechanisms causes amyloid accumulation (Mucke, 2009). As Aβ concentration increases, oligomers are formed, followed by plaques. Oligomers alter cell signaling and trigger release of toxic molecules by microglia. Oligomers and dimers prevent glutamate reuptake by astrocytes and neurons, leading to excitotoxicity, while plaques distort and damage axons and dendrites (Mucke, 2009; Selkoe, 2019; Zott et al., 2019). Tangle formation is due to Aβ activation of kinases catalyzing tau phosphorylation, neuroinflammation and cytokine release, reduced ability to degrade tau, and Aβ-induced impaired axonal transport (Blurton-Jones and Laferla, 2006; Silva et al., 2019).

Genetic evidence supports the AH. Mutations in three genes, *APP*, *PSEN1*, and *PSEN2*, contribute to early-onset AD. The *APP* gene encodes the amyloid precursor protein, while *PSEN1* and *PSEN2* encode presenilins (Lanoiselée et al., 2017). Genetic variants influencing Aβ and APP processing are also associated with later-onset dementia (dementia after 65) (Kunkle et al., 2019).

Mice models which overexpress APP develop plaques and memory impairment, but not NFTs. This may be due to absence of human tau in some mouse models (Selkoe and Hardy, 2016). Choi et al. (2014) demonstrated in human neural cell culture that mutations in *APP* and *PSEN1* produced extracellular amyloid plaques and tau pathology. Amyloid and tau were reduced through administration of β- or γ-secretase inhibitors, indicating that targeting Aβ peptide generation reduces plaques and tangles (Choi et al., 2014).

Further evidence in favor of the AH is described in Walsh and Selkoe (2020) and Selkoe and Hardy (2016). In Down's Syndrome an additional copy of Chromosome 21 produces an extra APP gene, causing the individual to display AD-like neuropathology. This is followed by microgliosis (proliferation and migration of microglia), astrocytosis (astrocyte proliferation in response to brain damage), and NFTs (Selkoe and Hardy, 2016). In contrast, mutations which reduce amyloid deposition protect against AD (Selkoe and Hardy, 2016). In general, early inherited AD is caused by APP mutations or in the proteins generating APP. These mutations, and corresponding biomarkers such as CSF Aβ concentration, may precede other pathologies including tau deposits (this may be disputed, see below), tissue atrophy, glucose hypometabolism, and cognitive decline by many years (Walsh and Selkoe, 2020). The apolipoprotein E4 (ApoE4) gene is expressed in more than 50 % of AD patients, and is the most common AD genetic risk factor (Safieh et al., 2019). ApoE4 increases Aβ production via its effect on γ-secretase activity, impairing lysosomal Aβ degradation, and possessing impaired ability to transport Aβ across the BBB (Safieh et al., 2019).

In contrast to the AH, some studies suggest Aβ is not the sole cause of AD. Tau correlates more strongly than amyloid with cognitive impairment (Bejanin et al., 2017). While genetic factors for late-onset AD include those affecting Aβ, others affect pathways related to tau binding proteins or alternate mechanisms (Kunkle et al., 2019). Subtle cognitive deficits may occur prior to or coincident with early amyloid build-up, suggesting AD may be initiated prior to amyloid pathology (Thomas et al., 2020). A counterargument in support of the AH is Aβ deposition may be an early event that initiates AD pathology and cognitive decline (Selkoe and Hardy, 2016). Aβ build-up may not be expected to correlate with cognitive performance in this interpretation.

Active immunization with Aβ prevents amyloid deposition in mouse models, although effectiveness of treatments is diminished in mice with extensive amyloid deposition (Das et al., 2001). Immunization causes mice to generate antibodies through Aβ exposure, enabling microglial to bind to and eliminate plaques. This therapy translated to humans reduced amyloid burden, however cognitive improvement was absent. Some patients demonstrated signs of severe dementia despite clearance of amyloid deposits (Holmes et al., 2008; Gallardo and Holtzman, 2017). Furthermore, 6% of immunized patients developed meningoencephalitis (Gilman et al., 2005).

Amyloid treatments may not be successful is amyloid removal via therapy causes amyloid to deposit on vessel walls, inducing hemorrhage and trapping toxic peptides within tissue in mice and humans (Wilcock et al., 2004; Patton et al., 2006). Another possibility is soluble Aβ surrounds the plaques and prevent the administered antibody from reaching the plaques in sufficient concentration (Dematteos et al., 2012).

Failures have also occurred with passive immunotherapies where an externally produced antibody is administered, as opposed to one internally generated through immunization. For example, bapineuzumab failed to reduce amyloid load or phosphorylated tau in cerebrospinal fluid (CSF) in phase 3 trials (Vandenberghe et al., 2016).

Several factors may contribute to failure of AH-based drugs beyond a simple assumption the AH is flawed. Amyloid deposition occurs many years prior to cognitive decline (Jack et al., 2013). Therapies may be administered by the time the effects of neuronal loss and tissue atrophy are irrevocable. This may be overcome in clinical trials using biomarkers to select patients with mild dementia attributable to early AD (Frisoni and Blennow, 2013). Selection of appropriate biomarkers to detect early AD or monitor progress is complex since numerous biomarkers are applicable, such as positron emission tomography (PET) amyloid imaging, fluorodeoxyglucose PET to detect

hypometabolism, CSF tau, MRI to detect brain atrophy, and CSF YKL-40 (an indicator of activated microglia) (Zetterberg and Bendlin, 2020).

In humans abnormally phosphorylated tau occurs in nerve cells or their processes prior to 30 years of age, and before extracellular amyloid plaques deposits (Braak and Del Tredici, 2011). Phosphorylated tau could spread to other brain regions, such as the brainstem and entorhinal cortex, contributing to AD (Jack et al., 2013). This appears to support the Tau Hypothesis (tau drives AD progression, see Section The Tau Hypothesis: Tau as a Driver of Neurodegeneration), suggesting that targeting amyloid may be ineffective if abnormal tau is not concurrently eliminated. An alternative interpretation is since tauopathy occurs in asymptomatic individuals, tauopathy may be an element of aging but not AD specifically (Jack et al., 2013). Tauopathy and Aβ pathology may occur independently, with tauopathy preceding Aβ deposition. Aβ accelerates tauopathy, eventually leading to NFTs in the neocortex (Musiek and Holtzman, 2012; Jack et al., 2013). This potentially occurs in mice, where breeding APP-transgenic with tau-transgenic mice increases tau deposition, but does not alter Aβ (Lewis et al., 2001; Selkoe and Hardy, 2016).

Aβ antibodies may not clear soluble oligomers, which are believed to more significantly influence synapse loss and cognition compared to plaques. Plaques serve as "reservoirs" of soluble and toxic Aβ, without being as directly toxic themselves (Koffie et al., 2009; Walsh and Selkoe, 2020). This characteristic may partially explain why some individuals with plaques do not appear to suffer cognitive consequences, since these cognitively normal individuals have a low ratio of soluble oligomer to plaque ratios (Walsh and Selkoe, 2020).

Challenges with drug therapies may not be due to Aβ specifically, but drug design. γ-secretase inhibitors potentially may inhibit Aβ accumulation by preventing cleavage at the γ-secretase site. Many γ-secretase inhibitors have been identified, however they are not specific for cleavage of APP. They also inhibit processing of Notch and other proteins involved in development, cell adhesion, hematopoiesis, and contacts between cells (Evin et al., 2006). This may induce serious side effects. Treatment with a γ-secretase inhibitor, semagacestat, was associated with cognitive decline and skin cancer as a side-effect. This skin cancer was potentially attributable to blocking Notch1 cleavage (Extance, 2010).

The Tau Hypothesis: Tau as a Driver of Neurodegeneration

In the Tau Hypothesis, tau (a microtubule-associated protein) replicates and spreads between cells. This causes neurodegeneration through mechanisms such as synaptic impairment and changes to mitochondrial structure and function through interactions between tau and actin (DuBoff et al., 2012; Kametani and Hasegawa, 2018). Phosphorylated tau induces cognitive deficits through decreasing the number of synapses and triggering cell death (Di et al., 2016).

In a PET study, the intensity of tau signal, but not Aβ, predicted the rate of tissue atrophy at early clinical AD stages (La Joie et al., 2020). Tau pathology could appear in healthy older adults without amyloid (Harrison et al., 2019), and may be present in brains of individuals with mild dementia absent Aβ pathology (de Paula et al., 2009). Extensive tau pathology is believed to occur as a result of Aβ accumulation, as demonstrated in neuronal cell cultures, mouse models, and genetic studies (Selkoe, 2011; Choi et al., 2014). This renders it unlikely to initiate AD by itself, although tau abnormalities may begin in childhood (Braak and Del Tredici, 2011).

Drugs targeting tau phosphorylation or aggregation have not successfully translated from mice to humans. For example, glycogen synthase kinase-3 (GSK3β) is a serine/threonine kinase facilitating tau hyperphosphorylation. In a mouse model overexpressing human mutant APP and tau, a GSK3β inhibitor affected multiple targets including reduced tau phosphorylation and amyloid deposition. This potentially protected against neuronal death and memory deficits through inhibiting the intrinsic mitochondrial signaling pathway to reduce cellular damage (Serenó et al., 2009). Clinical benefits were not obtained when a GSK-3 inhibitor, Tideglusib, was tested in clinical trials (Lovestone et al., 2015). Similar to Aβ therapies, possibly clinical trials of GSK-3 inhibitors are conducted at too late a disease stage to be effective (Hernandez et al., 2013).

Inflammation

In early AD, scavenger receptors (SRs) on microglia promote Aβ clearance (Wang et al., 2015). As amyloid builds, continual microglial interaction with Aβ via additional receptors (such as CD36) cause release of pro-inflammatory cytokines, leading to neuronal damage (Wang et al., 2015).

AD brains demonstrate chronic inflammation, with microglia displaying increased activity in AD patients (Liu et al., 2019). Amoeboid microglia indicating an activated inflammatory state are associated with Aβ, with microglial activation occurring following amyloidosis and neuronal injury, and possibly promoting tau accumulation (Suárez-Calvet et al., 2016; Hemonnot et al., 2019). Microglia may damage neurons directly as evident in axonal damage co-localizing with microglial cells *in vitro* (Park et al., 2018).

Inflammation may be a causative factor in AD. Epidemiology studies indicate a possible protective effective of anti-inflammatories (Andersen et al., 1995). Ibuprofen reduced amyloid deposition, cognitive decline, and inflammatory markers in transgenic mice (Lim et al., 2000; Van Dam et al., 2010). In wild type mice, a systemic prenatal immune challenge caused AD-like pathology, with elevation in inflammatory cytokines, increased hippocampal APP, and altered tau phosphorylation (Krstic et al., 2012).

A genetic risk associated with plaque clearance in AD is CD33 expression, a myeloid cell receptor expressed by microglia activated by glycoproteins and glycolipids and displayed on plaques (Hollingworth et al., 2011; Naj et al., 2011; Zhao, 2019). CD33 expression is elevated in AD, and deletion of the gene in the APP/PS1 mouse model reduces insoluble Aβ and plaque levels (Griciuc et al., 2013). The activated receptor recruits proteins such as SHP phosphatases that inhibit phagocytosis (Zhao, 2019). CD33 inhibitors are an area of drug development research,

although translation from mice to humans is challenging due to species differences in protein domain structure (Biber et al., 2019). Another transmembrane receptor found in microglia and neurons associated with AD is triggering receptor expressed by myeloid cells 2 (TREM2), which is involved in phagocytosis and preventing inflammatory mediator production (Doens and Fernández, 2014). TREM2 mutation reduces microglial clustering around plaques in mice and humans, resulting in enhanced neuritic dystrophy (Carmona et al., 2018).

Scheiblich et al., 2020 use a "Wave Model" to describe inflammation progression in AD. Pattern recognition receptors (PRRs) on microglia detect Aβ, followed by tau and other misfolded proteins. This activates proinflammatory pathways and toxic cytokines contributing to AD such as TNFα, IFNγ, ROS, and IL (interleukin)-1β, 4, 6, 9, 12, 23 (Mandrekar-Colucci and Landreth, 2010; Scheiblich et al., 2020). TNFα and IFNγ reduce levels of insulin degrading enzyme, impairing degradation of Aβ, and also impair microglial phagocytosis of Aβ (Mandrekar-Colucci and Landreth, 2010). The interleukins and TNFα trigger neuronal signaling leading to phosphatase inactivation and kinase activation, causing tau hyperphosphorylation, aggregation into toxic forms, and ultimately neuronal loss and dysfunction (Scheiblich et al., 2020). This neuronal loss is associated with altered concentrations of neurotransmitters, and enhanced astroglial and microglial proliferation (Scheiblich et al., 2020). An element of the inflammatory response is the NLRP3 inflammasome, which activates caspase-1 and ASC specks, which then bind to Aβ and induce its aggregation (Venegas et al., 2017; Scheiblich et al., 2020). The ASC specks may be absorbed by myeloid cells, resulting in sustained immunoactivity (Venegas et al., 2017).

Inflammation exerts effects on blood vessels through perivascular cells. In healthy tissue, perivascular macrophages (PVMs, macrophages contacting a vessel or within a cell thickness of a vessel) limit vessel permeability through maintenance of endothelial cell tight junctions, phagocytose pathogens, restrict inflammation, and control leukocyte movement across the vasculature (Lapenna et al., 2018). PVMs have a protective role by scavenging amyloid, as seen in a study in TgCRND8 mice where depletion of PVMs enhanced CAA load (Hawkes and McLaurin, 2009; Lapenna et al., 2018). However, Aβ stimulates PVM ROS release, contributing to cerebrovascular oxidative stress and vascular dysfunction through smooth muscle contraction (Lapenna et al., 2018). In wild-type mice where $A\beta_{40}$ was infused through the carotid artery, PVM depletion restores the ability of the vasculature to increase blood flow in response to functional stimulation or vasodilators (Park et al., 2017). The source of PVM-induced vascular dysfunction is Aβ in bloodstream that crosses the vascular wall, binding to CD36 (cell surface receptor) on PVMs and leading to Nox2 ROS production (Park et al., 2017; Lapenna et al., 2018).

Additional Factors Influencing Alzheimer's Progression

The Female Gender

Most AD patients are female (∼2/3), with females exhibiting reduced glucose metabolism in comparison with males (Mosconi et al., 2018). Menopause is believed to increase AD risk. Estrogen has protective effects such as reducing neuronal vulnerability to apoptosis through expression of anti-apoptotic proteins, and reducing oxidative stress through acting on mitochondria (Henderson and Brinton, 2010). Studies in 3xTg AD mice demonstrated ovariectomy reduced memory performance and increased Aβ accumulation (Carroll et al., 2007). Hormone replacement therapy has therefore been proposed to reduce AD risk. If administered prior to or at menopause in humans, glucose metabolism is preserved in regions susceptible to AD and prevents cognitive decline, potentially through increasing blood flow (Maki and Resnick, 2000; Brinton, 2008; Rasgon et al., 2014; Scheyer et al., 2018). This therapy is ineffective in postmenopausal women and is associated with an increased risk of AD (Savolainen-Peltonen et al., 2019). Long-term estrogen depletion may render an individual non-responsive to therapy due to decreased hippocampal estrogen-receptor-α (Scheyer et al., 2018). Alternatively, damage to mitochondria may cause estrogen to increase neurological damage (Brinton, 2008; Scheyer et al., 2018).

Abnormal Protein Disposal Mechanisms

Late onset AD is characterized by impaired Aβ clearance (Mawuenyega et al., 2010). Most Aβ is cleared through the BBB, although cerebrospinal fluid (CSF) contributes to Aβ clearance (Ramanathan et al., 2015). Subarachnoid CSF enters brain parenchyma through paravascular spaces around penetrating arteries. It mixes with interstitial fluid (ISF) in the brain interstitium, facilitated by aquaporin 4 (AQP4, a water channel protein) in astrocytes. This CSF-ISF mixture, via bulk flow or diffusion, travels through the tissue and is eliminated along paravascular spaces surrounding veins (Iliff et al., 2012; Reeves et al., 2020). The ISF bulk flow between these two pathways (i.e., para-arterial and paravenous routes) clears Aβ from the brain. Since ISF flow is mediated by AQP4 in cell membranes of astroglia, and due to its similarity to the lymphatic system, this pathway is termed the "glymphatic system" (Iliff et al., 2012). Ultimately, solutes (such as Aβ) and ISF diffuse to subarachnoid CSF, enter the bloodstream, or travel along the venular walls to the lymphatic system (Iliff et al., 2012). The importance of the glymphatic pathway is seen in the study by Xu et al. (2015), where AQP4 deletion in 12-month old APP/PS1 mice increased Aβ and cerebral amyloid angiopathy (CAA), as well as increased atrophy of astrocytes and memory impairment.

This fluid movement is driven largely by cardiac-generated penetrating arterial pulsation. This was shown in a mouse study where reducing pulsatility through internal carotid artery ligation reduces arterial pulsation and CSF-ISF exchange (Iliff et al., 2013). In a mathematical model, it was demonstrated that decreasing heart rate (and consequently arterial pulsations) and increasing arterial stiffness led to elevated brain Aβ deposition (Kyrtsos and Baras, 2015).

Plaque build-up along vessels contributes to reduced amyloid clearance. CAA increases arterial wall stiffness, reducing pulsatility and ISF movement (Reeves et al., 2020). Aβ deposition may also reduce space around arteries for fluid flow, increasing accumulation in tissue (Reeves et al., 2020).

Studies do not generally correlate vascular changes, such as microvessel density or tortuosity, with glymphatic clearance. Peng et al. (2016) found suppression of glymphatic transport in both aged (12–13 months) and young (3–4 months) APP/PS1 mice prior to significant Aβ deposits or CAA, when extensive vascular loss begins to occur. Since vessel density in APP/PS1 mice at 18-months does not differ between transgenic and age-matched controls (Hooijmans et al., 2007), it is reasonable to assume that the impaired glymphatic clearance at 3–13 months is not attributable to vessel loss. Mice models do experience changes in microvascular morphology at early time points prior to vascular loss (Durrant et al., 2020). It is conceivable that these morphological changes reflect dysfunctional vasculature, which could contribute to impaired Aβ clearance.

Aging contributes to impaired glymphatic clearance, since older mice experience a drop in penetrating arterial wall pulsatility, with a corresponding reduced ability to clear Aβ injected into brain tissue (Kress et al., 2014). In humans, loss of vascular compliance is associated with Aβ deposition, possibly due to structural changes in elastin (Fonck et al., 2009). Kress et al. (2014) propose that reduced compliance with aging is a contributor to reduced pulsatility. Alternatively, since astrocytes contact arteries via their endfeet, changes to astrocytes may occur during reactive astrogliosis that could affect arterial pulsatility (Kress et al., 2014).

Extracellular proteins may be degraded via cellular secretion of protein-degrading enzymes (Tarasoff-Conway et al., 2015). The two main routes of Aβ clearance in cells is through the ubiquitin-proteasome and autophagy-lysosome pathways (Perez et al., 2014). Due to reduced proteasome activity with aging, Aβ accumulates intracellularly, causing excessive lysosome activity that prevents cells from increasing protein degradation rate in response to stress (Ding et al., 2003; Perez et al., 2014).

Environmental Risk Factors

Nitrogen oxides and tobacco smoke are associated with greater dementia risk (Killin et al., 2016). Higher lead concentrations lead to an increased likelihood for AD, possibly attributable to astrocyte activation and alterations to tight junction proteins that induce BBB dysfunction (Killin et al., 2016).

While air particles may enter the body through lungs and blood stream, they commonly enter through the olfactory bulbs. A study (Calderón-Garcidueñas et al., 2010) of Mexico City residents found olfactory bulb inflammation and $A\beta_{42}$ accumulation in vessels, neurons, and glia. A significant contributor to $A\beta_{42}$ accumulation is ultrafine nanoparticles in the environment that promote oligomer formation/fibrillation (Linse et al., 2007; Calderón-Garcidueñas et al., 2010). They are dangerous because they are not bound to membranes, enabling access to organelles, and proteins (Calderón-Garcidueñas et al., 2010).

VASCULATURE IN ALZHEIMER'S DISEASE

Vessel damage in AD is present in vessels of all sizes. This includes flow reductions in large arteries in the Circle of Willis (Krucker et al., 2004) and penetrating arterioles displaying a twisted morphology (Dorr et al., 2012). Section Vasculature in Alzheimer's Disease below focuses on capillaries and microvasculature since capillary compression is a significant contributor to reduced CBF, and BBB damage may initiate or precede dementia (Cruz Hernández et al., 2019; Nation et al., 2019; Montagne et al., 2020).

The Aging Vasculature and Alzheimer's

Reduced capillary density with aging is attributed to diminished levels of angiogenic growth factors (such as VEGF), an imbalance between production of angiogenic and anti-angiogenic growth factors, and reduction of nitric oxide release and impaired vasodilation (Rivard et al., 1999; Ahluwalia et al., 2013; Ambrose, 2017).

Ambrose (2012) proposed the Neuroangiogenesis Hypothesis, wherein a decline in growth factors and angiogenic cytokines leads to a reduction in vessel density and cognition. Restoration of vessel density through administration of growth factors, such as VEGF, is proposed as a treatment to prevent development of AD symptoms (see Section Discussion).

In addition to vessel loss, aging is linked to increased capillary tortuosity and a thickened basement membrane (Østergaard et al., 2015). Pericytes are lost or become dysfunctional, causing BBB dysfunction and impaired flow regulation that decreases oxygen concentration in tissue (Kisler et al., 2017; Berthiaume et al., 2018). Aging may cause downregulation of the endothelial low density lipoprotein receptor 1 (LRP1) due to activation of protein kinase Cα (Silverberg et al., 2010). LRP1 eliminates Aβ proteins through the BBB, and its reduced concentration causes amyloid build-up.

Decreased neprilysin (the main Aβ degrading enzyme) in cells with aging leads to impaired amyloid clearance ability (Sasaguri et al., 2017). Aβ peptides (in particular the more soluble $A\beta_{40}$) therefore comprise a large proportion of atherosclerotic plaques (Kokjohn et al., 2011). Atherosclerosis develops prior to brain Aβ deposition and neural dysfunction in APP23 mice, indicating a possible contribution or connection between atherosclerosis and dementia (Tibolla et al., 2010). Most AD individuals display atherosclerosis in the Circle of Willis, with arteries to which blood is delivered by the Circle of Willis displaying decreased blood flow and increased pulsatility index (Gupta and Iadecola, 2015). Decreased blood flow causes tissue hypoxia and elevated Aβ production through increased β-secretase activity (Gupta and Iadecola, 2015). Increased arterial stiffening, as indicated by the elevated pulsatility index, transfers excessive pulsatile energy to capillaries (Wåhlin and Nyberg, 2019). This energy transfer leads to pericyte injury and BBB breakdown in the hippocampus, impairing memory function (Wåhlin and Nyberg, 2019).

Atherosclerosis and AD are associated with blood flow reductions, vessel occlusions, and arterial wall thickening. Differences exist between the conditions. Atherosclerosis is associated with cholesterol-rich arterial wall deposits, while AD is characterized by plaques and tangles leading to neuron loss. Deposition of Aβ plaques on blood vessels, as in CAA, further reduces blood flow. Whereas in atherosclerosis, many deposits are on major arteries (including outside the brain, such as the aorta), in AD deposits are located on intracerebral arterial

vasculature (Lathe et al., 2014), such as penetrating arterioles in TgCRND8 mice (Dorr et al., 2012) and capillaries in a human study (Hecht et al., 2018). Capillary deposits correspond to impaired blood flow in the APP23 mouse model (Thal et al., 2009). In humans, these deposits are associated with tissue microinfarcts in the hippocampus and cognitive decline (Hecht et al., 2018). In atherosclerosis, macrophages laden with cholesterol accumulate in vessel walls, diminishing blood flow to multiple tissues. Rupture of these plaques may lead to stroke or myocardial infarction (Lathe et al., 2014). While atherosclerosis and AD may share similarities, and atherosclerosis is a risk factor for AD, causes of reduced blood flow and tissue damage differ.

Vascular risk factors are prominent in aged populations. This may be due to aging-induced inflammation and cytokine release, leading to endothelial dysfunction and arterial stiffening (Sun, 2015). Hypertension is associated with microvascular abnormalities such as endothelial swelling and reduced capillary density (Boudier, 1999; Østergaard et al., 2015). This microvascular deficiency in hypertension is potentially aggravated by a deficiency in circulating insulin-like growth factor 1 (IGF-1) due to aging (Tarantini et al., 2016). However, a meta-analysis from our lab (ZP Feng) was not able to conclusively determine whether there was an increase or decrease in IGF-1 levels in AD subjects, indicating that IGF-1 may not be the source of microvascular dysfunction in AD (Ostrowski et al., 2016).

Cerebral Amyloid Angiopathy and the Vascular Hypothesis

In rodents, reductions in CBF increase Aβ deposition and induce memory deficits (Wang et al., 2016). Reduced blood flow may increase amyloid pathology through activation of β/γ-secretases that induces APP cleavage (Cai et al., 2017), through failure of Aβ drainage from the brain (Weller et al., 2008, 2009), or increased rate of tau phosphorylation (Koike et al., 2010). Aβ may deposit on artery walls or leptomeningeal vessels, and to a lesser extent capillaries (Preston et al., 2003; Thal et al., 2008; Weller et al., 2009). This is termed cerebral amyloid angiopathy (CAA), and is associated with vessel bleeding (Thal et al., 2009; Yates et al., 2014).

There are two main CAA subtypes: Type 1 occurs in cortical capillary walls, arterioles, leptomeningeal and cortical arteries, and venules/veins, whereas Type 2 does not occur in capillaries (Thal et al., 2002). Capillary CAA is regarded as a distinct CAA type, occurring in populations with a high ApoE4 allele frequency and correlating with AD pathology severity (Kövari et al., 2013). In arteries and veins, there is a higher ratio of $A\beta_{40}$:$A\beta_{42}$ compared to senile plaques, with a similar ratio in capillaries compared to senile plaques (Thal et al., 2008). Potentially, this higher ratio of $A\beta_{40}$ is due its solubility, enabling it move within perivascular drainage pathways and accumulate in vessel walls (Greenberg et al., 2020). CAA begins as small Aβ deposits on basement membranes of arteries, eventually depositing in the muscle cell layer (Thal et al., 2008). In severe cases, the smooth muscle cell layer deteriorates, and capillaries become occluded in mice and humans, reducing cerebral blood flow (Thal et al., 2008, 2009). CAA in mouse models is described in more detail by Klohs et al. (2014).

Understanding mechanisms by which CAA develops, or plaques deposit on the vasculature, is important in developing AD immunotherapies. Boche et al. (2008) analyzed brains of AD patients that died following immunization against $A\beta_{42}$. Compared to controls, immunized individuals demonstrated more frequent cortical microvascular lesions and microhemorrhages, with significantly more $A\beta_{42}$ deposited on cortical blood vessels and the leptomeninges. Solubilization of $A\beta_{42}$ via immunotherapies may overwhelm perivascular clearance pathways, leading to increased CAA (Greenberg et al., 2020).

Despite similarities between CAA and AD, these diseases are not identical. At least 60 % of individuals above 80 years old are afflicted with CAA, indicating CAA is not restricted to AD (Thal et al., 2008). CAA and AD share additional biomarkers such as cortical thinning and atrophy, cerebrovascular dysfunction, and tau deposition (Greenberg et al., 2020). Advanced CAA is associated with higher levels of cognitive impairment in AD (Greenberg et al., 2020), suggesting a link between aberrant vascular changes induced by CAA and AD development.

Linkages between vascular risk factors and dementia has led AD to be described as a vascular disorder. de la Torre and Mussivand (1993) proposed a hypothetical model where capillaries in brain aging undergo degeneration in response to amyloid deposits. This disturbs blood flow and causes proliferating glia produce APP (de la Torre and Mussivand, 1993; de la Torre, 1994). Factors contributing to brain dysfunction from impaired blood flow include decreased production of energy molecules such as ATP and failure to transmit signals between neurons.

Vascular-based hypotheses have implications for therapeutic targets. Anti-inflammatories, statins, and hypertension drugs are possible alternatives to targeting Aβ (Townsend and Praticò, 2005; Rius-Pérez et al., 2018). Anti-inflammatories reduce Aβ deposition and inflammation in mouse models (Yan et al., 2003; Heneka et al., 2005), with long-term administration of non-steroidal anti-inflammatory drugs lowering AD risk by 30–60% (Herrup, 2010).

Vascular Dysfunction and Morphology

Examples of abnormal capillary features include pits in vessel walls, loss of vascular innervation by neurons, and tortuous shaped vessels (Scheibel et al., 1989; de la Torre, 1994). An elevated number of non-perfused "string" vessels are present in AD, possibly explaining reduced flow despite occasional similar densities of capillaries between AD and healthy aging (Brown and Thore, 2011; Hunter et al., 2012).

Studies in mice support a role for Aβ in reducing CBF. Administration of $A\beta_{40}$ to cortex in wild type mice reduces cortical blood flow and diminishes CBF increases induced by vasodilators, probably through generation of ROS by $A\beta_{40}$ (Niwa et al., 2000). Mice over-expressing superoxide scavenging enzyme superoxide dismutase-1 (SOD1), or whose cortex was superfused with SOD, reverse vascular deficits induced by amyloid (Iadecola

et al., 1999; Niwa et al., 2000). $A\beta_{42}$ did not similarly influence resting CBF or endothelial response to vasodilators, suggesting that $A\beta_{40}$ may have a more significant vascular effect.

A potential mechanism underlying $A\beta_{40}$- and ROS-induced vascular dysfunction was elucidated in Park et al. (2014). Aβ activates innate immunity receptors on endothelial cells, leading to Nox2 production of superoxide. This superoxide reacts with nitric oxide (NO) produced in endothelial cells to produce peroxynitrite (PN). PN damages DNA, leading to a series of reactions that activate calcium-permeable ion channel TRPM2. This permits excessive Ca^{2+} entry into the cell, inducing the observed endothelial dysfunction such as vessel constriction, reduced blood flow, and vascular hyperpermeability. The potential of TRPM2 as a therapeutic target is evaluated further in the Section Discussion.

Endothelial dysfunction does not require plaque accumulation, only exposure to Aβ. This may explain blood flow reductions and observed microvascular abnormalities. Mice overexpressing APP and APP-derived Aβ peptides (Tg2123 and Tg2576) demonstrate blood flow reductions prior to plaque deposition, with the Tg2576 mouseline that possesses higher levels of Aβ demonstrating widespread reductions in CBF (Niwa et al., 2002). This may similarly occur in humans, as early CBF reductions occur prior to neuropathological changes and cerebrovascular responses to functional activation are impaired individuals at high AD risk (Smith et al., 1999; Niwa et al., 2000).

This suggests multiple phases of vascular dysfunction: one occurring prior to vessel loss, the second attributable to vascular destruction and regression. In humans, CBF deficits are present in the pre-dementia phase of AD, while blood volume changes indicative of vascular structural alterations are detected at the AD stage (Lacalle-Aurioles et al., 2014).

In the APP23 mouse model, at young ages prior to plaques, small deposits containing Aβ are found primarily attached to capillaries (Meyer et al., 2008). These deposits, associated with distorted microvessels, are proposed to alter local blood flow. This is believed to trigger increased amyloid production, ultimately resulting in vascular degeneration at older ages (Meyer et al., 2008). Since these deposits contain $A\beta_{42}$, this suggests a role for $A\beta_{42}$ in instigating vascular dysfunction, in addition to $A\beta_{40}$ discussed above. Similar capillary deposits have been observed in humans, lending support to the findings in mice (Miyakawa, 1997).

Studies in the APP/PS1 mouse model suggest capillary dysfunction prior to vessel loss. Despite similar cortical capillary length density in transgenic compared to wild-type mice at 18 months, cortical oxygen availability was reduced in the transgenic mice as indicated by reduced capillary blood flow and elevated capillary transit time heterogeneity at rest (Gutiérrez-Jiménez et al., 2018). This was attributed to factors such as abnormal cholinergic innervation of blood vessels, arterial contraction, or increased vessel tortuosity (Gutiérrez-Jiménez et al., 2018). Compared to wild types, APP/PS1 transgenic mice demonstrate increased blood flow and capillary flow homogenization in response to functional activation (Gutiérrez-Jiménez et al., 2018). The authors note in contrast to humans and other mouse models that display pericyte degeneration, pericyte numbers are not changed in the APP/PS1 model at 18-months. Vasodilation involving pericyte signaling, such as pericyte relaxation at the capillary wall (Hall et al., 2014), may be preserved, explaining the increased flow in response to functional activation (Gutiérrez-Jiménez et al., 2018).

In contrast to early blood flow reductions, some researchers record hyperperfusion in brain regions vulnerable to AD pathology in young, high-risk subjects (Fleisher et al., 2009; Bangen et al., 2012; Østergaard et al., 2013). This may be attributable to early capillary dysfunction that leads to reduced oxygen extraction by tissue from the microvasculature, causing a compensatory increase in CBF (Østergaard et al., 2013, 2015).

Angiogenesis and Alzheimer's Pathology

Vagnucci and Li (2003) proposed the "Angiogenesis Hypothesis." They observed drugs which reduce AD risk, such as statins, may possess anti-angiogenic properties. In addition, microvessel density is increased in AD (Perlmutter et al., 1990). In the Angiogenesis Hypothesis, neovascularization occurs in response to reduced blood flow and vascular injury due to inflammation. Pre-amyloid deposits on capillaries generate reactive oxygen species. This causes intravascular accumulation of thrombin and endothelial release of APP.

Studies in the Tg2576 mouse model suggest amyloid could trigger angiogenesis, causing BBB leakage and hypervascularity (Biron et al., 2011). This model demonstrates BBB disruption at 4-months, prior to plaque appearance (Ujiie et al., 2003). Aged (18–24 month old) Tg2576 mice displayed increased cortical microvessel density, similar to humans, corresponding with the degree of tight junction disruption (Biron et al., 2011). The hypervascularity observed in Tg2576 mice was reversed through immunization with Aβ (Biron et al., 2013). In mice, the anti-angiogenic bexarotene (an anti-cancer agent) clears Aβ and restores memory function (Cramer et al., 2012; Jefferies et al., 2013). However, angiogenic activation of endothelial cells occurs following cognitive decline in the APP23 mouse model (Schultheiss et al., 2006), suggesting angiogenesis may not initiate AD.

Some studies contradict the angiogenic properties of amyloid. Most human AD specimens display reduced vessel density (Brown and Thore, 2011). There is reduction in capillary density in white matter in 10-month old Tg2576 mice (Zhang et al., 2019), with Aβ inhibiting angiogenesis (Paris et al., 2004c) and potentially reducing vessel density in cortex and hippocampus (Paris et al., 2004a).

There are explanations for these discrepancies. Plaque deposits create "holes" in the vascular bed, while vessels proliferate around these holes (Meyer et al., 2008). An overall measure of vessel density may indicate loss of vessels due to holes, without accounting for the increase in vessels surrounding holes. A simultaneous loss and growth of vessels in human AD specimens has been observed (Desai et al., 2009). Despite the presence of angiogenic vessels in all brain regions, only the hippocampus demonstrated an increase in total capillary density (angiogenic plus non-angiogenic vessels) (Desai et al., 2009). Vessels may reside in a permanent angiogenic state, constantly growing and regressing in human studies (Desai

et al., 2009), resulting in no net change or even a loss of vessel density. See **Figure 1** for a diagram of vasculature in AD and healthy conditions.

Capillary density in AD models may be dependent on age or brain region. In the Tg2576 mouse model, at 5-months old cortical microvascular density is elevated, while at 27-months density is diminished (Giuliani et al., 2019). In the TgCRND8 mouse line, there is increased microvessel density at postnatal day 7 (Durrant et al., 2020), while in adulthood vessel density is reduced below controls in cortex (Religa et al., 2013). This elevated microvessel density at P7 was accompanied by increased microvessel tortuosity. This may indicate "pathological angiogenesis," or formation of dysfunctional blood vessels. In the same model (TgCRND8) at 6-months, a decrease in density was found in cortex, while it was increased in hippocampus relative to non-transgenic mice, suggesting a heterogenous angiogenic response depending on brain region (Maliszewska-Cyna et al., 2020).

The reduced vessel density at older ages might be attributable to the aging process and reduced expression of angiogenic growth factors. In brains without AD, decline in growth factors with aging, such as VEGF, fibroblast growth factor (FGF-1 and FGF-2), and angiopoietin, yield slow recovery in tissue wound injuries due to reduced angiogenic capabilities (Ambrose, 2017), or display reduced angiogenesis in response to hypoxia (Benderro and Lamanna, 2011). In a human study, Huang et al. (2013) found significant reduction in serum VEGF relative to both amnestic mild cognitive impairment and control (healthy) individuals. Transforming growth factor β1 (TGF-β1) (an angiogenic growth factor) serum concentration was reduced in AD, with the reduction in VEGF and TGF-β1 levels correlating with cognitive impairment severity (Huang et al., 2013). Huang et al. (2013) hypothesized this indicates reduction in angiogenic growth factors contribute to cognitive impairment. Since VEGF deposits with Aβ, it is possible that Aβ accumulation decreases available VEGF. This leads to reduced growth factor concentration available for angiogenesis, diminishing the number of blood vessels and inducing hypoperfusion (Huang et al., 2013). TGF-β1 reduction in AD patients has been recorded in another study, De Servi et al. (2002) verifying the findings of Huang et al. However, Kim and Kim (2012) recorded AD patients as possessing higher serum VEGF, while angiogenin (protein that stimulates angiogenesis) is reduced. Luppi et al. (2009) recorded significantly reduced VEGF, TGF- β1, and IGF-1 secreted by immune cells in AD patients. Together, these findings provide a potential explanation for reduced vessel density observed in AD.

Blood Brain Barrier Leakage and Disruption

The BBB is formed through tight junctions between endothelial cells, and regulates movement of ions and molecules between blood vessels and brain tissue. The BBB consists of multiple cell types in addition to endothelial cells, which together comprise the "Neurovascular Unit" (NVU). The cells types of the NVU include endothelial cells, pericytes, smooth muscle cells (arterial and venous), astrocytes, microglia, oligodendrocytes, and neurons (Sweeney et al., 2019).

This protects neural tissue from pathogens or toxins. BBB dysfunction due to brain injury is a risk factor for dementia, resulting in immune cell influx into tissue, perivascular inflammation, CBF alterations, and accumulation of molecules prone to aggregation (Abrahamson and Ikonomovic, 2020).

The BBB is a component of the Two-Hit Vascular Hypothesis (Sagare et al., 2012), where vasculature risk factors reduced blood flow or BBB dysfunction. Flow decreases may be induced by atherosclerosis (Gupta and Iadecola, 2015), while BBB damage could be caused by pericyte degeneration (Miners et al., 2018; Montagne et al., 2018; Wåhlin and Nyberg, 2019). These vascular risk factors and vascular damage are the "First Hit" which initiate Aβ deposition (the "Second Hit"). BBB dysfunction leads to neurotoxin accumulation and impaired Aβ clearance through the BBB. Reduced blood flow due to vascular damage also leads to elevated Aβ production. Together, accumulation of Aβ and hypoxic conditions initiate neuronal dysfunction, degeneration, and loss, causing dementia (Sagare et al., 2012).

BBB damage has consequences in not clearing Aβ and enabling toxins to enter brain tissue. In addition to LRP1 reduction with aging (see Section the Aging Vasculature and Alzheimer's), Receptor for Advanced Glycation End Products (RAGE) on endothelial cells binds circulating Aβ and transports it across the BBB (Deane et al., 2009). RAGE interaction with Aβ contributes to oxidative stress, reduced blood flow, and inflammation (Deane, 2012). BBB leakage causes plasma proteins such as albumin, fibrin, thrombin, and immune cells to enter tissue. These proteins and cells generate neuroinflammation and act on neurons and glia, damaging axons (Strickland, 2018; Klohs, 2019).

Since BBB impairment occurs prior to cognitive impairment or Aβ deposition (Klohs, 2019; Nation et al., 2019), BBB repair is an early target in AD. Due to the connection between neuronal damage, inflammation, and BBB, drugs developed to treat stroke have potential for translation to AD. 3K3A-APC, a drug for treating ischemic stroke, protects BBB through inhibition of endothelial apoptosis (Lazic et al., 2019). In a mouse model of AD administered 3K3A-APC daily for 4 months, neuronal production of Aβ was blocked through inhibition of β-secretase, neuroinflammation suppressed, BBB repaired, and CBF responses to stimulation restored (Lazic et al., 2019). This indicates a role for drugs that simultaneously reduce Aβ production, protect the vasculature, and suppress inflammation.

BBB leakage due to inflammation increases susceptibility to environmental pollutants. Tiny particles absorbed by alveoli circulate through the blood stream, where they may enter the brain, or trigger further inflammation (Peeples, 2020).

Imaging of Microvascular Dysfunction

One technique extensively applied to image the microvasculature in AD is 2-photon microscopy. 2-photon microscopy uses high intensity, long-wavelength laser light to excite fluorophores close to 1 mm deep into cortical tissue. The vasculature is typically imaged following a tail vein injection of a fluorescent

dye. Following imaging, the vasculature is segmented for quantification of structural properties of the network (Steinman et al., 2017, 2019). Blood flow simulations are performed on the vascular segmentations by approximating vessels as tubes (pipes), and application of equations which relate structural properties of the tube (length and diameter) to its blood flow resistance (Schmid et al., 2017).

An example of the benefits of flow simulations is seen in the study by Cruz Hernández et al. (2019), where blood flow reductions were calculated in simulations on mouse and human cortical vasculature due to capillary stalling. Observed flow reductions were attributed to the interconnectivity of the capillary network, where blockage of a single vessel reduces flow in downstream vessels.

Red blood cell (RBC) velocity in individual capillaries may be measured with 2-photon microscopy (Kleinfeld et al., 1998). This was demonstrated by Bennett et al. (2018) in tau P301L transgenic mice. Similar to Cruz Hernández et al. (2019), a number of very small diameter capillaries (<4 um diameter) contained leukocytes adhered to their walls, and flow that was restricted to plasma (i.e., RBCs were absent). These capillaries also demonstrated abnormal morphology, such as a spiral shape.

A metric of capillary network function is the variation in blood flow across the capillary network. In healthy tissue, there is a

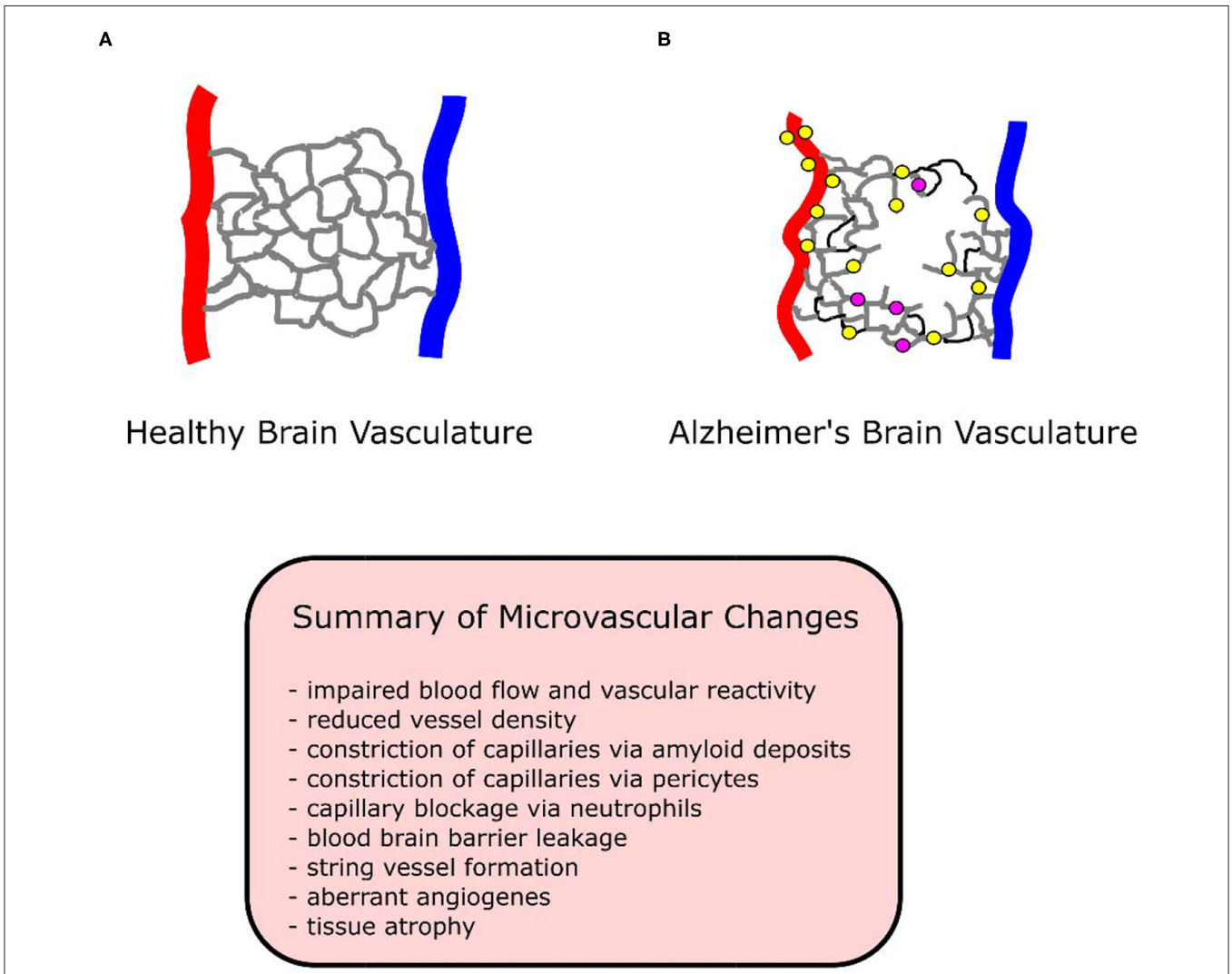

FIGURE 1 | Diagram of healthy and Alzheimer's brain vasculature. **(A)** Diagram of healthy brain vasculature. Penetrating arteries (*red*) and veins (*blue*) are connected via a capillary mesh (*gray*). **(B)** Diagram of Alzheimer's brain vasculature. Deposition of amyloid (*yellow dots*) in the vascular bed causes vascular dysfunction and loss in AD, with proliferation of vessels around missing vasculature (Meyer et al., 2008). String vessels (*black*) with no blood cells form as endothelial cells undergo apoptosis. Neutrophils (*purple dots*) stall a small portion (~2%) of capillaries, reducing blood flow in the network. Penetrating vessels have a tortuous shape, with a tendency to decrease in diameter with aging in AD (Dorr et al., 2012). Capillaries been reported to increase (trending) in diameter in APP/PS1 mice (Lu et al., 2019), experience swelling in APP23 mice (Meyer et al., 2008), decrease in diameter in P301L tau mice (Bennett et al., 2018), and to form "string" vessels with no flow or blood cells in humans (Hunter et al., 2012). Tissue undergoes atrophy, causing vascular shrinkage and functional brain deficits such as memory loss.

wide distribution of RBC velocities in capillaries, resulting in reduced oxygen extraction fraction (OEF) from blood vessels by tissues (Kleinfeld et al., 1998; Jespersen and Østergaard, 2012; Østergaard et al., 2015). In contrast, a more homogeneous RBC flux across capillaries and capillary oxygenation yields elevated OEF, which occurs in the case of neuronal stimulation (Li B. et al., 2019). Capillary flow patterns are affected by pericytes, dimensions of cells passing through capillaries, glycocalyx, blood composition, and adhesion of cells on vessel walls (Østergaard et al., 2015).

Capillary transit time (the time required for blood to pass through the capillary network) may be observed with 2-photon microscopy by monitoring the passage of a fluorescent dye through the network. A 2-photon study of the TgCRND8 mouse model demonstrated increased transit time dispersion (variability), together with increased transit time, indicative of decreased microvascular network efficiency (Dorr et al., 2012). Transit time dispersion was reduced to non-transgenic levels by treatment with scyllo-inositol, which reduces soluble and insoluble Aβ levels. Since Aβ damages endothelial cells, pericytes, and induces oxidative stress, removal of Aβ-induced endothelial dysfunction was interpreted as the reason for return to normal levels. These mice demonstrated an impaired hypercapnic response, which has been observed in both capillaries and arterioles in a transgenic rat model with amyloid and tau pathology (Joo et al., 2017). Impaired homogenization of transit times has been observed in the APP/PS1 mouse model in response to functional activation (Gutiérrez-Jiménez et al., 2018).

2-photon microscopy is not applicable to human studies as it requires invasive surgical procedures such as a craniotomy. Nielsen et al. (2017) performed perfusion MRI to calculate capillary transit time heterogeneity and mean transit time. Elevated mean transit time and capillary transit time heterogeneity in AD patients correlated with cortical thinning and poor cognitive performance. This study indicated a role for capillary dysfunction in contributing to cognitive decline in humans. Parameters measured in this study included CBF, microvascular cerebral blood volume, and tissue oxygen tension, whose reduction also correlated with poor cognitive performance (Nielsen et al., 2017).

In addition to transit time heterogeneity, MRI techniques (such as dynamic contrast enhanced MRI) may be used to evaluate BBB permeability (Raja et al., 2018).

The vascular changes discussed for the main mice models in this section (Section Vasculature in Alzheimer's Disease) are summarized in a **Table 1** below.

TABLE 1 | Summary of cerebral vascular changes in the main mouse models highlighted.

Mouseline	Vascular changes
TgCRND8	- Elevated cortical vessel density at P7 and increased microvascular tortuosity (Durrant et al., 2020) - Reduced cortical vascular density, increased hippocampal vessel density at 6 months (Maliszewska-Cyna et al., 2020). - Increased hippocampal non-capillary (arterial/venule) tortuosity (Maliszewska-Cyna et al., 2020). - Increased cortical penetrating arteriole tortuosity due to amyloid deposition. Longer transit time (relative to controls) and transit time variability. Hypercapnia results in transit time increase. No change in tortuosity of penetrating venules (Dorr et al., 2012; Lai et al., 2015)
Tg2576	- Widespread reductions in CBF at 2–3 months (Niwa et al., 2002) - BBB disruption at 4 months prior to plaques (Ujiie et al., 2003) - Increased cortical capillary density at 5 months when memory impaired and plaques not formed; capillary density diminished by 27 months (Giuliani et al., 2019) - Capillary density reduction in white matter at 10 months (Zhang et al., 2019)
APP/PS1	- Cerebral capillaries possess microaneurysms along their lengths, possible BBB breakdown, at 4–5 months prior to memory deficits; elevated cortical plaque number at this time point. No change in capillary diameter or length (Kelly et al., 2017) - No change in vessel density by 18 months, but elevated capillary transit time heterogeneity and reduced capillary blood flow at rest. Compared to wild types, demonstrate increased blood flow and capillary flow homogenization in response to functional activation (Gutiérrez-Jiménez et al., 2018)
APP23	- At young ages prior to plaques (4–6 months), deposits containing amyloid attach to capillaries; are associated with distorted blood vessels. The number and size of holes in the vascular bed increases. There are indicators of angiogenesis surrounding the holes (Meyer et al., 2008) - By 25–26 months, CAA-associated capillary occlusions in thalamus cause abnormal blood flow in perforating arteries (Thal et al., 2009)

DISCUSSION AND CONCLUDING THOUGHTS

Many research issues are unresolved. This includes, for example, the contributions of the various types of Aβ (monomers, soluble oligomers, and plaques/fibrillar Aβ) to AD (Hillen, 2019), and understanding why amyloid is unsuccessfully cleared and which mechanisms to clear plaques fail in a particular individual.

The AH was reviewed, including explanations for failures. Pathological mechanisms beyond amyloid were outlined. Interdisciplinary studies involving microvascular imaging and modeling in mouse models were highlighted, demonstrating microvascular malfunctions that exacerbate AD.

Despite promise in exploring alternative mechanisms, it is premature to abandon the AH. As noted in Walsh and Selkoe (2020), additional analyses of the Phase 3 aducanumab trials indicated that in one trial, there was an "∼40% less decline in activities of daily living than occurred on placebo." With another antibody (BAN2401) demonstrating success in a Phase 2b clinical trial (Walsh and Selkoe, 2020), there are indications that anti-Aβ therapies could reach a breakthrough.

It is important to investigate alternate avenues by which AD develops beyond Aβ. This affects strategies and approaches for designing research activities and development of treatments and drugs. For example, when plaques and tangles are both present, eliminating each simultaneously might be a preferred option rather than amyloid only. If neuroinflammation is widespread,

clearing amyloid without altering the inflammatory state may not reduce cognitive deficits.

There are numerous AD hypotheses in addition to Aβ, yet it is difficult to determine the relevancy of each hypothesis, since AD develops according to genetic, sex, and environmental factors that differ for each subject. AD could present in a variety of forms, with plaques and tangles in common (Frenkel, 2020). For example, atherosclerosis or cardiac dysfunction may appear in one AD patient, while be absent in another. This impacts the design of effective treatments since optimal therapies possibly should be "personalized" according to an individual's age, genetics, risk factors, and timing of diagnosis. Frenkel (2020) noted there is the potential of an "arsenal of drugs that can be used to personalize medicine for each patient in the spectrum of diseases associated with AD." This approach faces challenges, such as determining which "cocktail" of drugs to use and how drugs interact with one another.

Below are two approaches to treat AD with targeting Aβ: VEGF therapy and TRPM2 inhibition.

Non-amyloid Treatments

VEGF and Growth Factor Therapy

Due to reduced capillary density with aging, (Ambrose, 2012) proposed VEGF and growth factor administration for restoring capillary density and blood flow. A study in TgCRND8 AD mice overexpressing VEGF found partial recovery of vessel density and restoration of memory impairments, supporting enhancing vascular growth as a method for improving cognition (Religa et al., 2013).

There are factors to consider in applying this therapy to humans. VEGF in high concentrations may induce BBB leakage. Many newly formed vessels during angiogenesis are leaky with abnormal morphology (Vogel et al., 2004). Increasing vessel density alone does not necessarily elevate blood flow (Vogel et al., 2004). In VEGF-overexpressing mice subject to middle cerebral artery occlusion, flow is increased in regions outside the ischemic zone, but reduced within the ischemic/injured tissue core (Wang et al., 2005).

Ambrose (2012) reviews multiple methods for administering growth factors based on animal studies. These include: (1) intravenous delivery via a pump placed under the skin; (2) injection into CSF in ventricles; (3) injection into subarachnoid space above the cerebral hemispheres; (4) magnetic particles loaded with angiogenic factors that are held in the brain via a magnetic skullcap; (5) continuous release of growth factors via direct insertion of a growth factor releasing material into the brain; (6) surgical insertion (i.e., drilling holes in skull) of growth factor-loaded biodegradable material over cortex; (7) injection of growth factors into nasal cavity.

These delivery methods are complicated. For example, a pump placed under the skin would deliver VEGF throughout the body, not only the brain (Ambrose, 2012). Methods involving surgery (injection into CSF, drilling holes in skull) are invasive. A major issue is the growth factors to be delivered. Regrowth of vascular is more than increasing vessel number through administering VEGF. Newly formed vessels adjust their diameters, potentially differentiate into arteries or veins, and recruit support cells such as smooth muscle cells, pericytes, and fibroblasts to produce a functional vessel network (Gale and Yancopoulos, 1999). This network possesses optimal blood flow to satisfy tissue metabolic requirements, and may increase flow through adjusting diameters in response to functional activation of tissue. VEGF stimulates endothelial cell division and migration to form new vessels. Angiopoietin 1 (Ang1) facilitates communication between endothelial and support cells such as smooth muscle cells, stabilizing vessels and acting in conjunction with VEGF to produce a functional network (Gale and Yancopoulos, 1999). Delivery of a single growth factor, such as VEGF, risks producing vessel networks prone to leaks or hemorrhage (Yancopoulos et al., 2000). Expanding growth factor therapy to AD will require consideration of relative concentrations of naturally occurring growth factors unique to each subject and state of dementia, delivery method, and determining growth factors to administer (i.e., VEGF, Ang1 or 2, FGF, ephrins, etc.), quantity/concentration of growth factors to deliver, and length of time of treatment (i.e., single dose, multiple low-level doses, etc.).

A related therapy to growth factor administration that overcomes some deficiencies is exercise. Exercise increases concentration of a variety of angiogenic molecules such as Ang1 and 2, VEGF, fibroblast growth factor (FGF, upregulates VEGF, and induces vasodilation through nitric oxide), transforming growth factor (TGF, regulates extracellular matrix formation), and platelet derived growth factor (PDGF, mitogen for smooth muscle cells, fibroblasts, and glia cells) (Korivi et al., 2010). Mice provided access to running wheels demonstrated elevated brain microvascular efficiency (Dorr et al., 2017) and increased blood flow in the hippocampus (Cahill et al., 2017). In APP/PS1 mice, exercise restored vessel density and decreased capillary flow heterogeneity in cortex, likely indicating increased oxygen delivery (Lu et al., 2019). Exercise in TgCRND8 mice restored normal capillary density in cortex and hippocampus, and restored hippocampal arterial/venular tortuosity in AD mice to control levels (Maliszewska-Cyna et al., 2020). Since exercise did not alter parenchymal or vascular amyloid levels, improvements in short-term are possibly attributable to these vascular changes (Maliszewska-Cyna et al., 2020).

Inhibition of Transient Receptor Potential Melastatin 2 (TRPM2)

TRPM2 is a calcium-permeable ion channel expressed in multiple organs and cell types, including the brain (Turlova et al., 2018). It is activated in response to reactive oxygen species and oxidative stress, permitting calcium to enter the cell and causing neuronal death if the calcium concentration is sufficiently high (Turlova et al., 2018). Our labs demonstrated that eliminating TRPM2 expression or activity in neonatal hypoxic-ischemic injury improves behavioral performance and reduces tissue damage (Huang et al., 2017; Li F. et al., 2019).

Inhibition of TRPM2 activity demonstrates potential in AD. Ostapchenko et al. (2015) demonstrated that APP/PS1 TRPM2$^{-/-}$ mice display reduced microglial activation, reversal of memory deficits, and decreased synapse loss. Plaque load or soluble Aβ peptides were not altered, indicating potential for

recovery of cognitive function without directly affecting plaque concentration (Ostapchenko et al., 2015).

Activated TRPM2 damages tissue through several mechanisms. It promotes inflammation through cytokine production, and induces BBB dysfunction by allowing calcium into endothelial cells in response to oxidative stress (Belrose and Jackson, 2018). As previously mentioned, Aβ may cause endothelial and vascular dysfunction (such as arterial constriction) by increasing oxidative stress, activating a DNA repair enzyme that opens endothelial TRPM2 channels (Park et al., 2014). Since inhibiting or genetically deleting TRPM2 restores neural activity-induced CBF increases (Park et al., 2014), targeting TRPM2 has potential to restore cerebral vascular function in AD.

Potential mechanisms of TRPM2 action are highlighted in cell culture studies. In human pulmonary artery endothelial cell cultures, inhibition of TRPM2 via small interfering RNA decreased H_2O_2-induced intracellular calcium and the consequent increase in endothelial permeability (Hecquet et al., 2008). Ca^{2+} entry via TRPM2 may also initiate a process inducing endothelial dysfunction or apoptosis through actions on mitochondria. In cultured pancreatic β-cells in culture, increase in ROS activates TRPM2, causing Ca^{2+} cytoplasmic entry and Zn^{2+} release from lysosomes. Zn^{2+} binds to mitochondria, inhibiting the electron transport chain and leading to membrane potential loss that recruits dynamin-related protein1 (Drp1). Drp1 "slices" the mitochondria, causing mitochondrial fission and apoptosis (Li et al., 2017a,b). A similar process occurs in cultures of endothelial cells in response to increased ROS (Abuarab et al., 2017), with hippocampal neurons exposed to Aβ also demonstrating zinc accumulation in mitochondria and mitochondrial dysfunction (Li and Jiang, 2018).

Scalaradial, a marine extract, is a potent TRPM2 inhibitor, although it partially inhibits TRPM7 as well (Starkus et al., 2017). Its mechanism is unknown. Generally, while TRPM2 inhibitors exist, they lack potency or are non-specific (Starkus et al., 2017).

Looking Ahead and Thoughts

Restoring blood flow in early stages of AD progression could limit dementia progression. Korte et al. (2020) outline additional therapeutic approaches targeting blood flow. Capillary constriction via pericytes occurs via Aβ-oligomer production of ROS from pericytes and microglia and activation of endothelin A receptors that bind endothelin (a vasoconstrictor). Relaxing pericytes via voltage-gated calcium channel (VGCC) inhibition is a therapeutic target, with a VGCC-inhibitor (nilvadipine, normally used for hypertension) restoring cortical CBF in 13-month old Tg2576 mice, and hippocampal CBF in humans with mild-moderate AD (Paris et al., 2004b; de Jong et al., 2019; Korte et al., 2020). Additional therapies suggested by Korte et al. (2020) include preventing occluded capillaries through neutrophil targeting and anticoagulants to enhance blood flow. However, depletion of neutrophils may lead to infection, while anticlotting agents could induce hemorrhage (Korte et al., 2020).

A limitation in developing vascular-based drugs is animal models. A 3D microscopy analysis revealed amyloid plaques in human tissue were larger and more complex than those in mice, displaying a wider variety of sizes and shapes compared to those in mice (Liebmann et al., 2016). Consequently, successful removal of plaques from mice does not necessarily correspond to an identical situation in humans. Other limitations of transgenic rodent models are detailed in Braidy et al. (2012) such as difficulties in modeling tau pathology and lack of neurodegeneration. *In vitro* models, while valuable for investigating molecular mechanisms, face limits in translation to humans due to inability to account for multiple cellular interactions that affect endothelial cells. Progress has been made on this front through development of a 3D *in vitro* microfluidic culture model containing neurons (developed from progenitor cells) with mutations in APP and APP/PS1 genes, aggregation of extracellular Aβ, hyperphosphorylated tau, and mimicking BBB disruption with aggregation of Aβ on vascular wall (Choi et al., 2014; Kim et al., 2015; Shin et al., 2019). This culture model could be used to screen whether drugs cross the BBB and their effect on different cell types (Shin et al., 2019).

Despite our vascular focus, AD pathology may be improved through treatments that induce negative vascular effects. For example, nilotinib, a tyrosine kinase inhibitor normally used to treat leukemia, was administered to individuals with AD mild to moderate dementia in a phase 2 clinical trial (Turner et al., 2020). Nilotinib reduced CSF Aβ (40 and 42), minimized hippocampal volume loss, and reduced frontal lobe amyloid (Turner et al., 2020). However, nilotinib inhibits endothelial cell proliferation in culture, while inhibiting angiogenesis and blood flow following hind-limb ischemia in mice (Hadzijusufovic et al., 2017). Arterial occlusive disease developed in nilotinib-treated patients, while atherosclerosis and a pro-atherogenic phenotype was promoted in mice models and endothelial cultures respectively (Hadzijusufovic et al., 2017).

Early AD detection is necessary to deliver treatment prior to permanent tissue damage. Kosik (2013) proposed observing activity of collections of neurons, which may show subtle alterations not detectable with standard neuropsychological testing. Such changes could be detectable with resting state functional MRI to monitor connectivity between brain regions (Brier et al., 2014). This is supported by findings in mice, where regional neuronal activity determines location of Aβ deposition (Bero et al., 2011). Some studies note that in humans reduced blood flow precedes cognitive decline (Iturria-Medina et al., 2016), with impaired reactivity to hypercapnia a biomarker of disease (Glodzik et al., 2013).

It is necessary to consider multiple avenues by which AD develops beyond strictly Aβ in developing pharmacological approaches. The AH remains prominent, although reservations have been raised as to its underlying assumption of amyloid as the central feature of AD pathology. As research continues testing more hypotheses, a continued flexibility in approach is required beyond the belief that eliminating plaques/Aβ alone will lead to a cure.

A single treatment approach could be considered for early onset AD since this form of the disease is often dependent on APP-related genetics. Most cases, however, are late-onset

and depend on genetic elements beyond Aβ. Consideration should be given to treating multiple mechanisms simultaneously, such as removing plaques through antibodies and reducing inflammation through non-steroidal anti-inflammatories. This approach does not entail abandoning Aβ, but viewing it as an important element of AD pathology that acts in combination with other mechanisms.

To target multiple sites, there are issues to be addressed. For example, is amyloid build-up due to decreased LRP1 expression at the blood brain barrier, reduced neprilysin production, or the glymphatic system and arterial stiffening? And how can these be detected through imaging or biomarkers? To address these issues, the investigator requires understanding the biological mechanisms involved in disease progression, and consequences of therapeutic targeting of these mechanisms while omitting others.

Future research will continue to focus on the many issues covered in this review. Hopefully, this will lead to new research directions and treatments, and improve or prevent cognitive decline in patients.

AUTHOR CONTRIBUTIONS

All authors listed have made a substantial, direct and intellectual contribution to the work, and approved it for publication.

ACKNOWLEDGMENTS

This work was supported by grants from Canadian Institutes of Health Research to ZPF (PJT-153155) and the Natural Sciences and Engineering Research Council of Canada to HSS (RGPIN-2016-04574).

REFERENCES

Abrahamson, E. E., and Ikonomovic, M. D. (2020). Brain injury-induced dysfunction of the blood brain barrier as a risk for dementia. *Exp. Neurol.* 328:113257. doi: 10.1016/j.expneurol.2020.113257

Abuarab, N., Munsey, T. S., Jiang, L. H., Li, J., and Sivaprasadarao, A. (2017). High glucose-induced ROS activates TRPM2 to trigger lysosomal membrane permeabilization and Zn2+-mediated mitochonfrial fission. *Sci. Signal.* 10:eaa14161. doi: 10.1126/scisignal.aal4161

Ahluwalia, A., Jones, M. K., Deng, X., Sandor, Z., Szabo, S., and Tarnawski, A. S. (2013). An imbalance between VEGF and endostatin underlies impaired angiogenesis in gastric mucosa of aging rats. *Am. J. Physiol. Gastrointest. Liver Physiol.* 305, G325–G332. doi: 10.1152/ajpgi.00127.2013

Ambrose, C. T. (2012). Neuroangiogenesis: a vascular basis for Alzheimer's disease and cognitive decline during aging. *J. Alzheimers Dis.* 32, 773–788. doi: 10.3233/JAD-2012-120067

Ambrose, C. T. (2017). Pro-angiogenesis therapy and aging: a mini-review. *Gerontology* 63, 393–400. doi: 10.1159/000477402

Andersen, K., Launer, L. J., Ott, A., Hoes, A. W., Breteler, M. M., and Hofman, A. (1995). Do nonsteroidal anti-inflammatory drugs decrease the risk for Alzheimer's disease? The Rotterdam Study. *Neurology* 45, 1441–1445. doi: 10.1212/WNL.45.8.1441

Bangen, K. J., Restom, K., Liu, T. T., Wierenga, C. E., Jak, A. J., Salmon, D. P., et al. (2012). Assessment of Alzheimer's disease risk with functional magnetic resonance imaging: an arterial spin labeling study. *J. Alzheimers Dis.* 31(Suppl 3), S59–S74. doi: 10.3233/JAD-2012-120292

Bejanin, A., Schonhaut, D. R., La Joie, R., Kramer, J. H., Baker, S. L., Sosa, N., et al. (2017). Tau pathology and neurodegeneration contribute to cognitive impairment in Alzheimer's disease. *Brain* 140, 3286–3300. doi: 10.1093/brain/awx243

Belrose, J. C., and Jackson, M. F. (2018). TRPM2: a candidate therapeutic target for treating neurological diseases. *Acta Pharmacol. Sin* 39, 722–732. doi: 10.1038/aps.2018.31

Benderro, G. F., and Lamanna, J. C. (2011). Hypoxia-induced angiogenesis is delayed in aging mouse brain. *Brain Res.* 1389, 50–60. doi: 10.1016/j.brainres.2011.03.016

Bennett, R. E., Robbins, A. B., Hu, M., Cao, X., Betensky, R. A., Clark, T., et al. (2018). Tau induces blood vessel abnormalities and angiogenesis-related gene expression in P301L transgenic mice and human Alzheimer's disease. *Proc. Natl. Acad. Sci. U. S. A.* 115, E1289–E1298. doi: 10.1073/pnas.1710329115

Bero, A. W., Yan, P., Roh, J. H., Cirrito, J. R., Stewart, F. R., Raichle, M. E., et al. (2011). Neuronal activity regulates the regional vulnerability to amyloid-β deposition. *Nat. Neurosci.* 14, 750–756. doi: 10.1038/nn.2801

Berthiaume, A. A., Grant, R. I., McDowell, K. P., Underly, R. G., Hartmann, D. A., Levy, M., et al. (2018). Dynamic remodeling of pericytes *in vivo* maintains capillary coverage in the adult mouse brain. *Cell Rep.* 22, 8–16. doi: 10.1016/j.celrep.2017.12.016

Bertram, L., and Tanzi, R. E. (2019). Alzheimer disease risk genes: 29 and counting. *Nat. Rev. Neurol.* 15, 191–192. doi: 10.1038/s41582-019-0158-4

Biber, K., Bhattacharya, A., Campbell, B. M., Piro, J. R., Rohe, M., Staal, R. G. W., et al. (2019). Microglial drug targets in AD: opportunities and challenges in drug discovery and development. *Front. Pharmacol.* 10:840. doi: 10.3389/fphar.2019.00840

Biron, K. E., Dickstein, D. L., Gopaul, R., Fenninger, F., and Jefferies, W. A. (2013). Cessation of neoangiogenesis in Alzheimer's disease follows amyloid-beta immunization. *Sci. Rep* 3:1354. doi: 10.1038/srep01354

Biron, K. E., Dickstein, D. L., Gopaul, R., and Jefferies, W. A. (2011). Amyloid triggers extensive cerebral angiogenesis causing blood brain barrier permeability and hypervascularity in Alzheimer's disease. *PLoS One* 6:e23789. doi: 10.1371/journal.pone.0023789

Blurton-Jones, M., and Laferla, F. M. (2006). Pathways by which Abeta facilitates tau pathology. *Curr. Alzheimer Res.* 3, 437–448. doi: 10.2174/156720506779025242

Boche, D., Zotova, E., Weller, R. O., Love, S., Neal, J. W., Pickering, R. M., et al. (2008). Consequence of Abeta immunization on the vasculature of human Alzheimer's disease brain. *Brain* 131(Pt 12), 3299–3310. doi: 10.1093/brain/awn261

Boudier, H. A. (1999). Arteriolar and capillary remodelling in hypertension. *Drugs* 58, 37–40.

Braak, H., and Del Tredici, K. (2011). The pathological process underlying Alzheimer's disease in individuals under thirty. *Acta Neuropathol.* 121, 171–181. doi: 10.1007/s00401-010-0789-4

Bracko, O., Njiru, B. N., Swallow, M., Ali, M., Haft-Javaherian, M., and Schaffer, C. B. (2020). Increasing cerebral blood flow improves cognition into late stages in Alzheimer's disease mice. *J. Cereb. Blood Flow Metab.* 40, 1441–1452. doi: 10.1177/0271678X19873658

Braidy, N., Muñoz, P., Palacios, A. G., Castellano-Gonzalez, G., Inestrosa, N. C., Chung, R. S., et al. (2012). Recent rodent models for Alzheimer's disease: clinical implications and basic research. *J Neural Transm.* 119, 173–195. doi: 10.1007/s00702-011-0731-5

Brier, M. R., Thomas, J. B., and Ances, B. M. (2014). Network dysfunction in Alzheimer's disease: refining the disconnection hypothesis. *Brain Connect.* 4, 299–311. doi: 10.1089/brain.2014.0236

Brinton, R. D. (2008). The healthy cell bias of estrogen action: mitochondrial bioenergetics and neurological implications. *Trends Neurosci.* 31, 529–537. doi: 10.1016/j.tins.2008.07.003

Brown, W. R., and Thore, C. R. (2011). Review: cerebral microvascular pathology in ageing and neurodegeneration. *Neuropathol. Appl. Neurobiol.* 37, 56–74. doi: 10.1111/j.1365-2990.2010.01139.x

Cahill, L. S., Bishop, J., Gazdzinski, L. M., Dorr, A., Stefanovic, B., and Sled, J. G. (2017). Altered cerebral blood flow and cerebrovascular function

after voluntary exercise in adult mice. *Brain Struct. Funct.* 222, 3395–3405. doi: 10.1007/s00429-017-1409-z

Cai, Z., Liu, Z., Xiao, M., Wang, C., and Tian, F. (2017). Chronic cerebral hypoperfusion promotes amyloid-beta pathogenesis via activating β/γ-secretases. *Neurochem. Res.* 42, 3446–3455. doi: 10.1007/s11064-017-2391-9

Calderón-Garcidueñas, L., Franco-Lira, M., Henríquez-Roldán, C., Osnaya, N., González-Maciel, A., Reynoso-Robles, R., et al. (2010). Urban air pollution: influences on olfactory function and pathology in exposed children and young adults. *Exp. Toxicol. Pathol.* 62, 91–102. doi: 10.1016/j.etp.2009.02.117

Carmona, S., Zahs, K., Wu, E., Dakin, K., Bras, J., and Guerreiro, R. (2018). The role of TREM2 in Alzheimer's disease and other neurodegenerative disorders. *Lancet Neurol.* 17, 721–730. doi: 10.1016/S1474-4422(18)30232-1

Carroll, J. C., Rosario, E. R., Chang, L., Stanczyk, F. Z., Oddo, S., LaFerla, F. M., et al. (2007). Progesterone and estrogen regulate Alzheimer-like neuropathology in female 3xTg-AD mice. *J. Neurosci.* 27, 13357–13365. doi: 10.1523/JNEUROSCI.2718-07.2007

Choi, S. H., Kim, Y. H., Hebisch, M., Sliwinski, C., Lee, S., D'Avanzo, C., et al. (2014). A three-dimensional human neural cell culture model of Alzheimer's disease. *Nature* 515, 274–278. doi: 10.1038/nature13800

Cramer, P. E., Cirrito, J. R., Wesson, D. W., Lee, C. Y., Karlo, J. C., Zinn, A. E., et al. (2012). ApoE-directed therapeutics rapidly clear β-amyloid and reverse deficits in AD mouse models. *Science* 335, 1503–1506. doi: 10.1126/science.1217697

Cruz Hernández, J. C., Bracko, O., Kersbergen, C. J., Muse, V., Haft-Javaherian, M., Berg, M., et al. (2019). Neutrophil adhesion in brain capillaries reduces cortical blood flow and impairs memory function in Alzheimer's disease mouse models. *Nat. Neurosci.* 22, 413–420. doi: 10.1038/s41593-018-0329-4

Das, P., Murphy, M. P., Younkin, L. H., Younkin, S. G., and Golde, T. E. (2001). Reduced effectiveness of Aβ1-42 immunization in APP transgenic mice with significant amyloid deposition. *Neurobiol. Aging* 22, 721–727. doi: 10.1016/S0197-4580(01)00245-7

de Jong, D. L. K., de Heus, R. A. A., Rijpma, A., Donders, R., Olde Rikkert, M. G. M., Günther, M., et al. (2019). Effects of nilvadipine on cerebral blood flow in patients with Alzheimer disease. *Hypertension* 74, 413–420. doi: 10.1161/HYPERTENSIONAHA.119.12892

de la Torre, J. C. (1994). Impaired brain microcirculation may trigger Alzheimer's disease. *Neurosci. Biobehav. Rev.* 18, 397–401. doi: 10.1016/0149-7634(94)90052-3

de la Torre, J. C., and Mussivand, T. (1993). Can disturbed brain microcirculation cause Alzheimer's disease? *Neurol. Res.* 15, 146–153. doi: 10.1080/01616412.1993.11740127

de Paula, V. J. R., Guimarães, F. M., Diniz, B. S., and Forlenza, O. V. (2009). Neurobiological pathways to Alzheimer's disease: amyloid-β, TAU protein or both? *Dement. Neuropsychol.* 3, 188–194. doi: 10.1590/S1980-57642009DN30300003

De Servi, B., La Porta, C. A., Bontempelli, M., and Comolli, R. (2002). Decrease of TGF-β1 plasma levels and increase of nitric oxide synthase activity in leukocytes as potential biomarkers of Alzheimer's disease. *Exp. Gerontol.* 37, 813–821. doi: 10.1016/S0531-5565(02)00018-9

Deane, R., Bell, R. D., Sagare, A., and Zlokovic, B. V. (2009). Clearance of amyloid-beta peptide across the blood-brain barrier: implication for therapies in Alzheimer's disease. *CNS Neurol. Disord. Drug Targets* 8, 16–30. doi: 10.2174/187152709787601867

Deane, R. J. (2012). Is RAGE still a therapeutic target for Alzheimer's disease? *Future Med. Chem.* 4, 915–925. doi: 10.4155/fmc.12.51

Demattos, R. B., Lu, J., Tang, Y., Racke, M. M., Delong, C. A., Tzaferis, J. A., et al. (2012). A plaque-specific antibody clears existing β-amyloid plaques in Alzheimer's disease mice. *Neuron* 76, 908–920. doi: 10.1016/j.neuron.2012.10.029

Desai, B. S., Schneider, J. A., Li, J. L., Carvey, P. M., and Hendey, B. (2009). Evidence of angiogenic vessels in Alzheimer's disease. *J. Neural Transm.* 116, 587–597. doi: 10.1007/s00702-009-0226-9

Di, J., Cohen, L. S., Corbo, C. P., Phillips, G. R., El Idrissi, A., and Alonso, A. D. (2016). Abnormal tau induces cognitive impairment through two different mechanisms: synaptic dysfunction and neuronal loss. *Sci. Rep.* 6:20833. doi: 10.1038/srep20833

Ding, Q., Dimayuga, E., Martin, S., Bruce-Keller, A. J., Nukala, V., Cuervo, A. M., et al. (2003). Characterization of chronic low-level proteasome inhibition on neural homeostasis. *J. Neurochem.* 86, 489–497. doi: 10.1046/j.1471-4159.2003.01885.x

Doens, D., and Fernández, P. L. (2014). Microglia receptors and their implications in the response to amyloid β for Alzheimer's disease pathogenesis. *J. Neuroinflammation* 11:48. doi: 10.1186/1742-2094-11-48

Dorr, A., Sahota, B., Chinta, L. V., Brown, M. E., Lai, A. Y., Ma, K., et al. (2012). Amyloid-β-dependent compromise of microvascular structure and function in a model of Alzheimer's disease. *Brain* 135(Pt 10), 3039–3050. doi: 10.1093/brain/aws243

Dorr, A., Thomason, L. A., Koletar, M. M., Joo, I. L., Steinman, J., Cahill, L. S., et al. (2017). Effects of voluntary exercise on structure and function of cortical microvasculature. *J. Cereb. Blood Flow Metab.* 37, 1046–1059. doi: 10.1177/0271678X16669514

DuBoff, B., Götz, J., and Feany, M. B. (2012). Tau promotes neurodegeneration via DRP1 mislocalization *in vivo*. *Neuron* 75, 618–632. doi: 10.1016/j.neuron.2012.06.026

Durrant, C. S., Ruscher, K., Sheppard, O., Coleman, M. P., and Özen, I. (2020). Beta secretase 1-dependent amyloid precursor protein processing promotes excessive vascular sprouting through NOTCH3 signalling. *Cell Death Dis.* 11, 98. doi: 10.1038/s41419-020-2288-4

Evin, G., Sernee, M. F., and Masters, C. L. (2006). Inhibition of gamma-secretase as a therapeutic intervention for Alzheimer's disease: prospects, limitations and strategies. *CNS Drugs* 20, 351–372. doi: 10.2165/00023210-200620050-00002

Extance, A. (2010). Alzheimer's failure raises questions about disease-modifying strategies. *Nat. Rev. Drug Discov.* 9, 749–751. doi: 10.1038/nrd3288

Farkas, E., and Luiten, P. G. (2001). Cerebral microvascular pathology in aging and Alzheimer's disease. *Prog. Neurobiol.* 64, 575–611. doi: 10.1016/S0301-0082(00)00068-X

Ferretti, M. T., Iulita, M. F., Cavedo, E., Chiesa, P. A., Schumacher Dimech, A., Santuccione Chadha, A., et al. (2018). Sex differences in Alzheimer disease - the gateway to precision medicine. *Nat. Rev. Neurol.* 14, 457–469. doi: 10.1038/s41582-018-0032-9

Ferris, S. H., and Farlow, M. (2013). Language impairment in Alzheimer's disease and benefits of acetylcholinesterase inhibitors. *Clin. Interv. Aging* 8, 1007–1014. doi: 10.2147/CIA.S39959

Fleisher, A. S., Podraza, K. M., Bangen, K. J., Taylor, C., Sherzai, A., Sidhar, K., et al. (2009). Cerebral perfusion and oxygenation differences in Alzheimer's disease risk. *Neurobiol. Aging* 30, 1737–1748. doi: 10.1016/j.neurobiolaging.2008.01.012

Floden, A. M., Li, S., and Combs, C. K. (2005). Beta-amyloid-stimulated microglia induce neuron death via synergistic stimulation of tumor necrosis factor alpha and NMDA receptors. *J. Neurosci.* 25, 2566–2575. doi: 10.1523/JNEUROSCI.4998-04.2005

Fonck, E., Feigl, G. G., Fasel, J., Sage, D., Unser, M., Rüfenacht, D. A., et al. (2009). Effect of aging on elastin functionality in human cerebral arteries. *Stroke* 40, 2552–2556. doi: 10.1161/STROKEAHA.108.528091

Frenkel, D. (2020). Alzheimer's disease: a need for personalized therapeutic approaches. *Drug Dev. Res.* 81, 141–143. doi: 10.1002/ddr.21652

Frisoni, G. B., and Blennow, K. (2013). Biomarkers for Alzheimer's: the sequel of an original model. *Lancet Neurol.* 12, 126–128. doi: 10.1016/S1474-4422(12)70305-8

Gale, N. W., and Yancopoulos, G. D. (1999). Growth factors acting via endothelial cell-specific receptor tyrosine kinases: VEGFs, angiopoietins, and ephrins in vascular development. *Genes Dev.* 13, 1055–1066. doi: 10.1101/gad.13.9.1055

Gallardo, G., and Holtzman, D. M. (2017). Antibody therapeutics targeting Aβ and tau. *Cold Spring Harb. Perspect. Med.* 7:a024331. doi: 10.1101/cshperspect.a024331

Gilman, S., Koller, M., Black, R. S., Jenkins, L., Griffith, S. G., Fox, N. C., et al. (2005). Clinical effects of Aβ immunization (AN1792) in patients with AD in an interrupted trial. *Neurology* 64, 1553–1562. doi: 10.1212/01.WNL.0000159740.16984.3C

Giuliani, A., Sivilia, S., Baldassarro, V. A., Gusciglio, M., Lorenzini, L., Sannia, M., et al. (2019). Age-related changes of the neurovascular unit in the cerebral cortex of Alzheimer disease mouse models: a neuroanatomical and molecular study. *J. Neuropathol. Exp. Neurol.* 78, 101–112. doi: 10.1093/jnen/nly125

Glodzik, L., Randall, C., Rusinek, H., and de Leon, M. J. (2013). Cerebrovascular reactivity to carbon dioxide in Alzheimer's disease. *J. Alzheimers Dis.* 35, 427–440. doi: 10.3233/JAD-122011

Govindpani, K., McNamara, L. G., Smith, N. R., Vinnakota, C., Waldvogel, H. J., Faull, R. L., et al. (2019). Vascular dysfunction in Alzheimer's disease: a prelude to the pathological process or a consequence of it? *J. Clin. Med.* 8:651. doi: 10.3390/jcm8050651

Greenberg, S. M., Bacskai, B. J., Hernandez-Guillamon, M., Pruzin, J., Sperling, R., and van Veluw, S. J. (2020). Cerebral amyloid angiopathy and Alzheimer disease - one peptide, two pathways. *Nat. Rev. Neurol.* 16, 30–42. doi: 10.1038/s41582-019-0281-2

Griciuc, A., Serrano-Pozo, A., Parrado, A. R., Lesinski, A. N., Asselin, C. N., Mullin, K., et al. (2013). Alzheimer's disease risk gene CD33 inhibits microglial uptake of amyloid beta. *Neuron* 78, 631–643. doi: 10.1016/j.neuron.2013.04.014

Gupta, A., and Iadecola, C. (2015). Impaired Aβ clearance: a potential link between atherosclerosis and Alzheimer's disease. *Front. Aging Neurosci.* 7:115. doi: 10.3389/fnagi.2015.00115

Gutiérrez-Jiménez, E., Angleys, H., Rasmussen, P. M., West, M. J., Catalini, L., Iversen, N. K., et al. (2018). Disturbances in the control of capillary flow in an aged APP. *Neurobiol. Aging* 62, 82–94. doi: 10.1016/j.neurobiolaging.2017.10.006

Hadzijusufovic, E., Albrecht-Schgoer, K., Huber, K., Hoermann, G., Grebien, F., Eisenwort, G., et al. (2017). Nilotinib-induced vasculopathy: identification of vascular endothelial cells as a primary target site. *Leukemia* 31, 2388–2397. doi: 10.1038/leu.2017.245

Hall, C. N., Reynell, C., Gesslein, B., Hamilton, N. B., Mishra, A., Sutherland, B. A., et al. (2014). Capillary pericytes regulate cerebral blood flow in health and disease. *Nature* 508, 55–60. doi: 10.1038/nature13165

Hansen, D. V., Hanson, J. E., and Sheng, M. (2018). Microglia in Alzheimer's disease. *J. Cell Biol.* 217, 459–472. doi: 10.1083/jcb.201709069

Hardy, J. A., and Higgins, G. A. (1992). Alzheimer's disease: the amyloid cascade hypothesis. *Science* 256, 184–185. doi: 10.1126/science.1566067

Harrison, T. M., La Joie, R., Maass, A., Baker, S. L., Swinnerton, K., Fenton, L., et al. (2019). Longitudinal tau accumulation and atrophy in aging and alzheimer disease. *Ann. Neurol.* 85, 229–240. doi: 10.1002/ana.25406

Hawkes, C. A., and McLaurin, J. (2009). Selective targeting of perivascular macrophages for clearance of beta-amyloid in cerebral amyloid angiopathy. *Proc. Natl. Acad. Sci. U. S. A.* 106, 1261–1266. doi: 10.1073/pnas.0805453106

Hecht, M., Krämer, L. M., von Arnim, C. A. F., Otto, M., and Thal, D. R. (2018). Capillary cerebral amyloid angiopathy in Alzheimer's disease: association with allocortical/hippocampal microinfarcts and cognitive decline. *Acta Neuropathol.* 135, 681–694. doi: 10.1007/s00401-018-1834-y

Hecquet, C. M., Ahmmed, G. U., Vogel, S. M., and Malik, A. B. (2008). Role of TRPM2 channel in mediating H_2O_2-induced Ca^{2+} entry and endothelial hyperpermeability. *Circ. Res.* 102, 347–355. doi: 10.1161/CIRCRESAHA.107.160176

Hemonnot, A. L., Hua, J., Ulmann, L., and Hirbec, H. (2019). Microglia in Alzheimer disease: well-known targets and new opportunities. *Front. Aging Neurosci.* 11:233. doi: 10.3389/fnagi.2019.00233

Henderson, V. W., and Brinton, R. D. (2010). Menopause and mitochondria: windows into estrogen effects on Alzheimer's disease risk and therapy. *Prog. Brain Res.* 182, 77–96. doi: 10.1016/S0079-6123(10)82003-5

Heneka, M. T., Sastre, M., Dumitrescu-Ozimek, L., Hanke, A., Dewachter, I., Kuiperi, C., et al. (2005). Acute treatment with the PPARgamma agonist pioglitazone and ibuprofen reduces glial inflammation and Aβ1-42 levels in APPV717I transgenic mice. *Brain* 128(Pt 6), 1442–1453. doi: 10.1093/brain/awh452

Hernandez, F., Lucas, J. J., and Avila, J. (2013). GSK3 and tau: two convergence points in Alzheimer's disease. *J. Alzheimers Dis.* 33(Suppl 1), S141–S144. doi: 10.3233/JAD-2012-129025

Herrup, K. (2010). Reimagining Alzheimer's disease–an age-based hypothesis. *J. Neurosci.* 30, 16755–16762. doi: 10.1523/JNEUROSCI.4521-10.2010

Hillen, H. (2019). The beta amyloid dysfunction (BAD) hypothesis for Alzheimer's disease. *Front. Neurosci.* 13:1154. doi: 10.3389/fnins.2019.01154

Hollingworth, P., Harold, D., Sims, R., Gerrish, A., Lambert, J. C., Carrasquillo, M. M., et al. (2011). Common variants at ABCA7, MS4A6A/MS4A4E, EPHA1, CD33 and CD2AP are associated with Alzheimer's disease. *Nat. Genet.* 43, 429–435. doi: 10.1038/ng.803

Holmes, C., Boche, D., Wilkinson, D., Yadegarfar, G., Hopkins, V., Bayer, A., et al. (2008). Long-term effects of Aβ42 immunisation in Alzheimer's disease: follow-up of a randomised, placebo-controlled phase I trial. *Lancet* 372, 216–223. doi: 10.1016/S0140-6736(08)61075-2

Hooijmans, C. R., Graven, C., Dederen, P. J., Tanila, H., van Groen, T., and Kiliaan, A. J. (2007). Amyloid beta deposition is related to decreased glucose transporter-1 levels and hippocampal atrophy in brains of aged APP/PS1 mice. *Brain Res.* 1181, 93–103. doi: 10.1016/j.brainres.2007.08.063

Huang, L., Jia, J., and Liu, R. (2013). Decreased serum levels of the angiogenic factors VEGF and TGF-β1 in Alzheimer's disease and amnestic mild cognitive impairment. *Neurosci. Lett.* 550, 60–63. doi: 10.1016/j.neulet.2013.06.031

Huang, S., Turlova, E., Li, F., Bao, M. H., Szeto, V., Wong, R., et al. (2017). Transient receptor potential melastatin 2 channels (TRPM2) mediate neonatal hypoxic-ischemic brain injury in mice. *Exp. Neurol.* 296, 32–40. doi: 10.1016/j.expneurol.2017.06.023

Hunter, J. M., Kwan, J., Malek-Ahmadi, M., Maarouf, C. L., Kokjohn, T. A., Belden, C., et al. (2012). Morphological and pathological evolution of the brain microcirculation in aging and Alzheimer's disease. *PLoS One* 7:e36893. doi: 10.1371/journal.pone.0036893

Iadecola, C., Zhang, F., Niwa, K., Eckman, C., Turner, S. K., Fischer, E., et al. (1999). SOD1 rescues cerebral endothelial dysfunction in mice overexpressing amyloid precursor protein. *Nat. Neurosci.* 2, 157–161. doi: 10.1038/5715

Iliff, J. J., Wang, M., Liao, Y., Plogg, B. A., Peng, W., Gundersen, G. A., et al. (2012). A paravascular pathway facilitates CSF flow through the brain parenchyma and the clearance of interstitial solutes, including amyloid β. *Sci. Transl. Med.* 4:147ra111. doi: 10.1126/scitranslmed.3003748

Iliff, J. J., Wang, M., Zeppenfeld, D. M., Venkataraman, A., Plog, B. A., Liao, Y., et al. (2013). Cerebral arterial pulsation drives paravascular CSF-interstitial fluid exchange in the murine brain. *J. Neurosci.* 33, 18190–18199. doi: 10.1523/JNEUROSCI.1592-13.2013

Iturria-Medina, Y., Sotero, R. C., Toussaint, P. J., Mateos-Pérez, J. M., Evans, A. C., Initiative, A., et al. (2016). Early role of vascular dysregulation on late-onset Alzheimer's disease based on multifactorial data-driven analysis. *Nat. Commun.* 7:11934. doi: 10.1038/ncomms11934

Jack, C. R., Knopman, D. S., Jagust, W. J., Petersen, R. C., Weiner, M. W., Aisen, P. S., et al. (2013). Tracking pathophysiological processes in Alzheimer's disease: an updated hypothetical model of dynamic biomarkers. *Lancet Neurol.* 12, 207–216. doi: 10.1016/S1474-4422(12)70291-0

Jefferies, W. A., Price, K. A., Biron, K. E., Fenninger, F., Pfeifer, C. G., and Dickstein, D. L. (2013). Adjusting the compass: new insights into the role of angiogenesis in Alzheimer's disease. *Alzheimers. Res. Ther.* 5, 64. doi: 10.1186/alzrt230

Jespersen, S. N., and Østergaard, L. (2012). The roles of cerebral blood flow, capillary transit time heterogeneity, and oxygen tension in brain oxygenation and metabolism. *J. Cereb. Blood Flow Metab.* 32, 264–277. doi: 10.1038/jcbfm.2011.153

Joo, I. L., Lai, A. Y., Bazzigaluppi, P., Koletar, M. M., Dorr, A., Brown, M. E., et al. (2017). Early neurovascular dysfunction in a transgenic rat model of Alzheimer's disease. *Sci. Rep.* 7:46427. doi: 10.1038/srep46427

Kametani, F., and Hasegawa, M. (2018). Reconsideration of amyloid hypothesis and tau hypothesis in Alzheimer's disease. *Front. Neurosci.* 12:25. doi: 10.3389/fnins.2018.00025

Kelly, P., Denver, P., Satchell, S. C., Ackermann, M., Konerding, M. A., and Mitchell, C. A. (2017). Microvascular ultrastructural changes precede cognitive impairment in the murine APPswe/PS1dE9 model of Alzheimer's disease. *Angiogenesis* 20, 567–580. doi: 10.1007/s10456-017-9568-3

Killin, L. O., Starr, J. M., Shiue, I. J., and Russ, T. C. (2016). Environmental risk factors for dementia: a systematic review. *BMC Geriatr.* 16:175. doi: 10.1186/s12877-016-0342-y

Kim, Y. H., Choi, S. H., D'Avanzo, C., Hebisch, M., Sliwinski, C., Bylykbashi, E., et al. (2015). A 3D human neural cell culture system for modeling Alzheimer's disease. *Nat. Protoc.* 10, 985–1006. doi: 10.1038/nprot.2015.065

Kim, Y. N., and Kim, D. H. (2012). Decreased serum angiogenin level in Alzheimer's disease. *Prog. Neuropsychopharmacol. Biol. Psychiatry* 38, 116–120. doi: 10.1016/j.pnpbp.2012.02.010

Kisler, K., Nelson, A. R., Rege, S. V., Ramanathan, A., Wang, Y., Ahuja, A., et al. (2017). Pericyte degeneration leads to neurovascular uncoupling and limits oxygen supply to brain. *Nat. Neurosci.* 20, 406–416. doi: 10.1038/nn.4489

Kleinfeld, D., Mitra, P. P., Helmchen, F., and Denk, W. (1998). Fluctuations and stimulus-induced changes in blood flow observed in individual capillaries in layers 2 through 4 of rat neocortex. *Proc. Natl. Acad. Sci. USA*, 95: 15741–15746. doi: 10.1073/pnas.95.26.15741

Klohs, J. (2019). An integrated view on vascular dysfunction in Alzheimer's disease. *Neurodegener. Dis.* 19, 109–127. doi: 10.1159/000505625

Klohs, J., Rudin, M., Shimshek, D. R., and Beckmann, N. (2014). Imaging of cerebrovascular pathology in animal models of Alzheimer's disease. *Front. Aging Neurosci.* 6:32. doi: 10.3389/fnagi.2014.00032

Knowles, R. B., Wyart, C., Buldyrev, S. V., Cruz, L., Urbanc, B., Hasselmo, M. E., et al. (1999). Plaque-induced neurite abnormalities: implications for disruption of neural networks in Alzheimer's disease. *Proc. Natl. Acad. Sci. U. S. A.* 96, 5274–5279. doi: 10.1073/pnas.96.9.5274

Koffie, R. M., Meyer-Luehmann, M., Hashimoto, T., Adams, K. W., Mielke, M. L., Garcia-Alloza, M., et al. (2009). Oligomeric amyloid beta associates with postsynaptic densities and correlates with excitatory synapse loss near senile plaques. *Proc. Natl. Acad. Sci. U. S. A.* 106, 4012–4017. doi: 10.1073/pnas.0811698106

Koike, M. A., Green, K. N., Blurton-Jones, M., and Laferla, F. M. (2010). Oligemic hypoperfusion differentially affects tau and amyloid-β. *Am. J. Pathol.* 177, 300–310. doi: 10.2353/ajpath.2010.090750

Kokjohn, T. A., Van Vickle, G. D., Maarouf, C. L., Kalback, W. M., Hunter, J. M., Daugs, I. D., et al. (2011). Chemical characterization of pro-inflammatory amyloid-β peptides in human atherosclerotic lesions and platelets. *Biochim. Biophys. Acta* 1812, 1508–1514. doi: 10.1016/j.bbadis.2011.07.004

Korivi, M., Hou, C. W., Chen, C. Y., Lee, J.P., Kesireddy, S.R., and Kuo, C. H (2010). Angiogenesis: role of exercise training and aging. *Adapt. Med.* 2, 29–41. doi: 10.4247/AM.2010.ABA005

Korte, N., Nortley, R., and Attwell, D. (2020). Cerebral blood flow decrease as an early pathological mechanism in Alzheimer's disease. *Acta Neuropathol.* 140, 793–810. doi: 10.1007/s00401-020-02215-w

Kosik, K. S. (2013). Diseases: study neuron networks to tackle Alzheimer's. *Nature* 503, 31–32. doi: 10.1038/503031a

Kövari, E., Herrmann, F. R., Hof, P. R., and Bouras, C. (2013). The relationship between cerebral amyloid angiopathy and cortical microinfarcts in brain ageing and Alzheimer's disease. *Neuropathol. Appl. Neurobiol.* 39, 498–509. doi: 10.1111/nan.12003

Kress, B. T., Iliff, J. J., Xia, M., Wang, M., Wei, H. S., Zeppenfeld, D., et al. (2014). Impairment of paravascular clearance pathways in the aging brain. *Ann. Neurol.* 76, 845–861. doi: 10.1002/ana.24271

Krstic, D., Madhusudan, A., Doehner, J., Vogel, P., Notter, T., Imhof, C., et al. (2012). Systemic immune challenges trigger and drive Alzheimer-like neuropathology in mice. *J. Neuroinflammation* 9:151. doi: 10.1186/1742-2094-9-151

Krucker, T., Schuler, A., Meyer, E. P., Staufenbiel, M., and Beckmann, N. (2004). Magnetic resonance angiography and vascular corrosion casting as tools in biomedical research: application to transgenic mice modeling Alzheimer's disease. *Neurol. Res.* 26, 507–516. doi: 10.1179/016164104225016281

Kuchibhotla, K. V., Goldman, S. T., Lattarulo, C. R., Wu, H. Y., Hyman, B. T., and Bacskai, B. J. (2008). Aβ plaques lead to aberrant regulation of calcium homeostasis *in vivo* resulting in structural and functional disruption of neuronal networks. *Neuron* 59, 214–225. doi: 10.1016/j.neuron.2008.06.008

Kunkle, B. W., Grenier-Boley, B., Sims, R., Bis, J. C., Damotte, V., Naj, A. C., et al. (2019). Genetic meta-analysis of diagnosed Alzheimer's disease identifies new risk loci and implicates Aβ, tau, immunity and lipid processing. *Nat. Genet.* 51, 414–430. doi: 10.1038/s41588-019-0358-2

Kyrtsos, C. R., and Baras, J. S. (2015). Modeling the role of the glymphatic pathway and cerebral blood vessel properties in Alzheimer's disease pathogenesis. *PLoS One* 10:e0139574. doi: 10.1371/journal.pone.0139574

La Joie, R., Visani, A. V., Baker, S. L., Brown, J. A., Bourakova, V., Cha, J., et al.. (2020). Prospective longitudinal atrophy in Alzheimer's disease correlates with the intensity and topography of baseline tau-PET. *Sci. Transl. Med.* 12:eaau5732. doi: 10.1126/scitranslmed.aau5732

Lacalle-Aurioles, M., Mateos-Pérez, J. M., Guzmán-De-Villoria, J. A., Olazarán, J., Cruz-Orduña, I., Alemán-Gómez, Y., et al. (2014). Cerebral blood flow is an earlier indicator of perfusion abnormalities than cerebral blood volume in Alzheimer's disease. *J. Cereb. Blood Flow Metab.* 34, 654–659. doi: 10.1038/jcbfm.2013.241

Lai, A. Y., Dorr, A., Thomason, L. A., Koletar, M. M., Sled, J. G., Stefanovic, B., et al. (2015). Venular degeneration leads to vascular dysfunction in a transgenic model of Alzheimer's disease. *Brain* 138(Pt 4), 1046–1058. doi: 10.1093/brain/awv023

Lanoiselée, H. M., Nicolas, G., Wallon, D., Rovelet-Lecrux, A., Lacour, M., Rousseau, S., et al. (2017). APP, PSEN1, and PSEN2 mutations in early-onset Alzheimer disease: a genetic screening study of familial and sporadic cases. *PLoS Med.* 14:e1002270. doi: 10.1371/journal.pmed.1002270

Lapenna, A., De Palma, M., and Lewis, C. E. (2018). Perivascular macrophages in health and disease. *Nat. Rev. Immunol.* 18, 689–702. doi: 10.1038/s41577-018-0056-9

Lathe, R., Sapronova, A., and Kotelevtsev, Y. (2014). Atherosclerosis and Alzheimer–diseases with a common cause? Inflammation, oxysterols, vasculature. *BMC Geriatr.* 14:36. doi: 10.1186/1471-2318-14-36

Lazic, D., Sagare, A. P., Nikolakopoulou, A. M., Griffin, J. H., Vassar, R., and Zlokovic, B. V. (2019). 3K3A-activated protein C blocks amyloidogenic BACE1 pathway and improves functional outcome in mice. *J. Exp. Med.* 216, 279–293. doi: 10.1084/jem.20181035

Lewis, J., Dickson, D. W., Lin, W. L., Chisholm, L., Corral, A., Jones, G., et al. (2001). Enhanced neurofibrillary degeneration in transgenic mice expressing mutant tau and APP. *Science* 293, 1487–1491. doi: 10.1126/science.1058189

Li, B., Esipova, T. V., Sencan, I., Kil,iç, K., Fu, B., Desjardins, M., et al. (2019). More homogeneous capillary flow and oxygenation in deeper cortical layers correlate with increased oxygen extraction. *Elife* 8:e42299. doi: 10.7554/eLife.42299

Li, F., Abuarab, N., and Sivaprasadarao, A. (2017a). TRPM2: Shredding the mitochondrial network. *Channels (Austin)* 11, 507–509. doi: 10.1080/19336950.2017.1376982

Li, F., Munsey, T. S., and Sivaprasadarao, A. (2017b). TRPM2-mediated rise in mitochondrial Zn. *Cell Death Differ.* 24, 1999–2012. doi: 10.1038/cdd.2017.118

Li, F., Wong, R., Luo, Z., Du, L., Turlova, E., Britto, L. R. G., et al. (2019). Neuroprotective effects of AG490 in neonatal hypoxic-ischemic brain injury. *Mol. Neurobiol.* 56, 8109–8123. doi: 10.1007/s12035-019-01656-z

Li, X., and Jiang, L. H. (2018). Multiple molecular mechanisms form a positive feedback loop driving amyloid β42 peptide-induced neurotoxicity via activation of the TRPM2 channel in hippocampal neurons. *Cell Death Dis.* 9:195. doi: 10.1038/s41419-018-0270-1

Liebmann, T., Renier, N., Bettayeb, K., Greengard, P., Tessier-Lavigne, M., and Flajolet, M. (2016). Three-dimensional study of Alzheimer's disease hallmarks using the iDISCO clearing method. *Cell Rep.* 16, 1138–1152. doi: 10.1016/j.celrep.2016.06.060

Lim, G. P., Yang, F., Chu, T., Chen, P., Beech, W., Teter, B., et al. (2000). Ibuprofen suppresses plaque pathology and inflammation in a mouse model for Alzheimer's disease. *J. Neurosci.* 20, 5709–5714. doi: 10.1523/JNEUROSCI.20-15-05709.2000

Linse, S., Cabaleiro-Lago, C., Xue, W. F., Lynch, I., Lindman, S., Thulin, E., et al. (2007). Nucleation of protein fibrillation by nanoparticles. *Proc. Natl. Acad. Sci. U. S. A.* 104, 8691–8696. doi: 10.1073/pnas.0701250104

Liu, P. P., Xie, Y., Meng, X. Y., and Kang, J. S. (2019). History and progress of hypotheses and clinical trials for Alzheimer's disease. *Signal Transduct. Target Ther.* 4:29. doi: 10.1038/s41392-019-0063-8

Lovestone, S., Boada, M., Dubois, B., Hüll, M., Rinne, J. O., Huppertz, H. J., et al. (2015). A phase II trial of tideglusib in Alzheimer's disease. *J. Alzheimers Dis.* 45, 75–88. doi: 10.3233/JAD-141959

Lu, X., Moeini, M., Li, B., Lu, Y., Damseh, R., Pouliot, P., et al. (2019). A pilot study investigating changes in capillary hemodynamics and its modulation by exercise in the APP-PS1 Alzheimer mouse model. *Front. Neurosci.* 13:1261. doi: 10.3389/fnins.2019.01261

Luppi, C., Fioravanti, M., Bertolini, B., Inguscio, M., Grugnetti, A., Guerriero, F., et al. (2009). Growth factors decrease in subjects with mild to moderate Alzheimer's disease (AD): potential correction with dehydroepiandrosterone-sulphate (DHEAS). *Arch. Gerontol. Geriatr.* 49, 173–184. doi: 10.1016/j.archger.2009.09.027

Madav, Y., Wairkar, S., and Prabhakar, B. (2019). Recent therapeutic strategies targeting beta amyloid and tauopathies in Alzheimer's disease. *Brain Res. Bull.* 146, 171–184. doi: 10.1016/j.brainresbull.2019.01.004

Maki, P. M., and Resnick, S. M. (2000). Longitudinal effects of estrogen replacement therapy on PET cerebral blood flow and cognition. *Neurobiol. Aging* 21, 373–383. doi: 10.1016/S0197-4580(00)00123-8

Makin, S. (2018). The amyloid hypothesis on trial. *Nature* 559, S4–S7. doi: 10.1038/d41586-018-05719-4

Maliszewska-Cyna, E., Vecchio, L. M., Thomason, L. A. M., Oore, J. J., Steinman, J., Joo, I. L., et al. (2020). The effects of voluntary running on cerebrovascular morphology and spatial short-term memory in a mouse model of amyloidosis. *Neuroimage* 222:117269. doi: 10.1016/j.neuroimage.2020.117269

Mandrekar-Colucci, S., and Landreth, G. E. (2010). Microglia and inflammation in Alzheimer's disease. *CNS Neurol. Disord. Drug Targets* 9, 156–167. doi: 10.2174/187152710791012071

Mawuenyega, K. G., Sigurdson, W., Ovod, V., Munsell, L., Kasten, T., Morris, J. C., et al. (2010). Decreased clearance of CNS beta-amyloid in Alzheimer's disease. *Science* 330:1774. doi: 10.1126/science.1197623

Meyer, E. P., Ulmann-Schuler, A., Staufenbiel, M., and Krucker, T. (2008). Altered morphology and 3D architecture of brain vasculature in a mouse model for Alzheimer's disease. *Proc. Natl. Acad. Sci. U. S. A.* 105, 3587–3592. doi: 10.1073/pnas.0709788105

Miners, J. S., Schulz, I., and Love, S. (2018). Differing associations between Aβ accumulation, hypoperfusion, blood-brain barrier dysfunction and loss of PDGFRB pericyte marker in the precuneus and parietal white matter in Alzheimer's disease. *J. Cereb. Blood Flow Metab.* 38, 103–115. doi: 10.1177/0271678X17690761

Miyakawa, T. (1997). Electron microscopy of amyloid fibrils and microvessels. *Ann. N. Y. Acad. Sci.* 826, 25–34. doi: 10.1111/j.1749-6632.1997.tb48458.x

Montagne, A., Nation, D. A., Sagare, A. P., Barisano, G., Sweeney, M. D., Chakhoyan, A., et al. (2020). APOE4 leads to blood-brain barrier dysfunction predicting cognitive decline. *Nature* 581, 71–76. doi: 10.1038/s41586-020-2247-3

Montagne, A., Nikolakopoulou, A. M., Zhao, Z., Sagare, A. P., Si, G., Lazic, D., et al. (2018). Pericyte degeneration causes white matter dysfunction in the mouse central nervous system. *Nat. Med.* 24, 326–337. doi: 10.1038/nm.4482

Mosconi, L., Rahman, A., Diaz, I., Wu, X., Scheyer, O., Hristov, H. W., et al. (2018). Increased Alzheimer's risk during the menopause transition: a 3-year longitudinal brain imaging study. *PLoS One* 13:e0207885. doi: 10.1371/journal.pone.0207885

Mucke, L. (2009). Neuroscience: Alzheimer's disease. *Nature* 461, 895–897. doi: 10.1038/461895a

Musiek, E. S., and Holtzman, D. M. (2012). Origins of Alzheimer's disease: reconciling cerebrospinal fluid biomarker and neuropathology data regarding the temporal sequence of amyloid-beta and tau involvement. *Curr. Opin. Neurol.* 25, 715–720. doi: 10.1097/WCO.0b013e32835a30f4

Naj, A. C., Jun, G., Beecham, G. W., Wang, L. S., Vardarajan, B. N., Buros, J., et al. (2011). Common variants at MS4A4/MS4A6E, CD2AP, CD33 and EPHA1 are associated with late-onset Alzheimer's disease. *Nat. Genet.* 43, 436–441. doi: 10.1038/ng.801

Nation, D. A., Sweeney, M. D., Montagne, A., Sagare, A. P., D'Orazio, L. M., Pachicano, M., et al. (2019). Blood-brain barrier breakdown is an early biomarker of human cognitive dysfunction. *Nat. Med.* 25, 270–276. doi: 10.1038/s41591-018-0297-y

Nielsen, R. B., Egefjord, L., Angleys, H., Mouridsen, K., Gejl, M., Møller, A., et al. (2017). Capillary dysfunction is associated with symptom severity and neurodegeneration in Alzheimer's disease. *Alzheimers Dement.* 13, 1143–1153. doi: 10.1016/j.jalz.2017.02.007

Niwa, K., Carlson, G. A., and Iadecola, C. (2000). Exogenous A β1-40 reproduces cerebrovascular alterations resulting from amyloid precursor protein overexpression in mice. *J. Cereb. Blood Flow Metab.* 20, 1659–1668. doi: 10.1097/00004647-200012000-00005

Niwa, K., Kazama, K., Younkin, S. G., Carlson, G. A., and Iadecola, C. (2002). Alterations in cerebral blood flow and glucose utilization in mice overexpressing the amyloid precursor protein. *Neurobiol. Dis.* 9, 61–68. doi: 10.1006/nbdi.2001.0460

Nortley, R., Korte, N., Izquierdo, P., Hirunpattarasilp, C., Mishra, A., Jaunmuktane, Z., et al. (2019). Amyloid β oligomers constrict human capillaries in Alzheimer's disease via signaling to pericytes. *Science* 365:eaav9518. doi: 10.1126/science.aav9518

Ostapchenko, V. G., Chen, M., Guzman, M. S., Xie, Y. F., Lavine, N., Fan, J., et al. (2015). The transient receptor potential melastatin 2 (TRPM2) channel contributes to β-amyloid oligomer-related neurotoxicity and memory impairment. *J. Neurosci.* 35, 15157–15169. doi: 10.1523/JNEUROSCI.4081-14.2015

Østergaard, L., Aamand, R., Gutiérrez-Jiménez, E., Ho, Y. C., and Blicher, J. U., Madsen, S. M., et al. (2013). The capillary dysfunction hypothesis of Alzheimer's disease. *Neurobiol. Aging* 34, 1018–1031. doi: 10.1016/j.neurobiolaging.2012.09.011

Østergaard, L., Jespersen, S. N., Engedahl, T., Gutiérrez Jiménez, E., and Ashkanian, M., Hansen, M. B., et al. (2015). Capillary dysfunction: its detection and causative role in dementias and stroke. *Curr. Neurol. Neurosci. Rep.* 15:37. doi: 10.1007/s11910-015-0557-x

Ostrowski, P. P., Barszczyk, A., Forstenpointner, J., Zheng, W., and Feng, Z. P. (2016). Meta-analysis of serum insulin-like growth factor 1 in Alzheimer's disease. *PLoS One* 11:e0155733. doi: 10.1371/journal.pone.0155733

Paris, D., Patel, N., DelleDonne, A., Quadros, A., Smeed, R., and Mullan, M. (2004a). Impaired angiogenesis in a transgenic mouse model of cerebral amyloidosis. *Neurosci. Lett.* 366, 80–85. doi: 10.1016/j.neulet.2004.05.017

Paris, D., Quadros, A., Humphrey, J., Patel, N., Crescentini, R., Crawford, F., et al. (2004b). Nilvadipine antagonizes both Aβ vasoactivity in isolated arteries, and the reduced cerebral blood flow in APPsw transgenic mice. *Brain Res.* 999, 53–61. doi: 10.1016/j.brainres.2003.11.061

Paris, D., Townsend, K., Quadros, A., Humphrey, J., Sun, J., Brem, S., et al. (2004c). Inhibition of angiogenesis by Abeta peptides. *Angiogenesis*, 7, 75–85. doi: 10.1023/B:AGEN.0000037335.17717.bf

Park, J., Wetzel, I., Marriott, I., Dréau, D., D'Avanzo, C., Kim, D. Y., et al. (2018). A 3D human triculture system modeling neurodegeneration and neuroinflammation in Alzheimer's disease. *Nat. Neurosci.* 21, 941–951. doi: 10.1038/s41593-018-0175-4

Park, L., Uekawa, K., Garcia-Bonilla, L., Koizumi, K., Murphy, M., Pistik, R., et al. (2017). Brain perivascular macrophages initiate the neurovascular dysfunction of Alzheimer Aβ peptides. *Circ. Res.* 121, 258–269. doi: 10.1161/CIRCRESAHA.117.311054

Park, L., Wang, G., Moore, J., Girouard, H., Zhou, P., Anrather, J., et al. (2014). The key role of transient receptor potential melastatin-2 channels in amyloid-β-induced neurovascular dysfunction. *Nat. Commun.* 5:5318. doi: 10.1038/ncomms6318

Patton, R. L., Kalback, W. M., Esh, C. L., Kokjohn, T. A., Van Vickle, G. D., Luehrs, D. C., et al. (2006). Amyloid-beta peptide remnants in AN-1792-immunized Alzheimer's disease patients: a biochemical analysis. *Am. J. Pathol.* 169, 1048–1063. doi: 10.2353/ajpath.2006.060269

Peeples, L. (2020). News feature: how air pollution threatens brain health. *Proc. Natl. Acad. Sci. U. S. A.* 117, 13856–13860. doi: 10.1073/pnas.2008940117

Peng, W., Achariyar, T. M., Li, B., Liao, Y., Mestre, H., Hitomi, E., et al. (2016). Suppression of glymphatic fluid transport in a mouse model of Alzheimer's disease. *Neurobiol. Dis.* 93, 215–225. doi: 10.1016/j.nbd.2016.05.015

Perez, F. P., Bose, D., Maloney, B., Nho, K., Shah, K., and Lahiri, D. K. (2014). Late-onset Alzheimer's disease, heating up and foxed by several proteins: pathomolecular effects of the aging process. *J. Alzheimers Dis.* 40, 1–17. doi: 10.3233/JAD-131544

Perlmutter, L. S., Chui, H. C., Saperia, D., and Athanikar, J. (1990). Microangiopathy and the colocalization of heparan sulfate proteoglycan with amyloid in senile plaques of Alzheimer's disease. *Brain Res.* 508, 13–19. doi: 10.1016/0006-8993(90)91111-S

Preston, S. D., Steart, P. V., Wilkinson, A., Nicoll, J. A., and Weller, R. O. (2003). Capillary and arterial cerebral amyloid angiopathy in Alzheimer's disease: defining the perivascular route for the elimination of amyloid beta from the human brain. *Neuropathol. Appl. Neurobiol.* 29, 106–117. doi: 10.1046/j.1365-2990.2003.00424.x

Raja, R., Rosenberg, G. A., and Caprihan, A. (2018). MRI measurements of Blood-Brain Barrier function in dementia: a review of recent studies. *Neuropharmacology.* 134(Pt B), 259–271. doi: 10.1016/j.neuropharm.2017.10.034

Ramanathan, A., Nelson, A. R., Sagare, A. P., and Zlokovic, B. V. (2015). Impaired vascular-mediated clearance of brain amyloid beta in Alzheimer's disease:

the role, regulation and restoration of LRP1. *Front. Aging Neurosci.* 7:136. doi: 10.3389/fnagi.2015.00136

Rasgon, N. L., Geist, C. L., Kenna, H. A., Wroolie, T. E., Williams, K. E., and Silverman, D. H. (2014). Prospective randomized trial to assess effects of continuing hormone therapy on cerebral function in postmenopausal women at risk for dementia. *PLoS One* 9:e89095. doi: 10.1371/journal.pone.0089095

Reeves, B. C., Karimy, J. K., Kundishora, A. J., Mestre, H., Cerci, H. M., Matouk, C., et al. (2020). Glymphatic system impairment in Alzheimer's disease and idiopathic normal pressure hydrocephalus. *Trends Mol. Med*. 26, 285–295. doi: 10.1016/j.molmed.2019.11.008

Religa, P., Cao, R., Religa, D., Xue, Y., Bogdanovic, N., Westaway, D., et al. (2013). VEGF significantly restores impaired memory behavior in Alzheimer's mice by improvement of vascular survival. *Sci. Rep*. 3:2053. doi: 10.1038/srep02053

Rius-Pérez, S., Tormos, A. M., Pérez, S., and Taléns-Visconti, R. (2018). Vascular pathology: cause or effect in Alzheimer disease? *Neurologia* 33, 112–120. doi: 10.1016/j.nrleng.2015.07.008

Rivard, A., Fabre, J. E., Silver, M., Chen, D., Murohara, T., Kearney, M., et al. (1999). Age-dependent impairment of angiogenesis. *Circulation* 99, 111–120. doi: 10.1161/01.CIR.99.1.111

Safieh, M., Korczyn, A. D., and Michaelson, D. M. (2019). ApoE4: an emerging therapeutic target for Alzheimer's disease. *BMC Med*. 17:64. doi: 10.1186/s12916-019-1299-4

Sagare, A. P., Bell, R. D., and Zlokovic, B. V. (2012). Neurovascular dysfunction and faulty amyloid β-peptide clearance in Alzheimer disease. *Cold Spring Harb. Perspect. Med.* 2:a011452. doi: 10.1101/cshperspect.a011452

Sasaguri, H., Nilsson, P., Hashimoto, S., Nagata, K., Saito, T., De Strooper, B., et al. (2017). APP mouse models for Alzheimer's disease preclinical studies. *EMBO J.* 36, 2473–2487. doi: 10.15252/embj.201797397

Savolainen-Peltonen, H., Rahkola-Soisalo, P., Hoti, F., Vattulainen, P., Gissler, M., Ylikorkala, O., et al. (2019). Use of postmenopausal hormone therapy and risk of Alzheimer's disease in Finland: nationwide case-control study. *BMJ* 364:l665. doi: 10.1136/bmj.l665

Scheibel, A. B., Duong, T. H., and Jacobs, R. (1989). Alzheimer's disease as a capillary dementia. *Ann. Med*. 21, 103–107. doi: 10.3109/07853898909149194

Scheiblich, H., Trombly, M., Ramirez, A., and Heneka, M. T. (2020). Neuroimmune connections in aging and neurodegenerative diseases. *Trends Immunol*. 41, 300–312. doi: 10.1016/j.it.2020.02.002

Schenk, D., Barbour, R., Dunn, W., Gordon, G., Grajeda, H., Guido, T., et al. (1999). Immunization with amyloid-β attenuates Alzheimer-disease-like pathology in the PDAPP mouse. *Nature* 400, 173–177. doi: 10.1038/22124

Scheyer, O., Rahman, A., Hristov, H., Berkowitz, C., Isaacson, R. S., Diaz Brinton, R., et al. (2018). Female sex and Alzheimer's risk: the menopause connection. *J. Prev. Alzheimers Dis.* 5, 225–230. doi: 10.14283/jpad.2018.34

Schmid, F., Tsai, P. S., Kleinfeld, D., Jenny, P., and Weber, B. (2017). Depth-dependent flow and pressure characteristics in cortical microvascular networks. *PLoS Comput. Biol*. 13:e1005392. doi: 10.1371/journal.pcbi.1005392

Schultheiss, C., Blechert, B., Gaertner, F. C., Drecoll, E., Mueller, J., Weber, G. F., et al. (2006). *In vivo* characterization of endothelial cell activation in a transgenic mouse model of Alzheimer's disease. *Angiogenesis* 9, 59–65. doi: 10.1007/s10456-006-9030-4

Selkoe, D. J. (2011). Resolving controversies on the path to Alzheimer's therapeutics. *Nat. Med*. 17, 1060–1065. doi: 10.1038/nm.2460

Selkoe, D. J. (2019). Early network dysfunction in Alzheimer's disease. *Science* 365, 540–541. doi: 10.1126/science.aay5188

Selkoe, D. J., and Hardy, J. (2016). The amyloid hypothesis of Alzheimer's disease at 25 years. *EMBO Mol. Med*. 8, 595–608. doi: 10.15252/emmm.201606210

Serenó, L., Coma, M., Rodríguez, M., Sánchez-Ferrer, P., Sánchez, M. B., Gich, I., et al. (2009). A novel GSK-3β inhibitor reduces Alzheimer's pathology and rescues neuronal loss *in vivo*. *Neurobiol. Dis.* 35, 359–367. doi: 10.1016/j.nbd.2009.05.025

Sevigny, J., Chiao, P., Bussière, T., Weinreb, P. H., Williams, L., Maier, M., et al. (2016). The antibody aducanumab reduces Aβ plaques in Alzheimer's disease. *Nature* 537, 50–56. doi: 10.1038/nature19323

Shin, Y., Choi, S. H., Kim, E., Bylykbashi, E., Kim, J. A., Chung, S., et al. (2019). Blood-brain barrier dysfunction in a 3D *in vitro* model of Alzheimer's disease. *Adv. Sci. (Weinh)* 6:1900962. doi: 10.1002/advs.201900962

Silva, M. V. F., Loures, C. M. G., Alves, L. C. V., de Souza, L. C., Borges, K. B. G., and Carvalho, M. D. G. (2019). Alzheimer's disease: risk factors and potentially protective measures. *J. Biomed. Sci.* 26:33. doi: 10.1186/s12929-019-0524-y

Silverberg, G. D., Messier, A. A., Miller, M. C., Machan, J. T., Majmudar, S. S., Stopa, E. G., et al. (2010). Amyloid efflux transporter expression at the blood-brain barrier declines in normal aging. *J. Neuropathol. Exp. Neurol.* 69, 1034–1043. doi: 10.1097/NEN.0b013e3181f46e25

Smith, C. D., Andersen, A. H., Kryscio, R. J., Schmitt, F. A., Kindy, M. S., Blonder, L. X., et al. (1999). Altered brain activation in cognitively intact individuals at high risk for Alzheimer's disease. *Neurology* 53, 1391–1396. doi: 10.1212/WNL.53.7.1391

Smith, L. M., and Strittmatter, S. M. (2017). Binding sites for amyloid-β oligomers and synaptic toxicity. *Cold Spring Harb. Perspect. Med*. 7:a024075. doi: 10.1101/cshperspect.a024075

Stakos, D. A., Stamatelopoulos, K., Bampatsias, D., Sachse, M., Zormpas, E., Vlachogiannis, N. I., et al. (2020). The Alzheimer's disease amyloid-beta hypothesis in cardiovascular aging and disease: JACC focus seminar. *J. Am. Coll. Cardiol*. 75, 952–967. doi: 10.1016/j.jacc.2019.12.033

Starkus, J. G., Poerzgen, P., Layugan, K., Kawabata, K. G., Goto, J. I., Suzuki, S., et al. (2017). Scalaradial is a potent inhibitor of transient receptor potential melastatin 2 (TRPM2) ion channels. *J. Nat. Prod*. 80, 2741–2750. doi: 10.1021/acs.jnatprod.7b00515

Steinman, J., Cahill, L. S., Koletar, M. M., Stefanovic, B., and Sled, J. G. (2019). Acute and chronic stage adaptations of vascular architecture and cerebral blood flow in a mouse model of TBI. *Neuroimage* 202:116101. doi: 10.1016/j.neuroimage.2019.116101

Steinman, J., Koletar, M. M., Stefanovic, B., and Sled, J. G. (2017). 3D morphological analysis of the mouse cerebral vasculature: comparison of *in vivo* and *ex vivo* methods. *PLoS One* 12:e0186676. doi: 10.1371/journal.pone.0186676

Strickland, S. (2018). Blood will out: vascular contributions to Alzheimer's disease. *J. Clin. Invest*. 128, 556–563. doi: 10.1172/JCI97509

Suárez-Calvet, M., Araque Caballero, M., Kleinberger, G., Bateman, R. J., Fagan, A. M., Morris, J. C., et al. (2016). Early changes in CSF sTREM2 in dominantly inherited Alzheimer's disease occur after amyloid deposition and neuronal injury. *Sci. Transl. Med*. 8:369ra178. doi: 10.1126/scitranslmed.aag1767

Sun, Z. (2015). Aging, arterial stiffness, and hypertension. *Hypertension* 65, 252–256. doi: 10.1161/HYPERTENSIONAHA.114.03617

Sweeney, M. D., Zhao, Z., Montagne, A., Nelson, A. R., and Zlokovic, B. V. (2019). Blood-brain barrier: from physiology to disease and back. *Physiol. Rev*. 99, 21–78. doi: 10.1152/physrev.00050.2017

Swerdlow, R. H., Burns, J. M., and Khan, S. M. (2014). The Alzheimer's disease mitochondrial cascade hypothesis: progress and perspectives. *Biochim. Biophys. Acta* 1842, 1219–1231. doi: 10.1016/j.bbadis.2013.09.010

Tarantini, S., Tucsek, Z., Valcarcel-Ares, M. N., Toth, P., Gautam, T., Giles, C. B., et al. (2016). Circulating IGF-1 deficiency exacerbates hypertension-induced microvascular rarefaction in the mouse hippocampus and retrosplenial cortex: implications for cerebromicrovascular and brain aging. *Age (Dordr)* 38, 273–289. doi: 10.1007/s11357-016-9931-0

Tarasoff-Conway, J. M., Carare, R. O., Osorio, R. S., Glodzik, L., Butler, T., Fieremans, E., et al. (2015). Clearance systems in the brain-implications for Alzheimer disease. *Nat. Rev. Neurol*. 11, 457–470. doi: 10.1038/nrneurol.2015.119

Thal, D. R., Capetillo-Zarate, E., Larionov, S., Staufenbiel, M., Zurbruegg, S., and Beckmann, N. (2009). Capillary cerebral amyloid angiopathy is associated with vessel occlusion and cerebral blood flow disturbances. *Neurobiol. Aging* 30, 1936–1948. doi: 10.1016/j.neurobiolaging.2008.01.017

Thal, D. R., Ghebremedhin, E., Rüb, U., Yamaguchi, H., Del Tredici, K., and Braak, H. (2002). Two types of sporadic cerebral amyloid angiopathy. *J. Neuropathol. Exp. Neurol.* 61, 282–293. doi: 10.1093/jnen/61.3.282

Thal, D. R., Griffin, W. S., de Vos, R. A., and Ghebremedhin, E. (2008). Cerebral amyloid angiopathy and its relationship to Alzheimer's disease. *Acta Neuropathol.* 115, 599–609. doi: 10.1007/s00401-008-0366-2

Thomas, K. R., Bangen, K. J., Weigand, A. J., Edmonds, E. C., Wong, C. G., Cooper, S., et al. (2020). Objective subtle cognitive difficulties predict future amyloid accumulation and neurodegeneration. *Neurology* 94, e397–e406. doi: 10.1212/WNL.0000000000008838

Tibolla, G., Norata, G. D., Meda, C., Arnaboldi, L., Uboldi, P., Piazza, F., et al. (2010). Increased atherosclerosis and vascular inflammation in APP

transgenic mice with apolipoprotein E deficiency. *Atherosclerosis* 210, 78–87. doi: 10.1016/j.atherosclerosis.2009.10.040

Townsend, K. P., and Praticò, D. (2005). Novel therapeutic opportunities for Alzheimer's disease: focus on nonsteroidal anti-inflammatory drugs. *FASEB J.* 19, 1592–1601. doi: 10.1096/fj.04-3620rev

Turlova, E., Feng, Z. P., and Sun, H. S. (2018). The role of TRPM2 channels in neurons, glial cells and the blood-brain barrier in cerebral ischemia and hypoxia. *Acta Pharmacol. Sin*. 39, 713–721. doi: 10.1038/aps.2017.194

Turner, R. S., Hebron, M. L., Lawler, A., Mundel, E. E., Yusuf, N., Starr, J. N., et al. (2020). Nilotinib effects on safety, tolerability, and biomarkers in Alzheimer's disease. *Ann. Neurol*. 88, 183–194. doi: 10.1002/ana.25775

Ujiie, M., Dickstein, D. L., Carlow, D. A., and Jefferies, W. A. (2003). Blood-brain barrier permeability precedes senile plaque formation in an Alzheimer disease model. *Microcirculation* 10, 463–470. doi: 10.1080/mic.10.6.463.470

Vagnucci, A. H., and Li, W. W. (2003). Alzheimer's disease and angiogenesis. *Lancet* 361, 605–608. doi: 10.1016/S0140-6736(03)12521-4

Van Dam, D., Coen, K., and De Deyn, P. P. (2010). Ibuprofen modifies cognitive disease progression in an Alzheimer's mouse model. *J. Psychopharmacol.* 24, 383–388. doi: 10.1177/0269881108097630

Vandenberghe, R., Rinne, J. O., Boada, M., Katayama, S., Scheltens, P., Vellas, B., et al. (2016). Bapineuzumab for mild to moderate Alzheimer's disease in two global, randomized, phase 3 trials. *Alzheimers Res. Ther*. 8:18. doi: 10.1186/s13195-016-0189-7

Vandenberghe, R., and Tournoy, J. (2005). Cognitive aging and Alzheimer's disease. *Postgrad. Med. J.* 81, 343–352. doi: 10.1136/pgmj.2004.028290

Venegas, C., Kumar, S., Franklin, B. S., Dierkes, T., Brinkschulte, R., Tejera, D., et al. (2017). Microglia-derived ASC specks cross-seed amyloid-β in Alzheimer's disease. *Nature* 552, 355–361. doi: 10.1038/nature25158

Vogel, J., Gehrig, M., Kuschinsky, W., and Marti, H. H. (2004). Massive inborn angiogenesis in the brain scarcely raises cerebral blood flow. *J. Cereb. Blood Flow Metab*. 24, 849–859. doi: 10.1097/01.WCB.0000126564.89011.11

Wåhlin, A., and Nyberg, L. (2019). At the heart of cognitive functioning in aging. *Trends Cogn. Sci.* 23, 717–720. doi: 10.1016/j.tics.2019.06.004

Walsh, D. M., and Selkoe, D. J. (2020). Amyloid β-protein and beyond: the path forward in Alzheimer's disease. *Curr. Opin. Neurobiol*. 61, 116–124. doi: 10.1016/j.conb.2020.02.003

Wang, L., Du, Y., Wang, K., Xu, G., Luo, S., and He, G. (2016). Chronic cerebral hypoperfusion induces memory deficits and facilitates Aβ generation in C57BL/6J mice. *Exp Neurol*. 283(Pt A), 353–364. doi: 10.1016/j.expneurol.2016.07.006

Wang, W. Y., Tan, M. S., Yu, J. T., and Tan, L. (2015). Role of pro-inflammatory cytokines released from microglia in Alzheimer's disease. *Ann. Transl. Med*. 3:136. doi: 10.3978/j.issn.2305-5839.2015.03.49

Wang, Y., Kilic, E., Kilic, U., Weber, B., Bassetti, C. L., Marti, H. H., et al. (2005). VEGF overexpression induces post-ischaemic neuroprotection, but facilitates haemodynamic steal phenomena. *Brain* 128(Pt 1), 52–63. doi: 10.1093/brain/awh325

Weller, R. O., Boche, D., and Nicoll, J. A. (2009). Microvasculature changes and cerebral amyloid angiopathy in Alzheimer's disease and their potential impact on therapy. *Acta Neuropathol*. 118, 87–102. doi: 10.1007/s00401-009-0498-z

Weller, R. O., Subash, M., Preston, S. D., Mazanti, I., and Carare, R. O. (2008). Perivascular drainage of amyloid-beta peptides from the brain and its failure in cerebral amyloid angiopathy and Alzheimer's disease. *Brain Pathol*. 18, 253–266. doi: 10.1111/j.1750-3639.2008.00133.x

Wilcock, D. M., Rojiani, A., Rosenthal, A., Subbarao, S., Freeman, M. J., Gordon, M. N., et al. (2004). Passive immunotherapy against Aβ in aged APP-transgenic mice reverses cognitive deficits and depletes parenchymal amyloid deposits in spite of increased vascular amyloid and microhemorrhage. *J. Neuroinflamm.* 1:24. doi: 10.1186/1742-2094-1-24

Xu, Z., Xiao, N., Chen, Y., Huang, H., Marshall, C., Gao, J., et al. (2015). Deletion of aquaporin-4 in APP/PS1 mice exacerbates brain Aβ accumulation and memory deficits. *Mol. Neurodegener.* 10:58. doi: 10.1186/s13024-015-0056-1

Yan, Q., Zhang, J., Liu, H., Babu-Khan, S., Vassar, R., Biere, A. L., et al. (2003). Anti-inflammatory drug therapy alters beta-amyloid processing and deposition in an animal model of Alzheimer's disease. *J. Neurosci.* 23, 7504–7509. doi: 10.1523/JNEUROSCI.23-20-07504.2003

Yancopoulos, G. D., Davis, S., Gale, N. W., Rudge, J. S., Wiegand, S. J., and Holash, J. (2000). Vascular-specific growth factors and blood vessel formation. *Nature* 407, 242–248. doi: 10.1038/35025215

Yates, P. A., Desmond, P. M., Phal, P. M., Steward, C., Szoeke, C., Salvado, O., et al. (2014). Incidence of cerebral microbleeds in preclinical Alzheimer disease. *Neurology* 82, 1266–1273. doi: 10.1212/WNL.0000000000000285

Zetterberg, H., and Bendlin, B. B. (2020). Biomarkers for Alzheimer's disease-preparing for a new era of disease-modifying therapies. *Mol. Psychiatry*. doi: 10.1038/s41380-020-0721-9

Zhang, Y., Chao, F. L., Zhang, L., Jiang, L., Zhou, C. N., Chen, L. M., Lu, W., Jiang, R., and Tang, Y. (2019). Quantitative study of the capillaries within the white matter of the Tg2576 mouse model of Alzheimer's disease. *Brain Behav*. 9:e01268. doi: 10.1002/brb3.1268

Zhao, L. (2019). CD33 in Alzheimer's disease - biology, pathogenesis, and therapeutics: a mini-review. *Gerontology* 65, 323–331. doi: 10.1159/000492596

Zlokovic, B. V. (2005). Neurovascular mechanisms of Alzheimer's neurodegeneration. *Trends Neurosci*, 28: 202–208. doi: 10.1016/j.tins.2005.02.001

Zott, B., Simon, M. M., Hong, W., Unger, F., Chen-Engerer, H. J., Frosch, M. P., Sakmann, B., Walsh, D. M., and Konnerth, A. (2019). A vicious cycle of β amyloid-dependent neuronal hyperactivation. *Science* 365, 559–565. doi: 10.1126/science.aay0198

Conflict of Interest: The authors declare that the research was conducted in the absence of any commercial or financial relationships that could be construed as a potential conflict of interest.

frontiers in Aging Neuroscience

ORIGINAL RESEARCH
published: 25 January 2021
doi: 10.3389/fnagi.2020.627199

Motor Progression in Early-Stage Parkinson's Disease: A Clinical Prediction Model and the Role of Cerebrospinal Fluid Biomarkers

Ling-Yan Ma[1,2†], Yu Tian[3†], Chang-Rong Pan[3], Zhong-Lue Chen[4], Yun Ling[4], Kang Ren[4], Jing-Song Li[3] and Tao Feng[1,2,5*]*

[1] Department of Neurology, Center for Movement Disorders, Beijing Tiantan Hospital, Capital Medical University, Beijing, China, [2] China National Clinical Research Center for Neurological Diseases, Beijing, China, [3] Engineering Research Center of Electronic Medical Record (EMR) and Intelligent Expert System, College of Biomedical Engineering and Instrument Science, Zhejiang University, Ministry of Education, Hangzhou, China, [4] Gyenno Science Co. Ltd., Shenzhen, China, [5] Parkinson's Disease Center, Beijing Institute for Brain Disorders, Beijing, China

Background: The substantial heterogeneity of clinical symptoms and lack of reliable progression markers in Parkinson's disease (PD) present a major challenge in predicting accurate progression and prognoses. Increasing evidence indicates that each component of the neurovascular unit (NVU) and blood-brain barrier (BBB) disruption may take part in many neurodegenerative diseases. Since some portions of CSF are eliminated along the neurovascular unit and across the BBB, disturbing the pathways may result in changes of these substances.

Methods: Four hundred seventy-four participants from the Parkinson's Progression Markers Initiative (PPMI) study (NCT01141023) were included in the study. Thirty-six initial features, including general information, brief clinical characteristics and the current year's classical scale scores, were used to build five regression models to predict PD motor progression represented by the coming year's Unified Parkinson's Disease Rating Scale (MDS-UPDRS) Part III score after redundancy removal and recursive feature elimination (RFE)-based feature selection. Then, a threshold range was added to the predicted value for more convenient model application. Finally, we evaluated the CSF and blood biomarkers' influence on the disease progression model.

Results: Eight hundred forty-nine cases were included in the study. The adjusted R^2 values of three different categories of regression model, linear, Bayesian and ensemble, all reached 0.75. Models of the same category shared similar feature combinations. The common features selected among the categories were the MDS-UPDRS Part III score, Montreal Cognitive Assessment (MOCA) and Rapid Eye Movement Sleep Behavior Disorder Questionnaire (RBDSQ) score. It can be seen more intuitively that the model can achieve certain prediction effect through threshold range. Biomarkers had no significant impact on the progression model within the data in the study.

Conclusions: By using machine learning and routinely gathered assessments from the current year, we developed multiple dynamic models to predict the following year's

OPEN ACCESS

Edited by:
Dennis Qing Wang,
Southern Medical University, China

Reviewed by:
Angelo Antonini,
University of Padua, Italy
Xie Fen,
Southern Medical University, China

***Correspondence:**
Tao Feng
bxbkjys@sina.com
Jing-Song Li
ljs@zju.edu.cn

† These authors have contributed equally to this work

Received: *08 November 2020*
Accepted: *28 December 2020*
Published: *25 January 2021*

Citation:
Ma L-Y, Tian Y, Pan C-R, Chen Z-L, Ling Y, Ren K, Li J-S and Feng T (2021) Motor Progression in Early-Stage Parkinson's Disease: A Clinical Prediction Model and the Role of Cerebrospinal Fluid Biomarkers. Front. Aging Neurosci. 12:627199. doi: 10.3389/fnagi.2020.627199

motor progression in the early stage of PD. These methods will allow clinicians to tailor medical management to the individual and identify at-risk patients for future clinical trials examining disease-modifying therapies.

Keywords: Parksinon's disease, motor progression, predictive model, Parkinson's progression markers initiative, machine learning

INTRODUCTION

Parkinson's disease (PD) is a chronic progressive neurodegenerative disorder characterized by a broad spectrum of gradual motor and non-motor impairments (Selikhova et al., 2009). In the clinical course of PD, both linear (Gottipati et al., 2017; Holden et al., 2018) and non-linear (Vu et al., 2012; Reinoso et al., 2015) progression have been reported in the advancement of motor and non-motor symptoms. In an era of increasing focus on individualized management and disease-modifying therapies, there is a need to develop tools to predict motor progression at the individual level. However, the substantial heterogeneity (Foltynie et al., 2002; Selikhova et al., 2009; Ma et al., 2015; Qian and Huang, 2019) of clinical symptoms and lack of reliable progression markers present a major challenge in predicting accurate progression and prognoses.

The current literature on PD progression consists largely of associative analyses focusing on predictors such as gender, age, clinical subtype (Aleksovski et al., 2018), genes (Deng et al., 2019), cognitive status and baseline motor score (Reinoso et al., 2015). Greater progression of motor scores has been associated with several factors, such as male gender, older age at diagnosis, akinetic-rigid subtype, cognitive impairment (Reinoso et al., 2015), right-side onset (Baumann et al., 2014), orthostatic hypotension, and rapid eye movement sleep behavior disorder (Fereshtehnejad et al., 2015). Apart from associative analyses, a few prognostic models have been developed that focus on predicting different aspects of PD at the individual level, including logistic regression and Bayesian classification models to predict cognitive impairment (Schrag et al., 2017; Hogue et al., 2018; Gramotnev et al., 2019), machine-learning, random survival forests to predict time to initiation of symptomatic treatment (Simuni et al., 2016) and Bayesian machine-learning methods to predict motor progression (Latourelle et al., 2017) and data mining and classification techniques to predicting faster symptoms worsening at baseline patients evaluation (Tsiouris et al., 2017). Based on the Parkinson's Progression Markers Initiative (PPMI) database, Latourelle et al. developed comprehensive multivariable prognostic models to predict the annual rate of change in PD (Latourelle et al., 2017). The authors included relatively comprehensive indicators, including baseline molecular and clinical variables, to construct an ensemble of models to better clarify and analyze the predictors. However, due to the large heterogeneity of motor symptoms and the complexity of related factors, it was difficult to predict motor progression with high accuracy. The models yielded a cross-validated R^2 value of 41% for the PPMI cohort and 9% for the LABS-PD cohort.

Increasing evidence indicates that each component of the neurovascular unit and blood-brain barrier (BBB) disruption may take part in many neurodegenerative diseases (Yamazaki and Kanekiyo, 2017). Since some portions of Cerebrospinal Fluid (CSF) are eliminated along the neurovascular unit and across the BBB, disturbing the pathways may result in changes of these substances. CSF biomarkers in PD, such as α-synuclein species, lysosomal enzymes, markers of amyloid and tau pathology, and neurofilament light chain, have been suggested to possess potential diagnostic and prognostic value of PD (Parnetti et al., 2019). In large areas of undeveloped countries, costly tests, such as genetic and CSF testing, and image detection for PD (PET and MIBG), could exert a great burden on patients and medical security systems. Furthermore, the corresponding variables are not data routinely used for common clinical activities and are difficult to obtain. Considering clinical needs and utility, by using machine-learning methods with PD patient data from the PPMI database, we aim to develop multiple dynamic models to predict motor progression based on general information and classical clinical scales, displayed in the form of the Movement Disorder Society-Unified Parkinson's Disease Rating Scale (MDS-UPDRS) Part III score. We also explore the influence of CSF and blood biomarkers on the prediction model. The use of baseline assessments (e.g., age, gender, disease duration, motor and non-motor examination, validated self-report questionnaires), which are either already routinely performed or could be reasonably implemented during a typical neurologist's office visit, can facilitate widespread implementation of this cost-efficient predictive model in real world applications.

METHODS

Participants

Data used in the preparation of the article were obtained from the PPMI database. The PPMI is an international, multicenter, prospective study designed to discover, and validate biomarkers of disease progression in newly diagnosed PD participants (National Clinical Trials identifier NCT01141023). Each PPMI recruitment site received approval from an institutional review board or ethics committee on human experimentation before study initiation. Written informed consent for research was obtained from all individuals participating in the study. The PPMI database was accessed on December 9, 2020, to obtain data from baseline visits ($n = 474$) and follow-up visits (the numbers of follow-up visits for five separate years are 380, 323, 257, 259, 230). For up-to-date information on the study, please visit www.ppmi-info.org.

Model Variables

The main model outcomes of interest were motor function in the coming year. The primary outcome was the MDS-UPDRS Part

III score. Predictive variables included demographics, disease duration, and measures of motor (off state) and non-motor function. Motor assessments included the MDS-UPDRS Parts II-IV, Hoehn and Yahr Stage (H&Y), PD subtype evaluations (tremor dominant (TD), postural instability and gait difficulty (PIGD) and TD/PIGD scores). For non-motor evaluation, the Epworth Sleepiness Scale Score (ESS) and REM Sleep Behavior Disorder Screening Questionnaire Score (RBDSQ) were applied to measure a patient's sleep quality and disturbances. The Questionnaire for Impulsive-Compulsive Disorders in Parkinson's Disease (QUIP) score was used to evaluate PD impulse control disorders. The Geriatric Depression Scale (GDS) score was designed specifically to screen for depression in geriatric patients. The total score of the assessment of autonomic dysfunction in Parkinson's disease (SCOPA-AUT) was used to evaluate autonomic nervous function in the prior month. The MDS-UPDRS Part I score and component scores were used to evaluate mood and mentation.

In addition, we assessed whether biomarkers including CSF amyloid, CSF α-synuclein (and its ratio to CSF amyloid), serum uric acid had an impact on the progression model in the study.

Data Preprocessing

Each patient had a maximum of five samplings performed at different intervals. During data processing, we excluded negative differences in the MDS-UPDRS Part III score between the coming year and the prior year. According to the PPMI protocol, the "off state" was evaluated as more than 6 h after the last dose of dopaminergic therapy. Considering that the disease was always in a progressive state for all patients, a decrease in the MDS-UPDRS Part III score with increasing disease duration was thought to be unrealistic; therefore, patient samples that displayed this trend were discarded. Furthermore, as eliminating redundant information can improve the quality of the prediction model, we performed Spearman rank correlation analysis to ensure that no variables were correlated with a correlation coefficient of more than 0.5. Prior to model construction, all variables were transformed to a z-score by subtracting the mean value from each of the observed values and dividing by the standard deviation because the clinical phenotypes were measured on different scales and with different score ranges.

Regression Model Construction

First, the preprocessed data were divided into training and test sets. There were two dividing principles: (1) After ordering by diagnosis date, the first 75% of patients were included in the training data set; the remaining patients were included in the test set. (2) To avoid data overlapping, samples from the same patient were placed into either the training or test set.

We used five regression algorithms, including linear, ridge, Bayesian, random forest, and gradient boosting decision tree regression, to build the model with the training set. Features were selected using the recursive feature elimination (RFE) method. By evaluating model performance, the most irrelevant variables were eliminated in each iteration of the regression, and then the contributions of the remaining variables to the model were ranked. To select the best combination of features, RFE was performed with cross-validation to calculate the verification error of all subsets of features. The subset with the smallest error was regarded as the final feature combination. Next, regression models were built with parameter adjustment to achieve the best performance. Finally, the models were validated with the test set.

Assessment of Biomarkers' Influence on Parkinson's Disease Progression Model

Due to the great difference between the absence of biomarkers and other clinical variables, the initial inclusion would result in smaller amounts of data. So, biomarkers were added after model construction based on the clinical and scale scores data to evaluate their influence on the basic model. First, correlation analysis was performed between biomarkers and disease progression. Then the variables with significant correlation were selected to improve the models and we compared the model difference between before and after adding the biomarkers variables.

Statistical Analysis and Performance Measures

Descriptive statistics of the patients' demographic and clinical characteristics are summarized in **Table 1**. The Kolmogorov-Smirnov test was used to test the normality of continuous data. Continuous variables are described by the mean, standard deviation, maximum, and minimum. Categorical variables are expressed as percentages. The *t*-test was used to compare regression models before and after adding biomarkers variables. Two-tailed $p < 0.05$ were considered to indicate statistical significance.

The performance of the models was assessed by the root mean square error (RMSE) and the adjusted coefficient of determination (adjusted R-squared coefficient or adjusted R^2). R^2 is a statistical measure in the regression model, equal to the ratio of the regression sum of squares to the total sum of squares and which reflects the degree of agreement between the data and the model. The influence of the number of variables on the goodness is excluded in the adjusted R^2. Because doctors may score the same patient with minor differences in terms of the clinical significance of the symptom, we added a threshold range to each predicted value, which acted as the midpoint of the range, observed whether the true value fell within the range and calculated the accuracy for more convenient application of the model.

RESULTS

Patient Demographic and Clinical Characteristics

In this study, 474 (312 males and 162 females; M:F ratio 1.926:1; mean age 61.473 ± 9.753 years) PD patients were enrolled. The mean age of disease onset was 59.460 years, and the mean disease duration was 6.710 months at baseline. None of the continuous data were normally distributed according to the Kolmogorov–Smirnov test. Descriptive statistics of the

TABLE 1 | Descriptive statistics of the demographic and clinical variables of the Parkinson's progression markers initiative study participants.

Variables	Mean (SD; Min; Max)	Percentage (%)
Age	61.473 (9.753; 33.498; 84.884)	
Gender		Male: 65.823
		Female: 34.177
Age at symptom onset	59.460 (10.054; 25.370; 83.008)	
Side most affected at PD onset		Left: 39.873
		Right: 56.962
		Symmetric: 3.165
Family History of PD		First degree family w/PD: 14.768
		Non-1st degree family w/PD: 11.392
		No family w/PD: 73.840
Duration (Months)	6.710 (6.664; 0.400; 37.000)	
Total rigidity score	3.508 (2.703; 0.000; 13.000)	
Hoehn & Yahr stage		Stage 1:45.992
		Stage 2:53.376
		Stage 3: 0.633
TD/PIGD classification (OFF)		TD: 71.730
		PIGD: 17.300
		Indeterminate: 10.970
Tremor score (OFF)	4.340 (3.105; 0.000; 18.000)	
MDS-UPDRS part III score (OFF)	19.937 (9.141; 2.000; 51.000)	
ESS score	6.162 (3.758; 0.000; 20.000)	
RBDSQ score	4.162 (2.686; 0.000; 12.000)	
MOCA score	27.133 (2.325; 17.000; 30.000)	
QUIP score	0.325 (0.697; 0.000; 4.000)	
GDS score	2.464 (2.672; 0.000; 14.000)	
SCOPA-AUT total score	10.103 (6.760; 0.000; 44.000)	
MDS-UPDRS part I score	5.956 (4.571; 0.000; 27.000)	
Initial symptom (at diagnosis)—resting tremor		Symptom present at diagnosis: 78.692
Initial symptom (at diagnosis)—rigidity		Symptom present at diagnosis: 73.840
Initial symptom (at diagnosis)—bradykinesia		Symptom present at diagnosis: 82.068
Initial symptom (at diagnosis)—postural instability		Symptom present at diagnosis: 7.595

SD, Standard deviation; Min, Minimum; Max, Maximum; TD, Tremor Dominant; PIGD, Postural Instability/Gait Difficulty; MDS-UPDRS, Movement Disorder Society-Unified Parkinson's Disease Rating Scale; ESS, Epworth Sleepiness Scale; RBDSQ, REM Sleep Behavior Disorder Screening Questionnaire; MOCA, Montreal Cognitive Assessment; QUIP, Questionnaire for Impulsive-Compulsive Disorders in Parkinson's Disease; GDS, Geriatric Depression Scale; SCOPA-AUT, Assessment of autonomic dysfunction in Parkinson's disease.

general and total score variables are shown in **Table 1** and other detailed score variables are shown in **Supplementary Table 1**. A heatmap of the Spearman correlation coefficients between the variables are depicted in **Figure 1**. To reduce redundant information, we eliminated variables with strong correlations. So, most of the individual items were removed and the total scores were retained. In total, 24 features remained and are shown in **Table 2**. Apart from these, we also calculated the correlations between the 24 individual variables and the outcome event. The variables with the top five highest correlations were MDS-UPDRS Part III Score (0.882), Duration of Disease since Diagnosis (0.269), MDS-UPDRS Part I Apathy (0.197), SCOPA-AUT Total Score (0.196), and MDS-UPDRS Part I Fatigue (0.154). The correlation coefficients and probability values of all 24 variables are shown in **Supplementary Table 2**.

Prediction Model Construction and Performance Measures

After eliminating the missing data, a total of 849 cases were left, among which 633 cases were placed in the training set and 216 in the test set according to the aforementioned dividing principles. The disease progression as expressed by the MDS-UPDRS Part III score of the coming year was predicted based on the information from the previous year. We built regression models based on five algorithms, and their performances are shown in **Table 3**. The models can be divided into three categories: linear, Bayesian and ensemble methods. The adjusted R^2 of all the models reached above 0.75. The feature combinations obtained by the RFE method for models in the same category were similar and the feature importance or coefficient of each model is shown in **Table 4**. The models from each of the categories jointly selected the same three features: MDS-UPDRS Part III score, MOCA

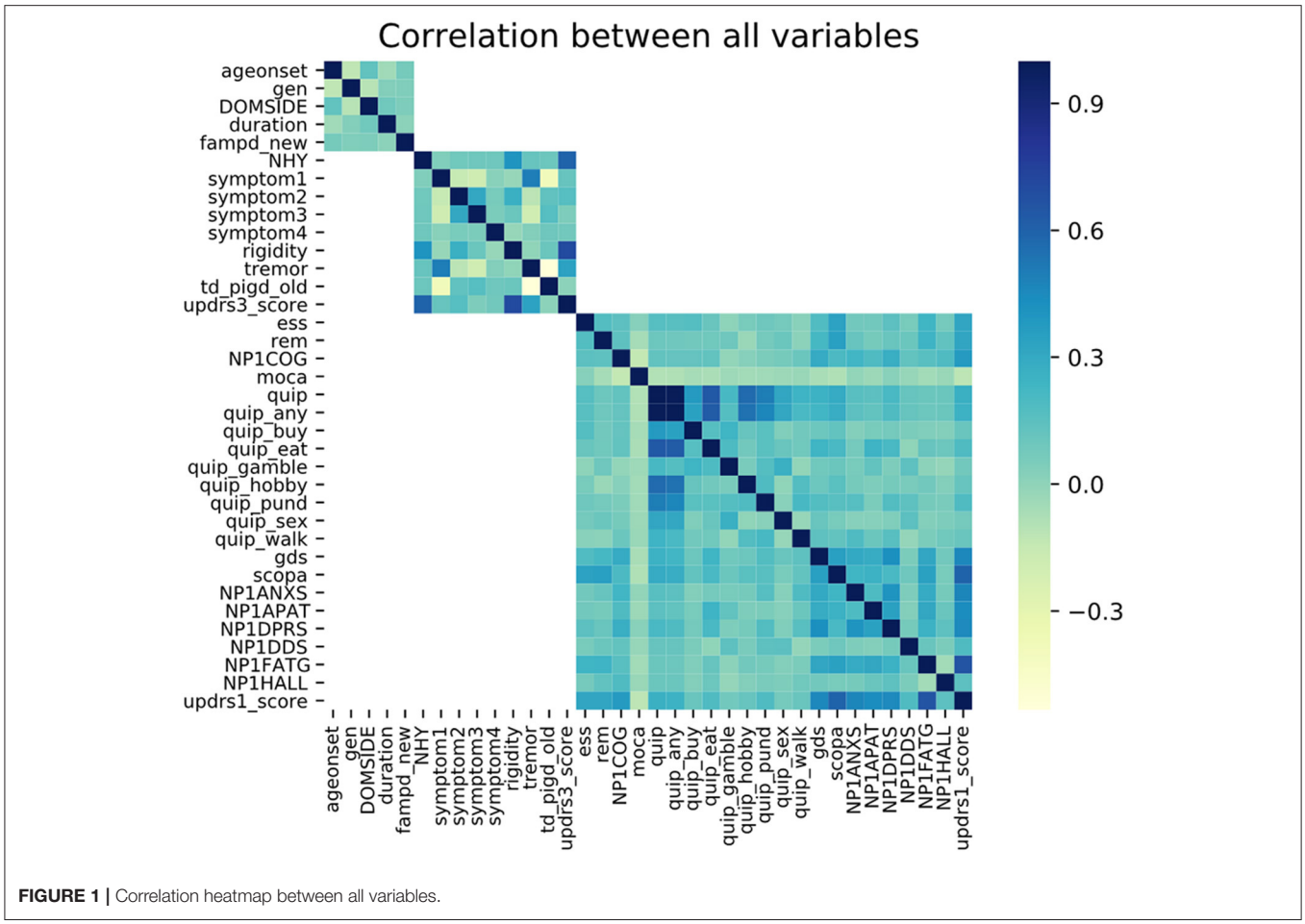

FIGURE 1 | Correlation heatmap between all variables.

TABLE 2 | The remaining 24 features after eliminating features with strong correlation.

Category	Features
General	Age at symptom onset gender side most affected at PD onset Duration (Months) family history of PD
Motor	Four initial symptoms at diagnosis TD/PIGD classification MDS-UPDRS Part III Score
Non-motor	ESS score RBDSQ score QUIP score GDS score SCOPA-AUT total score MOCA score MDS-UPDRS part I analytic score

TABLE 3 | The performance of five regression models.

Model category	Model	Adjusted R^2	RMSE
Linear methods	Linear regression	0.779	5.585
	Ridge regression	0.779	5.584
Bayesian method	Bayesian regression	0.778	5.579
Ensemble methods	Random forest	0.770	5.678
	Gradient boosting	0.753	5.918

Score and RBDSQ score. All coefficients of regression models are shown in **Table 5**.

Taking as an example, the random forest (RF) regression had an adjusted R^2 of 0.770 and an RMSE of 5.678. The importance of each feature in the model is computed as the total reduction in the criterion introduced by that feature and is shown in **Table 4**. **Figure 2** presents the evaluation of the predictions on the test set, with the predicted value as the midpoint of threshold ranges with half-range widths of 5, 6, and 7 for adjustment. Finally, we calculated the proportion of the true value that fell into the range as the accuracy.

Biomarkers Influence on Parkinson's Disease Progression Model

At the end of the study, the influence of biomarkers on Parkinson's disease progression model was analyzed. First, we performed spearman correlation analysis between biomarkers

TABLE 4 | The feature importance or coefficient of features selected through RFE method in five regression models.

Features selected through RFE method	Feature importance or coefficient				
	Linear regression	Ridge regression	Bayesian regression	Random forest	Gradient boosting
MDS-UPDRS part III score (OFF)	0.970	0.970	0.976	0.929	0.958
Age at symptom onset	/	/	/	0.009	0.002
Duration (months)	/	/	/	0.028	0.030
Family history of PD	0.523	0.521	0.326	/	/
MDS-UPDRS part I anxious mood	0.484	0.479	0.209	/	/
RBDSQ score	0.151	0.151	0.103	0.010	0.007
MDS-UPDRS part I features of dopamine dysregulation syndrome	−1.780	−1.738	−1.302	/	/
Initial symptom (at diagnosis)—postural instability	/	/	0.427	/	/
ESS score	/	/	/	0.010	/
SCOPA-AUT total score	/	/	/	0.007	/
MOCA score	−0.031	−0.031	−0.001	0.007	0.003

TABLE 5 | All coefficients of regression models.

Model	Coefficients
Linear regression	/
Ridge regression	Regularization strength = 1.32
Bayesian regression	Maximum number of iterations = 300
Random forest	The number of trees in the forest = 260
	The maximum depth of the tree = 4
	The function to measure the quality of a split = "the mean absolute error"
Gradient boosting	The number of boosting stages to perform = 30
	Learning rate = 0.1
	The function to measure the quality of a split = "the mean squared error with improvement score by Friedman"

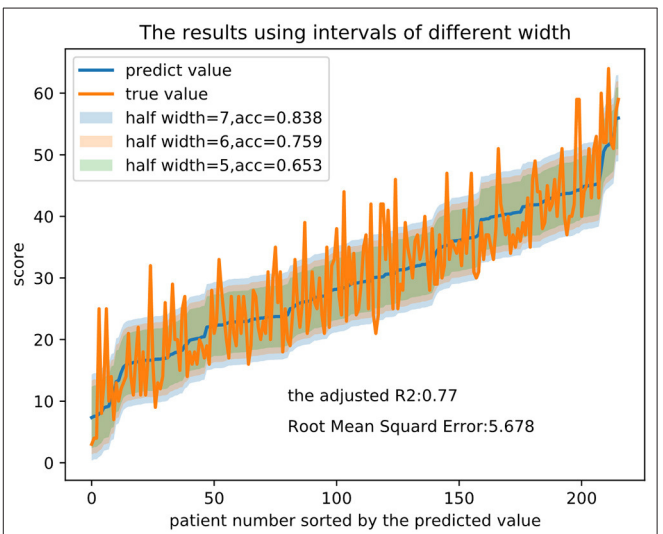

FIGURE 2 | Prediction results and intervals of different widths in the RF regression model. Note that half width represents half of the width of the threshold range and acc represents the proportion of the true value that falls into the range.

and disease progression and found that the CSF amyloid and CSF α-synuclein were significantly associated with disease progression, of which the correlation coefficient were, respectively, −0.132, −0.160. The correlation analysis results of other variables are shown in **Supplementary Table 1**. After incorporating the two variables into feature combinations selected by feature selection based on clinical characters and scales scores and eliminating the missing data, a total of 441 cases were left. The models were reconstructed based on the feature combinations before and after the inclusion of biomarkers variables and the performance of two sets of models were compared by *t*-test. The *P*-value were 0.408 and 0.883 respectively, showing no significant difference and indicating that these biomarkers had no significant impact on the progression model within the data in the study. The R^2 and RMSE of different regression models are shown in **Supplementary Table 3**.

DISCUSSION

In this study, we analyzed longitudinal data from the PPMI database to develop a predictive model for motor progression in patients with early PD. Five algorithms representing three model

categories (linear, ensemble and Bayesian) were developed; and the adjusted R^2 values of the models all reached 0.75. Our findings indicate that the models can practically predict the MDS-UPDRS Part III score of the coming year based on the clinically available characteristics obtained in the current year.

Our results suggest that all five algorithms (linear, ridge, Bayesian, RF and gradient boosting decision tree), categorized into linear, Bayesian and ensemble methods, have similar accuracies and features. Three common predictors were selected among the three categories: MDS-UPDRS Part III score, MOCA Score, and RBDSQ. In particular, functional status in the current year as measured by the MDS-UPDRS Part III (correlation coefficient 0.882; for more details, see the **Supplementary Table 2**) was consistent with and a relatively strong predictor of motor performance for the coming year. This is understandable, given that motor symptoms progress based on prior clinical features. Essentially, the results indicate that the worse one's baseline motor dysfunction is, the higher the MDS-UPDRS Part III score will be the following year.

Sleep disturbances such as disrupted circadian rhythm, insomnia, excessive daytime sleepiness (EDS), and rapid eye movement sleep behavior disorder (RBD) correlate with faster progression of motor symptoms and lower quality of life (Arnulf, 2005; Dulovic and Vos, 2018; Pagano et al., 2018). In our study, the scores of the scales used to evaluate RBD and EDS were important predictors for the progression of motor symptoms in the RF regression model, with RBD evaluation being a common predictor among the five algorithms. Subjective EDS in PD has been associated with advanced motor impairment and disease progression, male gender and the use of anti-parkinsonian medications (Arnulf, 2005; Dulovic and Vos, 2018). RBD is an aggravating factor of motor symptoms (Pagano et al., 2018), autonomic dysfunction, and dementia (Chahine et al., 2016). In a longitudinal analysis of early PD, the presence of RBD was found to predispose a patient toward a more aggressive phenotype characterized by a rapid progression of motor symptoms (Pagano et al., 2018). The promotion of neurodegeneration caused by sleep dysfunction has been proposed to drive further sleep alterations, creating a detrimental self-perpetuating cycle (Musiek and Holtzman, 2016).

Cognitive impairment at baseline is also significantly associated with faster disease progression and greater motor impairment, which has been identified in other studies (Velseboer et al., 2013; Fereshtehnejad et al., 2015; Reinoso et al., 2015). Fereshtehnejad et al. (2015) found that, besides UPDRS values, signs of cognitive impairment, orthostatic hypotension and rapid eye movement sleep behavior disorder at baseline evaluation, could suggest that patients will express a much faster decline in motor symptoms. This is mainly due to an increase in L-dopa non-responsive symptoms, which suggest a diffuse destruction of extra-nigrostriatal pathways in parallel with the nigrostriatal pathway (Velseboer et al., 2013).

There are some differences in the predictors selected among the models, which may be related to their different operating principles. The core idea underlying ensemble learning is to learn a series of basic classifiers from training data and then combine these relatively weak classifiers into a strong classifier. Then, the predictive ability of the categorical variables can be given full play, allowing the ensemble learning model to achieve a predictive effect with fewer variables. We observed this behavior among our ensemble learning models as well.

Parkinson's disease is a clinically heterogeneous disease with varied progression patterns (Qian and Huang, 2019; Beheshti et al., 2020; Haumesser et al., 2020; LeWitt et al., 2020; Shen et al., 2020). In addition to genetic factors (Gao et al., 2020), the availability of objective fluid biomarkers specifically associated with motor or cognitive trajectories of PD subtypes could allow reliable prediction of clinical outcomes (Qian and Huang, 2019; Xie et al., 2019). As for blood biomarkers, studies on blood oligomeric α-synuclein showed increased quantities in patients with PD both in serum (Williams et al., 2016) and in red blood cells(RBCs) (Wang et al., 2015; Zhao et al., 2016; Daniele et al., 2018). Similarly, plasma phosphorylated α-synuclein is higher in patients with Parkinson's disease compared with controls (Foulds et al., 2013). In addition to α-synuclein, there are several substances playing essential roles in PD. The lower plasma levels of serum superoxide dismutase (SOD), total cholesterol, high-density lipoprotein cholesterol (HDL-C), and low-density lipoprotein cholesterol (LDL-C) and increased level of high-sensitivity C-reactive protein (hsCRP) were found in PD, which might be important markers to assess the PD severity (Yang et al., 2020). One study showed a significant decrease in the ubiquitous mitochondrial creatine kinase (uMtCK) activity in the PD group and a correlation between serum uMtCK activities and the disease progression rate, duration, and age at onset in PD patients (Xu et al., 2019). Compared with healthy subjects, the serum levels of Trefoil factor 3 (TFF3) and cholinesterase activity were lower, while homocysteine (Hcy) was higher in patients with Parkinson's disease dementia (PDD) and vascular parkinsonism with dementia (VPD). Significant correlations between TFF3/ChE activity/Hcy levels and PDD/VPD severities were found, including motor dysfunction, declining cognition, and mood/gastrointestinal symptoms (Zou et al., 2018). To explore the vascular, inflammatory, metabolic risk factors of dementia in PD with type 2 diabetes mellitus (DM) (PD-DM), lower LDL, and higher fibrinogen were the most significant risk factors in PD-DM with dementia (Wang et al., 2020).

Evidence suggests that measures of CSF Aβ1-42, T-tau, P-tau181, and α-synuclein have prognostic and diagnostic potential in early-stage PD (Kang et al., 2013). Levels of α-synuclein in CSF are decreased in PD and other synucleinopathies and may serve as a marker to assist in diagnosis and prognosticating progression (Hong et al., 2010; Mollenhauer et al., 2011). Research has revealed that the NLR family pyrin domain containing 3 protein (NLRP3) inflammasome may facilitate the secretion of extracellular vesicles, as well as exosomal transmission of proteins like aggregated α-synuclein (Si et al., 2020). However, in prodromal and early PD, CSF α-synuclein does not correlate with PD's progression and does not reflect ongoing dopaminergic neurodegeneration (Mollenhauer et al., 2019). In our study, CSF biomarkers and serum uric acid had no significant impact on the progression model, indicating that easily accessible clinical assessments have sufficient capacity to predict disease progression.

Previouly, based on the PPMI database, Latourelle et al. developed comprehensive multivariable prognostic models to predict the annual rate of change in PD (Latourelle et al., 2017). There are several differences between the two studies. The first one concerns to be the methodology and objectives. The previous study mainly focused on causal analysis, which differs from our research on prediction analysis. Although the value of R^2 was small in the previous study, causal analysis can also be conducted to determine the effect of independent variables on dependent variables (Latourelle et al., 2017). In Latourelle's study, the R^2 value of the model was 41% for the PPMI database and 9% for the Lab-PD cohort. The shortcomings of a small R^2 can be offset by a large sample size. In our work, maximization of the R^2 value was critical for prediction. The adjusted R^2 value for the models in each of the three categories reached 0.75, indicating that the selected features had a good predictive ability for motor scores. In general, predicting the patient's future condition can assist doctors in making decisions on when to intervene. Second, the selected features varied between the two studies. The model variables in Latourelle et al.'s study included many clinical, genetic and laboratory examinations. However, the variables in our study were all general data and clinical evaluation indicators, which could be obtained by a single doctor in the outpatient department without the need for relatively complex laboratory and imaging examinations. Thus, the use of these variables can greatly enhance the clinical practicality of our model.

Our research possesses a number of strengths. First, our prediction model was developed based on data from the previous year in order to predict annual motor symptoms, a dynamic process that has a high degree of practical clinical application value. Additionally, this study included information that was easy to obtain in the patient interview process as model features, making the model feasible for practical application. Doctors can embed the model creation process in an electronic medical record system to predict the next year's motor function automatically based on the patient's current clinical data. Second, the PPMI database contains data from different hospitals in different regions, which helps improve the accuracy of prediction.

However, there are also several limitations in our study. First, the subtypes of PD were not considered, and only uniform predictions across subtypes were made. Second, only the MDS-UPDRS Part III total score was predicted as the model result, and no subdivision prediction was made for a single item or symptom category score (such as limb rigidity, central axis slowing, tremor, gait, etc.). It is possible that the relevant trends in variability would not be reflected in the total score. Third, our study focused on the early stage of PD. Thus, the model does not apply to patients with advanced PD.

CONCLUSIONS

In the present study, by using machine learning and routinely gathered assessments, we developed convenient predictive models synthesizing multiple clinical characteristics to provide 75% accuracy in predicting motor progression. CSF biomarkers and serum uric acid had no significant impact on the progression model, indicating that easily accessible clinical assessments have sufficient capacity to predict disease progression. The use of these models can predict motor evaluations at the individual level, allowing clinicians to tailor medical management for each patient and identify at-risk patients for future clinical trials investigating delaying motor progression. Future predictive models based on other large cohorts, assigned into training, and validation sets are needed to verify the accuracy of our results.

DATA AVAILABILITY STATEMENT

The datasets presented in this study can be found in online repositories. The names of the repository/repositories and accession number(s) can be found at: www.ppmi-info.org.

ETHICS STATEMENT

The studies involving human participants were reviewed and approved by Parkinson's Research and the National Institute of Neurological Disorders and Stroke (1P20NS092529-01). The patients/participants provided their written informed consent to participate in this study.

AUTHOR CONTRIBUTIONS

L-YM and YT participated in the design of the study, drafted the manuscript, and carried out the conceptualization of the study. C-RP, Z-LC, YL, and KR performed data analysis and drafted the manuscript. TF and J-SL carried out the conceptualization of the study, reviewing, and critiquing the article at the same time. All authors contributed to the article and approved the submitted version.

FUNDING

This research was supported by Natural Science Foundation of China (Nos. 82071422 and 81771367), National Key R&D Program of China (No. 2016YFC1306501), Capital Characteristic Clinic Project (No. Z171100001017041), Beijing Municipal Science and Technology Commission (Nos. Z151100003915117 and Z151100003915150), and Beijing Natural Science Foundation (No. 7164254). This work was also supported by grants from the Michael J. Fox Foundation for Parkinson's Research and the National Institute of Neurological Disorders and Stroke (Grant No. 1P20NS092529-01). PPMI—a public-private partnership—is funded by the Michael J. Fox Foundation for Parkinson's Research and funding partners, including Abbvie, Avid, Biogen, BioLegend, Bristol-Myers Squibb, GE Healthcare, Genentech, GlaxoSmithKline, Lilly, Lundbeck, Merck, Meso Scale Discovery, Pfizer, Piramal, Roche, Sanofi, Servier, Takeda, Teva, UCB, and Golub Capital.

SUPPLEMENTARY MATERIAL

The Supplementary Material for this article can be found online at: https://www.frontiersin.org/articles/10.3389/fnagi.2020.627199/full#supplementary-material

REFERENCES

Aleksovski, D., Miljkovic, D., Bravi, D., and Antonini, A. (2018). Disease progression in Parkinson subtypes: the PPMI dataset. *Neurol. Sci.* 39, 1971–1976. doi: 10.1007/s10072-018-3522-z

Arnulf, I. (2005). Excessive daytime sleepiness in parkinsonism. *Sleep Med. Rev.* 9, 185–200. doi: 10.1016/j.smrv.2005.01.001

Baumann, C. R., Held, U., Valko, P. O., Wienecke, M., and Waldvogel, D. (2014). Body side and predominant motor features at the onset of Parkinson's disease are linked to motor and nonmotor progression. *Mov. Disord.* 29, 207–213. doi: 10.1002/mds.25650

Beheshti, I., Mishra, S., Sone, D., Khanna, P., and Matsuda, H. (2020). T1-weighted MRI-driven brain age estimation in Alzheimer's disease and Parkinson's disease. *Aging Dis.* 11, 618–628. doi: 10.14336/AD.2019.0617

Chahine, L. M., Xie, S. X., Simuni, T., Tran, B., Postuma, R., Amara, A., et al. (2016). Longitudinal changes in cognition in early Parkinson's disease patients with REM sleep behavior disorder. *Parkinsonism Relat. Disord.* 27, 102–106. doi: 10.1016/j.parkreldis.2016.03.006

Daniele, S., Frosini, D., Pietrobono, D., Petrozzi, L., Lo Gerfo, A., Baldacci, F., et al. (2018). α-Synuclein heterocomplexes with β-amyloid are increased in red blood cells of Parkinson's disease patients and correlate with disease severity. *Front. Mol. Neurosci.* 11:53. doi: 10.3389/fnmol.2018.00053

Deng, X., Xiao, B., Allen, J. C., Ng, E., Foo, J. N., Lo, Y. L., et al. (2019). Parkinson's disease GWAS-linked park16 carriers show greater motor progression. *J. Med. Genet.* 56, 765–768. doi: 10.1136/jmedgenet-2018-105661

Dulovic, M., and Vos, M. (2018). Sleep dysfunction in Parkinson's disease: novel molecular mechanism and implications for therapy. *Mov. Disord.* 33, 1558–1559. doi: 10.1002/mds.27495

Fereshtehnejad, S. M., Romenets, S. R., Anang, J. B., Latreille, V., Gagnon, J. F., and Postuma, R. B. (2015). New clinical subtypes of parkinson disease and their longitudinal progression: a prospective cohort comparison with other phenotypes. *JAMA Neurol.* 72, 863–873. doi: 10.1001/jamaneurol.2015.0703

Foltynie, T., Brayne, C., and Barker, R. A. (2002). The heterogeneity of idiopathic Parkinson's disease. *J. Neurol.* 249:138–145. doi: 10.1007/PL00007856

Foulds, P. G., Diggle, P., Mitchell, J. D., Parker, A., Hasegawa, M., Masuda-Suzukake, M., et al. (2013). A longitudinal study on α-synuclein in blood plasma as a biomarker for Parkinson's disease. *Sci. Rep.* 3:2540. doi: 10.1038/srep02540

Gao, X., Huang, Z., Feng, C., Guan, C., Li, R., Xie, H., et al. (2020). Multimodal analysis of gene expression from postmortem brains and blood identifies synaptic vesicle trafficking genes to be associated with Parkinson's disease. *Brief Bioinform*. doi: 10.1093/bib/bbaa244. [Epub ahead of print].

Gottipati, G., Karlsson, M. O., and Plan, E. L. (2017). Modeling a composite score in Parkinson's disease using item response theory. *AAPS J.* 19, 837–845. doi: 10.1208/s12248-017-0058-8

Gramotnev, G., Gramotnev, D. K., and Gramotnev, A. (2019). Parkinson's disease prognostic scores for progression of cognitive decline. *Sci. Rep.* 9:17485. doi: 10.1038/s41598-019-54029-w

Haumesser, J. K., Beck, M. H., Pellegrini, F., Kühn, J., Neumann, W. J., Altschüler, J., et al. (2020). Subthalamic beta oscillations correlate with dopaminergic degeneration in experimental parkinsonism. *Exp. Neurol.* 335:113513. doi: 10.1016/j.expneurol.2020.113513

Hogue, O., Fernandez, H. H., and Floden, D. P. (2018). Predicting early cognitive decline in newly-diagnosed Parkinson's patients: a practical model. *Parkinsonism Relat. Disord.* 56, 70–75. doi: 10.1016/j.parkreldis.2018.06.031

Holden, S. K., Finseth, T., Sillau, S. H., and Berman, B. D. (2018). Progression of MDS-UPDRS scores over five years in *de novo* Parkinson disease from the parkinson's progression markers initiative cohort. *Mov. Disord. Clin. Pract.* 5, 47–53. doi: 10.1002/mdc3.12553

Hong, Z., Shi, M., Chung, K. A., Quinn, J. F., Peskind, E. R., Galasko, D., et al. (2010). DJ-1 and alpha-synuclein in human cerebrospinal fluid as biomarkers of Parkinson's disease. *Brain* 133, 713–726. doi: 10.1093/brain/awq008

Kang, J. H., Irwin, D. J., Chen-Plotkin, A. S., Siderowf, A., Caspell, C., Coffey, C. S., et al. (2013). Association of cerebrospinal fluid β-amyloid 1-42, T-tau, P-tau181, and α-synuclein levels with clinical features of drug-naive patients with early Parkinson disease. *JAMA Neurol.* 70, 1277–1287. doi: 10.1001/jamaneurol.2013.3861

Latourelle, J. C., Beste, M. T., Hadzi, T. C., Miller, R. E., Oppenheim, J. N., Valko, M. P., et al. (2017). Large-scale identification of clinical and genetic predictors of motor progression in patients with newly diagnosed Parkinson's disease: a longitudinal cohort study and validation. *Lancet Neurol.* 16, 908–916. doi: 10.1016/S1474-4422(17)30328-9

LeWitt, P. A., Kymes, S., and Hauser, R. A. (2020). Parkinson disease and orthostatic hypotension in the elderly: recognition and management of risk factors for falls. *Aging Dis.* 11, 679–691. doi: 10.14336/AD.2019.0805

Ma, L. Y., Chan, P., Gu, Z. Q., Li, F. F., and Feng, T. (2015). Heterogeneity among patients with Parkinson's disease: cluster analysis and genetic association. *J. Neurol. Sci.* 351, 41–45. doi: 10.1016/j.jns.2015.02.029

Mollenhauer, B., Caspell-Garcia, C. J., Coffey, C. S., Taylor, P., Singleton, A., Shaw, L. M., et al. (2019). Longitudinal analyses of cerebrospinal fluid α-synuclein in prodromal and early Parkinson's disease. *Mov. Disord.* 34, 1354–1364. doi: 10.1002/mds.27806

Mollenhauer, B., Locascio, J. J., Schulz-Schaeffer, W., Sixel-Döring, F., Trenkwalder, C., and Schlossmacher, M. G. (2011). α-Synuclein and tau concentrations in cerebrospinal fluid of patients presenting with parkinsonism: a cohort study. *Lancet Neurol.* 10, 230–240. doi: 10.1016/S1474-4422(11)70014-X

Musiek, E. S., and Holtzman, D. M. (2016). Mechanisms linking circadian clocks, sleep, and neurodegeneration. *Science* 354, 1004–1008. doi: 10.1126/science.aah4968

Pagano, G., De Micco, R., Yousaf, T., Wilson, H., Chandra, A., and Politis, M. (2018). REM behavior disorder predicts motor progression and cognitive decline in Parkinson disease. *Neurology* 91, e894-894.e905. doi: 10.1212/WNL.0000000000006134

Parnetti, L., Gaetani, L., Eusebi, P., Paciotti, S., Hansson, O., El-Agnaf, O., et al. (2019). CSF and blood biomarkers for Parkinson's disease. *Lancet Neurol.* 18, 573–586. doi: 10.1016/S1474-4422(19)30024-9

Qian, E., and Huang, Y. (2019). Subtyping of Parkinson's Disease - Where Are We Up To. *Aging Dis.* 10, 1130–1139. doi: 10.14336/AD.2019.0112

Reinoso, G., Allen, J. C. Jr, Au, W. L., Seah, S. H., Tay, K. Y., and Tan, L. C. (2015). Clinical evolution of Parkinson's disease and prognostic factors affecting motor progression: 9-year follow-up study. *Eur. J. Neurol.* 22, 457–463. doi: 10.1111/ene.12476

Schrag, A., Siddiqui, U. F., Anastasiou, Z., Weintraub, D., and Schott, J. M. (2017). Clinical variables and biomarkers in prediction of cognitive impairment in patients with newly diagnosed Parkinson's disease: a cohort study. *Lancet Neurol.* 16, 66–75. doi: 10.1016/S1474-4422(16)30328-3

Selikhova, M., Williams, D. R., Kempster, P. A., Holton, J. L., Revesz, T., and Lees, A. J. (2009). A clinico-pathological study of subtypes in Parkinson's disease. *Brain* 132, 2947–2957. doi: 10.1093/brain/awp234

Shen, Y. T., Yuan, Y. S., Wang, M., Zhi, Y., Wang, J. W., Wang, L. N., et al. (2020). Dysfunction in superior frontal gyrus associated with diphasic dyskinesia in Parkinson's disease. *NPJ Parkinsons. Dis.* 6:30. doi: 10.1038/s41531-020-00133-y

Si, X. L., Fang, Y. J., Li, L. F., Gu, L. Y., Yin, X. Z., Yan YP, et al. (2020). From inflammasome to Parkinson's disease: does the NLRP3 inflammasome facilitate exosome secretion and exosomal alpha-synuclein transmission in Parkinson's disease. *Exp Neurol.* doi: 10.1016/j.expneurol.2020.113525. [Epub ahead of print].

Simuni, T., Long, J. D., Caspell-Garcia, C., Coffey, C. S., Lasch, S., Tanner, C. M., et al. (2016). Predictors of time to initiation of symptomatic therapy in early Parkinson's disease. *Ann. Clin. Transl. Neurol.* 3, 482–494. doi: 10.1002/acn3.317

Tsiouris, K. M., Rigas, G., Gatsios, D., Antonini, A., Konitsiotis, S., Koutsouris, D. D., et al. (2017). Predicting rapid progression of Parkinson's disease at baseline patients evaluation. *Annu. Int. Conf. IEEE Eng. Med. Biol. Soc.* 2017, 3898–3901. doi: 10.1109/EMBC.2017.8037708

Velseboer, D. C., Broeders, M., Post, B., van Geloven, N., Speelman, J. D., Schmand, B., et al. (2013). Prognostic factors of motor impairment, disability, and quality of life in newly diagnosed PD. *Neurology* 80, 627–633. doi: 10.1212/WNL.0b013e318281cc99

Vu, T. C., Nutt, J. G., and Holford, N. H. (2012). Progression of motor and nonmotor features of Parkinson's disease and their response to treatment. *Br. J. Clin. Pharmacol.* 74, 267–283. doi: 10.1111/j.1365-2125.2012.04192.x

Wang, T., Yuan, F., Chen, Z., Zhu, S., Chang, Z., Yang, W., et al. (2020). Vascular, inflammatory and metabolic risk factors in relation to dementia

in Parkinson's disease patients with type 2 diabetes mellitus. *Aging* 12, 15682–15704. doi: 10.18632/aging.103776

Wang, X., Yu, S., Li, F., and Feng, T. (2015). Detection of α-synuclein oligomers in red blood cells as a potential biomarker of Parkinson's disease. *Neurosci. Lett.* 599, 115–119. doi: 10.1016/j.neulet.2015.05.030

Williams, S. M., Schulz, P., and Sierks, M. R. (2016). Oligomeric α-synuclein and β-amyloid variants as potential biomarkers for Parkinson's and Alzheimer's diseases. *Eur. J. Neurosci.* 43, 3–16. doi: 10.1111/ejn.13056

Xie, F., Gao, X., Yang, W., Chang, Z., Yang, X., Wei, X., et al. (2019). Advances in the research of risk factors and prodromal biomarkers of Parkinson's disease. *ACS Chem. Neurosci.* 10, 973–990. doi: 10.1021/acschemneuro.8b00520

Xu, J., Fu, X., Pan, M., Zhou, X., Chen, Z., Wang, D., et al. (2019). Mitochondrial creatine kinase is decreased in the serum of idiopathic Parkinson's disease patients. *Aging Dis.* 10, 601–610. doi: 10.14336/AD.2018.0615

Yamazaki, Y., and Kanekiyo, T. (2017). Blood-brain barrier dysfunction and the pathogenesis of Alzheimer's disease. *Int. J. Mol. Sci.* 18:1965. doi: 10.3390/ijms18091965

Yang, W., Chang, Z., Que, R., Weng, G., Deng, B., Wang, T., et al. (2020). Contra-directional expression of plasma superoxide dismutase with lipoprotein cholesterol and high-sensitivity C-reactive protein as important markers of Parkinson's disease severity. *Front. Aging Neurosci.* 12:53. doi: 10.3389/fnagi.2020.00053

Zhao, H. Q., Li, F. F., Wang, Z., Wang, X. M., and Feng, T. (2016). A comparative study of the amount of α-synuclein in ischemic stroke and Parkinson's disease. *Neurol. Sci.* 37, 749–754. doi: 10.1007/s10072-016-2485-1

Zou, J., Chen, Z., Liang, C., Fu, Y., Wei, X., Lu, J., et al. (2018). Trefoil factor 3, cholinesterase and homocysteine: potential predictors for Parkinson's disease dementia and vascular parkinsonism dementia in advanced stage. *Aging Dis.* 9, 51–65. doi: 10.14336/AD.2017.0416

Conflict of Interest: Z-LC, YL, and KR were employed by company Gyenno Science Co. Ltd., Shenzhen, China.

The remaining author declares that the research was conducted in the absence of any commercial or financial relationships that could be construed as a potential conflict of interest.

Advantages of publishing in Frontiers

OPEN ACCESS
Articles are free to read for greatest visibility and readership

FAST PUBLICATION
Around 90 days from submission to decision

HIGH QUALITY PEER-REVIEW
Rigorous, collaborative, and constructive peer-review

TRANSPARENT PEER-REVIEW
Editors and reviewers acknowledged by name on published articles

Frontiers
Avenue du Tribunal-Fédéral 34
1005 Lausanne | Switzerland

Visit us: www.frontiersin.org
Contact us: frontiersin.org/about/contact

REPRODUCIBILITY OF RESEARCH
Support open data and methods to enhance research reproducibility

DIGITAL PUBLISHING
Articles designed for optimal readership across devices

FOLLOW US
@frontiersin

IMPACT METRICS
Advanced article metrics track visibility across digital media

EXTENSIVE PROMOTION
Marketing and promotion of impactful research

LOOP RESEARCH NETWORK
Our network increases your article's readership